VOLUME 66
NUMBER 10 / NUMÉRO 10
OCTOBER / OCTOBRE
2009

An NRC Research Press
JOURNAL
Une REVUE des
Presses scientifiques du CNRC

Canadian Journal of FISHERIES AND AQUATIC SCIENCES

cjfas.nrc.ca

Journal canadien des SCIENCES HALIEUTIQUES ET AQUATIQUES

jcsha.cnrc.ca

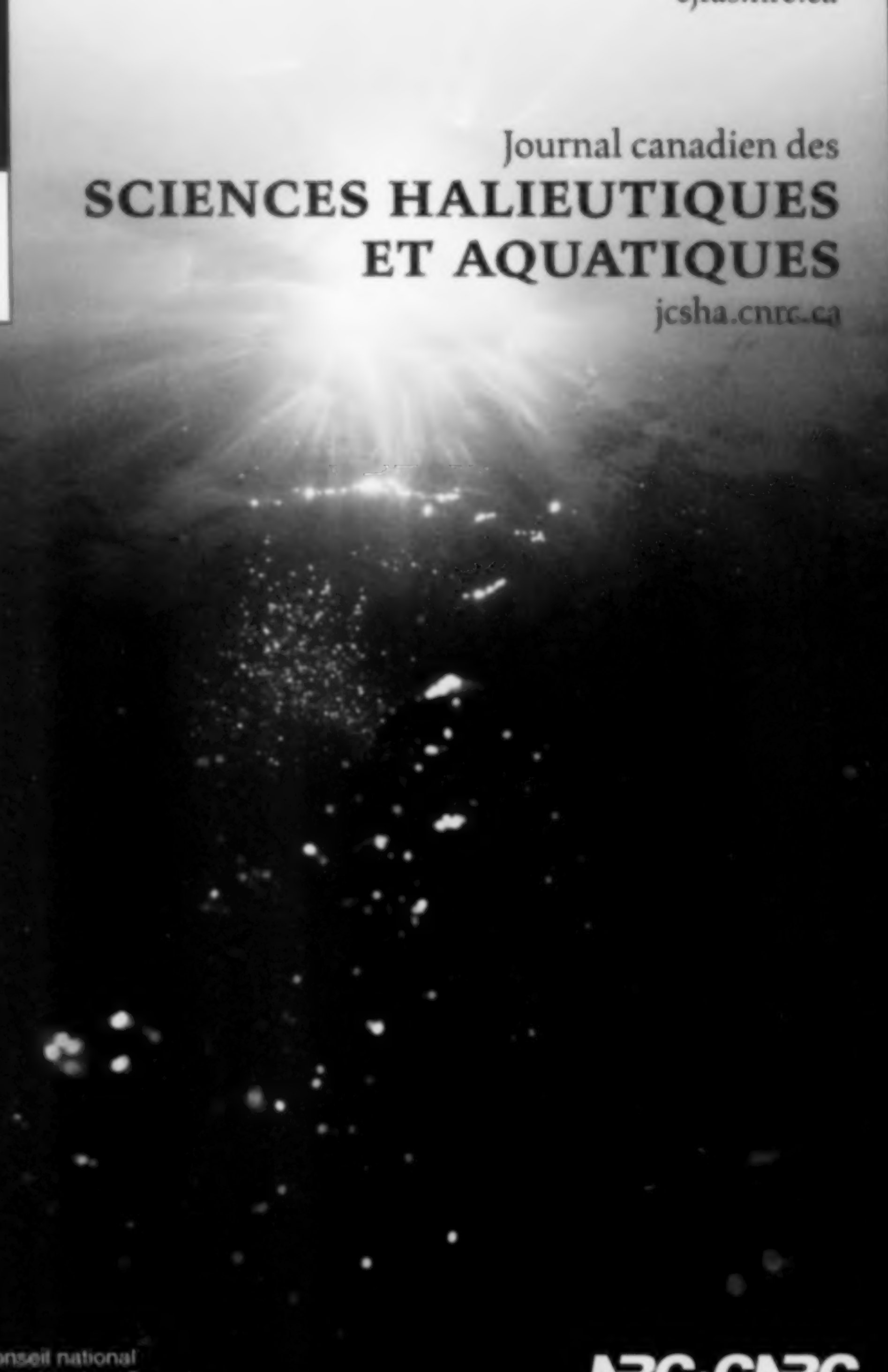

National Research Council Canada
Conseil national de recherches Canada
NRC·CNRC

ISSN 0706-652X / CJFSDX 66(10) 1635–1830 (2009)

The Canadian *Journal of Fisheries and Aquatic Sciences*, previously published as *Contributions to Canadian Biology* 1901–1925, *Contributions to Canadian Biology and Fisheries* 1926–1934, *Journal of the Biological Board of Canada* 1934–1937, and *Journal of the Fisheries Research Board of Canada* 1938–1979, is issued monthly to form annual volumes of 12 numbers plus supplements.

Editorial policy. The Journal publishes original research articles, perspectives (syntheses, critiques, reevaluations), discussions (comment and reply), and rapid communications. Manuscripts may concern cells, organisms, populations, communities, ecosystems, or processes that affect aquatic systems. They may cover a range of disciplines including biology and ecology of marine and freshwater organisms, limnology, oceanography, physiology, toxicology, genetics, economics, disease, and management. Preference will be given to manuscripts that emphasize understanding of observed phenomena and interpretation of experimental results. The Journal encourages papers that lead from clearly stated purpose or rationale and from testable hypotheses, concepts, or questions to identifiable conclusions or syntheses. Such papers may amplify, modify, question, or redirect accumulated knowledge embodied in contemporary perceptions of a particular state of aquatic sciences. The Journal discourages papers that are essentially descriptive, except in emerging disciplines; have only site-specific or local applications (a certain year, place, taxon, chemical compound, etc.); only confirm previously established principles; or apply standard techniques without breaking new methodological ground.

Manuscripts for publication should be submitted to the Editorial Office via NRC Research Press' online submission and peer review system (**OSPR**EY) at http://pubs.nrc-cnrc.gc.ca/cjfas/osprey. Alternatively, manuscripts may be submitted to the Editor, Canadian *Journal of Fisheries and Aquatic Sciences*, Department of Ecology and Evolutionary Biology, University of Toronto, Toronto, ON M5S 3G5, Canada (416-946-0609; fax: 866-523-4174 (Canada and United States) or 416-946-0509; e-mail: cjfas@utoronto.ca).

Submissions in either English or French are acceptable. The information must be original, that is, not copyrighted, published, or submitted elsewhere except in abstract form or unless by written consent of the Editor.

Correspondence concerning accepted manuscripts and corrected proofs should be sent to NRC Research Press, National Research Council of Canada, Ottawa, ON K1A 0R6, Canada (fax: 613-952-7656; e-mail: pubs@nrc-cnrc.gc.ca).

Instructions to Authors are published at cjfas.nrc.ca. The **Publishing Policy** of NRC Research Press is available at pubs.nrc-cnrc.gc.ca.

The Canadian *Journal of Fisheries and Aquatic Sciences*, ISSN 0706-652X, is published monthly, 12 times per year, by NRC Research Press, c/o USACAN Media Dist. Srv. Corp. at 26 Power Dam Way, Suite S1-S3, Plattsburgh, NY 12901, USA. Periodicals postage paid at Plattsburgh, NY. POSTMASTER: Send address changes to *Canadian Journal of Fisheries and Aquatic Sciences*, c/o NRC, P.O. Box 2888, Plattsburgh, NY 12901, USA.

Publié sans interruption depuis 1901, le *Journal canadien des sciences halieutiques et aquatiques* a paru sous plusieurs titres : *Contributions to Canadian Biology* 1901–1925, *Contributions to Canadian Biology and Fisheries* 1926–1934, *Journal of the Biological Board of Canada* 1934–1937, et *Journal of the Fisheries Research Board of Canada* 1938–1979. Le Journal paraît tous les mois, formant ainsi un volume de 12 numéros, et offre en plus jusqu'à deux suppléments par année.

Politique éditoriale. On publie, dans le Journal, des articles rendant compte de recherche originale, des perspectives (synthèses, critiques et réévaluations), des discussions (commentaires et réponses) et des communications rapides. Les documents peuvent porter sur les cellules, organismes, populations, communautés, écosystèmes ou processus qui affectent les systèmes aquatiques. Ils peuvent relever de divers domaines y compris la biologie et l'écologie des organismes marins et d'eau douce, la limnologie, l'océanographie, la physiologie, la toxicologie, la génétique, l'économie, la pathologie et la gestion. On accorde la préséance aux articles qui contribuent à la compréhension de phénomènes observés et à l'interprétation de résultats expérimentaux. On invite les auteurs à soumettre des articles ayant des objectifs précis ou relevant d'hypothèses, de concepts ou de questions vérifiables et se terminant par de solides conclusions ou d'utiles synthèses. Ces articles enrichissent, changent, mettent en question ou réorientent les connaissances acquises sur divers aspects des sciences aquatiques. On décourage toutefois la soumission d'articles simplement descriptifs (à moins qu'il ne s'agisse de nouvelles disciplines), d'application très limitée (applicables à une seule année, une seule région ou un seul taxon, portant sur un unique composé chimique, etc.); d'articles qui ne font que reprendre les principes énoncés dans des articles précédents; et d'articles rendant compte de l'application de normes sans gain de méthodologie.

Les auteurs sont invités à soumettre leur **manuscrit** au Bureau de la rédaction par le truchement du Système de soumission et d'examen en direct des articles (**OSPR**EY) des Presses scientifique du CNRC à http://pubs.nrc-cnrc.gc.ca/jcsha/osprey. Sinon, ils peuvent transmettre leur manuscrit par la poste au rédacteur en chef, *Journal canadien des sciences halieutiques et aquatiques*, Département d'écologie et de biologie évolutive, Université de Toronto, Toronto, ON M5S 3G5, Canada (416-946-0609; télécopieur : 866-523-4174 (Canada et États-Unis) ou 416-946-0509; courriel : cjfas@utoronto.ca).

Les contributions peuvent être en anglais ou en français. Elles doivent être originales, c.-à.-d. qu'elles ne doivent pas avoir fait l'objet d'un copyright, avoir été publiées ou soumises ailleurs, sauf sous forme abrégée ou avec le consentement du rédacteur en chef.

La correspondance ayant trait aux manuscrits acceptés et les **épreuves corrigés** doivent être envoyées aux Presses scientifiques du CNRC, Conseil national de recherches du Canada, Ottawa, ON K1A 0R6, Canada (télécopieur : 613-952-7656; courriel : pubs@nrc-cnrc.gc.ca).

Les **Recommandations aux auteurs** sont publiées au jcsha.cnrc.ca. La **Politique éditoriale** est disponible auprès des Presses scientifiques du CNRC ou au pubs.nrc-cnrc.gc.ca.

This Journal is indexed or abstracted in / Cette revue est signalée ou résumée dans

Aqualine; Aquatic Sciences and Fisheries Abstracts; BIOBASE; Biological and Agricultural Index; BIOSIS; CAB Abstracts; Canadian Fisheries Abstracts; Chemical Abstracts; Current Awareness in Biological Sciences; Current Abstracts; Current Contents; General Science Index; Oceanic Abstracts; PASCAL; Pollution Abstracts; Referativnyi Zhurnal; Science Citation Index; Water Resources Abstracts

Volume 66, Number 10, October 2009

Canadian Journal of Fisheries and Aquatic Sciences

Published by the National Research Council of Canada

Volume 66, numéro 10, octobre 2009

Journal canadien des sciences halieutiques et aquatiques

Publié par le Conseil national de recherches du Canada

Editors / Rédacteurs en chef Don Jackson and Rolf Vinebrooke

Assistant to the Editors / Adjointe au rédacteur en chef **Holly Foster**

Associate Editors / Comité de rédaction

M.J. Bradford, *DFO/MPO and Simon Fraser University*
D. Brickman, *DFO/MPO, Dartmouth*
S.E. Campana, *DFO/MPO, Dartmouth*
X. Chen, *Shanghai Fisheries University, Shanghai, China*
Y. Chen, *University of Maine, Orono, Maine*
I. Fleming, *Memorial University of Newfoundland*
B. Gillanders, *University of Adelaide, Australia*
J.W.A. Grant, *Concordia University*
M.M. Hansen, *Aarhus University, Denmark*
R. Hilborn, *University of Washington*
J.M. Jech, *NFSC/NOAA, Woods Hole, Mass.*
B. Jonsson, *Norwegian Institute for Nature Research, Oslo, Norway*
K.A. Kidd, *University of New Brunswick*
C. Kraft, *Cornell University, Ithaca, N.Y.*
D.L. MacLatchy, *University of New Brunswick, Saint John*
P. Magnan, *Université du Québec à Trois Rivières*
C.T. Marshall, *University of Aberdeen*
J. Post, *University of Calgary*
Y.T. Prairie, *Université du Québec à Montréal*
T.J. Quinn II, *University of Alaska–Fairbanks, Juneau, Alaska*
C.W. Ramcharan, *Laurentian University*
J.S. Richardson, *The University of British Columbia*
M.-J. Rochet, *IFREMER, Nantes, France*
K. Rose, *Louisiana State University, Baton Rouge, La.*
J. Rosenfeld, *British Columbia Ministry of Fisheries*
B. Sainte-Marie, *DFO/MPO, Mont-Joli*
R.E.H. Smith, *University of Waterloo*
S.J. Smith, *DFO/MPO, Dartmouth*
W.G. Sprules, *University of Toronto at Mississauga*
E.B. Taylor, *The University of British Columbia*
W. Tonn, *University of Alberta*
M. Trudel, *DFO/MPO, Pacific Biological Station, Nanaimo*
A. Vasemägi, *University of Turku, Turku, Finland*
C.J. Walters, *The University of British Columbia*
G. Weyhenmeyer, *Uppsala University, Sweden*

NRC Research Press / Presses scientifiques du CNRC

Fax / Télécopieur : 613-952-7656; e-mail / courriel : pubs@nrc-cnrc.gc.ca; URL / URL : pubs.nrc-cnrc.gc.ca

Editor-in-Chief / Directeur de la publication **Bruce P. Dancik**
Deputy Editor-in-Chief / Sous-directrice de la publication **Cindy E. Prescott**
Publisher / Éditeur **Cameron D. Macdonald**
Deputy Director / Directrice adjointe **Suzanne Kettley**

Business Manager / Gestionnaire des affaires commerciales **Mike Boroczki**
Advertising / Annonces publicitaires **Roxanne Landriault** (613-990-2254)
Subscriptions / Abonnements **Eileen Evans-Nantais** (613-990-7873)

Manager, Journals Program / Gestionnaire du Programme des revues **Carolyn Brown**
Managing Editor / Directrice de la rédaction **Cecily M. Pearson** (613-993-9099)
Scientific Publishing Editors / Réviseurs de publications scientifiques **Jennifer McColl, Thad Costigan, Peter Burke**
Editorial Publication Technicians / Techniciens à la publication éditoriale **Diana Leck, Luc Julien**
Editorial Applications Training and Support Officer / Agente de formation et de soutien à l'éditique **Susanne Lantos**

Production Manager / Gestionnaire de la production **Judy Hum**
Application Support Technician / Technicien au soutien de la production **Greg Boyce**
e-Publishing Technician / Technicien à l'édition électronique **Cory Klinkenberg**
Graphics Technician / Technicien en graphisme **Dario Ferrara, Davin P. Henrikson**
Web Technician / Technicien Web **Dennis Cafferty**

The National Research Council of Canada accepts no responsibility for statements or opinions expressed by a contributor. Acceptance of an advertisement, announcement, or other material does not imply endorsement by either the Journal's Editor or the National Research Council of Canada.

2009 National Research Council Canada or its licensors

For articles published in 2009 and later, copyright remains with the authors, whereas for articles published before 2009, copyright is held by the National Research Council Canada.

No part of the NRC Research Press journals may be reproduced, stored, or transmitted in any form or by any means, without the written permission of the publisher, except as stated below.

Under the Canadian *Copyright Act*, individuals may download or print single copies of articles for personal research or study. Any person may reproduce short excerpts from articles in the journals for any purpose that respects the moral rights of authors, provided that the source is fully acknowledged. As a courtesy, the consent of authors of such material should be obtained directly from the author.

Authorization to reproduce items for other than personal research or study, as stated above, may be obtained by clicking on the "Reprints and Permissions" link in the table of contents of the electronic article in question or via Access Copyright (http://www.accesscopyright.ca).

NRC Research Press also extends certain additional rights to authors.

The above rights do not extend to copying or reproduction for general distribution, for advertising or promotional purposes, for creating new collective works, or for resale. For such copying or reproduction, arrangements must be made with NRC Research Press (National Research Council Canada, Ottawa, ON K1A 0R6, Canada).

Subscription information

The *Canadian Journal of Fisheries and Aquatic Sciences* (ISSN 0706-652X) is published monthly by the National Research Council of Canada. The 2009 subscription rates are as follows. Institutional: electronic $1125; print, $1250; electronic + print, $1560. Personal: electronic, $290, print + electronic, $380. For all orders outside Canada, rates are in U.S. dollars. Print subscriptions include second class postage. For *air mail* add US$180 to the foreign rate. Canadian customers please include GST (business no. 12149 1807 RT 0275). Subscriptions are entered for the calendar year. Remittances should be made payable to the Receiver General for Canada, credit NRC. Price for regular single issues: institutional, $120.00; personal, $40.00. Supplements will be priced separately. Special rates apply to members of Canadian scientific and engineering societies if they subscribe through their respective societies.

Issues of the *Canadian Journal of Fisheries and Aquatic Sciences* are available on the Web. Pricing information can be found at pubs.nrc-cnrc.gc.ca.

There are no refunds on cancelled subscriptions once delivery has begun. Claims for missing issues should be made within four months (North America) or six months (outside North America) following the date of publication. The publisher expects to supply missing issues only when losses have occurred in transit and when the reserve stock will permit. For change of address and subscription enquiries: Subscription Office, NRC Research Press, National Research Council of Canada, Ottawa, ON K1A 0R6, Canada; tel.: 613-993-9084; fax: 613-952-7656; e-mail: pubs@nrc-cnrc.gc.ca.

Microform backfiles are available from UMI, P.O. Box 1346, Ann Arbor, MI 48106-1346, USA, and Micromedia Ltd., 20 Victoria St., Toronto, ON M5C 2N8, Canada.

Le Conseil national de recherches du Canada ne se tient en aucune façon responsable des opinions exprimées par un collaborateur ou des déclarations que pourrait faire ce dernier. La publication d'annonces publicitaires, d'avis et autres n'implique pas l'endossement de leur contenu par le rédacteur en chef de la Revue ou le Conseil national de recherches du Canada.

2009 Presses scientifiques du CNRC ou ses concédants de licence

Les auteurs détiennent les droits d'auteur sur les articles publiés en 2009 et plus tard, tandis que les Presses scientifiques du CNRC détiennent les droits d'auteurs sur les articles publiés avant 2009.

Il est interdit de reproduire, de sauvegarder ou de transmettre toute partie des revues des Presses scientifiques du CNRC dans quelque format ou de quelque façon que ce soit sans le consentement écrit de l'éditeur, sauf dans les cas énoncés ci-après.

Aux termes de la *Loi sur le droit d'auteur* du Canada, les particuliers peuvent télécharger ou imprimer des copies individuelles d'articles pour leurs études ou leurs recherches personnelles. Toute personne peut reproduire de courts extraits des articles d'une revue pourvu que les droits moraux de l'auteur soient respectés et que la source soit clairement indiquée. Il convient de demander directement à l'auteur son consentement.

On peut obtenir l'autorisation de reproduire du contenu à d'autres fins que l'usage personnel (tel que décrit ci-dessus), en cliquant sur le lien « Réimpressions et autorisations » dans la table des matières de l'article électronique en question ou par l'intermédiaire d'Access Copyright (http://www.accesscopyright.ca).

Les Presses scientifiques du CNRC accordent aussi des privilèges supplémentaires aux auteurs.

Les droits ci-dessus ne s'appliquent pas à la reproduction à grande échelle aux fins de distribution générale, de publicité ou de promotion, de compilation de nouveaux ouvrages collectifs ou de revente, par exemple. Les droits de reproduction de ce genre doivent faire l'objet d'une entente particulière avec les Presses scientifiques du CNRC (Conseil national de recherches du Canada, Ottawa, ON K1A 0R6, Canada).

Renseignements sur l'abonnement

Journal canadien des sciences halieutiques et aquatiques (ISSN 0706-652X) est une publication mensuelle du Conseil national de recherches du Canada. En 2009, les tarifs d'abonnement pour les organismes sont : 1125 $ pour la version électronique; 1250 $ pour l'imprimé; 1560 $ pour les deux versions. Pour leur part, les particuliers paient les tarifs suivants : 290 $ pour la version électronique; 380 $ pour la version électronique et l'imprimé. Les tarifs des commandes provenant de l'extérieur du Canada sont en dollars des États-Unis. L'abonnement à l'imprimé comprend le tarif du courrier de deuxième classe. L'expédition par avion exige des frais de 180 $ US en sus du prix d'abonnement à l'étranger. Les clients du Canada doivent ajouter la TPS (numéro d'entreprise 12149 1807 RT 0275). Les abonnements sont pour l'année civile. Tout paiement doit être adressé au Receveur général du Canada, crédit du CNRC. Le prix par numéro est de 120,00 $ pour les organismes et de 40,00 $ pour les particuliers. Le prix des hors-série varie. Les membres des sociétés canadiennes de sciences et de génie bénéficient de taux préférentiels en s'abonnant via leurs sociétés respectives.

Les numéros de *Journal canadien des sciences halieutiques et aquatiques* sont accessibles sur le Web. On trouvera des renseignements sur les tarifs à pubs.nrc-cnrc.gc.ca.

Aucun remboursement ne sera accordé ni aucune annulation acceptée une fois que les livraisons auront commencé. Les réclamations de numéros manquants devront être soumises dans les quatre mois (Amérique du Nord) ou dans les six mois (à l'extérieur de l'Amérique du Nord) suivant la date de publication. L'éditeur ne fournira de numéros manquants que si le document a été perdu pendant l'expédition et que si le stock le permet. Adressez tout changement d'adresse ou toute question quant à l'abonnement au : Bureau des abonnements, Presses scientifiques du CNRC, Conseil national de recherches Canada, Ottawa, ON K1A 0R6, Canada; téléphone : 613-993-9084; télécopieur : 613-952-7656; courriel : pubs@nrc-cnrc.gc.ca.

On peut obtenir les fichiers rétrospectifs sur **microforme** auprès de UMI, P.O. Box 1346, Ann Arbor, MI 48106-1346, É.-U., et auprès de Micromedia Ltée, 20, rue Victoria, Toronto, ON M5C 2N8, Canada.

Limnological properties of permafrost thaw ponds in northeastern Canada

Julie Breton, Catherine Vallières, and Isabelle Laurion

Abstract: Arctic warming has recently accelerated, triggering the formation of thaw ponds and the mobilization of a carbon pool that has accumulated over thousands of years. A survey of 46 thaw ponds in the Canadian arctic and subarctic regions showed that these ecosystems have high concentrations of dissolved organic matter (DOM) and nutrients and are relatively productive. This activity was reflected in the optical properties of DOM that indicated a dominance of allochthonous sources but a significant contribution of low molecular weight compounds. Several subarctic ponds were stratified in summer, resulting in a hypoxic hypolimnion. Most ponds were supersaturated in CO_2 and CH_4, with higher gas concentrations in bottom waters. However, arctic thaw ponds colonized by benthic microbial mats showed lower CO_2 concentrations, likely caused by active photosynthesis. CO_2 was correlated with both the quantity and the optical properties of DOM, suggesting the significant role of dissolved compounds from melting organic soils and catchment vegetation on the balance between heterotrophy and autotrophy. The large variability observed in limnological properties of this series of ponds precludes generalisations about their role in greenhouse gas production. However, the fact that all thaw ponds were supersaturated in CH_4 underscores the importance of estimating their global significance.

Résumé : Le réchauffement arctique s'est récemment accéléré, activant la formation des mares de fonte du pergélisol et la mobilisation d'une réserve de carbone accumulée sur plusieurs millénaires. L'étude de 46 mares de fonte en régions arctique et subarctique canadiennes montre que ces écosystèmes possèdent des concentrations élevées en matière organique dissoute (MOD) et en nutriments, ainsi qu'une productivité relativement élevée. Cette activité se reflète dans les propriétés optiques de la MOD qui indiquent une dominance des sources allochtones mais une contribution significative par les composés de faibles poids moléculaires. Plusieurs mares subarctiques étaient stratifiées l'été, avec présence d'un hypolimnion hypoxique. La plupart de ces mares étaient supersaturées en CO_2 et en CH_4, avec des concentrations de gaz supérieures au fond. Toutefois, les mares arctiques colonisées par d'épais tapis microbiens montraient de plus faibles concentrations en CO_2, probablement causées par l'activité photosynthétique. Le CO_2 était corrélé avec la quantité et les propriétés optiques de la MOD, suggérant le rôle significatif des composés dissous provenant de la fonte des sols organiques et des plantes du bassin versant sur l'équilibre entre l'hétérotrophie et l'autotrophie. La grande variabilité des conditions limnologiques observées dans cette série de mares nous garde de faire des généralisations sur leur rôle dans la production de gaz à effet de serre. Toutefois, le fait que toutes les mares étaient supersaturées en CH_4 souligne le besoin d'estimer leur importance globale.

Introduction

Thaw ponds and thermokarst ponds resulting from the thawing of permafrost are the most abundant types of aquatic ecosystems at circumpolar arctic and subarctic latitudes (Vincent et al. 2008). Processes involved in thermokarst formation include thawing, ponding, surface and subsurface drainage, surface subsidence, and erosion (Yoshikawa and Hinzman 2003). In continuous permafrost areas, thaw ponds develop on low-center polygons and in runnels over melting ice wedges (ice-filled soil cracks) at the surface of permafrost terrain (Fortier and Allard 2004). These ponds are a natural phenomenon associated with the active layer dynamics of organic soils but are likely increasing in importance with the accelerated warming and melting of permafrost. In discontinuous permafrost areas, thermokarst ponds are formed in depressions left after the ice has melted in surface soils (Calmels and Allard 2004; Arlen-Pouliot and Bhiry 2005). In this case, pond formation is associated with global warming trends (i.e., it requires more than seasonal warming of the active layer to form).

Permafrost is estimated to occupy about 24% of the northern hemisphere land surface (Zhang et al. 1999). In coming decades, increases in regional temperatures are expected to cause widespread degradation of permafrost, particularly in discontinuous permafrost zones (International Panel on Climate Change (IPCC) 2007). An increase in permafrost temperatures has been observed in northwestern Canada,

Received 1 August 2008. Accepted 22 May 2009. Published on the NRC Research Press Web site at cjfas.nrc.ca on 26 September 2009.
J20697

Paper handled by Associate Editor Yves Prairie.

J. Breton, C. Vallières, and I. Laurion.[1] Institut national de la recherche scientifique, Centre Eau, Terre et Environnement, 490 rue de la Couronne, Québec, QC G1K 9A9, Canada; Centre d'études nordiques, Université Laval, Québec, QC G1K 7P4, Canada.

[1] Corresponding author (e-mail: isabelle.laurion@ete.inrs.ca).

Can. J. Fish. Aquat. Sci. **66**: 1635–1648 (2009) doi:10.1139/F09-108 Published by NRC Research Press

Siberia, northern Europe, and Alaska over the last 20 years (Richter-Menge et al. (2006) and references therein). Woo et al. (1992) estimated that a 4–5 °C warming could lead to a 50% reduction in the area underlain by discontinuous permafrost in arctic and subarctic Canada. Recent deepening in the active layer of soils and the formation of thermokarst has been reported in both Europe (e.g., Zuidhoff 2002; Luoto and Seppälä 2003) and North America (e.g., Beilman et al. 2001; Jorgenson et al. 2006). In a subarctic peatland, Payette et al. (2004) observed that over the past 50 years, the surface area occupied by thermokarst ponds increased as permafrost melted. On the other hand, in some regions of Alaska, shrinking of pond surface areas has been observed (Yoshikawa and Hinzman 2003). This apparent contradiction can be explained using a continuum approach: initial permafrost warming leads to the development of thermokarst, followed by lake drainage as the permafrost degrades further (Smith et al. 2005). Exceptions to this model exist and may depend on specific soil geomorphology. For example, the discontinuous permafrost area of subarctic Quebec is underlain by postglacial marine silts (Calmels and Allard 2004) that render the soil below the ponds impermeable. Although drainage may not occur even after permafrost has completely disappeared, vegetation can colonize the system and cause the aquatic state to recede (Payette et al. 2004).

Among studies exploring permafrost disturbances, several have either focussed on hydrological regimes and geophysical description (e.g., Åkerman and Malmström 1986; Schwamborn et al. 2002) or explored the effect of permafrost degradation on vegetation (e.g., Lloyd et al. 2003). The type of vegetation seems to play an important role in greenhouse gas (CO_2 and CH_4) exchanges in tundra ecosystems (Oechel et al. 1993; Christensen et al. 1999). Subarctic wetlands disturbed by permafrost degradation have been investigated, with indications that plant species, soil moisture, and substrate availability to methanogens are key variables to greenhouse gas exchanges (Ström and Christensen (2007) and references therein). Changes in the thermokarst and aerial extent of wetlands, lakes, and ponds could alter globally the size and direction of greenhouse gas fluxes above these landscapes (Hamilton et al. 1994; Chapin et al. 2000). Walter et al. (2006) attributed a 58% CH_4 emission increase in northern Siberia to the expansion of thaw lakes between 1974 and 2000. Despite the potential role of thaw pond biology and ecosystem dynamics on global climate change, few studies have examined the limnological properties of these systems.

The present study was undertaken as part of a broader program to examine the evolution of this little-studied yet abundant type of ecosystem with regards to recent climate change. Our objectives were to describe the physicochemical and biological properties of thaw ponds located in contrasting permafrost conditions (subarctic discontinuous and arctic continuous permafrost regions) and to evaluate how these properties might affect their potential role as sources of greenhouse gases to the atmosphere. We considered the influence of thermal stratification and the microbial components of this ecosystem on greenhouse gas evasion. The relationship between dissolved organic matter (DOM) and greenhouse gas concentrations was also investigated in detail, as DOM has been identified as a major determinant of the role that lakes play in the carbon cycle (Cole et al. 2007).

Materials and methods

Field site description

An extensive study of 46 ponds was carried out in July and August of 2004 and 2005 in Nunavik in the subarctic discontinuous permafrost region (ponds named "KUJ" at 55°14′N 77°42′W and "KWK" at 55°20′N 77°30′W, both near the village of Whapmagoostui-Kuujjuarapik; "BON" at 57°44′N 76°14′W along Boniface River; "BGR" at 56°37′N 76°13′W near the village of Umiujaq) and in Sirmilik National Park, Bylot Island, Nunavut, in the arctic continuous permafrost region (ponds named "BYL" at 73°09′N 79°58′W near the village of Pond Inlet) (Figs. 1 and 2). The subarctic ponds are located in impermeable clay–silt beds and apparently are not part of a hydrologic network (requires further investigation). In contrast, arctic thaw ponds (only the runnels) were often interconnected (Fig. 2*f*).

The subarctic thaw ponds are surrounded by dense shrubs (*Betula glandulosa*, *Salix* spp., *Alnus* sp., *Myrica gale*) and sparse trees (*Picea mariana*, *Picea glauca*, *Larix laricina*; denser trees at BON), with some areas colonized by *Sphagnum* spp. mosses. Detailed environmental descriptions are available in Calmels and Allard (2004) for BGR, Arlen-Pouliot and Bhiry (2005) for KUJ, Payette et al. (2004) for BON, and Fortier and Allard (2004) for BYL. There is no existing description of the Kwakwatanikapistikw River site (KWK, at ~18 km north of the KUJ site). The soil forming the permafrost mounds at the BGR site (Fig. 2*c*) contained clays and silts with low organic matter content (<1.5%; Calmels and Allard 2004). However, some mounds were covered or surrounded with peat and had vegetation growing mainly on their ramparts. At the KWK site, mounds were also essentially mineral (no remaining peat cover), but only some of them were still apparent (i.e., permafrost had melted) and they had dense vegetal colonization (Fig. 2*a*). At the BON, KUJ, and BYL sites, peat cover (e.g., 2.7 m thick at KUJ; Arlen-Pouliot and Bhiry 2005) and dense vegetation were present (Fig. 2). The differing types of vegetation and soils in these five sites are most likely contributing to the observed differences in DOM and nutrient concentrations (see below). To our knowledge, only the ponds at the arctic site have previously been studied for benthic microbial mats and zooplankton grazing (Vézina and Vincent 1997; Rautio and Vincent 2006).

The study ponds were chosen to represent different water colors and development phases. Of the 46 ponds studied, four were investigated more closely (BGR1, BGR5, KWK1, and KWK2; these ponds were selected on-site), where profiles of several limnological characteristics were collected, including dissolved gases, nutrients, DOM optical properties, and bacterial abundance and production.

Physicochemistry

Temperature, dissolved oxygen, and pH were recorded in 2004 with an Ocean Seven probe (316; Idronaut Srl., Brugherio, Italy) and in 2005 with a multiparametric probe (600R; YSI Inc., Yellow Springs, Ohio). The temperatures at the

Fig. 1. Location of the sampling sites in the Canadian arctic and subarctic regions, as indicated by the stars.

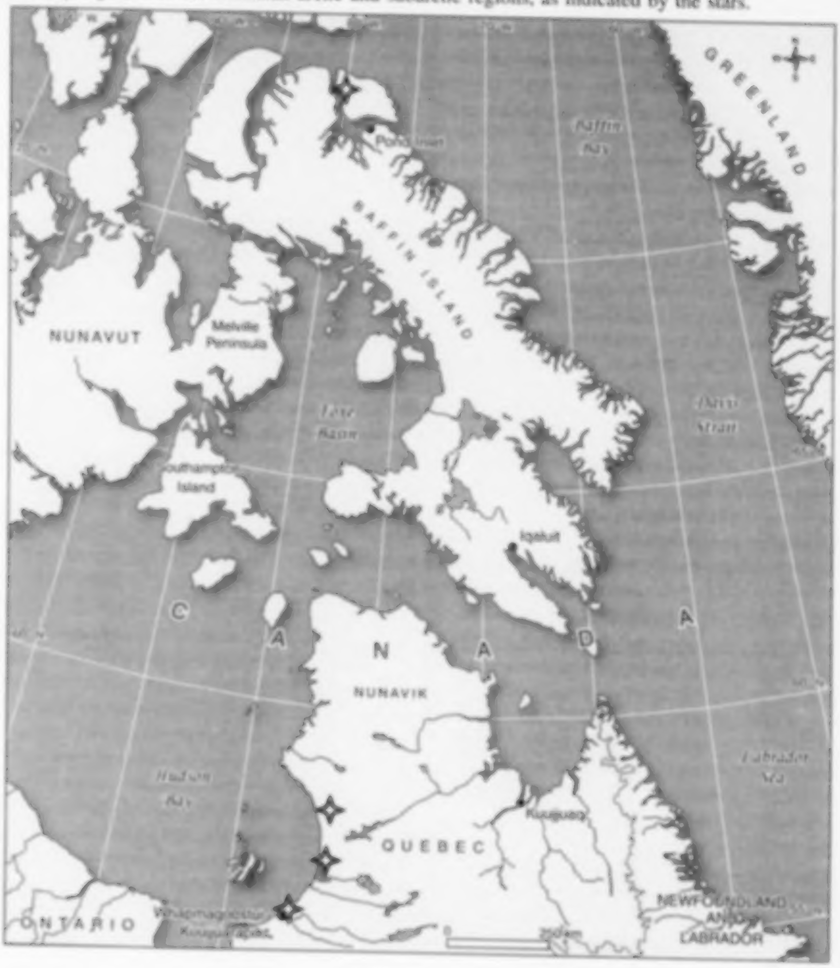
GREENLAND
Baffin Bay
Pond Inlet
BAFFIN ISLAND
NUNAVUT
Melville Peninsula
Foxe Basin
Davis Strait
Southampton Island
Iqaluit
C A N A D A
N
NUNAVIK
Labrador Sea
Hudson Bay
Kuujjuaq
QUEBEC
NEWFOUNDLAND AND LABRADOR
ONTARIO
Whapmagoostui
Kuujjuarapik
0
250 km

surface (0.3 m) and bottom (2.75 m) of pond BGR1 (56°37′N 76°13′W; maximum pond depth ~3.2 m) were measured continuously from July 2005 through July 2006, with the readings recorded every half hour (HOBOware™ U12 thermistors; Onset Computer Corp., Bourne, Massachusettes).

The total suspended solids (TSS) of surface water samples were collected onto precombusted and preweighed glass fiber filters (0.7 µm nominal mesh size; Advantec MFS Inc., Dublin, California) that were subsequently dried for 24 h at 60 °C. The quantity of solids volatilized at 500 °C (2 h) was used to estimate the organic fraction. The material that remained on the filter was considered an approximation of the inorganic fraction. Water samples were measured for total phosphorus (TP), soluble reactive phosphorus (SRP), nitrate (NO_3^-), and ammonium (NH_4^+) concentrations. For TP, H_2SO_4 was added to unfiltered water (0.15% final concentration). For SRP, NO_3^- and NH_4^+, water was filtered through prerinsed cellulose acetate filters (0.2 µm pore size; Advantec MFS Inc.). All samples were kept in prewashed Teflon-capped glass bottles and preserved at 4 °C until analysis. TP was measured by spectrophotometry as in Stainton et al. (1977). SRP and NH_4^+ were determined by flow injection analysis (Lachat Instruments, Loveland, California), and NO_3^- was determined by ionic chromatography (Dionex Corp., Sunnyvale, Colorado).

Biological components

Water samples were collected onto glass fiber filters for the determination of chlorophyll *a* concentrations (chl *a*). Filters were kept frozen at –80 °C until pigments were extracted in 95% aqueous MeOH. Chl *a* was determined by high-pressure liquid chromatography using the method adapted by Bonilla et al. (2005). Water samples for bacterial abundance were fixed with a filtered solution of paraformaldehyde (1% final concentration) and were kept at 4 °C until analysis. The bacteria were stained with 4′,6-diamidino-2-phenylindole (DAPI, 5 µg·L^{-1} final concentration) and counted using epifluorescence microscopy (Axiovert; Carl Zeiss MicroImaging Inc., Thornwood, New York). Bacterial production was estimated in 13 ponds from the subarctic BGR and KWK sites using the ^{3}H-leucine incorporation

Fig. 2. Thaw ponds study sites. Ponds formed on mineral mounds at an advanced stage of development in the discontinuous permafrost areas at (*a*) KWK, 55°19′N 77°30′W, (*b*) KUJ, 55°13′N 77°44′W (with a red algal bloom), and (*c*) BGR, 56°36′N 76°12′W (the arrow indicates a remaining patch of peat). (*d*) Pond formed along margins of a forested palsa (BON, 57°30′N 76°14′W). (*e*) Ponds colonized by *Sphagnum* spp. mosses near KWK site. (*f*) Ponds formed in melted ice wedges and above depressed polygons in the continuous permafrost area (BYL, 73°09′N 79°58′W). (*g*) Close-up of melted ice wedges with high-center polygons.

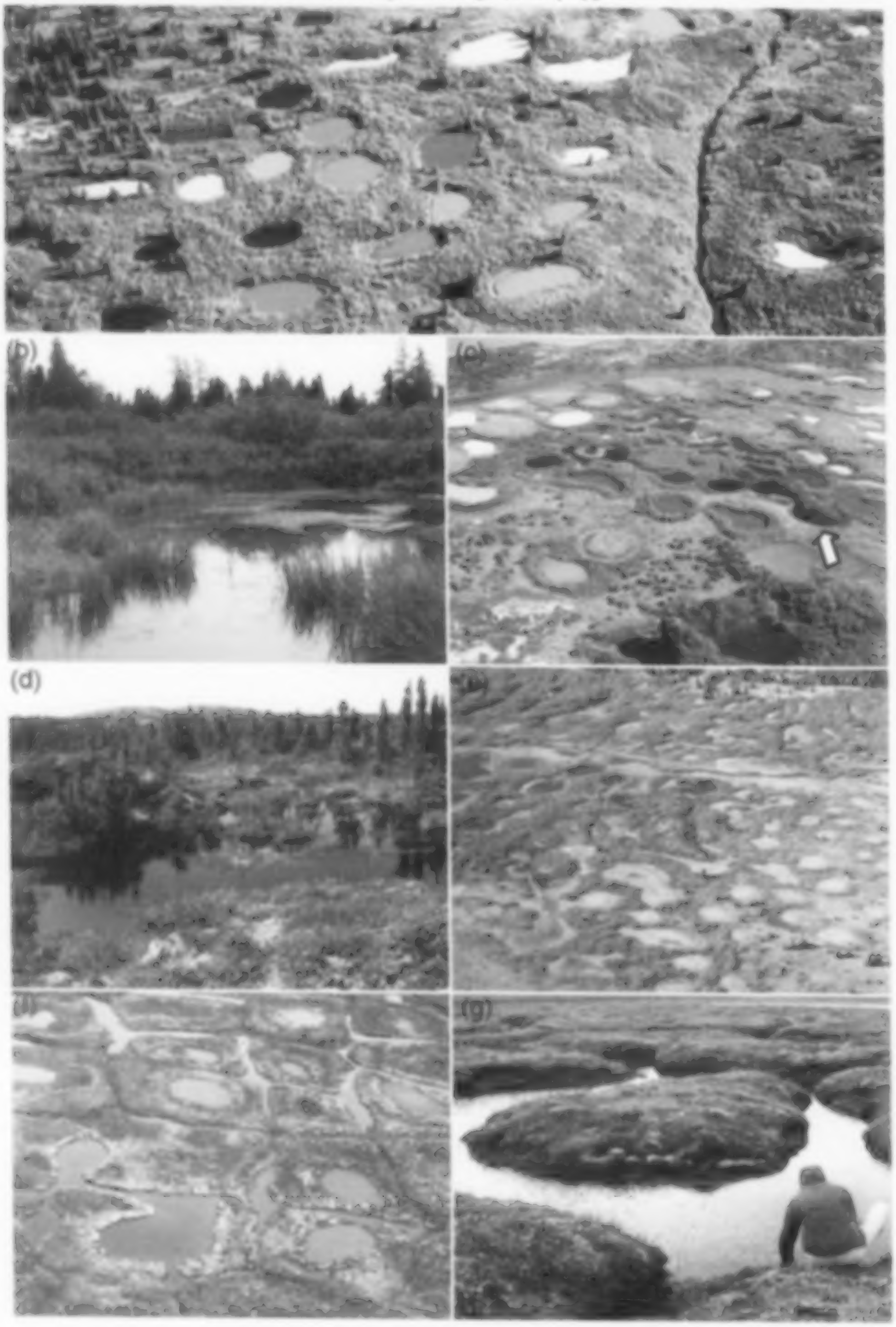

method as a measurement of protein synthesis by heterotrophic picoplankton (Kirchman 1993). The water was fractionated with 3 μm polycarbonate filters (47 mm, Poretics) to measure free-living (<3 μm) and total bacterial activity. For each measurement, five replicates of 2 mL water samples were incubated in sterile microvials; two of them were sterilized with trichloroacetic acid (TCA; 5% final concentration) to serve as controls. Microvials were then inoculated with ^{3}H-leucine (specific activity of 167 Ci·mmol^{-1}; Amersham Biosciences, Piscataway, New Jersey) to a final concentration of 10 nmol·L^{-1} (Simon and Azam 1989) and incubated in the dark at the pond in situ temperature (±3.5 °C) for 2 h. Protein synthesis was stopped by the addition of 5% TCA. To eliminate unlabelled ^{3}H-leucine, pellets were rinsed twice with 5% TCA (12 min centrifugation at 13 000 rpm; modified from Smith and Azam 1992) and then stored at –20 °C until analysis. A volume of 1 mL of scintillation liquid (OptiPhase "HiSafe" 2; Wallac scintillation products) was added to the samples, which were then radio-assayed 24 h later using a Beckman LS 6500 scintillation system. Carbon and phosphorus limitation to bacterial production was tested for two ponds at the BGR site in 2005 (BGR1 and BGR5). Polycarbonate bottles (1 L) were filled with unfiltered surface water, with enrichments as follows (triplicate bottles for each treatment; final concentrations are given): 5 μmol glucose·L^{-1} as a labile carbon source (C+), 5 μg K_2HPO_4·L^{-1} (P+), and the combination of both carbon and phosphorus (CP+). Triplicate bottles were kept unamended to serve as controls. The bottles were incubated in situ for 24 h in the dark. At the end of incubation, total bacterial production was measured as explained above.

DOM characterization

Water samples were filtered and stored as described above for nutrients (no signal is released by cellulose acetate filters when they are properly rinsed). Dissolved organic carbon (DOC) concentrations were measured using a Shimadzu TOC-5000A carbon analyzer calibrated with potassium biphthalate. To determine the chromophoric fraction of DOM (CDOM), absorbance scans were performed on a spectrophotometer from 250 to 800 nm (Cary 100; Varian; details in Mitchell et al. 2003). The absorption coefficient at 320 nm (a_{320}) was used to quantify CDOM. Two methods were used to further characterize DOM: synchronous fluorescence and a simple fluorescence emission scan. Synchronous fluorescence (SF) spectra (Peuravuori et al. 2002) were recorded over the excitation wavelength range 200–700 nm and a wavelength difference between excitation and emission beams of 14 nm (details in Belzile et al. 2002) using a spectrofluorometer (Cary Eclipse; Varian). Spectroscopic measurements were always run at natural pH and room temperature. Fluorescence data were corrected for scatter and inner-filter effect as in Mobed et al. (1996). Integrated areas under the three wavebands (Retamal et al. 2007) were used as an index of CDOM composition: low molecular weight compounds (LMW, emission range 280–323 nm), medium molecular weight compounds (MMW, 324–432 nm), and high molecular weight compounds (HMW, 433–593 nm). This index is used as a relative DOM composition index, but it is not appropriate to quantify the amount of each group of fluorophores (for example, the integration of excitation–emission matrix fluorescence peaks would be needed). A humification index (HI) was also determined as proposed in Kalbitz et al. (1999), where the ratio of SF intensity at 470 nm over 360 nm is considered a measure of polycondensation and degree of humification (although Kalbitz et al. (1999) used a slightly higher wavelength difference between excitation and emission beams of 18 nm). In addition, emission scans of fluorescence were obtained from 400 to 700 nm with an excitation wavelength at 370 nm (corrected as above). The fluorescence index (FI) developed by McKnight et al. (2001) was then calculated (ratio of fluorescence emission intensities at 450 nm over 500 nm) to characterize the source of the fulvic acid fraction of DOM (lower FI values for DOM derived from algal and microbial precursors compared with a terrestrial origin).

Dissolved CO_2 and CH_4 concentrations

Dissolved CO_2 and CH_4 ($Gas_{(aq)}$) were determined by the equilibration of 2 L of pond water into 20 mL of ambient air for 3 min, with the headspace sampled in duplicated vials (red-stopper Vacutainer®) previously flushed with helium and vacuum-sealed (Hesslein et al. 1990). Gas samples were kept at 4 °C until analysed by gas chromatography (Varian 3800, COMBI PAL Head Space injection system, CP-Poraplot Q 25 m × 0.53 mm column, flame ionization detector). The dissolved gases were calculated according to Henry's law:

$$(1)\qquad \mathrm{Gas}_{(aq)} = K_H \times p\mathrm{Gas}$$

where K_H is the Henry's constant adjusted for ambient water temperature and pGas is the partial pressure of CO_2 or CH_4 in the headspace. Although the CO_2 equilibrium in pond water is linked to pH, the method used (equilibrium of a headspace 100 times smaller than the water volume) was unlikely to change the pH sufficiently to affect dissolved CO_2 estimations. For CH_4, even though the effect was minor (<1%), gas movement during the equilibration was corrected for.

Results

Physicochemistry

Thaw ponds were deeper at the subarctic sites (1–3.3 m) than at the arctic sites (generally <1 m) and had small surface areas (81–605 m^2, as determined from a high spatial resolution Quickbird satellite image taken in 2006 at KWK, n = 34; I. Laurion, unpublished data). Surface water temperature at sampling varied from 7 to 21 °C in 2004 and from 7 to 28 °C in 2005. Most of the ponds were thermally stratified at the time of sampling, in particular the ponds at the BGR and KWK sites (Fig. 3). Several ponds showed a linear decrease in temperature with depth (i.e., without a defined thermocline; see the example of BGR1 in Fig. 3*a*), indicative of limited mixing during the sampling period. In ponds of the forested tundra (BON) and at the arctic sites (BYL), although a stable thermocline did not develop, short-term stratification was often observed. The year-long monitoring of surface and bottom water temperatures of subarctic pond BGR1 revealed persistent stratification despite its shallow depth (Fig. 4). The temperature difference between surface

Fig. 3. Profiles of temperature (dotted line, triangles) and dissolved oxygen (solid line, circles) in four subarctic thermokarst ponds: (*a*) BGR1 on 8 July 2005 starting at 1233 hours, (*b*) BGR4 on 6 July 2004 starting at 1345, (*c*) KWK1 on 17 July 2005 starting at 1323, and (*d*) KWK2 on 17 July 2005 starting at 1402. Profiles were obtained in 2004 with an Idronaut probe and in 2005 with a YSI probe.

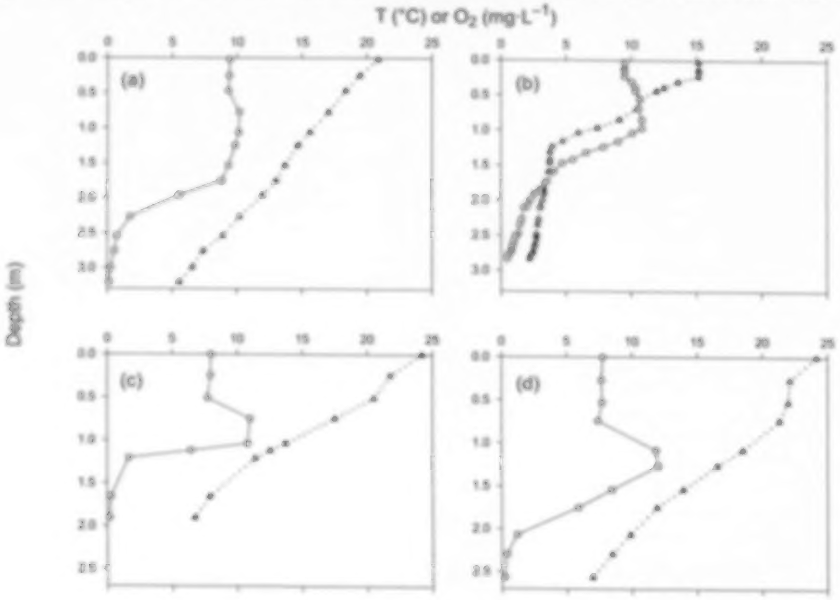

Fig. 4. Temperature at the surface (0.3 m, shaded line) and bottom (2.75 m, black line) of pond BGR1 (maximal depth ~3.2 m) (*a*) followed over one complete year from 13 July 2005 to 13 July 2006, (*b*) showing diurnal stratification during the autumnal mixing period, and (*c*) during spring mixing.

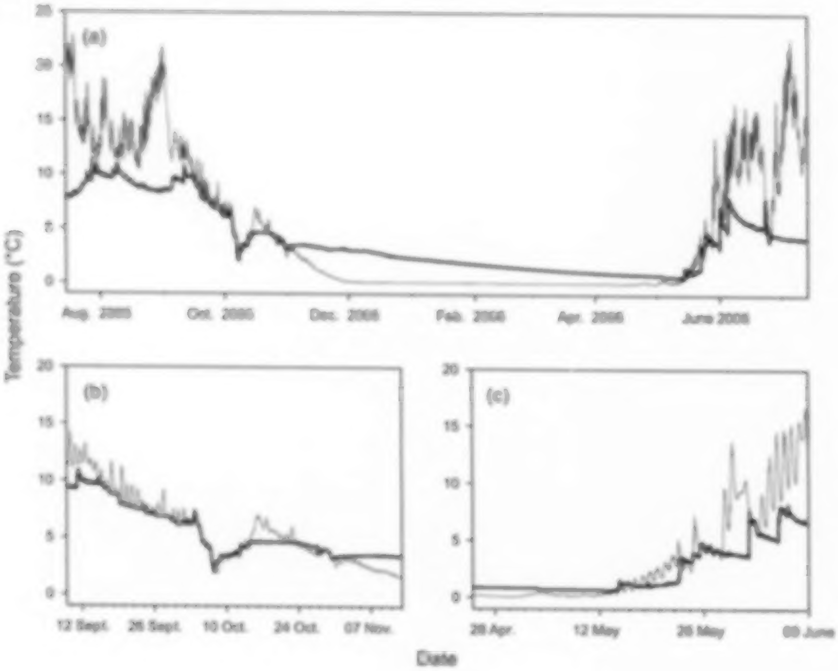

and bottom waters was larger than 1 °C for 71% of the year, with summer stratification occurring about 24% of the year. This pond was ice-covered from the end of November to the end of April, with two principal periods of mixing: a short episode in May–June (Fig. 4*b*) and a long episode beginning in September until the end of October (Fig. 4*c*). Short isolated "mixing events" were also observed during the summer (lasting for a total of less than 3 days in June–July). Temperature inversions occurred on 31 October and 18 May (ice cover). Winter water temperatures below the ice cover ranged from 0.5 to 3.6 °C, indicating that the pond did not freeze. Dissolved oxygen decreased with depth in most ponds, with an abrupt change below the thermocline in stratified ponds or with hypoxic waters near the sediments (0.5–4.1 mg $O_2 \cdot L^{-1}$ in 2004 and 0.1–1.4 mg $O_2 \cdot L^{-1}$ in 2005 in bottom waters; examples in Fig. 3). Even in some of the shallowest arctic ponds, oxygen gradients were observed (5.3–6.8 mg $O_2 \cdot L^{-1}$ in bottom waters compared with 7.1–10 mg $O_2 \cdot L^{-1}$ at the surface). The ponds presented a large range of pH values (Table 1), which did not change significantly with depth. The pH was higher in the arctic ponds above low-center polygons.

Several ponds were highly turbid at the subarctic sites, with a wide range of TSS values in surface waters (Table 1). Vertical extinction of photosynthetic available radiation was found to be controlled mainly by DOM absorption and the TSS diffusion of light (K_d ranged from 1.5 to 9.2 m^{-1} in 12 ponds sampled in 2006; I. Laurion, unpublished data). Ponds from the BGR and KWK sites (originating from melting ice under mineral mounds) had significantly higher TSS values than ponds from other sites (Mann–Whitney, $p < 0.001$). The ratio of volatile–inorganic solids (not presented) was always >1 at the BON and KUJ sites, and <1 at the BGR and KWK sites (except at KWK9). At the BYL sites, the ratio was variable (with five ponds out of 14 showing a ratio >1).

Nutrients were relatively high in thaw ponds compared with oligotrophic or dystrophic lakes more commonly studied in polar regions (e.g., Hamilton et al. 2001); TP ranged from 6 to 320 $\mu g\ P \cdot L^{-1}$ (mean ± standard deviation; 60 ± 70 $\mu g\ P \cdot L^{-1}$, $n = 30$), SRP from 1.5 to 48 $\mu g\ P \cdot L^{-1}$ (5 ± 10 $\mu g\ P \cdot L^{-1}$, $n = 21$), NO_3^- from 11 to 959 $\mu g\ N \cdot L^{-1}$ (167 ± 299 $\mu g\ N \cdot L^{-1}$, $n = 10$), and NH_4^+ from 39 to 287 $\mu g\ N \cdot L^{-1}$ (92 ± 60 $\mu g\ N \cdot L^{-1}$, $n = 28$). Nutrients were also generally higher in the bottom waters (not presented). Phosphorus concentrations (TP, SRP) were higher in subarctic ponds (on average twice as high, but differences were not significant) than in arctic ponds.

Biological components

Planktonic chl *a* concentrations ranged from 0.3 to 8.8 $\mu g \cdot L^{-1}$ (3.0 ± 2.5 $\mu g \cdot L^{-1}$). Blooms of algae (red or green filamentous) were observed in some subarctic ponds, indicative of a relatively productive system (Fig. 2*b*). Thick microbial mats were observed in the arctic ponds formed on low-center polygons, with a consortium of taxa dominated by oscillatorian cyanobacteria (Vézina and Vincent 1997). Planktonic bacterial abundance ranged from 0.9×10^6 to 30.6×10^6 $cells \cdot mL^{-1}$ ($6.2 \pm 5.0 \times 10^6$ $cells \cdot mL^{-1}$). There was a positive linear relationship between bacterial abundance and ammonium concentration ($r = 0.796$, $n = 29$, $p < 0.0001$), and a significant but weaker relationship with TP ($r = 0.499$, $n = 29$, $p = 0.005$). Samples taken from bottom waters generally showed higher bacterial abundance than surface waters (Table 2).

Bacterial production in the surface waters of subarctic ponds was lower (476 ± 76 pmol $leucine \cdot L^{-1} \cdot h^{-1}$, $n = 13$; Table 2), but not significantly different (*t* test, $p = 0.080$) from the production in bottom waters (757 ± 503 pmol $leucine \cdot L^{-1} \cdot h^{-1}$, $n = 4$). Results from size fractionation showed that 82% (BGR1) and 56% (BGR5) of bacterial ^{3}H-leucine uptake was associated with suspended particles >3 µm. The bacterial community in the two BGR ponds responded differently to carbon and phosphorus additions (Fig. 5). In pond BGR1, both carbon and phosphorus were limiting (one-way ANOVA, $p < 0.001$; Tukey, $p < 0.002$ for CP+ compared with other treatments), whereas in BGR5, carbon was the only limiting factor (one-way ANOVA, $p < 0.001$; Tukey, $p < 0.001$ for all comparisons except between CP+ and C+). In pond BGR1, bacterial activity increased by 2.6-fold in the CP+ treatment compared with the control, where there was a twofold increase in both C+ and CP+ treatments in pond BGR5.

DOM characterization

Pond DOM properties (DOC, a_{320}, FI, HI) are shown in Table 1. DOC presented a wide range of values and was significantly higher in arctic ponds than in subarctic ponds (means of 12.0 $mg \cdot L^{-1}$ and 8.8 $mg \cdot L^{-1}$, respectively; $p = 0.028$ for *t* test on square-root-transformed data). The specific absorption (defined as a_{320} per unit DOC) also varied widely (0.9–7.0 $L \cdot m^{-1} \cdot (mg\ DOC)^{-1}$) and was lower in the arctic ponds (average of 3.2 $L \cdot m^{-1} \cdot (mg\ DOC)^{-1}$ compared with 4.0 $L \cdot m^{-1} \cdot (mg\ DOC)^{-1}$ in subarctic ponds). The FI values varied from 1.12 to 1.36 at the surface of thaw ponds, which are below the range published by McKnight et al. (2001) but are still within the range reported in the literature for terrestrial reference fulvic acids (1.15–1.40; see Schwede-Thomas et al. (2005) and references therein). Differences observed between studies can be attributed to the unique optical design and light source of instruments (e.g., Schwede-Thomas et al. (2005) observed up to 0.26 unit differences between spectrofluorometers).

The synchronous fluorescence spectra were relatively similar in shape but differed in intensity (Fig. 6). The ponds featured eight principal peaks (emission wavelengths: 300 (I), 362 (II), 395 (III), 416 (IV), 439 (V), 487 (VI), 514 (VII), and 560–575 (VIII) nm), which were classified into LMW (peak I), MMW (peaks II to IV), and HMW (peaks V to VIII) fluorophore groups. Differences in relative proportions of these three groups of fluorophores were observed between subarctic ponds with a peat-containing catchment (12%, 43%, and 44% in LMW, MMW, and HMW fluorophores, respectively), subarctic ponds absent of peat (but with vegetation in their catchment and high turbidity; 16%, 47%, and 35%, respectively), and arctic ponds (19%, 50%, and 31%, respectively; Tukey multiple comparisons, $p < 0.05$). HI values varied from 0.3 to 1.4 (Table 1) and averaged 1.0, 0.6, and 0.5, respectively, in the above three types of pond catchment.

Dissolved CO_2 and CH_4 concentrations

The ponds were supersaturated in CO_2 and CH_4 in most

Table 1. Limnological characteristics of thaw ponds sampled in 2004 and 2005.

Pond type	Pond name	DOC	a_{320}	FI	HI	pH	TSS	$p\text{CO}_2$	$p\text{CH}_4$
Whapmagoostui–Kuujjuarapik, forest tundra (2005 unless specified)									
d, PP	KWK1	9.0	39.0	1.13	0.61	6.9	9.4	926	18.5
d, PP	KWK2	7.1	30.5	1.14	0.70	6.4	3.9	1283	37.1
d, PP	KWK2-B	25.4	56.5	1.30	0.86	na	64.6	1757	35.0
d, PP	KWK3 (2004)	3.4	10.5	na	na	7.1	7.8	750	4.0
d, PP	KWK5	9.3	42.0	1.15	0.83	na	na	1470	17.2
d, PP	KWK6	5.4	7.5	1.16	0.67	na	na	757	10.7
d, PP	KWK7	8.6	29.2	1.16	0.58	na	na	1048	53.8
d, PP	KWK8	10.1	44.0	1.15	0.61	na	na	1564	20.9
d, PP	KWK9 (2004)	4.5	20.2	1.23	0.54	7.0	2.8	1028	10.3
d, PR	KUJ1	24.5	171.0	1.24	0.85	5.8	5.4	7106	6.8
d, PR	KUJ6	26.0	23.8	na	na	6.9	11.4	2370	17.6
Umiujaq, Sheldrake River, shrub tundra (2004 unless specified)									
d, PP	BGR1	3.3	5.7	1.35	0.45	6.9	23.8	567	5.4
d, PP	BGR1 (2005)	2.5	4.5	1.36	0.50	7.1	5.3	364	10.0
d, PP	BGR2	3.0	12.9	1.18	0.84	6.4	271	2056	19.5
p, PR	BGR3	5.4	30.7	1.14	1.02	6.5	14.5	2608	33.0
d, PP	BGR4	2.5	8.7	1.27	0.95	7.0	39.7	835	5.6
d, PP	BGR5	1.3	5.9	1.24	0.51	na	na	na	na
d, PP	BGR5 (2005)	4.7	8.8	1.18	0.83	6.4	15.5	949	19.5
d, PP	BGR6	4.3	22.5	1.17	0.69	na	na	na	na
d, PR	BGR7	1.3	5.4	1.30	0.46	na	na	na	na
d, PR	BGR8	9.0	52.9	na	0.93	6.8	na	1158	32.3
d, PP	BGR9	2.7	5.8	1.24	0.49	8.5	na	na	na
d, PP	BGR10 (2005)	5.1	26.7	1.15	0.60	7.3	na	na	na
d, PP	BGR12 (2005)	4.3	4.0	1.18	0.53	7.0	na	na	na
p, PP	BGR16 (2005)	9.8	28.6	na	0.48	na	na	na	na
p, PP	BGR32 (2005)	7.3	24.5	1.12	0.77	na	na	na	na
p, PP	BGR33 (2005)	11.5	69.1	1.16	0.68	na	na	na	na
Boniface River, forest tundra (2004)									
p, PR	BON1	17.6	120.0	1.25	1.03	5.2	11.4	4166	11.6
p, PR	BON2	11.5	51.4	1.18	1.44	5.1	1.3	10 381	63.7
p, PR	BON4	9.3	42.2	na	na	5.4	3.5	2442	20.7
p, PR	BON5	9.4	49.5	1.18	0.90	6.3	na	1603	33.2
p, PR	BON8	11.8	56.8	1.19	1.28	5.8	0.7	3498	25.8
p, PR	BON9	20.6	109.0	1.28	0.97	4.7	7.3	na	na
Bylot Island, Arctic tundra (2005)									
d, PI	BYL1	9.4	20.9	1.20	0.52	9.2	2.0	275	10.1
p, PI	BYL2	19.7	109.0	1.31	0.38	7.4	2.8	3259	38.7
d, PI	BYL3	16.7	88.5	1.22	0.52	7.5	10.4	680	22.2
d, PI	BYL4	11.0	43.9	1.21	0.49	7.7	4.9	321	39.4
d, PI	BYL7	16.9	28.2	1.27	0.35	8.8	24.0	na	na
d, PI	BYL8	10.6	25.0	1.24	0.42	na	11.6	na	na
p, PI	BYL11	21.5	92.7	1.29	0.40	7.4	7.0	na	na
p, PI	BYL12	10.1	35.7	1.25	0.42	7.4	2.3	1132	11.6
p, PI	BYL13	10.5	33.6	1.26	0.42	7.5	3.4	na	na
p, PI	BYL14	8.6	22.3	1.23	0.47	8.0	0.4	440	10.3
d, PI	BYL15	7.9	19.6	1.21	0.54	8.0	1.7	na	na
d, PI	BYL16	8.6	14.4	1.26	na	9.1	1.0	86	7.5
d, PI	BYL17	10.1	19.3	1.23	0.45	8.7	5.0	na	na
p, PI	BYL18	11.0	42.4	1.27	0.47	7.4	5.4	na	na
d, PI	BYL20	6.8	17.8	1.26	0.51	na	na	na	na

Note: DOC, dissolved organic carbon (mg·L^{-1}); a_{320}, absorption coefficient of dissolved organic matter at 320 nm (m^{-1}); FI, fluorescence index (McKnight et al. 2001); HI, humification index (Kalbitz et al. 1999); TSS, total suspended solids (mg·L^{-1}); $p\text{CO}_2$ and $p\text{CH}_4$, partial pressure of carbon dioxide (μatm) and methane (μatm); d, depression; p, periphery; PR, peat-rich in subarctic area; PP, peat-poor in subarctic area; PI, polygonal ice-wedge formation in arctic area; na, not available.

Table 2. Bacterial abundance (BA, × 10^6 cells·mL^{-1}) and production (BP, pmol leucine·L^{-1}·h^{-1}; as estimated by leucine incorporation rate) in subarctic thermokarst ponds.

Pond name	Depth	Fraction	BA	BP	BP SD
BGR1	S	T	1.98	529	27
	S	<3	na	98	16
	B	T	4.43	1078	76
BGR5	S	T	11.60	1195	41
	S	<3	na	523	22
	B	T	6.61	1260	54
BGR9	S	T	4.21	192	9
BGR10	S	T	3.43	305	8
BGR12	S	T	3.93	103	8
BGR16	S	T	15.64	720	25
BGR32	S	T	9.40	190	32
KWK1	S	T	2.65	243	14
	B	T	13.66	167	30
KWK2	S	T	1.71	203	34
	B	T	1.98	523	57
KWK5	S	T	7.46	254	18
KWK6	S	T	4.09	413	20
KWK7	S	T	10.20	364	19
KWK8	S	T	7.65	359	19

Note: S, surface; B, bottom; T, total production; <3 µm, production associated with particles <3 µm; SD, standard deviation.

Fig. 5. Response of bacterial production (BP) to the addition of glucose (C+), phosphorus (P+), or both (CP+) compared with control in ponds (*a*) BGR1 and (*b*) BGR5. The error bars represent standard deviation from three replicates. The letters show the results of the Tukey multiple comparison test. Different letters indicate significant differences ($p < 0.002$).

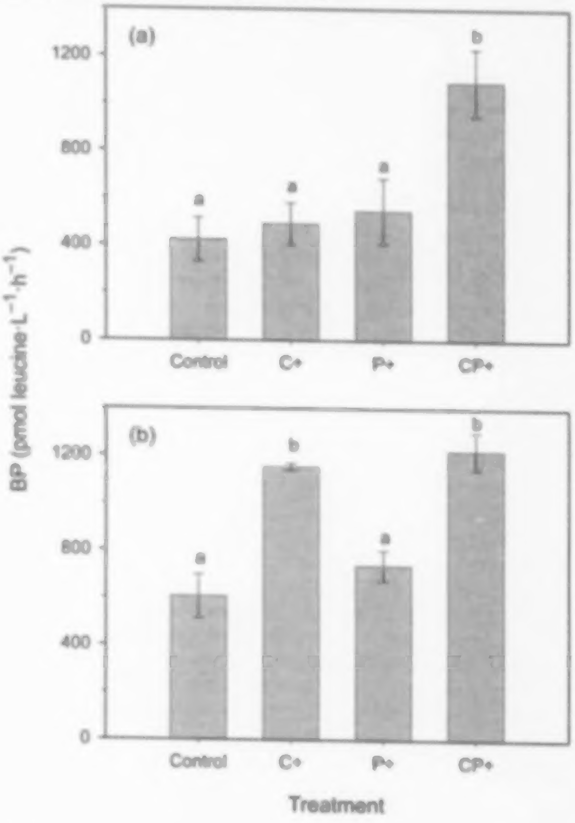

cases (assuming global values of atmospheric partial pressures equal to 379 µatm of CO_2 and 1.77 µatm of CH_4; IPCC 2007), although they presented a wide range of concentrations (gas partial pressure is presented in Table 1). Moreover, CO_2 was approximately 8 to 16 times higher in bottom waters than in surface waters (Table 3). CH_4 gradients were even more striking, with concentrations from 2 to 125 times higher in bottom waters. Because of its low solubility in water compared with CO_2, CH_4 was also likely escaping through ebullition, but this process was not evaluated in the present study. In low-center polygons colonized with benthic microbial mats where dissolved gases were measured (BYL1, BYL4, and BYL16), CO_2 was below the generic atmospheric concentration, but the ponds were still highly supersaturated in CH_4. Weak but positive correlations were found between CO_2 and DOM properties (DOC and HI are shown in Fig. 7; significant correlations also with a_{320} ($r = 0.577$, $p < 0.001$), a_{320}/DOC ($r = 0.474$, $p = 0.008$), and the proportion of HMW fluorophores ($r = 0.676$, $p < 0.001$)). Such correlations were not found between CH_4 and DOM properties or were only marginally significant, such as for the proportion of HMW fluorophores ($r = 0.402$, $p = 0.046$).

Discussion

High-latitude freshwater ecosystems are situated in a landscape with slow chemical weathering and minimal anthropogenic influences and typically produce ultraoligotrophic systems with low inputs of nutrients and organic carbon from their catchment (Pienitz et al. 1997; Hamilton et al. 2001; Lim et al. 2001). On the contrary, thaw ponds have relatively high nutrient concentrations. The high turbidity of most subarctic thaw ponds sampled in the present study may partly explain the high TP values measured (TP and TSS were correlated; $r = 0.536$, $p = 0.004$). Turbid systems often present high TP values due to the adsorption of phosphorus onto particles imported from land (Deborde et al. 2007), but even ponds with the lowest TSS (<5 mg·L^{-1}) had relatively high TP values (6.2–91 µg·L^{-1}). Fresh nutrients are also likely imported from the melting permafrost soils (Mack et al. 2004). Conversely, chl *a* concentrations were relatively low and did not correlate with TP. Primary production was likely limited by the availability of light in the most turbid and coloured ponds of the subarctic sites. This high nutrient – low light environment is likely promoting net heterotrophy in the more turbid subarctic ponds. CO_2 partial pressure was indeed higher in the subarctic ponds than in the arctic ponds ($p = 0.006$ for t test on log-transformed data), but CH_4 concentrations were similar in both types of systems.

The abundance of bacterioplankton was elevated in the ponds and comparable with densities found in eutrophic lakes (e.g., Nixdorf and Jander 2003). This abundant bacterial community presented high productivity compared with

Fig. 6. Synchronous fluorescence spectra (RFU, relative fluorescence units) obtained from thaw ponds sampled at BON1, KWK2, BGR16, and BYL3 sites. Vertical lines indicate the separation of three groups of fluorophores: low molecular weight (LMW), medium molecular weight (MMW), and high molecular weight (HMW) compounds.

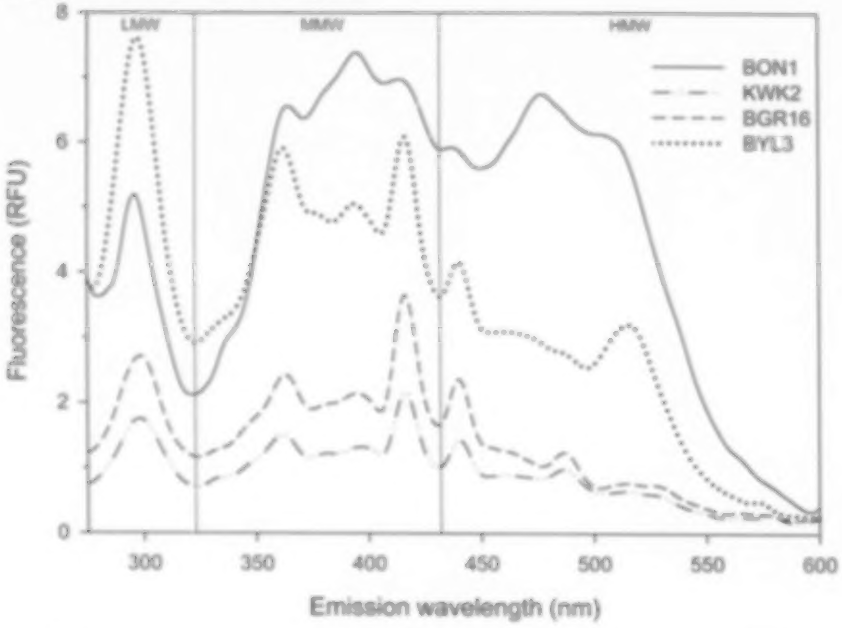

Table 3. Comparison of surface- and bottom-water characteristics of five thermokarst ponds in 2005.

Pond name	Depth	DOC	a_{320}	HI	$p\mathrm{CO}_2$	$p\mathrm{CH}_4$
BGR1	S	2.5	4.5	0.50	365	10.0
	B	2.5	2.2	0.53	3 090	23.9
BGR5	S	4.7	8.8	0.51	949	19.5
	B	3.0	9.0	0.71	9 258	1253.0
KWK1	S	9.0	39.0	0.61	927	18.5
	B	8.9	42.5	0.87	15 235	2309.0
KWK2	S	7.1	30.5	0.58	1 283	37.1
	B	6.8	35.5	0.70	17 382	3571.0
BYL11	S	21.5	92.7	0.40	na	na
	B	39.4	647.8	0.11	na	na

Note: S, surface; B, bottom; DOC, dissolved organic carbon (mg·L^{-1}); a_{320}, absorption coefficient of dissolved organic matter at 320 nm (m^{-1}); HI, humification index (Kalbitz et al. 1999); $p\mathrm{CO}_2$ and $p\mathrm{CH}_4$, partial pressure of carbon dioxide (μatm) and methane (μatm).

the ocean (0.04–230 pmol leucine·L^{-1}·h^{-1}; Steward et al. 1996) or a large subarctic river (132 pmol leucine·L^{-1}·h^{-1}; Vallières et al. 2008) and was found within the range obtained for temperate lakes (75–1229 pmol leucine·L^{-1}·h^{-1}, the maximal value being from an eutrophic lake; del Giorgio et al. 1997). The enrichment experiments in two BGR ponds indicated that the bacterial metabolism was carbon-limited when TP was high (63.4 μg P·L^{-1} in BGR5) and was both carbon- and phosphorus-limited under a lower TP concentration (26.7 μg P·L^{-1} in BGR1). Even though a large fraction of this phosphorus was likely adsorbed onto clay particles, it was possibly accessible through desorption. Clay – organic matter aggregates have been found to enhance bacterial production by providing a surface for attachment and concentrating DOM (Tietjen et al. 2005). A significant part of total bacterial activity in these two BGR ponds indeed came from particle-attached bacteria. The dominance of particle-based communities has also been observed in turbid, high-latitude rivers (Vallières et al. 2008). Particle-associated enzyme activity was frequently found to be much higher than the activity associated with free-living microbial communities (Arnosti 2003). Yet, the enrichment experiment results also suggest that planktonic bacterial activity was limited by the lability of the available organic carbon, despite significant DOC concentrations (4.7 mg·L^{-1} and 2.5 mg·L^{-1} in BGR1 and BGR5, respectively). There is a clear need to investigate if the carbon released to thaw ponds from melting permafrost watersheds is actually used by planktonic and benthic

Fig. 7. Relationship between carbon dioxide partial pressure (pCO$_2$) and (*a*) dissolved organic carbon (DOC) and (*b*) humification index (HI) calculated from the synchronous fluorescence spectra.

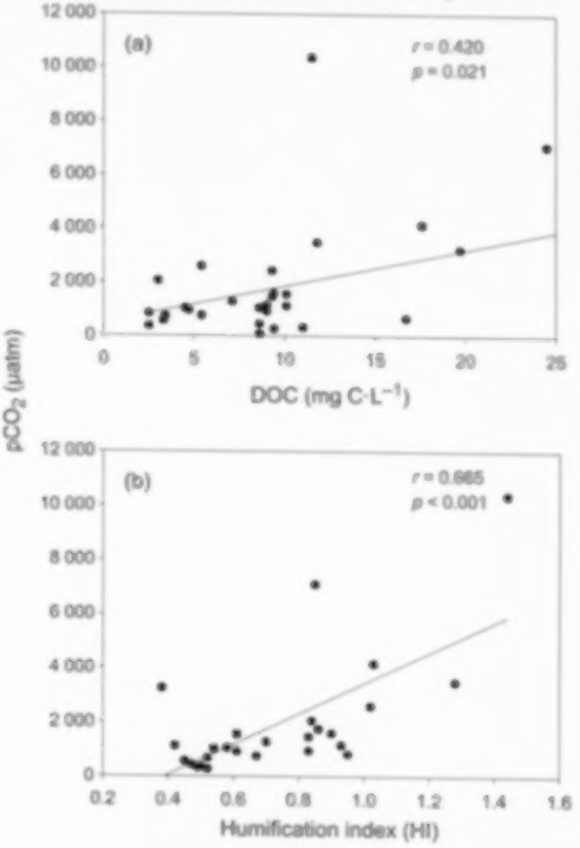

bacterial communities in relation to their role on DOM transformation and greenhouse gas production (e.g., using a stable isotope approach as in McCallister et al. 2004).

Steep thermal stratification was observed in many ponds in the discontinuous permafrost area, particularily in the most turbid ponds. The efficient absorption of photons at shorter wavelengths by CDOM and the diffusive properties of suspended solids promote the formation of temperature gradients, stable stratification, and therefore hypoxia in the bottom waters of these shallow ponds. Despite occasional short mixing periods during summer (probably associated with periods of strong winds and temperature cooling often observed at these latitudes), the water column in one typical pond was shown to be stable for most of the year. Such thermal stratification imposes restrictions on gas circulation. For example, the accumulated gases trapped in the hypolimnion are likely transferred to surface waters during mixing events. Therefore, autumn may be a period of intense degassing towards the atmosphere. Spring may also lead to increased gas fluxes in which accumulated gases, produced over the winter, are liberated upon ice break-up (Michmerhuizen et al. 1996), although this mixing period was quite short in the case of pond BGR1. Because the water remained liquid at the bottom of this pond during the whole winter, we can assume that most subarctic ponds with this depth range and at these latitudes could maintain some microbial activity in their bottom waters during the winter.

Kling et al. (1991) and Kortelainen et al. (2006) highlighted the importance of small lakes as gas conduits for transferring terrestrially fixed carbon into the atmosphere through CO$_2$ evasion. Despite large differences in several limnological characteristics, the thaw ponds sampled in the present study are no exception to this trend as they were all supersaturated in CO$_2$ and CH$_4$ (departures from saturation were, on average, 1512 and 22 µatm, respectively, for both gases); the exceptions were those arctic ponds on low-center polygons colonized with thick, actively photosynthesizing microbial mats and showing undersaturation in CO$_2$ but supersaturation in CH$_4$ (on average, –44 and 20 µatm, respectively). Most of the CH$_4$ evasion in Siberian thermokarst lakes was shown to occur through bubbling and sporadic hotspots in the study by Walter et al. (2006). Although CH$_4$ concentrations are likely underestimated in the present study, the high partial pressure measured nonetheless suggests that Canadian thaw ponds represent a significant source of CH$_4$ to the atmosphere. An estimation of the importance of CH$_4$ bubbling is required to accurately estimate evasion rates of this gas from thaw ponds on soils of a different nature and thickness than the yedoma organic sediments found beneath Siberian thaw lakes (Walter et al. 2006).

Because thaw ponds offer diverse habitats to microbial assemblages in terms of light availability, nutrients, and carbon sources, such a wide range of dissolved gas concentrations was expected. DOM was found to alter the metabolic balance and play a significant role on carbon evasion rates from freshwaters (Sobek et al. 2003; Cole et al. 2007). Our results suggest that the quantity and optical properties of DOM have a significant impact on thaw pond greenhouse gas concentrations. First, a significant positive correlation between CO$_2$ partial pressure and DOC was observed in surface waters, similar to the correlation found by Sobek et al. (2005) in a global-scale database. However, the correlation coefficient remained low and may indicate the difficulty in adequately describing the large variability in DOM reactivity in these systems simply by using bulk DOC. DOM is thought to be an important modifier of lake ecosystem metabolism (Hope et al. 1996), but the exact mechanisms may imply factors other than direct microbial DOM consumption. In fact, we did not find a correlation between CO$_2$ concentration and bacterioplankton abundance or productivity. The increasing concentration of CO$_2$ observed in the hypolimnion suggests that benthic respiration is the largest source of CO$_2$ in thaw ponds, as was the case in small boreal lakes (Kortelainen et al. 2006). DOM may indirectly affect benthic respiration through its control on temperature, stratification, and light regime (see Caplanne and Laurion 2008 and references therein), which, in turn, affect the oxygen content and the type of microbial metabolism. Large variations in the ratio of pond volume to sediment area may also affect these relationships. Finally, it is possible that part of the CO$_2$ measured in the thaw ponds originated from chemical weathering or soil microbial respiration in the catchment soils (especially where high concentrations were measured; up to 10 381 µatm in pond BON2), further reducing the strength of the relationship between CO_2 and DOM. Such possible sources of CO_2 need to be further investigated.

CO_2 partial pressure was also correlated with DOM optical properties. Pond water containing the most complex organic matter with the highest degree of humification (expressed as HI or as the proportion of HMW fluorophores) and aromaticity (expressed as a_{320}/DOC) had the highest concentrations of CO_2 (Fig. 7). This may suggest that a significant portion of CO_2 in the thaw ponds was produced by the photolysis of complex DOM molecules (Mopper et al. 2000). Several authors have demonstrated that photolysis is a major loss process of DOM in aquatic systems (e.g., Granéli et al. 1996; Vähätalo and Wetzel 2004). In the case of CH_4, the lower correlation with DOM properties (only significant with the proportion of HMW fluorophores) possibly results from a larger spatial and temporal variability in the production of this gas, such as shown by Walter et al. (2006). Overall, the relationship between greenhouse gases and HMW compounds, known for their higher precipitation rates compared with smaller DOM molecules, could be linked to the benthic microbial oxidation of precipitated organic matter (von Wachenfeldt et al. 2008).

As indicated by FI values, thaw pond DOM appeared to be derived mainly from terrestrial sources. However, these ponds should be considered active systems with a significant contribution to the DOM pool from photosynthesis and grazing, as indicated by the presence of LMW compounds identified in the SF spectra. The LMW peak (peak I at 300 nm) has been associated with dissolved proteins from recently produced organic matter (Coble et al. 1990). The higher exposure to sunlight and the occurrence of microbial mats in arctic ponds might explain their higher proportion of LMW DOM (19% ± 4%) and lower HI values (0.45 ± 0.06) as compared with subarctic ponds. How these properties affect bacterial production and respiration needs to be tested. Large differences were observed in the pond DOM properties and even within one site. For example, pond BGR2 had two times more CDOM (a_{320}), and its DOM was two times more absorbent (a_{320}/DOC) than BGR1, despite being located less than 25 m apart. Although differences in catchment and edaphic properties may exist on a small geographic scale, in situ processes such as differing inputs of autochthonous DOM (especially benthic algal colonization) and differing photochemical and microbial degradation rates of DOM (Obernosterer and Benner 2004) may have a greater influence on the DOM pool of thaw ponds, especially as they are not formed simultaneously (this asynchrony in pond formation can be observed at the BGR site shown herein). For example, clay mineral turbidity has been associated with increased photochemical degradation rates of DOM (Tietjen et al. 2005). Therefore, the quantity of clay particles and the developmental stage of the pond may indirectly affect its DOM. Differences in DOM properties may also be partly explained by the differing pH values observed in these ponds (Mobed et al. 1996; pH was not adjusted).

We hypothesize that the DOM properties of thaw ponds are not only linked to the presence of microbial mats, peat, or vegetation type in their catchment, but also to their development stage. For example, pond age may affect DOM properties through its influence on plants and macrophyte colonization, which stabilizes the shore and reduces the erosion of clays. If pond age is a crucial factor affecting its stability and trophic state, for example, through microbial community composition or colonization by plants (or mosses, such as observed in the subarctic region), it should affect the intensity and direction of carbon fluxes. The large variability observed in summer limnological properties of thaw ponds precludes generalisations about their role in greenhouse gas production. Measurements of temporal variability in greenhouse gas fluxes, in addition to accurate estimation of the aerial extent of thaw ponds in the Canadian subarctic and arctic landscapes (e.g., using remote sensing), are needed to fully evaluate their role in the global carbon balance.

Acknowledgements

We thank S. Caplanne, L. Laperrière, M.-J. Martineau, C. Martineau, S. Roy, and C. Tremblay for their assistance in the field and laboratory, G. Gauthier for letting us stay at their field camp in the Arctic, W.F. Vincent for inspiring discussions, C. Dupont, L. Retamal, F. Calmels, M. Allard, R.M. Cory, and P. Ramlal for sharing knowledge, L. Marcoux for drawing the map, K. Mueller for manuscript editing, P. Campbell, B. Beisner, and anonymous reviewers for their valuable comments. This study was supported by the Network of Centres of Excellence program ArcticNet, le Fonds québécois de la recherche sur la nature et les technologies, the Natural Sciences and Engineering Research Council of Canada, the Polar Continental Shelf Project (publication No. 042-07), Indian and Northern Affairs Canada, and the Centre d'études nordiques.

References

Åkerman, H.J., and Malmström, B. 1986. Permafrost mounds in the Abisko area, northern Sweden. Geogr. Ann. Ser. A, **68**(3): 155–165. doi:10.2307/521455.

Arlen-Pouliot, Y., and Bhiry, N. 2005. Palaeoecology of a palsa and a filled thermokarst pond in a permafrost peatland, subarctic Québec, Canada. Holocene, **15**(3): 408–419. doi:10.1191/0959683605hl818rp.

Arnosti, C. 2003. Microbial extracellular enzymes and their role in dissolved organic matter cycling. *In* Aquatic ecosystems: interactivity of dissolved organic matter. *Edited by* S.E.G. Findlay and R.L. Sinsabaugh. Academic Press, New York. pp. 316–342.

Beilman, D.W., Vitt, D.H., and Halsey, L.A. 2001. Localized permafrost peatlands in western Canada: definition, distributions, and degradation. Arct. Antarct. Alp. Res. **33**(1): 70–77. doi:10.2307/1552279.

Belzile, C., Gibson, J.A.E., and Vincent, W.F. 2002. Colored dissolved organic matter and dissolved organic carbon exclusion from lake ice: implications for irradiance transmission and carbon cycling. Limnol. Oceanogr. **47**: 1283–1293.

Bonilla, S., Villeneuve, V., and Vincent, W.F. 2005. Benthic and planktonic algal communities in a high Arctic lake: pigment structure and contrasting responses to nutrient enrichment. J. Phycol. **41**(6): 1120–1130. doi:10.1111/j.1529-8817.2005.00154.x.

Calmels, F., and Allard, M. 2004. Ice segregation and gas distribution in permafrost using tomodensitometric analysis. Permafrost Periglac. **15**(4): 367–378. doi:10.1002/ppp.508.

Caplanne, S., and Laurion, I. 2008. Effects of chromophoric dissolved organic matter on epilimnetic stratification in lakes. Aquat. Sci. **70**(2): 123–133. doi:10.1007/s00027-007-7006-0.

Chapin, F.S., III, Mcguire, A.D., Randerson, J., Pielke, R., Baldocchi, D., Hobbie, S.E., Roulet, N., Eugster, W., Kasischke, E., Rastetter, E.B., Zimov, S.A., and Running, S.W. 2000. Arctic and boreal ecosystems of western North America as components of the climate system. Glob. Change Biol. **6**(S1): 211–223. doi:10.1046/j.1365-2486.2000.06022.x.

Christensen, T.R., Jonasson, S., Callaghan, T.V., and Havström, M. 1999. On the potential CO_2 release from tundra soils in a changing climate. Appl. Soil Ecol. **11**(2-3): 127–134. doi:10.1016/S0929-1393(98)00146-2.

Coble, P.G., Green, S.A., Blough, N.V., and Gagosian, R.B. 1990. Characterization of dissolved organic matter in the Black Sea by fluorescence spectroscopy. Nature (London), **348**(6300): 432–435. doi:10.1038/348432a0.

Cole, J.J., Prairie, Y.T., Caraco, N.F., McDowell, W.H., Tranvik, L.J., Striegl, R.G., Duarte, C.M., Kortelainen, P., Downing, J.A., Middelburg, J.J., and Melack, J. 2007. Plumbing the global carbon cycle: integrating inland waters into the terrestrial carbon budget. Ecosystems (N.Y., Print), **10**(1): 171–184. doi:10.1007/s10021-006-9013-8.

Deborde, J., Anschutz, P., Chaillou, G., Etcheber, H., Commarieu, M.V., Lecroart, P., and Abril, G. 2007. The dynamics of phosphorus in turbid estuarine systems: example of the Gironde estuary (France). Limnol. Oceanogr. **52**: 862–872.

del Giorgio, P.A., Prairie, Y.T., and Bird, D.F. 1997. Coupling between rates of bacterial production and the abundance of metabolically active bacteria in lakes, enumerated using CTC reduction and flow cytometry. Microb. Ecol. **34**(2): 144–154. doi:10.1007/s002489900044. PMID:9230102.

Fortier, D., and Allard, M. 2004. Late Holocene syngenetic ice-wedge polygons development, Bylot Island, Canadian Arctic Archipelago. Can. J. Earth Sci. **41**(8): 997–1012. doi:10.1139/e04-031.

Granéli, W., Lindell, M., and Tranvik, L. 1996. Photo-oxidative production of dissolved inorganic carbon in lakes of different humic content. Limnol. Oceanogr. **41**: 698–706.

Hamilton, J.D., Kelly, C.A., Rudd, J.W.M., Hesslein, R.H., and Roulet, N.T. 1994. Flux to the atmosphere of CH_4 and CO_2 from wetland ponds on the Hudson Bay Lowlands (HBLs). J. Geophys. Res. Atmos. **99**(D1): 1495–1510. doi:10.1029/93JD03020.

Hamilton, P.B., Gajewski, K., Atkinson, D.E., and Lean, D.R.S. 2001. Physical and chemical limnology of 204 lakes from the Canadian Arctic Archipelago. Hydrobiologia, **457**(1/3): 133–148. doi:10.1023/A:1012275316543.

Hesslein, R.H., Rudd, J.W.M., Kelly, C., Ramlal, P., and Hallard, K.A. 1990. Carbon dioxide pressure in surface waters of Canadian lakes. *In* Air–water mass transfer. *Edited by* S.C. Wilhelms and J.S. Gulliver. American Society of Civil Engineers, Reston, Virginia. pp. 413–431.

Hope, D., Kratz, T.K., and Riera, J.L. 1996. Relationship between $p$$CO_2$ and dissolved organic carbon in northern Wisconsin lakes. J. Environ. Qual. **25**: 1442–1445.

International Panel on Climate Change. 2007. The physical science basis: summary for policymakers. Fourth Assessment Report. Cambridge University Press, New York.

Jorgenson, M.T., Shur, Y.L., and Pullman, E.R. 2006. Abrupt increase in permafrost degradation in Arctic Alaska. Geophys. Res. Lett. **33**(2): L02503. doi:10.1029/2005GL024960.

Kalbitz, K., Geyer, W., and Geyer, S. 1999. Spectroscopic properties of dissolved humic substances — a reflection of land use history in a fen area. Biogeochemistry, **47**(2): 219–238. doi:10.1007/BF00994924.

Kirchman, D.L. 1993. Leucine incorporation as a measure of biomass production by heterotrophic bacteria. *In* Handbook of methods in aquatic microbial ecology. *Edited by* P.F. Kemp, B.F. Sherr, E.B. Sherr, and J.J. Cole. Lewis, Boca Raton, Florida. pp. 509–517.

Kling, G.W., Kipphut, G.W., and Miller, M.C. 1991. Arctic lakes and streams as gas conduits to the atmosphere: implications for tundra carbon budgets. Science (Washington, D.C.), **251**(4991): 298–301. doi:10.1126/science.251.4991.298. PMID:17733287.

Kortelainen, P., Rantakari, M., Huttunen, J.T., Mattsson, T., Alm, J., Juutinen, S., Larmola, T., Silvola, J., and Martikainen, P.J. 2006. Sediment respiration and lake trophic state are important predictors of large CO_2 evasion from small boreal lakes. Glob. Change Biol. **12**(8): 1554–1567. doi:10.1111/j.1365-2486.2006.01167.x.

Lim, D.S.S., Douglas, M.S.V., Smol, J.P., and Lean, D.R.S. 2001. Physical and chemical limnological characteristics of 38 lakes and ponds on Bathurst Island, Nunavut, Canadian High Arctic. Int. Rev. Hydrobiol. **86**(1): 1–22. doi:10.1002/1522-2632(200101)86:1<1::AID-IROH1>3.0.CO;2-E.

Lloyd, A.H., Yoshikawa, K., Fastie, C.L., Hinzman, L., and Fraver, M. 2003. Effects of permafrost degradation on woody vegetation at Arctic treeline on the Seward Peninsula, Alaska. Permafrost Periglac. **14**(2): 93–101. doi:10.1002/ppp.446.

Luoto, M., and Seppälä, M. 2003. Thermokarst ponds as indicators of the former distribution of palsas in Finnish Lapland. Permafrost Periglac. **14**: 19–27. doi:10.1002/ppp.441.

Mack, M.C., Schuur, E.A.G., Bret-Harte, M.S., Shaver, G.R., and Chapin, F.S. 2004. Ecosystem carbon storage in arctic tundra reduced by long-term nutrient fertilization. Nature (London), **431**(7007): 440–443. doi:10.1038/nature02887. PMID:15386009.

McCallister, S.L., Bauer, J.E., Cherrier, J.E., and Ducklow, H.W. 2004. Assessing sources and ages of organic matter supporting river and estuarine bacterial production: a multiple-isotope ($\delta^{14}C$, $\delta^{13}C$, and $\delta^{15}N$) approach. Limnol. Oceanogr. **49**: 1687–1702.

McKnight, D.M., Boyer, E.W., Westerhoff, P.K., Doran, P.T., Kulbe, T., and Andersen, D.T. 2001. Spectrofluorometric characterization of dissolved organic matter for indication of precursor organic material and aromaticity. Limnol. Oceanogr. **46**: 38–48.

Michmerhuizen, C.M., Striegl, R.G., and McDonald, M.E. 1996. Potential methane emission from north-temperate lakes following icemelt. Limnol. Oceanogr. **41**: 985–991.

Mitchell, B.G., Kahru, M., Wieland, J., and Stramska, M. 2003. Determination of spectral absorption coefficients of particles, dissolved material and phytoplankton for discrete water samples. *In* Ocean optics protocols for satellite ocean color sensor validation. Revision 4. Vol. IV. *Edited by* J.L. Mueller, G.S. Fargion, and C.R. McClain. NASA/TM-2003-211621/R, Goddard Space Flight Center, Greenbelt, Md. pp. 39–56.

Mobed, J.J., Hemmingsen, S.L., Autry, J.L., and Mcgown, L.B. 1996. Fluorescence characterization of IHSS humic substances: total luminescence spectra with absorbance correction. Environ. Sci. Technol. **30**(10): 3061–3065. doi:10.1021/es960132l.

Mopper, K., Anesio, A.M., Granéli, W., and Aiken, G.R. 2000. Photoreactivity of humic substances and its effect on microbial availability of carbon in lakes water. *In* Effects of solar radiation on the abiotic and bacterially mediated carbon flux in aquatic systems. *Edited by* A.M. Anesio. Ph.D. thesis, Chapter 5, Lund University, Lund, Sweden.

Nixdorf, B., and Jander, J. 2003. Bacterial activities in shallow lakes — a comparison between extremely acidic and alkaline eutrophic hard water lakes. Hydrobiologia, **506–509**(1–3): 697–705. doi:10.1023/B:HYDR.0000008623.73250.c8.

Obernosterer, I., and Benner, R. 2004. Competition between biological and photochemical processes in the mineralization of dissolved organic carbon. Limnol. Oceanogr. **49**: 117–124.

Oechel, W.C., Hastings, S.J., Vourlitis, G., Jenkins, M., Riechers, G., and Grulke, N. 1993. Recent change of Arctic tundra ecosystems from a carbon dioxide sink to a source. Nature (London), **361**(6412): 520–523. doi:10.1038/361520a0.

Payette, S., Delwaide, A., Caccianiga, M., and Beauchemin, M. 2004. Accelerated thawing of subarctic peatland permafrost over the last 50 years. Geophys. Res. Lett. **31**(18): L18208. doi:10.1029/2004GL020358.

Peuravuori, J., Koivikko, R., and Pihlaja, K. 2002. Characterization, differentiation and classification of aquatic humic matter separated with different sorbents: synchronous scanning fluorescence spectroscopy. Water Res. **36**(18): 4552–4562. doi:10.1016/S0043-1354(02)00172-0. PMID:12418658.

Pienitz, R., Smol, J.P., and Lean, D.R.S. 1997. Physical and chemical limnology of 59 lakes located between the southern Yukon and the Tuktoyaktuk Peninsula, Northwest Territories (Canada). Can. J. Fish. Aquat. Sci. **54**(2): 330–346. doi:10.1139/cjfas-54-2-330.

Rautio, M., and Vincent, W.F. 2006. Benthic and pelagic food resources for zooplankton in shallow high-latitude lakes and ponds. Freshw. Biol. **51**(6): 1038–1052. doi:10.1111/j.1365-2427.2006.01550.x.

Retamal, L., Vincent, W.F., Martineau, C., and Osburn, C.L. 2007. Comparison of the optical properties of dissolved organic matter in two river-influenced coastal regions of the Canadian Arctic. Estuar. Coast. Shelf Sci. **72**(1-2): 261–272. doi:10.1016/j.ecss.2006.10.022.

Richter-Menge, J., Overland, J., Proshutinsky, A., Romanovsky, V., Bengtsson, L., Brigham, L., Dyurgerov, M., Gascard, J.C., Gerland, S., Graversen, R., Haas, C., Karcher, M., Kuhry, P., Maslanik, J., Melling, H., Maslowski, W., Morison, J., Perovich, D., Przybylak, R., Rachold, V., Rigor, I., Shiklomanov, A., Stroeve, J., Volker, R., Walker, D., and Walsh, J. 2006. State of the Arctic report. NOAA OAR Special Report. NOAA/OAR/PMEL, Seattle, Wash.

Schwamborn, G.J., Dix, J.K., Bull, J.M., and Rachold, V. 2002. High-resolution seismic and ground penetrating radar – geophysical profiling of a thermokarst lake in the western Lena Delta, northern Siberia. Permafrost Periglac. **13**(4): 259–269. doi:10.1002/ppp.430.

Schwede-Thomas, S.B., Chin, Y.P., Dria, K.J., Hatcher, P., Kaiser, E., and Sulzberger, B. 2005. Characterizing the properties of dissolved organic matter isolated by XAD and C-18 solid phase extraction and ultrafiltration. Aquat. Sci. **67**(1): 61–71. doi:10.1007/s00027-004-0735-4.

Simon, M., and Azam, F. 1989. Protein content and protein synthesis rates of planktonic marine bacteria. Mar. Ecol. Prog. Ser. **51**: 201–213. doi:10.3354/meps051201.

Smith, D.C., and Azam, F. 1992. A simple, economical method for measuring bacterial protein synthesis rates in seawater using ^{3}H-leucine. Mar. Microb. Food Webs, **6**: 107–114.

Smith, L.C., Sheng, Y., MacDonald, G.M., and Hinzman, L.D. 2005. Disappearing Arctic lakes. Science (Washington, D.C.), **308**(5727): 1429. doi:10.1126/science.1108142. PMID:15933192.

Sobek, S., Algesten, G., Bergström, A.K., Jansson, M., and Tranvik, L.J. 2003. The catchment and climate regulation of *p*CO$_2$ in boreal lakes. Glob. Change Biol. **9**(4): 630–641. doi:10.1046/j.1365-2486.2003.00619.x.

Sobek, S., Tranvik, L.J., and Cole, J.J. 2005. Temperature independence of carbon dioxide supersaturation in global lakes. Global Biogeochem. Cycles, **19**(2): GB2003. doi:10.1029/2004GB002264.

Stainton, M., Capel, M.J., and Armstrong, A. 1977. The chemical analysis of freshwater. 2nd ed. Can. Fish. Mar. Serv. Misc. Spec. Publ. No. 25.

Steward, G.F., Smith, D.C., and Azam, F. 1996. Abundance and production of bacteria and viruses in the Bering and Chukchi Seas. Mar. Ecol. Prog. Ser. **131**: 287–300. doi:10.3354/meps131287.

Ström, L., and Christensen, T.R. 2007. Below ground carbon turnover and greenhouse gas exchanges in a subarctic wetland. Soil Biol. Biochem. **39**(7): 1689–1698. doi:10.1016/j.soilbio.2007.01.019.

Tietjen, T., Vähätalo, A.V., and Wetzel, R.G. 2005. Effects of clay mineral turbidity on dissolved organic carbon and bacterial production. Aquat. Sci. **67**: 51–60. doi:10.1007/s00027-004-0753-2.

Vähätalo, A.V., and Wetzel, R.G. 2004. Photochemical and microbial decomposition of chromophoric dissolved organic matter during long (months–years) exposures. Mar. Chem. **89**(1-4): 313–326. doi:10.1016/j.marchem.2004.03.010.

Vallières, C., Retamal, L., Ramlal, P., Osburn, C.L., and Vincent, W.F. 2008. Bacterial production and microbial food web structure in a large arctic river and the coastal Arctic Ocean. J. Mar. Syst. **74**(3-4): 756–773. doi:10.1016/j.jmarsys.2007.12.002.

Vézina, S., and Vincent, W.F. 1997. Arctic cyanobacteria and limnological properties of their environment: Bylot Island, Northwest Territories, Canada (73°N, 80°W). Polar Biol. **17**: 523–534. doi:10.1007/s003000050151.

Vincent, W.F., Hobbie, J.E., and Laybourn-Parry, J. 2008. Introduction to the limnology of high latitude lake and river ecosystems. *In* Polar lakes and rivers: limnology of Arctic and Antarctic aquatic ecosystems. *Edited by* W.F. Vincent and J. Laybourn-Parry. Oxford University Press, New York. pp. 1–23.

von Wachenfeldt, E., Sobek, S., Bastviken, D., and Tranvik, L.J. 2008. Linking the allochthonous dissolved organic matter and boreal lake sediment carbon sequestration — the role of light mediated flocculation. Limnol. Oceanogr. **53**: 2416–2426.

Walter, K.M., Zimov, S.A., Chanton, J.P., Verbyla, D., and Chapin, F.S., III. 2006. Methane bubbling from Siberian thaw lakes as a positive feedback to climate warming. Nature (London), **443**(7107): 71–75. doi:10.1038/nature05040. PMID:16957728.

Woo, M., Lewkowicz, A.G., and Rouse, W.R. 1992. Response of the Canadian permafrost environment to climatic change. Phys. Geogr. **13**: 287–317.

Yoshikawa, K., and Hinzman, L.D. 2003. Shrinking thermokarst ponds and groundwater dynamics in discontinuous permafrost near Council, Alaska. Permafrost Periglac. **14**(2): 151–160. doi:10.1002/ppp.451.

Zhang, T., Barry, R.G., Knowles, K., Heginbottom, J.A., and Brown, J. 1999. Statistics and characteristics of permafrost and ground-ice distribution in the Northern Hemisphere. Polar Geogr. **23**(2): 132–154. doi:10.1080/10889379909377670.

Zuidhoff, F.S. 2002. Recent decay of a single palsa in relation to weather conditions between 1996 and 2000 in Laivadalen, northern Sweden. Geogr. Ann., Ser. A Physical Geogr. **84**(2): 103–111. doi:10.1111/j.0435-3676.2002.00164.x.

Benthic bioturbator enhances CH_4 fluxes among aquatic compartments and atmosphere in experimental microcosms

Marcos Paulo Figueiredo-Barros, Adriano Caliman, João J. F. Leal, Reinaldo L. Bozelli, Vinicius F. Farjalla, and Francisco A. Esteves

Abstract: We utilized laboratory microcosms to evaluate the effects of a benthic sediment bioturbator (*Heteromastus similis*; Polychaeta: conveyor-belt deposit feeder) on vertical distributions of CH_4 in sediment and net CH_4 fluxes across sediment–water–air interfaces. The effect of *H. similis* on sediment CH_4 concentration ($[CH_4]$) varied depending on sediment depth and was strongest at higher animal densities. In comparison with defaunated controls, microcosms with the highest density of *H. similis* exhibited an increase in $[CH_4]$ of 3.7-fold, on average, at the sediment surface (0–2 cm), but these concentrations decreased by ~2-fold in deeper sediment layers (2–8 cm). However, irrespective of sediment depth, the density of *H. similis* resulted in an overall nonlinear reduction of bulk sediment $[CH_4]$. Most of the observed CH_4 losses from the sediment were due to CH_4 oxidation, but the bioturbatory activities of *H. similis* also promoted significant increases in $[CH_4]$ in both the water column and the microcosm headspace. These results suggest that benthic invertebrates can mediate CH_4 turnover between compartments in aquatic ecosystems, with further consequences for the coupling between benthic–pelagic food chains via the methanotrophic-mediated microbial loop, as well as increase CH_4 emissions to the atmosphere.

Résumé : Des microcosmes de laboratoire nous ont servi à évaluer les effets d'un perturbateur biologique des sédiments benthiques (*Heteromastus similis*; polychète qui se nourrit de sédiments par convoyage) sur la répartition verticale de CH_4 dans le sédiment et les flux nets de CH_4 à travers les interfaces sédiment–eau–air. L'effet d'*H. similis* sur les concentrations de CH_4 ($[CH_4]$) varie en fonction de la profondeur du sédiment et est maximal aux plus fortes densités d'animaux. En comparaison des témoins sans animaux, les microcosmes avec les densités les plus élevées d'*H. similis* montrent une augmentation de $[CH_4]$ de 3,7 fois en moyenne à la surface des sédiments (0–2 cm), mais ces concentration diminuent de ~2 fois dans les couches plus profondes de sédiment (2–8 cm). Cependant, quelle que soit la profondeur des sédiments, la densité d'*H. similis* cause une réduction générale non linéaire du $[CH_4]$ du sédiment global. La plupart des pertes de CH_4 observées dans les sédiments sont dues à l'oxydation de CH_4; cependant, les activités de perturbation biologique d'*H. similis* provoquent aussi des augmentations significatives de $[CH_4]$, tant dans la colonne d'eau que dans l'espace de tête du microcosme. Ces résultats laissent croire que les invertébrés benthiques peuvent servir d'agents dans le circulation du CH_4 entre les compartiments des écosystèmes aquatiques, avec des conséquences additionnelles sur le couplage des chaînes alimentaires benthique et pélagique par l'intermédiaire de la boucle microbienne méthanotrophique, ainsi que sur l'accroissement des émissions de CH_4 vers l'atmosphère.

[Traduit par la Rédaction]

Received 6 January 2009. Accepted 22 June 2009. Published on the NRC Research Press Web site at cjfas.nrc.ca on 26 September 2009.
J20974

Paper handled by Associate Editor Gesa A. Weyhenmeyer.

M.P. Figueiredo-Barros, A. Caliman,[1,2] and R.L. Bozelli. Laboratório de Limnologia, Departamento de Ecologia, Instituto de Biologia, Universidade Federal do Rio de Janeiro, CCS, Cidade Universitária, Rio de Janeiro, RJ, CEP. 21940-590, Brazil.
J.J.F. Leal. Laboratório de Limnologia, Departamento de Ecologia, Instituto de Biologia, Universidade Federal do Rio de Janeiro, CCS, Cidade Universitária, Rio de Janeiro, RJ, CEP. 21940-590, Brazil; Centro Federal de Educação Tecnológica de Química, Rua Lucio Tavares 1045, Nilópolis, RJ, CEP.26530-060, Brazil.
V.F. Farjalla and F.A. Esteves. Laboratório de Limnologia, Departamento de Ecologia, Instituto de Biologia, Universidade Federal do Rio de Janeiro, CCS, Cidade Universitária, Rio de Janeiro, RJ, CEP. 21940-590, Brazil; Núcleo de Pesquisas em Ecologia e Desenvolvimento Sócio Ambiental de Macaé, Rodovia Amaral Peixoto, Km 181, Macaé, RJ, CEP. 27973-030, Brazil.

[1] Corresponding author (e-mail: caliman21@gmail.com).
[2] Present address: Universidade Federal do Rio Grande do Norte, Departamento de Botânica, Ecologia e Zoologia, Centro de Biociências, Natal, RN, Brasil.

Can. J. Fish. Aquat. Sci. **66**: 1649–1657 (2009) doi:10.1139/F09-111 Published by NRC Research Press

Introduction

Inland aquatic ecosystems such as wetlands, rice fields, and shallow lakes are major sources of the CH_4 that is released into the atmosphere (Bartlett and Harriss 1993; Whiting and Chanton 1993; Bastviken et al. 2004). The importance of aquatic communities in CH_4 emissions from aquatic ecosystems to the atmosphere has been reinforced by recent studies, but with a focus on aquatic macrophytes as the primary mediators (Joabsson et al. 1999). A few studies have recently demonstrated that the productivity of benthic invertebrates may rely strongly on foraging for methanotrophic bacteria (Eller et al. 2005). However, the effects of benthic invertebrates on CH_4 cycling through nontrophic, indirect mechanisms (e.g., bioturbation) still remain poorly understood (but see Kajan and Frenzel 1999; Leal et al. 2007).

Bioturbation is a biogenic process that has been considered an "archetype" of ecosystem bioengineering because it alters geophysical gradients and redistributes resources and organisms within sediment layers, as well as between the sediment and other benthic and pelagic compartments in aquatic ecosystems (Meysman et al. 2006). Bioturbation is an important process that alters sediment characteristics, and the production, oxidation (i.e., methanotrophy), and flux of CH_4 through the sediment–water interface may be strongly affected by invertebrate sediment reworking (Kajan and Frenzel 1999; Leal et al. 2007). Such changes in the sediment enhance benthic–pelagic coupling with great implications for ecosystem functioning, particularly in shallow aquatic ecosystems where the sediment is relatively important for sustaining pelagic communities and ecosystem-level processes (Schindler and Scheuerell 2002). For instance, recent studies have demonstrated that CH_4 released from sediment into the water column has the potential to sustain a considerable fraction of energy flux through planktonic food chains via carbon incorporation by methanotrophic bacteria (Bastviken et al. 2003). Moreover, the CH_4 released from the sediment into the water column may not be completely oxidized, and the extant amount may then diffuse into the atmosphere. However, no study to date has investigated whether the effects of bioturbation mediated by benthic invertebrates on CH_4 flux across the sediment–water interface translates into a significant increase in CH_4 emission into the atmosphere.

Furthermore, only a handful of studies has evaluated the effects of benthic infauna on CH_4 flux through the sediment–water interface, and such few efforts have focused on filter-feeder tube dwellers (Kajan and Frenzel 1999; Leal et al. 2007). However, benthic invertebrate species may differ with respect to their distribution and foraging strategies (i.e., different functional groups), which may lead to different sediment–water interfacial processes rates such as material and nutrient advection, as well as microbial activity (Heilskov and Holmer 2001; Mermillod-Blondin et al. 2001; Caliman et al. 2007). Thus, bioturbator invertebrates that belong to diverse functional groups must have different effects on CH_4 cycling across the sediment–water interface. Moreover, the density of invertebrates may also be an important factor because density-dependent effects may modify benthic–pelagic processes in very complex ways, depending on the effects of density on the foraging behavior and (or) intraspecific interactions of animals (Mermillod-Blondin et al. 2002; Marinelli and Williams 2003).

The aim of this study was to evaluate whether the presence and population density of *Heteromastus similis* (Polychaeta: Capitellidae), which is a conveyor-belt deposit feeder, alters the concentration of CH_4 (hereafter $[CH_4]$) in the sediment layer and if such changes affect the pelagic compartment and atmosphere. A laboratory experiment was designed to determine if the sediment bioturbation promoted by *H. similis* will result in the following: (*i*) altered sediment $[CH_4]$; (*ii*) increased $[CH_4]$ in the overlaying water and atmosphere; (*iii*) increased net CH_4 oxidation rates; and (*iv*) a dependence of these processes on the density of *H. similis*.

Material and methods

Study site and species characteristics

Individuals of *H. similis*, as well as sediment and water utilized in this experiment, were sampled from the central area (~0.9 m depth) of Imboassica Lagoon (latitude 22°50′S, longitude 44°42′W), which is a tropical, shallow, coastal freshwater ecosystem located in the state of Rio de Janeiro, Brazil. This coastal lagoon is separated from the Atlantic Ocean by a narrow sandbar, and there are no tidal influences as the lagoon is not directly connected to the sea. The total lagoon area is 326 ha, with a maximum volume of 3.56×10^6 m^3 and a mean depth of 1.1 m. The lagoon is subject to a wide range of anthropogenic impacts, including the discharge of untreated domestic sewage and occasional artificial breaching of the protective sandbar, reflecting changes in the physical, chemical, and biological features of the lagoon (Figueiredo-Barros et al. 2006; Santangelo et al. 2007).

Regarding the benthic community, the main species and groups present are Hydrobiidae gastropods (Figueiredo-Barros et al. 2006), chironomid midges, and Polychaeta (Callisto et al. 1998). Among the Polychaeta, *H. similis* is the most abundant species, with densities ranging from 132.6 to 9481.0 individuals·m^{-2}. *Heteromastus similis* is a conveyor-belt subsurface-deposit feeder that builds extensive semipermanent galleries in the sediment (Rao 1980). This species modifies the distribution of sediment organic matter and intensifies benthic–pelagic coupling by sediment advection and upward egestion of fecal pellets (Caliman et al. 2007).

Sediment and organism sampling and pre-incubation procedures

Sediment and individuals were sampled with a "corer" (8 cm internal diameter, 50 cm^2 surface area), modified from Ambühl and Bührer (1975). Water was collected with polyethylene bottles at the subsurface. In the laboratory, the sediment was washed with lagoon water on a sieve (0.5 mm mesh size) to select *H. similis* individuals and exclude other benthic infauna from the sediment. Individuals of *H. similis* were maintained for 10 days in an aerated aquarium that contained sediment and water from the sampling site, which allowed the animals to acclimatize to laboratory conditions. Concurrently, defaunated sediment was homogenized and allowed to settle (~20 cm thick layer) for 10 days in a 30 L aquarium with a layer of prefiltered (GF/C Whatman,

Fig. 1. Schematic representation of (*a*) pre-incubation phase (without *Heteromastus similis*) and (*b*) incubation phase (with *H. similis*).

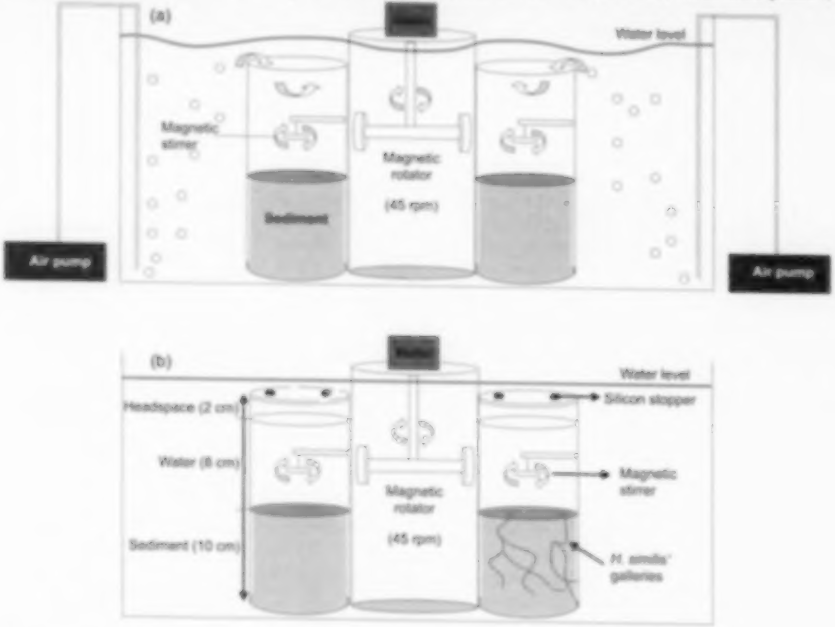

1.2 µm pore size) lagoon water with a depth of 10 cm. This procedure reduces the natural heterogeneity of the sediment and permits recovery of the microbial community and sediment biogeochemical depth gradient (Svensson 1998; Leal et al. 2007). After the stabilization period, 20 microcosms were established by introducing Plexiglas tubes (20 cm long × 4 cm internal diameter) into the stabilized sediment to a depth of 10 cm and maintaining overlaying water 9 cm deep. The microcosms were equipped with a rotating magnetic stirrer connected to the microcosm internal wall at 5 cm above the sediment surface. Microcosms were kept open at the top and placed around a rotating magnetic system according to the methods of Leal et al. (2007), and the whole system was submerged into a tank filled with filtered lagoon water (GF/C Whatman, 1.2 µm pore size), which was maintained under constant aeration for 12 h (Fig. 1*a*). This procedure was employed to homogenize starting abiotic conditions across all experimental microcosms.

Experimental design and incubations

After homogenization of the microcosms, five 8 mL water samples were collected from the tank to determine the initial [CH_4] in the water. Four microcosms were randomly chosen for determination of initial [CH_4] in sediment pore water across different sediment depths (0–2, 2–4, 4–6, and 6–8 cm). Three levels of *H. similis* density (4, 6, and 8 individuals per microcosm) and a defaunated control were replicated four times across the remaining 16 microcosms. The experimental range of *H. similis* density was comparable with the range of natural density observed for this species in Imboassica Lagoon (3175–6349 individuals·m^{-2}; M.P. Figueiredo-Barros, unpublished data). After addition of the animals, 20 mL of water was sampled from each microcosm to establish an internal headspace (atmosphere) ~2 cm high. The atmospheric [CH_4] in the experimental room was considered to correspond to initial [CH_4] in the atmosphere of the microcosms. The microcosms were then tightly sealed with silicon stoppers and incubated for 12 h (Fig. 1*b*). This incubation period was determined after a pilot experiment, in which we observed that in microcosms with sediment + eight animals, oxygen uptake never had an efficiency of greater than 50%. Hence, neither infaunal activity nor microbial methanotrophy was oxygen-limited in the experiment.

CH_4 samplings and analyses

At the end of the experiment, headspace air samples were taken with 1 mL syringes from each microcosm and immediately analyzed (see below). Water samples (8 mL) were collected from the overlaying water of the microcosms and injected into 12 mL glass capped vials at negative pressure to a final concentration of 20% NaCl by volume. To determine [CH_4] in sediment pore water, 5 mL of each sediment fraction was collected into 12 mL glass vials with 2 mL of NaOH (4%) and immediately sealed with rubber covers. For the determination of water content and sediment porosity, subsamples of fresh sediment were weighed in ceramic vessels, and weight loss was recorded after heating for 4 days at 60 °C according to Dalsgaard et al. (2000). Vials containing both water and sediment samples were stored in the dark at low temperature conditions (<10 °C) until analysis.

Syringes containing atmosphere samples and headspace subsamples (1 mL) taken from the vials containing sediment and water samples were analyzed for [CH_4] through gas chromatography using a Varian Star 3400 chromatograph equipped with a POROPAK-Q column (1 m, 60/100 mesh) at 85 °C, FID detector at 220 °C, injection at 120 °C, and N_2 was the carrier gas. The samples were injected using a Valvo C6W6 port loop valve (2.5 mL). A Star Chromatog-

Table 1. Results of bifactorial repeated-measures analysis of variance (RM-ANOVA) for individual and interactive effects of invertebrate density and sediment depth on sediment [CH_4].

Source of variation	df	MS	*F*	*P*
Between factor				
Density	3	2369.41	35.03	<0.0001
Error	12	67.62		
Within subject factors (Huynh–Feldt adjusted)				
Sediment depth	3	5881.79	56.50	<0.0001
Density × sediment depth	9	827.82	7.95	<0.0001
Error	36	104.09		

raphy workstation 5.51 (Varian, USA) was used to record data and for peak registration.

Data analysis

We estimate net CH_4 oxidation rates in response to invertebrate density as follows:

$$CH_{4\,oxi} = \frac{[\overline{S}_c - S_i] - [(W_i + A_i) - (\overline{W}_c + \overline{A}_c)]}{T}$$

where S_i, W_i, and A_i are the average [CH_4] in the bulk sediment, water, and air, respectively, at invertebrate density *i*. $\overline{S}_c$, $\overline{W}_c$, and $\overline{A}_c$ are the average [CH_4] in the bulk sediment, water, and air of microcosms without *H. similis* (controls), respectively, and *T* is the incubation time (12 h). To compare the effects of *H. similis* density on CH_4 oxidation rates, we first estimated ±95% confidence intervals (through bootstrap randomization with 3000 iterations) for each density level and then utilized comparisons of confidence intervals to determine if net CH_4 oxidation rates were different among density levels.

We used bifactorial repeated-measures analysis of variance (RM-ANOVA) to test the individual and interactive effects of *H. similis* density (between-subject factor) and sediment depth (within-subject factor) on sediment [CH_4]. The data were $\log_{10}$-transformed to improve variance homogeneity and adjusted (for the within-subject factor) by the Huynh–Feldt method to meet the assumption of circularity. Tukey's pairwise comparisons were performed to test if differences in sediment [CH_4] were among density levels or between the control and any density level (presence effect). Separate unifactorial analyses of variance (ANOVA) followed by Tukey's pairwise comparisons were used to test the effects of *H. similis* density on [CH_4] of the overlaying water and atmosphere. A significance level of $\alpha = 0.05$ was kept for all statistical analysis, using the software STATISTICA (version 7.0; StatSoft Inc., Tulsa, Oklahoma).

Results

Both the density of *H. similis* and sediment depth had significant individual and interactive effects on sediment [CH_4] (RM-ANOVA; Fig. 2; Table 1). For all treatments, sediment [CH_4] was a unimodal function of sediment depth, with the highest sediment [CH_4] observed at a depth of 4–6 cm. *Heteromastus similis* density caused an overall nonlinear reduction in sediment [CH_4], which was more pronounced (2.1× lower than control) in the highest density treatment (Fig. 3*c*; Tukey's post hoc test $P < 0.05$). Despite this significant overall negative effect of *H. similis* density on sediment [CH_4], the strength and direction of the effect of *H. similis* on sediment [CH_4] was also dependent on sediment depth, as indicated by the significant interactive effects (RM-ANOVA; Table 1). In comparison with controls, the bioturbational activities promoted by *H. similis* increased [CH_4] in the sediment surface (0–2 cm) on average 3.7 times but decreased [CH_4] over all deeper sediment layers (2–8 cm) on average 2.5 times (Fig. 2). Additionally, Tukey's pairwise comparisons demonstrated that with respect to sediment depth, the effect of *H. similis* density on sediment [CH_4] was consistent in the 4–6 cm layer, as both treatments with six and eight individuals per microcosm were significantly different from the treatment with only four individuals and the control (Fig. 2; Tukey's post hoc test $P < 0.05$). However, the presence of *H. similis* affected sediment [CH_4] at all sediment depths, which can be assessed by the significant differences between at least one *H. similis* treatment and controls (Fig. 2; Tukey's post hoc test $P < 0.05$). The strong effects of *H. similis* density on sediment [CH_4] at the sediment depth of 4–6 cm mirrored the effect observed in the bulk sediment [CH_4] (Fig. 3*c*), which suggests that complex interactions between density-dependent bioturbational behavior and depth-dependent microbial activities can substantially drive the overall effect of *H. similis* on bulk sediment [CH_4].

Fig. 2. Depth profiles (means ($n = 4$) ± standard error, SE) of [CH_4] in the sediment for the invertebrate density treatments after 12 h of incubations. "No animals" refers to the control treatments. Treatments within the same sediment depth displaying different letters are statistically different (Tukey's post hoc test, $P < 0.05$).

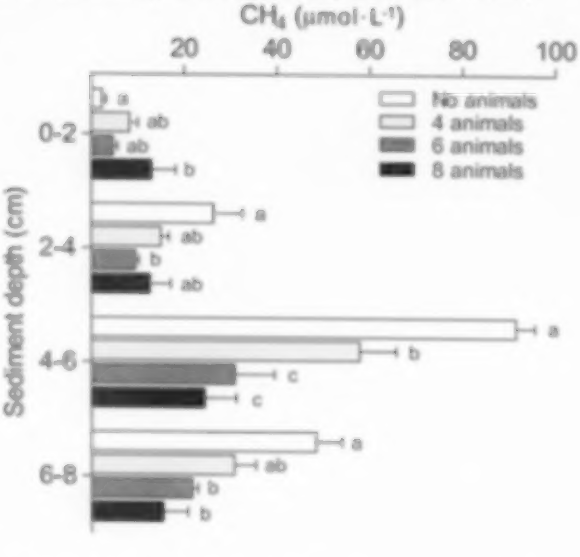

As observed for the sediment, *H. similis* density had a strong effect on both water (one-way ANOVA; $F = 325.8$, $P < 0.0001$) and air (one-way ANOVA; $F = 72.75$, $P < 0.0001$) [CH_4] (Figs. 3*a*–3*b*). The density of *H. similis* also had an increasingly positive effect on the [CH_4] for both overlaying water and air (Tukey's post hoc, $P < 0.05$). On average, [CH_4] for water and air were 150 times and 106

Fig. 3. CH_4 concentrations (means (n = 4) ± standard error, SE) measured in the (*a*) air (microcosm headspace), (*b*) water, and (*c*) sediment (depth average) of microcosms along different invertebrate densities. Values are final [CH_4] after 12 h of incubation. Different letters above treatments indicate statistically different values (Tukey's post hoc test, $P < 0.05$).

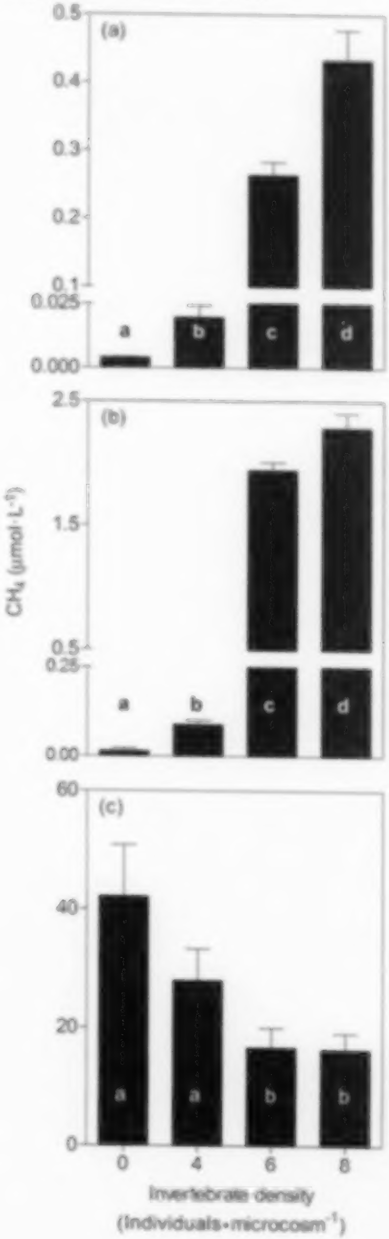

times higher, respectively, in the highest density treatment compared with controls.

The density of *H. similis* also had positive significant effects on net CH_4 oxidation rates. However, such effects exhibited a saturating response as density increased (Fig. 4). Confidence intervals were significantly different only for pairwise comparisons performed against the lowest density treatment.

Fig. 4. Net CH_4 oxidation rates (means n = 4) in response to invertebrate density. Different letters above treatments indicate statistically different values (error bars are ±95% confidence intervals).

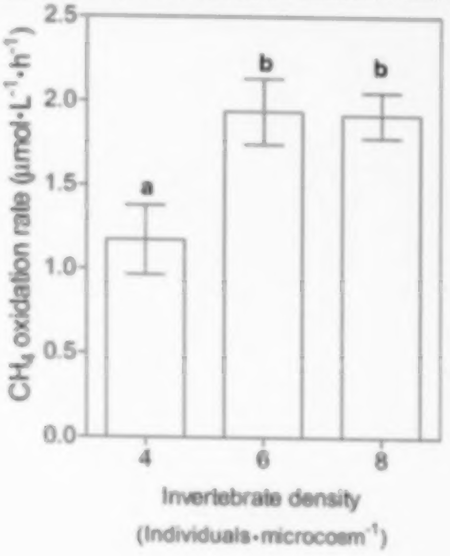

Discussion

These results demonstrate that bioturbation promoted by *H. similis* affected the processes related to CH_4 turnover in the sediment and between sediment–water–atmosphere interfaces. The presence of *H. similis* significantly altered the profiles of [CH_4] in the sediment (supporting hypothesis *i*), enhanced CH_4 flux from the sediment to water column and atmosphere (supporting hypothesis *ii*), and increased the net CH_4 oxidation rates (supporting hypothesis *iii*). Moreover, macroinvertebrate density also had significant effects on these processes (supporting hypothesis *iv*).

Effects of bioturbation on spatial dynamics of sediment [CH_4]

Heteromastus similis bioturbation had contrasting effects on vertical sediment [CH_4], increasing [CH_4] at the sediment surface (0–2 cm), but promoting overall reductions in [CH_4] at the three deeper sediment layers. Such polarization of sediment [CH_4] may be attributed to a set of non-mutually exclusive mechanisms mediated by the functional mode by of *H. similis* foraging within the sediment. First, bioadvection of surface particles (i.e., sediment mixing as a result of particle ingestion within the sediment and egestion at surface) might have decreased oxygen availability at the sediment boundary layer, limiting local CH_4 oxidation and (or) favoring methanogenesis at this sediment portion. Second, bioirrigation processes resulting from *H. similis* might have translocated CH_4-rich interstitial water from deeper sediment layers to the sediment surface and promoted CH_4 oxidation within deeper sediment layers (Fig. 5). Third, it has been recently shown that anaerobic microbial activity in the gut of benthic invertebrates may account for significant releases of nitrous oxide via fecal deposition by animals (Stief et al. 2009). Release, via fecal pellet deposition, of CH_4 produced in the gut of invertebrates might also have been important for the increase in [CH_4] at the sediment surface. Although, the deposition rates of fecal pellets was not monitored in our work, similar studies conducted with conveyor-belt deposit feeders have exhibited significant deposition of fecal pellets after relatively short-term incubation periods (van de Bund et al. 1994; Mermillod-Blondin et al. 2005). In addition, a recent study conducted with *H. filiformes* has also demonstrated that under nonflowing water conditions, oxygen consumption rates were 10 times higher within freshly egested fecal pellets than in the bulk surrounding sediment (Wild et al. 2005). Other studies have also reported significant increases in the abundance of active sediment bacteria associated with fecal pellets of tubificid worms, which generally have higher organic content than the surrounding sediment (van de Bund et al. 1994; Mermillod-Blondin et al. 2002). In fact, a greater amount of fecal mounds at the sediment surface of microcosms containing individuals of *H. similis* was observed at the end of incubation time, and the amount of fecal mounds was proportional to animal density. Therefore, the deposition of fecal pellets by *H. similis* might have intensified surficial diagenetic processes and promoted the formation of spatially heterogeneous microsites at the sediment surface characterized by anoxic conditions that favor methanogenesis and (or) limit CH_4 oxidation, thereby increasing [CH_4] at the sediment surface. A less obvious mechanism that might have contributed to the increase of [CH_4] at the sediment surface is that fecal pellet deposition on surficial sediments may have decreased the rates of diffusive processes across the sediment–water interface (van de Bund et al. 1994). Such a geochemical barrier might have retained part of the CH_4 transported upward by *H. similis* bioirrigation.

In comparison, the observed decrease of [CH_4] at the 2–8 cm sediment fractions in the presence of *H. similis* may be attributed to the stimulation of methanotrophy, as well as an upward transport of CH_4 to upper sediment layers. Bioturbatory activities of benthic invertebrates that build tubes or galleries are known to increase oxygen diffusion into the sediment (Svensson 1997; Leal et al. 2003), which affects metabolic processes due to alteration of the sediment redox potential (Kristensen 2000). Eller et al. (2005) reported that *Chironomus plumosus* might lead to a threefold increase of the sediment–water interface area. Furthermore, tubes built by invertebrate bioturbators have been proposed as an important microsite for CH_4 oxidation within the sediment (Kajan and Frenzel 1999). The increase in the sediment–water interface area in treatments with invertebrates may explain the density-dependent reduction of [CH_4] observed in deeper sediment layers (2–8 cm) in the presence of *H. similis*.

In accordance with recent studies regarding the nonconsumptive effects of benthic fauna on nutrient fluxes (Mermillod-Blondin et al. 2004; Michaud et al. 2006; Caliman et al. 2007), our results suggest that benthic invertebrate species from different functional groups can also differentially affect [CH_4] within sediment when compared with another study that evaluated the effects of invertebrate bioturbation on sediment [CH_4]. In a study of mayfly nymphs (*Campsurus notatus*), Leal et al. (2007) found that invertebrate bioturbation decreased [CH_4] in all sediment fractions. Such differences may be attributed to functional differences between *H. similis* and *C. notatus*. *Campsurus notatus* builds U- or J-shaped burrows within the sediment, which promotes a strong flux of water. However, this species does not deposit fecal pellets in the sediment surface like *H. similis*. Further studies should investigate how benthic bioturbator identity and diversity can affect the outcome of CH_4 turnover in the sediment of lake ecosystems, as benthic invertebrate species may differ in their impact upon sediment biogeochemical processes (Emmerson et al. 2001).

Fig. 5. Conceptual diagram illustrating the postulated causal connection between bioturbation by *Heteromastus similis* and spatial vertical dynamics of CH_4 cycling within the microcosms.

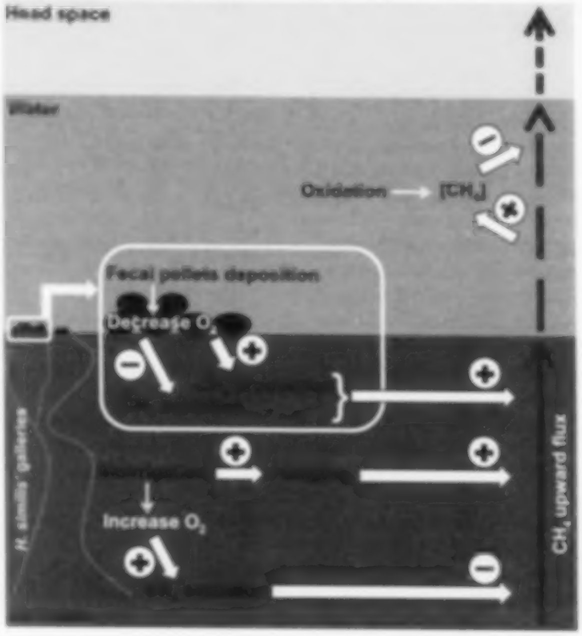

Effects of bioturbation on CH_4 flux through sediment–water–atmosphere interfaces

The observed effect of *H. similis* bioturbation on the spatial distribution of sediment [CH_4] was sufficient to cross sediment–water and water–atmosphere interfaces, as significant increases of [CH_4] in the overlaying water and headspace of microcosms inhabited by *H. similis* were observed. These results suggest that benthic invertebrates may affect CH_4 emissions from aquatic systems, and to our knowledge, this is the first study to experimentally demonstrate such an effect. However, the observed absolute [CH_4] in the water and atmosphere of microcosms was strikingly low in relation to the net reduction of bulk sediment [CH_4], as observed in the respective density treatments. Such a result shows that the impact of bioturbation promoted by *H. similis* was much greater on CH_4 oxidation than on CH_4 release to the water and headspace. The density of *H. similis* intensified net CH_4 oxidation. However, the main pathways of the net CH_4 oxidation could not be identified as CH_4 oxidation rates were not monitored at local scales (within sediment or in overlaying water). A great number of studies have demonstrated the importance of pelagic methanotrophy in the reduction of CH_4 emissions from water to the atmosphere (Utsumi et al. 1998; Sundh et al. 2005; Bastviken et al. 2008), but there is evidence that methanotrophy by sediment bacteria, mainly at the sediment–water interface, may greatly reduce the CH_4 flux from sediment to the water (Kajan and Frenzel 1999; Murase and Frenzel 2007). Both pathways of CH_4 oxidation were likely to have occurred in our experiment. As previously discussed, sediment bioadvection promoted by *H. similis* via surficial deposition of fecal pellets may translocate accumulated CH_4 in the sediment that is available for methanotrophy to the water column, while stimulating methanotrophy by sediment bacteria through oxygenating sediments via bioirrigation (Fig. 5). An additional complexity relies on the coupling of methanogenesis and methanotrophy, which greatly complicates our ability to derive conclusive pathways by which sediment reworking may affect CH_4 dynamics across aquatic compartments. Further studies regarding the effects of benthic infauna on CH_4 flux through benthic–pelagic compartments should investigate the mechanisms behind the spatial coupling between the origin and fate of CH_4 in aquatic systems.

Consequences of bioturbation to CH_4 cycling in aquatic systems and emissions from atmosphere

Our results demonstrated that bioturbatory activities by benthic infauna play an important role to the sediment CH_4 turnover and flux across sediment–water–atmosphere interfaces. These results suggest that bioturbation may be an important factor contributing to the coupling of carbon cycling between aquatic compartments, which has been demonstrated with nutrients such as N and P (Emmerson et al. 2001; Lohrer et al. 2004; Meysman et al. 2006). Recent studies have indicated a high reliance of secondary production of lake pelagic communities upon carbon and energy derived from CH_4 via trophic links among methanotrophic bacteria and higher trophic levels such as protozoa and zooplankton (Bastviken et al. 2003; Sundh et al. 2005; Taipale et al. 2008). For example, Taipale et al. (2007) have estimated that methanotrophic bacteria contributed 64%–87% of carbon incorporation by zooplankton during autumn in Mekkojärvi Lake. Therefore, mechanisms that enhance CH_4 transport from benthic to pelagic compartments, such as bioturbation, may indirectly affect carbon availability for pelagic food webs.

Regarding the effects of bioturbation on CH_4 emissions from aquatic systems to the atmosphere, this study demonstrated that sediment bioturbator organisms might contribute to aquatic systems as a source of greenhouse gases in the atmosphere. Considering the estimation of CH_4 emissions observed in the microcosms of intermediate invertebrate density (four individuals), bioturbation by *H. similis* might indirectly mediate the efflux of approximately 7.6 tonnes of CH_4 per year in Imboassica Lagoon. However, we are aware that important caveats associated with our experiment regarding the observed positive effects of *H. similis* on CH_4 emission should be considered. First, *H. similis* may prevent the formation of CH_4 bubbles by reducing $[CH_4]$ in the sediment, as CH_4 bubbles can form when CH_4 concentration in the sediment exceeds saturation. According to Nielsen et al. (2004), the maximum predicted $[CH_4]$ in pore water is 900 $\mu mol \cdot L^{-1}$ at 29 °C and 1 atm, which increases with increasing pressure (higher depths) and decreasing temperatures. In our experiment, the $[CH_4]$ observed in the sediment of microcosms was significantly lower than saturation values, which hinders bubble formation. Because CH_4 bubbles tend to pass through the water column without being oxidized, bioturbation by benthic invertebrates may play an important role in decreasing net CH_4 emission to the atmosphere from aquatic environments by forcing CH_4 sediment diffusion and oxidation throughout the water column. Second, CH_4 emissions may have been overestimated in our experiment due to the short water column of our microcosms, which decreases the probability of pelagic CH_4 oxidation. However, we believe that such an experimental artifact does not invalidate our results, as littoral regions of lakes and small ponds, which generally act as sources of CH_4 in the atmosphere (Bastviken et al. 2004; Bussmann 2005; Parsons et al. 2006), may exhibit water depths comparable with those of our experimental microcosms. Third, the generality of our results are constrained by the short-term experiment duration, and therefore, we are unable to assert to what extent the experimental results represent a transitional effect following colonization of sediment by benthic infauna or a more stable long-term effect of bioturbation. However, many studies have shown that the effects of invertebrate bioturbators on sediment reworking and materials and solute transfers across the sediment–water interface are consistent over temporal scales ranging from days to months (Emmerson et al. 2001; Marinelli and Williams 2003; Lohrer et al. 2004), which reinforce the validity of our results. However, to obtain a more precise knowledge about the effects of benthic infauna on CH_4 dynamics across sediment–water interfaces, further experiments should be conducted over larger temporal scales.

This study suggests that benthic invertebrate bioturbators may indirectly mediate CH_4 turnover among aquatic compartments and the atmosphere. Considering the effects of *H. similis* on CH_4 oxidation, these results demonstrate that bioturbatory activities promoted by invertebrate organisms may also indirectly subsidize carbon transformation and energy availability through enhancing methanotrophy, in addition to enhancing nutrient availability to pelagic production. These findings may be particularly important in understanding CH_4 turnover in shallow aquatic systems, where benthic-derived processes may be important drivers of ecosystem functioning.

Acknowledgements

We thank Albert Suhett for constructive comments that improved the final version of this manuscript. This work was supported by grants from Petrobras. Scholarships were provided by CNPq, CAPES, and FAPERJ.

References

Ambühl, H., and Bührer, H. 1975. Technik der entnahme ungestörter großproben von seesedimenten: ein verbessertes bohrlot. Schweiz. Z. Hydrol. **37**: 175–186. doi:10.1007/BF02505185.

Bartlett, K.D., and Harriss, R.C. 1993. Review and assessment of methane emissions from wetlands. Chemosphere, **26**(1–4): 261–320. doi:10.1016/0045-6535(93)90427-7.

Bastviken, D., Ejlertsson, J., Sundh, I., and Tranvik, L. 2003. Methane as a source of carbon and energy for lake pelagic food webs. Ecology, **84**(4): 969–981. doi:10.1890/0012-9658(2003)084[0969:MAASOC]2.0.CO;2.

Bastviken, D., Cole, J., Pace, M., and Tranvik, L. 2004. Methane emissions from lakes: dependence of lake characteristics, two regional assessments, and a global estimate. Global Biogeochem. Cycles, **18**(4): GB4009.1–GB4009.12. doi:10.1029/2004GB002238.

Bastviken, D., Cole, J.J., Pace, M.L., and de Bogert, M.C.V. 2008. Fates of methane from different lake habitats: connecting whole-lake budgets and CH_4 emissions. J. Geophys. Res. Biogeosci. **113**(G2): 13.

Bussmann, I. 2005. Methane release through resuspension of littoral sediment. Biogeochemistry, **74**(3): 283–302. doi:10.1007/s10533-004-2223-2.

Caliman, A., Leal, J.J.F., Esteves, F.A., Carneiro, L.S., Bozelli, R.L., and Farjalla, V.F. 2007. Functional bioturbator diversity enhances benthic–pelagic processes and properties in experimental microcosms. J. N. Am. Benthol. Soc. **26**(3): 450–459. doi:10.1899/06-050.1.

Callisto, M., Gonçalves-Junior, J.F., Leal, J.J.F., and Petrucio, M.M. 1998. Macroinvertebrados bentônicos nas lagoas Imboassica, Cabiúnas, e Comprida. *In* Ecologia das Lagoas Costeiras do Parque Nacional da Restinga de Jurubatiba e do Município de Macaé (RJ). *Edited by* F.A. Esteves. Nupem/Universidade Federal do Rio de Janeiro, Rio de Janeiro, Brazil. pp. 479–486.

Dalsgaard, T., Nielsen, L.P., Brotas, V., Viaroli, P., Underwood, G., Nedwell, D.B., Sundbäck, K., Rysgaard, S., Miles, A., Bartoli, M., Dong, L., Thornton, D.C.O., Ottosen, L.D.M., Castaldelli, G., and Risgaard-Petersen, N. 2000. Protocol handbook for NICE — nitrogen cycling in estuaries: a project under the EU research programe. Marine Science and Technology (MAST III), National Environmental Research Institute, Silkeborg, Denmark.

Eller, G., Deines, P., Grey, J., Richnow, H.H., and Kruger, M. 2005. Methane cycling in lake sediments and its influence on chironomid larval $\delta^{13}C$. FEMS Microbiol. Ecol. **54**(3): 339–350. doi:10.1016/j.femsec.2005.04.006. PMID:16332332.

Emmerson, M.C., Solan, M., Emes, C., Paterson, D.M., and Raffaelli, D. 2001. Consistent patterns and the idiosyncratic effects of biodiversity in marine ecosystems. Nature (London), **411**(6833): 73–77. doi:10.1038/35075055. PMID:11333979.

Figueiredo-Barros, M.P., Leal, J.J.F., Esteves, F.D., Rocha, A.D., and Bozelli, R.L. 2006. Life cycle, secondary production and nutrient stock in *Heleobia australis* (d'Orbigny 1835) (Gastropoda: Hydrobiidae) in a tropical coastal lagoon. Estuar. Coast. Shelf Sci. **69**(1–2): 87–95. doi:10.1016/j.ecss.2006.03.023.

Heilskov, A.C., and Holmer, M. 2001. Effects of benthic fauna on organic matter mineralization in fish-farm sediments: importance of size and abundance. ICES J. Mar. Sci. **58**(2): 427–434. doi:10.1006/jmsc.2000.1026.

Joabsson, A., Christensen, T.R., and Wallén, B. 1999. Vascular plant controls on methane emissions from northern peatforming wetlands. Trends Ecol. Evol. **14**(10): 385–388. doi:10.1016/S0169-5347(99)01649-3. PMID:10481199.

Kajan, R., and Frenzel, P. 1999. The effect of chironomid larvae on production, oxidation and fluxes of methane in a flooded rice soil. FEMS Microbiol. Ecol. **28**(2): 121–129. doi:10.1111/j.1574-6941.1999.tb00567.x.

Kristensen, E. 2000. Organic matter diagenesis at the oxic/anoxic interface in coastal marine sediments, with emphasis on the role of burrowing animals. Hydrobiologia, **426**(1–3): 1–24. doi:10.1023/A:1003980226194.

Leal, J.J.F., de Assis Esteves, F., Farjalla, V.F., and Enrich-Prast, A. 2003. Effect of *Campsurus notatus* on NH_4^+, DOC fluxes, O_2 uptake and bacterioplankton production in experimental microcosms with sediment–water interface of an Amazonian lake impacted by bauxite tailings. Int. Rev. Hydrobiol. **88**(2): 167–178. doi:10.1002/iroh.200390012.

Leal, J.J.F., dos Santos Furtado, A.L., de Assis Esteves, F., Bozelli, R.L., and Figueiredo-Barros, M.P. 2007. The role of *Campsurus notatus* (Ephemeroptera: Polymitarcytidae) bioturbation and sediment quality on potential gas fluxes in a tropical lake. Hydrobiologia, **586**(1): 143–154. doi:10.1007/s10750-006-0570-9.

Lohrer, A.M., Thrush, S.F., and Gibbs, M.M. 2004. Bioturbators enhance ecosystem function through complex biogeochemical interactions. Nature (London), **431**(7012): 1092–1095. doi:10.1038/nature03042. PMID:15470385.

Marinelli, R.L., and Williams, T.J. 2003. Evidence for density-dependent effects of infauna on sediment biogeochemistry and benthic–pelagic coupling in nearshore systems. Estuar. Coast. Shelf Sci. **57**(1–2): 179–192. doi:10.1016/S0272-7714(02)00342-6.

Mermillod-Blondin, F., Gérino, M., Degrange, V., Lensi, R., Chassé, J.-L., Rard, M., and des Châtelliers, M.C. 2001. Testing the functional redundancy of *Limnodrilus* and *Tubifex* (Oligochaeta, Tubificidae) in hyporheic sediments: an experimental study in microcosms. Can. J. Fish. Aquat. Sci. **58**(9): 1747–1759. doi:10.1139/cjfas-58-9-1747.

Mermillod-Blondin, F., Gerino, M., des Chatelliers, M.C., Degrange, V., Gerino, M., des Chatelliers, M.C., and Degrange, V. 2002. Functional diversity among 3 detritivorous hyporheic invertebrates: an experimental study in microcosms. J. N. Am. Benthol. Soc. **21**(1): 132–149. doi:10.2307/1468305.

Mermillod-Blondin, F., Rosenberg, R., François-Carcaillet, F., Norling, K., and Mauclaire, L. 2004. Influence of bioturbation by three benthic infaunal species on microbial communities and biogeochemical processes in marine sediment. Aquat. Microb. Ecol. **36**: 271–284. doi:10.3354/ame036271.

Mermillod-Blondin, F., Nogaro, G., Datry, T., Malard, F., and Gibert, J. 2005. Do tubificid worms influence the fate of organic matter and pollutants in stormwater sediments? Environ. Pollut. **134**(1): 57–69. doi:10.1016/j.envpol.2004.07.024. PMID:15572224.

Meysman, F.J.R., Middelburg, J.J., and Heip, C.H.R. 2006. Bioturbation: a fresh look at Darwin's last idea. Trends Ecol. Evol. **21**(12): 688–695. doi:10.1016/j.tree.2006.08.002. PMID:16901581.

Michaud, E., Desrosiers, G., Mermillod-Blondin, F., Sundby, B., and Stora, G. 2006. The functional group approach to bioturbation: II. The effects of the *Macoma balthica* community on fluxes of nutrients and dissolved organic carbon across the sediment–water interface. J. Exp. Mar. Biol. Ecol. **337**(2): 178–189. doi:10.1016/j.jembe.2006.06.025.

Murase, J., and Frenzel, P. 2007. A methane-driven microbial food web in a wetland rice soil. Environ. Microbiol. **9**(12): 3025–3034. doi:10.1111/j.1462-2920.2007.01414.x. PMID:17991031.

Nielsen, L.P., Enrich-Prast, A., and Esteves, F.A. 2004. Pathways of organic matter mineralization and nutrient regeneration in the sediment of five tropical lakes. Acta Limnol. Bras. **16**(2): 193–202.

Parsons, A.J., Newton, P.C.D., Clark, H., and Kelliher, F.M. 2006. Scaling methane emissions from vegetation. Trends Ecol. Evol. **21**(8): 423–424. doi:10.1016/j.tree.2006.05.017. PMID:16781006.

Rao, D.S. 1980. Ecology of *Heteromastus-Similis* Southern 1921 (Polychaeta, Capitellidae) in the Vasishta Godavari Estuary. Proc. Indian Acad. Sci. (Anim. Sci.), **89**(5): 407–414.

Santangelo, J.M., Rocha, A.de M., Bozelli, R.L., Carneiro, L.S., and Esteves, F.de A. 2007. Zooplankton responses to sandbar opening in a tropical eutrophic coastal lagoon. Estuar. Coast. Shelf Sci. **71**(3–4): 657–668. doi:10.1016/j.ecss.2006.09.021.

Schindler, D.E., and Scheuerell, M.D. 2002. Habitat coupling in lake ecosystems. Oikos, **98**(2): 177–189. doi:10.1034/j.1600-0706.2002.980201.x.

Stief, P., Poulsen, M., Nielsen, L.P., Brix, H., and Schramm, A. 2009. Nitrous oxide emission by aquatic macrofauna. Proc. Natl. Acad. Sci. U.S.A. **106**(11): 4296–4300. doi:10.1073/pnas.0808228106. PMID:19255427.

Sundh, I., Bastviken, D., and Tranvik, L.J. 2005. Abundance, activity, and community structure of pelagic methane-oxidizing bacteria in temperate lakes. Appl. Environ. Microbiol. **71**(11): 6746–6752. doi:10.1128/AEM.71.11.6746-6752.2005. PMID:16269705.

Svensson, J.M. 1997. Influence of *Chironomus plumosus* larvae on ammonium flux and denitrification (measured by the acetylene blockage and the isotope pairing technique) in eutrophic lake sediment. Hydrobiologia, **346**(1–3): 157–168. doi:10.1023/A:1002974201570.

Svensson, J.M. 1998. Emission of N_2O, nitrification and denitrification in a eutrophic lake sediment bioturbated by *Chironomus plumosus*. Aquat. Microb. Ecol. **14**(3): 289–299. doi:10.3354/ame014289.

Taipale, S., Kankaala, P., and Jones, R.I. 2007. Contributions of different organic carbon sources to *Daphnia* in the pelagic foodweb of a small polyhumic lake: results from mesocosm DI^{13}C-additions. Ecosystems (N.Y., Print), **10**(5): 757–772. doi:10.1007/s10021-007-9056-5.

Taipale, S., Kankaala, P., Tiirola, M., and Jones, R.I. 2008. Whole-lake dissolved inorganic ^{13}C additions reveal seasonal shifts in zooplankton diet. Ecology, **89**(2): 463–474. doi:10.1890/07-0702.1. PMID:18409435.

Utsumi, M., Nojiri, Y., Nakamura, T., Nozawa, T., Otsuki, A., and Seki, H. 1998. Oxidation of dissolved methane in an eutrophic, shallow lake: Lake Kasumigaura, Japan. Limnol. Oceanogr. **43**(3): 471–480.

van de Bund, W.J., Goedkoop, W., and Johnson, R.K. 1994. Effects of deposit-feeder activity on bacterial production and abundance in profundal lake sediment. J. N. Am. Benthol. Soc. **13**(4): 532–539. doi:10.2307/1467849.

Whiting, G.J., and Chanton, J.P. 1993. Primary production control of methane emission from wetlands. Nature (London), **364**(6440): 794–795. doi:10.1038/364794a0.

Wild, C., Roy, H., and Huettel, M. 2005. Role of pelletization in mineralization of fine-grained coastal sediments. Mar. Ecol. Prog. Ser. **291**: 23–33. doi:10.3354/meps291023.

Contribution of three life history types to smolt production in a Chinook salmon (*Oncorhynchus tshawytscha*) population

Timothy Copeland and David A. Venditti

Abstract: The most productive juvenile life history in the Pahsimeroi River Chinook salmon (*Oncorhynchus tshawytscha*; Idaho, USA) population (in terms of smolt production) is being eliminated. Length at emigration and survival from spawning areas to Lower Granite Dam within each of three juvenile phenotypes (age-0 smolts, fall parr, age-1 smolts) were influenced by initial cohort abundance. The proportion of age-1 emigrants reaching Lower Granite Dam was dome-shaped with respect to initial cohort abundance. As initial abundance increased, higher proportions of juveniles adopted the age-1 smolt phenotype or emigrated as fall parr. The age-0 smolt phenotype had the highest relative survival, and the fall parr phenotype, the lowest. The contributions of each emigrant type to cohort smolt production varied with circumstances; hence, the full expression of phenotypic diversity is important to the study population. However, there were no records of tagged age-0 smolts surviving to return from the Pacific Ocean. Given the potential productivity of this life history, management and recovery efforts should be directed at the age-0 smolt phenotype.

Résumé : Le cycle biologique juvénile le plus productif (en ce qui a trait à la production de saumoneaux) de la population de saumons chinook (*Oncorhynchus tshawytscha*) de la rivière Pahsimeroi, Idaho, É.-U., est en train d'être éliminé. La longueur à l'émigration et la survie depuis les sites de fraie jusqu'au barrage Lower Granite chez chacun des trois phénotypes juvéniles (saumoneaux d'âge 0, tacons d'automne et saumoneaux d'âge 1) sont influencées par l'abondance initiale de la cohorte. La proportion d'émigrants d'âge 1 qui atteint le barrage Lower Granite se répartit en dôme par rapport à l'abondance initiale de la cohorte. À mesure que l'abondance initiale augmente, des proportions plus élevées de jeunes adoptent le phénotype de saumoneau d'âge 1 ou émigrent comme tacons d'automne. Le phénotype d'âge 0 possède la survie relative la plus élevée et le phénotype de tacon d'automne la plus basse. Les contributions de chaque type d'émigrant à la production de saumoneaux de la cohorte varient selon les circonstances; l'expression de l'entière diversité phénotypique est donc importante dans l'étude de la population. Cependant, il n'existe aucune information concernant des saumoneaux d'âge 0 marqués ayant survécu jusqu'à leur retour du Pacifique. Étant donné la productivité potentielle de ce type de cycle biologique, on devrait concentrer des efforts de gestion et de conservation sur le phénotype de saumoneau d'âge 0.

[Traduit par la Rédaction]

Introduction

Intrapopulation diversity is important to population resilience (McElhany et al. 2000; Kendall and Fox 2002; Gamfeldt and Källström 2007). Life history diversity is diversity in time; multiple phenotypes are a population-level insurance policy against extinction (Healey and Prince 1995). Wilbur (1996) demonstrated theoretically that additional life history complexity could increase population productivity via niche expansion in time and space. Diversity of geographic and life history components increases regional resilience of a species (Hilborn et al. 2003). Managers need to understand how population components contribute to overall production and fitness for effective conservation. Here we document a case in which a major life history type in a Chinook salmon (*Oncorhynchus tshawytscha*) population has been compromised. Conservation of this population will be more effective with an understanding of how various juvenile life history types contribute to population functioning.

In Pacific salmon (*Oncorhynchus* sp.), adult life history diversity is well known but juvenile diversity may be greater and more important than currently understood (Hilborn et al. 2003). Juvenile life history types, defined with respect to timing of habitat use, contribute differentially to population productivity (Reimers 1973; Mobrand et al. 1997). Snake River spring–summer (SRSS) Chinook salmon generally exhibit a stream-type life history, rearing for 1 year in freshwater before migrating to the ocean (Healey 1991). However, a percentage of SRSS Chinook salmon juveniles exhibit an ocean-type life history, smolting and migrating to the ocean during their first year (Healey 1991; see also Connor et al. 2001). Emigration phenotypes in juvenile salmon may result from links between growth and smoltification (Thorpe et al. 1998; Beckman et al. 2007) as modified by the tradeoff between size and survival (Zabel and Achord 2004; Scheuerell 2005), genetic control (Taylor 1990), or density-dependent emigration (Dunham and Vinyard 1997; Grant et al. 1998; Dunham et al. 2000). The literature is am-

Received 22 October 2008. Accepted 31 May 2009. Published on the NRC Research Press Web site at cjfas.nrc.ca on 26 September 2009.
J20830

Paper handled by Associate Editor Bror Jonsson.

T. Copeland[1] **and D.A. Venditti.** Idaho Department of Fish and Game, 1414 East Locust Lane, Nampa, ID 83686, USA.

[1]Corresponding author (e-mail: tim.copeland@idfg.idaho.gov).

Can. J. Fish. Aquat. Sci. 66: 1658–1665 (2009) doi:10.1139/F09-110 Published by NRC Research Press

biguous as to whether migration types result from facultative responses or adaptive life history differences.

The existence of less productive phenotypes is a central problem in evolutionary biology (Reeve and Sherman 1993). Our study took advantage of a 13-year data set (1992 through 2004 cohorts) on a Chinook salmon population with multiple juvenile emigration phenotypes (age-0 smolt, fall parr, and age-1 smolt) to gain insight on this question. We assumed that the observed phenotypes arose as a tradeoff of long-term expectations versus short-term stochasticity (Stearns 1992; Roff 2002) and further that observed phenotypes will contribute under some circumstances. We used survival to Lower Granite Dam (Fig. 1) as our measure of fitness to avoid the influence of anthropogenic changes to the migratory corridor in the Snake and Columbia rivers (Waples et al. 2008). Our objectives were (*i*) to compare survival by phenotype, (*ii*) to describe the influence of growth and density on proportions of each phenotype in successful emigrants, and (*iii*) to model relative survival among phenotypes. Using the latter information, we considered how the study population functioned historically and how it is functioning currently.

Materials and methods

Study population

The study population was the Chinook salmon spawning in the Pahsimeroi River of central Idaho, USA (Fig. 1). The population is classified as summer-run, based on timing of adult entry into freshwater. It is part of the SRSS Chinook salmon Evolutionarily Significant Unit, which is listed as threatened under the Endangered Species Act. This is considered a key population for the recovery of the upper Salmon River major population group (MPG), and this MPG cannot be considered recovered without a viable Chinook salmon population in the Pahsimeroi River (Interior Columbia Technical Recovery Team (ICTRT) 2007). All SRSS Chinook salmon are considered to have a stream-type life history (Good et al. 2005), that is, they have an extended freshwater rearing phase and enter the ocean as yearlings, whereas ocean-type Chinook salmon typically enter the ocean as subyearlings (Healey 1991). Juvenile emigrants pass a total of eight dams on the Snake and Columbia rivers before reaching the Pacific Ocean; the first is Lower Granite Dam and the last is Bonneville Dam. A hatchery operates on the Pahsimeroi River with a weir 1.5 km upstream from the mouth. All hatchery-produced juveniles were marked with an adipose fin clip and excluded from this study. During the spawning run, marked adults were removed from the river at the weir, whereas unmarked fish were allowed to continue upstream.

The Pahsimeroi River is a tributary to the Salmon River, within the Snake River basin (Fig. 1), and historically supported a substantial, relatively productive Chinook salmon run (Good et al. 2005). The river lies in a dry intermontane sagebrush valley, with the mouth at an elevation of approximately 1500 m. Most tributaries are disconnected by irrigation diversions and the flow is often intermittent in the upper parts of the basin. Diverted water returns to the river via large springs near the center of the valley, so the lower Pahsimeroi River has substantial flow year-round and high connectivity to the Salmon River. Chinook salmon currently occupy the lower 20 km of the Pahsimeroi River. Within this reach, the river is a low-gradient stream dominated by groundwater flow, which moderates temperature (Trapani 2002). The channel is sinuous and well developed and has a large proportion of pool habitat. During the summer, submergent plants grow in a large proportion of the main channel, indicating a relatively high level of aquatic productivity, which sets the Pahsimeroi River apart from other tributaries in the Salmon River basin.

Fig. 1. Map showing the position of the Pahsimeroi River (Idaho, USA) in relation to the Snake and Columbia rivers. Locations of the rotary screw trap and Lower Granite Dam are marked. Inset map shows location within the US Pacific Northwest.

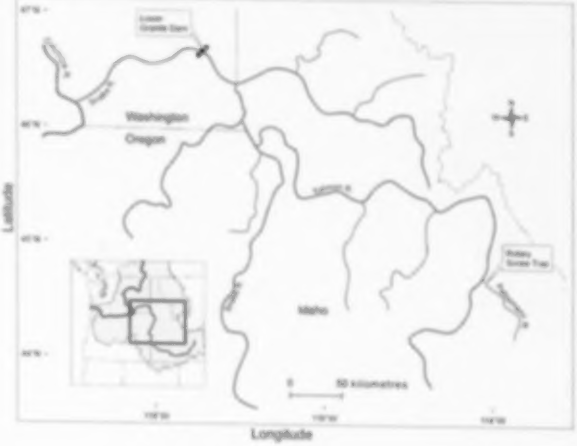

Juvenile Chinook salmon emigrating from the Pahsimeroi River display four distinct phenotypes. A group of fry exits the river soon after emergence in March. Because these fish were too small to be tagged with passive integrated transponder (PIT) tags, they were excluded from our study. From April to June, another group of subyearlings (age-0 smolts) leave the Pahsimeroi River, move through the Salmon River into the Snake River, and pass Lower Granite Dam, 619 km downstream (Fig. 1). Juvenile emigration from the Pahsimeroi River then essentially ceases until late August when a third group, fall parr, begins to emigrate. Fall parr spend the winter in the Salmon River and reach Lower Granite Dam the following spring. Lastly, yearling (age-1 smolts) leave the Pahsimeroi River during March and April, travel quickly to the Snake River, and pass Lower Granite Dam.

Data collection

Emigrating juveniles were collected by a rotary screw trap located 1.5 km upstream from the river mouth (Fig. 1). The trap was deployed as early as possible in the spring, usually in the last week of February or the first week of March, and operated until ice-up (usually the first week of December). For the first few years of the study (1992–1995), the trap was not operated in the summer (June–August).

Fish were processed at least once daily and were counted and measured, and a subsample was PIT-tagged. The transponder in these tags emits a unique code that can be read by a detector when the tag passes through a magnetic field (Prentice et al. 1990). All fish were anesthetized before processing with a buffered solution of tricaine methanesulfonate (MS-222). All fish were measured to the nearest 1 mm from the tip of the nose to the fork of the caudal fin (fork length, FL) and scanned for the presence of PIT tags. Fish ≥60 mm FL were eligible for tagging (see procedures below). After processing, all PIT-tagged fish were placed in a live box (a perforated container through which water could flow freely) 0.4 km upstream from the trap and released at dusk. Efficiency of the trap was calculated from recaptures of these fish. Recaptured fish and any individuals not tagged were placed in a second live box immediately below the trap and released at dusk.

Tagging procedures followed recommendations of the PIT Tag Steering Committee (1999). Tags were injected into the body cavity using a hypodermic needle. Needles and tags were sterilized in 70% ethanol for 10 min prior to and between uses. All age-1 smolts were tagged. All other groups (except fry) were tagged at a rate determined by the expected number of emigrants and the number of tags available for the year. Tagging data were recorded into a computer file each day and were uploaded to the central repository for all PIT-tagging activities in the Columbia basin (PTAGIS, www.ptagis.org) within 48 h.

Abundance of each emigrant type was estimated with a mark–recapture program specific to rotary screw trap data developed by Steinhorst et al. (2004). Each calendar year was partitioned into periods defined by changes in flow, subject to the constraint that at least seven recaptures occurred during the period. Population abundance of all emigrants from a cohort was estimated using a summation of Bailey's modified estimator (Ricker 1975):

$$N = \sum_{i=1}^{n} c_i(m_i + 1)/(r_i + 1)$$

where N is number of emigrants, n is the number of periods designated, c_i is the number of fish captured, m_i is the number of tagged fish released, and r_i is number of recaptures in period i. The estimator was computed using an iterative maximization of the log-likelihood, assuming that fish are captured independently with probability p_i (equivalent to trap efficiency) and tagged fish mix thoroughly with untagged fish.

Initial abundance of each cohort was indexed by multiple-pass redd counts. Redds are nests constructed in the stream gravel by spawning females and are a surrogate for the number of eggs spawned. The stream was surveyed three times annually between early September and early October. Trained observers walked the bank, scanning the stream substrate using polarized sunglasses to identify redds. To avoid double counting, each redd was marked by flagging a nearby bush or tree.

Emigrant survival was estimated from the detection of PIT-tagged individuals in the lower Snake and Columbia rivers. For this study, emigrants were considered successful if they passed Lower Granite Dam. Daily detection records were obtained by querying the PTAGIS database (www.ptagis.org) for all observations of fish tagged at the Pahsimeroi River trap by calendar year.

Data analyses

We categorized emigrant types by a combination of FL and day of tagging (Fig. 2*a*). Age-1 smolts were always distinct from age-0 smolts based on size and emigration date, but a subsample of ages was verified by scale examination (Lutch et al. 2003). After exclusion of the age-1 smolts, we separated age-0 smolt and fall parr types by constructing discriminant functions for each year using data from fish detected at downriver dams. Date and length at tagging were used to predict group membership. Individuals detected in the year of tagging were age-0 smolts, whereas individuals detected in the spring after tagging were fall parr. We applied the discriminant functions to all tagged fish. Abundance estimates were parsed into emigrant type for each estimation period by proportions of the tagged population.

We estimated survival to Lower Granite Dam by emigrant type within each cohort using a Cormack–Jolly–Seber model implemented by SURPH software (Lady et al. 2001). Model inputs were records of the PIT tags released at the Pahsimeroi River trap and their subsequent detection at downstream dams. Model outputs were the probability of being detected at Lower Granite Dam (based on detections there and downstream) and the probability of survival to Lower Granite Dam. The number of each emigrant type surviving to Lower Granite Dam was computed by multiplying abundance estimates at the Pahsimeroi River trap by survival probability.

We hypothesized that the expression of migratory phenotype is influenced by growth and abundance. The effect of abundance on growth was examined by plotting a growth index for each emigrant type versus the redd count for the year they were spawned. Power functions were used to describe the relationships (Grant and Imre 2005). These models were fit using a Gauss–Newton algorithm in SYSTAT (Systat Software Corporation 2004). Regressions were considered significant if their 95% Wald confidence interval (CI) did not contain zero, and the slopes of the functions differed if their CIs did not overlap. To index growth, we used mean FL of PIT-tagged emigrants in June for age-0 smolts, in November and December for fall parr, and all age-1 smolts collected. Mean lengths for age-0 smolts from the 1992 and 1993 cohorts were not calculated because the trap was not operated in June in those years. We also compared annual proportions of age-1 smolts surviving to Lower Granite Dam with initial cohort abundance, indexed by redd counts.

We examined the implications for population regulation with a deterministic model of relative survival contrasting age-0 smolts and fall parr to age-1 smolts. For prereproductive life stages, survival is equivalent to fitness (Roff 2002). The relevant question is how likely is a juvenile salmon to survive to Lower Granite Dam if it adopts a particular strategy? To understand fitness, a measure of survival prior to passing the trap is necessary. Therefore, we estimated two survival rates for each emigrant type to determine its relative survival: from the end of the cohort's first spring to emigration from the Pahsimeroi River ($S_{\mathrm{pah},k}$) and from the trap to Lower Granite Dam ($S_{\mathrm{lgd},k}$) for each emigrant type k. Relative survival (RS) was computed as

$$\mathrm{RS}_k = \frac{S_{\mathrm{pah},k} \times S_{\mathrm{lgd},k}}{\sum(S_{\mathrm{pah,age-1}} \times S_{\mathrm{lgd,age-1}})}$$

We used median S_{lgd} for the study period in the model as a measure of the central tendency in survival to reduce the ef-

Fig. 2. Patterns in Chinook salmon emigration from the Pahsimeroi River during 1999. (*a*) Fork length versus date of tagging by emigrant type for juvenile Chinook salmon tagged at the Pahsimeroi River trap. Age-1 smolts were spawned in 1997. Age-0 smolts and fall parr were spawned in 1998. Note that only a subsample of each type was tagged. (*b*) Cumulative percentage by emigrant type versus passage date at Lower Granite Dam. Age-1 smolts and fall parr were spawned in 1997. Age-0 smolts were spawned in 1998.

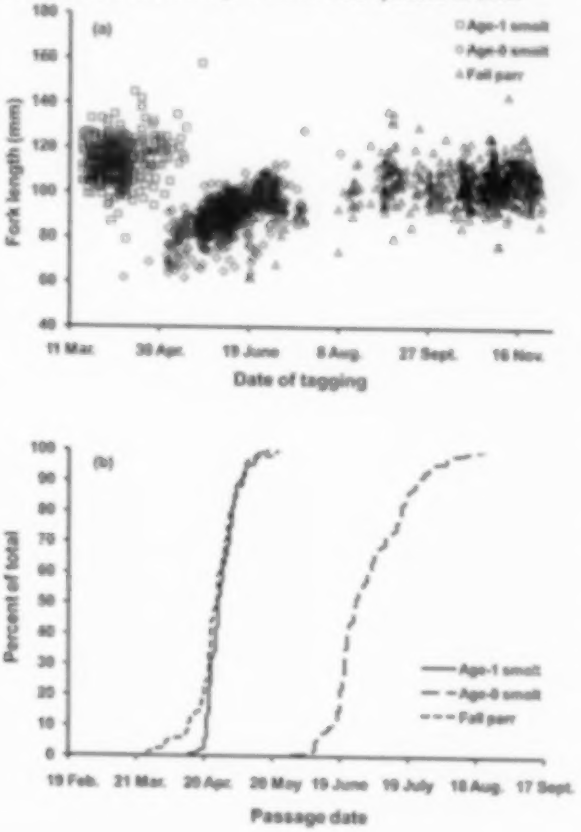

fect of extreme values. We assumed that daily survival was equivalent among all juveniles within the Pahsimeroi River and considered three scenarios about when mortality occurred: summer only, summer and fall only, or summer through winter. We further assumed that survival did not change appreciably with the seasons because flows were relatively stable and temperature was moderate throughout the year. Because age-0 smolts emigrate at the end of their first spring, $S_{\mathrm{pah,age\text{-}0}} = 1$. We iteratively solved for S_{pah} for fall parr and age-1 smolts while constraining model output such that

$$\frac{S_{\mathrm{pah,age\text{-}1}} \times S_{\mathrm{lgd,age\text{-}1}}}{\sum (S_{\mathrm{pah},k} \times S_{\mathrm{lgd},k})}$$

equaled the median ratio of age-1 smolts at Lower Granite Dam to total cohort production.

Results

The three life history types were present in every cohort studied and emigration followed a consistent pattern. Age-0 smolts were the first emigrants from each cohort, leaving the Pahsimeroi River in the spring after hatching (Fig. 2*a*) and continuing past Lower Granite Dam in the same year. Fall parr began emigrating during August (Fig. 2*a*) but did not pass Lower Granite Dam that year. In the following spring, age-1 smolts began emigrating in early March and usually were gone by mid-May. The first emigrant type from a cohort to reach Lower Granite Dam was the age-0 smolts, but when viewed from a calendar-year perspective, this emigrant type consistently passed the dam two months later than the other two types (Fig. 2*b*).

The discriminant functions were effective for distinguishing between age-0 smolts and fall parr. Classification accuracy of individuals with known life history averaged 97.5%. However, a small number of fish classified as age-0 smolts arrived at the dam in the year after tagging, i.e., they were actually fall parr. Classification of these fish as age-0 smolts did not alter survival estimates greatly (≤0.03). No juveniles classed as fall parr were detected as age-0 smolts. Age-1 smolts were quite distinct from age-0 smolts (Fig. 2*a*); hence, there was no need to use statistical techniques to classify them.

There were consistent differences in survival to Lower Granite Dam among emigrant types and FL at emigration (Table 1). Median survival to Lower Granite Dam of age-0 and age-1 smolts was similar. Age-0 smolt survival fluctuated more and was more similar to fall parr survival for 4 of 13 cohorts. Survival of fall parr was usually lower than that of age-1 smolts but was more stable. The lowest survival (0.13) was experienced by the age-0 smolts from the 2000 cohort, which emigrated during the extreme drought of 2001. Very high survivals (0.73–0.74) were experienced by age-1 and age-0 smolts in the 1997 cohort and age-1 smolts in the 1998 cohort. Length followed order of age; age-1 smolts were largest and age-0 smolts were smallest (Table 1). However, there was a wide range among annual means within each type. Mean FL for fall parr varied by up to 21.1 mm, but the range for age-0 smolts was only 14.1 mm.

Initial cohort abundance affected survival to Lower Granite Dam. Redd counts varied over an order of magnitude, from 11 in 1995 to 354 in 2003. The calculated slope of initial abundance on survival was steepest for age-0 smolts (Fig. 3), but because survival was highly variable, the slope was not significantly different from zero ($b = -0.20$; 95% Wald CI –0.44 to 0.03, mean corrected $r^2 = 0.27$). For fall parr, the slope of the relationship was significantly different from zero, although less steep than for age-0 smolts ($b = -0.16$, 95% Wald CI –0.25 to –0.06, mean corrected $r^2 = 0.55$). However, for age-1 smolts, survival was not related to cohort abundance ($b = 0.07$, 95% Wald CI –0.22 to 0.08, mean corrected $r^2 = 0.09$).

The relationship between initial cohort abundance and length at migration from the Pahsimeroi River was also well described by descending power functions (Fig. 4). The slopes for each type were similar and were significantly different from zero. The slope estimate was –0.04 (95% Wald

Table 1. Median probability of survival from the Pahimeroi River to Lower Granite Dam and mean fork length at emigration (mm) for each emigrant type.

Emigrant type	Median survival	Mean fork length
Age-0 smolt	0.51 (0.13–0.73)	90.8 (83.7–97.8)
Fall parr	0.27 (0.20–0.38)	105.2 (95.8–116.9)
Age-1 smolt	0.56 (0.33–0.74)	112.1 (104.0–124.0)

Note: Ranges of annual values are given in parentheses.

Fig. 3. Survival to Lower Granite Dam by type versus redd count, an index of initial cohort abundance. Lines are fitted power functions. Equations: for age-1 smolts (open squares), survival = $0.72(\text{redds})^{-0.07}$, mean corrected $r^2 = 0.09$; for age-0 smolts (solid diamonds), survival = $1.06(\text{redds})^{-0.20}$, mean corrected $r^2 = 0.27$; for fall parr (open triangles), survival = $0.52(\text{redds})^{-0.16}$, mean corrected $r^2 = 0.55$.

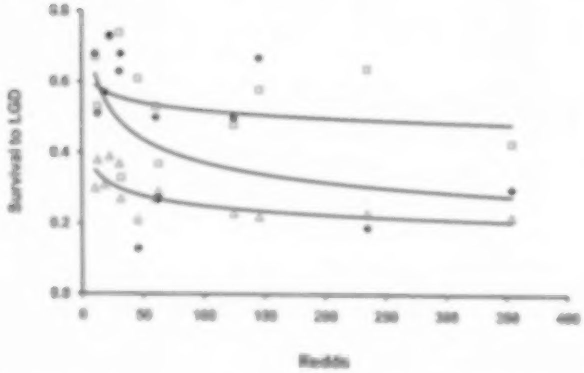

Fig. 4. Mean fork length at emigration by type versus redd count, an index of initial cohort abundance. Lines are fitted power functions. Equations: for age-1 smolts (open squares), length = $126.84(\text{redds})^{-0.03}$, mean corrected $r^2 = 0.49$; for age-0 smolts (open diamonds), length = $106.36(\text{redds})^{-0.04}$, mean corrected $r^2 = 0.82$; for fall parr (solid triangles), length = $131.43(\text{redds})^{-0.06}$, mean corrected $r^2 = 0.81$.

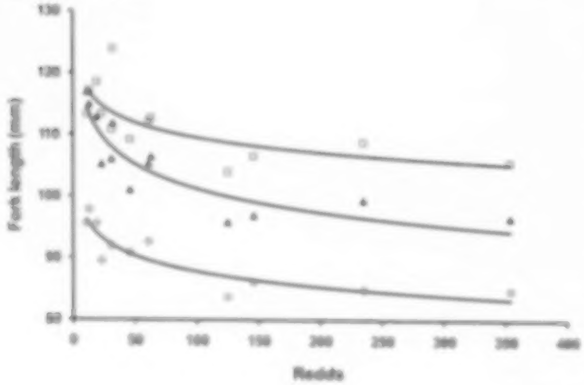

CI −0.06 to −0.03, mean corrected $r^2 = 0.82$) for age-0 smolts, −0.06 (95% Wald CI −0.08 to −0.04, mean corrected $r^2 = 0.81$) for fall parr, and −0.03 (95% Wald CI −0.05 to −0.01, mean corrected $r^2 = 0.49$) for age-1 smolts.

Fig. 5. Percentage of cohort surviving to Lower Granite Dam that emigrated as age-1 smolts versus initial cohort abundance as indexed by redd counts.

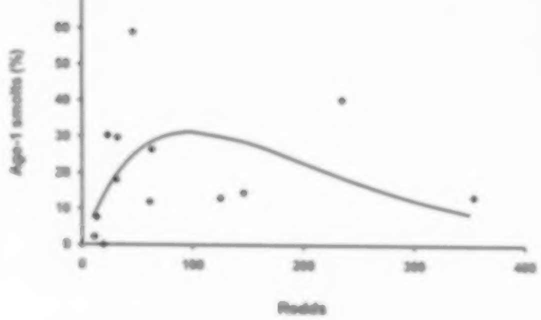

Fig. 6. Output of the relative survival model under three scenarios regarding in which season mortality occurs in Chinook salmon parr in the Pahsimeroi River: age-0 smolts, solid bars; fall parr, shaded bars; age-1 smolts, open bars.

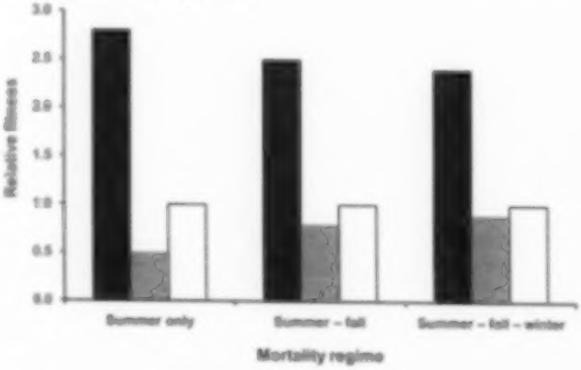

The relative importance of emigrant type changed with initial cohort abundance. The contribution of the age-1 smolt type, the group with highest survival from the trap to Lower Granite Dam, to the number of emigrants reaching Lower Granite Dam was dome-shaped with respect to redd counts (Fig. 5). The proportion of successful emigrants that left the Pahsimeroi River as age-1 smolts was above 33% of total smolt production only twice out of 13 cohorts. Relative survival, our surrogate for relative fitness, differed among the emigrant types and followed a consistent pattern. When scaled to age-1 egg-to-smolt survival, the age-0 smolt type consistently had the highest relative survival (2.4–2.8), and the fall parr type, the lowest (0.5–0.9) (Fig. 6). Results were robust to the exact timing of mortality within the Pahsimeroi River. Given the values of S_{lgd} observed, any mortality above the trap caused the relative survival of the age-0 smolts to become greater than that of the other types. We verified the model by replacing the median S_{lgd} values with survivals measured for cohorts with the worst and best survivals (2000 and 1997, respectively) and allowed the proportion of age-1 smolts at Lower Granite Dam to vary. The proportions predicted were close to proportions observed (50% predicted versus 54% observed for 2000 and 22% predicted versus 28% observed for 1997). Given this corroboration, we believe our simple model is a useful tool with which to gauge relative fitness.

Discussion

Population functioning in Pahsimeroi River Chinook salmon

The proportions of smolt production by each life history type varied with circumstances; hence, the full expression of phenotypic diversity is important to this population. Relative fitness patterns (as measured by egg-to-smolt survival) explained the dome-shaped relation of proportion of successful emigrants from juveniles tagged as age-1 smolts. In most years, if a young Chinook salmon can grow fast enough, it should emigrate immediately to maximize its chances of reaching the Snake River and the migration corridor to the ocean. If growth opportunity is not sufficient, then a salmon parr in the Pahsimeroi River should delay smoltification until becoming a yearling and then emigrate. At extreme low densities, few parr stay in the Pahsimeroi River to spend the winter. This framework is consistent with Lichatowich and Mobrand's (1995) hypothesis that sufficient growth opportunity and habitat connectivity lead to emergence of an age-0 emigrant life history as an important part of population productivity in stream-type Chinook salmon. In fact, stream-type Chinook salmon are able to smolt as subyearlings (Connor et al. 2001) given sufficient growth and an increasing photoperiod (Clarke et al. 1992).

We had no data on survival within the Pahsimeroi River. Instead, we modeled a survival regime (summer survival = 32.5%) that was reasonable given the data observed. Healey (1991) described Chinook salmon fry–smolt survival >30% as high but cited survivals up to 34%. The survival rate that we derived may be high, but the Pahsimeroi River is a relatively benign environment for young salmonids. The ground-water-dominated flow moderates temperatures and maintains flow throughout the year. The water is fertile and summer growth of aquatic vegetation provides shelter and food. The model results agreed well with the observed proportions of age-1 smolts; therefore, high and consistent survival in the Pahsimeroi River after the parr stage begins is reasonable.

An implicit assumption for this analysis was that smolt-to-adult return (SAR) rates were comparable for the three types, historically. Unfortunately, there are insufficient data (28 adult detections from 30 895 juveniles tagged during the study period; D. Venditti, unpublished data) to validate this assumption for this population. However, it is not necessary to assume that SARs were equal. For lifetime survival of age-0 and age-1 smolts to be equal, historic age-0 smolt survival through the migration corridor and ocean would have needed to be approximately one-third that of the age-1 smolts. Even with greatly reduced SARs, adult contribution from age-0 smolts would have been substantial.

Fitness implications should be inferred beyond the observed life stage to the entire life span to understand variability in performance (Zabel and Achord 2004). Although our study focused on juvenile life history, we obtained adult detections from juveniles tagged at the Pahsimeroi River trap at Snake and Columbia river dams from the PTAGIS database. No fish tagged as age-0 smolts were detected returning from the Pacific Ocean. However, a few adults that emigrated as age-0 smolts were observed at Bonneville Dam (Whiteaker and Fryer 2007) during the time when adults from Pahsimeroi were returning to freshwater.

We concluded that the age-0 smolt life history trajectory could no longer be completed. But why might this strategy be maintained? Length at emigration was influenced by initial cohort abundance. Survival was also influenced by initial abundance. The expression of life history type was influenced by density and thus growth conditions. The Pahsimeroi River population produces the largest age-1 smolts in Idaho and the age-0 smolts are similar in size to age-1 smolts in most other SRSS Chinook salmon populations (Lutch et al. 2003). However, age-0 smolts pass through the hydrosystem two months later and encounter a different set of hazards (discussed below). Enough of the other types survive to support the population, even though their fastest-growing progeny will become age-0 smolts. Thus, the unique growth potential present in the Pahsimeroi River allows a greater range of juvenile Chinook salmon life histories than typical for central Idaho.

Waples et al. (2004) argued that the age-0 emigrant life history is not viable for stream-type Chinook salmon populations in the interior Columbia River basin because they reach the ocean when conditions are not conducive for survival and growth for the migratory path that such populations follow. Why then does this life history persist if it was never viable? The Situk River in Alaska produces age-0 Chinook salmon smolts despite being in an area dominated by stream-type populations (Johnson et al. 1992). Similarly, in inland British Columbia, Canada, substantial numbers of both stream- and ocean-type juveniles are produced in the South Thompson River (Beacham et al. 2003). The alternative hypothesis is that the phenotype is recently evolved, which is unlikely given the lack of surviving adults. We argue that the age-0 life history in the Pahsimeroi River population is not an aberration but once was a viable alternative.

Importance of juvenile life history diversity to salmon conservation

Conservation of life history diversity is important to recovery of endangered species. Life history components may change in importance over time; small stocks today may be major producers tomorrow (Hilborn et al. 2003). Managers need to understand the fitness value of the population components to identify important elements of diversity for conservation and management. Management should address the full suite of phenotypes, not just the most common or obvious ones (Watters et al. 2003). This should include passage alternatives for young salmon emigrating through the main stem rivers late in the season.

Salmon conservation requires an understanding of what the fish need to complete their life history. It is important that all options remain viable. The current recovery plan emphasizes adult return timing without addressing juvenile life history types. Arguably, in this case, the juvenile phase is more constrained than the adult phase. Given that age-1 smolts from the Pahsimeroi River are very large, one might expect this population to be healthier than others in central Idaho. None of the SRSS Chinook salmon populations has met regional objectives for survival and recovery (Good et al. 2005; ICTRT 2007). Reliance on measures aimed at age-1 smolts may not raise this population's productivity because the most productive portion of the population is using a life history trajectory that cannot be completed.

In conclusion, we believe that potential opportunities for conservation of Pahsimeroi River Chinook salmon are greatest for age-0 smolts. Historically, improvements to the hydrosystem were aimed at age-1 smolts and did not benefit age-0 smolts (Raymond 1988). More recently, actions such as summer flow augmentation and temperature moderation from release of cool water from storage reservoirs has been used to improve migration conditions for subyearling migrants (Connor et al. 2003; National Oceanic and Atmospheric Adminstration Fisheries (NOAAF) 2008). A current line of applied research in the Columbia River basin is the use of new technologies to aid emigration through the main stem corridor (NOAAF 2008). Small increases in the survival of age-0 smolts to adulthood would have large impacts on the productivity of this population.

Acknowledgements

Fieldwork was conducted under a permit issued to the Idaho Department of Fish and Game by the National Marine Fisheries Service by authority of Section 10 of the Endangered Species Act. Bruce Barnett oversaw the collection and collation of the data. Doug Engemann, Todd Garlie, and Carmen Garlie helped in the field and provided logistical support. Paul Bunn provided the map. Jody White helped clarify some of our ideas. We thank Bill Schrader, Barry Berejikian, Charlie Petrosky, Dan Schill, and Jim Morrow for their helpful comments on an earlier draft. Criticisms from two anonymous reviewers and the associate editor were appreciated. Funding was provided by the Bonneville Power Administration (Projects 1989-098-00 and 1991-073-00).

References

Beacham, T.D., Supernault, K.J., Wetklo, M., Deagle, B., Labaree, K., Irvine, J.R., Candy, J.R., Miller, K.M., Nelson, R.J., and Withler, R.E. 2003. The geographic basis for population structure in Fraser River chinook salmon (*Oncorhynchus tshawytscha*). Fish. Bull. (Washington, D.C.), **101**: 229–242.

Beckman, B.R., Gadberry, B., Parkins, P., Cooper, K.A., and Arkush, K. 2007. State-dependent life history plasticity in Sacramento River winter-run Chinook salmon (*Oncorhynchus tshawytscha*): interactions among photoperiod and growth modulate smolting and early male maturation. Can. J. Fish. Aquat. Sci. **64**(2): 256–271. doi:10.1139/F07-001.

Clarke, W.C., Withler, R.E., and Shelbourn, J.E. 1992. Genetic control of juvenile life history pattern in Chinook salmon (*Oncorhynchus tshawytscha*). Can. J. Fish. Aquat. Sci. **49**: 2300–2306. doi:10.1139/f92-252.

Connor, W.P., Marshall, A.R., Bjornn, T.C., and Burge, H.L. 2001. Growth and long-range dispersal by wild subyearling spring and summer Chinook salmon in the Sanke River basin. Trans. Am. Fish. Soc. **130**(6): 1070–1076. doi:10.1577/1548-8659(2001)130<1070:GALRDB>2.0.CO;2.

Connor, W.P., Burge, H.L., Yearsley, J.R., and Bjornn, T.C. 2003. Influence of flow and temperature on survival of wild subyearling fall Chinook salmon in the Snake River. N. Am. J. Fish. Manage. **23**(2): 362–375. doi:10.1577/1548-8675(2003)023<0362:IOFATO>2.0.CO;2.

Dunham, J.B., and Vinyard, G.L. 1997. Relationships between body mass, population density, and the self-thinning rule in stream-living salmonids. Can. J. Fish. Aquat. Sci. **54**(5): 1025–1030. doi:10.1139/cjfas-54-5-1025.

Dunham, J.B., Dickerson, B.R., Beever, E., Duncan, R.D., and Vinyard, G.L. 2000. Effects of food limitation and emigration on self-thinning in experimental minnow cohorts. J. Anim. Ecol. **69**(6): 927–934. doi:10.1046/j.1365-2656.2000.00451.x.

Gamfeldt, L., and Källström, B. 2007. Increasing intraspecific diversity increases predictability in population survival in the face of perturbations. Oikos, **116**(4): 700–705. doi:10.1111/j.0030-1299.2007.15382.x.

Good, T.P., Waples, R.S., and Adams, P. (*Editors*). 2005. Updated status of federally listed ESUs of West Coast salmon and steelhead. NOAA Technical Memorandum No. NMFS-NWFSC-66.

Grant, J.W.A., and Imre, I. 2005. Patterns of density-dependent growth in juvenile stream-dwelling salmonids. J. Fish Biol. **67**(Suppl. B): 100–110. doi:10.1111/j.0022-1112.2005.00916.x.

Grant, J.W.A., Steingrímsson, S.Ó., Keeley, E.R., and Cunjak, R.A. 1998. Implications of territory size for the measurement and prediction of salmonid abundance in streams. Can. J. Fish. Aquat. Sci. **55**(Suppl. 1): 181–190. doi:10.1139/cjfas-55-S1-181.

Healey, M.C. 1991. Life history of Chinook salmon (*Oncorhynchus tshawytscha*). *In* Pacific salmon life histories. *Edited by* C. Groot and L. Margolis. UBC Press, Vancouver, British Columbia. pp. 311–393.

Healey, M.C., and Prince, A. 1995. Scales of variation in life history tactics of Pacific salmon and the conservation of phenotype and genotype. Am. Fish. Soc. Symp. **17**: 176–184.

Hilborn, R., Quinn, T.P., Schindler, D.E., and Rogers, D.E. 2003. Biocomplexity and fisheries sustainability. Proc. Natl. Acad. Sci. U.S.A. **100**(11): 6564–6568. doi:10.1073/pnas.1037274100. PMID:12743372.

Interior Columbia Technical Recovery Team. 2007. Salmon and steelhead recovery planning in the Snake River Basin, early draft plan chapters for public comment [online]. Available at http://www.idahosalmonrecovery.net/pdfs/5_5MPG_UpperSalmonRiverChinook.pdf [accessed March 2008].

Johnson, S.W., Thedinga, J.F., and Koski, K.V. 1992. Life history of juvenile ocean-type Chinook salmon (*Oncorhynchus tshawytscha*) in the Situk River, Alaska. Can. J. Fish. Aquat. Sci. **49**(12): 2621–2629. doi:10.1139/f92-290.

Kendall, B.E., and Fox, G.A. 2002. Variation among individuals and reduced demographic stochasticity. Conserv. Biol. **16**(1): 109–116. doi:10.1046/j.1523-1739.2002.00036.x.

Lady, J., Westhagen, P., and Skalski, J.R. 2001. SURPH (Survival under Proportional Hazards). Version 2.2b [online]. Available at www.cbr.washington.edu/paramest/surph/ [accessed February 2007].

Lichatowich, J.A., and Mobrand, L.E. 1995. Analysis of Chinook salmon in the Columbia River from an ecosystem perspective. Report to Bonneville Power Administration, Project 92-18, Portland, Oregon.

Lutch, J., Leth, B., Apperson, K.A., Brimmer, A., and Brindza, N. 2003. Idaho supplementation studies annual progress report, January 1, 1997 – December 31, 2001. Idaho Department of Fish and Game Report No. 03-37, Boise, Idaho.

McElhany, P., Ruckelshaus, M.H., Ford, M.J., Wainwright, T.C., and Bjorkstedt, E.P. 2000. Viable salmonids populations and the recovery of evolutionarily significant units. National Oceanic and Atmospheric Administration Technical Memorandum No. NMFS-NWFSC-42.

Mobrand, L.E., Lichatowich, J.A., Lestelle, L.C., and Vogel, T.S. 1997. An approach to describing ecosystem performance "through the eyes of salmon". Can. J. Fish. Aquat. Sci. **54**(12): 2964–2973. doi:10.1139/cjfas-54-12-2964.

National Oceanic and Atmospheric Administration Fisheries. 2008. Endangered Species Act 7(*a*) (2) consultation biological opinion and Magnuson–Stevens Fishery Conservation and Management Act essential fish habitat consultation. National Marine Fisheries Service, Northwest Region, Seattle, Washington.

PIT Tag Steering Committee. 1999. PIT tag marking station procedural manual. Version 2.0. Pacific States Marine Fisheries Commission, Portland, Oregon.

Prentice, E.F., Flagg, T.A., and McCutcheon, C.S. 1990. PIT-tag monitoring systems for hydroelectric dams and fish hatcheries. Am. Fish. Soc. Symp. **7**: 323–334.

Raymond, H.L. 1988. Effects of hydroelectric development and fisheries enhancement on spring and summer Chinook salmon and steelhead in the Columbia River basin. N. Am. J. Fish. Manage. **8**(1): 1–24. doi:10.1577/1548-8675(1988)008<0001:EOHDAF>2.3.CO;2.

Reeve, H.K., and Sherman, P.W. 1993. Adaptation and the goals of evolutionary research. Q. Rev. Biol. **68**(1): 1–32. doi:10.1086/417909.

Reimers, P.E. 1973. The length of residence of juvenile fall Chinook salmon in Sixes River, Oregon. Research Reports of the Fish Commission of Oregon, Portland, Oregon.

Ricker, W. E. 1975. Computation and interpretation of biological statistics of fish populations. Bull. Fish. Res. Board Can. No. 191.

Roff, D.A. 2002. Life history evolution. Sinauer Associates, Sunderland, Massachusetts.

Scheuerell, M.D. 2005. Influence of juvenile size on the age of maturity of individually marked wild Chinook salmon. Trans. Am. Fish. Soc. **134**(4): 999–1004. doi:10.1577/T04-206.1.

Stearns, S.C. 1992. The evolution of life histories. Oxford University Press, New York.

Steinhorst, K., Wu, Y., Dennis, B., and Kline, P. 2004. Confidence intervals for fish outmigration estimates using stratified trap efficiency methods. J. Agric. Biol. Environ. Stat. **9**(3): 284–299. doi:10.1198/108571104X3325.

Systat Software Corporation. 2004. SYSTAT. Version 11. Systat Software Corporation, Richmond, California.

Taylor, E.B. 1990. Phenotypic correlates of life-history variation in juvenile Chinook salmon *Oncorhynchus tshawytscha*. J. Anim. Ecol. **59**(2): 455–468. doi:10.2307/4874.

Thorpe, J.E., Mangel, M., Metcalfe, N.B., and Huntingford, F.A. 1998. Modelling the proximate basis of salmonid life-history variation, with application to Atlantic salmon. Evol. Ecol. **12**(5): 581–599. doi:10.1023/A:1022351814644.

Trapani, J. 2002. Stream habitat inventory report: Lemhi, Pahsimeroi, and the East Fork Salmon River, Idaho. Upper Salmon Basin Watershed Project, Salmon, Idaho. Available at http://www.modelwatershed.org/LIBRARY/habitatreport2.pdf

Waples, R.S., Teel, D.J., Myers, J.M., and Marshall, A.R. 2004. Life-history divergence in Chinook salmon: historic contingency and parallel evolution. Evolution, **58**(2): 386–403. doi:10.1554/03-323. PMID:15068355.

Waples, R.S., Zabel, R.W., Scheuerell, M.D., and Sanderson, B.L. 2008. Evolutionary responses by native species to major anthropogenic changes to their ecosystems: Pacific salmon in the Columbia River hydropower system. Mol. Ecol. **17**(1): 84–96. doi:10.1111/j.1365-294X.2007.03510.x. PMID:18268786.

Watters, J.V., Lema, S.C., and Nevitt, G.A. 2003. Phenotype management: a new approach to habitat restoration. Biol. Conserv. **112**(3): 435–445. doi:10.1016/S0006-3207(02)00343-9.

Whiteaker, J., and Fryer, J. 2007. Age and length composition of Columbia basin Chinook and sockeye salmon and steelhead at Bonneville Dam in 2006. Columbia River Inter-Tribal Fish Commission, Portland, Oregon.

Wilbur, H.M. 1996. Multistage life cycles. *In* Population dynamics in ecological space and time. *Edited by* O.E. Rhodes, R.K. Chesser, and M.H. Smith. University of Chicago Press, Chicago, Illinois. pp. 75–108.

Zabel, R.W., and Achord, S. 2004. Relating size of juveniles to survival within and among populations of Chinook salmon. Ecology, **85**(3): 795–806. doi:10.1890/02-0719.

Spawning time variation in Icelandic summer-spawning herring (*Clupea harengus*)

Guðmundur J. Óskarsson and Christopher T. Taggart

Abstract: Different fish stocks of the same species are defined by spatial and temporal differences in spawning, though spawning time can vary within and among stocks. Here we address spawning time variation in Icelandic summer-spawning (ISS) Atlantic herring (*Clupea harengus*). We do so by examining influencing factors that include variation in stock size structure, spawning experience (recruit vs. repeat spawners), spawning stock biomass (SSB), sea temperature, and combinations thereof. Our results, based on temporal variation in ovary weight (OW), relative ovary weight (RG), and maturation stage, across a time series of nearly 50 years and eight length classes of ISS herring, show that spawning occurs over a relatively invariant 30-day period defined by day-of-the-year. Logistic regression analyses and temporal development in OW and RG show that maximum spawning invariably occurs on day-of-the-year 200 ± 15 days, and seasonal variation in mesenteric fat content is physiologically consistent with the timing. We show that the smaller recruit spawners tend to spawn ~17 days later, on average, than the larger repeat spawners. Spawning occurs ~7 days later when SSB is greater than the long-term average, and spawning may be delayed by as much as 10 days during periods of colder than average ocean temperature.

Résumé : On définit les divers stocks d'une même espèce par les différences spatiales et temporelles dans la fraie, bien que le moment de la fraie puisse varier entre les stocks et à l'intérieur d'un même stock. Nous nous intéressons ici à la variation du moment de la fraie chez les harengs atlantiques (*Clupea harengus*) à fraie estivale d'Islande (ISS). Nous le faisons en examinant les facteurs explicatifs, y compris la variation dans la structure en taille du stock, l'expérience de fraie (recrues par rapport aux reproducteurs multipares), la biomasse du stock reproducteur (SSB), la température de la mer et les combinaisons de ces facteurs. Nos résultats, basés sur la variation temporelle de la masse ovarienne (OW), de la masse ovarienne relative (RG) et du stade de maturation dans une série chronologique de presque 50 ans qui comprend huit classes de longueurs de harengs ISS, montrent que la fraie se produit sur une période relativement invariable de 30 jours définie par le jour de l'année. Des analyses de régression logistique et l'évolution dans le temps de OW et de RG montrent que le maximum de la fraie a lieu au jour 200 ± 15 de l'année et que la variation saisonnière de la graisse mésentérique est physiologiquement compatible avec ce calendrier. Nous démontrons que les recrues plus petites qui se reproduisent ont tendance à le faire en moyenne ~17 jours plus tard que les reproducteurs multipares plus grands. La fraie se produit ~7 jours plus tard lorsque SSB est plus grande que la moyenne à long terme et la fraie peut être retardée de jusqu'à 10 jours durant les périodes où la température de l'océan est inférieure à la moyenne.

[Traduit par la Rédaction]

Introduction

Different fish stocks of the same species are defined, in part, by their spatial and temporal differences in spawning, which are hypothesized to be a consequence of "adaptation" to ensure a "match" between emergent larvae and their food resources (e.g., Cushing 1969; Bagenal 1971; Ware 1975). However, spawning time varies within, as well as among, stocks. Timing of maximum spawning in many north-temperate stocks varies annually due to variation in ocean temperature (Lambert 1987 and references therein; Hutchings and Myers 1994), age and size structure (e.g., Hutchings and Myers 1994; Marteinsdottir and Björnsson 1999), or a combination thereof (Carscadden et al. 1997). Spawning time in Baltic herring (*Clupea harengus membras*) can be a function of the feeding conditions experienced prior to spawning (Rajasilta 1992), and the same can be said of captive Pacific herring (*Clupea harengus pallasi*; Hay et al. 1988) and Atlantic cod (*Gadus morhua*; Kjesbu and Holm 1994). Photoperiod (Rijnsdorp and Vingerhoed 1994; Norberg et al. 1995) and tidal phase (e.g., Hay 1990) also appear to influence spawning time. In other cases, the time of maximum spawning is relatively invariant (e.g., Atlantic cod; Pedersen 1984).

There may be two or more spawning waves within a spawning season in some fish species and stocks (McPherson et al. 2003), with the recruit spawners (smaller and younger individuals) tending to spawn earlier (e.g., Hutchings and Myers (1994), protracted spawning for larger individuals; Morgan 2003) or later (Lambert (1987) and references therein for different herring stocks; Ware and Tanasichuk 1989; Slotte et al. 2000) than the larger and older spawners. One consequence of this age- or size-specific

Received 11 August 2008. Accepted 20 April 2009. Published on the NRC Research Press Web site at cjfas.nrc.ca on 26 September 2009.
J20721

Paper handled by Associate Editor Bror Jonsson.

G.J. Óskarsson[1,2] and C.T. Taggart. Department of Oceanography, Dalhousie University, Halifax, NS B3H 4J1, Canada.

[1]Corresponding author (e-mail: gjos@hafro.is).
[2]Present address: Marine Research Institute, Skulagata 4, P.O. Box 1390, 121 Reykjavik, Iceland.

Can. J. Fish. Aquat. Sci. **66**: 1666–1681 (2009) doi:10.1139/F09-095 **Published by NRC Research Press**

spawning determination is a contracted or protracted spawning period that depends on stock age or size structure and thus may reflect a mechanism that explains the relation between recruitment and the age (and presumably size) diversity in Icelandic Atlantic cod (Marteinsdottir and Thorarinsson 1998). Similarly, from a multistock herring analysis, it appears that better than average recruitment occurs as the number of age (and presumably size) classes in a stock increases due to protracted and geographically widespread spawning (Lambert 1987). Thus, it can be logically argued that variation in spawning time within and among different stock units will influence subsequent recruitment.

Here we address spawning time variation in Atlantic herring by using Icelandic summer-spawning (ISS) herring data to examine influencing factors that include variations in stock age and size structure, spawning experience (recruit vs. repeat spawners), spawning stock biomass (SSB), sea temperature, and combinations thereof. We do so, in part, because Cushing's (1969) original match–mismatch hypothesis focused on recruitment variation, primarily in herring, resulting from an invariant spawning time and larval emergence and variable timing in the availability of larval food. However, much of the literature has focussed on temporal variation in the production of food and less so on variation in spawning time, originally considered relatively invariant in Cushing's hypothesis.

Material and methods

Data sources

Our analyses are restricted to data on female herring drawn from archives at the Marine Research Institute (MRI) in Iceland. The MRI data include measurements of individual females collected over the period 1953 through 2000 from various research surveys (25%) and the commercial fishery (75%) among which sampling intensity differed within and among years in an irregular manner. The data include collection date and location, total length (±1.0 cm), whole-body weight (±1 g), gonad weight (±1 g; 10 181 of 11 370 fish; Table 1), maturity stages (1 to 8; Anonymous 1962), and a qualitative visual index of mesenteric fat content ranging from 0 (no fat) to 3 (organs fully covered with fat). For the latter, estimates are provided when the data are available (1962 through 2000) for female spawners at lengths 28 cm through 35 cm (smaller and larger being excluded due to the paucity of observations). Annual estimates of SSB (Table 1) are derived from sequential population analyses (SPA) conducted in 1992 (G. Stefánsson and J. Jakobsson, Marine Research Institute, Skulagata 4, P.O. Box 1390, 121 Reykjavik, Iceland, unpublished data) that provide stock estimates for 1962 through 1981 and more recently (Marine Research Institute 2002) for 1982 through 2001 (see Óskarsson 2005).

ISS spawning regions

In considering an area effect on the spawning time, we classified the herring samples according to two spawning regions (areas 1 and 2; Fig. 1) that are geographically separated (Fridriksson and Timmermann 1950; Jakobsson and Stefánsson 1999). The Irminger Current, a branch of the North Atlantic Drift (current) brings warm, high salinity water to the

Table 1. Summary of the total number of Icelandic summer-spawning female herring (*Clupea harengus*; *n*) collected for morphometric measurements at maturity stages 3 through 7 (Anonymous 1962) in each of areas 1 and 2 (see Fig. 1) over the period 1953 through 2000 and the combined spawning-stock biomass (SSB) estimates. Summary statistics are provided at the bottom of the table.

Year	Area-1 *n*	Area-2 *n*	SSB (× 10^3 t)
1953	574	21	108
1954	148		147
1955	149	1	169
1956	147		170
1957	18		180
1958	112		200
1959	135		278
1960			
1961	330		287
1962	347	1	310
1963	587		267
1964	194	15	189
1965			
1966	213		84
1967	304	19	89
1968	85		27
1969	703	42	17
1970	662	2	20
1971	466	155	13
1972	6	13	11
1973		60	29
1974	32	13	46
1975	49	28	117
1976	98	89	130
1977	136	187	134
1978	150	60	177
1979	352	257	198
1980	127	102	213
1981	13	10	186
1982	107	66	193
1983	41		220
1984	135	10	233
1985	101		251
1986			
1987	9	6	373
1988	71	54	444
1989	241	4	412
1990	122	94	371
1991	59	199	320
1992	99	79	381
1993	70	36	523
1994	280		532
1995			
1996	58		415
1997	148		417
1998	71	1	494
1999	269	114	496
2000	403	43	520
Summary statistics			
N	43	30	44
n	8401	1781	—
Mean ($n \cdot N^{-1}$)	195.4	59.4	236.2
SE mean	27.4	12.1	23.5

Note: Blank fields indicate no data available, therefore excluded in summary statistics. *N*, number of years for which there were data.

Fig. 1. Chart showing sampling locations in areas 1 and 2 (separation marked by broken lines) around Iceland and number (expanding symbols) of individual Icelandic summer-spawning herring (*Clupea harengus*; maturity stages 3 through 7) collected during 1953 through 2000 (n = 10 182). The locations of the primary spawning grounds (Jakobsson and Stefánsson 1999) are indicated with shading, and the locations (×) of repeated temperature measurements used for calculating the temperature index are noted for the Faxaflói, Reykjanes, Selvogsbanki, and Ingólfshöfði transects.

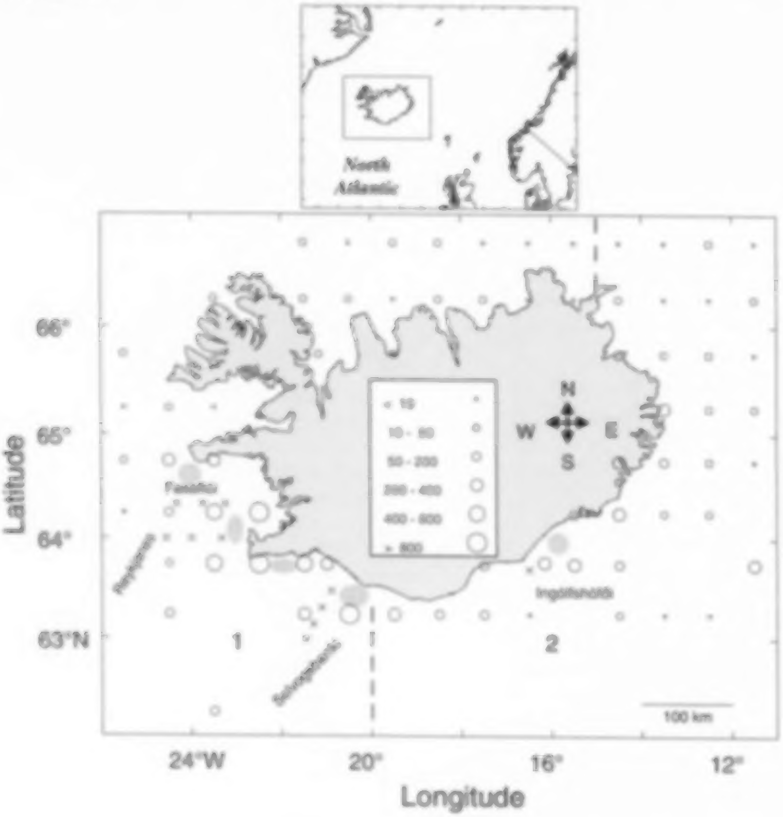

southern Iceland shelf where part of it is subsequently transported cyclonically around Iceland. Although both spawning regions are influenced by the current (see Stefánsson 1962), the onset of the spring phytoplankton bloom is generally earlier in area 1 than in area 2 (Thórdardóttir 1986), and consequently, higher concentrations of zooplankton are more frequently observed in area 1 (Astþórsson et al. 1983).

Annual indices

Three different indices are examined to assess interannual variation in ISS herring spawning time: sea temperature anomaly, body condition anomaly, and index of the age composition. The temperature (°C) anomaly is calculated using temperature data maintained at MRI (Malmberg 1980; Marine Research Institute 2001) that were collected annually at 50 and 100 m depths (z) during the months (m) of January through June over the years (Y) 1953 through 2000 at a suite of hydrographic stations (s) located off southern and southwestern Iceland (Fig. 1: 3 at Faxaflói; 3 at Reykjanes; 4 at Selvogsbanki; and 1 at Ingólfshöfði). Data are restricted to the above depths, months, and stations because they coincide with the depth and seasonal and geographic distribution of ISS herring during the period of ovarian growth and maturation each year. Average temperature at depth, location, and month ($\overline{T}_{z,s,m}$) was calculated across years. The difference between the average temperature and each datum provides the residual:

$$(1)\qquad R_{Y,z,s,m} = T_{Y,z,s,m} - \overline{T}_{z,s,m}$$

The annual temperature anomaly ($\overline{A}_Y$) is the average residual for each year (Y_i):

$$(2)\qquad \overline{A}_Y = \left(\sum_{i=1}^{n_Y} R_{Y_i,z,s,m}\right)\cdot(n_Y)^{-1}$$

where n_Y is the number of measurements in each year (Fig. 2). This formulation ensures that all depths, stations, and months in each region contribute equally to the index despite differences in measurement effort. If more than one datum occurred for each $T_{Y,z,s,m}$, the average value is used.

The MRI data were also used to estimate an annual body condition anomaly ($K_{\mathrm{anomaly},Y}$) among individual spawners by year (Y) for ISS herring during the prespawning season (February through June). Average condition ($\overline{K}_{L,C,R,I}$) among

Fig. 2. Time series of sea temperature anomaly ($\overline{A}_Y$) based on average 50 and 100 m depth measurements off southern and southwestern Iceland (solid line) for the months of January through June of 1953 through 2000. The dotted horizontal line separates negative and positive anomalies.

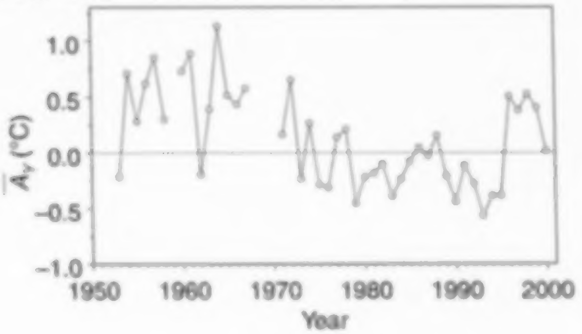

individuals within two length classes (LC; 28–31 cm and 32–35 cm inclusive), among five regions (*R*; covering the stock distribution), and at consecutive 15 day-of-the-year intervals (*I*) was calculated across all years. The five regions were chosen because body condition in ISS herring varies spatially within the same season (Óskarsson 2006). The difference between average and individual condition provides the residual

$$\text{(3)}\qquad \mathrm{KR}_{Y,LC,R,I} = K_{Y,LC,R,I} - \overline{K}_{LC,R,I}$$

The residuals averaged over each year (*Y*) provide the annual condition anomaly

$$\text{(4)}\qquad K_{\text{anomaly},Y} = \sum(\mathrm{KR}_{Y,LC,R,I})\cdot(n_Y)^{-1}$$

where n_Y is the number of individuals in each year. The standard deviation of the anomaly is calculated as

$$\text{(5)}\qquad \mathrm{SD}(K_{\text{anomaly},Y}) = \left((n_Y-1)^{-1}\sum(\mathrm{KR}_{Y,LC,R,I} - \overline{\mathrm{KR}}_{LC,R,I})^2\right)^{0.5}$$

where $\overline{\mathrm{KR}}_{LC,R,I}$ is the mean residual in year *Y*.

We use the skew in the frequency distribution of mature herring within each age class (X_i; ages 3 through 15) to estimate annual variation in the age composition of the spawning stock. The *r*th central moment of a sample (m_r) of *n* fish is defined as

$$\text{(6)}\qquad m_r = \frac{1}{n}\sum_{i=1}^{n}(X_i - \overline{X})^r$$

and for a given sample with 2nd and 3rd central moments (m_2 and m_3, respectively), the coefficient of skewness, b_I, becomes

$$\text{(7)}\qquad b_I = m_3(m_2^{3/2})^{-1}$$

The skew is used to describe the degree of departure from normality in the age distribution, i.e., a positive skew indicates a higher proportion of young spawners, and a negative skew, a lower proportion.

Table 2. Number (*n*) and percentage (%) of total of Icelandic summer-spawning herring (*Clupea harengus*) females collected during 1953 through 2000 (44 years, see Table 1) in both areas combined (Fig. 1) at maturity stages 3 through 7 and used in the analyses.

	Maturity stage					
	3	4	5	6	7	Total
n	3949	2826	2542	602	1451	11 370
%	35	25	22	5	13	

Spawning time determination

Monitoring of the ovary weight

A preliminary examination of ISS herring ovary weight (OW, g) demonstrated an exponential increase in OW from the onset of gonad growth through to spawning that was indicated by a marked decrease in OW. As herring are considered capital (sensu contracted spawning period and reproduction supported by energy reserves) or synchronous (eggs are spawned more or less at one time) spawners, a time series of variation in ovary weight can be used to assess development and thus spawning time. As OW is length (*L*, cm) dependent, we estimate relative ovary weight (RG = $100\cdot\mathrm{OW}\cdot L^{-3}$; g·cm^{-3}) as in Rijnsdorp (1991). To test the validity of RG as a reliable length-independent measure of OW, the median RG estimates at 5-day intervals for six length classes (28–33 cm, inclusive) are compared among classes. Following the evaluation of RG, we examine overall and length-specific variation in OW and RG over time by first calculating the median ($\tilde{x}_i$; $i = 1, 2, \ldots, 73$) OW and RG (statistically defined outliers excluded) in an incremental manner (day-of-the-year order) over sequential 5-day periods (blocks) for all years combined to provide the $\widetilde{\mathrm{OW}}$ and $\widetilde{\mathrm{RG}}$ series. We then smooth each series using a three-point running median ($\tilde{y}_j$ = median($\tilde{x}_{i-1}, \tilde{x}_i, \tilde{x}_{i+1}$), $j = 1, 2, \ldots, 71$) and used Webster's method (1973; see Legendre and Legendre 1998) to assess the magnitude of discontinuities in each series by first-differencing $d_k = (\tilde{y}_j - \tilde{y}_{j+1})$ ($k = 1, \ldots, 70$). The significance ($\alpha = 0.05$) of a discontinuity (change) in a series ($\Delta\widetilde{\mathrm{OW}}$or $\Delta\widetilde{\mathrm{RG}}$) is estimated using a *t* statistic: $t_k = |d_k|\mathrm{S}_{\tilde{x}}^{-1}$, where $\mathrm{S}_{\tilde{x}}$ is the standard deviation of the original series ($\tilde{x}_i$) above. We also determine length-specific discontinuities in $\widetilde{\mathrm{OW}}$ and median whole-body weight ($\widetilde{\mathrm{W}}$) as above. We use median estimates, as they are less sensitive than the mean to departures from normality.

A 5-day-interval average mesenteric fat index ($\overline{\mathrm{MF}}$) is determined using data aggregated over the period 1962 through 2000 among the 28 through 35 cm spawners at maturity stages 3 (mature) through 8 (recovering). This determines the nature of seasonal variation in comparison with ovary development and spawning time estimates.

Logistic regression on spawning stage

Female herring are divided into two classes based on maturation stage for the logistic regression. The dependent variable is binary: 0 (prespawning; maturity stages 3 to 5 inclusive) or 1 (spawning and postspawning; maturity stages 6 and 7, respectively). Stage 6 represents 5% of the observations and stage 7 represents 13% (see Table 2). Stage 7 is

Table 3. Summary of the independent variables used in logistic regression analyses to explain spawning time variation in Icelandic summer-spawning herring (*Clupea harengus*).

Variable	Symbol	Values or units
Day-of-the-year	D	1 through 365
Total length	x_1	±1 cm
Age	x_2	Number of years (scale annuli)
Spawning experience	x_3	0; recruit spawner (<30 cm)
		1; repeat spawner (≥30 cm)
Prespawning female mean annual body condition (Fulton's *K*)	x_4	$g \cdot cm^{-3}$
Spawning location	x_5	1; area 1
		0; area 2
Spawning-stock biomass (SSB)	x_6	Tonnes (t)
Spawning-stock biomass (SSB class)	x_7	0; <250 000 t
		1; >250 000 t
Skew in spawning-stock age distribution	x_8	Dimensionless coefficient[*]
Temperature index[†]	x_9	Anomaly, °C
Temperature index class	x_{10}	0: <average
		1: >average

[*] See Materials and methods, annual indices.

[†] Calculated using measurements at several stations off southern Iceland (Fig. 1) during January through June each year (see Materials and methods).

considered identifiable at ~15 days after spawning (Jakobsson et al. 1969), and we assume that the duration does not unduly compromise the analyses.

The independent variables that we examine include sample collection day-of-the-year (D), 10 presumed-relevant variables (x_1 to x_{10}; see Table 3), and various interaction terms. As there is variation in sampling intensity within and among locations and years (Table 1), it is necessary to combine some years and areas, though this is achieved in a systematic manner. For example, annual ISS data are aggregated according to low ($<250 \times 10^3$ tonnes (t)) and high ($\geq 250 \times 10^3$ t) estimates of SSB (Table 1; SSB class), where the divisional criterion approximates the average SSB for ISS (240×10^3 t) herring over the data series. Similarly, years are classified according to above- and below-average sea temperature (temperature-index class).

The logistic regression model is

$$\text{(8)} \qquad \operatorname{logit} y_i = \log_e(y_i(1-y_i)^{-1}) = \beta_0 + \beta_D D + \beta_1 x_1 + \ldots + \beta_n x_n$$

where i denotes individual fish, β represents the model constants and those associated with each variable ($x_1, \ldots, x_n$, etc.), and the reference model is the spawning characteristic (y_i) as a function of day-of-the-year (D). Models that include n other variables (x_n) are compared with the reference model using a decrease in deviance X^2 test (Ramsey and Schafer 1997) to determine the best model. Thus, the probability that a fish is spawning or has spawned ($y = 1$) is estimated as

$$\text{(9)} \qquad P(y=1) = \exp(\beta_0 + \beta_D D + \beta_1 x_1 + \ldots + \beta_n x_n) \times (1 + \exp(\beta_0 + \beta_D D + \beta_1 x_1 + \ldots + \beta_n x_n))^{-1}$$

A diagnostic procedure is applied to the best model using a deviance goodness-of-fit test (Neter et al. 1996). Inappropriate (poorly fitting) models are omitted here. To estimate the day-of-the-year when 50% spawning is achieved, $P(y = 0.5)$, the model becomes

$$\text{(10)} \qquad D = -(\beta_0 + \beta_1 x_1 + \ldots + \beta_n x_n)\beta_D^{-1}$$

where the confidence interval (CI) for D is defined using the standard error of the mean (SE) and the Z statistic with a standard normal distribution and confidence coefficient α, as

$$\text{(11)} \qquad \mathrm{CI}(y_i) = y_i \pm Z_{\alpha/2}(\mathrm{SE}(\beta_0)^2 + \mathrm{SE}(\beta_D)^2 D + \mathrm{SE}(\beta_1)^2 x_1 + \ldots + \mathrm{SE}(\beta_n)^2 x_n)$$

Results

Ovary weight

Median length-specific OW ordered across 5-day sequential intervals aggregated over all years shows a similar pattern for all length classes between 27 and 34 cm (Fig. 3). It is apparent that a marked decrease in $\widetilde{\mathrm{OW}}$ occurs around day 200, a change that we interpret as indicating spawning time. A comparison of the $\widetilde{\mathrm{OW}}$ estimates among length classes (Fig. 4) is consistent with the above interpretation for spawning time, although the largest herring (34 cm) display a secondary and sharp increase and decrease in $\widetilde{\mathrm{OW}}$ near day 210. This latter observation may be anomalous due to the influence of 12 prespawning herring in a total of 22 fish collected on the same day in 1967 in area 1. The discontinuity analyses (Fig. 5) of the $\widetilde{\mathrm{OW}}$ series indicate differences of approximately ±5 to ±10 days in spawning time, and there is no indication that spawning time varies with length class ($p \approx 1$). Around day 200 and among the eight length classes, there was one major discontinuity ($p \leq 0.05$) in the 29, 32, 33, and 34 cm length classes, one marginal discontinuity ($0.05 < p <$

Fig. 3. Box-and-whisker plots (median, +; 1st and 3rd quartile, box; non-outlier minimum and maximum, whiskers; extreme outliers beyond 1.5 interquartile range, ×) of Icelandic summer-spawning herring median ovary weight ($\widetilde{OW}$; g) at 5 day-of-the-year intervals aggregated over the period 1953 through 2000 among eight different length classes (27–34 cm) at maturity stages 3 (mature) through 7 (recently spawned).

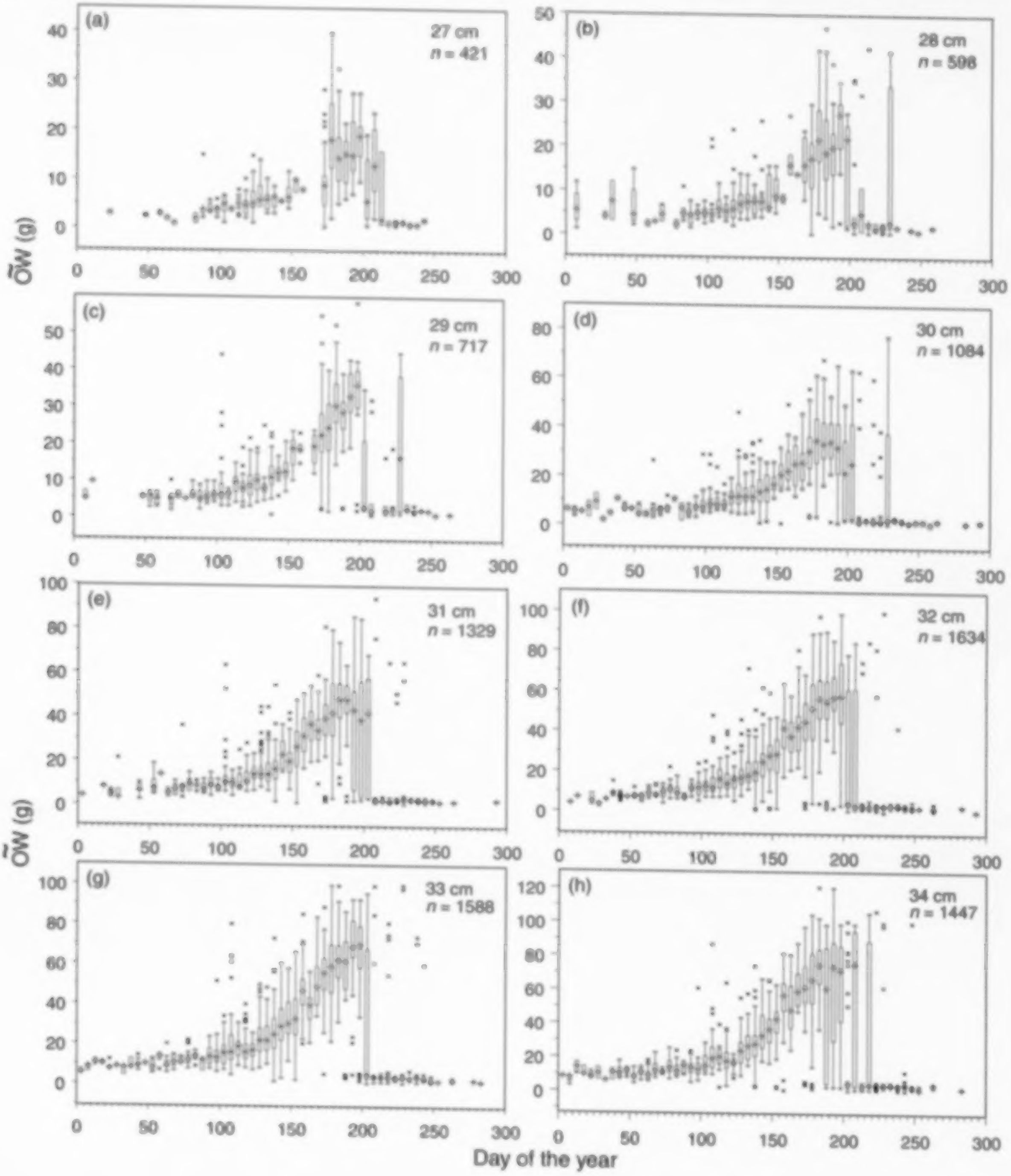

Fig. 4. Time series illustrating variation in Icelandic summer-spawning herring median ovary weight ($\widetilde{OW}$, g) at 5 day-of-the-year intervals aggregated over the period 1953 through 2000 among eight different length classes (27–34 cm) at maturity stages 3 (mature) through 7 (recently spawned).

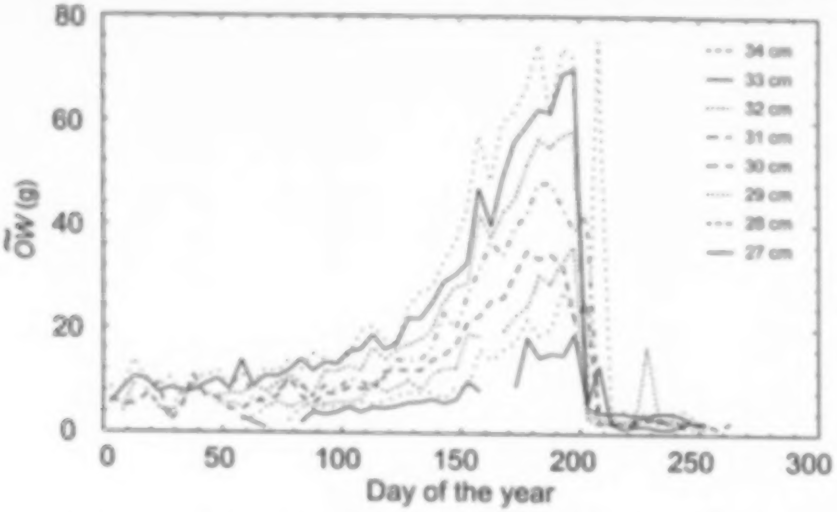

Fig. 5. Time series of discontinuities in median ovary weight ($\Delta\widetilde{OW}$ (g), ○) for Icelandic summer-spawning herring at 5 day-of-the-year intervals aggregated over the period 1953 through 2000 among eight different length classes (27–34 cm) at maturity stages 3 (mature) through 7 (recently spawned). Significant discontinuities: **, $p \le 0.05$; *, $0.05 < p < 0.1$.

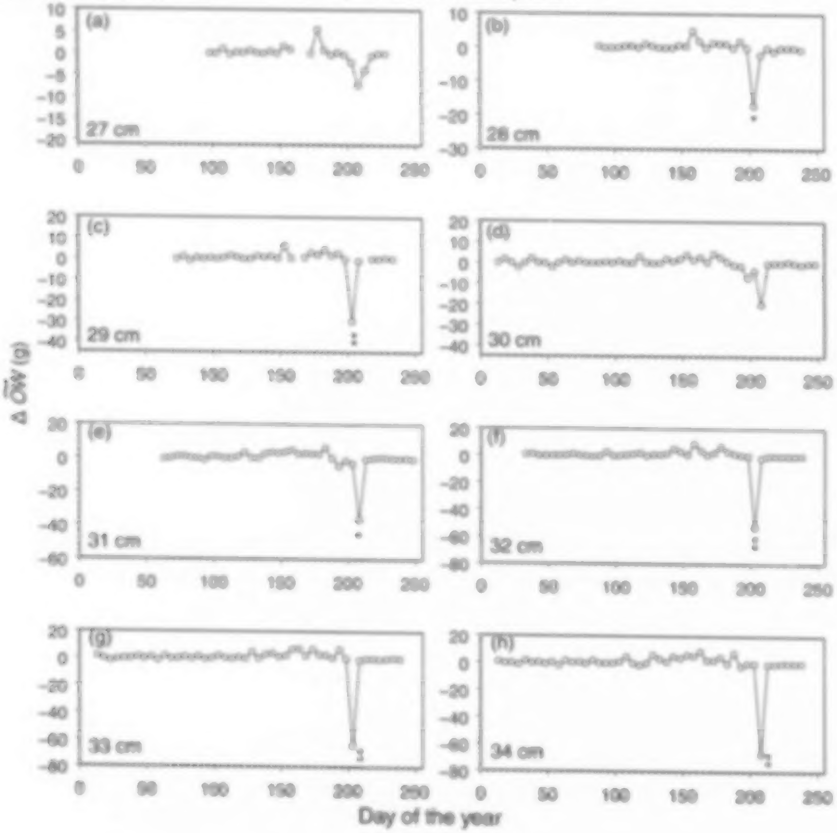

Fig. 6. Correlation matrix and the correlation coefficients ($p < 0.05$ in all cases) of median relative ovary weight ($\widetilde{RG}$, g·cm^{-1}) among the 28–33 cm length classes of summer-spawning Icelandic herring at 5 day-of-the-year intervals aggregated over the period 1953 through 2000 at maturity stages 3 (mature) through 7 (recently spawned).

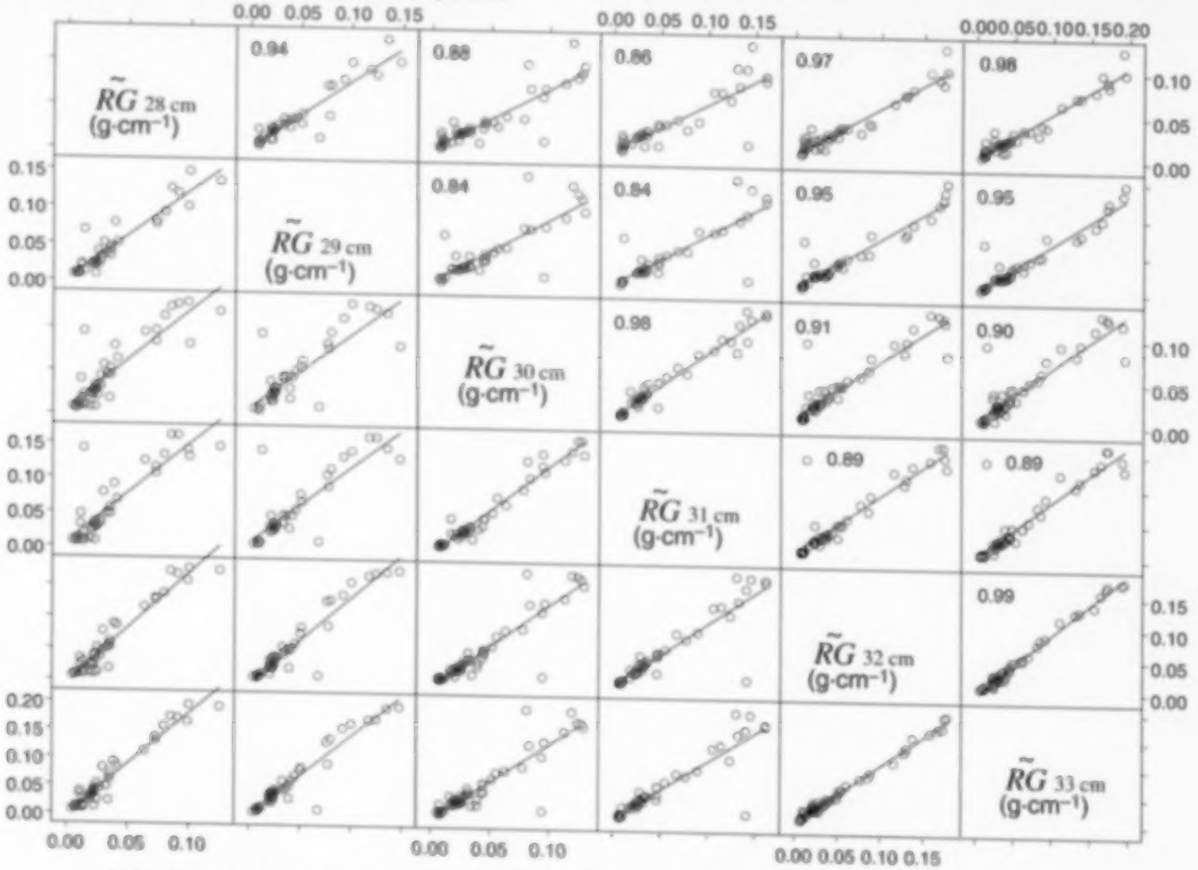

Table 4. Day-of-the-year (5-day interval combined over 1953 through 2000) serial cross-correlation estimates between median relative ovary weight ($\widetilde{RG}$, g·cm^{-1}) and median ovary weight ($\widetilde{OW}$, g) among the 27 through 34 cm length classes of female Icelandic summer-spawning herring at maturity stages 3 through 7, with number of observations (*n*, at all lags) in each length class and the lag-specific correlation coefficients.

$\widetilde{RG}$	$\widetilde{OW}_{27cm}$	$\widetilde{OW}_{28cm}$	$\widetilde{OW}_{29cm}$	$\widetilde{OW}_{30cm}$	$\widetilde{OW}_{31cm}$	$\widetilde{OW}_{32cm}$	$\widetilde{OW}_{33cm}$	$\widetilde{OW}_{34cm}$
n	16	41	42	53	43	50	51	51
lag −2	0.426	0.602	0.596	0.769	0.686	0.737	0.713	0.661
lag −1	**0.838**	0.813	0.769	0.886	0.815	0.869	0.854	0.783
lag 0	**0.837**	**0.963**	**0.946**	0.928	0.911	**0.994**	**0.990**	**0.897**
lag +1	0.547	0.825	0.842	**0.949**	**0.968**	0.886	0.883	0.793
lag +2	0.409	0.772	0.711	0.832	0.841	0.764	0.766	0.856

Note: Positive lag indicates that $\widetilde{RG}$ is leading $\widetilde{OW}$, and vice versa for negative lags. The largest coefficient is in bold type.

0.1) in the 28 and 31 cm length classes, and one questionable discontinuity in the 27 and 30 cm length classes.

All length-specific estimates of the median RG estimates at 5-day intervals for the six length classes (28–33 cm, inclusive) were strongly correlated: coefficients ranging between $r = 0.88$ and $r = 0.99$ (Fig. 6). From this, we infer that the $\widetilde{RG}$ series among length classes is similar to that observed for $\widetilde{OW}$ among length classes (see Figs. 3 and 4) and together they indicate synchronous increases beginning at around day 90, the apparent onset of maturation. The 5-day median estimates of RG indicate that spawning is most prevalent around day 200 (Fig. 7*a*), and this is consistent with the discontinuity analyses; i.e., $\Delta\widetilde{RG}$ (Fig. 7*b*). The serial cross-correlation between $\widetilde{OW}$ and $\widetilde{RG}$ for the different length classes also indicates that spawning time is consistent among length classes (Table 4) with the highest correlation

Fig. 7. (*a*) Box-and-whisker plot (median, +; 1st and 3rd quartiles, box; non-outlier minimum and maximum, whiskers; extreme outliers beyond 1.5 interquartile range, ×) of median relative ovary weight ($\widetilde{RG}$, g·cm^{-3}). (*b*) Time series of discontinuities in relative median ovary weight ($\Delta\widetilde{RG}$, ○) of Icelandic summer-spawning herring at 5 day-of-the-year intervals aggregated over the period 1953 through 2000 among all length classes (24–40 cm) at maturity stages 3 (mature) through 7 (recently spawned), where n = 10 182. Significant discontinuities: **, $p \leq 0.05$; *, $0.05 < p < 0.1$.

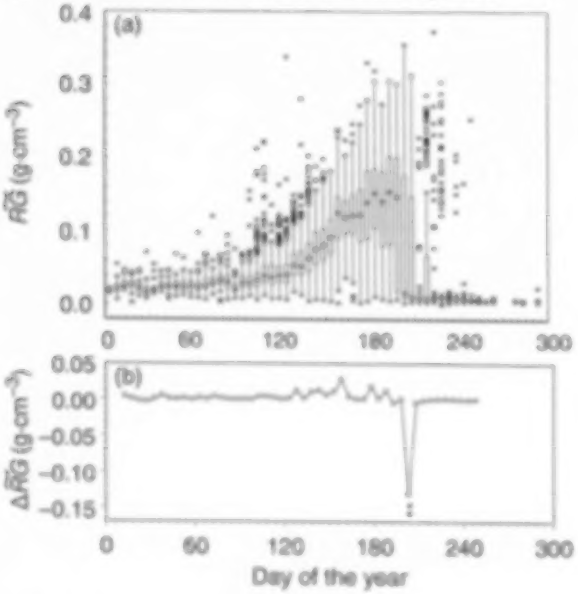

at lag 0 in all cases except for the 30 and 31 cm length classes (lag +1; i.e., $\widetilde{OW}$ 5 days later relative to $\widetilde{RG}$).

The 5-day-interval average mesenteric fat index ($\overline{MF}$) shows a clear seasonal cycle (Fig. 8*a*). The index reaches a minimum near day 190 (±10 days), consistent with the spawning time estimates described above. The $\overline{MF}$ index subsequently increases rapidly over a 3-month period to reach a maximum near day 280, presumably as a result of postspawning feeding. The index then decreases slowly over ~4 months through early winter, and subsequently, the decay accelerates over ~5 months during late winter and through to the early spring prespawning season. The $\widetilde{RG}$ and $\overline{MF}$ series are coupled as shown through a cross-correlation analysis with a maximum r = 0.76 (n = 53) at lag 0 and $\overline{MF}$ decays exponentially with increasing $\widetilde{RG}$ (Fig. 8*b*).

Fig. 8. (*a*) Illustration of time series of average (±2 standard error, SE) mesenteric fat index ($\overline{MF}$, 0 to 3; qualitative visual estimate) for Icelandic summer-spawning female herring at 5 day-of-the-year intervals aggregated over the period 1962 through 2000 among spawners (28–35 cm length) at maturity stages 3 (mature) through 8 (recovering), where n = 54 690 (n > 100 for each interval except between days-of-the-year 58 and 113). (*b*) Scattergram of observations (○) and least square regression (solid line) with 95% confidence interval around the regression (dotted lines) illustrating the decrease in the $\overline{MF}$ as a function of median relative ovary weight ($\widetilde{RG}$, g·cm^{-3}) at 5 day-of-the-year intervals aggregated over the period 1953 through 2000 among all length classes (24–40 cm) at maturity stages 3 (mature) through 7 (recently spawned), where $\overline{MF} = 1.76 \times 10^{-1}\,\widetilde{RG}^{-0.485}$; r^2 = 0.608, n = 57, $p < 0.0001$.

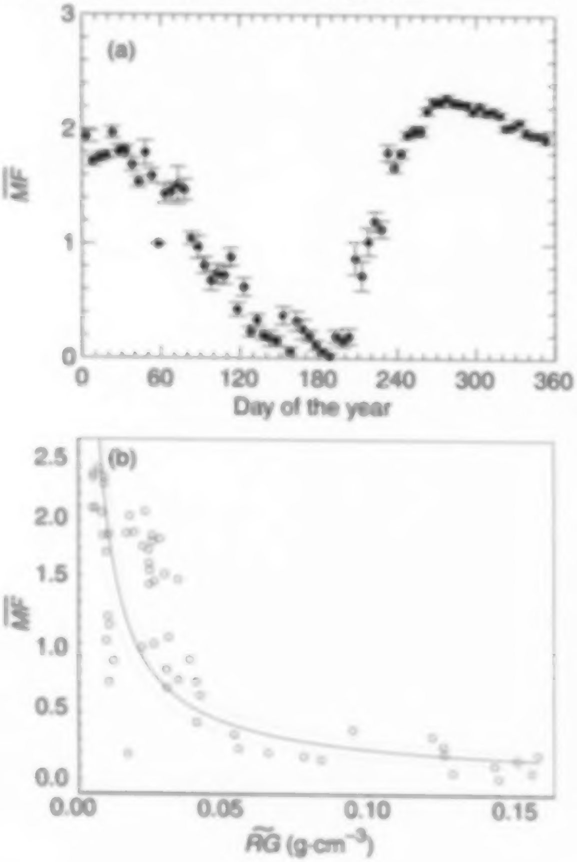

The potential influence of temperature on $\widetilde{RG}$, and thus spawning time, independent of length, is illustrated through a comparison of the relatively warm (1954 to 1967) and relatively cold (1979 to 1995) periods off southern and southwestern Iceland (Fig. 9). It appears that spawning is advanced by approximately 10 days during the warmer period, though close examination indicates that relatively few years were largely responsible for the observed difference. For example, during the warm period, the low $\widetilde{RG}$ values at days 173, 178, and 193 and the high $\widetilde{RG}$ values at day 198 resulted from a dominance of the 1967 samples, whereas the low $\widetilde{RG}$ at day 188 can be explained by few individuals (n = 5). During the cold period, the retardation in spawning was largely an effect of high median RG values in 1991, 1993, and 1994 and low $\widetilde{RG}$ values in 1980 and 1984 (i.e., earlier spawning near day 198). A serial (day-of-the-year) cross-correlation analysis of median RG in cold years with warm years showed the highest correlation coefficient at lag −2 (r = 0.78, n = 49), indicating that spawning was delayed by approximately 10 days during the cold period, as illustrated above.

Changes in median length-specific whole-body weight

Fig. 9. Box-and-whisker plots (median, +; 1st and 3rd quartiles, box; non-outlier minimum and maximum, whiskers; extreme outliers beyond 1.5 interquartile range, ×) of Icelandic summer-spawning herring median relative ovary weight ($\widetilde{RG}$, g·cm^{-3}) variation at 5 day-of-the-year intervals aggregated among all length classes (24–40 cm) at maturity stages 3 (mature) through 7 (recently spawned) over (*a*) a period of warm years off southern and southwestern Iceland (1954 through 1967; $n = 3032$) and (*b*) a period of cold years (1979 through 1995; $n = 2954$).

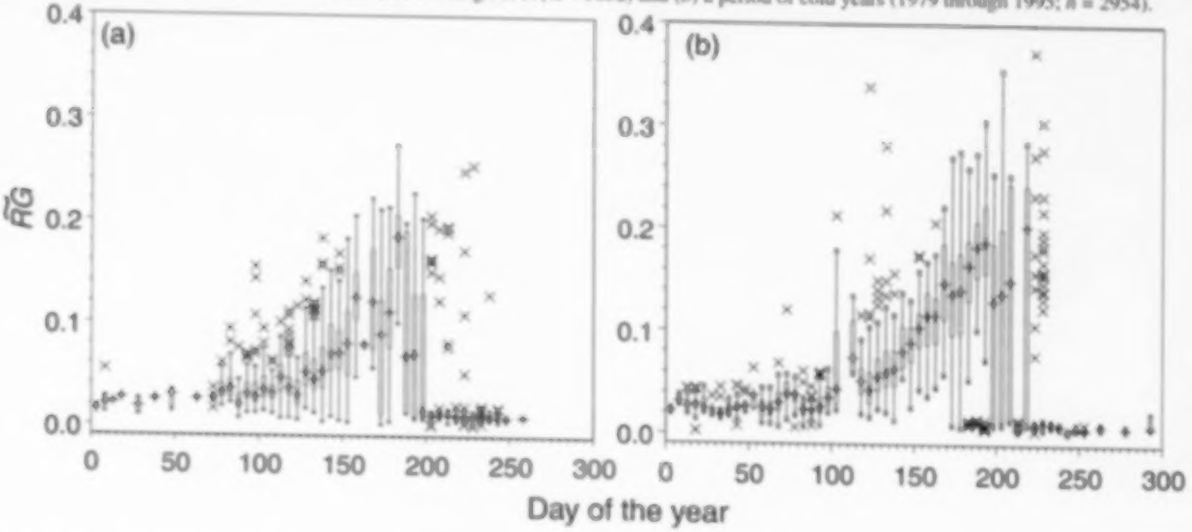

Fig. 10. Relations between median ovary weight ($\widetilde{OW}$, g) and median whole-body weight ($\widetilde{W}$, g) for Icelandic summer-spawning herring at 5 day-of-the-year intervals aggregated over the period 1953 through 2000 for four different length classes: (*a*) 29 cm, (*b*) 30 cm, (*c*) 31 cm, and (*d*) 32 cm at maturity stages 3 (mature) through 7 (recently spawned).

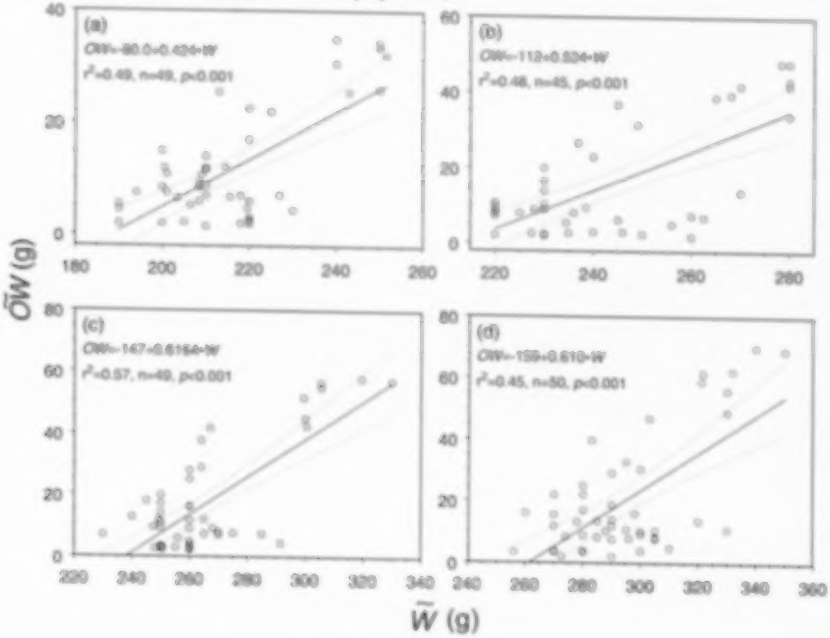

($\widetilde{W}$) with day-of-the-year are related to the changes in length-specific $\widetilde{OW}$ during the prespawning and spawning periods (Fig. 10) and all length classes reach a maximum near day 200, although all relations are insignificant ($p > 0.05$) when the data near spawning time (days-of-the-year 165 through 210) are excluded. The serial cross-correlation between $\widetilde{RG}$ and $\widetilde{W}$ among different length classes indicates that $\widetilde{W}$ generally leads $\widetilde{RG}$ by 5–10 days (Table 5), a lag likely reflecting the duration of physiological processes involved in gonad growth. Overall, it appears that spawning

Table 5. Day-of-the-year (5-day interval combined over 1953 through 2000) serial cross-correlation estimates between relative median ovary weight ($\widetilde{RG}$, g·cm^{-1}) and median whole-body weight ($\widetilde{W}$, g) among the 27 to 34 cm length classes of female Icelandic summer-spawning herring at maturity stages 3 through 7.

$\widetilde{RG}$	$\widetilde{W}_{27cm}$	$\widetilde{W}_{28cm}$	$\widetilde{W}_{29cm}$	$\widetilde{W}_{30cm}$	$\widetilde{W}_{31cm}$	$\widetilde{W}_{32cm}$	$\widetilde{W}_{33cm}$	$\widetilde{W}_{34cm}$
n	16	32	19	51	49	51	51	51
lag −2	0.104	0.289	0.230	0.426	0.340	0.359	0.325	0.357
lag −1	**0.630**	0.428	0.331	0.578	0.478	0.560	0.491	0.451
lag 0	0.524	0.555	**0.438**	0.633	0.550	0.730	0.625	0.512
lag +1	0.432	0.577	0.406	**0.686**	0.636	**0.775**	0.643	0.490
lag +2	0.314	**0.583**	0.352	0.575	**0.650**	0.748	**0.658**	**0.579**

Note: The table shows the number of observations (*n*, at all lags) in each length class and the lag-specific correlation coefficients, with the highest coefficient in bold type. Positive lag indicates $\widetilde{RG}$ is leading $\widetilde{W}$, and vice versa for negative lags.

Fig. 11. Time series of percent Icelandic summer-spawning herring females (*a*) at maturity stage 6 (spawning, *n* = 602) among all females at maturity stages 3 through 7 (*n* = 9919); and (*b*) at stage 6 or stage 7 (spawning and recently spawned, *n* = 2053) among all females at maturity stages 3 through 8 (*n* = 68 472) at 5 day-of-the-year intervals aggregated over the period 1953 through 2000.

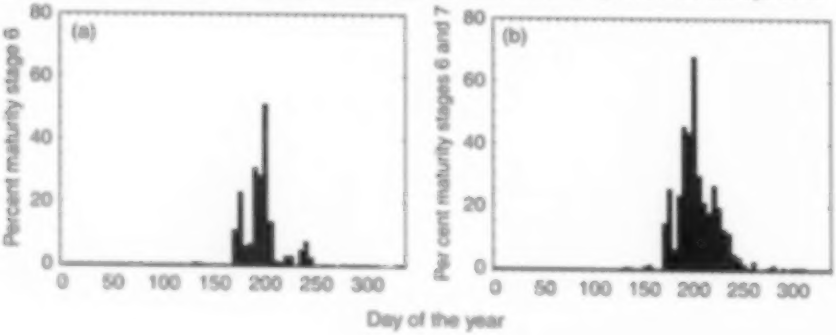

Fig. 12. Logistic regression estimates of the probability in time (day-of-the-year) that an Icelandic summer-spawning herring will be spawning or will have spawned under high (>250 × 10^3 tonnes) or low (<250 × 10^3 tonnes) spawning stock biomass (SSB) conditions and whether a recruit (<30 cm) or repeat (≥30 cm) spawner. Fifty percent of females are most likely to be spawning or to have spawned at the date at which the dotted horizontal line (0.5) intersects the probability curves.

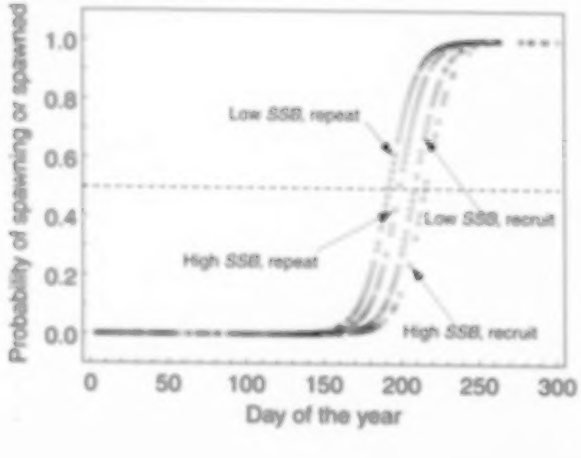

time can also be inferred from temporal changes in $\widetilde{W}$ that correspond to changes in $\widetilde{OW}$ (cf. Fig. 3).

Logistic regression on spawning stage

The proportional (percentage) distribution of the qualitative maturity indices for ISS females at stages 6 (spawning) and 7 (recently spawned), and aggregated over all length classes for the period 1953 to 2000, indicate that the majority of spawning occurs around day 200, though there is evidence that spawning can begin as early as day 170 and may not be entirely complete until as late as day 250 (Fig. 11). The logistic regression analyses show that depending on conditions (see below), 50% of the herring will be spawning or will have spawned near day-of-the-year 200 (Fig. 12). According to deviance goodness of fit ($X^2_{0.95,\,11\,334} > 11\,583$), the best-fitting logistic regression model describing ISS spawning probability includes day-of-the-year, SSB class (high or low), and spawning experience (Table 6). Using a 50% spawning or spawned criterion ($y_i = 0.5$), the estimated spawning day for recruit spawners is retarded by 17 days relative to repeat spawners and the 95% confidence intervals for the estimates do not overlap (Table 6; Fig. 12). Spawning is retarded when SSB is large relative to small, and though the uncertainties (95% CI) in the estimates do overlap (Table 6), the diagnostic deviance goodness-of-fit test (see Materials and methods) does not indicate an inap-

Table 6. (*a*) Parameters derived from logistic regression analyses (intercept, day-of-the-year, SSB class, and spawning experience) used to estimate spawning day (±95% confidence interval, CI) where $y = 0$ indicates maturity stages 3 to 5 inclusive and $y = 1$ indicates maturity stages 6 and 7 (see eq. 8) for Icelandic summer-spawning females aggregated over the years 1953 through 2000 where the null deviance of the model equals 10 714 on 11 337 *df*, giving pseudo-$r^2 = 0.643$ and (*b*) estimated spawning day (±95% CI) based on $y = 0.5$ (50% spawning or spawned; see eq. 10).

(*a*) Parameters derived from logistic regression analyses.

Variable	β	SE	95% CI(±)	Deviance	Total deviance (%)
Intercept	-2.278×10^{1}	6.081×10^{-1}	1.192		
Day-of-year	1.123×10^{-1}	2.969×10^{-3}	5.938×10^{-3}	6264	58.4
SSB class	-7.553×10^{-1}	8.682×10^{-2}	1.702×10^{-1}	388	3.6
Spawning experience	1.874	1.285×10^{-1}	2.518×10^{-1}	241	2.3
Total				6893	64.3

(*b*) Estimated spawning day.

SSB class	Spawning experience	Spawning day	Lower 95% CI	Upper 95% CI
1	1	192	185	199
1	0	209	202	215
0	0	202	195	208
0	1	185	179	192

Note: Variables are defined in Table 3.

Fig. 13. Time series of average Fulton's body condition anomaly ($K_{anomaly}$ ± 2 standard error, SE) for the period 1953 through 2000 for prespawning (February through June only) Icelandic summer-spawning female herring at lengths of 28 to 35 cm and maturity stages 3 (mature) through 5 (fully mature). No data were available in 1960, 1965, 1986, or 1995. The dotted horizontal line separates negative and positive anomalies.

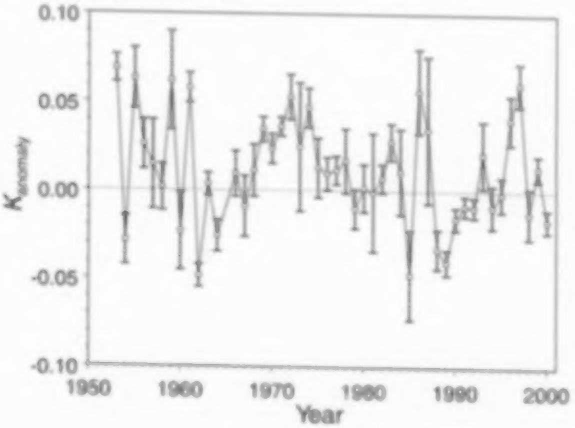

propriate model. None of total length, prespawning condition (Fulton's *K*; Fig. 13), spawning location, SSB, skew in the spawning-stock age distribution, or temperature (index or index class) provided significant contribution to an appropriate model.

Discussion

Spawning time in Icelandic summer-spawning herring appears relatively "fixed" near day-of-the-year 200 and contracted (±15 days). All of the above results related to measures and indices of spawning time are consistent with the interpretation that the majority of spawning in the ISS herring across nearly 50 years, eight length classes, and spawning grounds occurs over a relatively invariant 30-day period defined by day-of-the-year. The logistic regression results and the temporal variation in $\widetilde{OW}$ and $\widetilde{RG}$ are each consistent in showing that maximum spawning occurs around day-of-the-year 200 (±15 days). Seasonal variation in mesenteric fat content provides clear evidence that this interpretation is physiologically consistent. These results are surprisingly consistent with much earlier and very different observations made by Einarsson (1956), who used the occurrence of newly hatched larvae to estimate spawning time from early July (day 185) to mid-August (day 230).

Although spawning time appears relatively fixed in ISS herring overall, we provide new evidence of size dependency wherein recruit spawners (females <30 cm) appear to delay spawning by ~17 days relative to the repeat spawners (≥30 cm). We also provide new evidence of stock biomass dependency wherein subtle shifts in spawning time appear to be a function of SSB. Thus, there is some small but sufficient evidence to reject the null hypothesis that spawning time in the ISS stock is constant, though it is demonstrably limited to small temporally contracted shifts that are dependent on stock size structure and (or) SSB.

The logistic regression analyses that rely on the well-distinguished maturity stages 6 and 7 (at least relative to stages 3 through 5) appears sufficient in explaining spawning time variation that results from variation in spawning experience (recruit or repeat spawner) and SSB, despite the assertion that qualitative maturity indices are too subjective for such purpose (Ware and Tanasichuk 1989).

The analyses of ovary weight variation and the regression models showed some differences regarding size-specific spawning time in ISS herring. In the former, spawning time appears more or less fixed around days-of-the-year 200 through 210, where the range in timing appears to be retarded spawning due to smaller recruit spawners and advanced spawning due larger repeat spawners. Generally, it can be concluded that ISS recruit spawners spawn later than repeat spawners. It is typical for the smaller recruit spawners to spawn later in herring (e.g., Lambert (1987) and references therein; Slotte et al. 2000; Óskarsson et al. 2002) and in cod (e.g., Marteinsdottir and Petursdottir 1995; Bleil and Oeberst 1997), although the opposite is also observed in cod (Hutchings and Myers 1994) and American plaice (*Hippoglossoides platessoides*; Morgan 2003). Moreover, our results reflect the Slotte et al. (2000) results for Norwegian spring-spawning herring, using very different methods in which spawning time of repeat spawners is not a function of size or age, which had been postulated earlier by Lambert (1987) for the same stock. Delayed spawning among recruit spawners may be due to a delayed onset of maturation rather than protracted ovary development (Slotte et al. 2000), although the inverse has been observed (Ware and Tanasichuk 1989). Regardless of explanation, what is important in the context of this study is the question of what might be the effect of the observed spawning time variation on eventual recruitment? The positive influences of protracted spawning on recruitment that result from a large diversity in the size and age composition of a stock (e.g., Marteinsdottir and Thorarinsson 1998) were summarized above. Thus, a similar influence may be expected among ISS herring as some of our results indicate spawning time is, in part, size dependent. Absolute size composition in the stock may therefore influence recruitment of ISS herring through variation in spawning time over and above the variation attributable to relative fecundity (Óskarsson and Taggart 2006) and egg size (Óskarsson 2005).

The literature implies that the life history among different herring stocks in the North Atlantic varies considerably in terms of spawning time and migration pattern. Spawning occurs over a 30-day period or less among ISS herring (above), nearer 50 days among Norwegian spring spawners (Lambert 1987), and 90 days or more among Scotia–Fundy summer–autumn spawners (Óskarsson 2005). For the former two stocks, there is an indication of at least two spawning waves, whereas many disorganized waves are typically observed for the latter (Óskarsson 2005) when analysed in a manner similar to that described here. In all the three cases, the temporal distribution of spawning within the "fixed" spawning period can influence the recruitment success if linked to variation in the larval food production cycle (Cushing 1969), the basis of the match–mismatch hypothesis (Cushing 1975). However, spatial distribution can additionally influence recruitment indirectly. Spawning among ISS herring (Óskarsson 2005) and Norwegian spring-spawning herring (Slotte 1999) occurs upstream relative to the nursery grounds. In contrast, it is suggested that Scotia–Fundy herring larvae are retained near the spawning grounds (e.g., Iles and Sinclair 1982). Thus, the spatial and temporal distribution of spawning works to distribute the larvae spatially and temporally in relation to productive (larval food) regions. Accordingly, the "adaptation" to ensure a "match" between emergent larvae and their food resources can be either primarily dependent on spatial variation (e.g., ISS herring and Norwegian spring-spawning herring) as originally inferred by Hjort (1914), or temporal variation (e.g., Scotia–Fundy summer–autumn spawning herring) in spawning as inferred by Cushing (1969).

Spawning stock biomass had a small and marginally significant effect on spawning time in ISS herring. Similar findings of stock-dependent (SSB) effects on maturation have been observed for Baltic cod in which spawning time was found to be influenced by temperature, SSB, and food availability (Wieland et al. 2000). We postulate that the SSB effect on ISS herring spawning may be related to feeding conditions during the maturation process, when in high SSB years, more individuals would feed on the same (average) amount of food. This is reasonable as there is little difference in average zooplankton (dry weight) biomass ($g \cdot m^{-2}$, 0–50 m depth) off southern Iceland (Selvogsbanki) during years of low SSB and during years of high SSB over the period 1971 to 2000 (Marine Research Institute 2001). This implies that feeding success under high SSB may be reduced and lead to reduce ovary growth and thereby delayed spawning. It is well documented that feeding conditions and food availability during the prespawning season can affect the spawning time in herring (e.g., Hay et al. 1988; Rajasilta 1992). However, body condition ($K_{anomaly}$) did not contribute to explained variation in spawning time, as noted above, and has little influence on fecundity variation (Óskarsson and Taggart 2006). The appropriateness of using the $K_{anomaly}$ among prespawning herring to represent energy status has been questioned by Óskarsson (2008) due to hydration of both somatic and reproductive tissues during this period and due to the variability in stomach content.

The relatively low variation in the temperature anomaly off southern and southwestern Iceland, at least in comparison with other areas in Icelandic waters (Marine Research Institute 2001), appears to affect the spawning time of ISS herring as illustrated by temporal variation in $\widetilde{RG}$ and serial cross-correlation (warm years advancing spawning by about 10 days). However, the difference between warm years (1954 to 1967) and cold years (1979 to 1994) may be equally attributable to differences in SSB, as indicated by the logistic regression models. During the warm period, the average SSB was 198×10^3 t relative to 323×10^3 t during the cold period when spawning time was delayed. Furthermore, SSB consistently increased during the cold period. Given these facts, in addition to the results of the logistic regression in which SSB was found to contribute to the annual variation in spawning time but sea temperature did not, it is reasonable to conclude that SSB is more influential on spawning time of ISS herring than is temperature.

Warmer ocean temperatures have been documented to influence the spawning time of herring (Lambert (1987) and references therein; Ware and Tanasichuk 1989) and other species (e.g., haddock (*Melanogrammus aeglefinus*; Page and Frank 1989) and capelin (*Mallotus villosus*; Carscadden et al. 1997)) where it serves to advance spawning. In others cases, warmer temperature appears to retard spawning (e.g., English sole (*Parophrys vetulus*; Kruse and Tyler 1983); Atlantic cod (Hutchings and Myers 1994)). For ISS herring, there is no substantive evidence that the sea temperature influences the annual variation in spawning time when based on a typical temperature index such as we developed. Although a preferable measure such as the integral of the thermal environment experienced by the fish (e.g., degree-day; Neuheimer and Taggart 2007) is not easily accessible, it does raises the issue of how appropriate are such temperature indices. The existing, but limited information on the distribution of the ISS herring during the period of ovary growth (e.g., Jakobsson et al. 1993) suggest that it occurs within the spatial domain that we used to calculate the index; it is also the area of early phytoplankton blooms (e.g., Thórdardóttir 1986) and high productivity (e.g., AstÞórsson et al. 1983). However, the seasonal distributions and migration patterns of ISS herring exhibit periodic variation among years (e.g., Jakobsson 1980; Jakobsson and Stefánsson 1999), leading to the concern that such temperature indices might not adequately describe the thermal conditions experienced by a stock among years.

The relatively new insights provided by monitoring the variation in mesenteric fat of ISS herring are not only consistent with the analyses of the spawning time where the average MF was at minimum around day 190, they are generally consistent with Norwegian spring-spawning herring (Slotte 1999), and together they provide general implications for herring biology. The exponential rate of decay in mesenteric fat content ($\widetilde{MF}$), as a function of $\widetilde{RG}$, and the seasonal cycle in $\overline{MF}$ suggest that the fat accumulated over and above the metabolic demand during the spring feeding period and prior to spawning is used for reproduction, consistent with no accumulation of fat during the spring feeding period in March and April. However, as the fat content of gonads is generally low (Kaitaranta and Ackman 1981; Tocher and Sargent 1984) and gonad growth is mainly supplied by the translocation of proteins (Iles 1984; Bradford 1993), the fat must be responsible primarily for sustaining metabolic requirements during the prespawning season. Postspawning feeding likely provides the energy requirements needed for the overwintering period and somatic growth (Óskarsson 2008), whereas the fat remaining in the spring will presumably contribute to the pending spawning.

The herring data analysed here are derived from the commercial fleet (75%) and from research vessel surveys (25%). During the years 1953 to around 1970, most data were derived from the commercial fleet that was targeting herring during the prespawning period (Jakobsson 1980), whereas in the later years, the data were derived mainly from commercial bycatch and from research vessels. Could the results of the spawning time variation for the ISS herring be influenced by such sampling protocols that may bias the observations? The pattern of ISS herring $\widetilde{OW}$ variation is very well behaved (systematic and progressive) in all circumstances, even when aggregated over years with data mainly derived from a targeted fishery (1954 through 1967) and over years derived from bycatch and research surveys (1979 through 1995). Although the occurrence of maturity stage 6 relative to stages 3 through 7 illustrates the possibility of spawning waves, closer examination of the various maxima in the distribution can be traced to particular years. For example, the maximum around days 238 to 243 is a result of four repeat spawners in 1976 and five in 1977. It does indicate that some spawning was delayed in 1976 and 1977 but only to a small degree because postspawning fish were numerous around these days (33 fishes at stage 7 and 1600 fishes at stage 8). Further, examination of the data for the two years cited above showed that fish at maturity stage 5 (fully mature) around day 180 were as numerous as in other years. The explanation for this apparent delay in spawning in these two years is unknown, though there is no clear indication that sampling protocol is involved.

Several different methods can be used to estimate spawning time, and each is related to the purpose of the investigation. Spawning time can be estimated using abundance estimates and (or) developmental stages of eggs and (or) larvae (e.g., Einarsson 1956; Page and Frank 1989; Warlen 1994), but this excludes the ability to easily address phenotypic variation among the spawners. In some studies, oocyte size and growth and (or) development are used to estimate the spawning time (e.g., Juo and Musick 1991; Fargo and Tyler 1994; Óskarsson et al. 2002). Others focus on maturation stage (e.g., Hutchings and Myers 1994; Bleil and Oeberst 1997). Ovary growth rate or the ratio of ovary weight to body weight (the gonado-somatic index, GSI) can also be used (e.g., Ware and Tanasichuk 1989; Rijnsdorp 1991; Slotte et al. 2000). Generally, such studies rely on any one of the above methods, but typically only one. Here, we have used several methods and argue that two or more methods have the advantage of (*i*) overcoming data limitations, (*ii*) using different data sources, (*iii*) allowing for comparisons, (*iv*) validating assumptions and (or) inferences, and (*v*) determining consistency, including consistency with metabolic expectations. For ISS herring, the various series derived from monitoring maturity stage, ovary weight, and relative ovary weight not only illustrated spawning time variation, but also inferred consistency among years and size classes and one relatively invariant and contracted spawning time. The use of the logistic regression provided additional and consistent evidence, as well as new insights related to stock size structure and biomass.

Acknowledgements

We thank J. Jakobsson for vital support, L. Taylor and S.A. Malmberg at the Marine Research Institute in Iceland (MRI) for their assistance and influential discussions, R. Stephenson, K. Frank, T. Marshall, G. Marteinsdottir, and three anonymous referees for critical appraisals, and MRI for essential support. G.J.O. was supported by the Fishery Ministry of Iceland, the Icelandic Research Fund for Graduate Students, a NATO Science Fellowship, and a Natural Sciences and Engineering Research Council of Canada grant to C.T.T.

References

Anonymous. 1962. Recommendations adopted by the Herring Committee. Rapp. P.-V. Réun. Cons. Int. Explor. Mer. **1**: 1–73. [Append.]

AstÞórsson, Ó.S., Hallgrímsson, I., and Jónsson, G.S. 1983. Variations in zooplankton densities in Icelandic waters in spring during the years 1961–1982. Rit Fiskideildar, **7**: 71–113.

Bagenal, T.B. 1971. The interrelation of the size of fish eggs, the date of spawning and the production cycle. J. Fish Biol. **3**(2): 207–219. doi:10.1111/j.1095-8649.1971.tb03665.x.

Bleil, M., and Oeberst, R. 1997. The timing of the reproduction of cod (*Gadus morhua morhua*) in the Western Baltic and adjacent areas. ICES CM 1997/CC:2.

Bradford, R.G. 1993. Differential utilization of storage lipids and storage proteins by Northwest Atlantic herring (*Clupea harengus harengus*). J. Fish Biol. **43**(6): 811–824. doi:10.1111/j.1095-8649.1993.tb01157.x.

Carscadden, J., Nakashima, B.S., and Frank, K.T. 1997. Effects of fish length and temperature on the timing of peak spawning in capelin (*Mallotus villosus*). Can. J. Fish. Aquat. Sci. **54**(4): 781–787. doi:10.1139/cjfas-54-4-781.

Cushing, D.H. 1969. The regularity of the spawning season of some fishes. J. Cons. Int. Explor. Mer, **33**: 81–92.

Cushing, D.H. 1975. Marine ecology and fisheries. Cambridge University Press, London, UK.

Einarsson, H. 1956. Frequency and distribution of post-larval stages of herring (*Clupea harengus* L.) in Icelandic waters. Rit Fiskideildar, **2**: 1–33.

Fargo, J., and Tyler, A.V. 1994. Oocyte maturation in Hecate Strait English sole (*Pleuronectes vetulus*). Fish. Bull. (Washington, D.C.), **92**: 189–197.

Fridriksson, Á., and Timmermann, G. 1950. Rannsóknir á hrygningarstöðvum vorgotssíldar vorið 1950. Rit Fiskideildar, **1**: 1–32.

Hay, D.E. 1990. Tidal influence on spawning time of Pacific herring (*Clupea harengus pallasi*). Can. J. Fish. Aquat. Sci. **47**: 2390–2401. doi:10.1139/f90-266.

Hay, D.E., Brett, J.R., Bilinski, E., Smith, D.T., Donaldson, E.M., Hunter, G.A., and Solmie, A.V. 1988. Experimental impoundments of prespawning Pacific herring (*Clupea harengus pallasi*): effects of feeding and density on maturation, growth, and proximate analysis. Can. J. Fish. Aquat. Sci. **45**(3): 388–398. doi:10.1139/f88-047.

Hjort, J. 1914. Fluctuations in the great fisheries of northern Europe viewed in the light of biological research. Rapp. P.-V. Reun. Cons. Perm. Int. Explor. Mer. **20**: 1–228.

Hutchings, J.A., and Myers, R.A. 1994. Timing of cod reproduction: interannual variability and the influence of temperature. Mar. Ecol. Prog. Ser. **108**: 21–31. doi:10.3354/meps108021.

Iles, T.D. 1984. Allocation of resources to gonad and soma in Atlantic herring *Clupea harengus* L. *In* Fish reproduction: strategies and tactics. *Edited by* G.W. Potts and R.J. Wootton. Academic Press, London, UK. pp. 331–347.

Iles, T.D., and Sinclair, M. 1982. Atlantic herring: stock discreteness and abundance. Science (Washington, D.C.), **215**(4533): 627–633. doi:10.1126/science.215.4533.627. PMID:17842372.

Jakobsson, J. 1980. Exploitation of the Icelandic spring- and summer-spawning herring in relation to fisheries management, 1947–1977. Rapp. P.-V. Reun. Cons. Int. Explor. Mer, **177**: 23–42.

Jakobsson, J., and Stefánsson, G. 1999. Management of summer-spawning herring off Iceland. ICES J. Mar. Sci. **56**(6): 827–833. doi:10.1006/jmsc.1999.0542.

Jakobsson, J., Vilhjálmsson, H., and Schopka, S.A. 1969. On the biology of the Icelandic herring stocks. Rit Fiskideildar, **4**: 1–16.

Jakobsson, J., Gudmundsdóttir, Á., and Stefánsson, G. 1993. Stock-related changes in biological parameters of the Icelandic summer-spawning herring. Fish. Oceanogr. **2**(3–4): 260–277. doi:10.1111/j.1365-2419.1993.tb00141.x.

Joo, J.G., and Musick, J.A. 1991. Reproductive biology of the bay anchovy in Chesapeake Bay. Trans. Am. Fish. Soc. **120**(6): 701–710. doi:10.1577/1548-8659(1991)120<0701:RBOTBA>2.3.CO;2.

Kaitaranta, J.K., and Ackman, R.G. 1981. Total lipids and lipid classes of fish roe. Comp. Biochem. Physiol. B Comp. Biochem. **69**: 725–729.

Kjesbu, O.S., and Holm, J.C. 1994. Oocyte recruitment in first-time spawning Atlantic cod (*Gadus morhua*) in relation to feeding regime. Can. J. Fish. Aquat. Sci. **51**(8): 1893–1898. doi:10.1139/f94-189.

Kruse, H.K., and Tyler, A.V. 1983. Simulation of temperature and upwelling effects on the English dole (*Parophrys vetulus*) spawning season. Can. J. Fish. Aquat. Sci. **40**(2): 230–237. doi:10.1139/f83-033.

Lambert, T.C. 1987. Duration and intensity of spawning in herring *Clupea harengus* as related to the age structure of the mature population. Mar. Ecol. Prog. Ser. **39**: 209–220. doi:10.3354/meps039209.

Legendre, L., and Legendre, P. 1998. Numerical ecology. Elsevier Science B.V., Amsterdam, the Netherlands.

Malmberg, S.A. 1980. Hydrographic conditions in Icelandic waters in May–June 1978. Ann. Biol. **35**: 55–62.

Marine Research Institute. 2001. Environmental conditions in Icelandic waters 2000. Marine Research Institute, Iceland, Fjölrit No. 83.

Marine Research Institute. 2002. State of marine stocks in Icelandic waters 2001/2002, prospects for the quota year 2002/2003. Marine Research Institute, Iceland, Fjölrit No. 88.

Marteinsdottir, G., and Björnsson, H. 1999. Time and duration of spawning of cod in Icelandic waters. ICES CM 1999/Y:34.

Marteinsdottir, G., and Petursdottir, G. 1995. Spatial and temporal variation in reproduction of Icelandic cod at Selvogsbanki and nearby coastal area. ICES CM 1995/G:15.

Marteinsdottir, G., and Thorarinsson, K. 1998. Improving the stock–recruitment relationship in Icelandic cod (*Gadus morhua*) by including age diversity of spawners. Can. J. Fish. Aquat. Sci. **55**(6): 1372–1377. doi:10.1139/cjfas-55-6-1372.

McPherson, A.A., Stephenson, R.L., and Taggart, C.T. 2003. Genetically different Atlantic herring *Clupea harengus* spawning waves. Mar. Ecol. Prog. Ser. **247**: 303–309. doi:10.3354/meps247303.

Morgan, M.J. 2003. Variation with age in the timing and duration of spawning in American plaice. J. Fish Biol. **62**(2): 464–473. doi:10.1046/j.1095-8649.2003.00042.x.

Neter, J., Kutner, M.H., Nachtsheim, C.J., and Wasserman, W. 1996. Applied linear statistical models. 4th ed. WCB/McGraw-Hill, Boston, Massachusetts.

Neuheimer, A.B., and Taggart, C.T. 2007. Growing degree-day and fish size-at-age: the overlooked metric. Can. J. Fish. Aquat. Sci. **64**(2): 375–385. doi:10.1139/F07-003.

Norberg, B., Bjornsson, B.T., and Haux, C. 1995. Photoperiod controls the timing of reproduction in Atlantic cod (*Gadus morhua*). *In* Proceedings of the 5th International Symposium on the Reproductive Physiology of Fish. *Edited by* F.W. Goetz and P. Thomas. The University of Texas at Austin, Texas, USA, Fish Symposium 95. pp. 167–169.

Óskarsson, G.J. 2005. Pre-spawning factors and recruitment variation in Atlantic herring (Clupeidae; *Clupea harengus* L.): a comparative approach. Ph.D. thesis, Oceanography Department, Dalhousie University, Halifax, N.S.

Óskarsson, G.J. 2006. A comparison of the Icelandic summer-spawning herring off the east and west coast during 1997 to 2003. Marine Research Institute Report No. 123. pp. 31–42.

Óskarsson, G.J. 2008. Variation in body condition, fat content and growth rate of Icelandic summer-spawning herring *Clupea harengus* L. J. Fish Biol. **72**(10): 2655–2676. doi:10.1111/j.1095-8649.2008.01886.x.

Óskarsson, G.J., and Taggart, C.T. 2006. Fecundity variation in Icelandic summer-spawning herring and implications for reproductive potential. ICES J. Mar. Sci. **63**(3): 493–503. doi:10.1016/j.icesjms.2005.10.002.

Óskarsson, G.J., Kjesbu, O.S., and Slotte, A. 2002. Predictions of realised fecundity and spawning time in Norwegian spring-spawning herring (*Clupea harengus*): possible implications for subsequent recruitment. J. Sea Res. **48**: 59–79.

Page, F.H., and Frank, K.T. 1989. Spawning time and egg stage duration in Northwest Atlantic haddock (*Melanogrammus aeglifinus*) stocks with emphasis on Georges and Browns Bank. Can. J. Fish. Aquat. Sci. **46**(Suppl.): s68–s81. doi:10.1139/f89-279.

Pedersen, T. 1984. Variation of peak spawning of Arcto-Norwegian cod (*Gadus morhua* L.) during the period 1929–1982 based on indices estimated from fishery statistic. *In* The propagation of cod *Gadus morhua* L. *Edited by* E. Dahl, D.S. Danielsen, E. Moksness, and P. Solemdal. Flødevigen Rapportser. 1. pp. 301–316.

Rajasilta, M. 1992. Relationship between food, fat, sexual maturation, and spawning time of Baltic herring (*Clupea harengus membras*) in the Archipelago Sea. Can. J. Fish. Aquat. Sci. **49**(4): 644–654. doi:10.1139/f92-073.

Ramsey, F.L., and Schafer, D.W. 1997. The statistical sleuth, a course in methods of data analysis. Wadsworth Publishing Company, Belmont, California.

Rijnsdorp, A.D. 1991. Changes in fecundity of female North Sea plaice (*Pleuronectes platessa* L.) between three periods since 1900. ICES J. Mar. Sci. **48**(3): 253–280. doi:10.1093/icesjms/48.3.253.

Rijnsdorp, A.D., and Vingerhoed, B. 1994. The ecological significance of geographical and seasonal differences in egg size in sole *Solea solea* (L.). Neth. J. Sea Res. **32**(3–4): 255–270. doi:10.1016/0077-7579(94)90003-5.

Slotte, A. 1999. Effects of fish length and condition on spawning migration in Norwegian spring spawning herring (*Clupea harengus* L.). Sarsia, **84**: 111–127.

Slotte, A., Johannessen, A., and Kjesbu, O.S. 2000. Effects of fish size on spawning time in Norwegian spring-spawning herring. J. Fish Biol. **56**(2): 295–310. doi:10.1111/j.1095-8649.2000.tb02107.x.

Stefánsson, U. 1962. North Icelandic waters. Rit Fiskideildar, **3**: 1–269.

Thórdardóttir, T. 1986. Timing and duration of spring blooming south and southwest of Iceland. *In* The role of freshwater outflow in coastal marine ecosystems. *Edited by* S. Skreslet. NATO Advanced Study Institute Series, Vol. 7. pp. 345–360.

Tocher, D.R., and Sargent, J.R. 1984. Analyses of lipids and fatty acids in ripe roes of some Northwest European marine fish. Lipids, **19**(7): 492–499. doi:10.1007/BF02534481.

Ware, D.M. 1975. Relation between egg size, growth, and natural mortality of larval fish. J. Fish. Res. Board Can. **32**: 2503–2512.

Ware, D.M., and Tanasichuk, R.W. 1989. Biological basis of maturation and spawning waves in Pacific herring (*Clupea harengus pallasi*). Can. J. Fish. Aquat. Sci. **46**(10): 1776–1784. doi:10.1139/f89-225.

Warlen, S.M. 1994. Spawning time and recruitment dynamics of larval Atlantic menhaden, *Brevoortia tyrannus*, into a North Carolina estuary. Fish. Bull. (Washington, D.C.), **92**: 420–433.

Wieland, K., Teichmann, A.J., and Horbowa, K. 2000. Changes in the timing of spawning of Baltic cod: possible causes and implications for recruitment. ICES J. Mar. Sci. **57**(2): 452–464. doi:10.1006/jmsc.1999.0522.

Long-term declines in phosphorus export from forested catchments in south-central Ontario

M. Catherine Eimers, Shaun A. Watmough, Andrew M. Paterson, Peter J. Dillon, and Huaxia Yao

Abstract: Total phosphorus (TP) levels in many Canadian Shield lakes in central Ontario have declined over recent decades, despite increases in human activity in most watersheds. To investigate the contribution of changes in catchment export to long-term declines in lake TP, we examined temporal and spatial patterns in TP concentrations and export (1980–1981 to 2001–2002) across 11 subcatchments that drain into three lakes in which average ice-free TP levels have declined by approximately 35%. Annual stream export of TP decreased significantly by 30%–89% in eight of the 11 subcatchments, and decreases in export were driven by declines in TP concentration, not changes in stream flow. Annual average TP concentrations varied fivefold among adjacent subcatchments, and temporal patterns in annual average TP concentrations were poorly correlated. Seasonal patterns of TP concentration were most similar among streams in the spring (March–April–May), and TP export in the spring declined significantly in 10 of the 11 subcatchments. Because spring melt is the principal hydrologic event in these seasonally snow-covered basins, decreases in TP export during the spring were primarily responsible for declines observed in annual export. The drivers of changes in TP over time are unclear at this point but are the focus of current research.

Résumé : Les concentrations de phosphore total (TP) dans plusieurs lacs du Bouclier canadien du centre de l'Ontario ont diminué au cours des dernières décennies, malgré l'augmentation des activités humaines dans la plupart des bassins versants. Afin d'étudier la contribution des changements dans l'exportation de TP des bassins versants aux déclins à long terme du TP lacustre, nous examinons les patrons temporels et spatiaux de concentrations et d'exportation de TP (1980–1981 à 2001–2002) dans 11 sous-bassins qui se déversent dans trois lacs dans lesquels les concentrations de TP durant la période sans glace ont chuté d'environ 35 %. L'exportation annuelle de TP dans les cours d'eau a décru significativement de 30–89 % dans huit des 11 sous-bassins et les déclins de l'exportation de TP s'expliquent par des diminutions des concentrations de TP et non par des changements de débit des cours d'eau. Les concentrations annuelles moyennes de TP varient par un facteur de cinq dans des sous-bassins adjacents et les patrons temporels des concentrations annuelles moyennes sont faiblement corrélés. Les patrons saisonniers des concentrations de TP entre les cours d'eau ont la similarité la plus forte au printemps (mars–avril–mai) et l'exportation de TP au printemps a diminué significativement dans 10 des 11 sous-bassins versants. Parce que le dégel printanier est l'événement hydrologique principal dans ces bassins versants couverts de neige en saison, la diminution de l'exportation de TP au printemps est la cause principale des déclins observés dans l'exportation annuelle. Le ou les facteurs explicatifs des changements de TP au cours du temps restent obscurs, mais font actuellement l'objet de recherches.

[Traduit par la Rédaction]

Introduction

Declining total phosphorus (TP) concentrations have been reported recently in a number of oligotrophic Canadian Shield lakes in south-central Ontario that are remote from agricultural, industrial, and urban sources of P (Quinlan et al. 2008; Yan et al. 2008). These declines in TP levels in lakes have occurred despite general increases in human activity (e.g., cottage usage) in their watersheds, and recent regional lake water chemistry surveys indicate that TP levels have decreased over a much broader region by at least 30% over the past three decades (A. Paterson, unpublished data). Decreasing TP concentrations in oligotrophic systems are of particular concern because of the relationship between P availability and aquatic productivity (Hörnström 1999; Jeppesen et al. 2005) and shifts in aquatic community composition, such as an increase in the abundance of "taste and odour" algae, may occur in tandem with long-term declines in TP (Paterson et al. 2004).

Declines in lake TP concentrations could be a result of internal (i.e., within-lake) and (or) external (catchment) factors. Internal processes that could influence lake TP include lake water acidification (and changes in sediment organic matter mineralization and (or) Al complexation), changes in internal loading (e.g., changes in the reducing conditions in

Received 28 October 2008. Accepted 20 April 2009. Published on the NRC Research Press Web site at cjfas.nrc.ca on 26 September 2009.
J20844

Paper handled by Associate Editor Yves Prairie.

M.C. Eimers.[1] Department of Geography, Trent University, Peterborough, ON K9J 7B8, Canada.
S.A. Watmough and P.J. Dillon. Environmental and Resource Science Program, Trent University, Peterborough, ON K9J 7B8, Canada.
A.M. Paterson and H. Yao. Ontario Ministry of Environment, Dorset Environmental Science Centre, 1026 Bellwood Acres Road, Dorset, ON P0A 1E0, Canada.

[1] Corresponding author (e-mail: ceimers@trentu.ca).

Can. J. Fish. Aquat. Sci. **66**: 1682–1692 (2009) doi:10.1139/F09-101 Published by NRC Research Press

bottom sediments), biological changes (e.g., ecological shifts), and hydroclimatic changes (e.g., increases in water residence time, duration of the ice-free season, or stratification). However, because TP declines have been observed in a number of lakes across a relatively large area, including lakes with and without shoreline residential development, we hypothesize that the causal factors must operate on a regional scale and are not lake-specific. Furthermore, we are specifically interested in whether changes in external loading, i.e., declines in TP loads from the catchment and (or) the atmosphere, can account for declines in lake TP, and as such, we focus our investigation on catchment controls.

The export of TP from catchments to lakes is affected by a number of factors, many of which may change over time, including atmospheric deposition (phosphorus and acids), weathering, hydrology, climate, and land use. Changes in atmospheric deposition of P have an obvious direct impact on P inputs to lakes, and atmospheric inputs of P may be a large fraction of the P budget of lakes with relatively large surface-area to catchment-area ratios (Dillon et al. 1993) and where weathering fluxes are low (Jansson et al. 1986; Doskey and Ugoagwu 1989). Acid deposition may also affect lake TP levels, as elevated Al transport from acidified soils could result in the inactivation of P in lakes (Huser and Rydin 2005; Kopacek et al. 2007). Moreover, acidification of catchment soils could result in stronger adsorption of TP to soil mineral surfaces and lower leaching rates (e.g., McDowell et al. 2002).

Wetlands and riparian areas are particularly important loci of P cycling in undisturbed catchments, as they are a major source of dissolved organic matter (including dissolved organic P) in streams. In addition, redox processes within wetlands can alter stream P levels by affecting the solubility of iron–phosphorus (Fe–P) compounds, and Fe and TP are often correlated (increasing under reducing conditions; decreasing under oxic conditions) in wetland outflows (Devito and Dillon 1993*a*, 1993*b*; Carlyle and Hill 2001). Changes in land use, including wetland creation–degradation and forestry (reforestation or harvesting), can therefore increase or decrease P delivery to lakes by influencing the sources and pathways of P inputs (e.g., Hall and Smol 1996).

Changes in stream flow may also impact the delivery of P to lakes. Because of the tight biological cycling of P, the majority of P export from forested catchments occurs during relatively brief periods of high runoff, including storms and snowmelt (Meyer and Likens 1979). As such, changes in the magnitude and timing of high discharge events could influence P delivery to lakes. Hydroclimatic shifts could also influence the amount of labile P available for leaching by altering the rate of P uptake by biota or release from soils through mineralization.

It is clear that a variety of external factors could contribute to declining lake TP concentrations, and the relative importance of each factor may differ among catchments with different landscape characteristics (i.e., wetlands, slope, geology, etc.). To investigate the role of changes in the delivery of P to lakes, we examined long-term (1980–1981 to 2001–2002) trends in TP deposition and export from 11 streams that drain into three lakes in which TP levels have declined over the past two decades. The three lakes (Harp, Plastic, and Dickie) are located within 40 km of one another, are remote from point sources of TP deposition, and are not impacted by agriculture or urbanization. Plastic Lake is surrounded by intact coniferous forest, and there is no cottage development within its watershed. In contrast, Harp and Dickie lakes have substantial cottage populations (Harp, 110 residences in 2004; Dickie, 143 residences in 2001) and are surrounded by mixed hardwood forest and selective cutting by landowners has occurred in some of their subcatchments. All three watersheds receive similar inputs of bulk acidic and phosphorus deposition.

Specific objectives of this study are (*i*) to identify whether TP inputs to lakes in stream export and bulk deposition have changed over time, (*ii*) identify whether coherent seasonal changes in TP concentrations and export have occurred across the 11 study streams, (*iii*) examine relationships between TP and other chemical parameters to test for possible drivers of changes in TP, and (*iv*) determine whether changes in external inputs of TP to lakes can account for observed declines in lake TP.

Materials and methods

Study area

The 11 headwater subcatchments (HP3, HP3A, HP4, HP5, HP6, HP6A, DE5, DE6, DE8, DE10, PC1; Table 1) considered for this study are located in the District Municipality of Muskoka (Harp subcatchments, HP; Dickie subcatchments, DE) or Haliburton County (Plastic Lake subcatchment, PC) and are part of the Ontario Ministry of Environment Dorset Environmental Science Centre's (DESC) long-term monitoring program, which has been in operation since the mid- to late 1970s. The study area is located at the southern edge of the Canadian Shield and is typical of the shallow till – rock ridge physiographic region of south-central Ontario (Chapman and Putnam 1984). Plastic Lake is a small (32 ha; mean depth 7.9 m) headwater lake in an area of granitic gneiss bedrock overlain by a thin discontinuous layer of sandy basal till. Seven streams drain into Plastic Lake, six of which are ephemeral, draining a total watershed area of 92 ha. The largest inflow (Plastic Lake 1 (PC1); 23 ha) flows almost continuously (ceasing to flow only during particularly dry summers) and has been monitored for stream flow and chemistry using consistent methods since 1980. Plastic Lake has an average residence time (1980–2001) of 4.1 years. Upland soils at PC1 are generally thin (<50 cm), acidic ($\mathrm{pH}_{\mathrm{B\ horizon}}$ 4.2 – 4.7 in 0.01 mol $\mathrm{CaCl_2 \cdot L^{-1}}$), course-textured (>80% sand, <5% clay), weakly developed podzols (Neary et al. 1987).

Harp Lake is a slightly larger headwater lake (71 ha; mean depth 13 m) surrounded by a 471 ha watershed that is drained by six streams (HP3, HP3A, HP4, HP5, HP6, HP6A; Table 1), which have been monitored for stream flow and chemistry since 1976. Harp Lake has an average water residence time (1980–2001) of 3.3 years. Subcatchments within the HP watershed range in size from 9.97 to 190.5 ha and vary in average slope, till depth, and peatland coverage (Table 1; Eimers et al. 2008). The bedrock geology of the Harp Lake watershed is amphibolite and schist, overlain by a minor till plain. Soils are generally deeper at the HP catchments (1.5 to 25 m in areas of deep till) and are sandy, acidic (pH 4.2–4.6) podzols and brunisols.

Table 1. Catchment characteristics and average (1980–1981 to 2001–2002) stream chemistry.

	Area (ha)	Average slope (%)	Primary geology[a]	Average wetland (%)	Average [DOC] (mg·L^{-1})	Average [Fe] (µg·L^{-1})	Average [TP] (µg·L^{-1})	Average [Ca] (mg·L^{-1})
HP3	26.0	4	BHG, AS	9	8.4	284	16	3.2
HP3A	19.6	8	AS, BHG	3	3.4	52	6.0	2.9
HP4	119	5	AS, BHG	8	5.8	242	13	2.7
HP5	191	3	BHG	13	10.6	339	16	2.8
HP6	9.97	8	BHG	10	6.2	465	13	3.6
HP6A	15.3	10	DIOR, BHG	9	7.4	135	7.9	2.7
DE5	30.0	1	MIG	17	23	593	31	1.4
DE6	21.8	1.6	MIG	25	17	990	31	2.3
DE8	67.0	1	MIG	22	18	500	11	5.6
DE10	78.9	1	MIG	8	19	669	13	3.0
PC1	23.3	6	BHG, MIG	9	9.8	255	6.9	1.9

[a] BHG, biotite, horneblende, and gneiss; AS, amphibolite and schist; DIOR, diorite; MIG, migmatite.

Dickie Lake is the largest (94 ha) but shallowest (mean depth 5.0 m) of the three study lakes and is surrounded by a 406 ha catchment that is drained by five streams, four of which have been gauged continuously since 1976 (DE5, DE6, DE8, DE10; Table 1). The average (1980–2001) residence time of Dickie Lake is 1.9 years. The DE catchments are relatively flat compared with the HP catchments and PC1, are dominated by migmatite, and have a much larger wetland component (Table 1).

The study area lies at the southern limit of the Boreal ecozone, and forest composition ranges from predominantly coniferous at PC1 (*Pinus strobus*, *Tsuga canadensis*) to mixed hardwood at the Harp catchments (*Acer saccharum*, *Fagus grandifolia*, *Betula alleghenensis*) (Watmough and Dillon 2003*a*). Conifer (*Thuja occidentalis*, *Picea mariana*), mixed, and thicket swamps are the dominant peatland types (Devito et al. 1999), and wetland coverage ranges from 3% at HP3A to 25% at DE5 (Table 1). On average, wetlands cover 8%–10% of the landscape in this region (O'Connor 2007.).

Sampling

Precipitation depth was measured using Belfort gauges at three meteorological monitoring stations located in the study region, including sites at Harp, Plastic, and Heney lakes (located close to Dickie Lake). Bulk deposition of TP (wet + dry) was measured at the same sites in continuously open collectors fitted with Nitex screen (102 µm) to limit contamination by coarse particulates. Bulk deposition loads were calculated by multiplying the average TP concentration in deposition by the volume of precipitation received over the collection period. Average TP concentrations in deposition and loads represent the averages of measurements made at the three monitoring stations. Grab samples of stream water for chemical analysis were typically taken weekly to biweekly at the catchment outlet, and streams were sampled more frequently during periods of high discharge. Total phosphorus was measured in unfiltered stream water and bulk precipitation samples by ascorbic acid molybdate colorimetry following autoclave digestion with sulphuric acid (Dillon and Molot 2005); analytical methods for TP have been consistent since the beginning of the study.

Stream flow was monitored continuously at each catchment outflow at a V-notch or H-flume weir, and flow data from 1 June 1980 to 31 May 2002 were available for the 11 subcatchments. Total phosphorus fluxes were calculated using integrated daily estimates of discharge and concentration values and were summed for each hydrologic year (1 June – 31 May). Volume-weighted annual TP concentrations were calculated by dividing the total mass of TP exported by total stream discharge for each year. Seasonal fluxes and volume-weighted concentrations were calculated similarly and were summed for each three-month season (summer, June–August; fall, September–November; winter, December–February; spring, March–May).

Data analysis

Time trends in monthly volume-weighted TP concentration were evaluated using the nonparametric partial Mann–Kendall (PMK) test with monthly discharge as a covariate (Libiseller and Grimvall 2002). The seasonal MK test is commonly used to test for temporal trends in monthly measurements of water quality (e.g., Skjelkvåle et al. 2005), and discharge was considered as a covariate because of the potential influence of changes in stream flow on trends in phosphorus concentrations. The magnitude of any significant trend found was determined using the Sen slope estimator (Sen 1968).

To compare temporal patterns of TP among catchments (i.e., spatial consistency of temporal patterns), annual and seasonal values were transformed to Z scores by subtracting the 22-year mean from each observation and then dividing by the standard deviation (e.g., Arnott et al. 2003). Pearson's correlation coefficients (r) between seasonal and annual average standardized TP concentration and export values were used to estimate similarity in TP patterns among catchments. Relationships between average TP concentrations and selected catchment characteristics (e.g., average slope, percent wetland coverage) and chemical indicators of catchment properties (i.e., DOC indicates wetland coverage, Fe indicates redox cycling of TP, Ca indicates soil acidification status) were also examined to determine potential causes of spatial differences in TP.

As patterns in TP concentration were most coherent among catchments during the spring, and because the largest and most significant declines in TP concentration and export occurred during this season, we also examined correlations between average spring TP concentration and other chemical (e.g., average Fe, SO_4, and DOC concentrations) and physical parameters (runoff, deposition) in the spring at each catchment to gain insight into the processes controlling long-term trends in TP.

TP budgets (annual, seasonal) for individual subcatchments were calculated by comparing input in bulk deposition ($mg \cdot m^{-2}$) with stream export ($mg \cdot m^{-2}$). Inputs from cottages were not considered in budget calculations, because any cottages present in subcatchments were located downstream of stream gauging stations.

Results

Temporal trends in TP concentrations and export

Annual average TP concentrations and export declined significantly between 1980 and 2001 at seven and eight of the 11 catchments, respectively (Table 2). Total phosphorus concentrations and export were generally higher in the 1980s than in the 1990s, and most of the decline occurred between these two decades (Fig. 1). The magnitude of decrease in stream TP export between the first (1980–1984) and final five years of record (1997–2001) ranged from 16% at HP5 to 89% at DE5. Annual stream flow varied greatly between years, and there were no trends toward higher or lower flow over the period of record.

Seasonally, TP concentrations and export decreased significantly during the spring at 8 and 10 of the 11 catchments, respectively; only HP5 did not show any trend in spring export. Similar to annual averages, spring TP concentrations and export were generally higher in the 1980s than in the 1990s (Fig. 1). Spring runoff declined significantly ($p < 0.05$) at DE5 only. There was a tendency toward lower spring flow between 1980–1981 and 2001–2002 at HP6, DE10, and PC1, but the trends were not significant (p = 0.1; Table 2).

Decreases in TP concentration during the summer, fall, and winter were much less common, and declines in concentration were not always translated into decreased export, and TP export during the summer decreased significantly ($p <$ 0.05) at DE5 only (Table 2). Similarly, TP export declined significantly over time at only three (HP3, HP4, and DE5) and two (HP4 and DE5) streams in the fall and winter, respectively. Temporal patterns of annual average TP concentration were poorly correlated among catchments, and seasonal patterns were most similar in the spring (median r = 0.50), followed by the winter (median r = 0.39), and most disparate in the summer (median r = 0.21) and fall (median r = 0.31) (Fig. 1).

Correlations between average spring TP concentration and other chemical (e.g., average Fe, SO_4, and DOC concentrations) and physical (runoff, deposition) parameters provided little insight into the processes driving TP trends. Although average spring TP concentration was positively correlated with Fe at the majority of the streams (seven; Table 3), Fe concentrations (and export) only declined significantly at three (or four) of the 11 catchments, indicating that temporal patterns of Fe and TP were different. At many streams, particularly the wetland-dominated DE inflows, Fe concentrations were better correlated with DOC (Table 3). Sulphate was positively correlated with TP at three streams (Table 3). Overall, we could find no consistent correlates of TP at the

Table 2. Sen slopes and significance levels.

	HP3	HP3A	HP4	HP5	HP6	HP6A	DE5	DE6	DE8	DE10	PC1
Annual [TP]	-0.47***	-0.16**	-0.39***	—	—	—	-2.9***	—	-0.15*	-0.21+	-0.16**
Annual [TP] export	-0.46***	-0.13**	-0.31***	—	—	—	-1.5***	-0.52*	-0.18*	-0.22**	-0.12**
Annual flow	—	—	—	—	—	—	—	—	—	—	—
Summer [TP]	-1.4**	—	-0.51**	—	+0.68*	—	-5.2***	—	—	—	—
Summer [TP] export	-0.079+	—	—	—	—	—	-0.21**	—	—	—	—
Summer flow	—	—	—	—	—	—	—	—	—	—	—
Fall [TP]	-0.46*	—	-0.52***	—	—	—	-3.0***	—	—	—	—
Fall [TP] export	-0.13*	—	-0.078*	—	—	—	-0.40***	—	—	—	—
Fall flow	—	—	—	—	—	—	—	—	—	—	—
Winter [TP]	-0.41**	—	-0.41***	—	—	-0.07+	-3.1***	—	—	-1.7+	-0.14*
Winter [TP] export	—	—	-0.037*	—	—	—	-0.43**	—	—	—	—
Winter flow	—	—	—	—	—	—	—	—	—	—	—
Spring [TP]	-0.44**	-0.23*	-0.56***	—	—	—	-3.0***	-0.54*	-0.25**	-0.28**	-0.14**
Spring [TP] export	-0.19***	-0.076**	-0.16***	—	-0.073*	-0.033**	-0.65***	-0.24***	-0.09***	-0.13***	-0.066***
Spring flow	—	—	—	—	-321+	—	-1631*	—	—	-2776+	-938+
Spring [Fe]	—	-1.5**	-4.8*	—	—	—	—	+7.1**	—	+3.9+	—
Spring [Fe] export	-0.97*	-0.60***	-2.3***	-0.92+	—	-0.41**	—	—	—	—	-0.43+
Spring [Al]	+1.8*	—	—	—	—	+9.8+	—	—	—	—	+3.0*
Spring [Al] export	—	-1.0*	-1.2**	—	-1.3**	—	-0.60**	—	—	—	—
Spring [DOC]	+0.09*	—	—	—	+0.06*	+0.08*	-0.24*	—	—	+0.10+	+0.12***
Spring [DOC] export	—	—	-14*	—	—	—	-49*	—	—	—	—

Note: Significance levels (p): +, 0.1; *, 0.05; **, 0.01; ***, 0.001.

Fig. 1. Average volume-weighted phosphorus concentrations (µg·L^{-1}) in PC1 (△), HP3 (○), HP3A (+), HP4 (–), HP5 (–), HP6 (◇), HP6A (□), DE8 (×), and DE10 (◆) (all left axis) and DE5 (■) and DE6 (▲) (right axis) in (*a*) spring, (*b*) summer, (*c*) fall, (*d*) winter, and (*e*) annual time series.

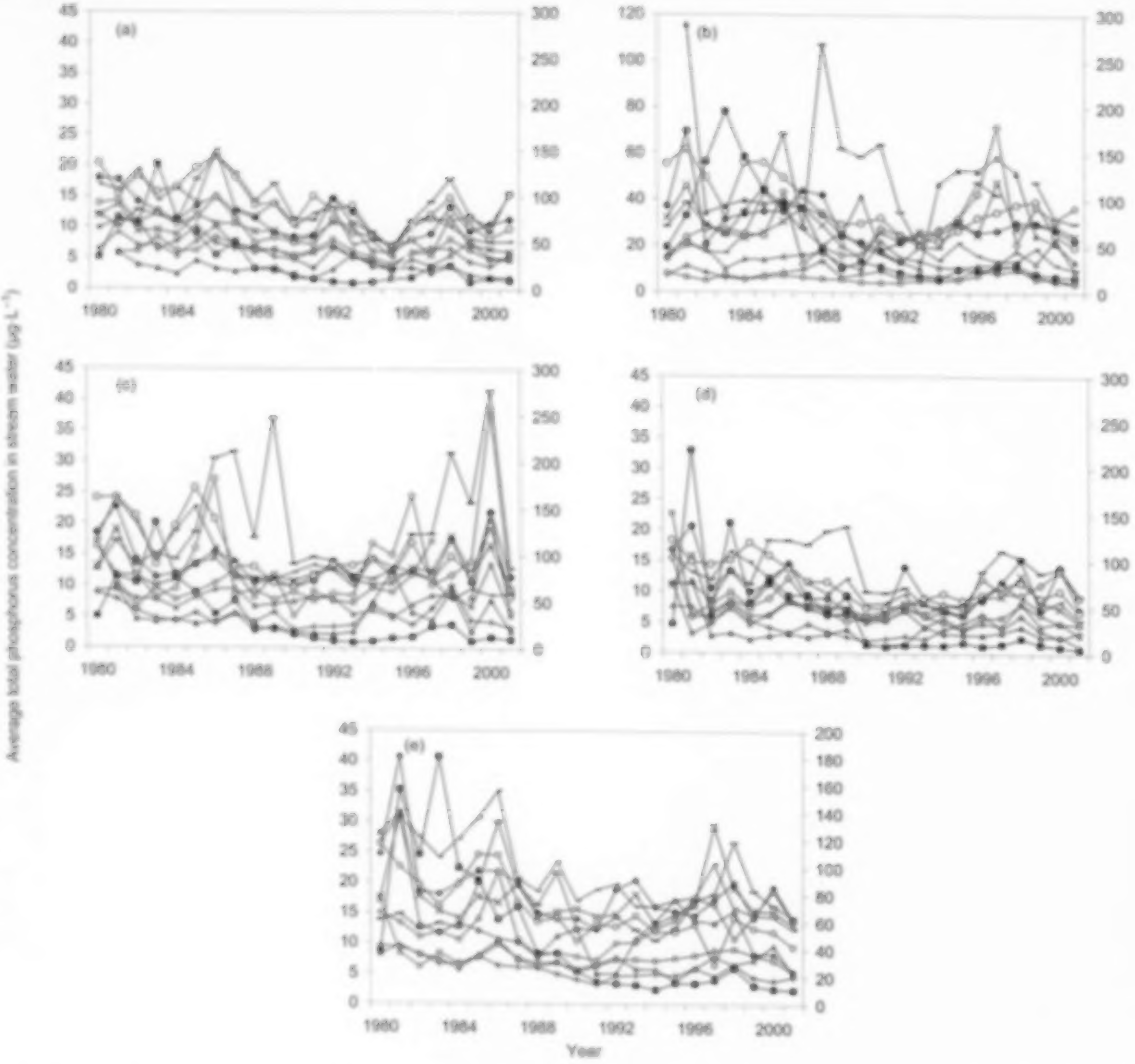

10 streams in which TP export declined significantly in the spring.

Phosphorus deposition

There was no significant trend in annual average TP concentration in bulk deposition or in TP loads (mg·m^{-2}) between 1980 and 2002; although three distinct periods can be identified within the deposition record. Between 1980 and 1990, TP deposition was relatively high and was generally greater than 15 mg·m^{-2}·annum^{-1} (1980 to 1990 inclusive; average = 18.2 mg·m^{-2}·annum^{-1}). In contrast, TP deposition was generally low between 1990 and 1998 and was almost always less than 14 mg·m^{-2}·annum^{-1} (excluding 1995 when deposition was 17 mg·m^{-2}; average$^{1991-1998}$ = 11.9 mg·m^{-2}·annum^{-1}; Fig. 2). TP loads and concentrations in deposition in 1999–2001 were higher and more similar to the first decade of record (average = 22 mg·m^{-2}). Interannual variations in TP loads were driven by changes in TP concentrations in deposition, rather than differences in precipitation (mm) inputs (Fig. 2).

Seasonally, TP deposition is highest in the spring (average 5.7 mg·m^{-2}; 26 µg·L^{-1}) and summer (average 5.4 mg·m^{-2}; 24 µg·L^{-1}) and substantially lower in the fall (average 3.1 mg·m^{-2}; 10 µg·L^{-1}) and winter (average 1.5 mg·m^{-2}; 6.4 µg·L^{-1}). TP loads in bulk deposition declined significantly in the summer only, by approximately 45% over the

Table 3. Pearson correlations between average spring TP concentration and other parameters (between years).

	[TP] vs. [Fe]	[Fe] vs. [DOC]	[TP] vs. [DOC]	[TP] vs. runoff (m^3)	[TP] vs. [SO_4]	[TP] vs. spring deposition ($mg \cdot m^{-2}$)
HP3	0.36	0.42	—	—	0.57	—
HP3A	0.77	—	—	—	0.51	—
HP4	0.66	—	—	—	—	—
HP5	0.49	0.85	0.45	—	—	—
HP6	—	—	—	—	—	0.46
HP6A	0.45	—	0.40	–0.44	0.45	—
DE5	—	0.69	0.57	—	—	—
DE6	—	0.54	—	—	—	0.48
DE8	0.57	0.68	0.37	—	—	—
DE10	—	0.40	—	—	—	—
PC1	0.46	0.44	—	—	—	—

Note: Units of TP and Fe ($\mu g \cdot L^{-1}$), DOC ($mg \cdot L^{-1}$). Catchments showing significant declines in spring TP export between 1980–1981 and 2001–2002 are indicated in bold.

Fig. 2. Annual total phosphorus deposition loads (◆, $mg \cdot m^{-2}$) and concentration (□, $\mu g \cdot L^{-1}$) and precipitation (bars, mm) for 1980 to 2001.

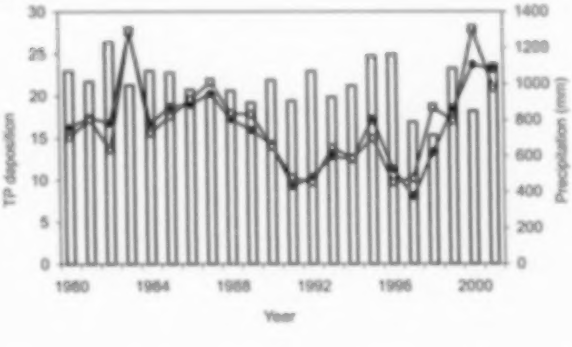

22-year period of record (Sen slope = –0.15 $mg \cdot m^{-2} \cdot annum^{-1}$; $p < 0.05$; data not shown). However, similar to annual data, there were obvious differences in seasonal deposition between the first (1980–1989) and second (1990–1999) decade of monitoring. For example, average spring deposition was 30% lower in 1990–1999 (4.6 $mg \cdot m^{-2}$) than in 1980–1989 (6.4 $mg \cdot m^{-2}$). In contrast, fall and winter depositions were relatively constant over time. There were no significant trends in precipitation amount (mm) in any season.

Mass balances

Comparisons of stream export with inputs in bulk deposition demonstrate that TP is retained within most catchments (i.e., atmospheric deposition exceeds stream output) at both the annual and seasonal scales (Table 4). Only at DE5 and DE6, where TP export is particularly large (especially in the early 1980s) was annual average TP input in approximate balance with export (Table 4). In general, TP retention was greatest in the summer (mean of 11 catchments: 76% of input was retained) and lowest in the winter, spring, and fall (32%, 39%, and 43% retention, respectively). In contrast to the other catchments, DE5 and DE6 were net sources of TP during the winter and spring, whereas TP inputs and outputs were in approximate balance in the fall (Table 4). There was substantial temporal variability in the magnitude of TP retention in catchments due to relatively large variation in atmospheric loads and stream export between years.

Spatial patterns in TP

Annual average TP concentrations and export varied almost fivefold across the 11 study catchments, despite their close proximity (Table 4; Fig. 1). Average (22-year) annual TP concentrations ranged from a high of around 31 $\mu g \cdot L^{-1}$ at DE5 and DE6 to lows of 6.0 and 6.9 $\mu g \cdot L^{-1}$ at HP3A and PC1, respectively. Average export similarly ranged from 3.5–3.7 $mg \cdot m^{-2}$ at HP3A and PC1 to over 16 $mg \cdot m^{-2}$ at DE5 and DE6. Seasonally, TP concentrations were highest and most variable among catchments in the summer (6.4–96 $\mu g \cdot L^{-1}$) when runoff is lowest and were lower and less variable among catchments in the fall (5.2–34 $\mu g \cdot L^{-1}$), spring (6.1–33 $\mu g \cdot L^{-1}$), and winter (4.4–42 $\mu g \cdot L^{-1}$) (Table 4).

Possible causes of differences in TP concentration among catchments were explored (Fig. 3). Average DOC concentration was positively correlated with TP, and higher DOC and TP concentrations occurred in flatter catchments with larger peatland components, suggesting that much of the TP originates from organic soil. However, removal of DE5 and DE6 (streams with exceptionally high DOC and TP concentrations) from the DOC vs. TP regression eliminated the statistical significance of the relationship. In contrast, average TP and Fe concentrations were significantly correlated across all 11 catchments, although the relationship between Fe and DOC was also strong (Fig. 3). Runoff and atmospheric deposition are virtually the same across catchments, and geology and forest composition are similar across many of the catchments, so these factors cannot explain the nearly fivefold difference in TP export among streams. Differences in stream Ca (which can be used to infer soil acidification status; Houle et al. 2006) similarly could not explain intercatchment differences in TP (Fig. 3).

Although land-use history may explain some of the interannual variation in TP within catchments, it is unlikely to account entirely for differences among catchments; for example, forest harvesting (selective cutting) has occurred at some of the HP catchments, yet average TP concentrations in the HP streams vary almost threefold. Cottages are present in most of the catchments; however, notably, TP lev-

Table 4. Average annual and seasonal TP export, concentrations, runoff, and percent TP retention (input – output/input × 100).

TP	HP3	HP3A	HP4	HP5	HP6	HP6A	DE5	DE6	DE8	DE10	PC1
Annual											
Export (mg·m^{-2})	9.3±4.2	3.5±1.5	7.0±2.7	9.5±2.9	7.4±2.9	3.8±1.9	16.3±15.1	17.0±14.8	5.9±2.1	6.6±2.6	3.7±1.2
[TP] (μg·L^{-1})	15.9±4.9	6.0±1.7	13.0±4.2	16.3±4.9	12.7±3.7	7.9±2.3	31.0±26.9	30.7±19.2	10.7±2.5	12.9±3.7	6.9±1.7
Runoff (m)	0.59±0.13	0.57±0.13	0.53±0.14	0.60±0.14	0.58±0.14	0.48±0.12	0.52±0.13	0.53±0.13	0.55±0.13	0.51±0.11	0.54±0.13
% retention	+44	+79	+57	+42	+55	+77	+0.5	–3.5	+64	+60	+77
Summer											
Export (mg·m^{-2})	1.8±1.6	0.30±0.26	1.0±0.8	1.7±1.4	1.5±1.4	0.17±0.17	2.2±2.9	3.0±2.9	1.0±0.92	1.4±0.88	0.51±0.56
[TP] (μg·L^{-1})	37.2±12.5	7.9±2.2	20.0±7.8	42.6±20.6	28.3±12.9	6.4±2.1	57.1±51.4	95.9±56.5	28.5±7.4	30.9±11.0	14.7±3.9
Runoff (m)	0.047±0.036	0.043±0.044	0.050±0.033	0.044±0.036	0.050±0.042	0.028±0.027	0.039±0.037	0.033±0.027	0.035±0.029	0.032±0.029	0.033±0.029
% retention	+67	+94	+81	+69	+72	+91	+59	+44	+82	+82	+91
Fall											
Export (mg·m^{-2})	2.1±1.7	0.60±0.54	1.7±1.3	2.5±2.1	1.8±1.2	0.93±0.77	3.0±3.0	3.2±2.6	1.3±0.81	1.4±0.88	0.93±0.49
[TP] (μg·L^{-1})	15.6±5.1	5.2±1.9	13.7±4.5	19.6±8.9	13.7±7.6	10.3±4.0	33.1±32.4	33.8±19.0	12.6±2.5	13.7±3.6	7.8±1.9
Runoff (m)	0.13±0.08	0.12±0.08	0.11±0.07	0.14±0.09	0.13±0.08	0.10±0.07	0.10±0.05	0.10±0.06	0.11±0.06	0.10±0.05	0.13±0.06
% retention	+31	+81	+46	+18	+43	+70	+4	–2	+57	+56	+70
Winter											
Export (mg·m^{-2})	1.2±0.8	0.53±0.48	1.0±0.6	1.8±0.8	0.89±0.54	0.68±0.78	3.1±3.7	1.7±0.9	0.81±0.35	1.0±0.51	0.55±0.28
[TP] (μg·L^{-1})	11.4±3.4	4.4±2.1	10.4±3.2	12.9±4.2	8.8±2.7	7.0±3.7	41.5±51.2	21.7±14.3	8.5±2.4	10.8±3.9	5.9±1.5
Runoff (m)	0.096±0.050	0.11±0.049	0.096±0.040	0.096±0.050	0.097±0.043	0.089±0.046	0.084±0.043	0.089±0.047	0.11±0.052	0.10±0.045	0.096±0.048
% retention	+23	+64	+33	+25	+41	+66	–109	–11.5	+97	+66	+64
Spring											
Export (mg·m^{-2})	4.2±1.5	2.0±0.9	3.2±1.3	4.1±1.5	3.2±0.9	1.6±0.3	8.0±7.0	6.3±2.5	2.7±0.81	3.2±1.0	1.7±0.5
[TP] (μg·L^{-1})	13.9±1.1	6.5±2.3	12.3±4.2	13.2±3.7	10.7±2.5	6.3±1.2	33.1±32.4	21.6±7.4	9.1±2.2	11.3±3.1	6.1±1.7
Runoff (m)	0.30±0.06	0.31±0.06	0.26±0.06	0.32±0.08	0.30±0.06	0.26±0.05	0.29±0.086	0.30±0.068	0.30±0.21	0.28±0.055	0.28±0.06
% retention	+27	+65	+42	+27	+44	+72	–40	–11	+53	+82	+70

Fig. 3. Correlations between average spring concentrations of (*a*) total phosphorus (TP) and Fe, (*b*) TP and dissolved organic carbon (DOC), (*c*) TP and Ca, and (*d*) Fe and DOC at the 11 study catchments.

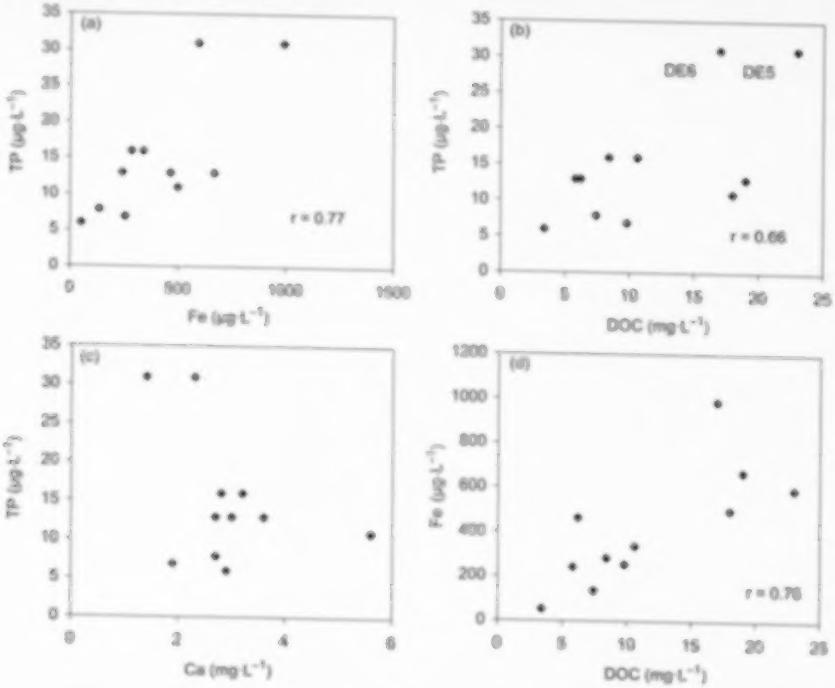

els have declined in catchments both with (e.g., HP4, HP3) and without (e.g., HP3A, PC1) cottage dwellings. It should also be noted that when present, cottages are typically located close to the lake shoreline and downstream of the stream water quality–quantity gauging station and are therefore unlikely to directly affect stream TP export, although inputs from septic systems may affect long-term changes in lake concentrations (Paterson et al. 2006).

Discussion

Results of this study have shown that annual average TP concentrations and stream export of TP vary almost fivefold among adjacent catchments. Despite large differences in TP across sites, the majority of catchments considered in this study (8/11) exhibited significant declines in TP concentrations and export (1980–1981 to 2001–2002), and declines were most consistent in the spring months, with 10 of the 11 catchments showing significant decreases in TP export. Decreases in catchment TP export can at least partly explain observed declines in lake TP, and processes occurring in the spring (and perhaps in the preceding winter months) are most important.

Temporal trends in TP

The fact that declines in stream TP concentrations and export were most apparent during the spring snowmelt season when temporal patterns in average TP were also the most coherent among catchments indicates the importance of the high-flow period for TP budgets. Because spring melt is the dominant hydrologic event in this region, comprising at least 50% of annual runoff, changes in TP export in this season are primarily responsible for changes observed in annual averages, as has been noted for DOC (Eimers et al. 2008). With the exception of DE5, spring stream flow did not change significantly over the period of record, indicating that declines in stream TP export during the spring cannot simply be attributed to decreases in stream flow. A decline in TP concentration implies a change in the process (or processes) that control TP retention–release within catchments during the spring; however, we were unable to find any clear driver of these declines, as TP levels were not consistently related to any of the chemical (Fe, DOC) or physical (flow) drivers that we investigated, and TP concentrations in spring deposition did not decline significantly over time.

Although previous studies have indicated the importance of wetlands as a source of stream TP, there is no evidence to suggest that either wetland coverage or the prevalence of reducing conditions have changed over time consistent with declines in stream TP (Dillon and Molot 2005). Furthermore, declines in stream TP occurred at both high DOC (e.g., DE5, DE6, PC1) and low DOC (e.g., HP3A, HP4) streams, and decreases were largest and most consistent among catchments during the spring. Spring is a time of year when stream flow is particularly high (due to snowmelt) and biological activity is relatively low (due to low temperatures), and neither condition supports a redox explanation. However, it is possible that changes in beaver pond area, for example, could contribute to the large interannual differences in TP export observed at some catchments (i.e., DE5 and DE6).

Lake studies have reported a relationship between SO_4 addition and TP release from sediment owing to disruption of the connections between the P and Fe cycles (e.g., Curtis 1989). The SO_4–Fe–TP relationship suggests that a decline in SO_4 availability would result in more efficient precipitation of P with Fe and therefore a decrease in P levels. However, although SO_4 levels declined in most of the streams, there were no consistent correlations between SO_4 and TP that would indicate a role of SO_4 in TP declines.

Long-term soil acidification may also contribute to declines in TP export from catchments as acidic soils tend to have more Al and Fe minerals available for P adsorption, and P adsorption is enhanced under acidic (i.e., greater H^+ availability) conditions (e.g., McDowell et al. 2002). Repeated soil sampling has shown that soil pH (particularly in the upper soil horizons) has declined at the HP and PC catchments over the past 20 years (Watmough and Dillon 2003*b*; Watmough and Dillon 2004); however, it is unclear how soil acidification could explain the magnitude of long-term declines in stream TP export or the scale of interannual variability. Detailed soil and lysimeter work is planned to examine this hypothesis.

One possible explanation for the lack of consistency among even adjacent catchments is the tendency for TP export to occur predominantly during high-flow events of relatively short duration (Meyer and Likens 1979; Prairie and Kalff 1988*b*). Numerous studies have reported a strong association between phosphorus and particulates, and the particulate P fraction is typically strongly correlated with stream flow due to the mobilization of particulate matter from surface soil and the stream channel during high-flow events (Meyer and Likens 1979; Prairie and Kalff 1988*a*, 1988*b*). It is possible that our inability to observe clear and consistent relationships between TP and other variables including flow is related to limited sampling during the time periods of maximum TP export. Studies that have documented relationships between, for example, TP and Al during episodic acidification events have used automated water samplers to purposely sample high-flow events at frequent (e.g., 2 h) intervals (Roy et al. 1999; Reinhardt et al. 2004). Sampling frequency therefore may compromise efforts to identify drivers of differences in TP among catchments or changes in TP over time, and runoff "quality" (rather than quantity) may be a better determinant of TP export from catchments. Targeted storm sampling is currently underway at two of the study catchments to test this hypothesis.

Spatial patterns in TP

We could find no clear landscape or chemical controls on differences in TP concentrations among streams using long-term monitoring data. Previous research in this region has indicated that catchments with greater wetland coverage and higher DOC concentrations have higher TP levels in stream water (Dillon et al. 1991; Dillon and Molot 1997). In this study, we found a significant relationship between slope and percent wetland, slope and average DOC concentration (i.e., flatter catchments have a larger proportion of wetlands and higher DOC concentration), and DOC and average TP concentration, suggesting that wetlands are important sources of TP. However, the relationship between DOC and TP disappeared when streams with the highest average DOC concentration (DE5 and DE6) were removed from the regression. In contrast, Fe was strongly correlated with TP across all 11 catchments. It is clear that wetlands are important sources of TP, as they supply both organic P (associated with dissolved organic matter) and P that is liberated from Fe compounds under reducing (low oxygen) conditions (Devito and Dillon 1993*a*, 1993*b*; Carlyle and Hill 2001). Correlations between TP and Fe, as well as temporal patterns of TP and Fe within years (data not shown), indicate that redox processes are important controls on TP variations in these streams. Redox processes, however, are only important in periodically saturated zones within catchments, e.g., wetlands and riparian areas (Surridge et al. 2007), and the lack of a consistent relationship between TP and DOC (e.g., HP3A and PC1 have similar TP concentrations yet very different DOC levels) indicates that wetland coverage is not the sole determinant of differences in TP export among catchments. It should be noted that we have classified all areas of flat, periodically saturated organic soil as "wetland" in our "percent wetland" categorization, yet wetland "type" (i.e., beaver pond vs. swamp vs. riparian wetland) may also have an important influence on TP release (Devito et al. 1989), and this distinction was not made here.

Soil acidity status may contribute to differences in TP export among catchments if P adsorption is enhanced in acidic mineral soil (e.g., McDowell et al. 2002). We used Ca concentrations in stream water to indicate soil acidity status (Houle et al. 2006) and found no relationship between concentrations of TP and Ca in stream water. However, it should be noted that stream chemistry is not necessarily a good indicator of soil pH, and stream pH or Ca levels may be more indicative of soil depth than the acidity of upper horizons (Watmough and Dillon 2003*a*).

Phosphorus deposition

"Back of the envelope" mass budget estimates indicate that changes in stream export are large enough to account for declines in lake TP, whereas changes in direct atmospheric deposition of TP to lake surfaces are not the primary driver of long-term declines in lake TP. Although TP loads in deposition were generally lower in the most recent decade of record, the magnitude of change in deposition between the 1980s and 1990s (~5 $mg \cdot m^{-2}$) was relatively small compared with the decline in lake burden. Similarly, the decline in spring TP deposition between the first and final 5 years of record (~1 $mg \cdot m^{-2}$), although large enough to account for decreases in spring export at a few streams (e.g., PC1; 1.4 $mg \cdot m^{-2}$), could not explain the very large decreases in export observed at streams such as HP4 (5.0 $mg \cdot m^{-2}$) or DE5 and DE6 (35 $mg \cdot m^{-2}$ and 23 $mg \cdot m^{-2}$, respectively). Other factors must contribute to TP declines at these catchments.

It should be noted that measurement of TP deposition is notoriously difficult, and deposition estimates are associated with a large degree of error due to the inevitable contamination from internal catchment sources such as bird feces and local dust and pollen (Doskey and Ugoagwu 1989). Indeed, we have found strong correlations between TP and potassium concentrations in deposition, which could indicate a biological source of phosphorus (C. Eimers, unpublished data). Given the inherent difficulties in measuring TP deposition, the presence or absence of a significant trend in deposition is perhaps less important than a general tendency toward lower or higher values, as was observed in the annual and seasonal (spring and summer) time series. In addition, it should be noted that the magnitude of TP input in deposition (1980–2001 average = 16 $mg \cdot m^{-2} \cdot annum^{-1}$) is large compared with stream export (3.5–9.5 $mg \cdot m^{-2} \cdot annum^{-1}$). Similar to other forested catchments (e.g., Wood et al. 1984), the majority of atmospheric input is retained within catchments in all seasons. Therefore, any change in catchment retention efficiency over time could have a substantial impact on stream and lake budgets, and further work is required to examine the role of deposition in long-term declines in lake TP.

Long-term declines in lake TP concentrations are as yet unexplained, although this study indicates that decreases in catchment export are a contributing factor. Furthermore, decreases in annual stream export are due to declines in the spring, when stream flow is highest. Despite relatively fast flushing rates in the spring, which would presumably limit contact time between runoff and catchment surfaces, TP concentrations and export remain highly variable among catchments in the spring, and the majority of catchments retain TP, indicating that catchment properties remain an important determinant of TP export even during the snowmelt season. The causes of long-term declines in spring export remain unclear and are the focus of current research efforts in this region.

Acknowledgements

The data used in this study were provided by the Ontario Ministry of Environment Dorset Environmental Science Centre and were produced through the hard work and dedication of a large number of staff and students, both past and present. This paper is a contribution to the Natural Sciences and Engineering Research Council of Canada (NSERC) Strategic Grant project examining catchment controls on TP declines in central Ontario lakes.

References

Arnott, S.E., Keller, B., Dillon, P.J., Yan, N.D., Paterson, M., and Findlay, D. 2003. Using temporal coherence to determine the response to climate change in Boreal Shield lakes. Environ. Monit. Assess. **88**(1–3): 365–388. doi:10.1023/A:1025537628078. PMID:14570423.

Carlyle, G.C., and Hill, A.R. 2001. Groundwater phosphate dynamics in a river riparian zone: effects of hydrologic flowpaths, lithology and redox chemistry. J. Hydrol. (Amst.), **247**(3–4): 151–168. doi:10.1016/S0022-1694(01)00375-4.

Chapman, L.J., and Putnam, D.F. 1984. The physiography of southern Ontario. Ontario Geological Survey, Toronto, Ont.

Curtis, P.J. 1989. Effects of hydrogen ion and sulphate on the phosphorus cycle of a Precambrian Shield lake. Nature (London), **337**(6203): 156–158. doi:10.1038/337156a0.

Devito, K.J., and Dillon, P.J. 1993*a*. The influence of hydrologic conditions and peat oxia on the phosphorus and nitrogen dynamics of a conifer swamp. Water Resour. Res. **29**(8): 2675–2685. doi:10.1029/93WR00622.

Devito, K.J., and Dillon, P.J. 1993*b*. Importance of runoff and winter anoxia to the P and N dynamics of a beaver pond. Can. J. Fish. Aquat. Sci. **50**(10): 2222–2234. doi:10.1139/f93-248.

Devito, K.J., Dillon, P.J., and LaZerte, B.D. 1989. Phosphorus and nitrogen retention in five Precambrian shield wetlands. Biogeochemistry, **8**(3): 185–204. doi:10.1007/BF00002888.

Devito, K.J., Hill, A.R., and Dillon, P.J. 1999. Episodic sulphate export from wetlands in acidified headwater catchments: prediction at the landscape scale. Biogeochemistry, **44**(2): 187–203. doi:10.1007/BF00992978.

Dillon, P.J., and Molot, L.A. 1997. Effect of landscape form on export of dissolved organic carbon, iron and phosphorus from forested stream catchments. Water Resour. Res. **33**(11): 2591–2600. doi:10.1029/97WR01921.

Dillon, P.J., and Molot, L.A. 2005. Long-term trends in catchment export and lake retention of dissolved organic carbon, dissolved organic nitrogen, total iron and total phosphorus: the Dorset, Ontario, study, 1978–1998. J. Geophys. Res. **110**: G01002. doi:10.1029/2004JG000003.

Dillon, P.J., Molot, L.A., and Scheider, W. 1991. Phosphorus and nitrogen export from forested stream catchments in central Ontario. J. Environ. Qual. **20**: 857–864.

Dillon, P.J., Reid, R.A., and Evans, H.E. 1993. The relative magnitude of phosphorus sources for small, oligotrophic lakes in Ontario, Canada. Verh. Int. Verein. Limnol. **25**: 355–358.

Doskey, P.V., and Ugoagwu, B.J. 1989. Atmospheric deposition of macronutrients by pollen at a semi-remote site in northern Wisconsin. Atmos. Environ. **23**(12): 2761–2766. doi:10.1016/0004-6981(89)90556-8.

Eimers, M.C., Buttle, J.M., and Watmough, S.A. 2008. Influence of seasonal changes in runoff and extreme events on dissolved organic carbon trends in wetland- and upland-draining streams. Can. J. Fish. Aquat. Sci. **65**(5): 796–808. doi:10.1139/F07-194.

Hall, R.J., and Smol, J.P. 1996. Paleolimnological assessment of long-term water quality changes in south-central Ontario lakes affected by cottage development and acidification. Can. J. Fish. Aquat. Sci. **53**(1): 1–17. doi:10.1139/cjfas-53-1-1.

Hörnström, E. 1999. Long-term phytoplankton changes in acid and limed lakes in SW Sweden. Hydrobiologia, **394**: 93–102. doi:10.1023/A:1003513521651.

Houle, D., Ouimet, R., Couture, S., and Gagnon, C. 2006. Base cation reservoirs in soil control the buffering capacity of lakes in forested catchments. Can. J. Fish. Aquat. Sci. **63**(3): 471–474. doi:10.1139/f06-007.

Huser, B.J., and Rydin, E. 2005. Phosphorus inactivation by aluminium in Lakes Gårdsjön and Härsvatten sediment during the industrial acidification period in Sweden. Can. J. Fish. Aquat. Sci. **62**(8): 1702–1709. doi:10.1139/f05-083.

Jansson, M., Persson, G., and Broberg, O. 1986. Phosphorus in acidified lakes: the example of Lake Gardsjon, Sweden. Hydrobiologia, **139**(1): 81–96. doi:10.1007/BF00770243.

Jeppesen, E., Jensen, J.P., Sondergaard, M., and Lauridsen, T. 2005. Response of fish and plankton to nutrient loading reduction in eight shallow Danish lakes with special emphasis on seasonal dynamics. Freshw. Biol. **50**(10): 1616–1627. doi:10.1111/j.1365-2427.2005.01413.x.

Kopacek, J., Maresova, M., Hejzlar, H., and Norton, S.A. 2007. Natural inactivation of phosphorus by aluminium in preindustrial lake sediments. Limnol. Oceanogr. **52**: 1147–1155.

Libiseller, C., and Grimvall, A. 2002. Performance of partial Mann–Kendall tests for trend detection in the presence of covariates. Environmetrics, **13**(1): 71–84. doi:10.1002/env.507.

McDowell, R.W., Brookes, P.C., Mahieu, N., Poulton, P.R., Johnston, A.E., and Sharpley, A.N. 2002. The effect of soil acidity on potentially mobile phosphorus in a grassland soil. J. Agric. Sci. **139**(01): 27–36. doi:10.1017/S0021859602002307.

Meyer, J.L., and Likens, G.E. 1979. Transport and transformation of phosphorus in a forest stream ecosystem. Ecology, **60**(6): 1255–1269. doi:10.2307/1936971.

Neary, A.J., Mistray, E., and Vanderstar, L. 1987. Sulphate relationships in some central Ontario forest soils. Can. J. Soil Sci. **67**: 341–352.

O'Connor, E.M. 2007. Modeling mercury concentrations in fish of the Muskoka River Watershed — a mass balance approach involving dissolved organic carbon and mercury models. M.Sc. thesis, Trent University, Peterborough, Ont., Canada.

Paterson, A.M., Cumming, B.F., Smol, J.P., and Hall, R.I. 2004. Marked recent increases of colonial scaled chrysophytes in Boreal lakes: implications for management of taste and odour events. Freshw. Biol. **49**(2): 199–207. doi:10.1046/j.1365-2427.2003.01170.x.

Paterson, A.M., Dillon, P.J., Hutchinson, N.J., Futter, M.N., Clark, B.J., Mills, R.B., Reid, R.A., and Scheider, W.A. 2006. A review of the components, coefficients and technical assumptions of Ontario's Lakeshore Capacity Model. Lake Reservior Manage. **22**(1): 7–18. doi:10.1080/07438140609353880.

Prairie, Y.T., and Kalff, J. 1988*a*. Dissolved phosphorus dynamics in headwater streams. Can. J. Fish. Aquat. Sci. **45**: 200–209. doi:10.1139/f88-023.

Prairie, Y.T., and Kalff, J. 1988*b*. Particulate phosphorus dynamics in headwater streams. Can. J. Fish. Aquat. Sci. **45**: 210–215. doi:10.1139/f88-024.

Quinlan, R., Hall, R.I., Paterson, A.M., Cumming, B.F., and Smol, J.P. 2008. Long-term assessments of ecological effects of anthropogenic stressors on aquatic ecosystems from paleoecological analyses: challenges to perspectives of lake management. Can. J. Fish. Aquat. Sci. **65**(5): 933–944. doi:10.1139/F08-027.

Reinhardt, R.L., Norton, S.A., Handley, M., and Amirbahman, A. 2004. Dynamics of P, Al and Fe during high discharge episodic acidification at the Bear Brook Watershed in Maine, U.S.A. Water Air Soil Pollut. Focus, **4**(2/3): 311–323. doi:10.1023/B:WAFO.0000028362.48966.17.

Roy, S., Norton, S.A., Fernandez, I., and Kahl, J. 1999. Linkages of P and Al export at high discharge at the Bear Brook Watershed in Maine. Environ. Monit. Assess. **55**(1): 133–147. doi:10.1023/A:1006187304113.

Sen, P.K. 1968. Estimates of the regression coefficient based on Kendall's tau. J. Am. Stat. Assoc. **63**(324): 1379–1389. doi:10.2307/2285891.

Skjelkvåle, B.L., Stoddard, J.L., Jeffries, D.S., Tørseth, K., Høgåsen, T., Bowman, J., Mannio, J., Monteith, D.T., Mosello, R., Rogora, M., Rzychon, D., Vesely, J., Wieting, J., Wilander, A., and Worsztynowicz, A. 2005. Regional scale evidence for improvements in surface water chemistry 1990–2001. Environ. Pollut. **137**(1): 165–176. doi:10.1016/j.envpol.2004.12.023. PMID:15944047.

Surridge, B.W.J., Heathwaite, A.L., and Baird, A.J. 2007. The release of phosphorus to porewater and surface water from river riparian sediments. J. Environ. Qual. **36**(5): 1534–1544. doi:10.2134/jeq2006.0490. PMID:17766834.

Watmough, S.A., and Dillon, P.J. 2003*a*. Base cation and nitrogen budgets for seven forested catchments in central Ontario, 1983–1999. For. Ecol. Manage. **177**(1–3): 155–177. doi:10.1016/S0378-1127(02)00320-1.

Watmough, S.A., and Dillon, P.J. 2003*b*. Base cation and nitrogen budgets for a mixed hardwood catchment in south-central Ontario. Ecosystems (N.Y., Print), **6**(7): 675–693. doi:10.1007/s10021-002-0164-y.

Watmough, S.A., and Dillon, P.J. 2004. Major element fluxes from a coniferous catchment in central Ontario, 1983–1999. Biogeochemistry, **67**(3): 369–398. doi:10.1023/B:BIOG.0000015792.42624.57.

Wood, T., Bormann, F.H., and Voigt, G.K. 1984. Phosphorus cycling in a northern hardwood forest: biological and chemical control. Science (Washington, D.C.), **223**(4634): 391–393. doi:10.1126/science.223.4634.391. PMID:17829887.

Yan, N.D., Somers, K.M., Girard, R.E., Paterson, A.M., Keller, W., Ramcharan, C.W., Rusak, J.A., Ingram, R., Morgan, G.E., and Gunn, J.M. 2008. Long-term trends in zooplankton of Dorset, Ontario, lakes: the probable interactive effects of changes in pH, total phosphorus, dissolved organic carbon, and predators. Can. J. Fish. Aquat. Sci. **65**(5): 862–877. doi:10.1139/F07-197.

Effects of predation from juvenile herring (*Clupea harengus*) on mortality rates of capelin (*Mallotus villosus*) larvae

Elvar H. Hallfredsson and Torstein Pedersen

Abstract: Predation has been suggested as a cause of substantial mortality of fish larvae to the degree that it might influence recruitment. This field-based study concludes that juvenile herring (*Clupea harengus*) as small pelagic predator can significantly affect mortality rates of the planktonic larvae of capelin (*Mallotus villosus*) in the Barents Sea. Surveys were carried out in the summers of 2001 and 2003. In 2001, juvenile herring were widely distributed and overlapped with capelin larvae over a wide area, whereas in 2003, the herring were more aggregated. The study focused on predation in the areas of predator–prey overlap. Capelin larvae were observed in the herring stomachs at 11 of 24 stations and at 8 of 16 stations where herring were caught in 2001 and 2003, respectively. At those stations, an estimated 7.3% and 9.9% of the capelin larvae were eaten by herring per day in 2001 and 2003, respectively. Statistical models revealed that density of capelin larvae and copepods and occurrence of euphausiids in the stomachs affected the number of capelin larvae per predator stomach. A simplified model with only capelin larvae density as predictor was converted to a functional response relationship using an experimentally derived digestion rate estimate for capelin larvae in herring stomachs.

Résumé : On a suggéré que la prédation était la cause d'une importante mortalité des larves de poissons au point de peut-être affecter le recrutement. Notre étude réalisée sur le terrain conclut que le rôle des jeunes harengs (*Clupea harengus*) comme petits prédateurs pélagiques peut affecter de façon significative les taux de mortalité des larves planctoniques de capelans (*Mallotus villosus*) dans la mer de Barents. Des inventaires ont été faits durant les étés 2001 et 2003. En 2001, les jeunes harengs avaient une répartition étendue qui chevauchait celle des larves de capelans sur une grande surface, alors qu'en 2003, les harengs avaient une répartition plus contagieuse. Notre étude s'est concentrée sur la prédation dans les zones de chevauchement des prédateurs et des proies. Les larves de capelans se sont retrouvées dans les estomacs de harengs dans respectivement 11 des 24 stations et 8 des 16 stations de capture de harengs en 2001 et 2003. Dans ces stations, nous estimons que respectivement 7,3 % et 9,9 % des larves de capelans étaient consommées quotidiennement par les harengs en 2001 et 2003. Des modèles statistiques montrent que la densité des larves de capelans, la densité des copépodes et la présence des euphausiidés dans les estomacs affectent le nombre de larves de capelans par estomac de prédateur. Nous avons converti un modèle simplifié, qui ne contient que la densité des larves de capelans comme variable prédictive, en une relation de réponse fonctionnelle, à l'aide d'une estimation du taux de digestion (provenant de travaux expérimentaux) des larves de capelans dans les estomacs de harengs.

[Traduit par la Rédaction]

Introduction

Pelagic planktivore fishes are major zooplankton consumers in many ecosystems, but their impact as predators on ichthyoplankton is poorly understood. However, planktivorous pelagic fishes have been pointed out as potential major sources for mortality of fish eggs and larvae (Hunter 1981; Bailey and Houde 1989; Takasuka et al. 2004). Due to methodological challenges such as the rapid digestion rates of fish larvae in predator stomachs and aggregation of predator and prey (Hunter 1981), there are few estimates of mortality rates that pelagic fish predators impose on fish eggs and larvae. Despite this, there are some promising quantitative studies of fish predation on early life stages (Köster and Möllmann 2000; Munk 2002; Pepin 2006).

The capelin (*Mallotus villosus*) stock in the Barents Sea is important both ecologically and commercially (Gjøsæter 1998) and has shown dramatic biomass fluctuations caused mostly by large recruitment variability (Gjøsæter and Bogstad 1998; Mikkelsen and Pedersen 2004). Observations of weak capelin year classes following the presence of a high abundance of juvenile herring (*Clupea harengus*) in the Barents Sea Hamre (1985, 1991, 1994) led to the hypothesis that the recruitment to the capelin stock was regulated by predation from juvenile herring. This was supported by other investigations (Moksness and Øiestad 1987; Gjøsæter and

Received 18 June 2008. Accepted 29 April 2009. Published on the NRC Research Press Web site at cjfas.nrc.ca on 26 September 2009.
J20625

E.H. Hallfredsson[1,2] and T. Pedersen. Department of Aquatic BioSciences, The Norwegian College of Fishery Science, University of Tromsø, N-9037 Tromsø, Norway.

[1] Corresponding author (e-mail: elvarh@imr.no).

[2] Present address: Institute of Marine Research, P.O. Box 6404, N-9294 Tromsø, Norway.

doi:10.1139/F09-105

Bogstad 1998; Huse and Toresen 2000), but estimates of predation mortality rates from juvenile herring on capelin larvae have been lacking. The strength of predator–prey interactions depends partly on the degree of overlap in space and time (Garrison et al. 2000; Hallfredsson and Pedersen 2007), and the spatial and temporal overlap of herring and the early life stages of capelin will be reflected by the life history of these two planktivore species.

The main spawning for the Barents Sea capelin is in March and April north of 68°N along the coast of northern Norway and northwest Russia, but in some years, a significant proportion of the spawning stock may spawn during May and June in the eastern spawning areas (Olsen 1968; Røttingen 1990; Gjøsæter 1998). Capelin spawn on coarse substrate close to the coast, and the larvae are advected offshore north- and east-wards (Gjøsæter 1998). Immature 1 year and older capelin inhabit the central and northern part of the Barents Sea. Practically all of the spawning stock dies after spawning, making the stock biomass largely reflecting variability in recruitment (Gjøsæter 1998; Gjøsæter et al. 2002; Christiansen et al. 2008). The Norwegian spring-spawning herring (NSSH) stock spawns mainly south of 68°N off the west coast of Norway, and the larvae drift north- and east-wards from the spawning grounds into the Barents Sea during their first summer (Fig. 1), and juveniles inhabit the southern part of the Barents Sea for 2–3 years (Dragesund et al. 1980; Røttingen 1990; Gjøsæter 1998). The recruitment of NSSH varies substantially (Dragesund 1970) with the result that biomass of juvenile herring in the Barents Sea during 1970–2000 ranged from almost absent to about 3 million tonnes (t) (Mikkelsen and Pedersen 2004). The year-class strength of NSSH is related to temperature variations, with larger year classes occurring more frequently in warmer years with extended inflow of Atlantic water (Hamre 1994; Ottersen and Loeng 2000).

In spring and summer, herring juveniles migrate from the eastern Barents Sea towards the south and west and enter the same waters as capelin larvae that are drifting north- and east-wards (Fig. 1). A belt-like distribution of juvenile herring along the northeastern part of the Finnmark coast appears to be common when juvenile herring are abundant in the Barents Sea (Huse and Toresen 2000; Johansen 2002; Lindstrøm et al. 2002). The juvenile herring are distributed south of the polar front during summer in the Barents Sea and tend to increase their distribution area during summer and early autumn (Fig. 1) (Johansen 2002). Predation from juvenile herring on capelin larvae has been observed (Huse and Toresen 2000; Godiksen et al. 2006), but it has been uncertain whether predation mortality is the main cause of the negative herring impact on capelin recruitment (Gjøsæter and Bogstad 1998; Mikkelsen and Pedersen 2004). Huse and Toresen (1995, 2000) found that the predation imposed by juvenile herring on capelin larvae during their investigation in 1992 and 1993 probably was an important mortality factor in those years, and they advocated that further process-oriented studies were necessary to estimate mortality rates from herring on capelin larvae. Identification of fish larvae and quantification of predation mortality are difficult in the field due to rapid digestion rates of fish larvae in predator stomachs (Folkvord 1993), but an estimate of digestion rate for capelin larvae preyed upon by herring is now available (Hallfredsson et al. 2007). Because digestion rates depend on temperature (Hunter and Kimbrell 1980), the relatively low temperature in the Barents Sea could be favourable for detection of fish larvae in predator stomachs.

In this study, we attempted to estimate the mortality rates of capelin larvae caused by juvenile herring based on two surveys in the southern Barents Sea in 2001 and 2003. The effects of spatial overlap between capelin larvae and juvenile herring are considered, as well as overlap with krill and copepods, which are alternative prey for the herring. We examined if predation intensity and capelin larvae density were correlated, and a functional response for herring preying on capelin larvae is derived.

Material and methods

Investigation area and trawl sampling

Data were collected on surveys with R/V *Johan Ruud* from 30 July to 10 August 2001 and R/V *Jan Mayen* from 23 June to 7 July 2003 (Table 1). The survey design was planned based on prior information about the abundance of capelin larvae and herring from surveys by the Institute of Marine Research in Norway conducted in June prior to our surveys both years (Institute of Marine Research 2001*a*, 2003*a*). Herring and other pelagic fish were sampled using a pelagic trawl, which had a 12 × 12 m opening and a codend liner with mesh size 4 mm. If no distinct aggregated registrations of fish were observed on the echosounder, the trawl was hauled with the headline at the surface using buoys. If aggregations were observed, trawling was attempted at the depth of the aggregations. Each haul lasted 20 min, except for the trawling on aggregations, where the trawling was terminated when the trawl had passed the aggregations. In 2001, when capelin spawned on both westerly and easterly spawning grounds, collections were made at 54 trawl stations between 19°E and 32°E. In 2003, capelin spawned mainly west of North Cape (26°E), and we covered an area from 24°E to 32°E with 41 trawl stations (Table 1). Distances between most stations were about 28 km in the north–south direction and about 37 km in the east–west direction. In 2003, a second coverage was conducted to search for herring schools without using the survey grid, and the stations were aimed at aggregations registered on the echosounder.

Vertical temperature profiles were measured at each station using a Seabird 911 Plus CTD recorder (Sea-Bird Electronics Inc., Bellevue, Washington).

Acoustical abundance estimation of herring

Abundance of herring was estimated using acoustic echo integration. The echosounder frequency was 38 kHz. In judging the acoustical echograms, the nautical area scattering coefficient (S_A) values were allocated to species groups based mostly on the species relative abundance in the pelagic trawl catches. The judging was done primarily by the first author, but in case of doubt, the second author and an experienced acoustics operator at the Norwegian Institute of Marine Research were consulted. Acoustic data from depths below 100 m were not used. To calculate the density of herring for each station, the S_A values were averaged to the nearest 10 nm^2 before and after the station. The target

Fig. 1. Overview of the Barents Sea with the major current patterns (based on Loeng 1989). Atlantic currents, solid arrows; Arctic currents, broken arrows; coastal currents, dotted arrows; polar front, broken lines; distribution of juvenile herring in September 2003, darker shading (from Institute of Marine Research 2003*b*). Labels on inset: NC, North Cape; NP, Nordkyn Peninsula; T, Tanafjord; VP, Varanger Peninsula; VF, Varangerfjord.

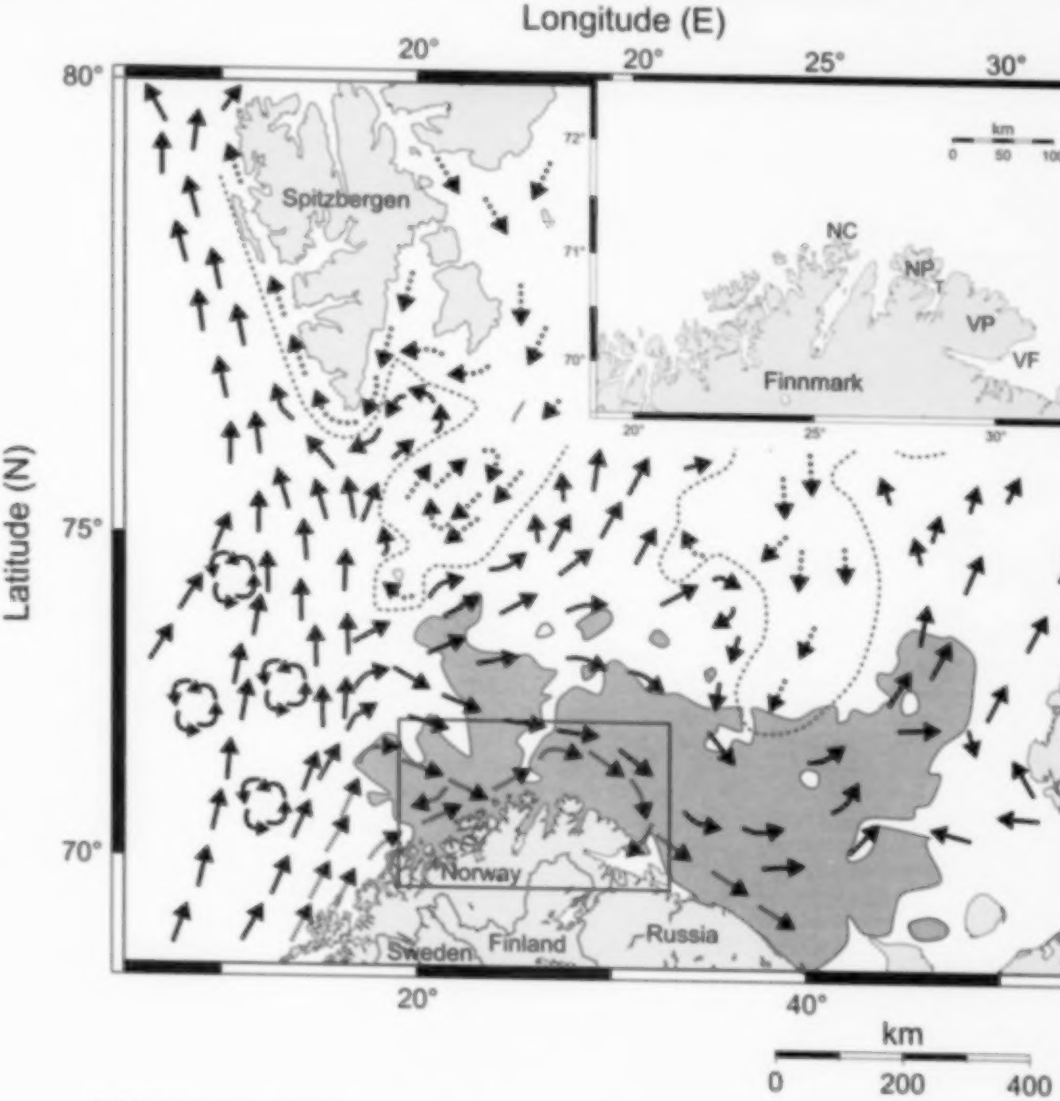

Table 1. Summary of surveys.

Date	Research vessel	No. of trawl hauls	Coverage number	No. of hauls with herring	No. of stomachs investigated
31 July – 10 August 2001	*Johan Ruud*	54	1	24	674
23 – 29 June 2003	*Jan Mayen*	41	1	8	87
29 June – 6 July 2003	*Jan Mayen*	40	2	8	335

strength (TS) of the herring was estimated using the average total length (L) at each station following the relation given by Foote (1987) ($TS = 20\log_{10}L - 71.9$). For stations in 2001 where herring were not present in the trawl catches, the average length at the nearest station with herring was used. For stations taken in 2003 with more infrequent herring catches resulting in long distances between stations with herring, the average length of the total catches of herring that year was used. Total length was converted from standard length (SL) as $L = 1.1507 \cdot SL$ (www.fishbase.org).

The body wet weight (*W*, grams) of herring was estimated using the relation $W = 0.0077{\cdot}\mathrm{SL}^{3.135}$, obtained from nonlinear regression based on the weights and standard lengths (SL in cm) from 2001 ($N = 1018$, $R^2 = 0.97$).

Abundance of capelin larvae and zooplankton

Shortly before or after each trawl haul, capelin larvae and zooplankton were sampled as close to the trawl trajectory as possible, using a GULF III high-speed plankton sampler with mesh size 375 µm (Alvheim 1984). With a vessel speed of 5 kn and a wire speed of $0.5\ \mathrm{m{\cdot}s^{-1}}$, the gear was lowered to a depth of about 60 m and then hauled up. In 2001, 250 m of wire was lowered from the gear, which corresponds to a depth of approximately 60 m. In 2003, the exact depth of the GULF III sampler was monitored using a Scanmar depth sensor. A flow meter was used to measure the water velocity through the net in the GULF III sampler, and the water volume filtered was subsequently calculated. The sampled capelin larvae and other fish larvae were counted, and the larvae and other zooplankton were conserved in 96% ethanol in separate bottles. Abundance estimates of the krill and copepods were estimated by counting from subsamples, and copepods were identified to species and stages.

Spearman rank correlation coefficient (r_S) was used to test whether abundances of capelin larvae, krill, and copepods estimated by GULF III sampler, numbers of capelin larvae caught per trawl haul, and acoustical estimate of herring were significantly correlated.

Stomach content analysis

Most of the herring were frozen immediately after hauling the trawl and kept at −18 °C until analysis at the laboratory. In 2003, 30 stomachs from each haul, if available, were analysed onboard the research vessel. The stomachs analysed onboard were kept cool on ice prior to analysis, and stomachs analysed in the laboratory were individually thawed. The SL and *W* of the herring were measured, and the stomachs were dissected. Presence of the characteristic double ventral row of melanophores was used as a secure identification of capelin larvae (Templeman 1948). Presence of a small vertebrae eye with lens (<1 mm in diameter) was taken as a secure identification of a fish larva. The numbers of capelin larvae were counted. For most of the stomachs, the presence of different zooplankton taxa was noted. The stomachs from 330 herring caught at three stations with trawling on a dense aggregation of herring in the second coverage in the 2003 survey reported by Godiksen et al. (2006) were included in the material of this investigation.

Mortality rates

The average number of capelin larvae eaten per juvenile herring per day (N_e) was estimated by the formula (Bajkov 1935; Munk 2002)

$$N_e = \mathrm{MSC} \cdot \mathrm{D} \cdot 24\ \mathrm{h}$$

where MSC is the mean number of capelin larvae found in the herring stomachs, and *D* is the digestion rate to disappearance, equal to $0.30{\cdot}\mathrm{h}^{-1}$ (standard error (SE) = 0.031) as estimated in digestion rate experiments by Hallfredsson et al. (2007). The average sea temperatures from surface to a depth of 50 m were 8.3 °C (standard deviation (SD) = 1.3) in 2001 and 6.6 °C (SD = 1.1) in 2003. This is close to the temperature of 7.6 °C in the digestion rate experiments of Hallfredsson et al. (2007), suggesting that the use of *D* may be appropriate for the field data. N_e was calculated for each station *i*, as well as combined for each year and coverage. Total numbers of capelin larvae eaten by herring at each station per day per square metre (N_{Tei}) was calculated as the product of N_e and juvenile herring abundance as estimated by the acoustics. Percentage daily predation mortality rate (DM) for each year and coverage was estimated as

$$\mathrm{DM} = 100\frac{\sum_{i=1}^{n} N_{Tei}}{\sum_{i=1}^{n} N_{Ci}}$$

where *i* is a station index, *n* is number of stations, and N_{Ci} is capelin larvae abundance at station *i* as estimated by the GULF III samples. Separate estimates of DM were calculated for all stations and for stations with herring in the trawl catches. Percentile confidence intervals for DM were estimated by bootstrapping (Efron and Tibshirani 1993).

The Spearman rank correlation coefficient (r_S) was used to investigate if abundance of capelin larvae and occurrence of capelin larvae in herring stomachs were correlated, as well as if abundance of capelin larvae and numbers of capelin larvae predated per herring per day were correlated. Stations with 10 or more herring in the trawl catches were included in the correlation tests.

Index of overlap O_{ij} was calculated according to Williamson (1993) for herring as predator and capelin larvae, krill, and copepods as prey. O_{ij} is equal to one when either prey or predator populations (or both) are uniformly distributed. Values of less than one represent lower overlap, with a theoretical lower limit of zero. When the values are greater than one, the overlap is greater than would be expected with uniform prey and predator distributions, and the upper limit is determined by the number of patches sampled (Williamson 1993).

Models

A model was constructed to predict the number of capelin larvae in the individual herring stomachs (SC) and fitted to data using log-likelihoods assuming a negative binomial error distribution. The negative binomial distribution has variance = mean + *k* mean^2, where *k* is a dispersion coefficient. If $k = 0$, the distribution equals Poisson distribution (variance = mean). If a log-likelihood ratio test showed that the negative binomial distribution gave a significantly better fit than the Poisson distribution, then the negative binomial distribution was preferred (Cameron and Trivedi 1998). The analysis was performed using the "mle" routine in the stats4 package in R (R Development Core Team 2008). In the function "dnbinom" for the negative binomial error distribution, *k* is represented by the parameter size equal to 1/*k*. The models (models 1 and 2) were fitted to individual herring with the number of capelin larvae in herring stomachs as the dependent variable; capelin larvae density as estimated by the GULF III samples (C_{capG}), numbers of capelin larvae in the pelagic trawl (C_{capT}), densities at stations (m^{-2}) of krill (× 10^{-3}, C_{krill}) and copepods (× 10^{-3}, C_{cop}), and occurrence of krill (O_{krill}) and copepods (O_{cop}) in the individual herring stomachs as the independent variables. O_{krill} and O_{cop} had values of either 0 or 1. A model assuming a linear relation between SC and capelin larvae density (model 1) (Holling type-I functional response; see Holling 1959), with parameters $P1$ to $P6$, was formulated as

$$\mathrm{SC} = (e^{P1} \cdot C_{\mathrm{capG}} + e^{P2} \cdot C_{\mathrm{capT}}) \times e^{(P3 \cdot \sqrt{C_{\mathrm{cop}}} + P4 \cdot \sqrt{C_{\mathrm{krill}}} + P5 \cdot O_{\mathrm{cop}} + P6 \cdot O_{\mathrm{krill}})} + C$$

where C is a parameter that was necessary because SC had to be positive and at some stations capelin larvae was registered in herring stomachs but no larvae were caught by GULF III and trawl (i.e., $C_{\mathrm{capG}} = 0$, $C_{\mathrm{capT}} = 0$). The rationale for using these two variables for expressing the capelin prey abundance for small and large capelin larvae, respectively, was that the GULF III probably underestimated the number of capelin larvae longer than 20 mm in length, whereas the pelagic trawl caught very few capelin larvae less than 20 mm in length (see fig. 5 in Hallfredsson and Pedersen 2007).

An alternative model (model 2) with a Holling type-II functional response (see Holling 1959) was formulated as

$$\mathrm{SC} = (e^{P1} \cdot C_{\mathrm{capG}} \cdot \mathrm{ks}/(\mathrm{ks} + C_{\mathrm{capG}}) + e^{P2} \cdot C_{\mathrm{capT}}) \times e^{(P3 \cdot \sqrt{C_{\mathrm{cop}}} + P4 \cdot \sqrt{C_{\mathrm{krill}}} + P5 \cdot O_{\mathrm{cop}} + P6 \cdot O_{\mathrm{krill}})} + C$$

where ks is the half-saturation coefficient.

The significance of variables in models 1 and 2 was determined applying a dynamic bottom-up approach as described by Posada and Crandall (2001), using log-likelihood ratio tests. Additionally, the sensitivity of the models with regard to the various significant parameters was examined.

A simplified model (model 3) without the terms for alternative prey effects and with capelin density estimates (C_{capG} and C_{capT}) as the only independent variables was fitted to the data as

$$\mathrm{SC} = e^{P1} \cdot C_{\mathrm{capG}} \cdot \mathrm{ks}/(\mathrm{ks} + C_{\mathrm{capG}}) + e^{P2} \cdot C_{\mathrm{capT}} + C$$

Visualization of spatial distributions

Colour-coded plots were produced to visualize spatial distributions of juvenile herring, capelin larvae, krill, and copepods by using the plot function in SYSTAT version 10.2 (SYSTAT 2004) and the DWLS (distance-weighted least-squares smoothing) routine with tension set to 0.1.

Results

Predation mortality

In total, for all stations where herring were caught, it was estimated that 7.3% (95% confidence interval (CI) = 1.8–18.4) of the capelin larvae were eaten by herring per day in 2001. In 2003, for all stations with herring, 9.9% (95% CI = 0.6–22.6) of the capelin larvae were estimated to be preyed upon by herring per day. If all stations were included when estimating the overall abundance of capelin larvae, 2.6% and 0.004% of the capelin larvae stock was estimated to be preyed upon by herring per day in 2001 and during the first coverage in 2003, respectively. At the three stations taken at the large aggregation of herring in the second coverage in 2003 north of 29°N (Fig. 2*b*), an average of 51% of the capelin larvae were estimated to be predated by herring per day.

Abundance and distribution

Herring were mainly distributed in the eastern part of the investigation area in both 2001 and 2003, but closer to the coast of the Varanger Peninsula in 2001 than in 2003 (Fig. 3*a*). The densities of capelin larvae captured by the GULF III sampler were generally low in 2001, with a maximum of 40 larvae·m^{-2} in the Varangerfjord area on a station at 31°20′E, 70°21′N (Fig. 3*b*). The krill abundance was also high in this area in 2001 (Fig. 4*a*), whereas copepods were most abundant in the western part of the investigation area in that year (Fig. 4*b*). In 2003, the density of capelin larvae was considerably higher than in 2001, with a maximum of 576 larvae·m^{-2} near the Nordkyn Peninsula (71°N, 28°E) (Fig. 3*b*). Abundances of capelin larvae, copepods, and krill were very low in the northeastern part of the investigation area in 2003, whereas herring were very abundant that year (Figs. 3 and 4). The catches of capelin larvae by pelagic trawl were more westerly distributed in both 2001 and 2003 compared with the abundance estimated from the GULF III samples (Figs. 3*a* and 4*b*).

The average standard length of herring was 15.8 cm (SD = 3.0 cm) and 11.1 cm (SD = 0.9 cm) in 2001 and 2003, respectively, with length showing a bimodal distribution in 2001 (Fig. 5). In 2001, herring were caught at 24 of 54 stations, and at seven of these stations, less than five herring were caught. In 2003, herring was caught at eight of 41 stations in the first coverage (Table 1); at six of these stations, less than five herring were caught. Fewer and larger schools were observed by the echosounder in 2003 than in 2001 (Table 2). This higher degree of aggregation was reflected in the relatively fewer number of stations with herring catches in the 2003 coverage with prelocated stations compared with the 2001 coverage (Table 1; Fig. 2). The average abundance of herring for the stations with overlap of capelin larvae and herring was 0.23 and 1.35 individuals·m^{-2} for 2001 and 2003, respectively. During the second coverage in 2003, a dense school of herring was found in the area outside Tanafjord (29°12′E, 71°04′N), with a horizontal extension of about 1.5 km, and the average biomass was estimated from three passes to be 8985 t (SD = 751). Three trawl stations were aimed at this school (Godiksen et al. 2006).

Occurrence of predation and numbers eaten

Frequency of occurrence of capelin larvae in the herring stomachs ranged from 0% to 42% at the stations in 2001 and from 0% to 62% at the stations in 2003 (Fig. 2*a*). The highest values in 2003 were at the stations where trawling was aimed for dense schools of herring. The estimated numbers of capelin larvae eaten by herring per square metre per day at stations with herring in the catches ranged from 0 to 4.6 (average = 0.30, SD = 0.93) in 2001 and from 0 to 62.1 (average = 6.77, SD = 17.82) in 2003 (Fig. 2*b*).

High occurrence (42%) of capelin larvae in the stomachs at low GULF III estimated abundance (1·m^{-2}) of capelin larvae was only observed at one station (station 48) in 2001 lo-

Fig. 2. (*a*) Occurrence (%) of capelin larvae in herring stomachs and (*b*) estimated numbers of capelin larvae preyed upon by herring (no.·m^{-2}·day^{-1}). The + symbols indicate stations where no herring were caught. The arrows indicate where three hauls were taken in 2003.

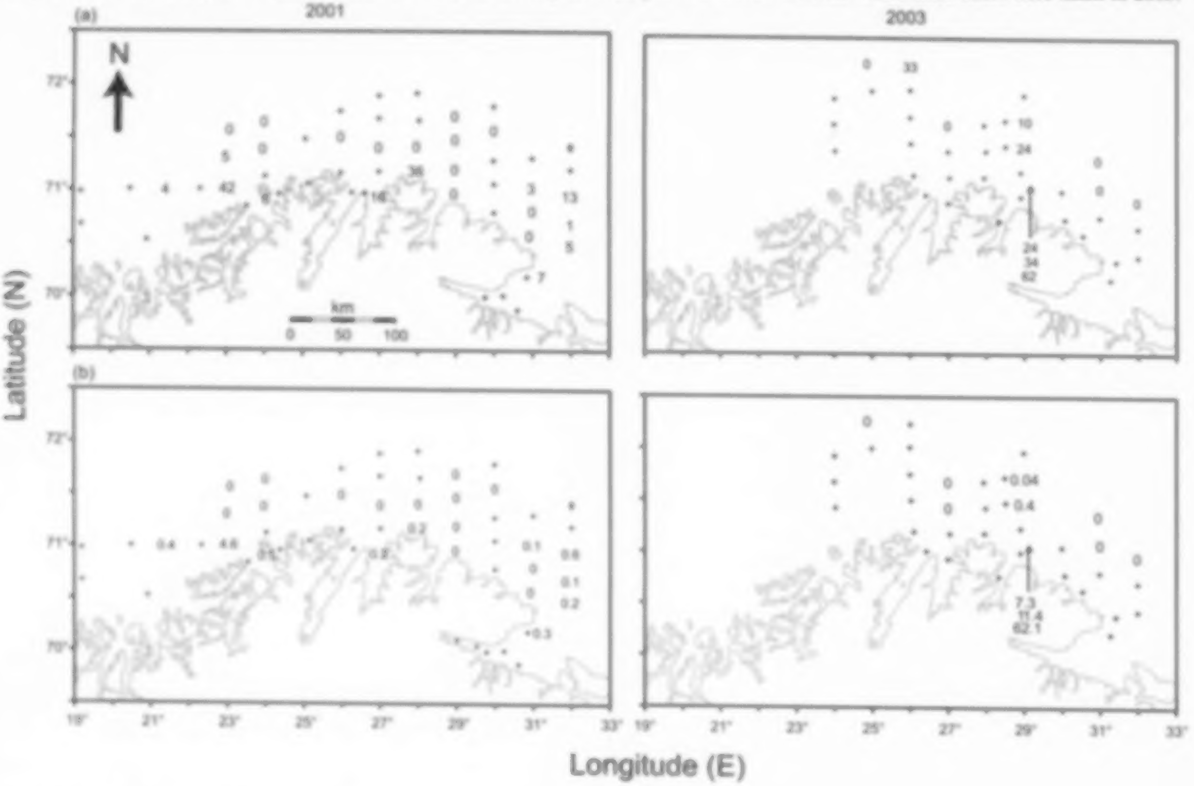

cated at 23°03′E, 71°01′N in the western part of the investigation area. At the same station, each herring had, on average, predated 17 capelin larvae per day, the second-most recorded number for the stations. At this station, capelin larvae were numerous in the trawl (Fig. 3*c*), which caught large capelin larvae relative to the GULF III samples.

Correlation between capelin larvae density and predation intensity

At all stations with herring where the abundance of capelin larvae was greater than 10·m^{-2}, capelin larvae were found in more than 7% of the herring stomachs (Fig. 6) and the numbers predated per herring per day for these station were generally greater than those found on stations where capelin larvae were less abundant (Fig. 7). The density of capelin larvae and occurrence of capelin larvae in the herring stomachs was significantly correlated ($r_S = 0.59$, *t* test, df = 17, $p = 0.008$) for stations with 10 or more herring in the trawl catches. The number of capelin larvae eaten per herring per day was also significantly correlated to density of capelin larvae ($r_S = 0.47$, *t* test, df = 17, $p = 0.041$) for stations with more than 10 herring in the trawl catches.

Predation models, spatial overlap, and functional response

The nonlinear Holling type-II formulation for number of larvae per predator stomach as a function of capelin larvae density in model 2 gave a better fit than the linear alternative in model 1 (Tables 3 and 4). The densities of copepods and occurrence of krill in the herring stomachs had significant negative and positive effects on SC, respectively (Tables 3 and 4), and the sensitivity analysis revealed that the effects of the alternative prey were large (Table 5).

A high mortality scenario (scenario 7, Table 5) with low copepod density and high krill occurrence increased the predation rate by 279% relative to the key scenario representing average conditions. In contrast, a low mortality scenario with high copepod density and low krill occurrence reduced the mortality by 92% relative to the key scenario (Table 5).

At the station level, densities of krill and capelin larvae sampled by GULF III were positively correlated for both years (Table 6). Copepods and capelin larvae as registered in the GULF III samples were not correlated, whereas copepods and krill were correlated. In 2003, herring was negatively correlated with krill and capelin larvae and not significantly correlated with copepods. The overlap index O_{ij} showed that overlap between herring and capelin larvae in 2001 was considerably higher than expected for uniform spatial distribution for both or one of the species, whereas it was less than expected for uniform distribution in 2003 (Table 7). The same applied for overlap between herring and krill. The overlap between herring and copepods in 2001 was as expected if one or both species were uniformly spatially distributed, whereas it was less than would be expected with uniform distribution in 2003.

Fig. 3. Spatial distributions of (*a*) herring (tonnes·km^{-2}), (*b*) capelin larvae densities (no.·m^{-2}) from the GULF III samples, and (*c*) capelin larvae catches in the pelagic trawl (numbers). To avoid extreme values masking the distribution of lover densities, a threshold value was chosen for each species. On stations with values higher than the threshold, the densities were fixed at the threshold value for the plots and the actual numbers are given on top. For other stations, the diameter of the circles reflects the densities as a proportion of the threshold value for that species. The arrows in (*a*) and (*b*) indicate the position of the herring aggregation where three hauls were taken in 2003.

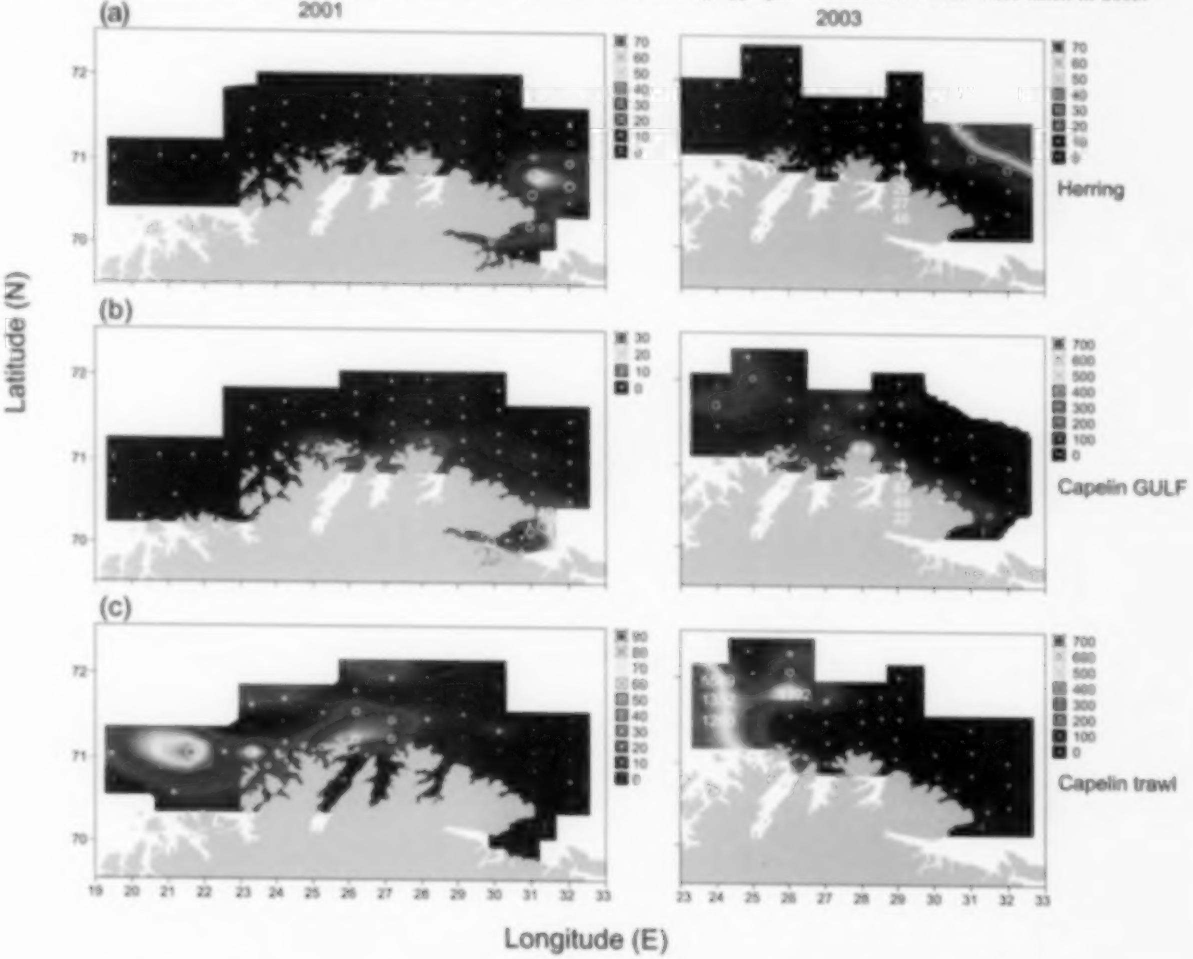

Model 3 fitted to the observed data gives SC = $e^{-2.84}$·C_{capG}·38.0/(38.0 + C_{capG}) + $e^{-4.86}$·C_{capT} + 0.02 (Table 3). By setting the number of capelin larvae caught per trawl (C_{capT}) in model 3 equal to zero and ignoring *C*, using the Bajkov formula and the estimate for digestion rate *D* of 0.3 h^{-1} from Hallfredsson et al. (2007), a functional response equation for the number predated per day per herring (N_e) as a function of capelin larvae abundance was obtained; N_e = SC·0.3 h^{-1}·24 h = 0.42·C_{capG}·(38.0/(38.0 + C_{capG})) (Fig. 8). This equation implies that the predation rate from one herring under 1 m^2 in the upper 60 m of the water column during one day in areas with spatial overlap will vary with larvae density.

Discussion

Studies on survival of fish larvae have focused to a large degree on bottom-up controlled mechanisms such as the match–mismatch concept (Cushing 1990). Top-down processes such as predation have been recognised as an important cause of mortality on eggs and larvae (Bailey and Houde 1989) but not as much studied, partly because of practical challenges such as difficulties of detecting larvae in predator stomachs due to rapid digestion. This study shows that predation mortality from herring on fish larvae may be quantified based on stomach samples. Predation from herring on early fish stages has been frequently observed in several ecosystems (Last 1989; Ellis and Nash 1997; Segers et al. 2007) and stock–recruitment modelling indicates a significant effect of herring predation on fish recruitment (Gjøsæter and Bogstad 1998; Mikkelsen and Pedersen 2004; Huse et al. 2008).

The average predation mortality of 7.3%·day^{-1} and 9.9%·day^{-1} in areas with prey–predator overlap in 2001 and 2003, respectively, suggests that herring may be a very sig-

Fig. 4. Spatial distributions of (*a*) krill and (*b*) copepods (no.·m^{-2}). To avoid extreme values masking the distribution of lower densities, a threshold value was chosen for each species or taxa. On stations with values higher than the threshold, the densities were fixed at the threshold value for the plots and the actual numbers are given on top. For other stations, the sizes of the circles reflect the densities as a proportion of the threshold value.

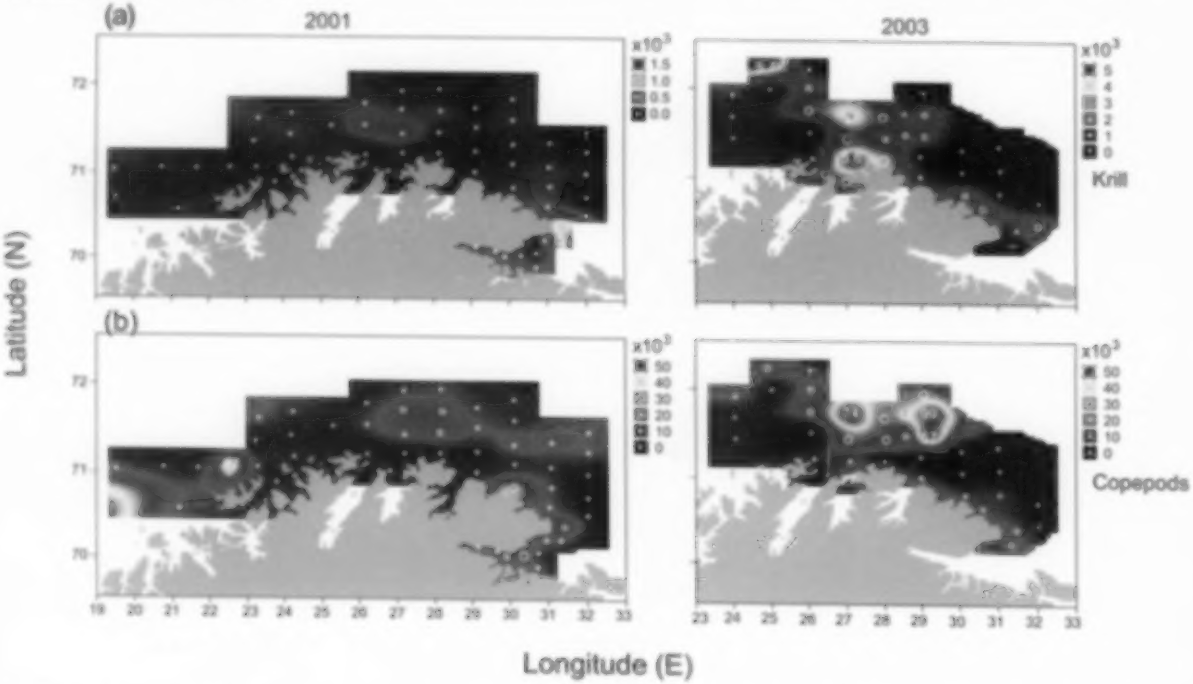
(a)
2001
2003
x10³
1.5
1.0
0.5
0.0
x10³
5
4
3
2
1
0
Krill
(b)
x10³
50
40
30
20
10
0
x10³
50
40
30
20
10
0
Copepods
Latitude (N)
72
71
70
19 20 21 22 23 24 25 26 27 28 29 30 31 32 33
23 24 25 26 27 28 29 30 31 32 33
Longitude (E)

Fig. 5. Length distribution for herring, weighted by acoustical densities for each station and averaged over all stations: 2001 data, solid bars; 2003 data, open bars.

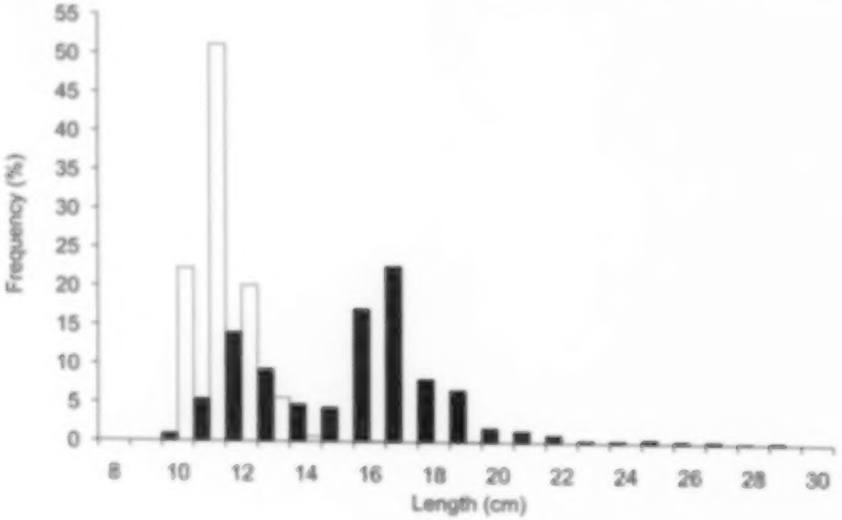

nificant predator of capelin larvae in the area of overlap. The total mortality rates in the field for fish larvae of other species with body sizes similar to that of the capelin larvae in this study are often in the range of 5%–15%·day^{-1} (Peterson and Wroblewski 1984; McGurk 1986; Houde 1997). In predator-free enclosure experiments, capelin larvae had low mortality rates of 1.3%·day^{-1}, indicating high survival potential in the absence of predators and at moderate prey levels (Ivarjord et al. 2008; Pedersen and Fossheim 2008). For fish predators preying on herring larvae in mesocosms,

Table 2. Herring schools encountered during the acoustic surveys.

Year	No. of registered schools	Estimated average biomass per school (tonnes)
2001	127	446 (698)
2003	54	2359 (3914)

Note: Standard deviation (SD) is given in parentheses. For 2003, only the schools registered in the first coverage are included.

Fig. 6. The relationship between the abundance and occurrence of capelin larvae in herring stomachs. Each data point refers to a single station with 10 or more herring in the trawl catches. 2001 data, solid circles; 2003 data, open triangles.

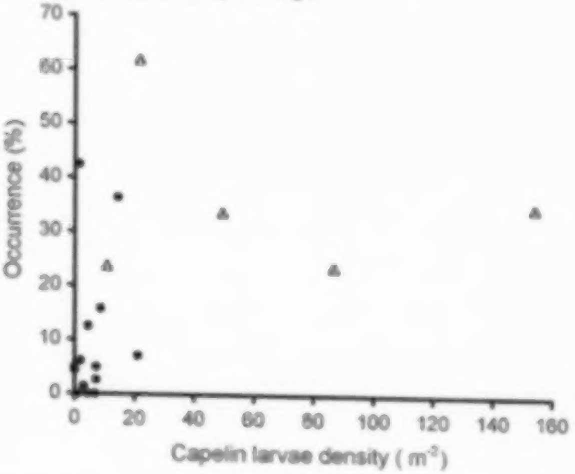

Fig. 7. Station averages for number of capelin larvae preyed upon per herring per day plotted against capelin larvae abundance from GULF III samples in 2001 and 2003. Each data point refers to a single station with 10 or more herring in the trawl catches. 2001 data, solid circles; 2003 data, open triangles.

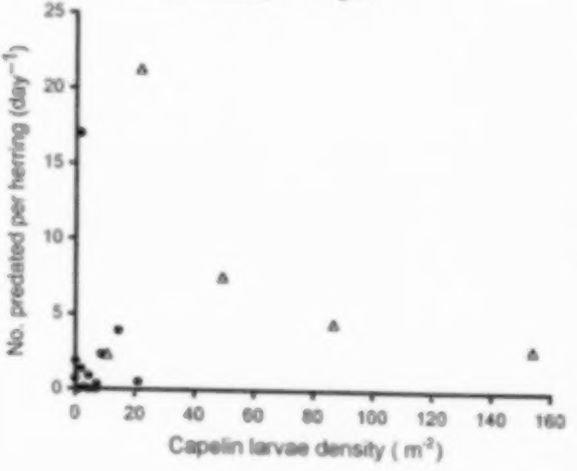

Table 3. Estimated parameter values for models predicting number of capelin (*Mallotus villosus*) larvae in herring (*Clupea harengus*) stomachs, with all significant variables.

	Parameter	CI low	CI high
Model 2			
C_{capG}	–4.08	–5.03	–3.31
ks	19.1	8.7	51.3
C_{capT}	–6.76	–7.82	–5.93
C_{cop}	–0.21	–0.32	–0.09
O_{krill}	2.70	2.05	3.59
C	0.013	0.002	0.041
K	0.20	0.16	0.24
Model 3			
C_{capG}	–2.84	–3.22	–2.39
C_{capT}	–4.86	–5.38	–4.37
ks	38.0	16.7	118.3
C	0.018	0.003	0.059
K	0.15	0.12	0.18

Note: Model 2 is the full model, whereas model 3 has only capelin larvae density in the GULF III samples and number of capelin larvae per trawl haul as variables. The 95% confidence intervals (CI low, CI high) are based on log-likelihood profiles, and $K = 1/k$, where k is the dispersion factor in the negative binomial distribution. For rationale of the constant C, see the Materials and methods section.

Fuiman and Gamble (1988) found that herring were less effective predators than sprat (*Sprattus sprattus*) and sandeels (*Hyperoplus lanceolatus* and *Ammodytes tobianus*), but our results show that herring are highly effective predators of capelin larvae in the field.

Because sampling year, capelin larvae densities, and size of herring were confounded, it was not possible to separate these possible effects in the predation model, but the effect of capelin density estimated by GULF III samples on the number of capelin larvae per herring stomach was similar in 2001 and 2003. In our study, the better fit of the nonlinear Holling type-II functional response function than the linear one seems to depend on data from two stations in 2003 with capelin larvae density higher than 50·m^{-3}. Further studies of predation by herring at high (>50·m^{-3}) larvae densities are needed to investigate whether a linear or nonlinear functional response is generally valid. It may be argued that it is unlikely that herring would become saturated by feeding on capelin larvae as long as krill and copepods were the main prey items. A linear relation between predation mortality rates and fish predator density has been observed for fish eggs and larvae by Smith et al. (1989) and Pepin et al. (2002). An increase in predation intensity with increasing capelin larvae abundance was also reflected by the positive correlations between abundance of capelin larvae and both occurrence of larvae and numbers of capelin larvae in herring stomachs.

There are several sources of errors in the estimates concerning prey and predator abundance, stomach content analysis, and digestion rate estimates. Because average temperatures in the field in 2003 and 2001 were lower and higher, respectively, than during the digestion rate experi-

Table 4. Selection of significant variables when modelling (models 1 and 2) the number of caplin (*Mallotus villosus*) larvae in juvenile herring (*Clupea harengus*) stomachs (SC).

Step	Variable	C_{capG}	ks	C_{capT}	C_{cop}	C_{krill}	O_{cop}	O_{krill}
1	LL	**−832.46**						
2	LL		−824.40	**−811.37**	−828.47	−826.23	−825.22	−821.51
	P		6×10^{-5}	$\mathbf{8\times10^{-11}}$	0.0047	0.0004	0.0001	3×10^{-6}
3	LL		−804.48		−808.65	−810.78	−803.99	**−785.54**
	P		0.0002		0.02	0.28	0.0001	$\mathbf{7\times10^{-13}}$
4	LL		**−771.09**		−776.86	−777.68	−784.20	
	P		$\mathbf{8\times10^{-8}}$		3×10^{-5}	7×10^{-5}	0.10	
5	LL				**−765.20**	−766.80	−769.94	
	P				**0.0006**	0.0034	0.13	
6	LL					−764.44	−763.39	
	P					0.22	0.058	

Note: LL, log-likelihood; *P*, significance probability associated with adding variables one at a time to the model according to the log-likelihood ratio test. For each step, the variable with the highest significance (values shown in bold) is included in the model. Station data are expressed in densities (no.·m^{-2}) of capelin larvae as estimated by the GULF III samples (C_{capG}), krill (*Thysanoessa* spp.) (× 10^2) (C_{krill}), and copepods (*Calanus* spp.) (× 10^3) (C_{cop}), and numbers of capelin larvae found in the trawl catches (C_{capT}). Occurrence of krill (O_{krill}) and copepods (O_{cop}) are given for individual herring stomachs.

Table 5. Sensitivity analysis of model 2, giving modelled number of capelin larvae per herring stomach (SC) as a function of copepod density (C_{cop}) and occurrence of krill (O_{krill}) in the stomachs.

No.	Scenario	C_{cop} (no.·m^{-2})	O_{krill} (%)	SC	Change (%)	Mortality (%)
1	Key	15 825	63	0.41	0	15
2	High C_{cop} and key O_{krill}	100 000	63	0.13	−69	5
3	Low C_{cop} and key O_{krill}	5 000	63	0.58	43	21
4	Key C_{cop} and low O_{krill}	15 825	0	0.09	−79	3
5	Key C_{cop} and high O_{krill}	15 825	100	1.09	165	39
6	High C_{cop} and low O_{krill}	100 000	0	0.03	−92	1
7	Low C_{cop} and high O_{krill}	5 000	100	1.56	279	56

Note: Density of capelin larvae was fixed at 20·m^{-2}. A key scenario shows SC for average values for 2001 and 2003 of C_{cop} (15 825·m^{-2}) and O_{krill} (63%). Values for the high and low copepod densities were selected close to minimum and maximum observed values of observed copepod densities. Percent mortality rate per predator per day per square metre was calculated as SC × *D* × 24 h × 20 m^{-2} × 100, where the digestion rate *D* was 0.3·h^{-1}.

ments of Hallfredsson et al. (2007), this may have contributed to a slight overestimation of predation mortality rates in 2003 and vice versa for 2001. Juvenile herring abundance may be underestimated because small schools of herring near the surface (above ~10 m depth) will not register on the echosounder. In 2001, catches of herring in the upper 10 m were frequent in the western part of the distribution area, whereas the estimated acoustical herring density was low in this area. Some stations had low catches of herring and few herring stomach analysed, affecting the precision of results at these stations. For instance, at 8 of 12 stations with no occurrence of predation in 2001, the number of herring stomachs was less then 10. The same applied for all stations with no predation in 2003. However, the predation model had individuals as sampling units and was not sensitive to low numbers of stomachs at some stations. Although it is difficult to estimate absolute densities of capelin larvae based on the trawl catches, they are useful as indicators of the presence of larger capelin larvae. The high numbers of relatively large capelin larvae (>25 mm long) in the trawl catches and low abundance estimated by the GULF III samples at some stations suggest that capelin larvae longer than 25 mm were underestimated by the GULF III samples (Hallfredsson and Pedersen 2007). The larger catches of capelin larvae in the pelagic trawl were more westerly distributed in both 2001 and 2003 compared with the densities estimated from the GULF III samples, possibly as a consequence of heavy predation on large larvae by herring in the eastern part of the area studied. Juvenile herring seem to prey selectively on large capelin larvae in the Barents Sea (Huse and Toresen 2000; Godiksen et al. 2006). The presence of larger larvae in the west can, however, also reflect earlier hatching, as earlier spawning in the westerly spawning areas is common (Gjøsæter 1998).

The presence of alternative prey for the predator can alter the predation pressure on fish eggs and larvae (Pepin and Shears 1995; Segers et al. 2007). That predation intensity in model 2 decreased with increasing density of copepods in the environment and with increasing prey occurrence of krill in the stomachs may indicate that herring feeding in small patches with high abundance of copepods prey less intensively on capelin larvae. Alternatively, it may reflect individual differences in preferences of zooplankton and capelin larvae. Copepods, mainly *Calanus finmarchicus*, were the dominating prey in the stomachs of herring in both years in this study. In herring stomachs from the three stations analysed by Godiksen et al. (2006), copepods constituted on average 61%–87% of the index of volume for the various

Table 6. Overview of Spearman rank correlations between abundances of capelin larvae (Cap_G and Cap_T for GULF III and trawl samples, respectively), krill and copepods ($Krill_G$ and Cop_G, respectively, for GULF III samples), and herring (Her_A, acoustical estimate).

Year	Variable	Cap_G	Cap_T	$Krill_G$	Cop_G
2001	Cap_T	–0.31*			
	$Krill_G$	0.28*	–0.31		
	Cop_G	–0.03	–0.20	0.51*	
	Her_A	0.42*	–0.39*	0.18	–0.17
2003	Cap_T	0.32*			
	$Krill_G$	0.61*	0.19		
	Cop_G	0.25	0.11	0.59*	
	Her_A	–0.44*	–0.42*	–0.32*	0.26

Note: An asterisk (*) denotes significance probability $P < 0.05$.

Table 7. Index of overlap (O_{ij}; Williamson 1993) with juvenile herring as predator and capelin larvae, krill, and copepods as prey.

Year	Capelin	Krill	Copepods
2001	1.59	1.41	0.99
2003	0.10	0.13	0.13

Fig. 8. Functional response for herring predation on capelin larvae as estimated by model 3 (continuous line), using a digestion rate of $0.3 \cdot h^{-1}$ (Hallfredsson et al. 2007). Broken lines are the 95% profile confidence intervals.

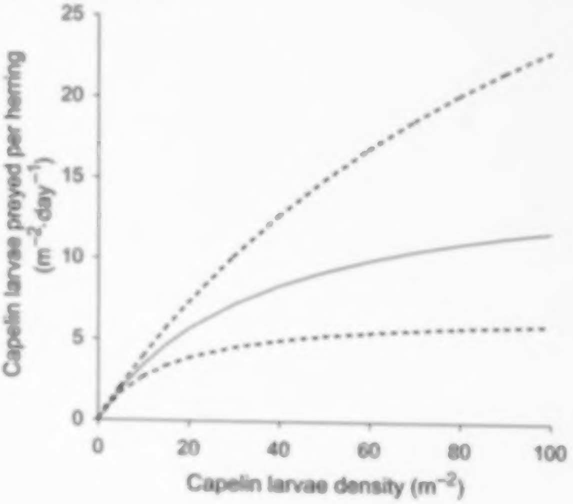

stations. Krill were preferred at all three stations in 2003, but the preference values for copepods and capelin larvae varied much between stations. The strong association between number of capelin larvae and mass of krill in the herring stomachs and the occurrence of layers with either copepods or krill and capelin larvae within the anterior part of the predator stomachs strongly indicated that individual herring switched between feeding on copepods and feeding on krill and capelin larvae (Godiksen et al. 2006). Godiksen et al. (2006) suggested that herring used a common searching image for these two types of prey. The prey switching may also reflect that the capelin larvae and krill are spatially co-occurring in the sea. In support of this, the densities of krill and capelin larvae sampled by GULF III were positively correlated both years. In the Norwegian Sea, herring seem to change diet during summer from copepods, mainly *Calanus finmarchicus*, to krill and other larger but less abundant prey (Dalpadado et al. 2000; Prokopchuk and Sentyabov 2006), probably reflecting the descent of *Calanus finmarchicus* to deeper water during summer (Falkenhaug et al. 1997). A similar change in herring diet is likely in the Barents Sea, although data on the diet of herring in the Barents Sea are scarcer than for herring in the Norwegian Sea.

The westwards movement of herring along the coast of Finnmark may be a response to heavy zooplankton predation and hence decreasing zooplankton abundance in areas with dense herring concentrations. As the herring feeding migrations are governed by abundant krill and copepods drifting with currents from the southwest, the capelin larvae will be preyed upon in the belt-like area with high herring densities. The dynamic behavior of this system was reflected to some extend in the data. There was a considerable difference between the years of investigation in the overlap of predator and the considered prey groups with regard to the O_{ij} overlap index. The very low abundances of copepods, krill, and capelin larvae in the area with high juvenile herring abundance north of the Varanger Peninsula suggest that they had been grazed down by herring in this area in 2003. Dense aggregations of herring were observed further west (northeast of Tanafjord, 29°12′E, 71°04′N) during the second coverage where herring abundance had been low during the first coverage one week earlier, indicating westward movement. The high predation intensity on capelin larvae during the second coverage in this area where the western "front" of high herring abundance encountered high abundance of capelin larvae prey (>100 larvae·m^{-2}) at about 29°E suggests that the high capelin larvae densities were grazed down as the "herring belt" moved westwards. This is supported by the high larvae abundance (>50·m^{-2}) extending about 90 km north of the Varanger Peninsula found in the capelin larvae survey conducted during 10–29 June prior to our survey by the Institute of Marine Research (Norway) (Institute of Marine Research 2003*a*). The high abundance of herring (20–60 t ww·km^{-2}) estimated in the area northeast (2001) and north (2003) of the Varanger Peninsula is far above the average biomass density of juvenile herring and capelin of 1–5 t ww·km^{-2} common for the whole Barents Sea (Bogstad et al. 2000). Similar high herring abundance was observed north of the Varanger Peninsula in 1999 (Sivertsen et al. 2006).

In 2001, the survey was conducted a month later than in 2003, and the herring was spread more westwards and was less aggregated, resulting in observed predation over a larger area. In 2001, the herring consisted mainly of 2- and 3-year-old herring (Institute of Marine Research 2001*b*), whereas in 2003, 1-year-old herring dominated. Much of the herring were probably migrating out of the Barents Sea during the summer of 2001, as there was very little herring in the Barents Sea in the summer of 2002 (Hallfredsson 2006). In

2003, herring had a wide spatial distribution in September (Institute of Marine Research 2003*b*), suggesting that the westward movement registered during our surveys continued during the summer and early autumn in 2003 as well.

Previously observed predation on capelin eggs and larvae might indicate the importance of predation regarding recruitment to the capelin stock. Predation mortality from pelagic 0-group cod (*Gadus morhua*) on capelin larvae in 2002 and 2003 in the Barents Sea was estimated to be about $1.5\%\cdot\text{day}^{-1}$ (Hallfredsson and Pedersen 2007), which would add to the herring predation mortality. In contrast to herring, the small pelagic 0-group cod will drift with the capelin larvae, resulting in a prolonged period of prey–predator overlap. There are also a number of other predators on capelin eggs and larvae: haddock (*Melanogrammus aeglefinus*), saithe (*Pollachius virens*), sandeel (*Ammodytes marinus*), and juvenile capelin (Godiksen et al. 2006; Huse and Toresen 1996; Hallfredsson 2006). With the exception of juvenile capelin, these predators are also distributed close to the coast of the southern Barents Sea, and the near-coastal area may be a high-mortality risk area for capelin larvae. However, these predators do not show the large interannual variability in biomass and extensive horizontal overlap with capelin larvae that are characteristic for juvenile herring in the Barents Sea.

Still, a study such as the present one can only give snapshots of the predation intensity at the time and place of the surveys. Because the predation from herring on capelin larvae in the Barents Sea occurs in a system in which capelin larvae are advected offshore north- and east-wards and herring migrate westwards against the prevailing currents, it is a future challenge to integrate the temporal and spatial effects of prey and predator movement to obtain the best estimates of the total effect of herring predation on capelin recruitment. Whether or not predation represents a significant constraint on capelin recruitment depends on the frequency and duration of predation incidences, as well as the presence of alternative prey. The present models might be suitable as submodels in larger models that address those aspects, and work on such a spatially resolved drifting model for the populations in questions is currently ongoing. The simplified functional response equation based on model 3 may be useful in time- and space-resolved models investigating the effects of herring predation on capelin larvae. In this context, the predation that happens where there is overlap is the most important.

In conclusion, a predation mortality of about 7%–$10\%\cdot\text{day}^{-1}$ caused by herring on capelin larvae in the area of overlap in 2001 and 2003 indicates that predation by juvenile herring may have a considerable impact on capelin larvae survival in years with high herring abundance.

Acknowledgement

The authors thank Ivan Ahlquist for his help with the processing of acoustical data and Rudi Cayers for refining figures. The authors also thank the crew members and scientific staff on both surveys and two anonymous reviewers for valuable comments. The present study was part of a research programme financed by the Research Council of Norway (BASECOEX, Project No. 140290/140).

References

Alvheim, O. 1984. Investigation of capelin larvae off Northern Norway and the Barents Sea. *In* The Proceedings of the Soviet–Norwegian Symposium on the Barents Sea Capelin, Bergen, 14–19 August 1984. *Edited* by H. Gjøsæter. Institute of Marine Research, Bergen, Norway. pp. 172–183.

Bailey, K.M., and Houde, E.D. 1989. Predation on eggs and larvae of marine fishes and the recruitment problem. Adv. Mar. Biol. **25**: 1–83. doi:10.1016/S0065-2881(08)60187-X.

Bajkov, A.D. 1935. How to estimate the daily food consumption of fish under natural conditions. Trans. Am. Fish. Soc. **65**(1): 288–289. doi:10.1577/1548-8659(1935)65[288:HTETDF]2.0.CO;2.

Bogstad, B., Haug, T., and Mehl, S. 2000. Who eats whom in the Barents Sea? NAMMCO Sci. Publ. **2**: 98–119.

Cameron, A.C., and Trivedi, P.K. 1998. Regression analysis of count data. Cambridge University Press, Cambridge, UK.

Christiansen, J.S., Præbel, K., Siikavuopio, S.I., and Carscadden, J.E. 2008. Facultative semelparity in capelin *Mallotus villosus* (Osmeridae) — an experimental test of a life history phenomenon in a sub-arctic fish. J. Exp. Mar. Biol. Ecol. **360**(1): 47–55. doi:10.1016/j.jembe.2008.04.003.

Cushing, D.H. 1990. Plankton production and year-class strength in fish populations — an update of the match mismatch hypothesis. Adv. Mar. Biol. **26**: 249–293. doi:10.1016/S0065-2881(08)60202-3.

Dalpadado, P., Ellertsen, B., Melle, W., and Dommasnes, A. 2000. Food and feeding conditions of Norwegian spring-spawning herring (*Clupea harengus*) through its feeding migrations. ICES J. Mar. Sci. **57**(4): 843–857. doi:10.1006/jmsc.2000.0573.

Dragesund, O. 1970. Factors influencing year-class strength of Norwegian spring spawning herring. Fiskeridir. Skr. Ser. Havunders. **15**: 381–450.

Dragesund, O., Hamre, J., and Ulltang, O. 1980. Biology and population dynamics of Norwegian spring-spawning herring. Rapp. P.-V. Reun. Cons. Int. Explor. Mer, **177**: 43–71.

Efron, B., and Tibshirani, R.J. 1993. An introduction to the bootstrap. Chapman and Hall, New York.

Ellis, T., and Nash, R.D.M. 1997. Predation by sprat and herring on pelagic fish eggs in a plaice spawning area in the Irish Sea. J. Fish Biol. **50**(6): 1195–1202. doi:10.1111/j.1095-8649.1997.tb01647.x.

Falkenhaug, T., Tande, K.S., and Semenova, T. 1997. Diel, seasonal and ontogenetic variations in the vertical distributions of four marine copepods. Mar. Ecol. Prog. Ser. **149**(1–3): 105–119. doi:10.3354/meps149105.

Folkvord, A. 1993. Prey recognition in stomachs of cannibalistic juvenile cod (*Gadus morhua* L). Sarsia, **78**(2): 97–100.

Foote, K.G. 1987. Fish target strengths for use in echo integration surveys. J. Acoust. Soc. Am. **82**(3): 981–987. doi:10.1121/1.395298.

Fuiman, L.A., and Gamble, J.C. 1988. Predation by Atlantic herring, sprat, and sandeels on herring larvae in large enclosures. Mar. Ecol. Prog. Ser. **44**(1): 1–6. doi:10.3354/meps044001.

Garrison, L.P., Michaels, W., Link, J.S., and Fogarty, M.J. 2000. Predation risk on larval gadids by pelagic fish in the Georges Bank ecosystem. I. Spatial overlap associated with hydrographic features. Can. J. Fish. Aquat. Sci. **57**(12): 2455–2469. doi:10.1139/cjfas-57-12-2455.

Gjøsæter, H. 1998. The population biology and exploitation of capelin (*Mallotus villsous*) in the Barents Sea. Sarsia, **83**(6): 453–496.

Gjøsæter, H., and Bogstad, B. 1998. Effects of the presence of herring (*Clupea harengus*) on the stock–recruitment relationship of Barents Sea capelin (*Mallotus villosus*). Fish. Res. **38**(1): 57–71. doi:10.1016/S0165-7836(98)00114-3.

Gjøsæter, H., Bogstad, B., and Tjelmeland, S. 2002. Assessment methodology for Barents Sea capelin, *Mallotus villosus* (Müller). ICES J. Mar. Sci. **59**(5): 1086–1095. doi:10.1006/jmsc.2002.1238.

Godiksen, J., Hallfredsson, E.H., and Pedersen, T. 2006. Effects of alternative prey on predation intensity from herring *Clupea harengus* and sandeel *Ammodytes marinus* on capelin *Mallotus villosus* larvae in the Barents Sea. J. Fish Biol. **69**(6): 1807–1823. doi:10.1111/j.1095-8649.2006.01250.x.

Hallfredsson, E.H. 2006. Fish predation on capelin larvae *Mallotus villosus* in the Barents Sea, in relation to recruitment. Doctor scientiarum thesis, The Norwegian College of Fishery Science / University of Tromsø, Norway.

Hallfredsson, E.H., and Pedersen, T. 2007. Effects of predation from 0-group cod (*Gadus morhua*) on mortality rates of capelin (*Mallotus villosus*) larvae in the Barents Sea. Can. J. Fish. Aquat. Sci. **64**: 1710–1722. doi:10.1139/F07-137.

Hallfredsson, E.H., Pedersen, T., and Præbel, K. 2007. Estimation of digestion rates for herring *Clupea harengus* L. feeding on fish larvae. J. Fish Biol. **70**(2): 638–643. doi:10.1111/j.1095-8649.2007.01312.x.

Hamre, J. 1985. Assessment and management of the Barents Sea capelin. *In* The Proceedings of the Soviet–Norwegian Symposium on the Barents Sea Capelin, Bergen, Norway, 14–17 August 1984. *Edited by* H. Gjøsæter. Institute of Marine Research, Bergen, Norway. pp. 5–24.

Hamre, J. 1991. Interrelation between environmental changes and fluctuating fish populations in the Barents Sea. *In* Long-term variability of pelagic fish populations and their environment. Proceedings of the International Symposium, Sendai, Japan. *Edited by* T. Kawasaki, S. Tanaka, Y. Toba, and A. Taniguchi. Pergamon Press, Oxford, UK. pp. 259–270.

Hamre, J. 1994. Biodiversity and exploitation of the main fish stocks in the Norwegian–Barents Sea ecosystem. Biodivers. Conserv. **3**(6): 473–492. doi:10.1007/BF00115154.

Holling, C.S. 1959. The components of predation as revealed by a study of small mammal predation of the European pine sawfly. Can. Entomol. **91**: 293–321.

Houde, E.D. 1997. Patterns and trends in larval-stage growth and mortality of teleost fish. J. Fish Biol. **51**(Suppl. A): 52–83. doi:10.1111/j.1095-8649.1997.tb06093.x.

Hunter, J.R. 1981. Feeding ecology and predation of marine fish larvae. *In* Marine fish larvae, morphology, ecology and relation to fisheries. *Edited by* R. Lasker. University of Washington Press, Seattle, Washington. pp. 33–77.

Hunter, J.R., and Kimbrell, C.A. 1980. Egg cannibalism in the northern anchovy, *Engraulis mordax*. Fish. Bull. U.S. **78**: 811–816.

Huse, G., and Toresen, R. 1995. Predation by juvenile herring (*Clupea harengus* L.) on Barents Sea capelin (*Mallotus villosus* Muller) larvae. *In* Precision and relevance of pre-recruit studies for fishery management related to fish stocks in the Barents Sea and adjacent waters. *Edited by* A. Hylen. Institute of Marine Research, Bergen, Norway. pp. 59–73.

Huse, G., and Toresen, R. 1996. A comparative study of feeding habits of herring (*Clupea harengus*, Clupeidae, L.) and capelin (*Mallotus villosus*, Osmoridae, Müller) in the Barents Sea. Sarsia, **81**(2): 143–153.

Huse, G., and Toresen, R. 2000. Juvenile herring prey on Barents Sea capelin larvae. Sarsia, **85**(5/6): 375–391.

Huse, G., Salthaug, A., and Skogen, M.D. 2008. Indications of a negative impact of herring on recruitment of Norway pout. ICES J. Mar. Sci. **65**(6): 906–911 . [Advance access.] doi:10.1093/icesjms/fsn074.

Institute of Marine Research. 2001*a*. Toktrapport Loddelarvetokt. Institute of Marine Research, Bergen, Norway, Survey Report. [In Norwegian; online.] Available at http://www.imr.no/publikasjoner/andre_publikasjoner/toktrapporter/2001/nb-no.

Institute of Marine Research. 2001*b*. Survey report from the joint Norwegian/Russian acoustic survey of pelagic fish in the Barents Sea, September–October 2001. Institute of Marine Research, Bergen, Norway, Survey Report. [Online.] Available at http://www.imr.no/publikasjoner/andre_publikasjoner/toktrapporter/2001/nb-no.

Institute of Marine Research. 2003*a*. Toktrapport Loddelarvetokt. Institute of Marine Research, Bergen, Norway, Survey Report No. 8-2003. [In Norwegian; online.] Available at http://www.imr.no/publikasjoner/andre_publikasjoner/toktrapporter/2003/nb-no.

Institute of Marine Research. 2003*b* Report from the joint Norwegian/Russian ecosystem survey in the Barents Sea, August–October 2003. Institute of Marine Research, Bergen, Norway, Survey Report No. 14-2003. [Online.] Available at http://www.imr.no/publikasjoner/andre_publikasjoner/toktrapporter/2003/nb-no.

Ivarjord, T., Pedersen, T., and Moksness, E. 2008. Effects of growth rates on the otolith increments deposition rate in capelin larvae (*Mallotus villosus*). J. Exp. Mar. Biol. Ecol. **358**(2): 170–177. doi:10.1016/j.jembe.2008.02.011.

Johansen, G.O. 2002. Temporal and spatial variation in predation on juvenile herring (*Clupea harengus* L.) by Northeast Arctic cod (*Gadus morhua* L.) in the Barents Sea in 1984–1997. ICES J. Mar. Sci. **59**(2): 270–292. doi:10.1006/jmsc.2001.1157.

Köster, F.W., and Möllmann, C. 2000. Trophodynamic control by clupeid predators on recruitment success in Baltic cod? ICES J. Mar. Sci. **57**(2): 310–323. doi:10.1006/jmsc.1999.0528.

Last, J.M. 1989. The food or herring, *Clupea harengus*, in the North Sea, 1983–1986. J. Fish Biol. **34**(4): 489–501. doi:10.1111/j.1095-8649.1989.tb03330.x.

Lindstrom, U., Haug, T., and Røttingen, I. 2002. Predation on herring, *Clupea harengus*, by minke whales, *Balaenoptera acutorostrata*, in the Barents Sea. ICES J. Mar. Sci. **59**(1): 58–70. doi:10.1006/jmsc.2001.1135.

Loeng, H. 1989. The influence of temperature on some fish population parameters in the Barents Sea. J. Northw. Atl. Fish. Sci. **9**: 103–113.

McGurk, M.D. 1986. Natural mortality of marine pelagic fish eggs and larvae — role of spatial patchiness. Mar. Ecol. Prog. Ser. **34**(3): 227–242. doi:10.3354/meps034227.

Mikkelsen, N., and Pedersen, T. 2004. How can stock–recruitment relationship on the Barents Sea capelin (*Mallotus villosus*) be improved by incorporating biotic and abiotic factors? Polar Res. **23**(1): 19–26. doi:10.1111/j.1751-8369.2004.tb00125.x.

Moksness, E., and Øiestad, V. 1987. Interaction of Norwegian spring spawning herring larvae (*Clupea harengus*) and Barents sea capelin larvae (*Mallotus villosus*) in a mesocosm study. J. Cons. Int. Explor.Mer, **44**: 32–42.

Munk, P. 2002. Larval sand lance (*Ammodytes* sp.) in the diet of small juvenile wolffish (*Anarhichas* spp.): predatory interactions in frontal water masses off western Greenland. Can. J. Fish. Aquat. Sci. **59**(11): 1759–1767. doi:10.1139/f02-147.

Olsen, S. 1968. Some results of the Norwegian capelin investigations 1960–1965. Rapp. P.-V. Reun. Cons. Int. Explor. Mer, **158**: 18–23.

Ottersen, G., and Loeng, H. 2000. Covariability in early growth and year-class strength of Barents Sea cod, haddock, and herring: the environmental link. ICES J. Mar. Sci. **57**(2): 339–348. doi:10.1006/jmsc.1999.0529.

Pedersen, T., and Fossheim, M. 2008. Diet of 0-group stages of capelin (*Mallotus villosus*), herring (*Clupea harengus*) and cod (*Gadus morhua*) during spring and summer in the Barents Sea. Mar. Biol. (Berl.), **153**(6): 1037–1046. doi:10.1007/s00227-007-0875-x.

Pepin, P. 2006. Estimating the encounter rate of Atlantic capelin (*Mallotus villosus*) with fish eggs, based on stomach content analysis. Fish. Bull. (Washington, D.C.), **104**(2): 204–214.

Pepin, P., and Shears, T.H. 1995. Influence of body size and alternate prey abundance on the risk of predation to fish larvae. Mar. Ecol. Prog. Ser. **128**(1–3): 279–285. doi:10.3354/meps128279.

Pepin, P., Dower, J.F., Helbig, J.A., and Leggett, W.C. 2002. Estimating the relative roles of dispersion and predation in generating regional differences in mortality rates of larval radiated shanny (*Ulvaria subbifurcata*). Can. J. Fish. Aquat. Sci. **59**(1): 105–114. doi:10.1139/f01-198.

Peterson, I., and Wroblewski, J.S. 1984. Mortality rate of fishes in the pelagic ecosystem. Can. J. Fish. Aquat. Sci. **41**(7): 1117–1120. doi:10.1139/f84-131.

Posada, D., and Crandall, K.A. 2001. Selecting the best-fit model of nucleotide substitution. Syst. Biol. **50**(4): 580–601. doi:10.1080/106351501750435121. PMID:12116655.

Prokopchuk, I., and Sentyabov, E. 2006. Diets of herring, mackerel, and blue whiting in the Norwegian Sea in relation to *Calanus finmarchicus* distribution and temperature conditions. ICES J. Mar. Sci. **63**(1): 117–127. doi:10.1016/j.icesjms.2005.08.005.

R Development Core Team. 2008. R: a language and environment for statistical computing. R Foundation for Statistical Computing, Vienna, Austria. ISBN 3-900051-07-0. Available at http://www.R-project.org.

Rottingen, I. 1990. A review of variability in the distribution and abundance of Norwegian spring spawning herring and Barents Sea capelin. Polar Res. **8**(1): 33–42. doi:10.1111/j.1751-8369.1990.tb00373.x.

Segers, F.H.I.D., Dickey-Collas, M., and Rijnsdorp, A.D. 2007. Prey selection by North Sea herring (*Clupea harengus*), with special reference to fish eggs. ICES J. Mar. Sci. **64**: 60–68.

Sivertsen, S., Pedersen, T., Lindstrom, U., and Haug, T. 2006. Prey partitioning between cod (*Gadus morhua*) and minke whale (*Balaenoptera acutorostrata*) in the Barents Sea. Mar. Biol. Res. **2**(2): 89–99. doi:10.1080/17451000600670952.

Smith, P.E., Santander, H., and Alheit, J. 1989. Comparison of the mortality rates of Pacific sardine, *Sardinops sagax*, and Peruvian anchovy, *Engraulis ringens*, eggs off Peru. Fish. Bull. (Washington, D.C.), **87**: 497–509.

SYSTAT. 2004. SYSTAT for Windows. Version 11. SYSTAT Software Inc., Richmond, California.

Takasuka, A., Oozeki, Y., Kimura, R., Kubota, H., and Aoki, I. 2004. Growth-selective predation hypothesis revisited for larval anchovy in offshore waters: cannibalism by juveniles versus predation by skipjack tunas. Mar. Ecol. Prog. Ser. **278**: 297–302. doi:10.3354/meps278297.

Templeman, W. 1948. The life history of the capelin (*Mallotus villosus* O.F. Muller) in Newfoundland waters. Newfoundland Govt. Lab. Bull. **17**: 1–151.

Williamson, C.E. 1993. Linking predation risk models with behavioral mechanisms — identifying population bottlenecks. Ecology, **74**(2): 320–331. doi:10.2307/1939295.

Evaluating recreational fisheries for an endangered species: a case study of taimen, *Hucho taimen*, in Mongolia

Olaf P. Jensen, David J. Gilroy, Zeb Hogan, Brant C. Allen, Thomas R. Hrabik, Brian C. Weidel, Sudeep Chandra, and M. Jake Vander Zanden

Abstract: Understanding the tradeoff between exploitation and conservation is difficult in data-poor situations, which are typical for most recreational fisheries, even in developed countries. In a developing country where the target species is endangered, the stakes are higher and the management resources are fewer. We combined a mark–recapture experiment, life history invariants, and meta-analysis to parameterize a delay-difference model for a population of the endangered giant Eurasian trout (taimen, *Hucho taimen*) in northern Mongolia. The model allowed us to evaluate the impacts of a recreational fishery for taimen based on a suite of population characteristics including equilibrium abundance, biomass, and mean weight. The Bayesian framework and Monte Carlo simulations combine disparate sources of information while keeping track of uncertainty as it propagates through the model. In the case of taimen in the Eg–Uur watershed, the existing catch–release recreational fishery has likely reduced taimen abundance, biomass, and mean weight by less than 10% compared with levels predicted in the absence of recreational fishing. In comparison, if all taimen caught in this fishery were retained (as they are elsewhere in Mongolia), there is a 57% chance that such harvest levels, if maintained, would lead to the eventual extirpation of the population.

Résumé : Il est difficile de comprendre le compromis entre l'exploitation et la conservation dans les pêches sportives lorsqu'il y a peu de données, ce qui est très souvent le cas, même dans les pays développés. Dans un pays en voie de développement lorsque l'espèce cible est menacée, les enjeux sont plus importants et les ressources de gestion moindres. Nous combinons une expérience de marquage–recapture, des invariants du cycle biologique et une méta-analyse afin de paramétrer un modèle de différence avec délais pour une population du huchon géant d'Eurasie (le taimen, *Hucho taimen*), une espèce menacée, dans le nord de la Mongolie. Le modèle nous permet d'évaluer l'impact d'une pêche sportive du taimen à partir d'une série de caractéristiques démographiques, dont l'abondance à l'équilibre, la biomasse et la masse moyenne. Le cadre bayésien et la méthode de Monte Carlo combinent des sources disparates de renseignements, tout en tenant compte de l'incertitude à mesure qu'elle se propage dans le modèle. Dans le cas du taimen de l'Eg–Uur, la pêche sportive actuelle avec remise à l'eau des prises a vraisemblablement réduit l'abondance, la biomasse et la masse moyenne du taimen par moins de 10 %, par comparaison aux valeurs prédites en l'absence de pêche sportive. D'un autre côté, si tous les taimens capturés dans cette pêche étaient gardés (comme ils le sont ailleurs en Mongolie), il y a une probabilité de 57 % qu'une telle intensité de capture, si elle devait se maintenir, aboutirait à une extirpation éventuelle de la population.

[Traduit par la Rédaction]

Introduction

There is a growing realization that recreational fisheries have the capacity to severely reduce the abundance of fished species (Post et al. 2002; Coleman et al. 2004; Cooke and Cowx 2004). Yet recreational fisheries often produce large economic benefits (Haab et al. 2001; Cowx 2002; Kelch et al. 2006), particularly in rural areas where alternative economic activities are limited. They also provide an economic incentive for protecting the ecosystems on which target species depend. Size limits and catch–release policies can limit the negative impacts of recreational fishing, but even mandatory catch–release may be insufficient to protect long-

Received 20 September 2008. Accepted 22 May 2009. Published on the NRC Research Press Web site at cjfas.nrc.ca on 26 September 2009.
J20783

Paper handled by Associate Editor John Post.

O.P. Jensen,[1,2] D.J. Gilroy, B.C. Weidel, and M.J. Vander Zanden. Center for Limnology, University of Wisconsin – Madison, 680 N. Park Street, Madison, WI 53706, USA.
Z. Hogan and B.C. Allen. Tahoe Environmental Research Center, P.O. Box 633, 2400 Lake Forest Road, Tahoe City, CA 96145, USA.
T.R. Hrabik. University of Minnesota, Duluth Campus, 1110 Kirby Drive, Duluth, MN 55812, USA.
S. Chandra. Department of Natural Resources and Environmental Science, University of Nevada – Reno, 1000 Valley Road, Reno, NV 89512, USA.

[1] Corresponding author (e-mail: ojensen@u.washington.edu).

[2] Present address: University of Washington, School of Aquatic and Fishery Sciences, Box 355020, Seattle, WA 98195-5020, USA.

Can. J. Fish. Aquat. Sci. **66**: 1707–1718 (2009) doi:10.1139/F09-109 Published by NRC Research Press

lived, low productivity species when fishing effort is high and postrelease survival is low (Coggins et al. 2007). The general lack of stock assessments for recreational fisheries, even in developed countries (Post et al. 2002), results in management that is often focused on restoring degraded fisheries. Such a retroactive focus is extremely risky for target species that are globally threatened.

Newly developing fisheries present serious stock assessment challenges, as well as a unique opportunity to gather information about fish population dynamics from relatively unexploited populations. Good management advice at the start of a fishery's development can be critical; yet without time series data, the available analytical tools are quite limited. There is a need for models of population dynamics that can combine prior information from life history invariants (Beverton and Holt 1959; Charnov 1993) and meta-analysis of other species or other populations of the same species (Myers et al. 1999) with data from limited surveys or mark–recapture experiments. These models must also be able to accurately portray uncertainty in parameters, processes, and model output. Although uncertainty in these early models is likely to be high, the relevant management questions for recreational fisheries are often quite basic (e.g., can fishing effort safely be doubled or is current effort already too high?). An early but approximate answer to such questions is more valuable than a precise postmortem. New life-history-based approaches to estimating maximum sustainable yield (MSY) and F_{MSY} have recently been developed (Beddington and Kirkwood 2005), but analogous tools applicable to recreational fisheries are lacking.

In Mongolia, recreational fisheries targeting taimen, *Hucho taimen*, are developing rapidly (Vander Zanden et al. 2007). Taimen are the world's largest salmonid, reaching a maximum size of 2 m in length and 100 kg in mass (Holčík et al. 1988). Taimen have declined in abundance throughout their range in the large rivers of the Volga/Caspian, Arctic, and Pacific drainages of northern Eurasia (Holčík et al. 1988; Matveyev et al. 1998) and are listed as endangered on the Mongolian, Russian, and Chinese red lists (Holčík 1995; Ocock et al. 2006). Healthy populations still exist, however, in the relatively unexploited and undeveloped rivers of northern Mongolia. There is little cultural tradition of fishing or fish consumption in Mongolia, though Russians and Chinese immigrants living in Mongolia have imported these practices, and both fishing and fish consumption are becoming increasingly common (Chandra et al. 2005). Private tourist companies have expanded since the end of the Soviet occupation in 1990, and many offer guided taimen fishing. Some, but not all, of these outfitters encourage or require catch–release for taimen (Ocock et al. 2006). Commercial harvest of taimen is officially illegal; however, there is little enforcement and taimen are openly sold or bartered in small numbers. Recreational fisheries represent a potentially important source of income in the undeveloped regions of northern Mongolia. Fishing offers an alternative economic activity to mining, which has caused significant habitat damage in some watersheds (Stubblefield et al. 2005). Management of recreational taimen fisheries in Mongolia consists of a license requirement and seasonal closures, though enforcement is minimal.

Management of taimen throughout their remaining range is hampered by a general lack of knowledge about the life history and population dynamics of this species. Assessments of recreational taimen fisheries in Mongolia are urgently needed for three reasons. (*i*) Taimen are a globally threatened species. Their long life span and relatively high age at maturity (at least 30 years and approximately 3–8 years, respectively; Holčík et al. 1988) suggest that they are vulnerable to overfishing. (*ii*) High-value catch–release fisheries for trophy-sized taimen may not be sustainable if fishing pressure leads to substantially reduced abundance or average size of taimen. Taimen require at least 10 years to grow to a length of 1 m (Holčík et al. 1988; Matveyev et al. 1998), and individuals this age have disappeared in less than 20 years from exploited rivers in which they were formerly abundant (Matveyev et al. 1998). (*iii*) Unexploited systems provide a unique opportunity to estimate unfished abundance, a critical unknown in stock assessments (Hilborn and Walters 1992). In many fisheries, time series data are only available after the onset of heavy exploitation. Consequently, baseline abundance may be significantly lower than unfished abundance, and the expectations of scientists and fishermen underestimate the population's true potential. This "shifting baseline syndrome" (Pauly 1995) can be avoided by studying populations early in the development of a fishery.

We began an assessment of a developing taimen recreational fishery in Mongolia in 2004. Although length–frequency and growth information exist for taimen populations in Russia (Holčík et al. 1988; Matveyev et al. 1998), there are no reliable time series of abundance, catch, or effort; estimates of natural or fishing mortality rates; or data on stock–recruitment relationships. Our objectives were (*i*) to estimate growth, unfished abundance and biomass, and recreational postrelease mortality and (*ii*) to develop a population model that will allow policy-makers to anticipate the population level consequences of maintaining or expanding an existing recreational catch–release fishery. Such a model must make efficient use of all available data, while accurately representing the effects of parameter uncertainty on model output.

Materials and methods

Study site and field methods

We sampled taimen populations in the Eg and Uur rivers near their confluence in northern Mongolia (Fig. 1) from May 2004 through October 2007. The Eg is the main outlet of one of Mongolia's largest lakes, Lake Hovsgol. After joining with the Uur, the Eg flows into the Selenge River, a tributary of Lake Baikal. Near their confluence, the Eg and the Uur have typical discharges of 40 and 75 $m^3 \cdot s^{-1}$, respectively, during the spring and fall (mid-May and mid-October) and higher discharges, >54 and 370 $m^3 \cdot s^{-1}$, respectively, during July and August (D.J. Gilroy, unpublished data). The climate of the region is temperate, with average water temperatures of 9 °C in May and 14 °C in August in the Eg and 12 °C in May and 17 °C in August in the Uur. The Eg and Uur typically freeze in late November and thaw in early May (Gilroy 2007). Fish communities include a small number of cold-water species, predominantly lenok (*Brachymystax lenok*), Arctic grayling (*Thymallus arcticus arc-*

Fig. 1. Study area in the Eg–Uur watershed of northern Mongolia. River sections in bold represent the extent of the mark–recapture study. Shaded sections represent the extent of the extended telemetry surveys.

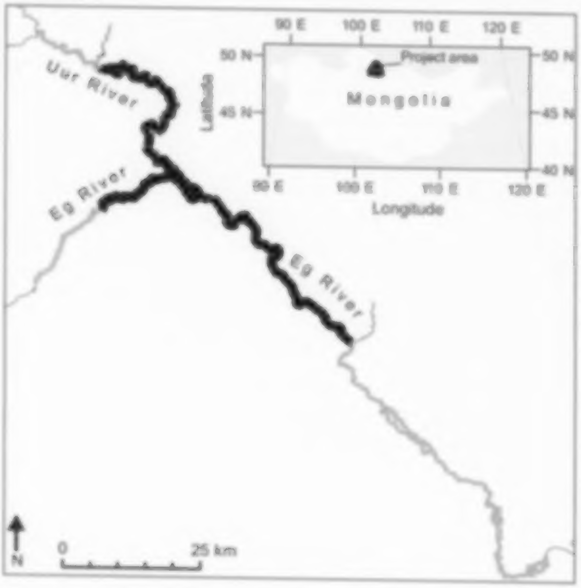

ticus), Eurasian minnow (*Phoxinus phoxinus*), and Arctic cisco (*Coregonus autumnalis*), with taimen as the top predator. The field season was divided into spring (early May to late June or early July) and fall (late August to mid-October) sampling periods. The study region is remote and is fished almost exclusively by clients of a single fly-fishing guide service, which practices strict catch–release fishing using single barbless hooks.

Fish were sampled by angling with barbless hooks. Other methods proved to be ineffective or impractical (e.g., backpack or boat electrofishing and beach seining) or would likely have resulted in unacceptable mortality (e.g., gill nets). Captured fish were checked for tags and marks, measured to the nearest millimetre (total length), and weighed to the nearest 100 g in a net with a hanging scale. Untagged fish were tagged with individually numbered plastic t-bar anchor tags (Hallprint model TBA) as part of a multiple-season mark–recapture study (n = 612 over nine seasons). The posterior third of the anal fin was clipped on 124 of the t-bar tagged individuals during the spring and fall 2007 sampling seasons to estimate the tag shedding rate.

Radio (Lotek MCFT series, n = 27) and acoustic (Vemco V16, n = 17) tags were surgically implanted in a subset of captured fish to study movements (Gilroy 2007) and to estimate postrelease mortality. Two additional individuals were tagged with both types of tags for a separate detection efficiency study. All radio- and acoustic-tagged fish were anesthetized with MS-222 (tricaine methanesulfonate) prior to surgery, irrigated during surgery, and held in instream enclosures until they were swimming strongly (average of 30 min). Mobile radio and acoustic tracking surveys were conducted by boat once every 15–30 days during the ice-free season and, on average, once every two months during the winter over a 60 km stretch of river (Gilroy 2007) within the 120 km mark–recapture study area fished by Sweetwater Travel. Six telemetry surveys were conducted over a larger area (200–250 km) that encompassed the entire mark–recapture study area.

Length at age was determined for 11 individual taimen based on sectioned saggitae otoliths. Otoliths were collected from those fish that were either found dead (n = 6) or died during capture (n = 4) or tag implantation surgery (n = 1). Epoxy-mounted otoliths were sectioned in the transverse plane through the origin using a low-speed saw (Casselman 1983). Annuli interpretations and counts were made directly from polished sections by an experienced salmonid otolith reader. Aging using scales was found to be ineffective due to abrasion of outer growth rings, a common problem with salmonid scales (Sharp and Bernard 1988).

Population model

We used a delay-difference population model (Deriso 1980; Schnute 1985, 1987) to simulate changes through time (t) in abundance (N_t), biomass (B_t), and mean weight ($\bar{w}_t$) of taimen recruited to the fishery (i.e., large enough to be vulnerable to fishing gear used to target adult taimen) within the Eg–Uur study region. The delay-difference model represents a compromise between surplus production models, in which recruitment, mortality, and individual growth are condensed into a single intrinsic rate of growth, and fully age-structured models, which track individual cohorts. Production models are unable to predict changes in size, a crucial model output for recreational fisheries, whereas fully age-structured models require age-specific information on vulnerability to fishing, natural mortality, and fecundity. The delay-difference model incorporates two separate equations for numbers and biomass in year t + 1 (modified from Walters and Martell 2004):

$$(1) \qquad B_{t+1} = S_t(cN_t + \rho B_t) + w_k R_{t+1}$$

$$(2) \qquad N_{t+1} = S_t N_t + R_{t+1}$$

The parameter w_k is the weight at age k, the age at recruitment. For taimen in the Eg–Uur study area, the age at recruitment to the fishery is ~4 years and is similar to the age at sexual maturity (3–8 years for males and 4–8 years for females; Holčík et al. 1988). The annual total survival rate, S_t, is a function of the instantaneous natural mortality rate (M) and the annual exploitation rate (h), i.e., the fraction of the population removed due to harvest or postrelease mortality:

$$(3) \qquad S_t = \mathrm{e}^{-M}(1 - h)$$

The parameters c and ρ are the intercept and slope, respectively, of the Ford–Brody body weight equation for predicting weight at age a + 1:

$$(4) \qquad w_{a+1} = c + \rho w_a$$

Recruitment in year t + 1 (R_{t+1}) is frequently modeled as a function of biomass in the previous year (B_t), unfished recruitment (R_0), a steepness parameter (z) (Mace and Doonan 1988) representing the proportion of R_0 produced by 20% of the unfished biomass (B_0), and φ_0, the spawning biomass per recruit at unfished equilibrium (B_0/R_0). Of all the possible stock–recruit functions, the Beverton and Holt

$$(5)\qquad R_{t+1} = \frac{0.8R_0 z B_t}{0.2\varphi_0(1-z)+(z-0.2)B_t}$$

is the most commonly observed in empirical analyses of stock–recruit data (Myers and Barrowman 1996; Myers et al. 1999; Walters et al. 2006) and has a strong theoretical basis related to risk-sensitive foraging behavior (Walters and Korman 1999).

Although the stock–recruit functions are typically parameterized based on unfished equilibrium biomass and recruitment (B_0 and R_0), they can also be parameterized based on an arbitrary point (B^*, R^*) on the stock–recruit curve (Kimura 1988). In that case, steepness (z^*) does not have the same meaning. However, for higher values of steepness and B^* not much less than B_0, z^* is nearly the same as z. For example, for $z = 0.8$ and $B^* = 0.8B_0$, the ratio of $z^*:z$ is 0.96 (Appendix A).

Data analysis and parameter estimation

We used lengths, ages, and weights from individuals captured in the Eg–Uur study area, taimen lengths and ages from published literature, an empirical relationship between growth and natural mortality (Pauly 1980; Jensen 1996), and data from the mark–recapture experiment to estimate c, ρ, M, B_1, and N_1 (the time subscript 1 is used to indicate the current state, which was not assumed to be the same as the unfished state). The annual total survival rate, S_t, was estimated from its components (M and h) as described in the next section. All of these data sources were combined in an integrated analysis in which posterior distributions of model parameters were estimated by Markov chain Monte Carlo (MCMC) sampling using AD Model Builder software (ADMB, Otter Research Ltd., Sidney, British Columbia).

A von Bertalanffy (VB) growth model of length at age (L_a)

$$(6)\qquad L_a = L_\infty\left(1-e^{-K(a-t_0)}\right)$$

was fit to age and length data from 31 taimen stocks (303 age–length combinations; Holčík et al. 1988; Matveyev et al. 1998) using a nonlinear mixed effects model (R, nlme package) where asymptotic length (L_∞) was allowed to vary among stocks. The maximum likelihood estimates (MLEs) of L_∞, age at length zero (t_0), and the VB growth rate parameter (K), and their standard deviations (random effect standard deviation for L_∞) were used to set priors on these three parameters for a second round of fitting to the ages and lengths from the 11 aged individuals from the Eg–Uur study area. Embedded in this second round of fitting were four separate growth and mortality submodels: (*i*) a regression, $M = gK$ (Jensen 1996), using the 175 stocks from Pauly (1980), (*ii*) an application of this formula to predict M for taimen using the estimated regression coefficient, g, and the estimated VB K parameter, (*iii*) a length–weight regression, $W = \alpha L^\beta$, based on the lengths and weights of 56 individuals sampled from the Eg–Uur study area, and (*iv*) a Ford–Brody body weight regression (eq. 4) using simulated data for ages 1 to 30 from the VB growth model and the length–weight regression. Simulated data were used in this last growth submodel because the relationship between w_{a+1} and w_a is slightly nonlinear when weights at age are estimated from the VB length growth model and a length–weight regression, thus there is no analytical solution for the Ford–Brody weight relationship as there is for the L_{a+1} vs. L_a relationship (Hilborn and Walters 1992). There is little weight at age information in the published literature on taimen, making it difficult to estimate the Ford–Brody weight parameters directly.

A Jolly–Seber (JS) mark–recapture model (Jolly 1965; Seber 1965) including tag shedding was used to estimate the average abundance of taimen over the study period. In the m_{ij}-array form of the JS model, the probability of the observed number of recaptures in period j of individuals marked in period i (m_{ij}) is estimated conditional on the number of releases of marked fish in period i (R_i). The predicted number of recaptures, $\hat{m}_{ij}$, is

$$(7)\qquad \hat{m}_{ij} = \frac{R_i \cdot D \cdot C_j \cdot A^{(j-i)/2}}{N_0}$$

where D is the tag retention rate (assuming that all tag shedding occurs between the time of tagging and the following sampling period), C_j is the total number of individuals (both tagged and untagged) captured in period j, and $A^{(j-i)/2}$ is the apparent survival between the tagging period (i) and the recapture period (j). Mortality and emigration are confounded in the apparent survival parameter, A, making it difficult to estimate the natural mortality rate (M) directly from the mark–recapture experiment. We assumed a constant apparent survival rate and population size. Short-term fluctuations in the number of fully recruited individuals for this long-lived species are likely to be small in the absence of large and recent anthropogenic mortality sources, and a single population size can be estimated with greater precision than could sampling period-specific population sizes.

Assuming that the m_{ij} are independent samples from Poisson distributions with means given by eq. 7 and ignoring likelihood terms involving only the data, the log-likelihood kernel ($\log L$), for all of the m_{ij} given the parameters (θ) is

$$(8)\qquad \log L(m|\theta) = \sum_{j>i=1}^{k}\left(-\hat{m}_{ij} + m_{ij}\log(\hat{m}_{ij})\right)$$

(Coggins et al. 2006). If the same fish is recaptured multiple times, then the m_{ij} are not independent (Coggins et al. 2006); however, in this study, the number of recaptures was relatively low (total = 40, not counting individuals recaptured in the same sampling period, which are not used in the JS model), and only two of these individuals were recaptured more than once. Although excellent software is available for analysis of mark–recapture experiments, the most widely used program (MARK; White and Burnham 1999) does not allow for the inclusion of a tag loss rate and has limited options for estimating population size. Our abundance estimate was within 10% of an estimate obtained by analyzing our data with another widely used program designed to estimate abundance from mark–recapture experiments (JOLLY; Pollock et al. 1990).

The double-marking (tag and anal fin clip) experiment provided an estimate of the tag retention rate (Guy et al.

1996). Fifteen of the double-marked individuals were recaptured, of which 14 had retained their tags. If no other prior information on tag retention is available and these 15 observations are considered as independent binomial trials, then the distribution of the tag retention rate is a beta distribution, Beta(16, 2), with a mode at 0.94. We used this distribution as a prior on the tag retention rate. Because the mark–recapture data contain little information about tag retention, the prior and posterior distributions are very similar; however, the posterior distributions of A and abundance reflect this uncertainty in tag retention.

The stock–recruit model steepness parameter, z, could not be estimated from any of the data that we collected in our field study. The parameters of stock–recruit models are typically estimated by fitting a model to time series of spawning stock size and recruitment. Myers et al. (1999) estimated values of z from more than 700 such time series to get empirical probability distributions of z for many different fish species and stocks. To develop a prior for z, which can range between 0.2 and 1, for any particular species, Myers et al. (2002) recommend using the distribution of z for either taxonomically or ecologically related species or estimating a distribution of z using life history and environmental covariates. Similar distributions of z resulted from the taxonomic and ecological approaches. There are two species of nonanadromous salmonids for which z was estimated by Myers et al. (1999), five populations of brook trout (*Salvelinus fontinalis*; median $z = 0.87$) and one population of lake trout (*Salvelinus namaycush*; $z = 0.86$). Myers et al.'s (2002) "domain 3" group of species (older age at maturity, low natural mortality rate, and high fecundity) was the closest ecologically similar group to taimen. The probability distribution of z estimated for this group is centered on 0.84 and is closely approximated by Beta(28.5, 6.2). We drew random samples of z from this distribution for the Monte Carlo simulations described below. The other stock–recruit parameter, $\varphi_1 = B_1/R_1$, was calculated from the estimated current biomass B_1 and current recruitment assuming the population is at equilibrium, $R_1 = (1 - S_1)N_1$.

We used the radio- and acoustic-tagged individuals to estimate an upper bound on the release mortality rate. Individuals relocated at more than one location more than 7 days after release were considered to have survived. Of 52 radio- and acoustic-tagged individuals, 47 survived according to this definition. We consider $1 - (47/52) = 0.096$ to be an upper bound on the release mortality rate as these individuals experienced greater trauma (tag implantation surgery) than fish released by the fishing guides, and there is some probability that an individual may not be relocated due to tag malfunction or emigration beyond the surveyed area.

Five of 122 fish landed in the recreational fishery in fall 2007 and examined for signs of injury were observed to be bleeding heavily from the gill area. We used this fraction (0.04) as a lower bound on postrelease mortality as these individuals were likely to die and some of the other individuals released alive without obvious injuries may have subsequently died from unseen injuries or stress sustained during the capture and release process. Between 2005 and 2007 (years for which complete catch records were available), the recreational catch in the Eg–Uur study area averaged 240 fish per year. Given this catch and the range of release mortality rates, deaths due to recreational fishing within the study area ranged between 10 and 23 fish per year, on average.

Although the study area is remote, some subsistence or artisanal harvest and (or) poaching does occur. We refer to such harvest generically as "subsistence harvest", as the disposition of the catch (consumed by fishermen or sold) and the legality of the fishing activity are generally unknown and irrelevant to the population model. This harvest is essentially unregulated and entirely undocumented. When we observed the disappearance of telemetry-tagged fish from locations within the core tracking area where they had previously been found, we attempted to ascertain through interviews with fishing guides (who traverse the core tracking area on a daily basis) and local residents whether any fishing activity had been observed in the area. On three occasions, these interviews led to confirmation that the telemetry-tagged fish had been harvested. The telemetry study resulted in a total of 1304 tag months of effort. Based on the three confirmed fish harvested, the monthly harvest rate is then 2.3×10^{-3}, which is equivalent to an annual harvest rate of 0.027. We used this rate as an estimate of the current subsistence harvest rate with the recognition that this measure is imprecise and potentially an underestimate of the true subsistence harvest rate.

Monte Carlo simulations

We estimated the probability distributions of unfished equilibrium biomass, population size, and mean weight using the maximum and minimum estimates of postrelease survival and the estimated subsistence harvest rate combined with random samples from the distributions of the model parameters. Current abundance and biomass, as estimated from the mark–recapture model, were assumed to be the equilibrium values achieved by the population under the current recreational and subsistence fishing mortality rate. The fishing mortality components of the annual total survival rate, S_t, were removed and the delay-difference model (eqs. 1 and 2) was run to approximate equilibrium (200 years). This procedure was repeated using 10 000 MCMC samples of the joint posterior distribution of the delay-difference model parameters. These MCMC samples represent every 500th trial from a 6 000 000 trial chain, where the first 1 000 000 trials were discarded as a burn-in period.

For each of these 10 000 parameter combinations, we also calculated the biomass, population size, survival to age 10, and mean weight at equilibrium for absolute harvest rates (number of fish killed per year) ranging from 0 to 500 fish per year. This range of harvest rates is equivalent to management scenarios ranging from stopping the recreational and subsistence fisheries to allowing the recreational fishery to approximately double its annual catch and switch to a 100% retention policy. At some level of constant harvest, the population is reduced to the point at which the harvest level exceeds the projected population size, i.e., a continued harvest at that level would lead to eventual extirpation of the population. For each harvest rate, we calculated the probability of extirpation as the fraction of the 10 000 simulations for which the harvest rate would exceed the population size within 200 years.

Results

Length at age for taimen in the Eg–Uur study area was similar to values observed in other locations (Fig. 2). The posteriors obtained using uniform priors on the von Bertalanffy growth parameters were broad (Fig. 3), indicating that much of the information on growth rate came from the prior distributions derived from meta-analysis of published lengths at age. The posterior modes and 95% Bayesian credible intervals of the parameters of the von Bertalanffy growth model were as follows: K = 0.09·year^{-1} (0.08–0.10), L_{∞} = 147 cm (136–160), and a_0 = –0.16 years (–0.41–0.10) (Table 1).

Annual natural survival estimated from the growth rate using the Jensen (1996) method was 0.86 (0.84–0.88). Estimated abundance of recruited taimen (>age 4) in the study area averaged over the 4-year study period was 2320 individuals (1363–4517), yielding a density over the 120 km study area of 19 individuals·km^{-1} (11–38).

The population model results suggest that at the current size of the fishery, the effects of catch–release mortality on abundance, biomass, mean weight, and survival from recruitment to age 10 are minimal, even when the higher release mortality estimate was used. Equilibrium biomass was more sensitive than the other three indicators (abundance, mean weight, and survival to age 10) and was estimated to have been reduced to 90% (82%–94%) of levels expected in the absence of recreational fishing under the higher release mortality rate. The effects of the recreational fishery on other population characteristics were smaller (Fig. 4; Table 2). An annual harvest rate of 24 individuals, equivalent to the number of fish killed by the recreational fishery under the higher release mortality rate, resulted in zero risk of extirpation due to harvest (Fig. 5; Table 2).

In contrast, without catch–release, the effects of a recreational fishery of this size could be severe. An annual harvest of 130 individuals (approximately equivalent to a 50% release rate assuming the higher release mortality) would likely result in a reduction in equilibrium population size to 69% (0%–84%), biomass to 50% (0%–72%), mean weight to 73% (0%–90%), and survival to age 10 to 68% (0%–84%) of levels expected in the absence of a recreational fishery (Fig. 4). Note that a value of zero in the confidence limits indicates extirpation. The probability of extirpation if this level of harvest were maintained indefinitely is 4% (Fig. 5). Above this level of recreational harvest, extirpation risk rises rapidly. For example, a switch to 100% retention in the current recreational fishery (annual harvest of 240 individuals) would result in a probability of extirpation due to fishing of 57%. The effects of the estimated level of subsistence harvest appear to be greater than the effects of the recreational catch–release fishery; however, uncertainty in the subsistence harvest rate is high and cannot be quantified.

Discussion

The growth and natural mortality estimates and the population model results all suggest that taimen populations are likely to be very sensitive to fishing mortality. Holčík et al. (1988) found that in most taimen populations, sexual maturity is attained at a weight of ~1 kg for males and ~2 kg for females. In the Eg–Uur population, this is equivalent to an age of 4 years for males and 5 years for females. The relatively slow growth, low natural mortality, late maturation, and low fecundity (10 000 – 30 000 eggs per female; Holčík et al. 1988) of taimen place them with many other salmonids between the "periodic" and "equilibrium" life history strategies (Winemiller and Rose 1992). The natural mortality rate and growth rate that we estimated for taimen are both low relative to those of other salmonids but similar to some cold-water populations of lake trout, brook trout, and lake whitefish (*Coregonus clupeaformis*; Froese and Pauly 2008). Many other species with slow growth and high longevity have proven to be especially vulnerable to overexploitation (Musick 1999).

Fig. 2. Length and age data from the published literature (open squares; Holčík et al. 1988; Matveyev et al. 1998) and from individuals collected in the Eg–Uur study area (solid triangles). von Bertalanffy growth models fit to the literature data (broken line) and to the Eg–Uur data using the parameter estimates from a mixed-effects model based on the literature data as priors (solid line).

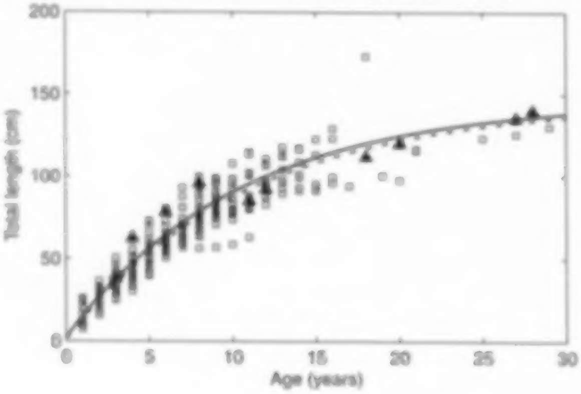

Our modeling approach makes use of correlations among life history characteristics (Pauly 1980; Jensen 1996) and meta-analysis of stock–recruitment relationships (Myers et al. 1999, 2002) to reduce uncertainty in the survival rate and the stock–recruitment steepness parameter. Such approaches are frequently used to develop informative priors for stock assessments based on time series data (e.g., McAllister et al. 2001). When time series data are not yet available, life history correlates and meta-analysis can also be used (as we have shown here) to parameterize models that provide general predictions about the likely impacts of different levels of fishing. These initial models can later be combined with time series data in a fully integrated assessment framework advocated by Maunder (2004).

The Bayesian modeling approach linked to Monte Carlo simulation allowed us to keep track of uncertainty as it propagated through the model. For example, uncertainty in survival rate derives from both uncertainty in the growth rate (K) and variability in the natural mortality (M) vs. K relationship. Other approaches to quantifying this uncertainty exist. Gunderson et al. (2003), for example, used the delta method to estimate the standard error of M based on the Jensen (1996) method. However, by combining the

Fig. 3. Gaussian kernel densities of marginal posterior distributions (solid lines), prior distributions (shaded lines), and posterior distributions resulting from a uniform prior (broken lines) for the von Bertalanffy growth parameters (*a*) asymptotic length, (*b*) growth rate, and (*c*) the intercept; (*d*) the length–weight coefficient and (*e*) exponent; (*f*) the annual natural survival rate estimated using the Jensen (1996) method; (*g*) population density; (*h*) apparent survival; and (*i*) tag retention rate. Posterior densities are based on 10 000 systematic samples from a Markov chain Monte Carlo (MCMC) chain of length 6 000 000, where the first 1 000 000 were discarded to allow for convergence. Uniform priors are not shown.

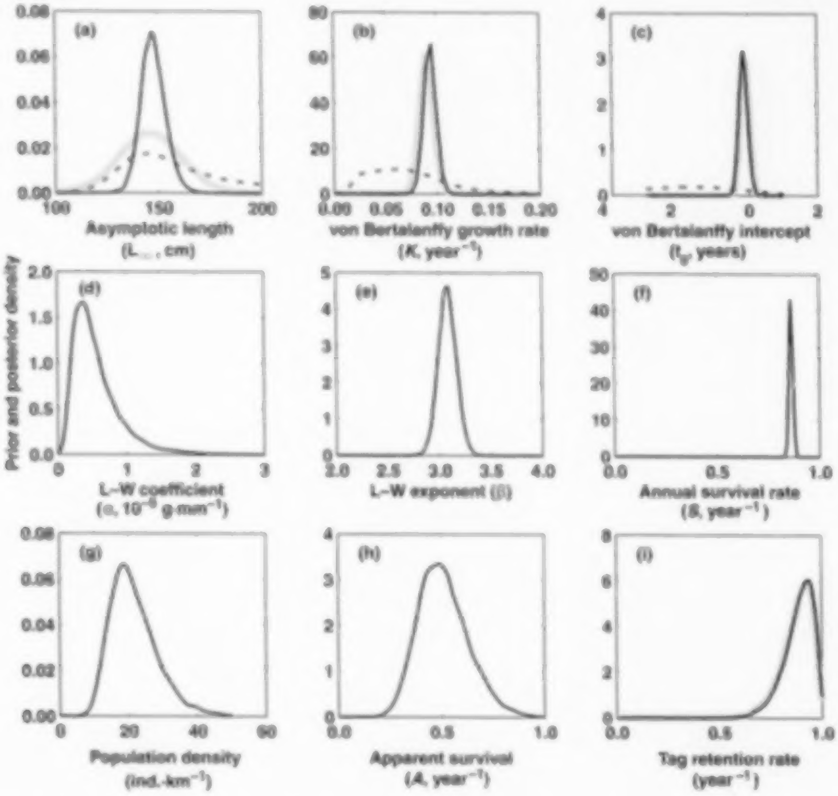

Table 1. Median values of parameters used in the delay difference model.

Parameter	Value	Unit	Method and (or) source
Growth parameters			
von Bertalanffy growth rate (K)	0.09 (0.08–0.10)	year^{-1}	Fit to length and age
von Bertalanffy asymptotic length (L_∞)	147 (136–160)	cm	Fit to length and age
von Bertalanffy age intercept (a_0)	−0.16 (−0.41–0.10)	years	Fit to length and age
Length–weight coefficient (α)	4.7 (1.5–15.0) × 10^{-6}	g·mm^{-1}	Fit to length and weight
Length–weight exponent (β)	3.1 (2.9–3.2)	—	Fit to length and weight
Population dynamics parameters			
Current abundance (N_1)	2320 (1363–4517)	individuals	Mark–recapture model
Current mean weight ($\bar{w}_1$)	5810 (4920–6700)	grams	Mean of weighed individuals
Annual natural survival rate (S_0)	0.86 (0.84–0.88)	year^{-1}	Jensen (1996) method
Steepness (z)	0.83 (0.70–0.92)	—	Myers et al. (2002)

Note: The 95% Bayesian credible interval (95% confidence interval for mean weight) is given in parentheses.

analysis of growth with the estimation of natural mortality in a Bayesian framework, we were also able to preserve correlation between growth and survival. The Monte Carlo simulations draw from the joint posterior of S_0 and K. Thus, relatively unlikely combinations such as high growth rate and high survival are appropriately more rare than if these parameters were drawn from two independent distributions.

Survival rate and steepness, together with population size, are the most important parameters in the delay-difference

Fig. 4. (*a*) Equilibrium abundance, (*b*) biomass, (*c*) mean weight, and (*d*) survival to age 10 relative to unfished conditions plotted against absolute harvest rate (individuals per year). Medians (solid lines) and upper and lower 95% confidence intervals (broken lines) are based on 10 000 simulations. Vertical shaded lines indicate the range of harvest rates equivalent to the mortality resulting from the existing catch–release fishery. The equivalent relative annual harvest rate at the beginning of each simulation is shown on the top *x* axis.

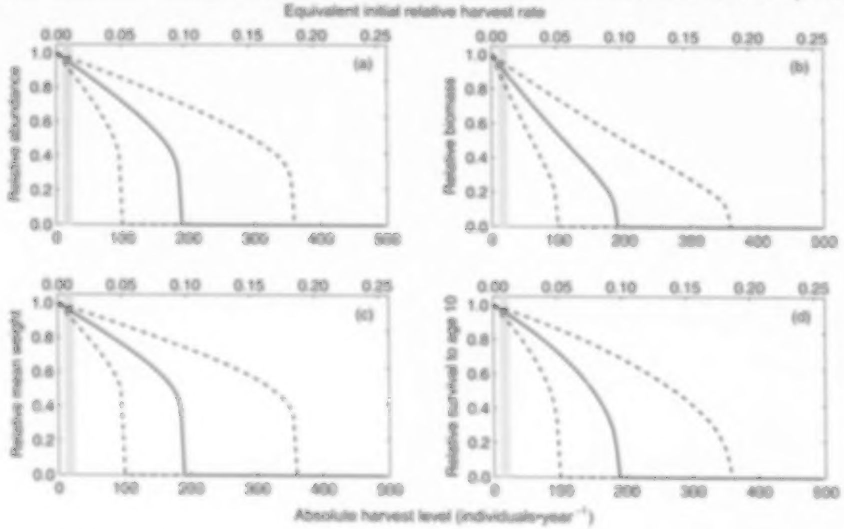

Table 2. Equilibrium abundance (*N*), biomass (*B*), mean weight ($\overline{W}$), survival to age 10 (S_{10}), and probability of extirpation ($p(E)$) for several exploitation scenarios (SH, current subsistence harvest levels; 2SH, double current subsistence harvest levels; CR low, CR high, and 2CR high, catch–release based on the low and high estimates of release mortality and a doubling of the recreational catch; RH, 100% retention (i.e., no catch–release) of fish caught in the recreational fishery).

Scenario	*N*	*B*	$\overline{W}$	S_{10}	$p(E)$
CR low (10)	0.98 (0.96–0.99)	0.96 (0.93–0.98)	0.98 (0.96–0.99)	0.98 (0.96–0.99)	0.00
CR high (23)	0.94 (0.90–0.97)	0.90 (0.82–0.94)	0.95 (0.91–0.97)	0.95 (0.91–0.97)	0.00
2CR high (46)	0.90 (0.81–0.94)	0.82 (0.68–0.90)	0.91 (0.83–0.95)	0.91 (0.82–0.95)	0.00
SH + CR low (73)	0.83 (0.68–0.91)	0.70 (0.49–0.83)	0.85 (0.72–0.92)	0.83 (0.68–0.91)	0.00
SH + CR high (86)	0.80 (0.63–0.89)	0.66 (0.42–0.81)	0.83 (0.67–0.91)	0.81 (0.62–0.90)	0.00
SH (63)	0.85 (0.73–0.92)	0.74 (0.55–0.85)	0.87 (0.76–0.93)	0.86 (0.73–0.93)	0.00
RH (240)	0.00 (0.00–0.69)	0.00 (0.00–0.50)	0.00 (0.00–0.73)	0.00 (0.00–0.67)	0.57
2SH + CR high (149)	0.63 (0.00–0.80)	0.43 (0.00–0.67)	0.68 (0.00–0.83)	0.61 (0.00–0.81)	0.09

Note: All scenarios are based on an assumption of constant harvest at the level indicated in parentheses next to the scenario. All values except $p(E)$ are expressed relative to the unfished state and represent medians from the Monte Carlo simulations. The 95% confidence interval is given in parentheses. Note that a value of *zero* indicates extirpation. No confidence interval can be calculated for $p(E)$.

model for predicting the relative impact of different harvest rates. Although there remains substantial uncertainty in all of these parameters, the data requirements of this approach are minimal and the results are sufficiently precise to provide useful answers to the key motivating question: is the existing catch–release fishery having a substantial adverse impact on this population of taimen? Based on our analysis, the answer is clearly no. A fishery of this size, however, has the potential to seriously endanger this population if fish are retained or if postrelease mortality rates are higher (e.g., due to more harmful fishing gear such as live bait or lures with multiple-barbed hooks). Proper management of any more intense exploitation of this population would require better estimates of all parameters and adequate monitoring of exploitation rates. Our model is clearly not sufficient for management that aims to maintain a harvest fishery near some optimal exploitation rate (e.g., F_{MSY}).

We chose to express our harvest scenarios in terms of an absolute harvest rate (individuals·year^{-1}) rather than a relative harvest rate (fraction of the population·year^{-1}), as is more commonly done when displaying the results of fisheries population models. Using a relative harvest rate would reduce the uncertainty in model output that derives from uncertainty in the population size. An absolute harvest rate is, however, more readily interpretable by managers of developing fisheries who may know the absolute harvest from a population (how many fish were caught) but are unlikely to know the exploitation rate (what fraction of the population

Fig. 5. Probability of extirpation vs. absolute harvest rate (individuals per year). The vertical shaded line indicates the range of harvest rates equivalent to the mortality resulting from the existing catch–release fishery. The equivalent relative annual harvest rate at the beginning of each simulation is shown on the top *x* axis.

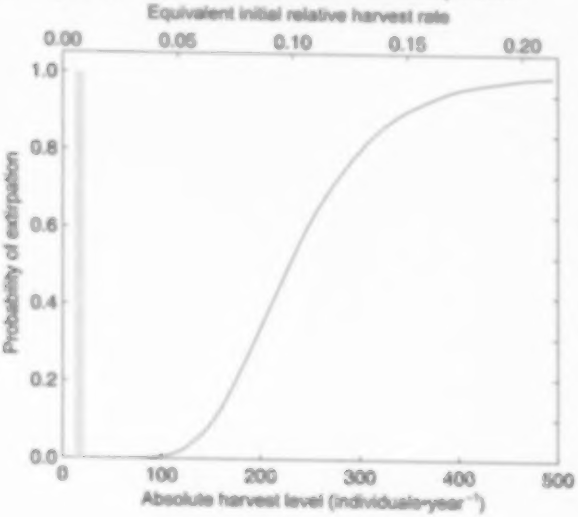

was caught). Of course, model results expressed in terms of an absolute harvest rate are not directly transferable to other populations that differ in size.

Several other rivers in Mongolia support recreational fisheries for taimen, and the potential exists to develop such fisheries elsewhere. Our results suggest that these fisheries can have minimal impact if fishermen practice strict catch–release and if fishing effort does not grow too large. Intense recreational catch–release effort and (or) harvest fisheries, however, have the potential to threaten the continued persistence of this species in one of its last strongholds. Harvest fisheries may also threaten the economic viability of valuable catch–release fisheries if they contribute to a decline in catch rates and abundance of large fish. Fishery management and enforcement capabilities are poorly developed in Mongolia, making top-down management approaches unlikely to succeed. If fisheries for taimen are to be both sustainable and profitable, the economic incentives must be aligned in such a way that conservation is encouraged (Ostrom et al. 1999; Hilborn et al. 2005; Grafton et al. 2006).

One possible approach is to develop a system of concessions, i.e., sections of river within which one recreational fishing company has exclusive access. The value of a concession would depend on maintaining high abundance of large taimen. Strict catch–release may not be appropriate for all concessions, as some anglers value the experience of landing and keeping a fish (Holland and Ditton 1992; Arlinghaus et al. 2007). Yet limits on harvest may be necessary, and some river sections could be set aside as reserves to ensure that overharvest within one or more concessions did not threaten the viability of the entire population. Such concession systems have a long history in Europe, where many freshwater recreational fisheries are privately owned and managed (Arlinghaus 2006). Without a concession system or effective law enforcement, there is less incentive to protect taimen populations as recreational fishing companies that deplete local populations can simply move to other locations. Such serial depletion of recreational fisheries is apparent in other locations where management has been lax (Post et al. 2002; Carpenter and Brock 2004).

In our experience in the Eg–Uur study area, the presence of a recreational fishing company operating in this area is, by itself, a deterrent to harvest, even though the fishing company has no official law enforcement authority. The fishing company hires local guides, camp cooks, and assistants, thus creating an economic incentive for the community to maintain a viable recreational fishery. Local residents working for the fishing company discourage others from fishing. In the absence of nearby markets for taimen or access to refrigeration, such social pressure appears to be effective in limiting illegal harvest. Anglers in this fishery are primarily wealthy individuals from North America, Western Europe, and Japan, with many alternative fishing options. If recreational fishing intensity or illegal harvest increased to the point that catch rates of large taimen seriously declined, the commercial viability of this fishery would be threatened. Our experience suggests that a collapse of this recreational fishery would likely lead to increased fishing mortality rates due to the loss of the deterrent effect.

In considering the impact of the recreational fishery on taimen in the Eg–Uur study area, we ignored secondary effects on the local ecosystem, which can be serious (Cowx 2002). Examples of such effects could include the impact of recreational fishing gear on habitat (e.g., Asoh et al. 2004) or the impact of jet boats on riverbank erosion (McConchie and Toleman 2003) or, potentially, on taimen survival (although a study of effects of boat traffic on Chinook salmon (Reid 2007) found little effect).

We also did not consider immigration and emigration in our population dynamics simulations. Immigration and emigration were incorporated in the analysis of the mark–recapture data through the use of an open population model. On the one hand, movement of taimen into the study area could potentially offset some of the decline in abundance predicted at higher harvest levels. On the other hand, declining abundance within the study area could lead to declines beyond its boundaries through a reduction in net emigration. The overall effect of movement is to reduce the local impact of harvest, while spreading it over a wider area.

Little is known about the scales of population connectivity in taimen. The telemetry study (Gilroy 2007), which tracked taimen for over 2.5 years, found a mean home range size (maximum distance between relocations) of 16.8 km, with 90% of telemetry-tagged individuals showing home ranges smaller than 53 km. Yet some individuals tagged within the study area were found outside it during the extended telemetry surveys. The difference between apparent survival from the mark–recapture analysis and survival estimated from growth rate also suggests that movement could be important. Population genetics studies are needed to determine the optimum scale of analysis for modeling population dynamics of taimen.

The existing recreational fishery for taimen provides economic benefits with little risk to the long-term persistence of the local taimen population. However, this fishery represents an extreme: low fishing effort, spread over a large area, with 100% release and minimum-impact fishing techniques. Our results indicate that a fishery of similar intensity managed as a 100% harvest fishery would seriously threaten the persistence of this population of the endangered taimen. Although recreational fisheries clearly have the potential to adversely impact target species, well-managed catch–release fisheries are not necessarily incompatible with conservation of an endangered species.

Acknowledgements

We thank Brian Roth, Norman Mercado-Silva, Gonzorik, Tsogsaikhan, the Taimen Conservation Fund, Sweetwater Travel, and Hovsgol Travel for field assistance. Bill Pine provided helpful comments on the analysis of mark–recapture data. Financial support was provided by the Taimen Conservation Fund, National Geographic, and the University of Wisconsin Vilas and Anna Grant Birge travel grants.

References

Arlinghaus, R. 2006. Overcoming human obstacles to conservation of recreational fishery resources, with emphasis on central Europe. Environ. Conserv. **33**(1): 46–59. doi:10.1017/S0376892906002700.

Arlinghaus, R., Cooke, S.J., Lyman, J., Policansky, D., Schwab, A., Suski, C., Sutton, S.G., and Thorstad, E.B. 2007. Understanding the complexity of catch-and-release in recreational fishing: an integrative synthesis of global knowledge from historical, ethical, social, and biological perspectives. Rev. Fish. Sci. **15**(1–2): 75–167. doi:10.1080/10641260601149432.

Asoh, K., Yoshikawa, T., Kosaki, R., and Marschall, E.A. 2004. Damage to cauliflower coral by monofilament fishing lines in Hawaii. Conserv. Biol. **18**(6): 1645–1650. doi:10.1111/j.1523-1739.2004.00122.x.

Beddington, J.R., and Kirkwood, G.P. 2005. The estimation of potential yield and stock status using life-history parameters. Philos. Trans. R. Soc. Lond. B Biol. Sci. **360**(1453): 163–170. doi:10.1098/rstb.2004.1582. PMID:15713595.

Beverton, R.J.H., and Holt, S.J. 1959. A review of the lifespans and mortality rates of fish in nature and the relation to growth and other physiological characteristics. *In* Ciba Foundation Colloquium on Ageing. Vol. 5. The lifespan of animals. Little, Brown and Co., Boston, Mass. pp. 142–177.

Carpenter, S.R., and Brock, W.A. 2004. Spatial complexity, resilience, and policy diversity: fishing on lake-rich landscapes. Ecol. Soc. **9**(1): 8.

Casselman, J.M. 1983. Age and growth assessment of fish from their calcified structures — techniques and tools. NOAA (Natl. Ocean. Atmos. Adm.) Tech. Rep. NMFS (Natl. Mar. Fish. Serv.), **8**: 1–17.

Chandra, S., Gilroy, D., Purevdorj, S., and Erdenebat, M. 2005. The feeding behaviour of fish from the upper Lake Baikal watershed of the Eroo River in Mongolia. Mongolian J. Biol. Sci. **3**(1): 39–45.

Charnov, E. 1993. Life history invariants. Oxford University Press, New York.

Coggins, L.G., Pine, W.E., Walters, C.J., and Martell, S.J.D. 2006. Age-structured mark–recapture analysis: a virtual-population-analysis-based model for analyzing age-structured capture–recapture data. N. Am. J. Fish. Manage. **26**(1): 201–205. doi:10.1577/M05-133.1.

Coggins, L.G., Catalano, M.J., Allen, M.S., Pine, W.E., and Walters, C.J. 2007. Effects of cryptic mortality and the hidden costs of using length limits in fishery management. Fish Fish. **8**: 196–210.

Coleman, F.C., Figueira, W.F., Ueland, J.S., and Crowder, L.B. 2004. The impact of United States recreational fisheries on marine fish populations. Science (Washington, D.C.), **305**(5692): 1958–1960. doi:10.1126/science.1100397. PMID:15331771.

Cooke, S.J., and Cowx, I.G. 2004. The role of recreational fishing in global fish crises. Bioscience, **54**(9): 857–859. doi:10.1641/0006-3568(2004)054[0857:TRORFI]2.0.CO;2.

Cowx, I.G. 2002. Recreational fisheries. *In* Handbook of fish biology and fisheries. Vol. II. *Edited by* P.B.J. Hart and J.D. Reynolds. Blackwell Science, Oxford, UK. pp. 367–390.

Deriso, R.B. 1980. Harvesting strategies and parameter estimation for an age-structured model. Can. J. Fish. Aquat. Sci. **37**(2): 268–282. doi:10.1139/f80-034.

Froese, R., and Pauly, D. 2008. FishBase [online]. Available at www.fishbase.org [accessed 7 December 2008].

Gilroy, D. 2007. Home range and seasonal movements of taimen, *Hucho taimen*, in the Eg and Uur rivers, Mongolia. M.S. thesis, Limnology and Marine Science, University of Wisconsin – Madison, Madison, Wisc.

Grafton, R.Q., Arnason, R., Bjorndal, T., Campbell, D., Campbell, H.F., Clark, C.W., Connor, R., Dupont, D.P., Hannesson, R., Hilborn, R., Kirkley, J.E., Kompas, T., Lane, D.E., Munro, G.R., Pascoe, S., Squires, D., Steinshamn, S.I., Turris, B.R., and Weninger, Q. 2006. Incentive-based approaches to sustainable fisheries. Can. J. Fish. Aquat. Sci. **63**(3): 699–710. doi:10.1139/f05-247.

Gunderson, D.R., Zimmerman, M., Nichol, D.G., and Pearson, K. 2003. Indirect estimates of natural mortality rate for arrowtooth flounder (*Atheresthes stomias*) and darkblotched rockfish (*Sebastes crameri*). Fish. Bull. **101**: 175–182.

Guy, C.S., Blankenship, H.L., and Nielsen, L.A. 1996. Tagging and marking. *In* Fisheries techniques. *Edited by* B.R. Murphy and D.W. Willis. American Fisheries Society, Bethesda, Md. pp. 353–379.

Haab, T., Whitehead, J.C., and McConnell, T. 2001. The economic value of marine recreational fishing in the southeast United States: 1997 southeast economic data analysis. US Department of Commerce, National Oceanic and Atmospheric Administration, National Marine Fisheries Service, NOAA Technical Memorandum NMFSC-SEFSC-446.

Hilborn, R., and Walters, C.J. 1992. Quantitative fisheries stock assessment. Chapman & Hall, London, UK.

Hilborn, R., Orensanz, J.M., and Parma, A.M. 2005. Institutions, incentives and the future of fisheries. Philos. Trans. R. Soc. Lond. B Biol. Sci. **360**(1453): 47–57. doi:10.1098/rstb.2004.1569. PMID:15744918.

Holčík, J. 1995. Threatened fishes of the world — *Hucho hucho* (Linnaeus, 1758) (Salmonidae). Environ. Biol. Fishes, **43**(1): 105–106. doi:10.1007/BF00001822.

Holčík, J., Hensel, K., Nieslanik, J., and Skacel, L. 1988. The Eurasian huchen, *Hucho hucho*, largest salmon of the world. Kluwer Academic Publishers, Boston, Mass.

Holland, S.M., and Ditton, R.B. 1992. Fishing trip satisfaction: a typology of anglers. N. Am. J. Fish. Manage. **12**(1): 28–33. doi:10.1577/1548-8675(1992)012<0028:FTSATO>2.3.CO;2.

Jensen, A.L. 1996. Beverton and Holt life history invariants result from optimal trade-off of reproduction and survival. Can. J. Fish. Aquat. Sci. **53**(4): 820–822. doi:10.1139/cjfas-53-4-820.

Jolly, G.M. 1965. Explicit estimates from capture–recapture data with both death and immigration-stochastic model. Biometrika, **52**: 225–247. PMID:14341276.

Kelch, D., Lichtkoppler, F., Sohngen, B., and Daigneault, A. 2006. The value of steelhead (*Onchorhynchus mykiss*) angling in Lake Erie tributaries. J. Gt. Lakes Res. **32**(3): 424–433. doi:10.3394/0380-1330(2006)32[424:TVOSOM]2.0.CO;2.

Kimura, D. 1988. Stock–recruitment curves as used in the stock-reduction analysis model. J. Cons. Int. Explor. Mer. **44**: 253–258.

Mace, P.M., and Doonan, I.J. 1988. A generalized bioeconomic simulation model for fish dynamics. Fisheries Research Center, P.O. Box 297, Wellington, New Zealand.

Matveyev, A.N., Pronin, N.M., Samusenok, V.P., and Bronte, C.R. 1998. Ecology of Siberian taimen *Hucho taimen* in the Lake Baikal Basin. J. Gt. Lakes Res. **24**(4): 905–916.

Maunder, M.N. 2004. Population viability analysis based on combining Bayesian, integrated, and hierarchical analyses. Acta Oecol. **26**(2): 85–94. doi:10.1016/j.actao.2003.11.008.

McAllister, M.K., Pikitch, E.K., and Babcock, E.A. 2001. Using demographic methods to construct Bayesian priors for the intrinsic rate of increase in the Schaefer model and implications for stock rebuilding. Can. J. Fish. Aquat. Sci. **58**(9): 1871–1890. doi:10.1139/cjfas-58-9-1871.

McConchie, J.A., and Toleman, I.E.J. 2003. Boat wakes as a cause of riverbank erosion: a case study from the Waikato River, New Zealand. J. Hydrol. (Amst.), **42**: 163–179.

Musick, J. 1999. Life in the slow lane: ecology and conservation of long-lived marine animals. American Fisheries Society, Bethesda, Md.

Myers, R.A., and Barrowman, N.J. 1996. Is fish recruitment related to spawner abundance. Fish. Bull., **94**: 707–724.

Myers, R.A., Bowen, K.G., and Barrowman, N.J. 1999. Maximum reproductive rate of fish at low population sizes. Can. J. Fish. Aquat. Sci. **56**(12): 2404–2419. doi:10.1139/cjfas-56-12-2404.

Myers, R.A., Barrowman, N.J., Hilborn, R., and Kehler, D.G. 2002. Inferring Bayesian priors with limited direct data: applications to risk analysis. N. Am. J. Fish. Manage. **22**(1): 351–364. doi:10.1577/1548-8675(2002)022<0351:IBPWLD>2.0.CO;2.

Ocock, J., Baasanjav, G., Baillie, G., Erdenebat, M., Kottelat, M., Mendsaikhan, B., and Smith, K. 2006. Summary conservation action plans for Mongolian fishes. Zoological Society of London, London, UK.

Ostrom, E., Burger, J., Field, C.B., Norgaard, R.B., and Policansky, D. 1999. Revisiting the commons: local lessons, global challenges. Science (Washington, D.C.), **284**(5412): 278–282. doi:10.1126/science.284.5412.278. PMID:10195886.

Pauly, D. 1980. On the interrelationships between natural mortality, growth parameters, and mean environmental temperature in 175 fish stocks. J. Cons. Int. Explor. Mer. **39**: 175–192.

Pauly, D. 1995. Anecdotes and the shifting base-line syndrome of fisheries. Trends Ecol. Evol. **10**(10): 430. doi:10.1016/S0169-5347(00)89171-5.

Pollock, K.H., Nichols, J.D., Brownie, C., and Hines, J.E. 1990. Statistical inference for capture–recapture experiments. Wildlife Monographs No. 107.

Post, J.R., Sullivan, M., Cox, S., Lester, N.P., Walters, C.J., Parkinson, E.A., Paul, A.J., Jackson, L., and Shuter, B.J. 2002. Canada's recreational fisheries: the invisible collapse? Fisheries, **27**(1): 6–17. doi:10.1577/1548-8446(2002)027<0006:CRF>2.0.CO;2.

Reid, I.S. 2007. Influence of motorboat use on thermal refuges and implications to salmonid physiology in the lower Rogue River, Oregon. N. Am. J. Fish. Manage. **27**(4): 1162–1173. doi:10.1577/M06-061.1.

Schnute, J.T. 1985. A general theory for analysis of catch and effort data. Can. J. Fish. Aquat. Sci. **42**(3): 414–429. doi:10.1139/f85-057.

Schnute, J.T. 1987. A general fishery model for a size-structured fish population. Can. J. Fish. Aquat. Sci. **44**(5): 924–940. doi:10.1139/f87-111.

Seber, G.A.F. 1965. A note on multiple-recapture census. Biometrika, **52**: 249–259. PMID:14341277.

Sharp, D., and Bernard, D.R. 1988. Precision of estimated ages of lake trout from five calcified structures. N. Am. J. Fish. Manage. **8**(3): 367–372. doi:10.1577/1548-8675(1988)008<0367:POEAOL>2.3.CO;2.

Stubblefield, A., Chandra, S., Eagan, S., Tuvshinjargal, D., Davaadorzh, G., Gilroy, D., Sampson, J., Thorne, J., Allen, B.C., and Hogan, Z. 2005. Impacts of gold mining and land use alterations on the water quality of central Mongolian rivers. Integr. Environ. Assess. Manag. **1**(4): 365–373. doi:10.1897/1551-3793(2005)1[365:IOGMAL]2.0.CO;2. PMID:16639903.

Vander Zanden, M.J., Joppa, L.N., Allen, B.C., Chandra, S., Gilroy, D., Hogan, Z., Maxted, J.T., and Zhu, J. 2007. Modeling spawning dates of *Hucho taimen* in Mongolia to establish fishery management zones. Ecol. Appl. **17**(8): 2281–2289. doi:10.1890/06-1781.1. PMID:18213968.

Walters, C.J., and Korman, J. 1999. Linking recruitment to trophic factors: revisiting the Beverton–Holt recruitment model from a life history and multispecies perspective. Rev. Fish Biol. Fish. **9**(2): 187–202. doi:10.1023/A:1008991021305.

Walters, C.J., and Martell, S.J.D. 2004. Fisheries ecology and management. Princeton University Press, Princeton, N.J.

Walters, C.J., Martell, S.J.D., and Korman, J. 2006. A stochastic approach to stock reduction analysis. Can. J. Fish. Aquat. Sci. **63**(1): 212–223. doi:10.1139/f05-213.

White, G.C., and Burnham, K.P. 1999. Program MARK: survival estimation from populations of marked animals. Bird Study, **46**(Suppl.): 120–139. doi:10.1080/00063659909477239.

Winemiller, K.O., and Rose, K.A. 1992. Patterns of life-history diversification in North American fishes: implications for population regulation. Can. J. Fish. Aquat. Sci. **49**(10): 2196–2218. doi:10.1139/f92-242.

Appendix A

Beverton–Holt stock–recruit functions are frequently parameterized based on one known point on the curve (B^*, R^*) and a steepness parameter (z), defined as the proportion of unfished recruitment (R_0) produced by 20% of the unfished biomass (B_0) (Mace and Doonan 1988). B^* and R^* can be any arbitrary point on the stock–recruit curve (Kimura 1988). However, when B^* and R^* are not equal to B_0 and R_0, the proportion of R^* produced by 20% of B^* (z^*) is not necessarily the same as z. In many cases, B_0 and R_0 are unknown, but current biomass can be estimated from surveys or mark–recapture experiments, and current equilibrium recruitment can be estimated as the product of current abundance and the annual mortality rate. When current biomass is not substantially lower than B_0, there may be little harm in using z instead of z^*. We investigated this possibility by calculating z^* for different values of z and B^*/B_0 (Table A1). For modestly depleted populations with relatively high steepness, the effect on the stock–recruitment curve of using B^*, R^*, and z instead of z^* is minor (Fig. A1).

Table A1. The ratio of steepness defined relative to current biomass and recruitment (z^*) to steepness defined relative to unfished biomass and recruitment (z).

	Current biomass (B^*) / unfished biomass (B_0)										
Steepness (z)	0.50	0.55	0.60	0.65	0.70	0.75	0.80	0.85	0.90	0.95	0.99
0.50	0.77	0.80	0.82	0.85	0.87	0.90	0.92	0.94	0.96	0.98	1.00
0.55	0.77	0.80	0.83	0.85	0.88	0.90	0.92	0.94	0.96	0.98	1.00
0.60	0.78	0.81	0.83	0.86	0.88	0.90	0.93	0.95	0.96	0.98	1.00
0.65	0.79	0.82	0.84	0.87	0.89	0.91	0.93	0.95	0.97	0.98	1.00
0.70	0.81	0.83	0.86	0.88	0.90	0.92	0.94	0.96	0.97	0.99	1.00
0.75	0.83	0.85	0.87	0.89	0.91	0.93	0.95	0.96	0.98	0.99	1.00
0.80	0.85	0.87	0.89	0.91	0.93	0.94	0.96	0.97	0.98	0.99	1.00
0.85	0.88	0.90	0.92	0.93	0.94	0.96	0.97	0.98	0.98	0.99	1.00
0.90	0.91	0.93	0.94	0.95	0.96	0.97	0.98	0.98	0.99	0.99	1.00
0.95	0.95	0.96	0.97	0.97	0.98	0.98	0.99	0.99	0.99	1.00	1.00
0.99	0.99	0.99	0.99	0.99	1.00	1.00	1.00	1.00	1.00	1.00	1.00

Fig. A1. A true Beverton–Holt stock–recruitment curve (solid line) defined using unfished biomass (B_0), unfished recruitment (R_0), and steepness (z) defined relative to B_0 (1000) and R_0 (100) and an estimated stock–recruit curve (broken line) defined using the points B^* (800), R^* (98.5), and z, where $z = 0.8$ and $B^* = 0.8\,B_0$. Units are arbitrary.

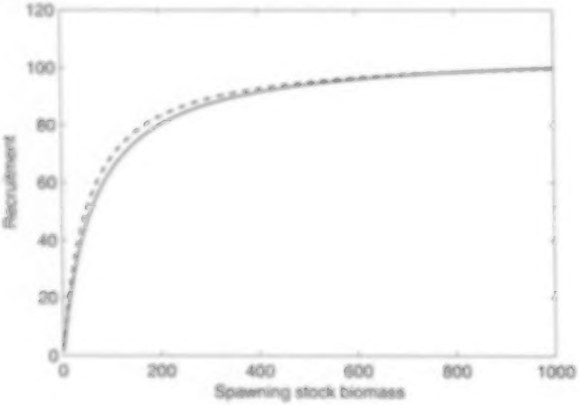

References

Kimura, D. 1988. Stock–recruitment curves as used in the stock-reduction analysis model. J. Cons. Int. Explor. Mer. **44**: 253–258.

Mace, P.M., and Doonan, I.J. 1988. A generalized bioeconomic simulation model for fish dynamics. Fisheries Research Center, P.O. Box 297, Wellington, New Zealand.

Temporal trends in probabilistic maturation reaction norms and growth of Atlantic cod (*Gadus morhua*) on the Icelandic shelf

Heidi Pardoe, Anssi Vainikka, Gudmundur Thórdarson, Gudrun Marteinsdóttir, and Mikko Heino

Abstract: Decreasing temporal trends in probabilistic maturation reaction norm (PMRN) midpoints, symptomatic of earlier maturation despite environmentally induced variation in growth, have been observed in many exploited fish stocks. Here, we studied the growth and maturation trends of female and male Icelandic cod (*Gadus morhua*) by estimating PMRN midpoints for cohorts 1964–1999 and found evidence that a shift towards maturation at smaller sizes and younger ages has occurred independently of changes in growth, condition, and temperature. Weighting the data with regional survey abundance estimates to account for spatial heterogeneity in maturity status and sampling intensity did not qualitatively affect the temporal trends. Length-at-age also decreased through the study period, which, through simulations, could be attributed to the energetic costs of earlier maturity at maturing age groups but not at younger ages. These findings support the hypothesis that such changes in maturation schedules are not caused by environmental factors alone but could also reflect a genetic change, potentially in response to intensive fishing.

Résumé : On a observé chez plusieurs stocks de poissons exploités des tendances temporelles à la baisse dans les points médians des normes probabilistes de réaction de la maturation, ce qui est un symptôme d'une maturation précoce malgré la variation de la croissance sous influence environnementale. Nous étudions ici les tendances de croissance et de maturation des femelles et des mâles de morues (*Gadus morhua*) islandaises en estimant les points médians des normes probabilistes de réaction de la maturation pour les cohortes de 1964 à 1999. Nous trouvons qu'il est apparu une tendance vers la maturation à des tailles plus petites et des âges plus jeunes indépendamment des changements de croissance, de condition et de température. Une pondération des données avec les estimations des abondances d'inventaire régionales, pour tenir compte de l'hétérogénéité spatiale du statut de maturité et de l'intensité de l'échantillonnage, n'affecte pas qualitativement les tendances temporelles. La longueur en fonction de l'âge a aussi diminué durant la période d'étude, ce qui, dans des simulations, peut s'expliquer par le coût énergétique de la maturité plus précoce chez les groupes en maturation, mais non chez les groupes plus jeunes. Ces résultats appuient l'hypothèse qui veut que de tels changements dans le calendrier de la maturation ne soient pas causés par les seuls facteurs environnementaux, mais qu'ils puissent aussi refléter un changement génétique, peut-être en réaction à la pêche intensive.

[Traduit par la Rédaction]

Introduction

Trends towards maturation at younger ages and smaller sizes have been observed in many exploited fish stocks (e.g., Trippel 1995; Hutchings and Baum 2005; Jørgensen et al. 2007). Such changes are relevant for fisheries management, since earlier maturation may have negative implications for population growth rates (reviewed by Hutchings and Fraser 2008) and yield (Law and Grey 1989; Stokes and Law 2000; Conover and Munch 2002) through decreased growth rates and size of fish in the catch (Heino 1998) and the reduced reproductive ability of a spawning stock comprising smaller individuals and a higher proportion of first-time spawners (Marteinsdóttir and Begg 2002; Hutchings 2005). Shifts towards earlier maturity may also increase variability in population abundance (Stergiou 2002;

Received 26 September 2008. Accepted 15 July 2009. Published on the NRC Research Press Web site at cjfas.nrc.ca on 6 October 2009. J20796

Paper handled by Associate Editor C. Tara Marshall.

H. Pardoe.[1] Marine Research Institute, Skúlagata 4, P.O. Box 1390, 121 Reykjavik, Iceland; Institute of Biology, University of Iceland, Sturlugata 7, 101 Reykjavik, Iceland.
A. Vainikka. Institute of Coastal Research, Swedish Board of Fisheries, Box 109, SE-742 22 Öregrund, Sweden.
G. Thórdarson. Marine Research Institute, Skúlagata 4, P.O. Box 1390, 121 Reykjavik, Iceland.
G. Marteinsdóttir. Institute of Biology, University of Iceland, Sturlugata 7, 101 Reykjavik, Iceland.
M. Heino. Department of Biology, University of Bergen, Box 7800, N-5020 Bergen, Norway; Institute of Marine Research, Box 1870 Nordnes, N-5817 Bergen, Norway; Evolution and Ecology Program, International Institute for Applied Systems Analysis, A-2361 Laxenburg, Austria.

[1] Corresponding author (e-mail: heidi@hafro.is).

Can. J. Fish. Aquat. Sci. **66**: 1719–1733 (2009) doi:10.1139/F09-132 Published by NRC Research Press

Anderson et al. 2008; Stenseth and Rouyer 2008) and adversely affect the ability of a population to recover from overharvesting (Hutchings 2005; Walsh et al. 2006; Enberg et al. 2009). Consequently, monitoring life history traits and the potential causes of significant trends is essential for the effective long-term conservation and management of the resource (Trippel 1995; Jørgensen et al. 2007).

Phenotypic variability in the maturation pattern of a stock typically arises through plastic responses to environmental changes that may also be density dependent. For example, relaxed competition for food in a fished-down stock may lead to accelerated growth and in turn earlier maturation (Trippel 1995; Law 2000). However, given that the maturation process is a complex physiological cascade, it is likely to be affected by ontogenetic processes related to not only growth but also environmental conditions and individual experience preceding and at the point at which the "decision" to mature is made (e.g., see Wright 2007). Consequently, factors such as temperature (Dhillon and Fox 2004; Kraak 2007) and the status of energy reserves, reflected by condition (Yoneda and Wright 2005; Thorpe 2007), are potential proximate triggers of the maturation process (Wright 2007). However, these factors are often not taken into consideration when temporal trends in maturation patterns are studied (however, see Grift et al. 2007; Mollet et al. 2007).

In addition to plastic responses, fishing has been identified as a potentially strong selective force in shaping the life history traits of exploited fish populations (Law and Grey 1989; Conover and Munch 2002; Dunlop et al. 2009). Harvest mortality may favour adaptations in traits such as size and age at maturation, growth rate, reproductive effort, and behaviours related to feeding and mating, with changes being more pronounced when exploitation is size selective (e.g., Heino and Godø 2002; Conover et al. 2005; Reznick and Ghalambor 2005). Aquaculture studies reporting moderate to high heritabilities for traits such as age at maturation and weight-at-age in cod ($h^2 = 0.12–0.56$ and 0.20–0.51, respectively; Kolstad et al. 2006) and salmonids (Henryon et al. 2002; Kause et al. 2003) support the hypothesis that these traits are susceptible to genetic change, including that mediated through fishing.

The Icelandic stock of Atlantic cod (*Gadus morhua*) has supported an important fishery for decades (Fig. 1*a*), although both the stock (Fig. 1*b*) and the catches have been below historic levels for many years (Anonymous 2007). Although no formal quantification is currently available, the fishery is considered to be highly size selective, targeting large individuals (Anonymous 2007). Bottom trawling (conforming to codend mesh size regulations of 155 mm from 1977 and 135 mm for the past decade) provides the majority of the catch (Anonymous 2007). Icelandic cod become fully recruited to the fishery at age 5 or 6 at which between approximately 25% and 55% are mature according to recent data (Anonymous 2007). Intensive exploitation during the last decades has led to truncation in the age structure of the stock (Marteinsdóttir and Thórarinsson 1998). Concurrently, declines in age and size at 50% maturity have been observed (Marteinsdóttir and Begg 2002; Anonymous 2007).

In this study, we assess trends in the maturation schedules of female and male Icelandic cod between cohorts 1964 and 1999, utilizing probabilistic maturation reaction norms (PMRNs) as our primary tool. We investigate whether there have been simultaneous trends in potential explanatory variables, namely water temperature or cod condition, or potential sampling biases related to the demographic effects of spatially segregated fishing or geographically differing cod characteristics, which would influence our interpretation of the PMRNs. We hypothesize that residual changes not explainable by environmental variables may be due to the effects of fishing but note that a causal relationship cannot be demonstrated through such a descriptive study. We also introduce a novel method to examine whether changes in maturation could, through energetic trade-offs, explain those observed in length-at-age or whether independent changes could have occurred in growth.

Materials and methods

Data

Data were obtained from the Marine Research Institute (MRI), Reykjavik, Iceland. All data were collected by bottom trawling but originated from three sources: the annual spring (March) groundfish survey (GSD), which began in 1985, long-term ad hoc research surveys (SD), and commercial catches (CD). The CD consisted of samples collected by observers from the Icelandic Directorate of Fisheries onboard commercial trawlers using 135 or 155 mm mesh size in the codend. GSD were collected using a bottom trawl with a 40 mm mesh size in the codend (Pálsson et al. 1989), and therefore, only those SD collected with the same mesh size were selected. During MRI research surveys (SD and GSD), samples were taken randomly across the area of the continental shelf of Iceland occupied by cod, whereas the spatial coverage of CD was more limited (Fig. 2). For the purposes of our analysis, GSD and SD were considered comparable (see Discussion). PMRNs were estimated from CD so that they could be compared with PMRNs from SD/GSD but were excluded from all trend analyses, since CD are less representative.

For all data types, location and date were recorded, total length was measured to the nearest 1 cm, otoliths were collected for age determination, sex was recorded, and maturity stage (1, immature; 2, ripening; 3, spawning; 4, spent) was determined macroscopically according to the stages defined in Powles (1958). All fish were then reclassified as either juvenile (class 1) or mature (classes 2–4). From 1993, body, gutted, and liver weights were also measured to the nearest 1 g during the annual spring groundfish survey (GSD). Cod in Icelandic waters spawn from late March to May–June (Marteinsdóttir et al. 2000), and therefore, only those data collected between February and April were selected to maximize the likelihood of accurate maturity stage estimation and also to provide consistency between the different sources. The final data set was divided into three temporally overlapping groups: SD, years 1967–1984, CD, years 1977–1995, and GSD (with some SD), years 1989–2007 (Table 1; Fig. 2). To verify that combining data in the most recent time period was appropriate, temporal trends in PMRNs estimated from GSD alone and GSD combined with SD (GSD/SD) were compared using analysis of covariance (ANCOVA). For each age and sex combination, an ANCOVA explaining the Lp50 estimates (length at which the

Fig. 1. (*a*) Average fishing mortality (ages 5–10) and (*b*) biomass (solid line, total for ages 4+; broken line, spawning stock) of the Icelandic cod stock since 1955 (Anonymous 2007).

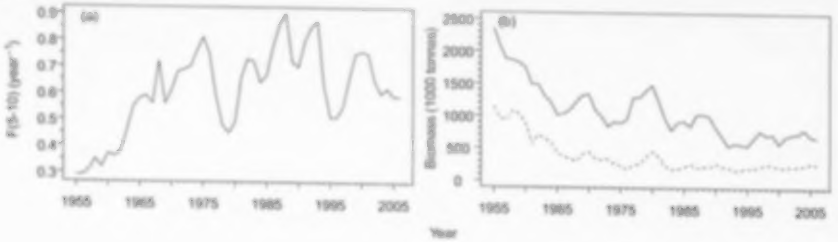

Fig. 2. Sampling locations for three data types and time periods ((*a*) SD, 1967–1984, (*b*) CD, 1977–1995, and (*c*) GSD/SD, 1989–2007) (also see Table 1). Bar plots show the percentage of samples from the southern region (hatched bars) and northern region (solid bars). The 500 m depth contour is marked (thin line).

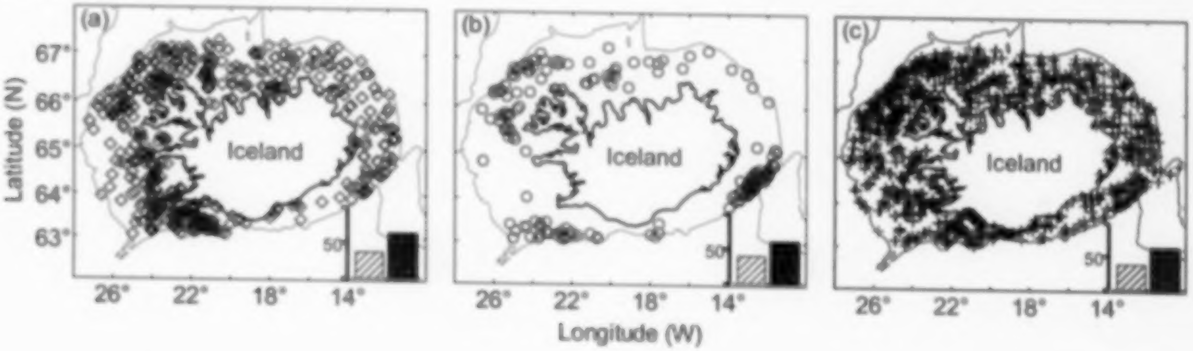

Table 1. Data summary for Icelandic cod.

Data type, years	Age (years) 3	4	5	6	7	8	Total	% for females
SD, 1967–1984 (Fig. 2*a*)								
Total	2743	5032	4667	4229	3515	2178	22364	48
Mean per cohort[a]	115	298	271	267	220	112		
Mean % mature, females[a]	0	2	12	35	61	82	29	
Mean % mature, males[a]	1	4	20	54	78	90	40	
CD, 1977–1995 (Fig. 2*b*)								
Total	183	2446	4698	3971	2615	924	14837	50
Mean per cohort[b]	8	116	270	241	165	48		
Mean % mature, females[b]	5	10	15	30	53	66	27	
Mean % mature, males[b]	5	9	23	41	64	73	35	
GSD/SD, 1989–2007 (Fig. 2*c*)								
Total	11373	14650	13899	11413	7375	3375	62085	50
Mean per cohort[c]	574	762	694	579	374	180		
Mean % mature, females[c]	0	5	22	52	75	86	37	
Mean % mature, males[c]	1	13	42	66	81	90	50	

Note: For each time period and data type (survey data (SD), commercial data (CD), and groundfish survey data (GSD)): age-specific total sample size, mean per cohort, and mean proportion mature for females and males are shown. Percentage of data for females is also shown.

[a] For cohorts 1964–1976.

[b] For cohorts 1974–1987.

[c] For cohorts 1985–1999.

probability to mature is 50%) as a function of data source (categorical variable, GSD or GSD/SD) and cohort (continuous variable), weighted by the inverse of the bootstrap variance (see below), was used to test for differences between the intercepts and slopes of the two Lp50 time series.

PMRN estimation

PMRNs describe age- and size-specific population-level probabilities for an average individual to mature (Heino et al. 2002*a*). These maturation probabilities are thus conditional on an individual having attained a certain combination of age and size. Based on the assumption that a significant component of maturation plasticity results from environmentally induced variation in growth and survival and that these processes are the principle determinants of that age–size combination being reached, maturation reaction norms are considered to be largely unaffected by changes in average growth and mortality (Heino et al. 2002*a*; Dieckmann and Heino 2007; Heino and Dieckmann 2008). As it is not possible to separate first-time and repeat spawning Icelandic cod, retrospective PMRNs were estimated using the demographic method of Barot et al. (2004*a*), which relies on individual records of age (a), size (s) (in this case length), and maturity status. PMRNs were estimated separately for males and females in each data group and were determined for each age and cohort (c) in three stages: estimation of (*i*) the maturity ogive $o(a, s, c)$, (*ii*) growth rate as the annual increment in average length Δs, and (*iii*) the cohort-specific probability to mature at a certain age and size:

$$(1) \qquad p(a, s, c) = \frac{o(a, s, c) - o(a - 1, s - \Delta s, c)}{1 - o(a - 1, s - \Delta s, c)}$$

Temporal trends were visualized using PMRN midpoints (Lp50s) calculated by linear interpolation between the lengths associated with maturation probabilities immediately above and below 50% (Barot et al. 2004*b*). Further details of these procedures, performed in R (version 2.6.0) (R Development Core Team, R Foundation for Statistical Computing, Vienna, Austria), are provided below. We focused our analyses on ages 4–8, thus also requiring cod of age 3 for estimation of growth increments and maturity. In the majority of cases, the final age- and cohort-specific sample sizes (Table 1) fulfilled the minimum recommended sample size (100) for PMRN analysis (Barot et al. 2004*a*). However, for some ages and cohorts with very low sample sizes, it was not possible to compute the Lp50.

The most important data requirement of the PMRN method is that proportions of mature fish within each age and length class are unbiased (Barot et al. 2004*b*). Differing sampling intensity between the northern and southern regions of Iceland could lead to a violation of this requirement because a significant proportion of the immature and mature cod are spatially segregated during the spawning season (Astthorsson et al. 1994; Marteinsdóttir et al. 2000; Begg and Marteinsdóttir 2003). Consequently, we considered weighting the proportions of mature and immature fish in our data with regional abundance estimates. This procedure makes the resulting estimates of population parameters less biased. Survey indices, estimates of the relative abundances of fish in the north and south (from the annual spring groundfish survey; Anonymous 2007), were available for data group 3 (cohorts 1985–1999) only. Those data (GSD/SD) were thus weighted by the age-, region-, and year-specific survey index divided by the corresponding age-, region-, and year-specific sample size. ANCOVAs (see Data section above) were used to test for differences between temporal trends in Lp50s estimated from unweighted and weighted (data source in ANCOVA models) data.

Maturity ogives

The proportions of mature fish as a function of age and size, i.e., maturity ogives, were estimated using logistic regression. Candidate models (including the cohort effect) were first examined using stepwise forward and backward selection procedures in SPSS (version 15.0.0) (SPSS Inc., Chicago, Illinois), allowing for all possible first-order interactions, with log-likelihood tests used to compare competing models. The final model was chosen based on the proportion of correctly classified observations and Nagelkerke's R^2 (coefficient of determination for the logistic regression):

$$(2) \qquad \text{logit}[o] \sim \text{age} + \text{size} + \text{factor(cohort)} + \text{age} \times \text{factor(cohort)} + \text{size} \times \text{factor(cohort)}$$

where size refers to length in centimetres. Age was entered as a continuous variable, since the age-specific sample sizes were sometimes too low to allow full factorial estimation of the effects. The predictive power of the chosen model was similar to that in which age was factorial, but the Akaike information criterion was lower. The age × length interaction was omitted, since its inclusion caused "swapping" in the reaction norm, i.e., in some samples, the probability to mature was higher at smaller sizes, likely an artefact of low sample sizes (Barot et al. 2004*a*).

Growth

Age- and cohort-specific growth increments were estimated by predicting average length at age a in year y using the model

$$(3) \qquad \text{Size} \sim \text{age} + \text{factor(year)} + \text{age} \times \text{factor(year)}$$

and then calculating the difference between estimated lengths at age a in year y and at age $a - 1$ in year $y - 1$. A linear effect of age was chosen because of insufficient data in some samples for full factorial estimation of the effects and for consistency with the ogive estimation.

Confidence intervals

Since obtaining direct estimates of the error associated with the reaction norm midpoints is beyond realistic options (Barot et al. 2004*a*), the PMRN estimation procedure was repeated 1000 times by year stratified bootstrapping of the original data. Confidence intervals (CI) were estimated as the 2.5 and 97.5 percentiles of the 1000 bootstrapped Lp50 estimates for each age and cohort. Low sample sizes in the resampled data, particularly for those ages where few individuals mature, can result in wide CI for the Lp50s or even make it impossible to compute the PMRN for those bootstrap samples (Barot et al. 2004*a*). If Lp50s were not successfully calculated in ≥90% of the 1000 bootstrap samples, that age/cohort was removed from further analyses.

Analysis of trend and sex differences

To test for an age-specific trend in Lp50s between cohorts 1964 and 1999, the reaction norm midpoints were regressed against cohort (as a continuous variable) and weighted by the inverse of the bootstrap variance (Grift et al. 2003).

To determine whether males and females have different PMRNs, we used a randomization test (Barot et al. 2004*b*). Observed sex values were redistributed randomly across the data set and age- and cohort-specific Lp50s were estimated from these new data, for each sex separately, using the method described above. These Lp50s were modelled as a function of age, cohort, and sex (all considered as factors) and the parameter corresponding to the effect of sex was recorded. The randomization procedure was repeated 1000 times, separately for each data group. The same parameter was collected for the original, nonrandomized data sets. The effect of sex was then considered to be significant if this parameter estimate fell within or beyond the upper 5% tail (one-tailed test: H_1 being females have higher PMRNs than males) of the distribution of the 1000 coefficients obtained from the randomization procedure.

Potential explanatory variables of Lp50 trends

In principle, fishing in northern Icelandic waters where immature cod are located in greatest abundance (Astthorsson et al. 1994) could result in their selective removal, particularly during the spawning season (Thórarinsson and Jóhannesson 1997; Begg and Marteinsdóttir 2003), and thus lead to a sampling bias towards mature cod (at each size and age class) in research data. Fishing might then cause false trends in the estimated Lp50s, simply as an artefact of sampling, particularly if this bias increased through time. To address this, we investigated potential correlations between fishing mortality F (per year) and age- and sex-specific PMRN midpoints using linear regressions weighted by the inverse of the bootstrap variance. Fishing mortality F was available as both average annual mortality of ages 5–10 (F(5–10)) (Fig. 1*a*) and age- and cohort-specific estimates (Anonymous 2007).

Factors such as condition and temperature could also directly affect maturation decisions and thereby explain changes in PMRNs (Kraak 2007; Marshall and McAdam 2007; Thorpe 2007). Average condition, represented by the hepatosomatic index (HSI) (percent) and relative body condition index (K_r), was calculated from GSD separately for immature and mature Icelandic cod aged 4–8 years in the spring of 1993–2007 using the method described in Pardoe et al. (2008). Because of the potential error associated with assignment of maturity status in the autumn, immature and mature cod were combined before estimating these indices from MRI autumn (October) groundfish survey data for the period 1995–2007.

Temperature (degrees Celsius) time series collected by MRI on the main spawning grounds in the southwest (Selvogsbanki) and off the central north coast (Siglunes) were used to qualitatively assess if Lp50 trends reflected those observed in temperature and quantitatively examine correlations between Lp50s and average temperature. For the former, annual temperature measurements made at 50–150 m in February–March were deemed most representative of the long-term conditions in Icelandic waters (H. Valdimarsson, MRI, Skúlagata 4, 121 Reykjavik, Iceland, personal communication (2008)). For the latter, measurements from the third quarter, when temperature might be expected to directly influence the maturation decision of cod that will spawn in the following spring, were available for the majority of years between 1968 and 2007 (north, 50–150 m) and between 1971 and 2007 (southwest, 0–200 m). Correlations were investigated according to Kraak (2007) with the exception that the positive trends in temperature (north: $P = 0.0039$, southwest: $P = 0.001$) were removed prior to the analyses. This was necessary, since temporal covariation between trends in Lp50s and temperature would otherwise confound these analyses. Linear regression (weighted by the inverse of the bootstrap variance) was used to test for an effect of detrended temperature measured 1 ($t_{\text{year-1}}$), 2 ($t_{\text{year-2}}$), and 3 ($t_{\text{year-3}}$) years prior to the assessment of maturity status (t_{year}) on the Lp50 trends.

Growth trends

Trends in average length were investigated using a generalized linear model (GLM) that included (*i*) the main effect of age, (*ii*) first-order interactions between age and cohort, cohort and sex, cohort and maturity, cohort and region (south or north), cohort and data group (SD or GSD/SD), age and region, age and maturity, age and data group, age and sex, maturity and region, and maturity and data group, and (*iii*) second-order interactions between cohort, age, and maturity and cohort, age, and data group. All variables were factorial with the exception of cohort. The model was based primarily on those effects and interactions considered to be biologically meaningful, although the final model also had the lowest Akaike information criterion out of all those examined.

Effect of earlier maturation on growth

Owing to the allocation of limited energy to reproduction, maturation usually leads to slower growth (Roff 1983; Lester et al. 2004; Heino et al. 2008). To investigate the relationship between the observed lengths-at-age and maturation schedules, we simulated cohorts of 100 000 individuals that matured according to the results of our PMRN analyses and grew according to the Lester et al. (2004) fixed investment model. The model was parameterized for Icelandic cod by first estimating the average gonadosomatic index (GSI) (11.0% and 7.5% for males and females, respectively) from GSD combined for all ages (4–8 years), for the period 1994–2007, and then converting this to an energetic GSI (average GSI × 1.73 yielding 19.0% and 13.0% for males and females, respectively; Lester et al. 2004). Juvenile growth rates matching the GSIs and observed lengths-at-age were then found using the least squares method (11.5 and 11.6 $\text{cm}\cdot\text{year}^{-1}$ for males and females, respectively). The lengths-at-age used in the fitting were averages of the whole time period (cohorts 1964–1999) estimated from SD/GSD. In addition, a value of 30%, representing a "high" energetic GSI and corresponding to juvenile growth increments of 11.7 and 11.9 $\text{cm}\cdot\text{year}^{-1}$ for males and females, respectively, was used to estimate the upper limits of the predicted change in growth. Sex-specific maturation probabilities at age (4–8 years) and at a fixed length (average lengths-at-age described above) were derived from the PMRN analysis of GSD/SD. On completion of the simulation, the average lengths-at-age of all individuals (regardless of maturity status) were calculated and linear regressions were used to estimate the average age-specific change between cohorts 1964 and 1999. These predicted changes were compared with those resulting from linear regression, weighted by the cohort- and age-specific sample sizes, of the average lengths-at-age estimated for the PMRN analyses (eq. 3). There was no mortality in the simulation.

Results

Length-at-age

Short-term fluctuations in average length (estimated using eq. 3) were generally similar across all ages and sexes (Fig. 3). For those cohorts where both GSD/SD and CD were available, average length-at-age from CD, in comparison with GSD/SD, tended to be higher for the youngest ages but lower for the oldest ages (Fig. 3). A number of trends in average length were revealed (see Growth trends section above) (Fig. 4): all of the modelled interactions were significant (along with the main effect of age) ($P < 0.001$). Notably, however, average length of Icelandic cod had decreased during the study period (Fig. 4).

PMRNs

We first evaluated the influence of data source (GSD or GSD/SD and unweighted or weighted GSD/SD) on the PMRN estimates in the most recent time period (cohorts 1985–1999). For the majority of age–sex combinations, temporal trends in Lp50s estimated from GSD only and GSD/SD did not differ (ANCOVA, $P = 0.11–0.91$). The only exceptions were age 4 and 5 males for which there were significant differences in the intercepts ($P = 0.031$ and $P = 0.027$, respectively) and slopes ($P = 0.033$ and $P = 0.027$, respectively) of the regression lines. However, after Bonferroni correction, these too would have been nonsignificant ($P > 0.05$). It was therefore deemed appropriate to combine GSD and SD in this time period.

Comparison of PMRNs based on unweighted and weighted (see Materials and methods) GSD/SD showed that weighting produced visually higher PMRN midpoints for most age and cohort combinations (Fig. 5). However, ANCOVAs did not reveal any differences between the intercepts or slopes of the weighted and unweighted Lp50 time series ($P = 0.10–0.84$). It was therefore concluded that using unweighted data in all subsequent analyses was acceptable.

The negative slopes of the maturation reaction norms (Fig. 6) signify that the length at which Icelandic cod attains a certain probability to mature decreases with age. A significant downward trend in the reaction norm slopes (i.e., they had become more negative) was found for female cod ($P = 0.021$) but not for male cod ($P = 0.68$), indicating that the effect of age on female maturation probabilities had increased over time. PMRNs based on research survey data (SD and GSD/SD) showed that recent cohorts of Icelandic cod attained maturity at a smaller size than those of the early 1970s (Fig. 6).

These downward trends are evident in the time series of cohort-specific Lp50s, despite short-term variation in the midpoints at all ages, and wide CI for many age and cohort combinations (Fig. 7). Short-term fluctuations in the Lp50s could not be attributed to any biological anomalies in the data but most likely reflect "noise" in the data (see Discussion). Significant estimates for the decrease in Lp50 between cohorts 1964 and 1999 varied between 6.2 and 14.3 cm for females and 6.4 and 12.9 cm for males (Table 2). For age 7 female and male Icelandic cod, this corresponds to a decrease of 0.23 and 0.27 $cm \cdot year^{-1}$, or 0.33 and $0.44\% \cdot year^{-1}$, respectively (Table 2). There was no significant trend in the Lp50s of age 4 and 5 females (Table 2). Lp50 estimates from CD tended to be higher than those from SD and GSD/SD, and the majority were either associated with large CI (Figs. 6 and 7) or excluded (and therefore not shown) owing to data limitations.

Randomization tests revealed differences in the Lp50s of male and female cod: nonrandomized parameter estimates for the effect of sex fell within and beyond (SD, cohorts 1964–1976 and GSD/SD, cohorts 1985–1999, respectively) the upper 5% tail of the distribution of the 1000 coefficients obtained from the randomization procedure, indicating that females attain 50% maturation probability at a significantly larger size than males.

Potential variables explaining trends in PMRNs

Spatial heterogeneity in fishing could lead to a sampling bias towards mature Icelandic cod in research data and therefore underestimation of PMRN midpoints. Furthermore, a positive trend in this bias through time could explain the decrease in Lp50s. However, no relationships between Lp50s and fishing mortality F of cod aged 4–6 years were observed, and for cod aged 7 and 8 years, relationships were in fact weakly positive. For age 8 females, the correlation between Lp50 and $F(5–10)$ was significant ($P = 0.045$, $R^2 = 0.178$), as was that with age- and cohort-specific F ($P = 0.019$, $R^2 = 0.24$).

As changes in PMRNs could also result from the direct influence of environmental factors on the maturation process, we examined trends in average condition of Icelandic cod and temperature of Icelandic waters. An overall decline in condition, measured as HSI and K_r, of immature and mature cod was present between 1993 and 2007 (Fig. 8). This trend is the opposite of that which would explain the facilitated maturation illustrated by the PMRNs. Temperature southwest and north of Iceland varied notably between years. However, prior to 1995, there was an overall decrease in average temperature, a trend that has since reversed markedly (Fig. 8). No significant relationships between detrended temperature (southwest and north of Iceland in the third quarter of t_{year-1}, t_{year-2}, or t_{year-3}) and PMRN midpoints (t_{year}) were found ($P > 0.05$).

Effect of earlier maturation on growth

Simulations to investigate the influence of earlier maturation, as predicted by the PMRN analyses, on average length-at-age revealed that this would have the greatest effect in the oldest age groups. For those ages, the observed shift in maturation probability was predicted to result in a decrease in average length of as much as 3.8 cm when the average GSI was converted to an energetic GSI; at ages 7 and 8, the predicted changes in average length were comparable with those observed (Table 3). When a "high" energetic GSI

Fig. 3. Average length of (*a*) female and (*b*) male Icelandic cod aged 4–8 years (bottom to top line) estimated for probabilistic maturation reaction norm analyses of survey (black lines) and commercial (grey lines) data. Predictions made from a GLM (eq. 3).

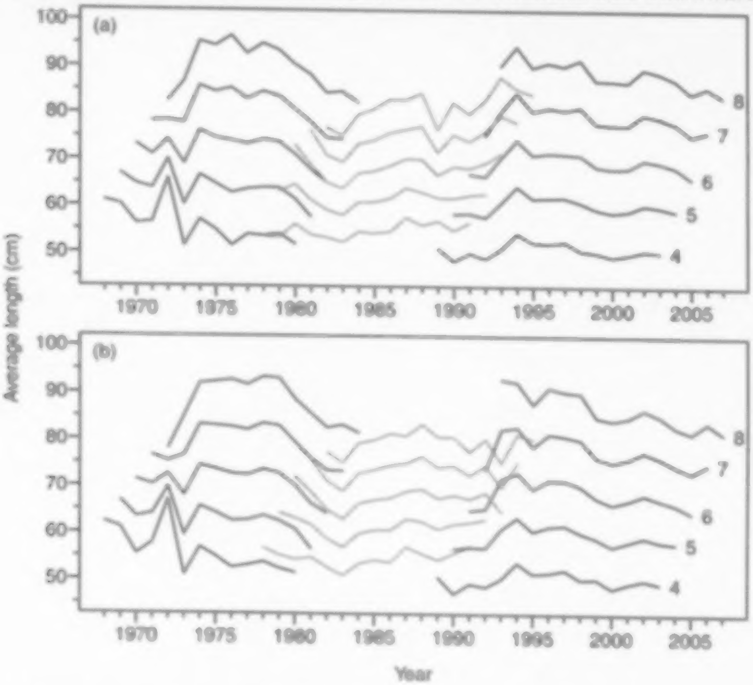

Fig. 4. Estimated trends in growth from GLM of survey data shown for immature Icelandic cod (top panels) of ages (*a*) 4 and (*b*) 5 and mature cod (bottom panels) of ages (*c*) 6 and (*d*) 7. For each group, average length is predicted for males (solid lines) and females (broken lines) in the northern region (lower thin lines) and southern region (upper thick lines).

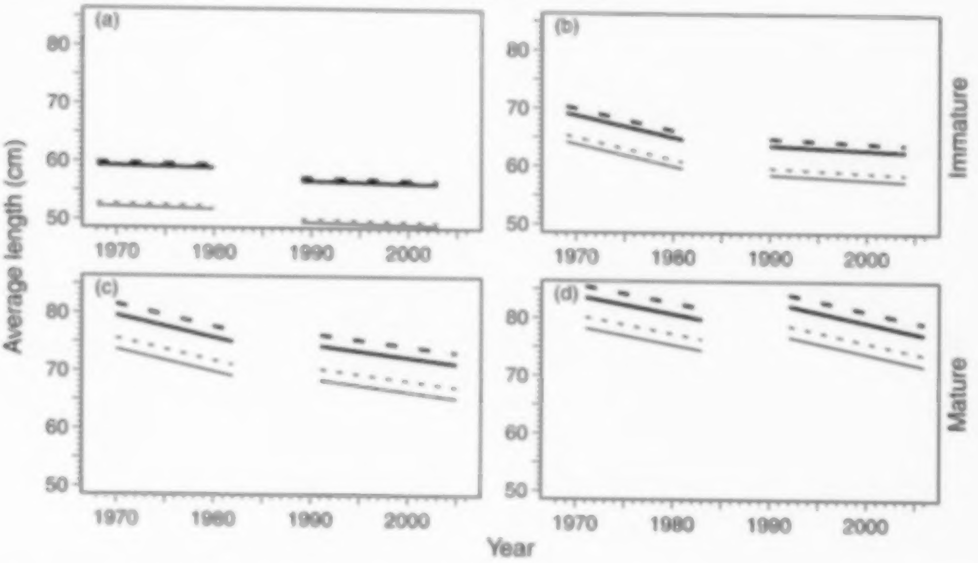

value of 30% was assumed, average length declined even more (Table 3). However, even for the high GSI, earlier maturation could not fully account for the observed declines at the youngest ages.

Discussion

In this study, we found that the size at 50% maturation probability of female and male Icelandic cod had decreased between the 1964 and 1999 cohorts. The corresponding ma-

Fig. 5. Probabilistic maturation reaction norm midpoints (Lp50s) for (*a*–*e*) female and (*f*–*j*) male Icelandic cod (ages 4–8) of cohorts 1985–1999 (plotted by year). Lp50s were estimated using unweighted (triangles) and weighted (circles) research survey data. Bootstrapped 95% confidence intervals are shown for weighted data (vertical bars) only; see Fig. 7 for confidence intervals of unweighted data. Note the different scales on the *y*-axes (set to the minimum possible scale).

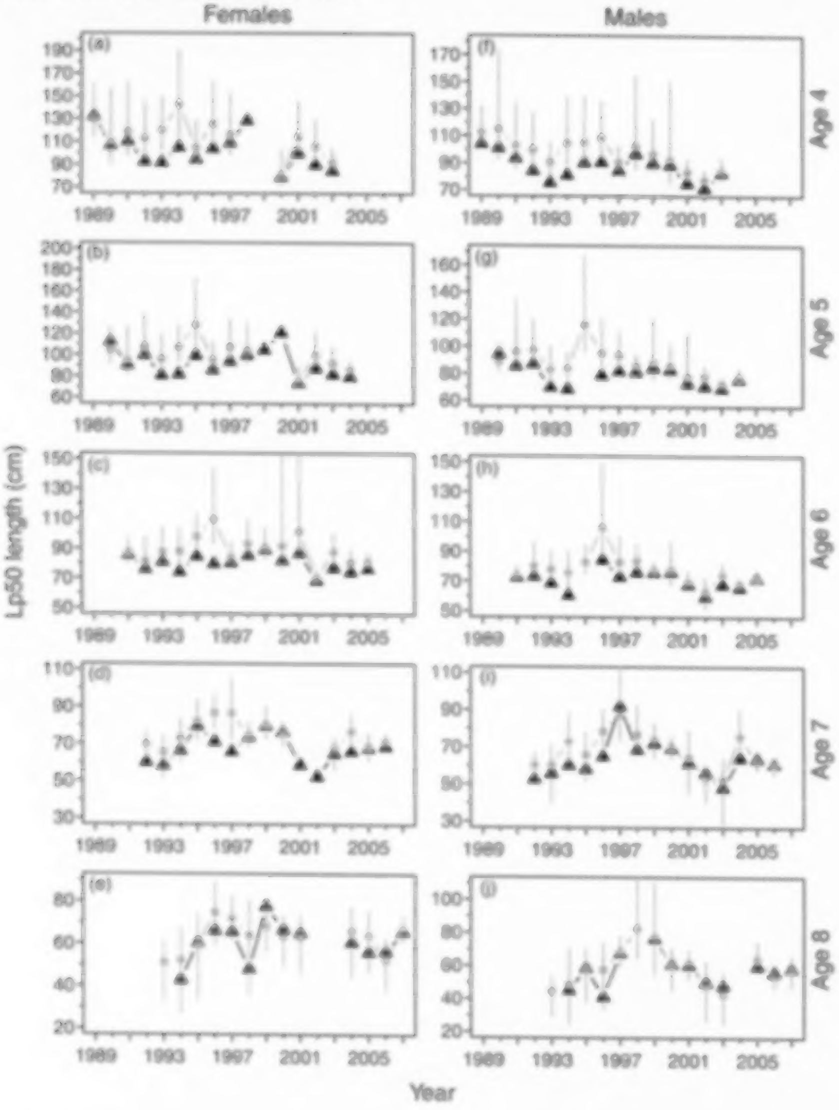

turation probabilities at a fixed length (the average length of cod at a certain age) had increased: for example, for cod of age 6 years, the probability to mature had risen from 16% to 44% and from 29% to 53% for females of 71 cm and males of 70 cm, respectively. The observed PMRN trends could not be explained by those in water temperature or fish condition, which have been proposed as alternative explanations for previously published PMRN trends (e.g., Kraak 2007; Marshall and McAdam 2007; Wright 2007). We also found no support for the hypothesized effects of potential sampling biases related to spatial variation in fishing and maturity. Furthermore, we demonstrated that the observed declines in average length of mature age groups could result from the long-term shifts towards earlier maturation.

Although we have made significant progress in our quest to establish how and why maturation in the Icelandic cod stock has changed, the relative contributions of residual phenotypic plasticity and alterations to the genetic composition of the stock cannot be determined from this correlative study alone (Dieckmann and Heino 2007; Marshall and Browman 2007; Browman et al. 2008). Because age and size are only proxies of the physiological factors that trigger maturation (Marshall and Browman 2007), PMRNs cannot provide a description of maturation tendency that is immune

Fig. 6. Probabilistic maturation reaction norms of (*a*) female and (*b*) male Icelandic cod estimated as the average Lp50 for cohorts 1970–1973 (crosses on dotted black line), cohorts 1980–1983 (triangles on solid grey line), and cohorts 1996–1999 (squares on dashed black line). Grey lines show estimates from commercial data; these are considered less representative than survey data (black lines). Lines without points show the average length-at-age for the corresponding cohorts.

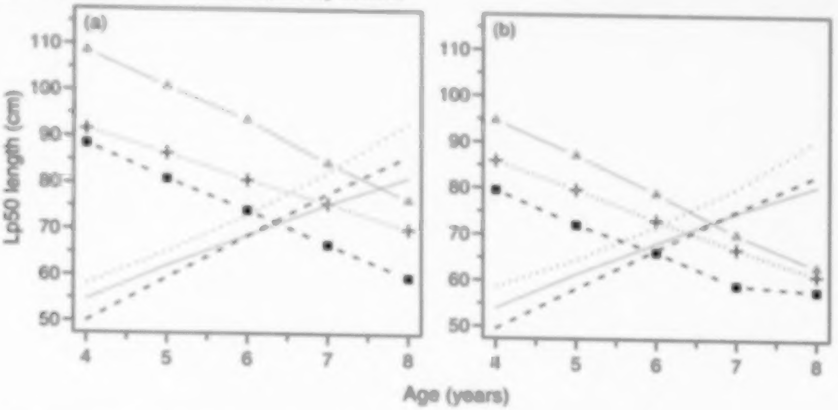

to environmental influences. Indeed, there is ample evidence that age- and size-based PMRNs are influenced by the environment (e.g., Heino et al. 2002*b*; Law 2007), including residual growth-related effects (Morita and Fukuwaka 2006). While we have failed to identify environmental influences that could explain the PMRN trends in our study, absence of evidence is no proof of absence. Nevertheless, it seems unlikely that the large changes identified in this study, and in several other studies, could be fully ascribed to some important but yet unidentified change in the environment. At the same time, life history theory predicts that increased mortality, particularly the size-selective mortality associated with commercial fishing, will bring about evolutionary change in maturation schedules (Stearns 1992; Law 2000). Accordingly, this has been proposed as the most parsimonious explanation for comparable PMRN trends in a number of exploited stocks (Jørgensen et al. 2007; Heino and Dieckmann 2008). Clearly, no definitive conclusions can be made in the absence of genetic evidence, and until those genes that code for maturation are identified, and genotypic and phenotypic correlations are understood, that task remains elusive (Kuparinen and Merilä 2008; Naish and Hard 2008). To assess whether fishing could have caused our observed trends, the predicted rates of change should be quantitatively compared with estimates of selection differentials generated by fishing (Law 2007; Swain et al. 2007). This is beyond the scope of the current study, although eco-genetic models developed for cod-like populations suggest that fishing is capable of driving fast evolution in PMRNs (Dunlop et al. 2009; Enberg et al. 2009).

Alongside maturation schedules, there are potential implications of intensive size-selective harvesting for individual growth rates in exploited fish stocks (Ricker 1981; Sinclair et al. 2002; Swain et al. 2007). Because variation in growth is partially environmentally driven and partially genetic (Imsland and Jonassen 2001; Conover and Munch 2002; Kolstad et al. 2006), fishing could invoke both phenotypically plastic and evolutionary responses in this trait. PMRN trends paralleled by a trend in growth might therefore implicate a genetic shift in one or both of these traits if they are linked by sufficiently strong genetic covariance (Dieckmann and Heino 2007). In a recent study of southern Gulf of St. Lawrence cod, Swain et al. (2007) found evidence of a genetic response, in the form of slower growth, to selection on body size. However, reduced growth rates could also reflect confounded changes in the maturation schedule or reproductive investment because of energetic trade-offs (Heino et al. 2008). In an attempt to address this issue, we ran a simple simulation to investigate what effect the observed changes in maturation might have on average length of Icelandic cod according to the Lester et al. (2004) growth model. This exercise suggested that the declines in growth detected in the present study could be explained by the energetic costs of earlier maturation in the older, mostly mature age groups only. For the younger juvenile ages, without reproductive costs, earlier maturation could not account for the observed decreases. Whether the observed declines in growth of Icelandic cod, particularly in the younger age groups, are purely phenotypic or also have a genetic component therefore remains unresolved. However, our method provides a tool that could be combined with that of Swain et al. (2007) to investigate the propensity for direct selection on growth rates in this, and other, fish stocks.

To facilitate comparison with other cod studies utilizing PMRNs, we quantified the magnitude and rate of the reduction in the PMRN midpoints of Icelandic cod over 36 cohorts following the methodology of Jørgensen et al. (2007, see their table S2). We estimated the total change to be 8%–20% (average 13%) and the rate as $2.2 \times 10^3 - 6.3 \times 10^3$ darwins (average 3.8×10^3 darwins). This suggests that the magnitude and rate of change in the maturation schedule of Icelandic cod are comparable with those observed in other stocks of Atlantic cod (e.g., Heino et al. 2002*b*; Barot et al. 2004*b*; Olsen et al. 2005). However, it is interesting to note that for the latest maturing stocks, Icelandic cod and Northeast Arctic cod (Trippel 1995; Anonymous 2007), this change has been relatively small; the magnitude of change over 67 cohorts was calculated to be 12% at a rate of 2.1×10^3 darwins for Northeast Arctic cod (Jørgensen et al. 2007).

Female Icelandic cod were found to reach 50% matura-

Fig. 7. Probabilistic maturation reaction norm midpoints (Lp50s) of (*a*–*e*) female and (*f*–*j*) male Icelandic cod aged 4–8 years with bootstrapped 95% confidence intervals (vertical bars) for survey (triangles) and commercial (circles) data. Significant linear regressions of Lp50s estimated from research survey data (GSD and SD), weighted by the inverse bootstrap variances, are shown by the broken lines.

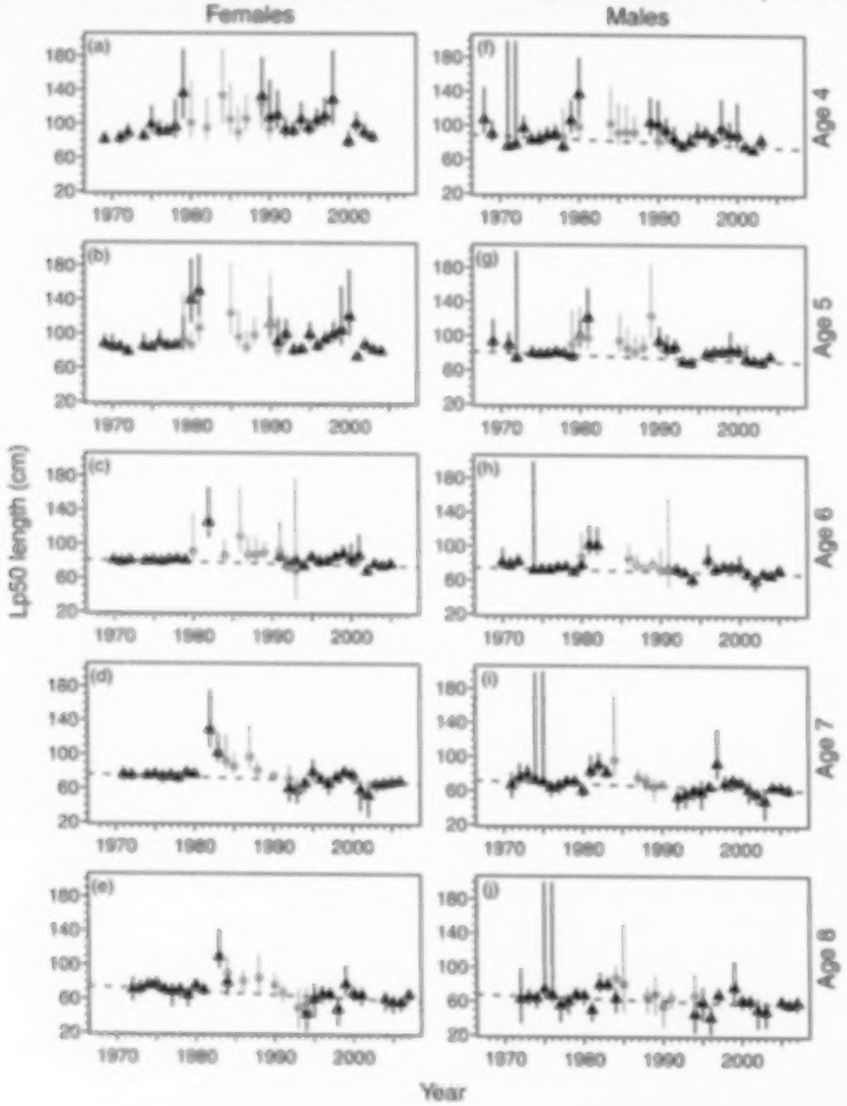

tion probability at a larger size than males, indicating that sex differences in age- and length-based maturity ogives (Marteinsdóttir and Begg 2002) are not the result of variation in growth or survival alone. Similar sex differences have been found in other cod stocks such as those off Labrador and Newfoundland (Olsen et al. 2005). In contrast, variation between the sexes of Georges Bank and Gulf of Maine cod only existed at ages 2 and 3, respectively, and in these cases, females had a marginally higher tendency to mature at a given age and size than males (Barot et al. 2004*b*).

The estimation of PMRNs through the demographic method (Barot et al. 2004*a*), as it is usually applied, relies on two simplifying assumptions: that both growth and survival are, within an age group, independent of maturity status and size. The method has been shown to be robust to moderate violations of these assumptions, however (Barot et al. 2004*a*). Unfortunately, we are unaware of any available empirical evidence that would either attest or refute similar growth rates of immature and mature Icelandic cod, or size-independent growth, within an age class. However, it is possible that differences exist between the survival of immature and mature Icelandic cod within an age class. Fishing in northern Icelandic waters, particularly during the spawning season, could result in the selective removal of immature cod (Thórarinsson and Jóhannesson 1997) and therefore lead to a sampling bias towards mature cod in research

Table 2. Estimated change (weighted linear regression of estimates from research survey data) in Icelandic cod probabilistic maturation reaction norm midpoints (Lp50s) between 1964 and 1999 cohorts.

		Estimated change in Lp50		
Age (years)	Sex	cm	%·year^{-1}	*P*
4	Female	6.1[a]	0.20	0.2091
4	Male	–12.9	–0.36	0.0101
5	Female	–2.3	–0.07	0.0535
5	Male	–10.5	–0.33	0.0052
6	Female	–6.2	–0.22	0.0192
6	Male	–6.4	–0.23	0.0233
7	Female	–8.4	–0.33	0.0027
7	Male	–9.6	–0.44	0.0157
8	Female	–14.3	–0.63	0.0002
8	Male	–10.7	–0.52	0.0222

[a] No estimate for 1964 cohort.

data. In the present study, Lp50s estimated from CD would suggest that the fishery is immature biased. However, the CD originate from bottom trawling during a select few months and so are unlikely to be representative of the Icelandic cod fishery as a whole. This is even more apparent when the contribution of gears such as gillnets and longlines, which target the mature component of the stock, to mean fishing mortality and the total catch is considered (Begg and Marteinsdóttir 2003; Anonymous 2007). The positive correlations observed between fishing mortality and Lp50s of the older ages are in agreement with this last statement and thereby support the hypothesis that the observed decreasing trends were not simply artefacts of sampling.

Our analyses were based on three data groups corresponding to three overlapping time periods. Potential sources of error or bias existed in the CD, as reliability of the maturity classifications is somewhat debatable (S. Schopka, MRI, Skúlagata 4, 121 Reykjavik, Iceland, personal communication (2008)), and these data were collected in a limited area of the Icelandic shelf with larger meshes. However, by selecting data from one gear type and a restricted period of the year, we were able to minimize variation between the data groups. Despite this, we excluded CD Lp50 estimates from our trend analyses. Consequently, we were able to compare PMRN and growth analyses of research data and CD while avoiding any misleading influence of CD on our results. In doing so, we found quite notable differences in our estimates from the two data types. Inconsistency between GSD and other research SD, particularly those SD collected early in the time series, was also a possibility because of discrepancies in sampling design and intensity. Despite this, preliminary exploration of the data did not reveal anything obviously problematic for the analyses, and we were careful that our data selection only minimized this variation and not that which might be biologically meaningful. We therefore do not consider this to have significantly influenced our findings. Furthermore, the observed short-term variability in the Lp50s does not alter our conclusion of an overall downward trend in the PMRNs of Icelandic cod. Instead, such fluctuations, which are often observed (e.g., see Olsen et al. 2005; Mollet et al. 2007; Vainikka et al. 2009), are to be expected given that there will be plastic effects that have not been accounted for, for example originating from the short-term variation in temperature and condition. Some residual noise is also unavoidable owing to small sample sizes, measurement errors, and variable sampling (Heino and Dieckmann 2008).

Temperature in Icelandic waters has increased since 1995; however, no corresponding changes in reaction norm midpoints were observed. Furthermore, no correlative relationships between Lp50s and temperature were detected. It is therefore unlikely that temperature has made a consistent contribution to the changes in maturation. As a cautionary note, although these temperature time series are thought to represent average conditions in Icelandic waters, individual cod may still experience different ambient temperatures at the time relevant for the maturation decision.

There was a general decline in condition of Icelandic cod in the period since 1993. Since good condition is assumed to promote earlier maturation (Marshall and McAdam 2007), the opposite trend would have led us to suspect some influence of condition on the observed shift towards earlier maturation. As weight data are lacking prior to 1993, no conclusive statements can be made regarding the role of condition in the observed maturation trends. However, it is unlikely that changes in condition are responsible for the overall downward trend in maturation, although it is feasible that short-term variation in condition (Pardoe et al. 2008) may have contributed to the observed variability in Lp50s. In four previous PMRN studies of plaice (*Pleuronectes platessa*) (Grift et al. 2007), sole (*Solea solea*) (Mollet et al. 2007), and Atlantic cod in the Baltic (Vainikka et al. 2009) and off Newfoundland (Baulier et al. 2006), inclusion of condition as a third explanatory variable of maturation probability did not alter the conclusion of a decreasing temporal trend in the PMRN midpoints. For cod, the major storage location of lipids is the liver (Eliassen and Vahl 1982*a*; Holdway and Beamish 1984), and so HSI is an obvious candidate for three-dimensional PMRN studies of this species. However, mature cod have been found to have higher liver condition than immature cod (Eliassen and Vahl 1982*b*; Vitale et al. 2006; Pardoe et al. 2008), suggesting that better condition may be the consequence, rather than cause, of maturation (Rijnsdorp 1990). If this is the case, it could mean the false interpretation of a positive effect of condition on maturation probability (Grift et al. 2007) and should therefore be considered in future experimental investigations.

The influence of social factors on maturation cannot be determined from this study, as accounting for such effects is practically impossible with the available data. If maturation of subordinate juvenile cod is suppressed by the presence of dominant adults, as has been found in other, admittedly more sedentary, fish species (e.g., Fricke and Fricke 1977; Borowsky 1978; Jones and Thompson 1980), truncation in the age structure of Icelandic cod (Marteinsdóttir and Thórarinsson 1998) could account for some of the observed PMRN changes. Furthermore, changes in the density and size structure of the stock are directly related to fishing mortality, i.e., selection, and it therefore becomes impossible to disentangle the direct within-cohort effects of fishing (viability selection) from potentially evolutionary factors (truly inherited changes).

Fig. 8. Average condition: (*a*) hepatosomatic index (HSI) and (*b*) relative body condition index (K_r) for immature (circles) and mature (squares) Icelandic cod in the spring (March) and all cod in the autumn (October) (triangles). Temperature in (*c*) northern (Siglunes section) and (*d*) southwestern (Selvogsbanki) Icelandic waters: measurements from 50–150 m in May–June (thin line, north and southwest), 50–150 m in July–September (thick line, north), and 0–200 m in July–September (thick line, southwest).

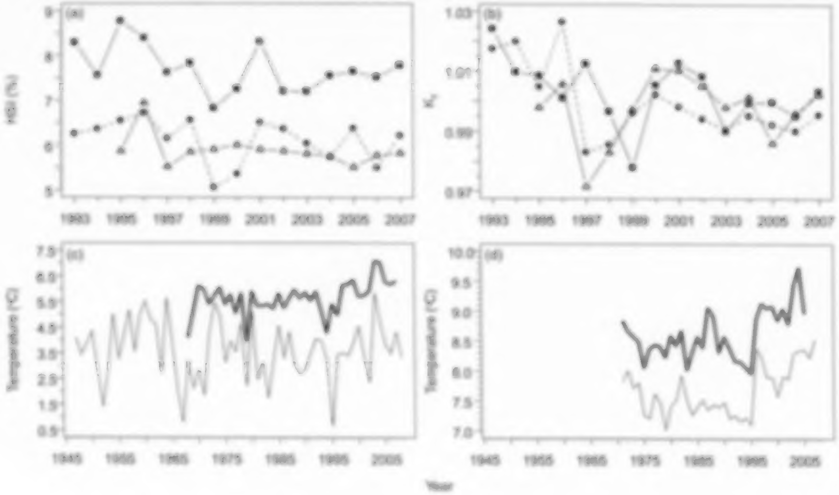

Table 3. Changes in average length of Icelandic cod between 1964 and 1999 cohorts observed in probabilistic maturation reaction norm analyses compared with those predicted by a simulation exercise examining the effects of earlier maturation on growth.

			Predicted change (cm)	
Age (years)	Sex	Observed change (cm)	Average GSI	High GSI
4	Female	–5.2	–0.1	–0.2
4	Male	–5.3	–0.4	–0.6
5	Female	–4.3	–0.6	–1.4
5	Male	–5.1	–1.7	–2.6
6	Female	–3.7	–1.8	–3.8
6	Male	–4.4	–3.3	–4.9
7	Female	–2.1	–2.4	–5.1
7	Male	–2.8	–3.8	–5.5
8	Female	–3.5	–2.3	–4.6
8	Male	–4.0	–3.5	–5.0

Note: Predictions made using an average energetic gonadosomatic index (GSI) and a "high" energetic GSI.

Phenotypic (Marteinsdóttir and Begg 2002; Jónsdóttir et al. 2006; Pardoe et al. 2008) and, more recently, genetic (Pampoulie et al. 2006) and behavioural (Pálsson and Thorsteinsson 2003; Pampoulie et al. 2008; V. Thorsteinsson, MRI, Skúlagata 4, 121 Reykjavik, Iceland, unpublished data) structure within the Icelandic cod stock has been detected. Most prominent is the variation in life history traits between the northern and southern regions, with cod in the former maturing at older ages and larger sizes than their conspecifics in the south (Jónsson 1954; Marteinsdóttir and Begg 2002). In addition, the stock structure is temporally variable. A significant proportion of the mature stock migrates between the main feeding and spawning grounds in the northwest and southwest, respectively, and is contrasted by seemingly resident behaviour of other stock components (Jónsson 1954; Pampoulie et al. 2006). Consequently, variation in sampling intensity between the regions, or even on a finer spatial scale, could introduce biases to analyses such as those performed in the present study. To address this, we weighted data from the most recent time period with available regional estimates of stock abundance in such a way that observations from the more poorly sampled (and immature-dominated) northern region had greater weight. As long as it is reasonable to assume that this bias has remained approximately constant, this weighting would not appear essential for the evaluation of a temporal trend in the trait of interest, illustrated by comparison of the weighted and unweighted Lp50 time series. Instead, this method's value is apparent for the estimation of the position and form of the actual PMRN.

Icelandic cod is not an exception: spatial population structure has been detected in a large number of commercial fish stocks (e.g., Hutchinson et al. 2001; Knutsen et al. 2003; Ruzzante et al. 2006). The accurate detection of persistent changes in life history traits within such stocks would therefore appear dependent on our capacity to disaggregate such trends between relevant stock components, or even behavioural types (Biro and Post 2008). But why do we consider this important? First, there is the possibility that divergent life history responses to environmental change or selective pressures will emerge within these components, and these may go undetected, or lead to erroneous conclusions, when studies are performed at an inappropriate spatial resolution. Second, replacement of one depleted population by another (Hutchinson et al. 2003) could feasibly be interpreted as a phenotypic or evolutionary shift in the life history tactic of the stock, or dominant sub-component. It is therefore important to bear in mind that if any of the aforementioned cases apply to the Icelandic cod stock, or indeed if there are population components that are genetically distinct in their maturation properties, our stock-level PMRN analyses, along with the weighting method, would be inappropriate and perhaps misleading. Unfortunately, phenotypic and in particular behavioural and genetic complexity in the Icelandic cod stock is still poorly understood. Consequently, in light of what is known and the data that are available, we have to assume that our analyses are appropriate. We therefore encourage future investigation of the potential implications of stock complexity, both genetic and phenotypic, for the detection of directional responses to natural or anthropogenic environmental change.

We have detected declining trends in age and size at maturation of Icelandic cod that could not be explained by demographic effects, variation in phenotypic growth, characteristics of the environment represented by ambient temperature and average condition, or sampling biases. Regardless of its origin, earlier maturation may have negative implications for the biological and commercial productivity of the stock (e.g., Heino 1998; Stokes and Law 2000; Stenseth and Rouyer 2008). Furthermore, reversal of any genetic change is predicted to be slow, or even unachievable, because of relatively weak natural selection pressures (Law 2000; Enberg et al. 2009). On a more positive note, the ability to adapt to a changing environment, in this case through the age and size at which Atlantic cod mature, could be regarded in a positive light if we consider it as a buffer against stock collapse. Nevertheless, our findings call for a comprehensive monitoring scheme of spatial and temporal variation in maturation and other life history traits, along with a retrospective and prospective investigation of the propensity for fisheries-induced evolution within the stock, based on past and future exploitation patterns and management strategies.

Acknowledgements

We thank Loïc Baulier, Tim Grabowski, Richard Law, Bruce McAdam, Fabian Mollet, Davnah Urbach, and Héðinn Valdimarsson, along with two anonymous referees and the *Journal*'s editorial team, for their valuable input and comments, which enabled us to greatly improve the manuscript. We also thank the scientists and crews at the Marine Research Institute who were involved in the sampling and preparation of the data used in this study. This research was supported by the European Marie Curie Research Training Network FishACE (Fisheries-induced Adaptive Changes in Exploited Stocks) (contract MRTN-CT-2004-005578) and the Specific Targeted Research Project Fisheries-induced Evolution (FinE) (contract SSP-2006-044276) funded through the European Community's Sixth Framework Programme. The support of the Marine Research Institute, the Icelandic Centre for Research, and the Bergen Research Foundation is gratefully acknowledged.

References

Anderson, C.N.K., Hsieh, C.H., Sandin, S.A., Hewitt, R., Hollowed, A., Beddington, J., May, R.M., and Sugihara, G. 2008. Why fishing magnifies fluctuations in fish abundance. Nature, **452**(7189): 835–839. doi:10.1038/nature06851. PMID:18421346.

Anonymous. 2007. Report of the ICES North-Western Working Group (NWWG). ICES CM 2007/ACFM:17.

Astthorsson, O.S., Gislason, A., and Gudmundsdóttir, A. 1994. Distribution, abundance, and length of pelagic juvenile cod in Icelandic waters in relation to environmental conditions. ICES Mar. Sci. Symp. **198**: 529–541.

Barot, S., Heino, M., O'Brien, L., and Dieckmann, U. 2004*a*. Estimating reaction norms for age and size at maturation when age at first reproduction is unknown. Evol. Ecol. Res. **6**: 659–678.

Barot, S., Heino, M., O'Brien, L., and Dieckmann, U. 2004*b*. Long-term trend in the maturation reaction norm of two cod stocks. Ecol. Appl. **14**(4): 1257–1271. doi:10.1890/03-5066.

Baulier, L., Heino, M., Lilly, G.R., and Dieckmann, U. 2006. Body condition and evolution of maturation of Atlantic cod in Newfoundland. ICES CM 2006/H:19.

Begg, G.A., and Marteinsdóttir, G. 2003. Spatial partitioning of relative fishing mortality and spawning stock biomass of Icelandic cod. Fish. Res. **59**(3): 343–362. doi:10.1016/S0165-7836(02)00025-5.

Biro, P.A., and Post, J.R. 2008. Rapid depletion of genotypes with fast growth and bold personality traits from harvested fish populations. Proc. Natl. Acad. Sci. U.S.A. **105**(8): 2919–2922. doi:10.1073/pnas.0708159105. PMID:18299567.

Borowsky, R. 1978. Social inhibition of maturation in natural populations of *Xiphophorus variatus* (Pisces: Poeciliidae). Science, **201**(4359): 933–935. doi:10.1126/science.201.4359.933. PMID: 17729573.

Browman, H.I., Law, R., Marshall, C.T. 2008. The role of fisheries-induced evolution. Science, **320**(5872): 47. doi:10.1126/science.320.5872.47b. PMID:18388275.

Conover, D.O., and Munch, S.B. 2002. Sustaining fisheries yields over evolutionary time scales. Science, **297**(5578): 94–96. doi:10.1126/science.1074085. PMID:12098697.

Conover, D.O., Arnott, S.A., Walsh, M.R., and Munch, S.B. 2005. Darwinian fishery science: lessons from the Atlantic silverside (*Menidia menidia*). Can. J. Fish. Aquat. Sci. **62**(4): 730–737. doi:10.1139/f05-069.

Dhillon, R.S., and Fox, M.G. 2004. Growth-independent effects of temperature on age and size at maturity in Japanese medaka (*Oryzias latipes*). Copeia, **2004**(1): 37–45. doi:10.1643/CI-02-098R1.

Dieckmann, U., and Heino, M. 2007. Probabilistic maturation reaction norms: their history, strengths, and limitations. Mar. Ecol. Prog. Ser. **335**: 253–269. doi:10.3354/meps335253.

Dunlop, E.S., Heino, M., and Dieckmann, U. 2009. Eco-genetic modeling of contemporary life-history evolution. Ecol. Appl. **19**(7): 1815–1834.

Eliassen, J.-E., and Vahl, O. 1982*a*. Seasonal variations in the gonad size and the protein and water content of cod, *Gadus morhua* (L.), muscle from northern Norway. J. Fish Biol. **20**(5): 527–533. doi:10.1111/j.1095-8649.1982.tb03953.x.

Eliassen, J.-E., and Vahl, O. 1982*b*. Seasonal variations in biochemical composition and energy content of liver, gonad and muscle of mature and immature cod, *Gadus morhua* (L.) from Balsfjorden, northern Norway. J. Fish Biol. **20**(6): 707–716. doi:10.1111/j.1095-8649.1982.tb03981.x.

Enberg, K., Jørgensen, C., Dunlop, E.S., Heino, M., and Dieckmann, U. 2009. Implications of fisheries-induced evolution for stock rebuilding and recovery. Evol. Appl. **2**(3): 394–414. doi:10.1111/j.1752-4571.2009.00077.x.

Fricke, H., and Fricke, S. 1977. Monogamy and sex change by aggressive dominance in coral reef fish. Nature, **266**(5605): 830–832. doi:10.1038/266830a0. PMID:865603.

Grift, R.E., Rijnsdorp, A.D., Barot, S., Heino, M., and Dieckmann, U. 2003. Fisheries-induced trends in reaction norms for maturation in North Sea plaice. Mar. Ecol. Prog. Ser. **257**: 247–257. doi:10.3354/meps257247.

Grift, R.E., Heino, M., Rijnsdorp, A.D., Kraak, S.B.M., and Dieckmann, U. 2007. Three-dimensional maturation reaction norms for North Sea plaice. Mar. Ecol. Prog. Ser. **334**: 213–224. doi:10.3354/meps334213.

Heino, M. 1998. Management of evolving fish stocks. Can. J. Fish. Aquat. Sci. **55**(8): 1971–1982. doi:10.1139/cjfas-55-8-1971.

Heino, M., and Dieckmann, U. 2008. Detecting fisheries-induced life-history evolution: an overview of the reaction-norm approach. Bull. Mar. Sci. **83**: 69–93.

Heino, M., and Godø, O.R. 2002. Fisheries-induced selection pressures in the context of sustainable fisheries. Bull. Mar. Sci. **70**: 639–656.

Heino, M., Dieckmann, U., and Godø, O.R. 2002*a*. Measuring probabilistic reaction norms for age and size at maturation. Evolution, **56**(4): 669–678. PMID:12038525.

Heino, M., Dieckmann, U., and Godø, O.R. 2002*b*. Reaction norm analysis of fisheries-induced adaptive change and the case of the Northeast Arctic cod. ICES CM 2002/Y:14.

Heino, M., Baulier, L., Boukal, D.S., Dunlop, E.S., Eliassen, S., Enberg, K., Jørgensen, C., and Varpe, Ø. 2008. Evolution of growth in Gulf of St Lawrence cod? Proc. R. Soc. Lond. B Biol. Sci. **275**(1639): 1111–1112. doi:10.1098/rspb.2007.1429.

Henryon, M., Jokumsen, A., Berg, P., Lund, I., Pedersen, P.B., Olesen, N.J., and Slierendrecht, W.J. 2002. Genetic variation for growth rate, feed conversion efficiency, and disease resistance exists within a farmed population of rainbow trout. Aquaculture, **209**(1-4): 59–76. doi:10.1016/S0044-8486(01)00729-3.

Holdway, D.A., and Beamish, F.W.H. 1984. Specific growth rate and proximate body composition of Atlantic cod (*Gadus morhua* L.). J. Exp. Mar. Biol. Ecol. **81**(2): 147–170. doi:10.1016/0022-0981(84)90003-0.

Hutchings, J. 2005. Life history consequences of overexploitation to population recovery in Northwest Atlantic cod (*Gadus morhua*). Can. J. Fish. Aquat. Sci. **62**(4): 824–832. doi:10.1139/f05-081.

Hutchings, J.A., and Baum, J.K. 2005. Measuring marine fishes biodiversity: temporal changes in abundance, life history and demography. Philos. Trans. R. Soc. Lond. B Biol. Sci. **360**(1454): 315–338. doi:10.1098/rstb.2004.1586. PMID:15814348.

Hutchings, J.A., and Fraser, D.J. 2008. The nature of fisheries- and farming-induced evolution. Mol. Ecol. **17**(1): 294–313. doi:10.1111/j.1365-294X.2007.03485.x. PMID:17784924.

Hutchinson, W.F., Carvalho, G.R., and Rogers, S.I. 2001. Marked genetic structuring in localised spawning populations of cod *Gadus morhua* in the North Sea and adjoining waters, as revealed by microsatellites. Mar. Ecol. Prog. Ser. **223**: 251–260. doi:10.3354/meps223251.

Hutchinson, W.F., van Oosterhout, C., Rogers, S.I., and Carvalho, G.R. 2003. Temporal analysis of archived samples indicates marked genetic changes in declining North Sea cod (*Gadus morhua*). Proc. R. Soc. Lond. B Biol. Sci. **270**(1529): 2125–2132. doi:10.1098/rspb.2003.2493.

Imsland, A.K., and Jonassen, T.M. 2001. Regulation of growth in turbot (*Scophthalmus maximus* Rafinesque) and Atlantic halibut (*Hippoglossus hippoglossus* L.): aspects of environment × genotype interactions. Rev. Fish Biol. Fish. **11**(1): 71–90. doi:10.1023/A:1014240430779.

Jones, G.P., and Thompson, S.M. 1980. Social inhibition of maturation in females of the temperate wrasse *Pseudolabrus celidotus* and a comparison with the blennioid *Tripterygion varium*. Mar. Biol. (Berl.), **59**(4): 247–256. doi:10.1007/BF00404748.

Jónsdóttir, I.G., Campana, S.E., and Marteinsdóttir, G. 2006. Stock structure of Icelandic cod *Gadus morhua* L. based on otolith chemistry. J. Fish Biol. **69**(Suppl. C): 136–150. doi:10.1111/j.1095-8649.2006.01271.x.

Jónsson, J. 1954. On the Icelandic stock of cod during the years 1928–1953. Rapp. P.-v. Réun. Cons. Int. Explor. Mer, **136**: 51–57.

Jørgensen, C., Enberg, K., Dunlop, E.S., Arlinghaus, R., Boukal, D.S., Brander, K., Ernande, B., Gårdmark, A., Johnston, F., Matsumura, S., Pardoe, H., Raab, K., Silva, A., Vainikka, A., Dieckmann, U., Heino, M., and Rijnsdorp, A.D. 2007. Ecology: managing evolving fish stocks. Science, **318**(5854): 1247–1248. doi:10.1126/science.1148089. PMID:18033868.

Kause, A., Ritola, O., Paananen, T., Mäntysaari, E., and Eskelinen, U. 2003. Selection against early maturation in large rainbow trout *Oncorhynchus mykiss*: the quantitative genetics of sexual dimorphism and genotype-by-environment interactions. Aquaculture, **228**(1-4): 53–68. doi:10.1016/S0044-8486(03)00244-8.

Knutsen, H., Jorde, P.E., André, C., and Stenseth, N.C. 2003. Fine-scaled geographical population structuring in a highly mobile marine species: the Atlantic cod. Mol. Ecol. **12**(2): 385–394. doi:10.1046/j.1365-294X.2003.01750.x. PMID:12535089.

Kolstad, K., Thorland, I., Refstie, T., and Gjerde, B. 2006. Body weight, sexual maturity, and spinal deformity in strains and families of Atlantic cod (*Gadus morhua*) at two years of age at different locations along the Norwegian coast. ICES J. Mar. Sci. **63**(2): 246–252. doi:10.1016/j.icesjms.2005.11.007.

Kraak, S.B.M. 2007. Does the probabilistic maturation reaction norm approach disentangle phenotypic plasticity from genetic change? Mar. Ecol. Prog. Ser. **335**: 295–300. doi:10.3354/meps335295.

Kuparinen, A., and Merilä, J. 2008. The role of fisheries-induced evolution. Science, **320**(5872): 47–48. doi:10.1126/science.320.5872.47b. PMID:18396481.

Law, R. 2000. Fishing, selection, and phenotypic evolution. ICES J. Mar. Sci. **57**(3): 659–668. doi:10.1006/jmsc.2000.0731.

Law, R. 2007. Fisheries-induced evolution: present status and future directions. Mar. Ecol. Prog. Ser. **335**: 271–277. doi:10.3354/meps335271.

Law, R., and Grey, D.R. 1989. Evolution of yields from populations with age-specific cropping. Evol. Ecol. **3**(4): 343–359. doi:10.1007/BF02285264.

Lester, N.P., Shuter, B.J., and Abrams, P.A. 2004. Interpreting the von Bertalanffy model of somatic growth in fishes: the cost of reproduction. Proc. R. Soc. Lond. B Biol. Sci. **271**(1548): 1625–1631. doi:10.1098/rspb.2004.2778.

Marshall, C.T., and Browman, H.I. 2007. Disentangling the causes of maturation trends in exploited fish populations. Mar. Ecol. Prog. Ser. **335**: 249–251.

Marshall, C.T., and McAdam, B.J. 2007. Integrated perspectives on genetic and environmental effects on maturation can reduce potential errors of inference. Mar. Ecol. Prog. Ser. **335**: 301–310. doi:10.3354/meps335301.

Marteinsdóttir, G., and Begg, G.A. 2002. Essential relationships incorporating the influence of age, size and condition on variables required for estimation of reproductive potential in Atlantic cod *Gadus morhua*. Mar. Ecol. Prog. Ser. **235**: 235–256. doi:10.3354/meps235235.

Marteinsdóttir, G., and Thórarinsson, K. 1998. Improving the stock–recruitment relationship in Icelandic cod (*Gadus morhua*) by including age diversity of spawners. Can. J. Fish. Aquat. Sci. **55**(6): 1372–1377. doi:10.1139/cjfas-55-6-1372.

Marteinsdóttir, G., Gunnarsson, B., and Suthers, I.M. 2000. Spatial variation in hatch date distributions and origin of pelagic juvenile cod in Icelandic waters. ICES J. Mar. Sci. **57**(4): 1182–1195. doi:10.1006/jmsc.2000.0880.

Mollet, F.M., Kraak, S.B.M., and Rijnsdorp, A.D. 2007. Fisheries-induced evolutionary changes in maturation reaction norms in North Sea sole *Solea solea*. Mar. Ecol. Prog. Ser. **351**: 189–199. doi:10.3354/meps07138.

Morita, K., and Fukuwaka, M.A. 2006. Does size matter most? The effect of growth history on probabilistic reaction norm for salmon maturation. Evolution, **60**(7): 1516–1521. PMID:16929668.

Naish, K.A., and Hard, J.J. 2008. Bridging the gap between the genotype and the phenotype: linking genetic variation, selection and adaptation in fishes. Fish Fish. **9**: 396–422. doi:10.1111/j.1467-2979.2008.00302.x.

Olsen, E.M., Lilly, G.R., Heino, M., Morgan, M.J., Brattey, J., and Dieckmann, U. 2005. Assessing changes in age and size at maturation in collapsing populations of Atlantic cod (*Gadus morhua*). Can. J. Fish. Aquat. Sci. **62**(4): 811–823. doi:10.1139/f05-065.

Pálsson, Ó.K., and Thorsteinsson, V. 2003. Migration patterns, ambient temperature, and growth of Icelandic cod (*Gadus morhua*): evidence from storage tag data. Can. J. Fish. Aquat. Sci. **60**(11): 1409–1423. doi:10.1139/f03-117.

Pálsson, Ó.K., Jónsson, E., Schopka, S.A., Stefánsson, G., and Steinarsson, B.Æ. 1989. Icelandic groundfish survey data used to improve precision in stock assessments. J. Northwest Atl. Fish. Sci. **9**: 53–72.

Pampoulie, C., Ruzzante, D.E., Chosson, V., Jörundsdóttir, T.D., Taylor, L., Thorsteinsson, V., Daníelsdóttir, A.K., and Marteinsdóttir, G. 2006. The genetic structure of Atlantic cod (*Gadus morhua*) around Iceland: insight from microsatellites, the *Pan* I locus, and tagging experiments. Can. J. Fish. Aquat. Sci. **63**(12): 2660–2674. doi:10.1139/F06-150.

Pampoulie, C., Jakobsdóttir, K.B., Marteinsdóttir, G., and Thorsteinsson, V. 2008. Are vertical behaviour patterns related to the pantophysin locus in the Atlantic cod (*Gadus morhua* L.)? Behav. Genet. **38**(1): 76–81. doi:10.1007/s10519-007-9175-y. PMID:17978867.

Pardoe, H., Thordarson, G., and Marteinsdóttir, G. 2008. Spatial and temporal trends in condition of Atlantic cod (*Gadus morhua* L.) on the Icelandic shelf. Mar. Ecol. Prog. Ser. **362**: 261–277. doi:10.3354/meps07409.

Powles, P. 1958. Studies of reproduction and feeding of Atlantic cod (*Gadus callarias* L.) in the southwestern Gulf of St. Lawrence. J. Fish. Res. Board Can. **15**: 1383–1402.

Reznick, D.N., and Ghalambor, C.K. 2005. Can commercial fishing cause evolution? Answers from guppies (*Poecilia reticulata*). Can. J. Fish. Aquat. Sci. **62**(4): 791–801. doi:10.1139/f05-079.

Ricker, W.E. 1981. Changes in the average size and average age of Pacific salmon. Can. J. Fish. Aquat. Sci. **38**(12): 1636–1656. doi:10.1139/f81-213.

Rijnsdorp, A.D. 1990. The mechanism of energy allocation over reproduction and somatic growth in female North Sea plaice, *Pleuronectes platessa* L. Neth. J. Sea Res. **25**(1/2): 279–289. doi:10.1016/0077-7579(90)90027-E.

Roff, D.A. 1983. An allocation model of growth and reproduction in fish. Can. J. Fish. Aquat. Sci. **40**(9): 1395–1404. doi:10.1139/f83-161.

Ruzzante, D.E., Mariani, S., Bekkevold, D., Andre, C., Mosegaard, H., Clausen, L.A.W., Dahlgren, T.G., Hutchinson, W.F., Hatfield, E.M.C., Torstensen, E., Brigham, J., Simmonds, E.J., Laikre, L., Larsson, L.C., Stet, R.J.M., Ryman, N., and Carvalho, G.R. 2006. Biocomplexity in a highly migratory pelagic marine fish, Atlantic herring. Proc. Natl. Acad. Sci. U.S.A. **273**: 1459–1464.

Sinclair, A.F., Swain, D.P., and Hanson, J.M. 2002. Measuring changes in the direction and magnitude of size-selective mortality in a commercial fish population. Can. J. Fish. Aquat. Sci. **59**(2): 361–371. doi:10.1139/f02-015.

Stearns, S.C. 1992. The evolution of life histories. Oxford University Press, New York.

Stenseth, N.C., and Rouyer, T. 2008. Ecology: destabilized fish stocks. Nature, **452**(7189): 825–826. doi:10.1038/452825a. PMID:18421343.

Stergiou, K.I. 2002. Overfishing, tropicalization of fish stocks, uncertainty and ecosystem management: resharpening Ockham's razor. Fish. Res. **55**: 1–9.

Stokes, K., and Law, R. 2000. Fishing as an evolutionary force. Mar. Ecol. Prog. Ser. **208**: 307–309.

Swain, D.P., Sinclair, A.F., and Hanson, J.M. 2007. Evolutionary response to size-selective mortality in an exploited fish population. Proc. R. Soc. Lond. B Biol. Sci. **274**(1613): 1015–1022. doi:10.1098/rspb.2006.0275.

Thórarinsson, K., and Jóhannesson, G. 1997. Correcting for variation in catchability: maturity-related catchability variation in Icelandic cod. ICES J. Mar. Sci. **54**(5): 787–796. doi:10.1006/jmsc.1996.0199.

Thorpe, J.E. 2007. Maturation responses of salmonids to changing developmental opportunities. Mar. Ecol. Prog. Ser. **335**: 285–288. doi:10.3354/meps335285.

Trippel, E.A. 1995. Age at maturity as a stress indicator in fisheries. Bioscience, **45**(11): 759–771. doi:10.2307/1312628.

Vainikka, A., Gårdmark, A., Bland, B., and Hjelm, J. 2009. Two- and three-dimensional maturation reaction norms for the eastern Baltic cod, *Gadus morhua*. ICES J. Mar. Sci. **66**(2): 248–257. doi:10.1093/icesjms/fsn199.

Vitale, F., Svedäng, H., and Cardinale, M. 2006. Histological analysis invalidates macroscopically determined maturity ogives of the Kattegat cod (*Gadus morhua*) and suggests new proxies for estimating maturity status of individual fish. ICES J. Mar. Sci. **63**(3): 485–492. doi:10.1016/j.icesjms.2005.09.001.

Walsh, M.R., Munch, S.B., Chiba, S., and Conover, D.O. 2006. Maladaptive changes in multiple traits caused by fishing: impediments to population recovery. Ecol. Lett. **9**(2): 142–148. doi:10.1111/j.1461-0248.2005.00858.x. PMID:16958879.

Wright, P.J. 2007. Understanding the maturation process for field investigations of fisheries-induced evolution. Mar. Ecol. Prog. Ser. **335**: 279–283. doi:10.3354/meps335279.

Yoneda, M., and Wright, P.J. 2005. Effects of varying temperature and food availability on growth and reproduction in first-time spawning female Atlantic cod. J. Fish Biol. **67**(5): 1225–1241. doi:10.1111/j.1095-8649.2005.00819.x.

Behavioral thermoregulation and associated mortality trade-offs in migrating adult steelhead (*Oncorhynchus mykiss*): variability among sympatric populations

Matthew L. Keefer, Christopher A. Peery, and Brett High

Abstract: We used radiotelemetry to assess thermoregulatory behaviors for 14 populations (n = 3985) of adult summer steelhead (*Oncorhynchus mykiss*) as they passed through the Columbia River migration corridor. Steelhead use of small cool-water tributaries ("thermal refugia") rapidly increased when the Columbia River reached a temperature threshold of about 19 °C. When main stem temperatures were warmest (i.e., >21 °C), more than 70% of the tagged fish used refugia sites and these fish had median refugia residence times of 3–4 weeks. Thermoregulatory responses were similar across populations, but there were large among-population differences in the incidence and duration of refugia use likely linked to population-specific migration timing patterns. In survival analyses using 1285 known-origin steelhead, fish that used thermal refugia were significantly less likely to survive to natal basins, were harvested at relatively high rates in refugia tributaries, and had greater unknown mortality in the main stem. These results highlight the trade-off between the presumed physiological benefits of thermal refugia use and a likely increase in harvest and other mortality risks that arise when preferred thermal habitats are severely constricted.

Résumé : La radiotélémétrie nous a servi à évaluer le comportement thermorégulateur de 14 populations (n = 3 985) de truites arc-en-ciel anadromes (*Oncorhynchus mykiss*) adultes d'été lors de leur passage à travers le corridor de migration du fleuve Columbia. L'utilisation par les truites arc-en-ciel anadromes de petits tributaires d'eau froide (« refuges thermiques ») augmente rapidement quand la température du Columbia atteint un seuil d'environ 19 °C. Lorsque les températures du cours principal sont maximales (c'est-à-dire >21 °C), plus de 70 % des poissons marqués utilisent les sites de refuge et la durée médiane du séjour de ces poissons dans les refuges est de 3–4 semaines. Les réactions de thermorégulation sont les mêmes dans les diverses populations, mais il y a d'importantes différences entre les populations en ce qui concerne la fréquence et la durée de l'utilisation des refuges, vraisemblablement liées aux patrons temporels de migration spécifiques à chaque population. Des analyses de survie impliquant 1 285 truites arc-en-ciel anadromes d'origine connue montrent que les poissons qui utilisent les refuges thermiques sont significativement moins susceptibles de survivre jusqu'à leur retour à leur bassin versant de naissance, qu'ils sont récoltés à des taux relativement élevés dans les tributaires refuges et qu'ils ont une mortalité de cause inconnue plus forte dans le cours principal. Ces résultats mettent en évidence le compromis entre les bénéfices physiologiques présumés de l'utilisation des refuges thermiques et une vraisemblable augmentation de la récolte et des autres risques de mortalité qui apparaissent lorsque les habitats thermiques préférés sont grandement réduits.

[Traduit par la Rédaction]

Received 3 November 2008. Accepted 23 July 2009. Published on the NRC Research Press Web site at cjfas.nrc.ca on 29 September 2009.
J20855

Paper handled by Associate Editor Michael Bradford.

M.L. Keefer[1] and C.A. Peery.[2] Fish Ecology Research Laboratory, Department of Fish and Wildlife Resources, College of Natural Resources, University of Idaho, Moscow, ID 83844-1136, USA.
B. High. Idaho Department of Fish and Game, 4279 Commerce Circle, Idaho Falls, ID 83401, USA.

[1] Corresponding author (e-mail: mkeefer@uidaho.edu).
[2] Present address: Idaho Fishery Resource Office, US Fish and Wildlife Service, 4147 Ahsahka Road, Ahsahka, ID 83520-0018, USA.

Introduction

Water temperature is a controlling factor in the distribution, ecology, physiology, and behavior of poikilothermic fishes (Brett 1971; Angilletta et al. 2002; Perry et al. 2005), and most species have relatively narrow thermal preferences where physiological and metabolic processes are optimized (Beitinger and Fitzpatrick 1979; Magnuson et al. 1979). Many also have well-defined thermal tolerance thresholds where exposure marks dramatic reductions in performance, survival, and fitness (Eaton et al. 1995; Beitinger et al. 2000; Pörtner and Knust 2007). Some fishes regularly encounter thermal thresholds, particularly in temperate systems where large seasonal temperature fluctuations constrict or eliminate preferred habitats. These fish must balance use of favored thermal niches with other biological needs such as feeding, predator avoidance, reproduction, and migration (e.g., Fischer et al. 1987; Baird and Krueger 2003).

Can. J. Fish. Aquat. Sci. 66: 1734–1747 (2009) doi:10.1139/F09-131 Published by NRC Research Press

One of the principal strategies for living in marginal or complex thermal environments is behavioral thermoregulation, where animals actively avoid stressful temperatures or seek preferred thermal habitats (Reynolds and Casterlin 1979; Adolph 1990; Holland et al. 1992). In fishes, behavioral thermoregulation has been documented for a diverse group of saltwater (e.g., Holland et al. 1992; Hight and Lowe 2007) and freshwater species (e.g., Magnuson et al. 1979; Schaefer et al. 2003). There has been particular research interest in the coldwater Salmonidae (e.g., Biro 1998; Torgersen et al. 1999; Sutton et al. 2007) both because they are vulnerable at relatively moderate temperatures and because climate warming may rapidly constrict suitable habitats for many populations (Eaton and Scheller 1996; Hari et al. 2006; Battin et al. 2007). As a group, anadromous salmonids can confront temperature challenges throughout their complex life cycle, with thermoregulatory behaviors reported during freshwater rearing (Ebersole et al. 2001; Breau et al. 2007), juvenile outmigration (Sauter et al. 2001), and ocean residency (Tanaka et al. 2000), along adult migration corridors (Newell and Quinn 2005; Goniea et al. 2006), and in spawning tributaries (Berman and Quinn 1991; Torgersen et al. 1999).

In all environments, behavioral thermoregulation is adaptive and presumably results in beneficial fitness outcomes. However, the behavior has inherent mortality risks because fish often become spatially or temporally concentrated in otherwise marginal habitats. Such aggregations are vulnerable to a variety of threats, including predation, disease transmission, and human harvest. A dramatic fisheries example occurs in the lower Columbia River where thousands of adult summer steelhead (anadromous rainbow trout) (*Oncorhynchus mykiss*) move into small, cool-water tributaries as the main migration corridor warms (Keefer et al. 2004). Many steelhead use these thermal refugia for days to months during summer (High et al. 2006) and attract intensive recreational and tribal fisheries. Harvest from these aggregations is controversial because the steelhead are seeking refuge from stressful conditions and because most fish derive from upriver populations (i.e., from river basins distant from the harvest sites). These include dozens of genetically distinct steelhead populations (e.g., Brannon et al. 2004) and several metapopulations (Snake River, mid-Columbia River, and upper Columbia River) that are listed as threatened under the US Endangered Species Act (National Marine Fisheries Service 1997; Good et al. 2005). Despite likely impacts on protected fish, uncertainty about the demographics of the thermoregulating group has restricted management options.

To investigate the relationships between behavioral thermoregulation, population demographics (i.e., fish size and origin), and mortality risks, we reconstructed adult migration histories for several thousand radio-tagged summer steelhead. The study had four basic objectives. First, the telemetry data were used to identify main stem water temperatures associated with thermoregulatory responses in migrating steelhead. Second, we assessed among-population differences in thermal refugia use, including residency times and percentages of each population recorded in refugia sites. Third, we tested for associations between refugia use and fish fate (i.e., main stem harvest, unknown main stem mortality, nonnatal tributary harvest/mortality, and successful return to spawning tributaries). Fourth, we examined potential delayed effects of refugia use on fish fate in upstream river reaches. The last two objectives were addressed using a subsample of the tagged fish for which juvenile origin was known. This was a prerequisite for differentiating harvest of thermoregulating fish from harvest of returning local stocks. The combined objectives tested two hypotheses: (1) that the degree and duration of behavioral thermoregulation differ among Columbia River steelhead populations as a function of stock-specific migration timing and migration corridor temperatures and (2) that mortality risks associated with thermoregulation vary among populations, with greater risk for populations with proportionately greater refugia use and longer refugia residency times.

Materials and methods

Study system

Adult steelhead were monitored at main stem Columbia and Snake River dams (fixed location telemetry sites described in Keefer et al. 2005) and at all major tributaries from Bonneville Dam (river kilometre (rkm) 235) upstream to Priest Rapids Dam (rkm 639) on the Columbia River and Hells Canyon Dam (rkm 919) on the Snake River (Fig. 1). Additional tributaries were monitored continuously in the Snake River Basin and intermittently in the upper Columbia River Basin. Thermoregulatory behaviors were studied at the confluence areas of eight Columbia River tributaries to the two most downstream reservoirs. Bonneville reservoir (~73 rkm long) extends to the tailrace of The Dalles Dam (rkm 308), and The Dalles reservoir (~38 rkm long) extends to the tailrace of John Day Dam (rkm 346). The eight tributaries (Wind, Little White Salmon, White Salmon, Klickitat, Hood, and Deschutes rivers and Herman and Eagle creeks) drain the Cascade Range and are routinely 2–7 °C cooler than the main stem Columbia River in summer and fall (Goniea et al. 2006).

The summer steelhead run is protracted at Bonneville Dam, with the earliest fish arriving in April and continuous passage through November (Busby et al. 1996; Robards and Quinn 2002). Most fish pass Bonneville Dam from June to September, coincident with seasonally high main stem water temperatures as recorded at dams (Fig. 2). Columbia River temperatures typically reach 20 °C in mid- to late July and remain at 20–23 °C until early to mid-September. In the study years, a mean of ~370 000 steelhead (range = ~204 000 – 636 000) were counted at Bonneville Dam and ~281 000 (range = ~154 000 – 481 000) were counted at John Day Dam (available from www.cbr.washington.edu/dart/). At a minimum, these data indicate that about 75% of the steelhead that passed Bonneville Dam were from interior populations (i.e., from Idaho and eastern Oregon and Washington). Actual interior population percentages were likely higher because fish counts at John Day Dam were truncated on 31 October in most years and harvest removed a portion of the interior runs in the Bonneville to John Day reach.

Collection, tagging, and monitoring

Adult steelhead were trapped and intragastrically implanted with radiotransmitters at Bonneville Dam from late

Fig. 1. Map of the Columbia and Snake River basins where radio-tagged adult summer steelhead (*Oncorhynchus mykiss*) were monitored at dams, in reservoirs, and while using cool-water tributaries during migration. Tagged fish were assigned to one of 14 populations upstream from The Dalles Dam: Deschutes River (A), John Day River (B), Umatilla River (C), Walla Walla River (D), Yakima River (E), Hanford Reach (F), upper Columbia River (G), Lyons Ferry Hatchery (H), Tucannon River (I), Snake River upstream from Lower Granite Dam (J), Clearwater River (K), Grande Ronde River (L), Salmon River (M), and Imnaha River (N). Thermoregulatory behaviors were monitored at eight sites: Herman Creek (1), Eagle Creek (2), Wind River (3), Little White Salmon River (4), White Salmon River (5), Klickitat River (6), Hood River (7), and Deschutes River (8).

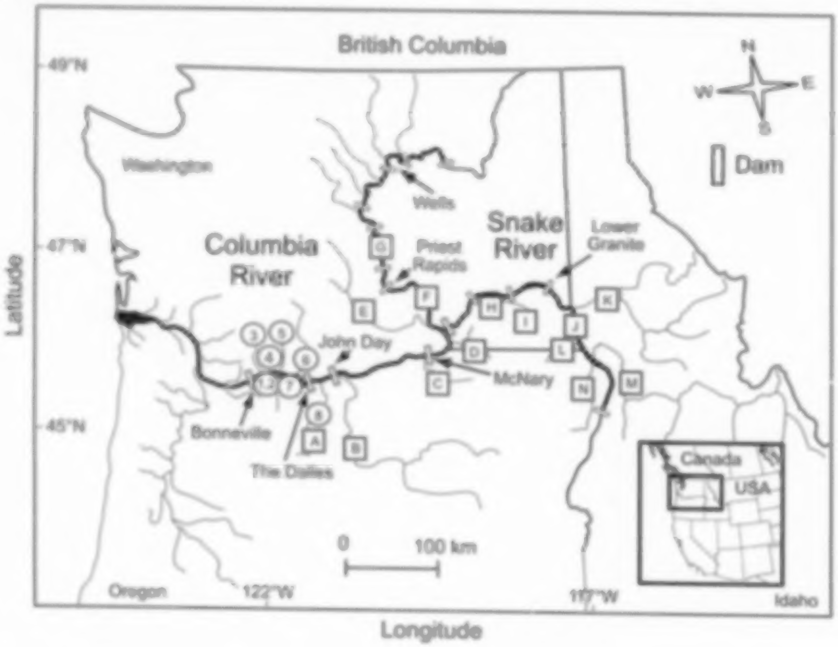

May or early June through October during 6 years (1996–1997 and 2000–2003). Details of the trap facility, tagging methods, and types and sizes of radiotransmitters are described in Keefer et al. (2004, 2005). In 1996, 1997, and 2000, steelhead were nonselectively sampled in approximate proportion to the runs, with a slight bias for later timed fish to ensure adequate samples for evaluations at Snake River dams (see Keefer et al. 2004). Total samples in these years were 765 (1996), 975 (1997), and 1160 (2000); 200 fish (7%) were excluded from analyses because they never passed Bonneville Dam or they lost transmitters during migration and refugia use could not be evaluated (Table 1).

In 2001–2003, we used an automated system to identify fish with passive integrated transponder (PIT) tags as they passed through the Bonneville adult trap. PIT tags indicated where fish were tagged as juveniles and we refer to this group as "known-origin" fish. Radio-tagging of known-origin fish allowed for direct tests of thermoregulation effects on fish fate because harvested fish and those with unknown fate could be assigned to specific populations, unlike for the unselective samples in earlier years. The availability of known-origin steelhead depended on unrelated juvenile tagging projects and so these groups were not random with respect to population. The largest known-origin sample (n = 684) (Table 1) was for two steelhead groups PIT-tagged at Lower Granite Dam on the Snake River as part of an ongoing National Marine Fisheries Service project (e.g., Buchanan et al. 2006). As juveniles, these fish were either transported downstream in barges or migrated in-river. There were year-to-year differences in juvenile selection protocols at Lower Granite Dam, but all wild and hatchery populations upstream from the dam should have been represented. Adult distributions of the sampled barged and in-river groups were nearly identical among those fish that passed Lower Granite Dam, with about 16% last recorded in the Clearwater River, 10% in the Grande Ronde River, 22%–26% in the Salmon River, and ~50% last recorded in the main stem Snake River. The second largest known-origin group was PIT-tagged at Wells Hatchery (near Wells Dam) (Fig. 1) or collected and tagged at other upper Columbia River dams (n = 465). The remaining 136 known-origin fish were PIT-tagged in Snake River tributaries (Table 1).

Adult radio-tagged steelhead movements were monitored at a series of approximately 170 receiver sites that operated from April through late fall, with some tributary and dam sites in place all year (see Keefer et al. 2008*a*). Aerial antennas were used in reservoirs, in the tailraces of dams, and in tributaries; underwater antennas monitored passage inside dam fishways and at fish ladder exits. In all years, the six larger tributary rivers in the Bonneville to John Day reach (Wind, Little White Salmon, White Salmon, Klickitat, Hood, and Deschutes) had fixed aerial antennas within 2 rkm of their confluences with the Columbia River. These sites were far enough upstream so that fish passing in the

Fig. 2. Numbers of adult summer steelhead (*Oncorhynchus mykiss*) counted passing fish ladders at Bonneville (shaded area) and John Day (solid line) dams on the Columbia River. (*a*) 1996; (*b*) 1997; (*c*) 2000; (*d*) 2001; (*e*) 2002; (*f*) 2003. Dotted lines represent mean daily Columbia River water temperatures at the water quality monitoring site at Bonneville Dam. Dashed horizontal lines at 19 °C represent a possible thermoregulatory threshold.

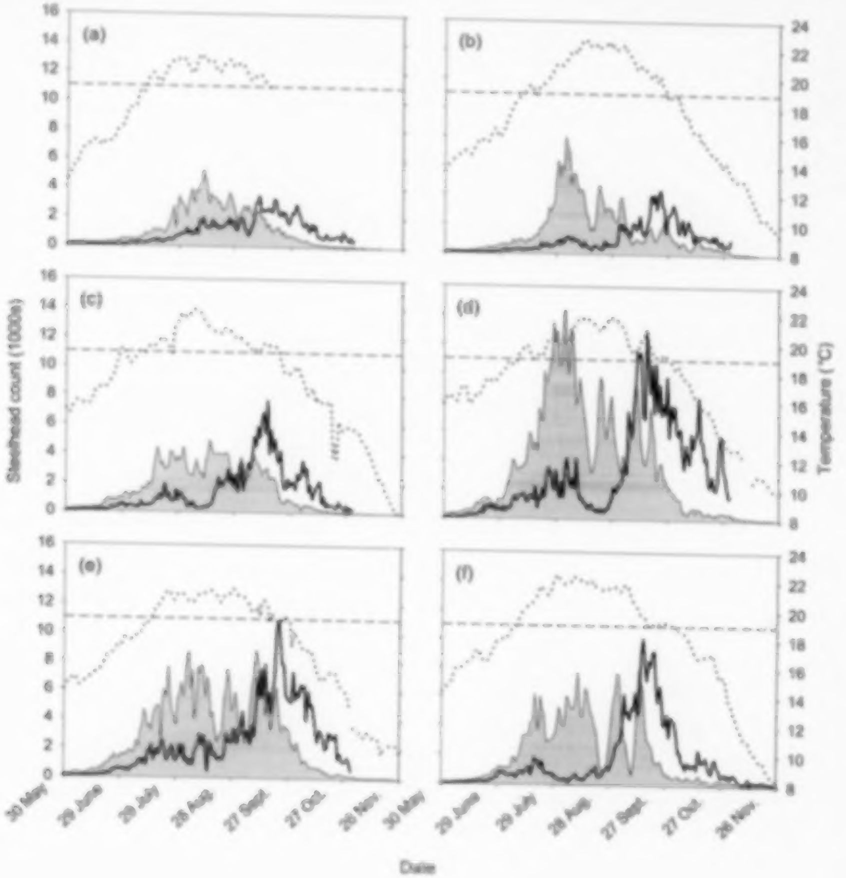

main Columbia River channel would rarely be detected. Additional aerial antennas were used to monitor fish entries and exits from tributary plumes and confluence areas at the Wind, Little White Salmon, White Salmon, and Deschutes rivers. An aerial antenna was installed inside the low-discharge Herman Creek in 2001–2003 and this site was also monitored daily (2000) or periodically (1996–1997) using truck- or boat-mounted aerial antennas (see High et al. 2006). The low-discharge Eagle Creek was periodically monitored with mobile antennas in all years. The lower monitoring effort at the creeks relative to the larger tributary rivers resulted in some underestimation of thermoregulatory behavior.

Tributary use and passage time estimation

The time that steelhead spent in cool-water tributaries along the Bonneville to John Day reach was calculated from the first to last telemetry records at antennas inside tributaries, and multiple times were summed when individuals exited and reentered one or more tributaries. At the creeks without fixed aerial antennas, repeated mobile records of fish were required to establish use of the site. Each of these measures were conservative estimates of the time that fish spent inside cool-water refugia because tracking with mobile antennas indicated that many fish were also in tributaries downstream from fixed antennas, in tributary plumes where temperatures were lower than the main stem (High 2002), and in confluence areas for extended periods. For analyses, steelhead were considered to have "used" tributaries if their cumulative time inside tributaries was >12 h. This cutoff was selected to minimize the number of fish that used tributaries only incidentally (e.g., during exploratory movements or at night). Passage times through three study reaches (Bonneville to The Dalles, Bonneville to John Day, and The Dalles to John Day) were calculated from the dates fish passed each dam. Times were calculated using passage dates determined from telemetry records; use of dates rather than dates plus times allowed us to include fish that passed top-of-ladder sites during receiver outages but had other telemetry records that clearly identified passage date.

Table 1. Numbers of adult steelhead (*Oncorhynchus mykiss*) that were collected and radio-tagged at Bonneville Dam during 6 study years.

	Unknown-origin samples				Known-origin samples			
	1996	1997	2000	Total	2001	2002	2003	Total
Total tagged	765	975	1160	2900	655	548	82	1285
Used in analyses	712	904	1084	2700	655	548	82	1285
Hatchery (%)	84	86	73	80	68	34	22	51
Wild (%)	16	14	27	20	32	66	78	49
Populations: based on final fish locations (unknown-origin) or juvenile tag site (known-origin)								
Deschutes River	86	78	69	265				
John Day River	21	33	36	90				
Umatilla River	4	8	12	24				
Walla Walla River	8	17	16	41				
Yakima River	4	5	8	17				
Hanford Reach	12	15	18	45				
Upper Columbia River	18	25	46	89	324	140	1	465
Lyons Ferry Hatchery	8	10	6	24				
Tucannon River	9	9	1	19				
Snake River above Lower Granite Dam	92	81	92	265				
Clearwater River	65	84	166	315	20	34	2	56
Grande Ronde River	18	38	30	86	3	18	2	23
Salmon River	72	92	114	278	16	10	4	30
Imnaha River					14	7	6	27
Lower Granite Dam (barged)[a]					160	213	51	424
Lower Granite Dam (in-river)[a]					118	126	16	260

Note: "Unknown-origin" fish were randomly collected. Natal basins for "known-origin" fish were identified from PIT tags implanted when fish were juveniles. Population assignment for unknown-origin fish was by final recorded location outside the monitored Columbia – Snake River Hydrosystem.

[a] Includes fish from Clearwater, Grande Ronde, Salmon, and Imnaha rivers and from the Snake River and its smaller tributaries upstream from Lower Granite Dam.

Stock and fate assignments

All unknown- and known-origin steelhead last recorded in tributaries or hatcheries upstream from The Dalles Dam or that passed Lower Granite Dam or Priest Rapids Dam were assigned to one of 14 populations (Table 1). Ten of the 14 populations were delineated by major tributary basins and one was a hatchery adjacent to the Snake River (Lyons Ferry). The three remaining groups were not tributary based: the "upper Columbia River" included all fish that passed the uppermost Columbia River monitoring site (Priest Rapids Dam), "Snake River above Lower Granite Dam" included fish that passed this dam but were not subsequently recorded in secondary tributaries, and "Hanford Reach" included fish last recorded in the Columbia River between the Snake River confluence and Priest Rapids Dam (Fig. 1). Each of the study populations supports multiple distinct spawning stocks and further separation is possible (e.g., Brannon et al. 2004; Winans et al. 2004; Keefer et al. 2008*a*). However, we elected to combine stocks within basin to more clearly demonstrate basic patterns. Unknown-origin fish that were harvested or that were last recorded at main stem sites were not assigned to populations. Some steelhead were almost certainly last recorded in nonnatal locations (i.e., they were "strays") and their population assignment was therefore incorrect. In previous analyses, Snake River steelhead were most likely to stray into the Deschutes and John Day rivers (Keefer et al. 2008*b*), and this should be considered in the interpretation of results. For example, some fish assigned to the Deschutes and John Day rivers were likely from upriver populations, adding a small bias of unknown direction to thermoregulatory estimates for these stocks.

Each known-origin steelhead was assigned to one of five fate categories. Successful migrants were those that returned to natal tributaries or hatcheries or that passed the uppermost monitored dams (Lower Granite and Priest Rapids). Fish whose transmitters were returned from commercial gillnet, sport, and tribal fisheries through a reward program (US$10–100) were assigned to either main stem or nonnatal tributary harvest categories based on reported harvest location. Known-origin fish last recorded at antennas in nonnatal tributaries were considered strays, and those last recorded at main stem sites between dams were assigned unknown fate. Both stray and unknown main stem fate categories included unreported harvest as well as nonharvest mortality.

Statistical analyses

To identify potential thermoregulatory threshold temperatures, each fish was assigned a reservoir entry temperature using mean daily Columbia River temperatures from water quality monitoring sites at Bonneville or The Dalles (www.cbr.washington.edu/dart/river.html). Run-of-river reservoirs in the Columbia River have little thermal stratification and temperatures at these sites were strongly correlated. Temperature at date of reservoir entry was selected because fish could easily reach refugia sites within 8–12 h after entering either reservoir. Daily data were also reasonable as steelhead that do not use refugia generally pass through the study reservoirs in <1–3 days (Keefer et al. 2004). Reservoir entry temperatures were summarized for fish that subsequently did or did not use refugia sites for both the aggregated populations and individual populations (successful migrants) and years separately. Logistic regression was used to model population-specific refugia use probabilities in the Bonneville reservoir.

We tested for associations between refugia use and known-origin steelhead fate (2001–2003 only) using Pearson's χ^2 tests. The four fate classes were successful migrant, main stem harvest, nonnatal tributary, and main stem unknown fate. In these tests, the nonnatal tributary group included strays and fish reported harvested in the tributaries. Approximately a third of the nonnatal tributary group was reported harvest, and unreported harvest was a likely fate for the majority of the remainder because almost no fish were reported on spawning grounds and many transmitter signals ceased, consistent with harvest removal. We note that strays are typically considered a loss from source populations, ecologically equivalent, in this case, to harvest or unknown loss. Within the fate analyses, hatchery and wild fish were evaluated separately and in aggregation, because management implications differ for the two groups.

Because harvest tends to be higher for larger fish and both behavior and fate differ seasonally (e.g., Keefer et al. 2005; Hard et al. 2008), steelhead length and migration timing at Bonneville Dam were compared among fate classes using ANOVA. Models used to evaluate potential delayed effects upstream were similar to the Pearson tests described above for overall fish fate, except that steelhead had to pass the dam upstream from refugia sites (The Dalles Dam for Bonneville tributary sites and John Day Dam for all study sites) to be included in comparisons. In other words, fish in these comparisons had survived their initial thermoregulatory behavior and resumed upstream migration. Importantly, tests for delayed effects did not include premature mortality (harvest or otherwise) that occurred upstream from Lower Granite Dam or Priest Rapids Dam because monitoring of these areas was spatially and temporally limited.

Results

Thermoregulatory behavior

Across all study years, steelhead use of thermal refugia in Bonneville reservoir tributaries rapidly increased after mean daily main stem water temperatures reached ~19 °C (Fig. 3). Fish that entered the reservoir when temperatures were <19 °C passed from Bonneville Dam to The Dalles Dam in a median of 3 days (n = 689), with 10% recorded in cool-water tributaries. At reservoir entry temperatures of 19–21 °C, the median passage time was 6 days (n = 1802) and 49% used tributaries. Above 21 °C, the median time was 25 days (n = 731) and 71% used tributaries. The telemetry data from tributary and confluence antennas strongly indicated that steelhead with passage times >3 days spent most of the additional migration time inside refugia tributaries or in tributary plume areas where cool tributary water mixed with the main stem near confluences. Notably, Columbia River temperature profiles varied among years (Fig. 2), but steelhead behavior in relation to temperature was consistent (i.e., annual cool-water refugia use increased severalfold as temperatures rose above ~19 °C).

Fig. 3. Steelhead (*Oncorhynchus mykiss*) passage times from the top of Bonneville Dam to the top of The Dalles Dam (~73 rkm) by water temperature at the Bonneville water quality monitoring site on the date that each fish entered the Bonneville reservoir. Box plots show median, quartile, and 10th and 90th percentiles pooled across study years; 5th and 95th percentiles are marked by open circles. The solid line with solid circles shows the percentage of steelhead recorded in cool-water Bonneville reservoir tributaries for >12 h.

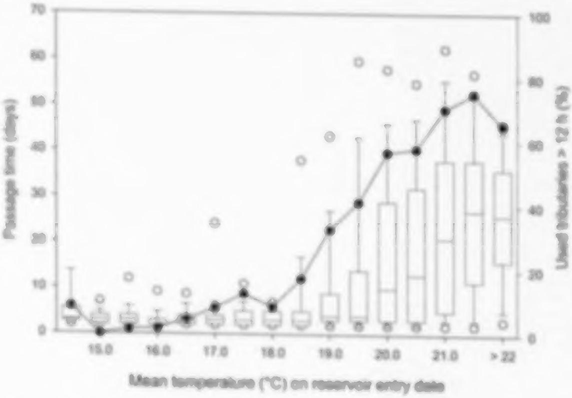

Steelhead use of the Deschutes River where it enters The Dalles reservoir similarly increased as Columbia River temperatures rose. However, fewer fish had thermoregulatory behaviors in The Dalles reservoir because most entered the reach relatively later in the migrations and encountered cooler conditions. Across years, median steelhead reservoir entry dates were 24 August at Bonneville Dam near peak temperatures versus 13 September, when temperatures were decreasing, at The Dalles Dam (Fig. 2). Overall, 27% of steelhead that entered The Dalles reservoir (n = 3222) and 28% of those that eventually passed John Day Dam (n = 2762) were recorded in the Deschutes River. Median passage times through the 38 rkm reach were 15 days for fish that used the Deschutes River (n = 744) versus 2 days for fish that did not (n = 1953). Median passage times through the combined Bonneville to John Day reach were five times longer for fish recorded using cool-water tributaries (32 days, n = 1662) than for fish not recorded in tributaries (6 days, n = 1046).

Stock-specific refugia use patterns by successful migrants paralleled those for the aggregate runs, with consistent evidence for a thermoregulatory threshold near 19 °C and rapidly increasing duration of use at higher temperatures. Stock-specific logistic regression models of refugia use in the Bonneville reservoir were consistent for the seven stocks with the largest sample sizes (Fig. 4*a*). Predicted use probabilities were more variable among stocks with small sample sizes and lower statistical power, although the overall response was similar (Fig. 4*b*). The two populations with the greatest modeled difference from the aggregate sample had the smallest sample sizes (Tucannon River, n = 23; Yakima River, n = 26).

Both the percentage of fish that used refugia and the duration of use differed more than twofold among populations (Fig. 5). Differences were related to stock-specific migration

Fig. 4. Population-specific refugia use probabilities estimated by logistic regression models. The predictor variable was water temperature at the Bonneville water quality monitoring site on the date that steelhead (*Oncorhynchus mykiss*) entered the Bonneville reservoir and the dependent variable was use of a Bonneville refugia tributary for >12 h. (*a*) Populations with large sample sizes: Deschutes River, John Day River, upper Columbia River, Snake River upstream from Lower Granite Dam, Clearwater River, Grande Ronde River, and Salmon River. (*b*) Populations with small sample sizes: Umatilla River, Walla Walla River, Yakima River, Hanford Reach, Tucannon River, Lyons Ferry Hatchery, and Imnaha River. Solid lines show modeled probabilities for all 14 populations combined and dashed lines show population-specific probabilities.

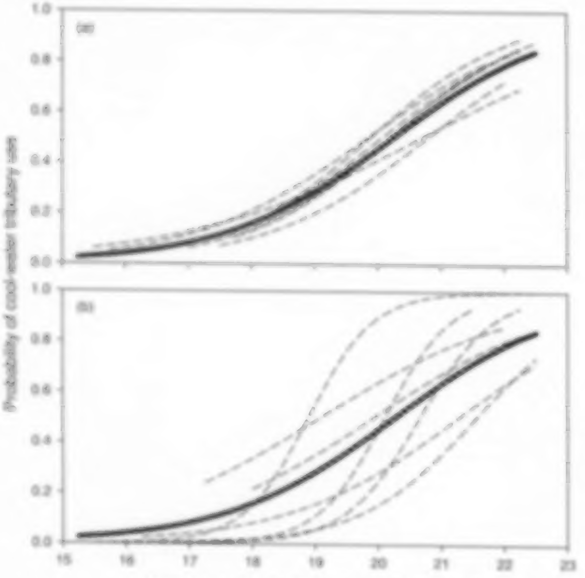

Fig. 5. Relationships between median population-specific steelhead (*Oncorhynchus mykiss*) passage times from the top of Bonneville Dam to the top of John Day Dam (~112 rkm) and the percentages of steelhead that were (solid circles) and were not (open circles) recorded in cool-water tributaries for >12 h. Results pooled for successful migrants across study years. TUC, Tucannon River; HAN, Hanford Reach; LFH, Lyons Ferry Hatchery; UCR, Upper Columbia River; WWR, Walla Walla River; CWR, Clearwater River; SAL, Salmon River; SNK, Snake River above Lower Granite Dam; YAK, Yakima River; IMR, Imnaha River; GRR, Grande Ronde River; UMA, Umatilla River; JDR, John Day River.

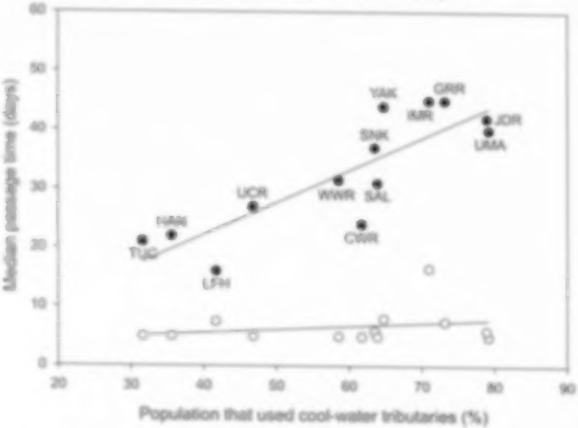

Fig. 6. Migration timing distributions (median, quartiles, and 10th and 90th percentiles) at Bonneville Dam for steelhead (*Oncorhynchus mykiss*) that successfully returned to tributaries or hatcheries pooled across study years. Populations were identified by final fish locations. The vertical dotted lines show mean first and last dates that Columbia River water temperature was 19 °C; the shaded area shows dates with mean temperature ≥21 °C.

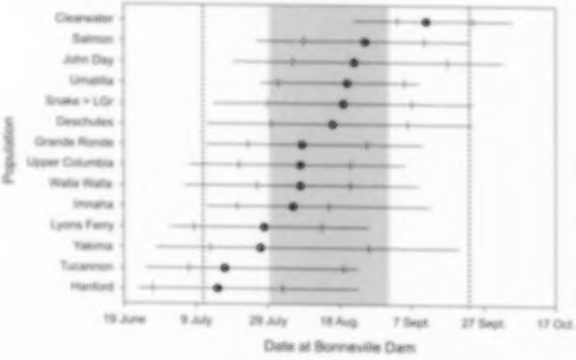

timing and associated seasonal warming and cooling (Fig. 6). On average, stocks migrating earliest (Tucannon, Hanford Reach, and Lyon's Ferry) encountered the lowest mean daily temperatures in the Bonneville reservoir, were least likely to use refugia, and passed through the Bonneville to John Day reach fastest. The latest timed stock (Clearwater) also encountered relatively cool main stem temperatures and had migration rates most similar to those of early migrants. In contrast, stocks with the longest passage times and highest rates of refugia use (Grande Ronde, Imnaha, John Day, and Umatilla) had migration timing distributions that coincided with the warmest migration conditions (Figs. 5 and 6). Migration times for fish not recorded in tributaries were consistent across populations, with median Bonneville to John Day passage times of 5–8 days. The single exception was the small sample of Imnaha steelhead (median = 16.5 days, *n* = 9).

Fish fate

Final fates of known-origin steelhead in 2001–2003 indicated lower overall migration success for fish that used thermal refugia (Fig. 7). With all groups combined, mean annual homing success was 8.1% lower for steelhead that used tributaries (68.7%) than for those that did not (76.8%). Differences were 4.5% for wild steelhead (68.5% versus 73.0%) and 10.6% for hatchery steelhead (73.0% versus 83.6%). Allocations among unsuccessful categories (main stem harvest, unknown fate, and harvest in refugia/permanent straying) showed higher unknown loss for fish that used tributaries and relatively high harvest rates in refugia sites (Fig. 7). In contrast, main stem harvest (which included both gillnet and recreational fisheries) tended to be higher for fish not re-

Fig. 7. Mean annual estimates of homing, main stem harvest, straying, and unknown fate for known-origin steelhead (*Oncorhynchus mykiss*) that were (shaded bars) or were not (open bars) recorded using tributary thermal refugia in the lower Columbia River during the 2001–2003 migrations. (*a*) All fish; (*b*) wild fish; (*c*) hatchery fish. The "strayed" category includes permanent strays to nonnatal basins and fish reported harvested inside monitored tributary refugia.

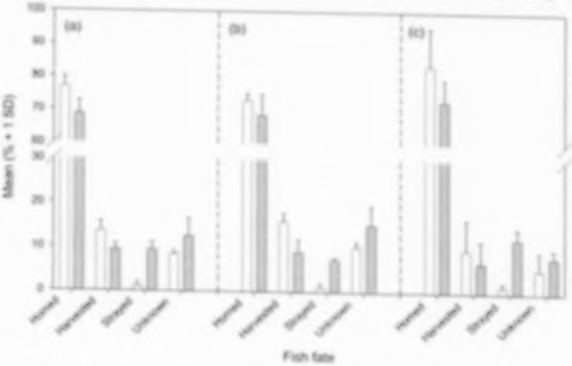

corded in refugia. Distributions among the four fate classes differed significantly for wild fish in 2001 ($\chi^2 = 7.9$, df = 3, $P = 0.048$, $n = 208$) and 2002 ($\chi^2 = 17.0$, df = 3, $P < 0.001$, $n = 357$) but not in 2003 ($\chi^2 = 1.9$, df = 3, $P = 0.591$, $n = 63$). Similarly, differences were significant for hatchery fish in 2001 ($\chi^2 = 17.5$, df = 3, $P < 0.001$, $n = 447$) and 2002 ($\chi^2 = 11.5$, df = 3, $P = 0.009$, $n = 185$) but not in 2003 ($\chi^2 = 1.8$, df = 3, $P = 0.403$, $n = 20$). We note that many fish harvested in the main stem were reported captured near tributary mouths where they may have been using cool-water tributary plumes. Treating these fish as "not using" refugia sites likely reduced the power to detect statistical differences among categories.

Fate patterns for individual populations were more mixed (Table 2), at least in part due to among-stock migration timing and demographic differences that affected harvest. For the predominantly (96%) hatchery origin upper Columbia group, steelhead last recorded in refugia were larger (75.0 cm) than fish harvested in the main stem (72.2 cm), fish that homed (70.6 cm), and fish with unknown fate (70.0 cm) (ANOVA: $F = 5.18$, df = 464, $P = 0.002$). Mean migration timing at Bonneville Dam was latest for upper Columbia fish harvested in the main stem (13 August) and progressively earlier for fish that homed (7 August), that were last recorded in refugia (6 August), and with unknown fate (3 August) ($F = 2.52$, df = 464, $P = 0.057$). Sample sizes were limiting for several of the Snake River known-origin groups. However, with all Snake River wild fish combined, main stem harvested fish were largest (74.4 cm) followed by fish that homed (72.3 cm), fish with unknown fate (69.7 cm), and fish last recorded in refugia (68.7 cm) ($F = 3.57$, df = 613, $P = 0.014$). Both Snake River wild and hatchery steelhead last recorded in refugia migrated earlier (8–14 days on average) than fish in other fate classes; these timing differences were not statistically significant ($P > 0.26$).

Snake River steelhead fates did differ ($\chi^2 = 13.1$, df = 3, $P = 0.004$) for wild versus hatchery fish. With all Snake River groups combined, wild fish were twice as likely to have unknown fate (12.9%, $n = 614$) as hatchery fish (6.3%, $n = 206$). Further, more wild (10.8%) than hatchery fish (8.3%) were reported harvested in main stem fisheries, more hatchery (9.7%) than wild fish (4.7%) were last recorded in refugia sites, and more hatchery (75.7%) than wild fish (71.5%) returned to Lower Granite Dam or Snake River tributaries.

Delayed effects

There was little evidence that steelhead survival upstream from The Dalles and (or) John Day dams was affected by thermoregulatory behavior in reservoir reaches downstream from these sites. For example, of all known-origin fish that passed The Dalles Dam, those that used refugia downstream in Bonneville reservoir homed and were harvested at similar rates as fish that did not use Bonneville refugia (Table 3). Similarly, fates of fish that passed John Day Dam did not differ with downstream refugia use in Bonneville or The Dalles reservoirs. Nonsignificant ($P > 0.05$) results were consistent for hatchery and wild fish separately and for individual years. In delayed effects tests using individual populations, upstream fates differed with thermoregulatory behavior only for the Snake River barged group that passed John Day Dam (all fish pooled across years). In this case, barged fish recorded in tributaries were less likely to home (76.3%) and were more likely to be harvested (4.7%), to last be recorded in nonnatal tributaries (8.8%), and to have unknown fate (10.2%) than fish not recorded in tributaries (home = 87.3%, harvest = 1.4%, nonnatal tributary = 2.8%, and unknown = 8.5%) ($\chi^2 = 9.1$, df = 3, $P = 0.028$, $n = 357$). Results were nonsignificant ($P > 0.05$) when the barged group was separated into groups based on origin (hatchery or wild) or year.

Discussion

Behavioral thermoregulation

The first study objective was to identify temperatures that provoked behavioral thermoregulation in adult steelhead. An apparent threshold for the initiation of refugia use was associated with Columbia River warming to ~19 °C, when about a third of the telemetered migrants were recorded in cool-water tributary areas. By comparison, <10% were detected in refugia when main stem temperatures were between 14 and 18 °C. With continued warming, the likelihood of thermoregulation rapidly increased, with >70% of the aggregate run using refugia at the warmest times (i.e., ≥21 °C). Typical refugia residence times were on the scale of hours to days at 19 °C but increased to weeks and even months when temperatures were 20 °C and higher. Temperatures associated with the initiation of refugia use were relatively constant across populations, and large percentages of all groups used refugia when main stem temperatures were highest.

Steelhead thermoregulatory behaviors differed substantially from those of Columbia River fall-run Chinook salmon (*Oncorhynchus tshawytscha*) that comigrate with steelhead in August–October. In a concurrent study by Goniea et al. (2006), fall Chinook salmon experienced similar peak temperatures and used the same refugia as steelhead, but only 9% stayed more than 12 h and typical residence times were 3–5 days. A fall Chinook salmon thermoregula-

Table 2. Summary of known-origin steelhead (*Oncorhynchus mykiss*) fates by natal basin, rearing type (hatchery, wild), and use of cool-water tributaries in the Bonneville or The Dalles reservoir.

				Fate					
Stock	Rearing type	Tributary use	n	Successful	Main stem harvest	Nonnatal tributary[a]	Main stem unknown	χ^2	P
UpperColumbia	All	No	234	76.5	14.1	1.3	8.1	25.3	<0.001
		Yes	228	63.6	13.2	12.7	10.5		
	Hatchery	No	226	76.1	14.2	1.3	8.4	25.1	<0.001
		Yes	217	64.1	12.4	13.4	10.1		
	Wild	No	8	87.5	12.5			2.7	0.263
		Yes	11	54.6	27.3		18.2		
Snake (barged)	All	No	170	72.9	12.9	2.4	11.7	17.6	<0.001
		Yes	248	66.1	6.5	11.7	15.7		
	Hatchery	No	24	83.3	4.2	4.2	8.3	2.8	0.424
		Yes	42	66.7	7.1	16.7	9.5		
	Wild	No	146	71.2	14.4	2.1	12.3	16.3	0.001
		Yes	206	66.0	6.3	10.7	17.0		
Snake (in-river)	All	No	114	75.6	17.5	0.9	7.0	10.6	0.014
		Yes	144	79.9	8.3	6.9	4.9		
	Hatchery	No	28	75.0	14.3	3.6	7.1	6.8	0.077
		Yes	48	83.3	2.1	12.5	2.1		
	Wild	No	86	74.4	18.6		7.0	5.3	0.154
		Yes	96	78.1	11.5	4.2	6.3		
Snake (other[b])	All	No	50	78.0	14.0	2.0	6.0	2.3	0.514
		Yes	86	77.9	8.1	5.8	8.1		

Note: Steelhead in the Snake River barged and in-river groups were PIT-tagged at Lower Granite Dam and either transported downstream or released back to the river. Those in the Snake River (other) group were PIT-tagged in tributaries or at hatcheries upstream from Lower Granite Dam. Statistical results from Pearson χ^2 tests.

[a] Permanent strays to nonnatal basins and fish reported harvested inside monitored tributary refugia.

[b] Clearwater (n = 56), Grande Ronde (n = 23), Salmon (n = 30), and Imnaha (n = 27).

Table 3. Tests for delayed effects of cool-water tributary use on main stem fates of known-origin steelhead (*Oncorhynchus mykiss*) after they passed over The Dalles and (or) John Day dams.

				Fate					
Dam passed	Rearing type	Tributary use	n	Successful	Main stem harvest	Nonnatal tributary[a]	Main stem unknown	χ^2	P
The Dalles	All	No	622	81.4	7.2	3.4	8.0	0.5	0.919
		Yes	517	80.1	7.4	4.1	8.5		
	Hatchery	No	321	81.9	8.1	3.4	6.5	0.5	0.930
		Yes	252	81.0	7.5	3.6	7.9		
	Wild	No	301	80.7	6.3	3.3	9.6	0.8	0.856
		Yes	265	79.3	7.2	4.5	9.1		
John Day	All	No	478	89.3	3.1	1.5	6.1	5.5	0.137
		Yes	574	85.9	4.4	3.5	6.3		
	Hatchery	No	258	89.2	3.9	1.6	5.4	0.7	0.876
		Yes	269	88.1	5.2	1.9	4.8		
	Wild	No	220	89.6	2.3	1.4	6.8	6.0	0.111
		Yes	305	83.9	3.6	4.9	7.5		

Note: Tributary use was limited to tributaries to the Bonneville reservoir for fish that passed The Dalles Dam and to tributaries to the Bonneville or The Dalles reservoir for fish that passed John Day Dam.

[a] Permanent strays to nonnatal basins and fish reported harvested inside monitored tributary refugia.

tory threshold was identified at about 20 °C (Goniea et al. 2006). Behavioral differences between these species reflect divergence in life history and migration timetables. The Chinook salmon are obligate fall spawners with a relatively narrow migration window (Dauble and Watson 1997), whereas steelhead have temporally plastic migrations in the seasons preceding spring spawning (Brannon et al. 2004; Quinn 2005). The migration schedule of a third Columbia River salmonid, sockeye salmon (*Oncorhynchus nerka*), overlaps the first half of the steelhead migration and presents a third strategy. Peak adult sockeye passage in the study reach is from mid-June to mid-July when mean daily temperatures are mostly 15–19 °C (Quinn et al. 1997), and the run rapidly passes through the lower river with little evidence of refugia use (Naughton et al. 2005). Instead, sockeye salmon often encounter high water temperatures at upriver sites closer to spawning grounds where extended migration delays (Major and Mighell 1967; Hyatt et al. 2003) and refugia use (Keefer et al. 2008*c*) have been reported at temperatures of 20–21 °C.

The behaviors and migration schedules of the three species may reflect alternative evolutionary approaches to avoiding stressful or lethal Columbia River temperatures. Fall-spawning sockeye and fall Chinook salmon migrate mostly before (sockeye) or after (Chinook) historic peak main stem temperatures. Variations of these two patterns are repeated throughout the species' Pacific Rim ranges, with site-specific adaptations to long-term temperature and flow regimes (Groot and Margolis 1991; Myers et al. 1998; Hodgson and Quinn 2002). Historically, Columbia River summer steelhead may have used the same temperature avoidant strategies as both Chinook and sockeye salmon, as their passage distributions in the lower river were bimodal with a nadir in late summer during temperature peaks (Robards and Quinn 2002). However, with development of the Columbia River Hydrosystem, main stem temperatures have significantly increased and bimodality in the steelhead run has shifted to a relatively flat distribution that overlaps the warmest temperatures (Robards and Quinn 2002). Earlier spring warming, higher summer temperatures, and later fall cooling (e.g., Quinn et al. 1997) means that many more steelhead now encounter high water temperatures, and it is likely that a larger proportion of the run thermoregulates during migration compared with historically. It is not clear, however, whether the recent run timing shift can be explained by environmental changes and attendant behavioral responses by steelhead or if other factors (i.e., loss of native stocks and proliferation of hatchery fish (Busby et al. 1996)) are responsible.

Importantly, neither the fitness consequences of cumulative temperature exposure during migration nor the potential for thermal refugia use to ameliorate temperature effects has been directly evaluated for steelhead in unregulated systems. This will be an important next step in the evaluation of the population-level effects of refugia use. For adults, potential negative temperature impacts include elevated physiological and energetic demands (Brett 1995; Lee et al. 2003; MacNutt et al. 2006), greater susceptibility to disease incidence and severity (e.g., Wagner et al. 2005), and higher prespawn mortality (Crossin et al. 2008; Keefer et al. 2008*c*). High temperature exposure also lowers reproductive success, egg viability, and the fitness of progeny (e.g., Flett et al. 1996; King et al. 2007). Behavioral thermoregulation during migration, like premature and multiphase migrations, may therefore have developed in response to selective constraints on adults and subsequent effects on juveniles (e.g., emergence timing, fry growth, and survival) (Dodson 1997; Quinn 2005).

Variability among populations

In addressing the second objective, we found that the percentage of thermoregulating fish and the duration of thermoregulation significantly varied among study populations. Refugia use patterns strongly supported our first hypothesis, as the behavior appeared to be a function of population-specific migration timing and attendant among-population differences in encountered river temperatures. Relatively early- and late-migrating populations encountered lower mean water temperatures in the study reach each year. These populations had fewer individuals use refugia sites, and those that did typically remained for relatively shorter periods. On average, the longest refugia use times were for populations with median migration dates in the last week of July or first week of August, coincident with mean Columbia River water temperatures reaching ~21 °C. A third group, the populations with the highest percentages of fish using refugia, had median passage dates in mid-August, or about the time of peak main stem temperatures. We did not attempt to untangle the effects of migration timing (i.e., date effects) from the effects of main stem temperature, as the two were strongly correlated in all years. However, it is possible that timing-related factors unassociated with water temperature, such as river discharge, photoperiod, or conspecific abundance, also affected steelhead behaviors.

Migration timing distributions for the 14 study populations varied considerably, with median passage dates at Bonneville Dam ranging from mid-July to mid-September. The most temporally distinctive distribution was for the relatively late-migrating Clearwater River steelhead, which are part of a Snake River population complex that spends an additional year in the ocean. These larger fish are believed to have been historically abundant in the late mode of the Columbia River run (Busby et al. 1996; Brannon et al. 2004). Among-population timing differences presumably reflect selective pressures that parallel those for the among-species differences in migration timing. For example, it is likely that conditions in spawning tributaries influenced divergence in adult migration timing given the strong organizing effects of environmental conditions during spawning and subsequent juvenile life stages (Quinn et al. 2000; Waples et al. 2004). Migration distance and seasonal migration obstacles (e.g., falls, low flows, temperature barriers, etc.) in both the main stem and tributaries may also have shaped the divergent timing patterns. As additional data become available, it should be possible to better define migration timing distributions for the Columbia's many subbasin steelhead populations. We expect that more nuanced behavioral differences among groups will also be identified. Improving upon our relatively coarse-scale population analyses will be useful for predicting how many fish from either individual or aggregated populations will have thermoregulatory responses within a given year or at specific temperature criteria. Such data can be used to develop appropriate management plans for steelhead with conservation priority.

The overall behavioral consistency among populations suggests exposure to a shared historic selective regime, perhaps during the postglacial period of salmon and steelhead recolonization of the interior basin (e.g., McPhail and Lindsey 1986; Waples et al. 2008). Such a regime potentially predated divergence among Columbia River steelhead populations. Steelhead also may have adapted similar thermoregulatory responses across populations through a process of parallel evolution (e.g., across-population exposure to extreme events or similarity in hydrologic regimes across spatially separated sites; Waples et al. 2004; Beechie et al. 2006).

We note that there was substantial individual variability among steelhead from all identified populations. Some fish showed no thermoregulatory behavior despite migrating at the warmest times, while others remained in refugia for weeks to months after fall cooling (e.g., Keefer et al. 2008*a*). Similarly, some steelhead used multiple refugia sites with repeated entries and exits, while others showed high fidelity to single locations (see High et al. 2006). This variability echoes steelhead activities in winter when Columbia River fish hold for varying lengths of time, move up- and downstream past dams, and temporarily enter nonnatal tributaries (Keefer et al. 2008*a*). Behavioral plasticity across seasons results in mixed stock aggregations that are spatially distributed over long segments of the migration route. Taken together, these behaviors reflect either a remarkable evolutionary legacy of adaptation to stochastic environments (e.g., Hilborn et al. 2003; Dickerson et al. 2005; Wilbur and Rudolf 2006) or a more recent, less adaptive consequence of rapid demographic and environmental changes (e.g., Araki et al. 2008; Hutchings and Fraser 2008).

Mortality trade-offs

Our third objective was to assess associations between refugia use and known-origin steelhead fate. The survival results strongly suggested that use of thermal refugia, a normally adaptive behavior, might carry a relatively high mortality risk in this system. The negative outcome is characteristic of an "ecological trap" where animals respond to a reliable evolutionary cue but then experience reduced survival or reproductive success (Coutant 1987; Schlaepfer et al. 2002; Robertson and Hutto 2006). In our samples, steelhead that used refugia were about 8% less likely to complete migration through the monitored Hydrosystem, and survival costs were significant for both hatchery (~11%) and wild (~5%) fish. The mortality appeared to be most directly related to fisheries inside refugia where reported harvest rates were about 13% for upper Columbia steelhead populations and ranged from 4%–17% for the various Snake River groups. Importantly, a portion of the negative thermoregulatory effect may have been indirect, particularly if steelhead in poor physical condition (i.e., with pathogens or relatively low energetic reserves) were more likely to use refugia sites. Unknown loss in the main stem was also higher for the thermoregulating group in most known-origin populations, likely reflecting unreported harvest near confluence areas and possible indirect effects on natural mortality. Overall, we believe that differences in overall mortality estimates between fish that did or did not use refugia may be conservative for two reasons. First, information returned with transmitters suggested that some "nonthermoregulating" fish harvested in the main stem were almost certainly caught in cool-water plumes from refugia tributaries (i.e., they were incorrectly identified as not using refugia). Second, several dozen known-origin fish were harvested in the main stem before they had an opportunity to enter refugia, a bias that would lead to underestimation of refugia effects.

The mortality and migration timing patterns provided compelling, but indirect, support for our hypothesis that mortality risks associated with thermoregulation differ among populations. Although mortality trade-offs related to refugia use likely vary among populations, we are hesitant to extrapolate results from the known-origin samples to the Columbia's many steelhead stocks given demographic (i.e., hatchery or wild), selective harvest, and migration timing differences among populations. On balance, we expect that population-level risk of harvest inside thermal refugia is likely greatest for fish that enter the study reach during the peak of thermoregulatory behavior from late July through early September. The presumed mortality for strays that were not reported harvested is also likely highest for those entering during the thermoregulatory peak. Risk of main stem harvest is presumably highest for early and late migrants when fisheries effort is concentrated outside refugia. This early-season harvest hypothesis is supported by the escapement summaries for unknown-origin steelhead reported in Keefer et al. (2005), which showed that Hydrosystem survival was lowest for steelhead that passed Bonneville Dam in late May and June. Low survival during this period was related to both main stem harvest and unknown main stem mortality. Risks also clearly differed for wild and hatchery steelhead because some protection was afforded wild fish (i.e., mandatory release of rod-caught fish with intact adipose fins). However, relatively high percentages of wild fish in the sampled known-origin populations had unknown fates, indicating either illegal harvest, greater susceptibility to "natural" mortality, or possible handling mortality following catch and release (e.g., Bendock and Alexandersdottir 1993). The latter may be of special concern given the combined negative effects of fish handling and high water temperatures (Dempson et al. 2002; Cooke and Suski 2005).

In the fourth objective, we tested for delayed mortality effects with the expectation that steelhead might be targeted after exiting refugia sites as temperatures decreased in the fall. However, we found little evidence that harvest rates in upstream reaches differed between steelhead that did and did not use the studied refugia. Unlike during the onset of high water temperatures, when fisheries in the study area efficiently shifted from main stem to refugia sites, there was no indication of a large-scale shift to main stem fisheries as temperatures decreased. The general lack of delayed effects may have been because fish were not spatially aggregated after exiting refugia or because there was no clear threshold temperature for refugia exit timing. The single statistically significant delayed effect was that Snake River fish that were barged as juveniles had lower upstream survival, consistent with a broader pattern of reduced homing and increased migration mortality for transported fish (Keefer et al. 2008*b*).

In summary, migrations of Columbia River summer-run steelhead are spatially and temporally complex, in large part because adults encounter a wide range of environmental conditions that include water temperatures near both upper tolerance limits (21–25 °C) and annual minima (1–5 °C). Steelhead have adapted by migrating in phases, with bouts of upstream movement when conditions are favorable and holding or refuge seeking when conditions are stressful. During summer temperature peaks, cool-water habitats are spatially constricted and patchily distributed, resulting in dense adult aggregations in midmigration. The refugia that steelhead used in this study were clustered along the margins of a relatively short (<100 rkm) section of the lower migration corridor, hundreds to more than 1000 km downstream from spawning grounds. Despite their small spatial extent, these few refugia sites were used by >75% of the tagged steelhead from some upriver populations, with many fish holding for weeks to months. The behaviors underscore the critical importance of thermal refugia in the Columbia River system where decades-long warming of the migration corridor (e.g., Quinn et al. 1997) is forecast to accelerate with regional climate change (Hamlet and Lettenmaier 1999; Battin et al. 2007).

Despite the apparent survival costs, the presumed benefits of steelhead refugia use should not be discounted. Experiments with rainbow trout, Atlantic salmon (*Salmo salar*), and sockeye salmon have all shown that exposure to high water temperature can have large negative effects on fish performance, maturation, survival, and productivity (e.g., Pankhurst et al. 1996; King et al. 2007; Crossin et al. 2008). The recorded steelhead use of refugia almost certainly reduced these effects to varying degrees. The behaviors also presumably helped conserve energy needed to complete migration, compete for redd sites, and spawn (e.g., Berman and Quinn 1991; Newell and Quinn 2005). Future biotelemetry studies that monitor both migration behaviors and reproductive success (e.g., Mann and Peery 2005) or laboratory-based experiments that simulate thermal histories and monitor survival outcomes (e.g., Crossin et al. 2008) will provide a more complete cost–benefit accounting of steelhead refugia use. In the Columbia River system, where many important refugia have already been identified, managers must now balance demands for fisheries with more conservative restrictions in refugia sites to protect populations listed under the Endangered Species Act.

Acknowledgements

Many people provided time and assistance during the course of this study. We especially thank D. Clugston, R. Kalamacz, M. Langeslay, T. Mackey, M. Shutters, and K. Zelch (US Army Corps of Engineers) for project oversight and funding. T. Bjornn, R. Ringe, K. Tolotti, M. Jepson, S. Lee, C. Boggs, G. Naughton, T. Reischel, W. Daigle, C. Caudill, P. Keniry, M. Heinrich, M. Morasch, T. Dick, C. Morat, and D. Joosten (University of Idaho) helped with project oversight, field operations, fish tagging, and telemetry data processing. L. Stuehrenberg, A. Matter, B. Burke, M. Moser, T. Bohn, and S. McCarthy (NOAA Fisheries) helped with data management. Personnel at the Grant, Chelan, and Douglas County Public Utility Districts cooperated with telemetry data collection. Hatchery and agency staff and anglers and tribal fishers basin-wide cooperated in the transmitter return programs.

References

Adolph, S.C. 1990. Influence of behavioral thermoregulation on microhabitat use by two *Sceloporus* lizards. Ecology, **71**(1): 315–327. doi:10.2307/1940271.

Angilletta, M.J., Jr., Niewiarowski, P.H., and Navas, C.A. 2002. The evolution of thermal physiology in ectotherms. J. Therm. Biol. **27**(4): 249–268. doi:10.1016/S0306-4565(01)00094-8.

Araki, H., Berejikian, B.A., Ford, M.J., and Blouin, M.S. 2008. Fitness of hatchery-reared salmonids in the wild. Evol. Appl. **1**(2): 342–355. doi:10.1111/j.1752-4571.2008.00026.x.

Baird, O.E., and Krueger, C.C. 2003. Behavioural thermoregulation of brook and rainbow trout: comparison of summer habitat use in an Adirondack river, New York. Trans. Am. Fish. Soc. **132**(6): 1194–1206. doi:10.1577/T02-127.

Battin, J., Wiley, M.W., Ruckelshaus, M.H., Palmer, R.N., Korb, E., Bartz, K.K., and Imaki, H. 2007. Projected impacts of climate change on salmon habitat restoration. Proc. Natl. Acad. Sci. U.S.A. **104**(16): 6720-6725. doi:10.1073/pnas.0701685104. PMID:17412830.

Beechie, T., Buhle, E., Ruckelshaus, M., Fullerton, A., and Holsinger, L. 2006. Hydrologic regime and the conservation of salmon life history diversity. Biol. Conserv. **130**(4): 560–572. doi:10.1016/j.biocon.2006.01.019.

Beitinger, T.L., and Fitzpatrick, L.C. 1979. Physiological and ecological correlates of preferred temperature in fish. Am. Zool. **19**(1): 319–329.

Beitinger, T.L., Bennett, W.A., and McCauley, R.W. 2000. Temperature tolerances of North American freshwater fishes exposed to dynamic changes in temperature. Environ. Biol. Fishes, **58**(3): 237–275. doi:10.1023/A:1007676325825.

Bendock, T., and Alexandersdottir, M. 1993. Hooking mortality of chinook salmon released in the Kenai River, Alaska. N. Am. J. Fish. Manag. **13**(3): 540–549. doi:10.1577/1548-8675(1993)013<0540:HMOCSR>2.3.CO;2.

Berman, C.H., and Quinn, T.P. 1991. Behavioural thermoregulation and homing by spring chinook salmon, *Oncorhynchus tshawytscha* (Walbaum), in the Yakima River. J. Fish Biol. **39**(3): 301–312. doi:10.1111/j.1095-8649.1991.tb04364.x.

Biro, P.A. 1998. Staying cool: behavioral thermoregulation during summer by young-of-year brook trout in a lake. Trans. Am. Fish. Soc. **127**(2): 212–222. doi:10.1577/1548-8659(1998)127<0212:SCBTDS>2.0.CO;2.

Brannon, E.L., Powell, M.S., Quinn, T.P., and Talbot, A. 2004. Population structure of Columbia River basin chinook salmon and steelhead trout. Rev. Fish. Sci. **12**(2-3): 99–232. doi:10.1080/10641260490280313.

Breau, C., Cunjak, R.A., and Bremset, G. 2007. Age-specific aggregation of wild juvenile Atlantic salmon *Salmo salar* at cool water sources during high temperature events. J. Fish Biol. **71**(4): 1179–1191. doi:10.1111/j.1095-8649.2007.01591.x.

Brett, J.R. 1971. Energetic responses of salmon to temperature. A study of some thermal relations in the physiology and freshwater ecology of sockeye salmon (*Oncorhynchus nerka*). Am. Zool. **11**: 99–113.

Brett, J.R. 1995. Energetics. *In* Physiological ecology of Pacific salmon. *Edited by* C. Groot, L. Margolis, and W.C. Clarke. University of British Columbia Press, Vancouver, B.C. pp. 3–68.

Buchanan, R.A., Skalski, J.R., and Smith, S.G. 2006. Estimating the effects of smolt transportation from different vantage points and management perspectives. N. Am. J. Fish. Manag. **26**(2): 460–472. doi:10.1577/M05-080.1.

Busby, P.J., Wainwright, T.C., Bryant, E.J., Lierheimer, L.J., Waples, R.S., Waknitz, F.W., and Lagomarsino, I.V. 1996. Status review of west coast steelhead from Washington, Idaho, Oregon, and California. NOAA Tech. Memo. NMFS-NWFSC-27. NOAA, Washington, D.C.

Cooke, S.J., and Suski, C.D. 2005. Do we need species-specific guidelines for catch-and-release recreational angling to effectively conserve diverse fishery resources? Biodivers. Conserv. **14**(5): 1195–1209. doi:10.1007/s10531-004-7845-0.

Coutant, C.C. 1987. Thermal preference: when does an asset become a liability? Environ. Biol. Fishes, **18**(3): 161–172. doi:10.1007/BF00000356.

Crossin, G.T., Hinch, S.G., Cooke, S.J., Welch, D.W., Patterson, D.A., Jones, S.R.M., Lotto, A.G., Leggatt, R.A., Mathes, M.T., Shrimpton, J.M., Van Der Kraak, G., and Farrell, A.P. 2008. Exposure to high temperature influences the behaviour, physiology, and survival of sockeye salmon during spawning migration. Can. J. Zool. **86**(2): 127–140. doi:10.1139/Z07-122.

Dauble, D.D., and Watson, D.G. 1997. Status of fall chinook salmon populations in the Mid-Columbia River, 1948–1992. N. Am. J. Fish. Manag. **17**(2): 283–300. doi:10.1577/1548-8675(1997)017<0283:SOFCSP>2.3.CO;2.

Dempson, J.B., Furey, G., and Bloom, M. 2002. Effects of catch and release angling on Atlantic salmon, *Salmo salar* L., of the Conne River, Newfoundland. Fish. Manag. Ecol. **9**(3): 139–147. doi:10.1046/j.1365-2400.2002.00288.x.

Dickerson, B.R., Brinck, K.W., Willson, M.F., Bentzen, P., and Quinn, T.P. 2005. Relative importance of salmon body size and arrival time at breeding grounds to reproductive success. Ecology, **86**(2): 347–352. doi:10.1890/03-625.

Dodson, J.J. 1997. Fish migration: an evolutionary perspective. *In* Behavioural ecology of teleost fishes. *Edited by* J.-G.J. Godin. Oxford University Press, New York. pp.10–36.

Eaton, J.G., and Scheller, R.M. 1996. Effects of climate warming on fish thermal habitat in streams of the United States. Limnol. Oceanogr. **41**(5): 1109–1115.

Eaton, J.G., McCormick, J.H., Goodno, B.E., O'Brien, D.G., Stefany, H.G., Hondzo, M., and Scheller, R.M. 1995. A field information-based system for estimating fish temperature tolerances. Fisheries, **20**(4): 10–18. doi:10.1577/1548-8446(1995)020<0010:AFISFE>2.0.CO;2.

Ebersole, J.L., Liss, W.J., and Frissell, C.A. 2001. Relationship between stream temperature, thermal refugia and rainbow trout *Oncorhynchus mykiss* abundance in arid-land streams in the Northwestern United States. Ecol. Freshwat. Fish, **10**(1): 1–10. doi:10.1034/j.1600-0633.2001.100101.x.

Fischer, R.U., Jr., Standora, E.A., and Spotila, J.R. 1987. Predator-induced changes in thermoregulation of bluegill, *Lepomis macrochirus*, from a thermally altered reservoir. Can. J. Fish. Aquat. Sci. **44**(9): 1629–1634. doi:10.1139/f87-197.

Flett, P.A., Van Der Kraak, G., and Leatherland, J.F. 1996. Overripening as the cause of low survival to hatch in Lake Erie coho salmon (*Oncorhynchus kisutch*) embryos. Can. J. Zool. **74**(5): 851–857. doi:10.1139/z96-099.

Goniea, T.M., Keefer, M.L., Bjornn, T.C., Peery, C.A., Bennett, D.H., and Stuehrenberg, L.C. 2006. Behavioral thermoregulation and slowed migration by adult fall Chinook salmon in response to high Columbia River water temperatures. Trans. Am. Fish. Soc. **135**(2): 408–419. doi:10.1577/T04-113.1.

Good, T.P., Waples, R.S., and Adams, P. 2005. Updated status of federally listed ESUs of West coast salmon and steelhead. NOAA Tech. Memo. NMFS-NWFSC-66. NOAA, Washington, D.C.

Groot, C., and Margolis, L. 1991. Pacific salmon life histories. University of British Columbia Press, Vancouver, B.C.

Hamlet, A.F., and Lettenmaier, D.P. 1999. Effects of climate change on hydrology and water resources in the Columbia River basin. J. Am. Water Resour. Assoc. **35**(6): 1597–1623. doi:10.1111/j.1752-1688.1999.tb04240.x.

Hard, J.J., Gross, M.R., Heino, M., Hilborn, R., Kope, R.G., Law, R., and Reynolds, J.D. 2008. Evolutionary consequences of fishing and their implications for salmon. Evol. Appl. **1**(2): 388–408. doi:10.1111/j.1752-4571.2008.00020.x.

Hari, R.E., Livingstone, D.M., Siber, R., Burkhardt-Holm, P., and Güttinger, H. 2006. Consequences of climatic change for water temperature and brown trout populations in Alpine rivers and streams. Glob. Change Biol. **12**(1): 10–26. doi:10.1111/j.1365-2486.2005.001051.x.

High, B. 2002. Effect of water temperature on adult steelhead migration behavior and survival in the Columbia River basin. Master's thesis, University of Idaho, Moscow, Idaho.

High, B., Peery, C.A., and Bennett, D.H. 2006. Temporary staging of Columbia River summer steelhead in coolwater areas and its effect on migration rates. Trans. Am. Fish. Soc. **135**(2): 519–528. doi:10.1577/T04-224.1.

Hight, B.V., and Lowe, C.G. 2007. Elevated body temperatures of adult female leopard sharks, *Triakis semifasciata*, while aggregating in shallow nearshore embayments: evidence for behavioral thermoregulation? J. Exp. Mar. Biol. Ecol. **352**(1): 114–128. doi:10.1016/j.jembe.2007.07.021.

Hilborn, R., Quinn, T.P., Schindler, D.E., and Rogers, D.E. 2003. Biocomplexity and fisheries sustainability. Proc. Natl. Acad. Sci. U.S.A. **100**(11): 6564–6568. doi:10.1073/pnas.1037274100. PMID:12743372.

Hodgson, S., and Quinn, T.P. 2002. The timing of adult sockeye salmon migration into fresh water: adaptations by populations to prevailing thermal regimes. Can. J. Zool. **80**(3): 542–555. doi:10.1139/z02-030.

Holland, K.N., Brill, R.W., Chang, R.K.C., Sibert, J.R., and Fournier, D.A. 1992. Physiological and behavioural thermoregulation in bigeye tuna (*Thunnus obesus*). Nature, **358**(6385): 410–412. doi:10.1038/358410a0. PMID:1641023.

Hutchings, J.A., and Fraser, D.J. 2008. The nature of fisheries- and farming-induced evolution. Mol. Ecol. **17**(1): 294–313. doi:10.1111/j.1365-294X.2007.03485.x. PMID:17784924.

Hyatt, K.D., Stockwell, M.M., and Rankin, D.P. 2003. Impact and adaptation responses of Okanagan River sockeye salmon (*Oncorhynchus nerka*) to climate variation and change effects during freshwater migration: stock restoration and fisheries management implications. Can. Water Resour. J. **28**: 689–713.

Keefer, M.L., Peery, C.A., Bjornn, T.C., Jepson, M.A., and Stuehrenberg, L.C. 2004. Hydrosystem, dam, and reservoir passage rates of adult chinook salmon and steelhead in the Columbia and Snake rivers. Trans. Am. Fish. Soc. **133**(6): 1413–1439. doi:10.1577/T03-223.1.

Keefer, M.L., Peery, C.A., Daigle, W.R., Jepson, M.A., Lee, S.R., Boggs, C.T., Tolotti, K.R., and Burke, B.J. 2005. Escapement, harvest, and unknown loss of radio-tagged adult salmonids in the Columbia River – Snake River hydrosystem. Can. J. Fish. Aquat. Sci. **62**(4): 930–949. doi:10.1139/f04-246.

Keefer, M.L., Boggs, C.T., Peery, C.A., and Caudill, C.C. 2008*a*. Overwintering distribution, behavior, and survival of adult summer steelhead: variability among Columbia River populations. N. Am. J. Fish. Manag. **28**(1): 81–96. doi:10.1577/M07-011.1.

Keefer, M.L., Caudill, C.C., Peery, C.A., and Lee, S.R. 2008*b*. Transporting juvenile salmonids around dams impairs adult migration. Ecol. Appl. **18**(8): 1888–1900. doi:10.1890/07-0710.1. PMID:19263886.

Keefer, M.L., Peery, C.A., and Heinrich, M.J. 2008*c*. Temperature-mediated en route migration mortality and travel rates of endangered Snake River sockeye salmon. Ecol. Freshwat. Fish, **17**(1): 136–145. doi:10.1111/j.1600-0633.2007.00267.x.

King, H.R., Pankhurst, N.W., and Watts, M. 2007. Reproductive sensitivity to elevated water temperatures in female Atlantic salmon is heightened at certain stages of vitellogenesis. J. Fish Biol. **70**(1): 190–205. doi:10.1111/j.1095-8649.2006.01295.x.

Lee, C.G., Farrell, A.P., Lotto, A., MacNutt, M.J., Hinch, S.G., and Healey, M.C. 2003. The effect of temperature on swimming performance and oxygen consumption in adult sockeye (*Oncorhynchus nerka*) and coho (*O. kisutch*) salmon stocks. J. Exp. Biol. **206**(18): 3239–3251. doi:10.1242/jeb.00547. PMID:12909705.

MacNutt, M.J., Hinch, S.G., Lee, C.G., Phibbs, J.R., Lotto, A.G., Healey, M.C., and Farrell, A.P. 2006. Temperature effects on swimming performance, energetics, and aerobic capacities of mature adult pink salmon (*Oncorhynchus gorbuscha*) compared with those of sockeye salmon (*Oncorhynchus nerka*). Can. J. Zool. **84**(1): 88–97. doi:10.1139/z05-181.

Magnuson, J.J., Crowder, L.B., and Medvick, P.A. 1979. Temperature as an ecological resource. Am. Zool. **19**: 331–343.

Major, R.L., and Mighell, J.L. 1967. Influence of Rocky Reach Dam and the temperature of the Okanogan River on the upstream migration of sockeye salmon. Fish. Bull. (Wash., D C.), **66**: 131–147.

Mann, R., and Peery, C. 2005. Effects of water temperature exposure on spawning success and developing gametes of migrating anadromous fish – 2004. Progress Report, University of Idaho, Moscow, Idaho.

McPhail, J.D., and Lindsey, C.C. 1986. Zoogeography of the freshwater fishes of Cascadia (the Columbia system and rivers north to the Stikine). *In* The zoogeography of North American freshwater fishes. *Edited by* C.H. Hocutt and E.O. Wiley. John Wiley & Sons, New York. pp. 615–638.

Myers, J.M., Kope, R.G., Bryant, G.J., Teel, D., Lierheimer, L.J., Wainwright, T.C., Grant, W.S., Waknitz, F.W., Neely, K., Lindley, S.T., and Waples, R.S. 1998. Status review of chinook salmon from Washington, Idaho, Oregon, and California. NOAA Tech. Memo. NMFS-NWFSC-35. NOAA, Washington, D.C.

National Marine Fisheries Service. 1997. Endangered and threatened species: listing of several evolutionarily significant units (ESUs) of West Coast steelhead. Fed. Regist. **62**(159): 43937–43954.

Naughton, G.P., Caudill, C.C., Keefer, M.L., Bjornn, T.C., Stuehrenberg, L.C., and Peery, C.A. 2005. Late-season mortality during migration of radio-tagged adult sockeye salmon (*Oncorhynchus nerka*) in the Columbia River. Can. J. Fish. Aquat. Sci. **62**(1): 30–47. doi:10.1139/f04-147.

Newell, J.C., and Quinn, T.P. 2005. Behavioral thermoregulation by maturing adult sockeye salmon (*Oncorhynchus nerka*) in a stratified lake prior to spawning. Can. J. Zool. **83**(9): 1232–1239. doi:10.1139/z05-113.

Pankhurst, N.W., Purser, G.J., Kraak, G.V.D., Thomas, P.M., and Forteath, G.N.R. 1996. Effect of holding temperature on ovulation, egg fertility, plasma levels of reproductive hormones and in vitro ovarian steroidogenesis in the rainbow trout *Oncorhynchus mykiss*. Aquaculture, **146**(3–4): 277–290. doi:10.1016/S0044-8486(96)01374-9.

Perry, A.L., Low, P.J., Ellis, J.R., and Reynolds, J.D. 2005. Climate change and distribution shifts in marine fishes. Science, **308**(5730): 1912–1915. doi:10.1126/science.1111322. PMID:15890845.

Pörtner, H.O., and Knust, R. 2007. Climate change affects marine fishes through the oxygen limitation of thermal tolerance. Science, **315**(5808): 95–97. doi:10.1126/science.1135471.

Quinn, T.P. 2005. The behavior and ecology of Pacific salmon and trout. American Fisheries Society, Bethesda, Md.

Quinn, T.P., Hodgson, S., and Peven, C. 1997. Temperature, flow, and the migration of adult sockeye salmon (*Oncorhynchus nerka*) in the Columbia River. Can. J. Fish. Aquat. Sci. **54**(6): 1349–1360. doi:10.1139/cjfas-54-6-1349.

Quinn, T.P., Unwin, M.J., and Kinnison, M.T. 2000. Evolution of temporal isolation in the wild: genetic divergence in timing of migration and breeding by introduced chinook salmon populations. Evolution, **54**(4): 1372–1385. PMID:11005303.

Reynolds, W.W., and Casterlin, M.E. 1979. Behavioral thermoregulation and the "final preferendum" paradigm. Am. Zool. **19**: 211–224.

Robards, M.D., and Quinn, T.P. 2002. The migratory timing of adult summer-run steelhead in the Columbia River over six decades of environmental change. Trans. Am. Fish. Soc. **131**(3): 523–536. doi:10.1577/1548-8659(2002)131<0523:TMTOAS>2.0.CO;2.

Robertson, B.A., and Hutto, R.L. 2006. A framework for understanding ecological traps and an evaluation of existing evidence. Ecology, **87**(5): 1075–1085. doi:10.1890/0012-9658(2006)87[1075:AFFUET]2.0.CO;2. PMID:16761584.

Sauter, S.T., Crawshaw, L.I., and Maule, A.G. 2001. Behavioural thermoregulation by juvenile spring and fall chinook salmon, *Oncorhynchus tshawytscha*, during smoltification. Environ. Biol. Fishes, **61**(3): 295–304. doi:10.1023/A:1010849019677.

Schaefer, J.F., Marsh-Matthews, E., Spooner, D.E., Gido, K.B., and Matthews, W.J. 2003. Effects of barriers and thermal refugia on local movement of the threatened leopard darter, *Percina pantherina*. Environ. Biol. Fishes, **66**(4): 391–400. doi:10.1023/A:1023906424075.

Schlaepfer, M.A., Runge, M.C., and Sherman, P.W. 2002. Ecological and evolutionary traps. Trends Ecol. Evol. **17**(10): 474–480. doi:10.1016/S0169-5347(02)02580-6.

Sutton, R.J., Deas, M.L., Tanaka, S.K., Soto, T., and Corum, R.A. 2007. Salmonid observations at a Klamath River thermal refuge under various hydrological and meteorological conditions. River Res. Appl. **23**(7): 775–785. doi:10.1002/rra.1026.

Tanaka, H., Takagi, Y., and Naito, Y. 2000. Behavioural thermoregulation of chum salmon during homing migration in coastal waters. J. Exp. Biol. **203**(Pt. 12): 1825–1833. PMID:10821740.

Torgersen, C.E., Price, D.M., Li, H.W., and McIntosh, B.A. 1999. Multiscale thermal refugia and stream habitat associations of chinook salmon in northeastern Oregon. Ecol. Appl. **9**(1): 301–319. doi:10.1890/1051-0761(1999)009[0301:MTRASH]2.0.CO;2.

Wagner, G.N., Hinch, S.G., Kuchel, L.J., Lotto, A., Jones, S.R.M., Patterson, D.A., Macdonald, J.S., Van Der Kraak, G., Shrimpton, M., English, K.K., Larsson, S., Cooke, S.J., Healey, M.C., and Farrell, A.P. 2005. Metabolic rates and swimming performance of adult Fraser River sockeye salmon (*Oncorhynchus nerka*) after a controlled infection with *Parvicapsula minibicornis*. Can. J. Fish. Aquat. Sci. **62**(9): 2124–2133. doi:10.1139/f05-126.

Waples, R.S., Teel, D.J., Myers, J.M., and Marshall, A.R. 2004. Life-history divergence in Chinook salmon: historic contingency and parallel evolution. Evolution, **58**(2): 386–403. doi:10.1554/03-323. PMID:15068355.

Waples, R.S., Pess, G.R., and Beechie, T. 2008. Evolutionary history of Pacific salmon in dynamic environments. Evol. Appl. **1**(2): 189–206. doi:10.1111/j.1752-4571.2008.00023.x.

Wilbur, H.M., and Rudolf, V.H.W. 2006. Life-history evolution in uncertain environments: bet hedging in time. Am. Nat. **168**(3): 398–411. doi:10.1086/506258. PMID:16947114.

Winans, G.A., Paquin, M.M., Van Doornik, D.M., Baker, B.M., Thornton, P., Rawding, D., Marshall, A., Moran, P., and Kalinowski, S. 2004. Genetic stock identification of steelhead in the Columbia River basin: an evaluation of different molecular markers. N. Am. J. Fish. Manag. **24**(2): 672–685. doi:10.1577/M03-052.1.

Light-dependent predation by the invertebrate planktivore *Bythotrephes longimanus*

Kevin L. Pangle and Scott D. Peacor

Abstract: We evaluated predation by the invasive invertebrate planktivore *Bythotrephes longimanus* on a Lake Michigan prey assemblage as a function of light intensity. *Daphnia mendotae* was the only prey type significantly reduced and light intensity strongly affected this reduction. Specifically, *Bythotrephes* consumption of *D. mendotae* was not detected under low light intensity (<1 $\mu mol \cdot m^{-2} \cdot s^{-1}$) but increased with greater light intensity and leveled off under high light intensity (>100 $\mu mol \cdot m^{-2} \cdot s^{-1}$) at which point *Bythotrephes* ingestion rate was 2.3 *Daphnia* per hour. These results indicate that *Bythotrephes* predation is more sensitive to light than previously thought, a discrepancy that can be explained after considering the ability of *D. mendotae* to detect *Bythotrephes*' hydromechanic disturbance. The observed effect of light intensity on *Bythotrephes* predation is more like that of planktivorous fish than that of other previously studied invertebrate planktivores. Our findings elucidate the role that *Bythotrephes* plays in the food web and provide a novel explanation for its tendency to invade lakes of high water clarity. The importance of light-dependent predation found here may extend to other visually oriented predatory cladocerans.

Résumé : Nous évaluons la prédation par l'invertébré envahissant planctonophage *Bythotrephes longimanus* sur un ensemble de proies du lac Michigan en fonction de l'intensité lumineuse. *Daphnia mendotae* est le seul type de proie à subir une réduction significative et l'intensité lumineuse affecte fortement cette réduction. En particulier, on ne décèle pas de consommation de *D. mendotae* par *Bythotrephes* aux faibles intensités lumineuses (<1 $\mu mol \cdot m^{-2} \cdot s^{-1}$); la consommation augmente cependant aux intensités lumineuses plus élevées et atteint un plateau aux fortes intensités lumineuses (>100 $\mu mol \cdot m^{-2} \cdot s^{-1}$) et à ce point, le taux d'ingestion de *Bythotrephes* est de 2,3 *Daphnia* par heure. Ces résultats indiquent que la prédation de *Bythotrephes* est plus sensible à la lumière qu'on ne le croyait antérieurement, un écart qui peut s'expliquer si l'on tient compte de la capacité de *D. mendotae* à détecter la perturbation hydraulique causée par *Bythotrephes*. L'effet de l'intensité lumineuse observé sur la prédation chez *Bythotrephes* ressemble plus à celui qui se produit chez les poissons planctonophages que chez les autres invertébrés planctonophages étudiés. Nos observations mettent en lumière le rôle joué par *Bythotrephes* dans le réseau alimentaire et apportent une explication inédite à la tendance qu'a *Bythotrephes* à envahir les lacs à eau très claire. L'importance de la prédation dépendante de la lumière s'applique peut-être aussi à d'autres cladocères prédateurs à orientation visuelle.

[Traduit par la Rédaction]

Introduction

Light can strongly influence the composition and dynamics of communities in aquatic systems (Interlandi and Kilham 2001; Wissel et al. 2003; Sørnes and Aksnes 2006). One mechanism underlying this effect relates to the role that light plays in predator–prey interactions (Aksnes 2007). For example, some planktivores have consumption rates that are order-of-magnitudes greater in lit environments than in the dark because they rely on visual cues to detect prey (Ali 1959). Such predation pressure can drive visually conspicuous prey to extirpation (Brooks and Dodson 1965) and shift habitat use of remaining prey (Clark and Levy 1988; De Meester et al. 1998), both having potentially strong indirect effects on aquatic communities (Carpenter and Kitchell 1993).

Since planktivores can play a dominant role in aquatic communities, the potential consequences of the invasive predatory cladoceran *Bythotrephes longimanus* in the Laurentian Great lakes and surrounding inland lakes have received much attention (Boudreau and Yan 2003; Barbiero and Tuchman 2004; Strecker et al. 2006). Since its arrival in the Great Lakes two decades ago, *Bythotrephes* has been implicated in the extirpation and reduction in density of several zooplankton species (Lehman and Cáceres 1993; Yan et

Received 6 October 2008. Accepted 17 July 2009. Published on the NRC Research Press Web site at cjfas.nrc.ca on 13 October 2009.
J20808

Paper handled by Associate Editor Charles Ramcharan.

K.L. Pangle.[1,2] Department of Fisheries and Wildlife, Michigan State University, 13 Natural Resources Building, East Lansing, MI 48824-1222, USA.
S.D. Peacor. Department of Fisheries and Wildlife, Michigan State University, 13 Natural Resources Building, East Lansing, MI 48824-1222, USA; National Oceanic and Atmospheric Administration, Great Lakes Environmental Research Laboratory, 2205 Commonwealth Boulevard, Ann Arbor, MI 48105-2945, USA.

[1] Corresponding author (e-mail: pangle.3@osu.edu).
[2] Present address: Aquatic Ecology Laboratory, The Ohio State University, 1314 Kinnear Road, Columbus, OH 43212-1156, USA.

Can. J. Fish. Aquat. Sci. **66**: 1748–1757 (2009) doi:10.1139/F09-133 Published by NRC Research Press

al. 2002). This disruption to pelagic food webs can have indirect consequences on other organisms, including fish (Hoffman et al. 2001) and rotifers (Hovius et al. 2007). Understanding the long-term effects of *Bythotrephes* will require continued monitoring (Neilson et al. 2003) and a better understanding of the mechanisms governing its effect (Schulz and Yurista 1999; Boudreau and Yan 2003).

Muirhead and Sprules (2003) showed that *Bythotrephes*' ability to detect prey increased with increased light intensity using experiments that measured the response of tethered *Bythotrephes* to prey. This type of prey detection is different from that associated with more commonly studied invertebrate planktivores, such as *Chaoborus* spp. and predatory copepods, which depend primarily on hydromechanical cues for tactile detection of prey. In confirmation of the importance of light, *Bythotrephes* generally inhabit the most lit portions (i.e., epi- and metalimnion) of the water column (Evans 1988; Lehman and Cáceres 1993), and their depth selection is best explained by a trade-off between risk from planktivorous fish and access to sufficient light to feed effectively (Young and Yan 2008). Further, field surveys (Lehman and Cáceres 1993; Pangle et al. 2007) and laboratory experiments (Pangle and Peacor 2006) indicate that *Bythotrephes* induce a strong downward migration in prey during the day but not at night. Such behavioral responses are presumably an adaptive response to reduce predation risk associated with light intensity (reviewed in DeMeester et al. 1998).

Despite its importance to accurately quantifying and modeling *Bythotrephes* predation rate as a function of time and among systems, the functional relationship between *Bythotrephes* predation and light intensity is still not well understood. To our knowledge, there has not been a study that has experimentally measured predation rate of *Bythotrephes* at different light intensities. This gap in knowledge is also true for predatory cladocerans in general, despite their dominance in many lakes (Manca et al. 2000; Pichlová and Brandl 2003; McNaught et al. 2004). Further, when quantifying *Bythotrephes* predation rate using encounter models (Muirhead and Sprules 2003), *Bythotrephes* is predicted to consume prey even in the absence of light; however, we found that *Bythotrephes* predation rates were below detection limits in an experiment using low light intensity (<0.1 μmol·m^{-2}·s^{-1}; K.L. Pangle, unpublished data). The goal of this study was to evaluate the effect of light intensity on *Bythotrephes* predation using experiments designed to encompass the variation of light intensity and prey observed in nature. Our findings will improve predictions of *Bythotrephes* influence on pelagic communities across its current and expanding geographical range.

Materials and methods

We conducted two separate predation experiments in which *Bythotrephes* were incubated with prey at different light intensities, one occurring on 1 September 2005 and the other on 13 October 2005. Each experiment had three light intensity treatments, which we labeled high, mid, and low for Experiment 1 and mid, low, and lowest for Experiment 2 (Table 1). The second experiment explored a light intensity gradient lower than the first gradient; the lowest light intensity was 30 times lower than the low light intensity treatment in the first experiment and the low and mid treatments approximated those in the first experiment (Table 1). The labels for the different treatments were chosen to cover a range from lowest to high, with the names common to the two experiments (i.e., mid and low) describing nearly equivalent light levels.

Table 1. Summary of the different *Bythotrephes* densities and light intensities used for each treatment in Experiments 1 and 2.

Light treatment	*Bythotrephes* per bottle	Light intensity (μmol·m^{-2}·s^{-1}) Minimum	Mean	Maximum
Experiment 1				
High	1	55	170	397
Mid	1	8	25	60
Low	3	1	3	8
Control	0	55	170	397
Experiment 2				
Mid	1	8	22	71
Low	3	1	3	11
Lowest	3	0.02	0.06	0.21
Control	0	8	22	71

The prey consisted of a natural assemblage of zooplankton to make our results most applicable to predation occurring in natural systems (Colton 1987). For both experiments, 4 L glass bottles containing *Bythotrephes* and prey were submerged in an incubation chamber and predation rate was estimated by comparing the final density of zooplankton in bottles that contained *Bythotrephes* with that in control bottles lacking *Bythotrephes*. To manipulate light intensity among treatments, bottles were wrapped with varying layers of neutral-density vinyl screening to reduce the fraction of light entering the bottle during the experiment. We designed the experiments so that the loss of zooplankton due to *Bythotrephes* predation would be kept low enough to avoid severe prey depletion and high enough to still be detectable statistically (Vanderploeg et al. 1982; Båmstedt et al. 2000). Zooplankton densities were also chosen to be within a range observed in the field (K.L. Pangle, unpublished data).

Our incubator chamber allowed for 36 bottles per experiment. Consequently, we decided to only have one control treatment using the highest light intensity of each experiment (i.e., the high light intensity for Experiment 1 and the mid light intensity for Experiment 2 (Table 1)), thus allowing for more replicates of each treatment. We choose to have the single control in the highest light intensity treatment because it is in this treatment that the potential for prey loss is highest in the absence of *Bythotrephes* because predation rate is likely greatest from other predators in the community sampled (e.g., *Epischura lacustris*, *Polyphemus pediculus*, and *Leptodora kindtii*), which may also display light-dependent predation (Young and Taylor 1987). While we expected minor prey loss in the absence of *Bythotrephes*, we believe that our use of a high light intensity control would, if anything, lead to underestimates of the effects of light intensity on *Bythotrephes* predation rates and thus is conservative in the context of this experiment.

On the day of each experiment, live *Bythotrephes* and zooplankton prey were obtained from Lake Michigan at a site 5 km west of Muskegon, Michigan (43°11′29″N, 86°25′92″W; bottom depth = 45 m). Prior to the initiation of each experiment, approximately equal densities of zooplankton were added to each *Bythotrephes* treatment bottle (27 bottles) and each control bottle (nine bottles). An additional 18 samples of zooplankton were also taken using the same technique and used to assess initial zooplankton densities. At the start of each experiment, *Bythotrephes* were added into *Bythotrephes* treatment bottles (27 bottles total), while control treatment bottles received no *Bythotrephes*. We anticipated lower predation rates as light intensity decreased and therefore added more *Bythotrephes* to treatments with lower light (Table 1).

Bythotrephes were collected by towing a 1 m diameter, 500 μm mesh plankton net equipped with a 4 L collection bottle from 25 m depth to the surface. Captured *Bythotrephes* were immediately transferred into 15 mL vials (one individual per vial) that were filled with lake water that had been passed through a 64 μm filter to remove all zooplankton prey. To reduce variability among *Bythotrephes*, we separated individuals by instar and used individuals of the second instar in the experiments (mean individual weight in both experiments was 0.3 mg dry weight). The experiment started when *Bythotrephes* were poured from the vials into the experimental bottles.

Zooplankton prey were collected using a 0.5 m diameter, 64 μm mesh plankton net equipped with a 1 L collection bottle at the cod end towed over the same area. Captured zooplankton prey were gently poured into a 30 L aquarium that was filled with filtered lake water. Cetyl alcohol was added to the aquarium to prevent zooplankton from adhering to the surface of the water (Desmarais 1997). Zooplankton prey were added to the experimental bottles by taking 10 mL subsamples of water from the center of the aquarium and releasing subsamples into the bottles. We took subsamples by lowering an 8 mm diameter cylinder into the water until it touched the bottom of the aquarium, at which point we capped the top of the cylinder to retain the water and organisms inside. This subsampling approach allowed us to capture organisms regardless of their vertical position in the aquarium and also did not require producing a suction field that could potentially be sensed and avoided by some zooplankton. Subsamples were transferred to bottles according to a randomized-block design, a technique that minimized the variation in zooplankton density between bottles, and one subsample was added to each bottle (both the thirty-six 4 L experimental bottles and the eighteen 0.5 L sample bottles for estimates of initial zooplankton densities) sequentially until each bottle received 16 subsamples in total. Initial zooplankton density samples were preserved with buffered sugar–formalin solution.

The incubation chamber in which experiments were carried out was 2000 L in size and maintained an environment similar to that observed in Lake Michigan. The incubation chamber was illuminated with natural sun. In addition to manipulating light as it entered individual bottles, light entering the chamber passed through theatrical gels (Peacock Blue Roscolux) (Rosco Laboratories Inc., Stamford, Connecticut) that mimicked the pelagic light spectra and neutral-density vinyl screening that reduced light intensity (Lohrenz et al. 2004). Ambient light intensity was measured using a 4 pi sensor over the course of the experiments, and the number of neutral vinyl layers was changed as sunlight intensity changed. In comparing light intensities maintained during the experiments (Table 1) with those observed in Lake Michigan's water column, the mid and high light intensity treatments would be typical at the thermocline and at the center of epilimnion, respectively, on a summer day, whereas the lowest light intensity treatment would be typical at the surface on a moonlit night (K.L. Pangle, unpublished data). Water temperature inside the incubation chamber was kept at a level typical of the Lake Michigan metalimnion (16 °C) using an external water chiller.

Bottles were attached to a motorized cage located inside the incubation chamber that rotated the bottles end-over-end during the experiment at a constant rate (approximately 0.5 rpm). The bottles were rotated to maintain spatial homogeneity of zooplankton, a commonly used method in invertebrate predation (e.g., Wong 1981; McClatchie and Boyd 1983; Greene and Landry 1988) and one previously used to evaluate *Bythotrephes* predation (Vanderploeg et al. 1993). Both experiments ran for 7 h from 1300 to 2000 EDT. The time length of our predation experiments represented a trade-off between allowing time for detectable predation to occur and ending the experiment before prey depletion became so great that it would confound our estimates of clearance and ingestion rates (Båmstedt et al. 2000). While many recent predation studies have used shorter experimental durations (10 min to 4 h) (e.g., Packard 2001; Koski and Johnson 2002; Fulford et al. 2006), it was necessary to extend the length of our experiments given the relatively low predation rates observed for *Bythotrephes* (Vanderploeg et al. 1993).

At the end of each experiment, bottles were removed from the incubation chamber and organisms were immediately narcotized by adding Alka-Seltzer tablets to each bottle. Organisms were siphoned from the bottles onto a 64 μm filter and then transferred into 0.2 L bottles with buffered sugar–formalin solution. Later, all zooplankton prey and *Bythotrephes* were identified and counted using a microscope and their body lengths were measured using a drawing tube and digitizer (Roff and Hopcroft 1986). Prey were grouped into one of seven prey types including *Daphnia mendotae*, *Bosmina longirostris*, copepod nauplii, juvenile *Diaptomus* spp., adult *Diaptomus* spp., juvenile *Diacyclops thomasi*, and adult *D. thomasi*. The composition of prey types observed corresponded to the dominant prey types found in Lake Michigan, indicating that *Bythotrephes* in our experiments were exposed to a natural array of prey.

Statistical analyses and predation rate calculations

Prior to analyses of light effect, we first tested assumptions of normality and homogeneity of variance using the Wilks–Shapiro test and the Levene's test, respectively. In addition, we evaluated whether prey density was substantially different in the control bottles at the end of the experiment from what it was at the start of the experiment due to predation by other predators in the community sampled. This was done by comparing the average initial prey density based on the preserved initial samples with the average prey density in the control bottles at the end of the experiment. While the predatory copepod *Epischura lacustris* was found in two and 17 bottles in Experiments 1 and 2, respectively, its presence did not vary among treatments (one-way analysis of variance (ANOVA): both $p > 0.05$) and the prey density in initial samples and control treatments did not differ significantly (Student's t test: all $p > 0.05$) in both experiments. Other predatory cladocerans, including the invasive *Cercopagis pengoi* and the native *L. kindtii* and *P. pediculus*, were never found in either experiment. We removed one mid light intensity replicate and one low light intensity replicate in Experiment 1 and one mid light intensity replicate in Experiment 2 from the analyses because an individual *Bythotrephes* was not found in these bottles at the end of the experiments. We never found more *Bythotrephes* than intended in the bottles.

We tested the hypothesis that light intensity led to different final densities of each zooplankton prey type using one-way ANOVAs. Because we repeated the analyses for multiple prey types, we used critical p values that were calculated following a sequential Bonferroni procedure (Benjamini and Hochberg 1995). When significant differences were found among treatments for a prey type's final density, we separated differences between specific treatments using Tukey's honestly significant difference (HSD) tests (Zar 1999). We then calculated estimated clearance rates (F) (litres per hour per predator) and ingestion rates (I) (prey per hour per predator) for prey types that were significantly depleted and (*i*) tested for variation in clearance and ingestion rates for each experiment by one-way ANOVA and (*ii*) combined data from the two experiments to estimate a relationship between ingestion rate and light intensity. Clearance rate was calculated as

$$(1)\qquad F = \frac{-\ln(N_f/\widehat{N}_i)V}{tP}$$

where N_f is final prey density (individuals per litre) in a *Bythotrephes* bottle, $\widehat{N}_i$ is the average final prey density (individuals per litre) in the control bottles, V is the volume of the bottle (litres), t is the duration of the experiment (hours), and P is the number of *Bythotrephes* in the bottle (Båmstedt et al. 2000). Ingestion rate was calculated as

$$(2)\qquad I = F\widehat{N}_i$$

We used standard error propagation techniques (Meyer 1975) to calculate standard errors associated with mean clearance and ingestion rates of each *Bythotrephes* treatment. Propagated standard errors are reported with treatment means and used in a subsequent analysis but not included in ANOVAs of clearance and ingestion rates because the error associated with the initial prey density was common among *Bythotrephes* treatments.

We pooled estimates of ingestion rates from both experiments to better describe *Bythotrephes* consumption over a broad range of light intensity (0.06–170 $\mu\text{mol}\cdot\text{m}^{-2}\cdot\text{s}^{-1}$). Using weighted nonlinear least squares regression, the relationship between light intensity and *Bythotrephes* ingestion rate was fit to the logistic model

$$(3)\qquad I = \frac{a}{1 + (L/b)^c}$$

where a, b, and c are fitted parameters representing the maximum ingestion rate, the light intensity at which ingestion rate is half of its maximum, and the exponential rate of increase, respectively, and L is light intensity (micromoles per square metre per second). Data used for the regression were treatment means weighted with their respective propagated standard error (Gurevitch and Hedges 1999). We chose this logistic model because, for visual predators, ingestion rate is often constant over low light intensities and then increases to an asymptote as light intensity increases (Fraser and Metcalfe 1997). We chose to use ingestion rate rather than clearance rate in this analysis because the prey densities, specifically that of *D. mendotae*, used in both experiments were greater than that at which *Bythotrephes* predation is saturated at high light intensities (K.L. Pangle, unpublished data.).

Results

In both experiments, *D. mendotae* density was significantly reduced (Experiment 1: $F_{[3,30]} = 21.04$, $p < 0.01$; Experiment 2: $F_{[3,31]} = 3.64$, $p = 0.02$) (Fig. 1). In Experiment 1, *Bythotrephes* clearance and ingestion rates of *D. mendotae* did not differ significantly between the mid and high light intensity treatments; however, rates in these treatments were significantly greater than those in the low light intensity treatment (Table 2), with values approximately four times greater in the highest than in the lowest light intensity treatment. The other six prey types were not significantly affected by *Bythotrephes*.

In Experiment 2, *Bythotrephes* clearance and ingestion rates of *D. mendotae* were significantly greater in the mid light intensity treatment than those in the low and lowest light intensity treatments (Table 2). An additional analysis using data from only the lowest light intensity treatment showed that clearance and ingestion rates at this light intensity did not differ significantly from zero (Student's t test: $t_{[8]} = 0.50$, $p = 0.63$ and $t_{[8]} = 0.13$, $p = 0.90$, respectively) and had upper bounds of 0.05 $\text{L}\cdot\text{h}^{-1}$ and 0.31 *Daphnia*$\cdot\text{h}^{-1}$ in 95% confidence intervals.

We pooled ingestion rate data found in Experiments 1 and 2 to examine the functional relationship between *Bythotrephes* consumption of *D. mendotae* and light intensity. The combined data fit a logistic model well ($r^2 = 0.98$) (Fig. 2) with a half-saturation point at 5.97 $\mu\text{mol}\cdot\text{m}^{-2}\cdot\text{s}^{-1}$ and maximum ingestion rate at 2.35 *Daphnia*$\cdot\text{h}^{-1}$.

Discussion

Light strongly influenced the predation rate of the invasive planktivore *Bythotrephes* on the cladoceran *D. mendotae*, a prey type shown to be highly selected for by *Bythotrephes* (Vanderploeg et al. 1993; Lehman and Branstrator 1995; Dumitru et al. 2001). Consumption of *Daphnia* was not detectable under low light intensity (<1 $\mu\text{mol}\cdot\text{m}^{-2}\cdot\text{s}^{-1}$) but increased with greater light intensity and eventually leveled off at high light intensity (>100 $\mu\text{mol}\cdot\text{m}^{-2}\cdot\text{s}^{-1}$). The steepness of the increase in predation rate at intermediate light intensities is difficult to ascertain given our experimental design;

Fig. 1. Densities of different prey types in *Bythotrephes* and control treatments in (*a*) Experiment 1 and (*b*) Experiment 2. In each experiment, bottles were exposed to different light intensities and received zero, one, or three *Bythotrephes* depending on the treatment (see the legends on the figure). Bars are means with standard errors and reflect total, not per capita, predator effect. Prey types included *Daphnia mendotae* (D.m.), *Bosmina longirostris* (B.l.), copepod nauplii, immature *Diaptomus* (I. Diap.), adult *Diaptomus* (A. Diap.), immature *Diacyclops thomasi* (I. Diac.), and adult *Diacyclops thomasi* (A. Diac.). Asterisks denote significant differences.

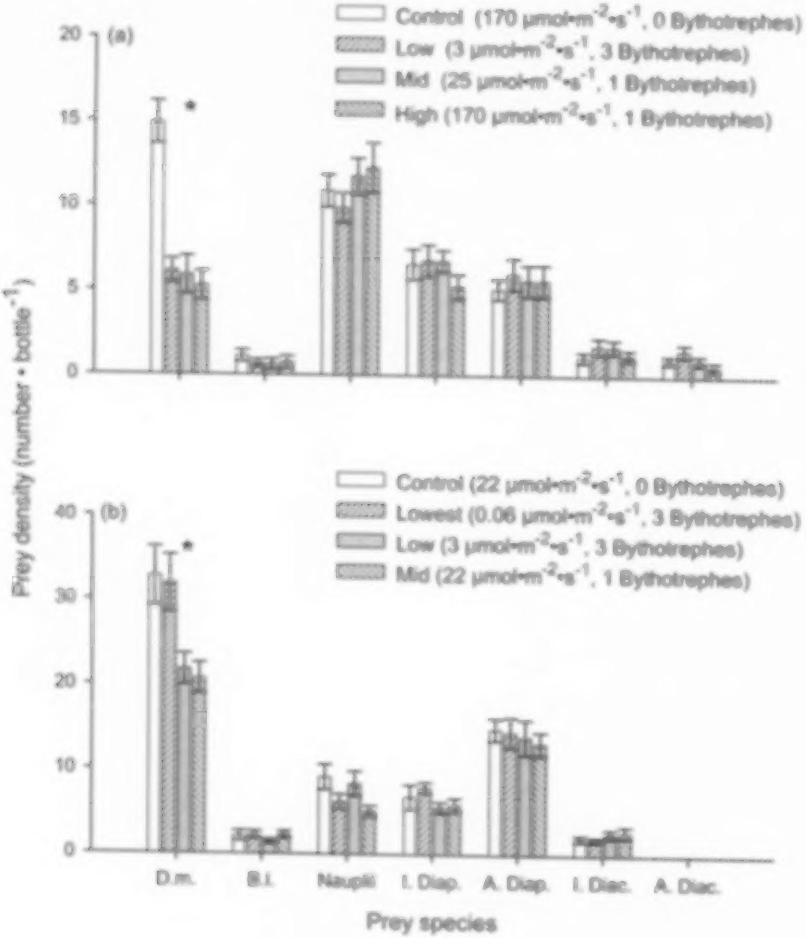

however, the increase depicted here is similar to the increase that Muirhead and Sprules (2003) found for the reaction distance of *Bythotrephes* to prey over a similar range of light intensities.

We did not observe consumption of prey other than *D. mendotae* at any light intensity. Our ability to detect predation for some of these prey may have been limited due to their low density, particularly *B. longirostris*, which is another preferred prey of *Bythotrephes* (Vanderploeg et al. 1993). In addition, *Bythotrephes* is known to have higher selectivity for *Daphnia* spp. than for juvenile and adult copepods (Vanderploeg et al. 1993), which may account for the lack of predation on these copepods in our experiments. Although the influence of light on predation by *Bythotrephes* is likely general to all instars (e.g., all instars are equipped with a large eye), our decision to use only second-instar *Bythotrephes* for the experiments may have played a role in prey selection as well. Burkhardt and Lehman (1994) showed that *Bythotrephes* were more capable at handling large prey items as they increased in instar. Further, experimental evidence suggests that selectivity for small prey items, such as copepod nauplii, is greater for first-instar *Bythotrephes* than for older instars (K.L. Pangle, unpublished data), thus providing an explanation for the lack of predation on copepod nauplii during our experiments.

Our data indicate that *Bythotrephes* predation rates on *D. mendotae* are negligibly low at very low light levels. A potentially confounding factor of the lower predation rates observed at the lower light intensity treatments is that the higher number of *Bythotrephes* used per bottle at lower light levels may have led to predator interference, particularly because *Bythotrephes* is cannibalistic (Schulz and Yurista

Table 2. *Bythotrephes* clearance rates and ingestion rates of *Daphnia mendotae* observed in Experiments 1 and 2 at different intensities (description of light intensities given in Table 1).

Variable	Light intensity treatment			
	Lowest	Low	Mid	High
Experiment 1				
Clearance rate (L·h^{-1})		0.17±0.03a	0.61±0.11b	0.62±0.09b
Ingestion rate (number·h^{-1})		0.62±0.10a	2.28±0.40b	2.30±0.34b
Experiment 2				
Clearance rate (L·h^{-1})	0.02±0.02a	0.08±0.02a	0.28±0.07b	
Ingestion rate (number·h^{-1})	0.12±0.20a	0.68±0.19a	1.83±0.70b	

Note: Values are means ± propagated standard errors and were calculated using eqs. 1 and 2. Mean row values with different lowercase letters were significantly different as determined by ANOVA and Tukey's HSD tests ($p < 0.05$).

Fig. 2. Effect of light intensity on *Bythotrephes* ingestion rate. Data of ingestion rates of *Daphnia mendotae* in Experiments 1 and 2 (circles and triangles, respectively) were combined to evaluate *Bythotrephes* predation over a broad range of light intensities. Points are means with propagated standard error bars that were calculated using eqs. 1 and 2. In this analysis, the relationship between light intensity and ingestion rate was described using a logistic regression model ($y = 2.35/[1 + (x/5.97)^{-1.49}]$) shown by the fitted line.

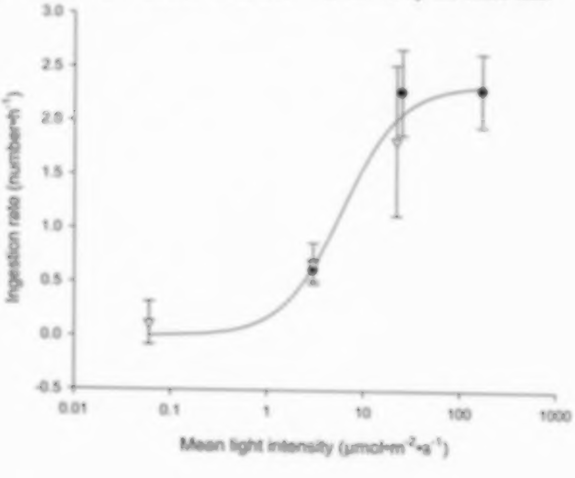

1999). We used higher *Bythotrephes* levels at low light treatments to increase our ability to measure predation at the lower light levels where we suspected that predation rates would be lower. We believe that several lines of evidence support that low light levels, and not predator interference, were responsible for the negligible predation rates. First, in Experiment 2, there was a significant difference in the final number of *Daphnia* between the lowest and low light treatments, both of which held three *Bythotrephes* per bottle; thus, the difference between treatments can be attributed to light intensity differences and not predator interference. Second, in a pilot experiment, we observed no significant predation loss in one-*Bythotrephes*-per-bottle treatments (one treatment at high and one at low prey density) that were held at low-light conditions (average 0.015 μmol·m^{-2}·s^{-1}) over a 28 h period. Lastly, predator interference could reduce predation rates, but it would unlikely reduce predation rates on a preferred prey to the negligible levels observed.

Previous studies indicate that invertebrate planktivores primarily use tactile, rather than visual, cues as the primary means to detect prey (Pastorok 1981; Kiørboe and Visser 1999). Exceptions include studies on predation by mysids (Ramcharan and Sprules 1986) and notonectids (Dieguez and Gilbert 2003); however, in both of these cases, these invertebrate planktivores still relied strongly on tactile means to detect prey and, in contrast with *Bythotrephes*, their feeding was not substantially reduced in total darkness. Thus, the strong dependence of *Bythotrephes* on light intensity found here is unique among known aquatic invertebrates and is comparable with planktivorous fish predation, which is often strongly affected by light intensity. Indeed, zooplankton prey have evolved behavior known as diel vertical migration to avoid overlap with fish in areas and at times of high light intensity (DeMeester et al. 1998). Laboratory experiments (Pangle and Peacor 2006) and field observations (Pangle et al. 2007) have shown that zooplankton prey also migrate vertically in the presence of *Bythotrephes*, suggesting that *Bythotrephes* may be driving selection for zooplankton to perceive its risk and respond behaviorally.

A previous laboratory study by Muirhead and Sprules (2003) that evaluated prey detection by *Bythotrephes* as a function of light also predicted that *Bythotrephes* predation rate decreased with decreasing light intensity, but the predicted light effect was less than what we found in our experiments. Their predictions were derived from a model of the rate of prey encountered by a single *Bythotrephes* given the density and swimming velocity of *Bythotrephes* and prey, and *Bythotrephes* reaction distance, which is a function of light intensity (details of the model and its application provided in Appendix A). The model was parameterized with data from laboratory observations of tethered *Bythotrephes*' detection of prey. Given the densities in Experiment 2, the number of *D. mendotae* encountered by *Bythotrephes* is predicted by the model to decline 29.1% as light intensity changes from the low to the lowest light intensity treatment (Appendix A); in contrast, the observed mean decline in ingestion rate was actually 100%.

The discrepancy between our results and the model predictions may result from the ability of *D. mendotae* to detect *Bythotrephes*, which is not included in the model. Zooplankton prey are known to avoid predators through hydromechanical signals prior to an attack (Heath 1993; Viitasalo et al. 1998) such that the ability of prey to detect predators is not dependent on light. To test the role of predator detection by *Daphnia* on *Bythotrephes* predation rate at low light, we can apply models developed by Tiselius and Jonsson (1990) parameterized with data from our study and other studies of *Daphnia* and *Bythotrephes* (Brewer et al. 1999; Muirhead and Sprules 2003). These models predict the hydromechanical signals produced by *Bythotrephes* and the distance from *Bythotrephes* that *D. mendotae* would be able to detect these signals (details of the model and its application provided in Appendix B). Results of the hydromechanical models show that the predicted distance at which *Bythotrephes* is able to detect prey is less than the predicted distance at which *D. mendotae* can detect *Bythotrephes* at the magnitude of the lowest light intensity treatment, but *Bythotrephes*' detection distance becomes greater that *D. mendotae*'s detection distance at the magnitude of the low light intensity treatment. The model predictions suggest that *D. mendotae* may be able to perceive *Bythotrephes* before being attacked at light intensities less than 2.7 $\mu mol \cdot m^{-2} \cdot s^{-1}$, which could account for the dramatic decrease in predation observed and the discrepancy with the predation rate prediction by the Muirhead and Sprules (2003) model. These idealized models provide a qualitative explanation for the patterns observed in our study; however, more research is needed on prey detection ability and how it influences predation by *Bythotrephes* on *D. mendotae*. For example, *Daphnia* spp. are more likely to perform escape behavior as light intensity increases (Pijanowska and Kowalczewski 1997); thus, light may influence the interaction between *Bythotrephes* and *Daphnia* beyond expanding *Bythotrephes*' reaction distance. Building on previous studies that have emphasized the importance of prey escape capabilities (Drenner et al. 1978; Heath 1993; Viitasalo et al. 1998), our results suggest that light-mediated changes to the relative ability of prey and predator to detect each other can substantially affect predation rate.

Light-dependent predation has implications for predicting *Bythotrephes*' impact on zooplankton communities. Our results suggest that *Bythotrephes*' effect could be strongly influenced by the depth and time at which *Bythotrephes* and zooplankton overlap. For example, there are periods in Lake Michigan in which the only overlap in the vertical distribution of *D. mendotae* and *Bythotrephes* occurs at night (Pangle et al. 2007); thus, *Bythotrephes*' ability to consume *D. mendotae* would be greatly reduced. *Bythotrephes* is also known to migrate downward itself when facing fish predation (Straile and Halbich 2000). In lakes with high fish predation, predation by *Bythotrephes* that are forced to inhabit deeper, darker regions of the water column would also be greatly reduced (Lehman and Cáceres 1993; Palmer et al. 2001).

Given the potential impact of *Bythotrephes* on lake ecosystems (Yan et al. 2001; Barbiero and Tuchman 2004), the spread of *Bythotrephes* is of concern to lake management of lake ecosystems. Understanding factors controlling the establishment of *Bythotrephes* in a lake can aid in identifying lakes on which to focus management efforts (Muirhead and MacIsaac 2005). Our results suggest that the success of *Bythotrephes*, in terms of its predation, would increase in lakes with increased water transparency; indeed, this relationship has been observed in nature. MacIsaac et al. (2000) found that high Secchi depth values, an indication of high water transparency, were a strong predictor of *Bythotrephes* presence in lakes within *Bythotrephes*' native range. In addition, Branstrator et al. (2006) reported a similar finding in Minnesota lakes that were recently invaded by *Bythotrephes*. These studies propose different explanations for why *Bythotrephes* were found more often in clear lakes. MacIsaac et al. (2000) suggested that high transparency was indicative of systems with low productivity that could not support high densities of planktivorous fish, thereby providing *Bythotrephes* a release from both a predator and a competitor. Branstrator et al. (2006) suggested that high transparency was not the primary reason for the establishment of *Bythotrephes* but rather an indicator that the systems also have a warm, low-light middepth water layer. This layer may be beneficial to *Bythotrephes* populations by acting as a visual refuge from warmwater fish and a thermal refuge from coldwater fish (Yan et al. 2001). Based on our results, we propose that light-dependent predation by *Bythotrephes* should be added to the list of potential factors contributing to its establishment in clear lakes.

There is evidence that the type of predation observed in this study may be general to other predatory cladocerans. An experiment using *P. pediculus* found that its predation varied with light intensity and was not detectable in the absence of light (A.T. Packard, Department of Biology, Saint Joseph's College of Maine, 278 Whites Bridge Road, Standish, ME 04084, USA, unpublished data). A large, complex eye like the one that *Bythotrephes* and *Polyphemus* use to detect prey is a trait common to *C. pengoi*, *L. kindtii*, and ponids (Rivier 1998). The maintenance of a large eye is costly because it makes predatory cladocerans more visible to fish (Branstrator and Holl 2000). This large cost must be associated with a large benefit, suggesting that the eye plays an important role in detecting prey. In addition, the distribution of predatory cladocerans in natural systems indicates that light influences their prey consumption, as they primarily inhabit well-lit areas, such as the littoral zone and the epi- and metalimnion of the pelagic (Palmer et al. 2001; Benoit et al. 2002). Future studies of light-dependent predation in other predatory cladocerans may aid in better understanding the role that these organisms play in aquatic communities and their relative success in different systems.

Acknowledgments

We thank C. Bergeon, W. Burns, D. Donahue, K. Krieger, and J. Workman for their assistance with setting up and performing the experiments, particularly J. Workman, who devised a clever way to attach bottles to a motorized cage. We thank G. Fahnenstiel and H. Vanderploeg for lending their valuable advice and equipment to the study. We are grateful to J. Bence, G. Horst, O. Johannsson, E. Loew, J. Muirhead, O. Sarnelle, W. Pangle, the Associate Editor, and four anonymous reviewers whose comments improved this manuscript. Funding for this study was provided by the Fishery Research Program of the Great Lakes Fisheries Commission, the National Oceanic and Atmospheric Administration, the Michigan Agricultural Experiment Station, and National Science Foundation grant DEB-0089809 to E.

Werner and S.D. Peacor. This is Great Lakes Environmental Research Laboratory contribution 1525.

References

Aksnes, D.L. 2007. Evidence of visual constraints in large marine fish stocks. Limnol. Oceanogr. **52**: 198–203.

Ali, M.A. 1959. The ocular structure, retinomotor and photo-behavioral responses of juvenile Pacific salmon. Can. J. Zool. **37**(6): 965–996. doi:10.1139/z59-092.

Båmstedt, U., Gifford, D.J., Irigoien, X., Atkinson, A., and Roman, M. 2000. Feeding. *In* Zooplankton methodology manual. *Edited by* R.P. Harris, P.H. Wiebe, J. Lenz, H.R. Skjoldal, and M. Huntley. Academic Press, New York. pp. 297–400.

Barbiero, R.P., and Tuchman, M.L. 2004. Changes in the crustacean communities of Lakes Michigan, Huron, and Erie following the invasion of the predatory cladoceran *Bythotrephes longimanus*. Can. J. Fish. Aquat. Sci. **61**(11): 2111–2125. doi:10.1139/f04-149.

Benjamini, Y., and Hochberg, Y. 1995. Controlling the false discovery rate: a practical and powerful approach to multiple testing. J. R. Stat. Soc. Ser. B (Methodol.), **57**: 289–300.

Benoit, H.P., Johannsson, O.E., Warner, D.M., Sprules, W.G., and Rudstram, L.G. 2002. Assessing the impact of a recent predatory invader: the population dynamics, vertical distribution, and potential prey of *Cercopagis pengoi* in Lake Ontario. Limnol. Oceanogr. **47**: 626–635.

Boudreau, S.A., and Yan, N.D. 2003. The differing crustacean zooplankton communities of Canadian Shield lakes with and without the nonindigenous zooplanktivore *Bythotrephes longimanus*. Can. J. Fish. Aquat. Sci. **60**(11): 1307–1313. doi:10.1139/f03-111.

Branstrator, D.K., and Holl, C.M. 2000. Planktivory by bluegill (*Lepomis macrochirus*) on *Leptodora kindtii* in a small North American lake. Hydrobiologia, **437**(1/3): 101–106. doi:10.1023/A:1026530201948.

Branstrator, D.K., Brown, M.E., Shannon, L.J., Thabes, M., and Heimgartner, K. 2006. Range expansion of *Bythotrephes longimanus* in North America: evaluating habitat characteristics in the spread of an exotic zooplankter. Biol. Invasions, **8**(6): 1367–1379. doi:10.1007/s10530-005-5278-7.

Brewer, M.C., Dawidowicz, P., and Dodson, S.I. 1999. Interactive effects of fish kairomones and light on *Daphnia* escape behavior. J. Plankton Res. **21**(7): 1317–1335. doi:10.1093/plankt/21.7.1317.

Brooks, J.L., and Dodson, S.I. 1965. Predation, body size, and composition of plankton. Science, **150**(3692): 28–35. doi:10.1126/science.150.3692.28.

Burkhardt, S., and Lehman, J.T. 1994. Prey consumption and predatory effects of an invertebrate predator (*Bythotrephes*: Cladocera, Cercopagidae) based on phosphorus budgets. Limnol. Oceanogr. **39**: 1007–1019.

Carpenter, S.R., and Kitchell, J.F. 1993. The trophic cascade in lakes. Cambridge University Press, Cambridge, England.

Clark, C.W., and Levy, D.A. 1988. Diel vertical migration by sockeye salmon and the antipredation window. Am. Nat. **131**(2): 271–290. doi:10.1086/284789.

Colton, T.F. 1987. Extending functional response models to include a second prey type: an experiment test. Ecology, **68**(4): 900–912. doi:10.2307/1938361.

DeMeester, L., Dawidowicz, P., van Gool, E., and Loose, C.J. 1998. Ecology and evolution of predator-induced behavior of zooplankton: depth selection behavior and diel vertical migration. *In* The ecology and evolution of induced defenses. *Edited by* R. Tollrian and C.D. Harvell. Princeton University Press, Princeton, N.J. pp. 160–177.

Desmarais, K.H. 1997. Keeping *Daphnia* out of the surface film with cetyl alcohol. J. Plankton Res. **19**(1): 149–154. doi:10.1093/plankt/19.1.149.

Dieguez, M.C., and Gilbert, J.J. 2003. Predation by *Buenoa macrotibialis* (Insecta, Hemiptera) on zooplankton: effect of light on selection and consumption on prey. J. Plankton Res. **25**(7): 759–769. doi:10.1093/plankt/25.7.759.

Drenner, R.W., Strickler, J.R., and O'Brien, W.J. 1978. Capture probability: the role of zooplankter escape in the selective feeding of planktivorous fish. J. Fish. Res. Board Can. **35**: 1370–1373.

Dumitru, C., Sprules, W.G., and Yan, N.D. 2001. Impact of *Bythotrephes longimanus* on zooplankton assemblages of Harp Lake, Canada: an assessment based on predator consumption and prey production. Freshw. Biol. **46**(2): 241–251. doi:10.1046/j.1365-2427.2001.00649.x.

Evans, M.S. 1988. *Bythotrephes cederstroemi*: its new appearance in Lake Michigan. J. Gt. Lakes Res. **14**: 234–240.

Fraser, N.H.C., and Metcalfe, N.B. 1997. The costs of becoming nocturnal: feeding efficiency in relation to light intensity in juvenile Atlantic salmon. Funct. Ecol. **11**(3): 385–391. doi:10.1046/j.1365-2435.1997.00098.x.

Fulford, R.S., Rice, J.A., Miller, T.J., Binkowski, F.P., Dettmers, J.M., and Belonger, B. 2006. Foraging selectivity by larval yellow perch (*Perca flavescens*): implications for understanding recruitment in small and large lakes. Can. J. Fish. Aquat. Sci. **63**(1): 28–42. doi:10.1139/f05-196.

Greene, C.H., and Landry, M.R. 1988. Carnivorous suspension feeding by the subarctic calanoid copepod *Neocalanus cristatus*. Can. J. Fish. Aquat. Sci. **45**(6): 1069–1074. doi:10.1139/f88-130.

Gurevitch, J., and Hedges, L.V. 1999. Statistical issues in ecological meta-analyses. Ecology, **80**: 1142–1149.

Heath, M.R. 1993. The role of escape reaction in determining the size distribution of prey captured by herring larvae. Environ. Biol. Fishes, **38**(4): 331–344. doi:10.1007/BF00007527.

Hoffman, J.C., Smith, M.E., and Lehman, J.T. 2001. Perch or plankton: top-down control of *Daphnia* by yellow perch (*Perca flavescens*) or *Bythotrephes cederstroemi* in an inland lake? Freshw. Biol. **46**(6): 759–775. doi:10.1046/j.1365-2427.2001.00716.x.

Hovius, J.T., Beisner, B.E., McCann, K.S., and Yan, N.D. 2007. Indirect food web effects of *Bythotrephes* invasion: responses by the roifer *Conochilus* in Harp Lake, Canada. Biol. Invasions, **9**(3): 233–243. doi:10.1007/s10530-006-9028-2.

Interlandi, S.J., and Kilham, S.S. 2001. Limiting resources and the regulation of diversity in phytoplankton communities. Ecology, **82**: 1270–1282.

Kiørboe, T., and Visser, A.W. 1999. Predator and prey perception in copepods due to hydromechanical signals. Mar. Ecol. Prog. Ser. **179**: 81–95. doi:10.3354/meps179081.

Koski, M.L., and Johnson, B.M. 2002. Functional response of kokanee salmon (*Oncorhynchus nerka*) to *Daphnia* at different light levels. Can. J. Fish. Aquat. Sci. **59**(4): 707–716. doi:10.1139/f02-045.

Lehman, J.T., and Branstrator, D.K. 1995. A model for growth, development, and diet selection by the invertebrate predator *Bythotrephes cederstroemi*. J. Gt. Lakes Res. **21**: 610–619.

Lehman, J.T., and Cáceres, C.E. 1993. Food-web responses to species invasion by a predatory invertebrate: *Bythotrephes* in Lake Michigan. Limnol. Oceanogr. **38**: 879–891.

Lohrenz, S.E., Fahenstiel, G.L., Millie, D.F., Schofield, O.M.E., Johengen, T., and Bergmann, T. 2004. Spring phytoplankton photosynthesis, growth, and primary production and relationships to a recurrent coastal sediment plume and river inputs in southeastern Lake Michigan. J. Geophys. Res. Oceans, **109**(C10): C10S14. doi:10.1029/2004JC002383.

MacIsaac, H.J., Ketelaars, H.A.M., Grigorovich, I.A., Ramcharan, C.W., and Yan, N.D. 2000. Modeling *Bythotrephes longimanus* invasions in the Great Lakes basin based on its European distribution. Arch. Hydrobiol. **149**: 1–21.

Manca, M., Ramoni, C., and Comoli, P. 2000. The decline of *Daphnia hyalina* in Lago Maggiore: a comparison of the population dynamics before and after oligotrophication. Aquat. Sci. **62**(2): 142–153. doi:10.1007/PL00001328.

McClatchie, S., and Boyd, C.M. 1983. Morphological study of sieve efficiencies and mandibular surfaces in the Antarctic krill, *Euphausia superba*. Can. J. Fish. Aquat. Sci. **40**: 955–967.

McNaught, A.S., Kiesling, R.L., and Ghadouani, A. 2004. Changes to zooplankton community structure following colonization of a small lake by *Leptodora kindtii*. Limnol. Oceanogr. **49**: 1239–1249.

Meyer, S.L. 1975. Data analysis for scientists and engineers. Wiley & Sons, Inc., Hoboken, N.J.

Muirhead, J.R., and MacIsaac, H.J. 2005. Development of inland lakes as hubs in an invasion network. J. Appl. Ecol. **42**(1): 80–90. doi:10.1111/j.1365-2664.2004.00988.x.

Muirhead, J., and Sprules, W.G. 2003. Reaction distance of *Bythotrephes longimanus*, encounter rate and index or prey risk for Harp Lake, Ontario. Freshw. Biol. **48**(1): 135–146. doi:10.1046/j.1365-2427.2003.00986.x.

Neilson, M.A., Painter, D.S., Warren, G., Hites, R.A., Basu, I., Weseloh, D.V.C., Whittle, D.M., Christie, G., Barbiero, R., Tuchman, M., Johannsson, O.E., Nalepa, T.F., Edsall, T.A., Fleischer, G., Bronte, C., Smith, S.B., and Baumann, P.C. 2003. Ecological monitoring for assessing the state of the nearshore and open waters of the Great Lakes. Environ. Monit. Assess. **88**(1–3): 103–117. doi:10.1023/A:1025500619900. PMID: 14570412.

Packard, A.T. 2001. Clearance rates and prey selectivity of the predaceous cladoceran *Polyphemus pediculus*. Hydrobiologia, **442**(1/3): 177–184. doi:10.1023/A:1017582323631.

Palmer, A., Stich, H.B., and Maier, G. 2001. Distribution patterns and predation risk of the coexisting cladocerans *Bythotrephes longimanus* and *Leptodora kindtii* in a large lake — Lake Constance. Hydrobiologia, **442**(1/3): 301–307. doi:10.1023/A:1017530305884.

Pangle, K.L., and Peacor, S.D. 2006. Non-lethal effect of the invasive predator *Bythotrephes longimanus* on *Daphnia mendotae*. Freshw. Biol. **51**(6): 1070–1078. doi:10.1111/j.1365-2427.2006.01555.x.

Pangle, K.L., Peacor, S.D., and Johannsson, O.E. 2007. Large nonlethal effects of an invasive invertebrate predator on zooplankton population growth rate. Ecology, **88**(2): 402–412. doi:10.1890/06-0768. PMID:17479758.

Pastorok, R.A. 1981. Prey vulnerability and size selection by *Chaoborus* larvae. Ecology, **62**(5): 1311–1324. doi:10.2307/1937295.

Pichlová, R., and Brandl, Z. 2003. Predatory impact of *Leptodora kindtii* on zooplankton community in the Slapy Reservoir. Hydrobiologia, **504**(1–3): 177–184. doi:10.1023/B:HYDR.0000008517.64246.fd.

Pijanowska, J., and Kowalczewski, A. 1997. Predators can induce swarming behavior and locomotory response in *Daphnia*. Freshw. Biol. **37**(3): 649–656. doi:10.1046/j.1365-2427.1997.00192.x.

Ramcharan, C.W., and Sprules, W.G. 1986. Visual predation in *Mysis relicta* Loven. Limnol. Oceanogr. **31**: 414–420.

Rivier, I.K. 1998. The predatory cladocera (Onychopoda: Podonidae, Polyphemoidae, Cercopagidae) and Leptodoridae of the world. Backhuys Publishers, Leiden, The Netherlands.

Roff, J.C., and Hopcroft, R.R. 1986. High-precision microcomputer based measuring system for ecological research. Can. J. Fish. Aquat. Sci. **43**: 2044–2048. doi:doi:10.1139/f86-251.

Schulz, K.L., and Yurista, P.M. 1999. Implications of an invertebrate predator's (*Bythotrephes cederstroemi*) atypical effects on a pelagic zooplankton community. Hydrobiologia, **380**(1/3): 179–193. doi:10.1023/A:1003484813672.

Sornes, T.A., and Aksnes, D.L. 2006. Concurrent temporal patterns in light absorbance and fish abundance. Mar. Ecol. Prog. Ser. **325**: 181–186. doi:10.3354/meps325181.

Straile, D., and Halbich, A. 2000. Life history and multiple antipredator defenses of an invertebrate pelagic predator, *Bythotrephes longimanus*. Ecology, **81**: 150–163.

Strecker, A.L., Arnott, S.E., Yan, N.D., and Girard, R. 2006. Variation in the response of crustacean zooplankton species richness and composition to the invasive predator *Bythotrephes longimanus*. Can. J. Fish. Aquat. Sci. **63**(9): 2126–2136. doi:10.1139/F06-105.

Tiselius, P., and Jonsson, P.R. 1990. Foraging behaviour of six calanoid copepods: observations and hydrodynamic analysis. Mar. Ecol. Prog. Ser. **66**: 23–33. doi:10.3354/meps066023.

Vanderploeg, H.A., Bowers, J.A., Chapelski, O., and Soo, H.K. 1982. Measuring in situ predation by *Mysis relicta* and observations on underdispersed microdistributions of zooplankton. Hydrobiologia, **93**(1–2): 109–119. doi:10.1007/BF00008104.

Vanderploeg, H.A., Liebig, J.R., and Omair, M. 1993. *Bythotrephes* predation on Great Lakes zooplankton measured by an in situ method: implications for zooplankton community structure. Arch. Hydrobiol. **127**: 1–8.

Viitasalo, M., Kiørboe, T., Flinkman, J., Pedersen, L.W., and Visser, A.W. 1998. Predation vulnerability of planktonic copepods: consequences of predator foraging strategies and prey sensory abilities. Mar. Ecol. Prog. Ser. **175**: 129–142. doi:10.3354/meps175129.

Wissel, B., Boeing, W.J., and Ramcharan, C.W. 2003. Effects of water color on predator regimes and zooplankton assemblages in freshwater lakes. Limnol. Oceanogr. **48**: 1965–1976.

Wong, C.K. 1981. Predatory feeding behavior of *Epischura lacustris* (Copepoda, Calanoida) and prey defense. Can. J. Fish. Aquat. Sci. **38**: 275–279. doi:doi:10.1139/f81-039.

Yan, N.D., Blukacz, A., Sprules, W.G., Kindy, P.K., Hackett, D., Girard, R.E., and Clark, B.J. 2001. Changes in zooplankton and the phenology of the spiny water flea, *Bythotrephes*, following its invasion of Harp Lake, Ontario, Canada. Can. J. Fish. Aquat. Sci. **58**(12): 2341–2350. doi:10.1139/cjfas-58-12-2341.

Yan, N.D., Girard, R., and Boudreau, S. 2002. An introduced invertebrate predator (*Bythotrephes*) reduces zooplankton species richness. Ecol. Lett. **5**(4): 481–485. doi:10.1046/j.1461-0248.2002.00348.x.

Young, J.D., and Yan, N.D. 2008. Modifications of the diel vertical migration of *Bythotrephes longimanus* by the cold-water planktivore, *Coregonus artedi*. Freshw. Biol. **53**(5): 981–995. doi:10.1111/j.1365-2427.2008.01954.x.

Young, S., and Taylor, V.A. 1987. Spontaneous and evoked eyemovements in *Polyphemus pediculus* (Cladocera, Crustacea) — a case of open-loop tracking. J. Exp. Biol. **131**: 323–336.

Zar, J.H. 1999. Biostatistical analysis. 4th ed. Prentice-Hall, Inc., Englewood Cliffs, N.J.

Appendix A

Gerritsen and Strickler (1977) developed a model that predicted how predators encountered prey in aquatic systems assuming that predator and prey are randomly distributed, swim in random directions, swim at an average velocity, and encounter each other when prey are within a reaction space around the predator. This reaction space is described by a solid angle (s) using the equation

$$s = \sin\theta d\theta d\phi \tag{A1}$$

where θ is the polar angle and ϕ is the azimuthal angle. An encounter model was adapted specifically for *Bythotrephes*–prey encounters by Muirhead and Sprules (2003). In this model, the rate of prey encounter (Z) (number per hour) by a single *Bythotrephes* is estimated using the equation

$$Z = \frac{R^2N}{2}\int_0^{2\pi}\int_0^{\frac{\pi}{2}} \sin\theta\sqrt{u^2 + v^2 - 2uv\cos\theta}\,d\theta d\phi \tag{A2}$$

where R is the reaction distance of the predator (metres), N is prey density (number per cubic metre), and u and v are the swimming velocities (metres per hour) of the prey and predator, respectively. Using a series of laboratory experiments, Muirhead and Sprules (2003) related *Bythotrephes* reaction distance (millimetres) to light intensity (L) (micromoles per square metre per second) according to the set of equations

$$R = \begin{cases} 6.61, \; L < 2 \\ -7.69 + 36.97\log_{10}(L+1) - 21.88\log_{10}(L+1)^2 + 3.93\log_{10}(L+1)^3, \; 2 \le L \le 500 \\ 9.995, \; L > 500 \end{cases} \tag{A3}$$

We estimated the difference in *D. mendotae* encounter rate between the lowest- and low-light treatments of Experiment 2 using this model given our experimental conditions. From the literature, we found average swimming velocities (millimetres per second) for second-instar *Bythotrephes* (16.03; Muirhead and Sprules 2003) and *D. mendotae* (1.2; Gerritsen 1980). Model predictions were compared with the difference between encounter rates observed in lowest and low light intensity treatments in Experiment 2. Encounter rates were calculated using the experimental ingestion rates (I) and the equation

$$I = N\{1 - \exp[-Z(T - hI)]\} \tag{A4}$$

where T (hours) is the total duration of the experiment and h (hours) is an experimentally derived estimate of the handling time associated with the consumption of individual *Daphnia* by *Bythotrephes* (K.L. Pangle, unpublished data). This recursive equation allowed us to estimate encounter rate for *Bythotrephes* exposed to a saturating level of prey density (Hassel 1978).

References

Gerristen, J. 1980. Adaptive response to encounter problems. *In* Evolution and ecology of zooplankton communities. *Edited by* W.C. Kerfoot. University Press New England, Hanover, N.H. pp. 52–62.

Gerristen, J., and Strickler, J.R. 1997. Encounter probabilities and community structure in zooplankton: a mathematical model. J. Fish. Res. Board Can. **34**: 73–82.

Hassel, M.P. 1978. The dynamics of arthropod predator-prey systems. Princeton University Press, Princeton, N.J.

Muirhead, J., and Sprules, W.G. 2003. Reaction distance of *Bythotrephes longimanus*, encounter rate and index or prey risk for Harp Lake, Ontario. Freshw. Biol. **48**(1): 135–146. doi:10.1046/j.1365-2427.2003.00986.x.

Appendix B

A swimming planktivore produces water velocity gradients that can alert zooplankton of its presence. Studies have shown that zooplankton are particularly sensitive to the deformation rate (per second) component of water velocity gradients caused by a predator (Kiørboe and Visser 1999; Kiørboe et al. 1999). Assuming that a planktivore produces water velocity gradients that are similar to that of a sphere with radius r (centimetres) and velocity v (centimetres per second) and assuming that zooplankton respond to a planktivore when deformation rate surpasses some critical threshold Δ (per second), the distance D (centimetres) that zooplankton can detect a planktivore can be calculated using the equation

$$D = r\sqrt{\frac{3v}{4r\Delta}\left(1 + \sqrt{1 - \frac{8r\Delta}{3v}}\right)} \text{ for } \Delta \le \frac{3v}{8r} \tag{B1}$$

Using this model, we estimated the distance that *D. mendotae* could detect *Bythotrephes* using a critical threshold found for *Daphnia* (1.8·s^{-1}; Brewer et al. 1999), *Bythotrephes* swimming velocity (1.6 cm·s^{-1}; Muirhead and Sprules 2003), and the mean thoracic radius of *Bythotrephes* used in the experiment (0.15 cm).

References

Brewer, M.C., Dawidowicz, P., and Dodson, S.I. 1999. Interactive effects of fish kairomones and light on *Daphnia* escape behavior. J. Plankton Res. **21**(7): 1317–1335. doi:10.1093/plankt/21.7.1317.

Kiørboe, T., and Visser, A.W. 1999. Predator and prey perception in copepods due to hydromechanical signals. Mar. Ecol. Prog. Ser. **179**: 81–95. doi:10.3354/meps179081.

Kiørboe, T., Saiz, E., and Visser, A. 1999. Hydrodynamic signal perception in the copepod *Acartia tonsa*. Mar. Ecol. Prog. Ser. **179**: 97–111. doi:10.3354/meps179097.

Muirhead, J., and Sprules, W.G. 2003. Reaction distance of *Bythotrephes longimanus*, encounter rate and index or prey risk for Harp Lake, Ontario. Freshw. Biol. **48**(1): 135–146. doi:10.1046/j.1365-2427.2003.00986.x.

Ancestry, population structure, and conservation genetics of Arctic grayling (*Thymallus arcticus*) in the upper Missouri River, USA

Douglas P. Peterson and William R. Ardren

Abstract: We genotyped Arctic grayling (*Thymallus arcticus*) at 10 microsatellite loci in 18 samples (n = 726) from Montana, Wyoming, and Saskatchewan to determine genetic relationships among native, captive, and naturalized populations in the upper Missouri River basin, to assess patterns in genetic diversity, and to infer recent demographic histories. Substantial genetic subdivision was observed among sample populations (global F_{ST} = 0.10). Canadian populations have been isolated from Missouri River populations long enough for mutation to cause genetic differences between regions (mean pairwise F_{ST} = 0.18, R_{ST} = 0.54). Within the Missouri River basin, most naturalized lacustrine populations traced their ancestry to Red Rock lakes. Two populations in headwater lakes within the Big Hole River watershed appear to be native. We found neither evidence for introgression of Canadian-origin grayling nor any effect of hatchery stocking in native populations. The native fluvial Big Hole River group was genetically distinct and most diverse (H_E = 0.89), whereas native Madison River and Red Rock lakes populations exhibited lower genetic diversity (H_E = 0.74 and 0.80, respectively) and evidence of recent bottlenecks. The existing Big Hole and Red Rock populations are at low abundance but do not appear to be at immediate risk of inbreeding depression (N_e = 207.7–228.2).

Résumé : Nous avons déterminé le génotype d'ombres arctiques (*Thymallus arcticus*) à 10 locus microsatellites dans 18 échantillons (n = 726) provenant du Montana, du Wyoming et de la Saskatchewan afin de déterminer les relations génétiques entre les populations indigènes, captives et naturalisées dans le bassin supérieur de la rivière Missouri, d'évaluer les patrons de diversité génétique et de déduire leur histoire démographique récente. Il existe une importante subdivision génétique des populations échantillonnées (F_{ST} global = 0,10). Les populations canadiennes ont été isolées assez longtemps des populations de la rivière Missouri pour que des mutations produisent des différences génétiques entre les régions (F_{ST} apparié moyen = 0,18, R_{ST} = 0,54). Au sein du bassin versant du Missouri, la plupart des populations lacustres naturalisées retracent leur origine aux lacs Red Rock. Deux populations dans des lacs d'amont du bassin versant de la rivière Big Hole semblent être indigènes. Il n'y a aucune indication d'introgression de la part d'ombres arctiques d'origine canadienne, ni d'effet de l'empoissonnement à partir des piscicultures sur les populations indigènes. Le groupe indigène fluvial de la Big Hole est distinct génétiquement et très diversité (H_E = 0,89), alors que les populations indigènes de la Madison et des lacs Red Rock possèdent une diversité génétique plus basse (respectivement H_E = 0,74 et 0,80) et montrent des signes de goulots d'étranglement récents. Les populations actuelles de Big Hole et de Red Rock ont une abondance faible, mais ne semblent pas courir à court terme de risque de dépression par consanguinité (N_e = 207,7 – 228,2).

[Traduit par la Rédaction]

Introduction

Understanding population-level consequences of patterns in neutral genetic variation has become a preliminary step in the development of conservation programs for many commercially exploited or sensitive species. In addition to helping determine ancestral relationships and phylogeny, these patterns are commonly used to infer genetic connectivity among demes and help define populations (Waples and Gaggiotti 2006), the logical focus of conservation and management (Morris and Doak 2002). Microsatellite DNA markers can help identify cryptic population structure (e.g., So et al. 2006) and reconstruct demographic histories for rare species (e.g., Nielsen et al. 1999). Genetic-based methods can both characterize and distinguish between historical and contemporary factors that influence the demographic histories of extant populations (Pearse and Crandall 2004), for example, glacial events across tens of thousands of years (Bernatchez and Wilson 1998) versus recent habitat fragmentation, human exploitation, nonnative species invasions,

---

Received 4 November 2008. Accepted 31 May 2009. Published on the NRC Research Press Web site at cjfas.nrc.ca on 13 October 2009. J20860

Paper handled by Associate Editor Eric Taylor.

D.P. Peterson.[1] US Fish and Wildlife Service, Division of Ecological Services, 585 Shepard Way, Helena, MT 59601, USA.
W.R. Ardren.[2] US Fish and Wildlife Service, Conservation Genetics Program, Abernathy Fish Technology Center, 1440 Abernathy Creek Road, Longview, WA 98632, USA.

[1] Corresponding author (e-mail: Doug_Peterson@fws.gov).

[2] Present address: Western New England Complex, US Fish and Wildlife Service, 11 Lincoln Street, Essex Junction, VT 05452, USA.

Can. J. Fish. Aquat. Sci. 66: 1758–1774 (2009)   doi:10.1139/F09-113   Published by NRC Research Press

or other impacts over tens or hundreds of years (e.g., Koskinen et al. 2002*a*; Stamford and Taylor 2005). These properties make microsatellite markers particularly amenable to understanding the conservation status of northern freshwater fishes, e.g., Arctic grayling, (*Thymallus articus*), that have been strongly influenced by both types of factors.

Arctic grayling are stenothermic cold-water, salt-water-intolerant salmonids. They are native to Arctic Ocean drainages of Alaska and northwestern Canada, as far east as Hudson's Bay, and westward across northern Eurasia to the Ural mountains (Scott and Crossman 1973; Froufe et al. 2005; Weiss et al. 2006). In North America, they are also native to northern Pacific Ocean drainages as far south as the Stikine River in British Columbia. To the south and east of the main species distribution, two disjunct groups of Arctic grayling are native to the coterminous United States: one in Michigan (extirpated in the late 1930s; Hubbs and Lagler 1949), and one in the upper Missouri River basin in Montana and Wyoming (extant). The Michigan and Missouri River populations were isolated from northern drainages by Wisconsin glaciation (Pielou 1991), but the latter apparently began to diverge genetically before that time (i.e., >70 000 years ago; Redenbach and Taylor 1999). Glacial history and genetic data suggest that the Missouri River population was founded from individuals that survived Pleistocene glacial advance in a refuge in the upper Missouri River system or southwestern Alberta, or in both places (Redenbach and Taylor 1999; Stamford and Taylor 2004).

The historical distribution of Arctic grayling in Wyoming and Montana was thought to encompass approximately 2000 km of lotic habitat in the upper Missouri River system above the Great Falls (Kaya 1992). A migratory, river-dwelling (fluvial) life history presumably predominated, based on historical reports of Arctic grayling in the mainstem Missouri River and its major tributaries (e.g., Madison, Jefferson, and Gallatin rivers) and the paucity of lakes accessible for colonization (Vincent 1962; Kaya 1992). The current distribution of native Arctic grayling in the Missouri River system is only a fraction (<5%) of the historical estimate (Kaya 1992). The combined effects of overexploitation, dams, stream dewatering, and interaction with nonnative trout species are suspected in this decline (Vincent 1962; Kaya 1992, 2000). Currently, native Arctic grayling occur only in southwestern Montana at three locations: (*i*) the Big Hole River and perhaps two small lakes in that drainage; (*ii*) Red Rock lakes, which are two small natural lakes in the headwaters of the Beaverhead River system; and (*iii*) Ennis Reservoir on the Madison River. The Big Hole River population has received special conservation focus as the only remaining fluvial Arctic grayling population in the coterminous US (Montana Fish, Wildlife and Parks (MFWP) 1995).

Until recently, fluvial Arctic grayling in Montana were considered a candidate species for listing under the Endangered Species Act (US Fish and Wildlife Service (USFWS) 2007), and the decision not to extend US federal protection to this population remains controversial. Nonetheless, conservation efforts continue to focus on improving habitat conditions in the Big Hole River and re-establishing other fluvial populations in historic waters using fish derived from the Big Hole River (MFWP 1995, 2007). Ironically, although native Arctic grayling in the upper Missouri River have declined precipitously in the past 100 years, culture and stocking of grayling within and beyond the region has been extensive (Kelly 1931; Kaya 1990; MFWP 2005*b*). Dozens of naturalized Arctic grayling populations have been established in Montana lakes (MFWP 2005*b*). Through the mid-20th century, millions of hatchery-reared Arctic grayling of uncertain origin were planted in Montana waters containing extant native populations, including the Big Hole River, raising concerns that interbreeding with introduced fish has altered indigenous gene pools (Everett 1986), which potentially disrupts local adaptation (e.g., Allendorf et al. 2001).

Existing genetic data support the long-term geographic isolation of Arctic grayling from the upper Missouri River (Everett 1986; Redenbach and Taylor 1999; Stamford and Taylor 2004). These same data provide less insight into ancestral relationships among the extant native and introduced populations within the Missouri River system. In general, allozymes may exhibit less variation in recently diverged populations (Hedrick 1999), which may explain why protein electrophoresis has proven only moderately informative for distinguishing among Arctic grayling populations in Montana and Wyoming (Everett 1986; Campton 2006; R. Leary, Montana Fish, Wildlife and Parks, University of Montana, Division of Biological Sciences, Missoula, MT 59812, USA, unpublished data, 2005). The existing mtDNA data are uninformative within this region, as 24 of 25 individuals from the Big Hole River, Red Rock lakes, and Madison River populations had the same composite haplotype (Redenbach and Taylor 1999). In contrast, a genetic signature of population structure is often detected at the basin or subbasin scales for philopatric freshwater fishes such as salmonids (e.g., Costello et al. 2003; Hendry et al. 2004). Indeed, Hop and Gharrett (1989) used electrophoresis to determine the population structure of Arctic graying in the Chena River, Alaska, and studies of European grayling (*Thymallus thymallus*) have found significant population structuring within a river system (e.g., Weiss et al. 2002; Gum et al. 2003; Meldgaard et al. 2003) or even within the same lake (Koskinen et al. 2001). Fine-scale genetic analyses of North American Arctic grayling using microsatellites are few (see Stamford and Taylor 2005) but may help answer important conservation questions.

Our general objective was to use microsatellite markers to more clearly characterize ancestral relationships and genetic differentiation among native and naturalized Arctic grayling populations in the upper Missouri River. Specifically, we used these markers to infer the genetic origin of introduced populations, to determine if significant admixture between indigenous and introduced fish has resulted from past stocking, and to characterize the population structure among native populations at the basin scale (i.e., upper Missouri River). At the subbasin scale within the Big Hole River, we sought to establish whether the fluvial population functions genetically as a single, panmictic population or as a set of demes linked by occasional gene flow. For the supported native population groupings, we used genetic data to deduce their demographic histories and identify if, and when, abrupt population declines have occurred. Results are discussed relative to the genetic status and conservation of native populations with special emphasis on the Big Hole River and continuing efforts to restore fluvial populations in indigenous waters within the upper Missouri River basin.

Materials and methods

Study area and sample collection

We collected samples thought to represent native populations and their derivatives, introduced populations of Montana or Canadian origin, and a reference population in northeast Saskatchewan, Canada (Table 1; Fig. 1).

Native or putative native populations and derived conservation populations

From the Big Hole River, we obtained Arctic grayling samples from five discrete but hydrologically connected locations (populations 1–5; Table 1) thought to represent different demes based on occurrence of young-of-the-year fish (e.g., Liknes and Gould 1987; MFWP 2005*a*, 2007). Mussigbrod (6) and Miner (7) are samples from small (<50 ha) headwater lakes in the upper Big Hole River system, which are now isolated from the main stem by a diversion dam and by habitat degradation, respectively. Red Rock lakes (8) includes adfluvial grayling collected during their spawning migration into Red Rock Creek. Madison River – Ennis Reservoir (9) are grayling collected in, or upstream from, Ennis Reservoir. This reservoir was formed by construction of an impassible dam in 1903 (Fig. 1).

Waters containing populations 1–9 were extensively stocked with grayling, primarily from the Washoe Park Hatchery (Table 2). Kelly (1931) reported that the Washoe Park (Anaconda) Hatchery and a population in nearby Georgetown Lake were founded with grayling eggs from Red Rock lakes (Elk Springs Creek) and the Madison River (Meadow Creek). The Bozeman National Fish Hatchery population was founded from Red Rock lakes grayling (Kelly 1931).

The Ruby River (10), Axolotl Lake (11), and Bozeman Fish Technology Center (12) samples are derived from Big Hole River grayling taken into captivity for conservation purposes. The Ruby River has been stocked with captive-spawned juvenile graying in an attempt to re-establish a fluvial population (MFWP 2004, 2007). Axolotl Lake is a closed-basin lake that contains a brood reserve established 20 years ago (MFWP 2007). Grayling (manually) spawned from Axolotl Lake have been transplanted to the Ruby River and elsewhere in the upper Missouri River system (MFWP 2007). The Bozeman Fish Technology Center was a hatchery genetic reserve established between 1988 and 1992 (M. Toner, US Fish and Wildlife Service, Bozeman Fish Technology Center, 4050 Bridger Canyon Road, Bozeman, MT 59715, USA, personal communication).

Introduced and Canadian-origin populations

Odell (13) and Bobcat lakes (16) are small (<15 ha) headwater lakes in the Wise River system, a major tributary to the Big Hole River (Fig. 1). We could not locate any stocking records for these locations (Table 1). Grebe Lake (15) is a headwater lake (<40 ha) in the Madison River system within Yellowstone National Park. Grebe Lake is isolated by a natural geologic barrier, but grayling were introduced in 1921 and the lake became a major source of grayling eggs shipped throughout western US (Kaya 2000). Sunnyslope Canal (17) contains an introduced population derived from the stocking of its source reservoir between 1937 and 1943 (Barndt and Kaya 2000).

Fuse Lake (14) is in the Columbia River basin and contains a population introduced in 1952 from the Mackenzie River system, Canada (Everett 1986; Kaya 1990). We included this sample to determine if Canadian-origin grayling were further transplanted within the upper Missouri River. The Fond du Lac (18) area in northeastern Saskatchewan is also part of the Mackenzie River system, and Fond du Lac grayling were included as a reference population.

Samples from most locations consisted of fin clips collected from adults representing multiple cohorts. Native grayling were so rare in the Big Hole and Madison rivers that samples were pooled across years (Table 1) and generally included all available individuals, including young-of-the-year when present. Swamp Creek and Wisdom samples were primarily young-of-the-year from two different cohorts because adults were not present. Only young-of-the-year were present at the time of sample collection in Steel Creek, so we systematically selected a subsample of individuals for genotyping to reduce the probability of including full siblings. Scales were the DNA source for the 1996 Madison River – Ennis Reservoir samples (9) and the entire Fond du Lac sample (18).

DNA extraction and genotyping of microsatellite loci

For genomic DNA extraction, a 1 mm^2 piece of fin tissue or a single scale was placing in 200 µL of 5% chelex containing 0.2 mg·mL^{-1} of proteinase K; the mixture was incubated for 2 h at 56 °C, boiled for 8 min at 100 °C, and vortexed for 30 s. We used 2 µL of the supernatant in 15 µL PCR reactions to amplify 10 microsatellite loci (Table 3). Conditions for polymerase chain reaction (PCR) amplification, primer sequences, and methods for determining multilocus genotypes for all loci are reported in Diggs and Ardren (2008).

Data analyses

Within-population diversity

Average population gene diversities (H_E; Nei 1987) and allelic richness for each locus were estimated using the program HP-RARE 1.0 (Kalinowski 2005). Allelic richness was estimated using a rarefaction procedure to account for unequal sample sizes (Kalinowski 2004). The allele permutation test in FSTAT 2.9.3.2 (Goudet 2001) was used to test for differences between groups of populations in the mean values of allelic richness and H_E. Conformance of genotypic frequencies to Hardy–Weinberg expectations (HWE) was evaluated using the methods of Guo and Thompson (1992) via the program GENEPOP 4.0.7 (Raymond and Rousset 1995). Tests for genotypic disequilibrium at all pairs of loci in each sample were also calculated using GENEPOP 4.0.7, with 10 000 dememorizations, 10 000 batches, and 10 000 iterations per batch. Statistical significance levels used to detect deviations from HWE or genotypic equilibrium ratios were adjusted for the number of simultaneous tests by the sequential Bonferroni correction (Rice 1989).

Sample collections containing close relatives have the po-

Table 1. Presumed origin, location, sample size (N), and sample collection years for 18 native and introduced Arctic grayling (*Thymallus arcticus*) populations in the upper Missouri River and one from the Mackenzie River system, Canada.

No.	Sample population	Latitude (°N)	Longitude (°W)	Elevation (m)	N	Years
Native — upper Missouri River basin						
Connected Big Hole River						
1	Steel Creek[a]	45.66682	−113.46601	1826	27	2006
2	Swamp Creek[a]	45.64978	−113.44271	1823	38	2005, 2006
3	Big Hole River near Wisdom, Montana[a]	45.61755	−113.45758	1844	22	2006
4	Fishtrap Creek[a]	45.8697	−113.22847	1779	28	2005, 2006
5	Lamarche Creek[a]	45.8834	−113.20211	1780	29	2005, 2006
Upper Big Hole River watershed						
6	Mussigbrod Lake[b]	45.79078	−113.61149	1979	48	2006
7	Miner Lake[b]	45.3248	−113.56747	2125	37	2006
Red Rock lakes, Beaverhead River						
8	Red Rock Creek	44.61359	−111.68807	2016	48	2005
Madison River						
9	Madison River – Ennis Reservoir	45.40931	−111.69449	1469	27	1996 (n = 23), 1999 (1), 2004 (1), 2006 (2)
Captive reserve or conservation — derived from Big Hole River						
10	Ruby River	45.00863	−111.96207	1880	48	2006
11	Axolotl Lake	45.2258	−111.8713	2229	55	2006
12	Bozeman Fish Technology Center (BFTC)	45.70802	−110.9774	1497	48	2005
Introduced — other sources (source)						
13	Odell Lake (unknown)	45.57523	−113.23231	2543	46	2006
14	Fuse Lake (Canada)	46.24785	−113.72297	2347	47	2006
15	Grebe Lake (upper Missouri River)	44.75083	−110.55778	2447	47	2002, 2005
16	Bobcat Lake (unknown)	45.6219	−113.2206	2569	47	2006
17	Sunnyslope Canal (unknown)	47.60490	−112.09710	1293	50	2006
Native population — Saskatchewan, Canada						
18	Fond du Lac, Athabaska River system	59.24341	−106.41357	202	34	1987

[a] Putative demes for fluvial Arctic grayling within the Big Hole River and connected tributaries.

[b] Putative remnant populations presently isolated by habitat degradation and water development.

tential to bias population genetic measures of diversity. Many of the samples for this study were collected from populations that have experienced recent declines, thus increasing the chance of the sample containing relatives. In addition, the tendency for juvenile salmonids to remain in close proximity during their juvenile life stage often results in the sampling of family groups (Allendorf and Phelps 1981). We estimated the level of relatedness in each sample by calculating the mean pairwise identity (I; Belkhir et al. 2002). The probability that each sample was a random draw from a panmictic population was estimated in IDENTIX (Belkhir et al. 2002) by permutating across genotypes and generating 1000 randomized pseudosamples under the assumption of no relatedness. The proportion of pseudosamples that produced a larger mean pairwise identity than the observed mean pairwise identity was used to calculate the p value for the null hypothesis that the sample represented a random draw from a panmictic population.

Population structure

We used contingency tests of allele frequency homogeneity to test the null hypothesis of panmixia between any pair of sample collections. Contingency tests were conducted using the methods of Raymond and Rousset (1995) as implemented in GENEPOP 4.0.7. For each locus, we estimated the exact probability that the observed allele frequencies were drawn from the same population using the Markov chain Monte Carlo (MCMC) methods to provide an unbiased estimate of the exact probability for each randomization test. We ran 100 batches of 5000 replicates each, with 10 000 dememorisation steps. For each comparison, we used the Fisher's combined probability test (χ^2_F) as a composite test over all loci and the false discovery rate (FDR) method of Narum (2006) to set a experiment-wise α at the 0.05 level that accounts for multiple tests.

The level of genetic variation among populations was estimated by F_{ST} using the θ statistic of Weir and Cockerham (1984). Pairwise F_{ST} values were estimated in GENEPOP 4.0.7. Estimates of F_{ST} over all sample locations and associated 95% confidence intervals, generated by bootstrap sampling over loci, were calculated in FSTAT 2.9.3.2 (Goudet 2001). Testing for different ancestral histories between populations was accomplished by comparing global variance in allelic identity (i.e., F_{ST}) and allelic size (i.e., R_{ST}) measures of genetic difference. Under the null hypothesis ($R_{ST} = F_{ST}$), differentiation is caused mainly by drift, whereas under the alternative hypothesis ($R_{ST} > F_{ST}$), stepwise mutations have contributed to differentiation (Hardy et al. 2003). SPAGEDI

Fig. 1. Location of Arctic grayling (*Thymallus arcticus*) sample populations. (*a*) The species historical distribution in western North America is shaded and includes a disjunct set of populations that occur in the upper Missouri River basin. (*b*) In the upper Missouri River, grayling were native to the main stem Missouri River (shaded area) and most of its major tributaries (dark lines). The present range of native grayling that express a fluvial life history is restricted to the upper Big Hole River (dark bold line). Major dams are denoted by white bars. (*c*) In the Big Hole River drainage, samples were collected from a number of discrete locations. In all panels, triangles indicate presumed native populations, squares denote introduced (naturalized) populations, and circles are the location of captive or introduced conservation populations derived from Arctic grayling native to the Big Hole River.

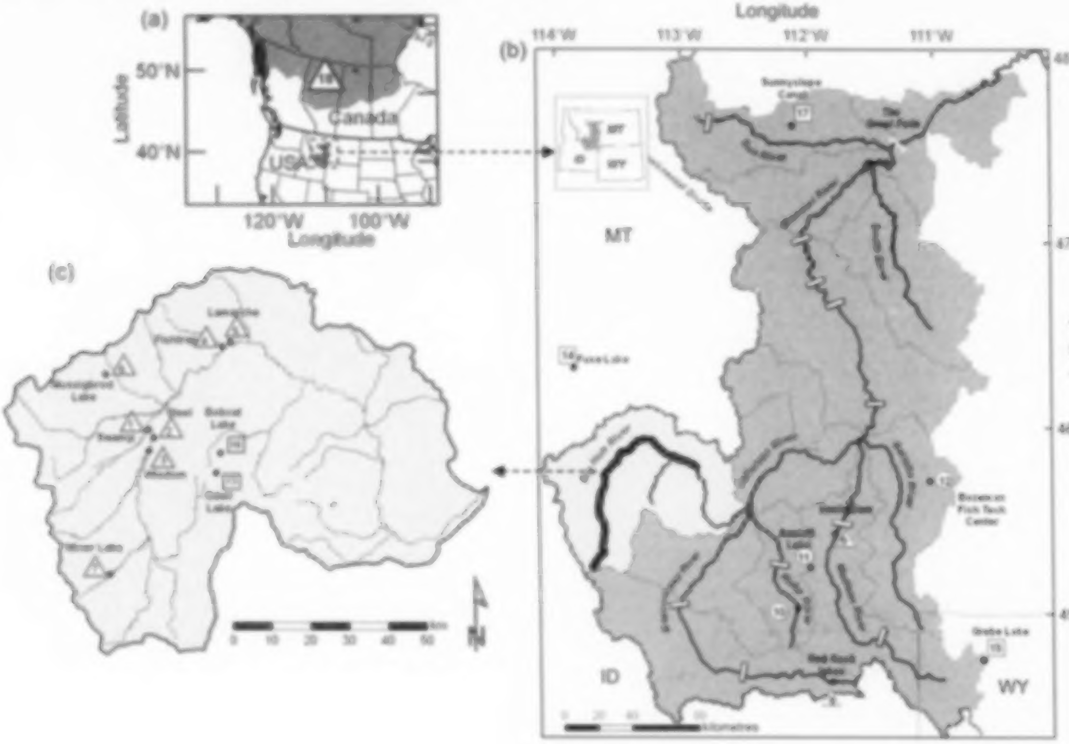

Table 2. Documented stocking of hatchery-cultured Arctic grayling (*Thymallus arcticus*) into waters containing indigenous or presumed indigenous populations.

No.	Population	Years stocked	Total number stocked	Hatchery source
1–5	Big Hole River group	1937–1957	14 732 193[a]	Washoe Park Hatchery (MFWP 2005*b*)[b]
6	Mussigbrod Lake	1934–1955	5 951 847	Washoe Park Hatchery (MFWP 2005*b*)[b]
7	Miner Lake	1933–1952	3 220 776	Washoe Park Hatchery (MFWP 2005*b*)[b]
8	Red Rock	1899–1938	Unknown	Bozeman National Fish Hatchery (Randall 1978)
		1946–1962	103 704	Ennis National Fish Hatchery (Randall 1978; MFWP 2005*b*)
9	Madison River – Ennis Reservoir	1928–1961	2 690 729[c]	Washoe Park during 1928–1934, Ennis National Fish Hatchery during 1946–1962 (MFWP 2005*b*)

[a] Number includes records for Arctic grayling planted into the Big Hole River and its tributaries. Number excludes 1080 Arctic grayling from Somers Hatchery (also known as Flathead Lake Salmon Hatchery) planted in 1962 and 622 Arctic grayling from the Bozeman Fish Technology Center planted in 1992 and 1993.

[b] The Washoe Park Hatchery is operated by the state of Montana and was historically referred to as the "Anaconda Hatchery".

[c] Numbers for the Madison River includes records for Arctic grayling planted into Odell Creek, Ennis Reservoir, the lower, middle, and upper segments of the Madison River, and the South Fork Madison River (MFWP 2005*b*).

v1.2 (Hardy and Vekemans 2002) was used to calculate R_{ST} and to test for significant differences between F_{ST} and R_{ST} using the allele size permutation test of Hardy et al. (2003) ($\alpha = 0.05$ with FDR adjustment). We used standard error estimates from SPAGEDI v1.2 to calculate 95% confidence intervals for the average pairwise R_{ST} estimates over all populations. To test for geographic structure and consistency with a stepping-stone model of gene flow among native pop-

Table 3. Population genetic characteristics for 18 Arctic grayling (*Thymallus arcticus*) sample populations across 10 microsatellite loci.

No.	Sample population	N	N_A	N_A^{36}	N_P	H_O	H_E	HWE	LD	I
Native — upper Missouri River basin										
Connected Big Hole River										
1	Steel Creel	27	14.5	12.9	—	0.89	0.88	0	0	0.1569
2	Swamp Creek	38	16.7	13.5	—	0.87	0.89	0	0	0.1503
3	Big Hole River	22	14.7	13.7	—	0.86	0.89	0	0	0.1365
4	Fishtrap Creek	28	14.3	12.8	—	0.90	0.89	0	0	0.1480
5	Lamarche Creek	29	15.4	13.2	—	0.88	0.89	0	0	0.1532
1–5	Big Hole River group[a]	144	19.3	13.3[b]	5	0.88	0.89	0	0	0.1438
Upper Big Hole River watershed										
6	Mussigbrod Lake	48	10.9	9.1	1	0.78	0.78	0	0	0.2437
7	Miner Lake	37	13.1	10.7	3	0.79	0.82	1	0	0.2101
Red Rock lakes, Beaverhead River										
8	Red Rock Creek	48	13.3	10.4	2	0.79	0.80	0	0	0.2181
Madison River										
9	Madison River – Ennis Reservoir	27	8.4	7.7	0	0.73	0.74	0	0	0.3285
Captive reserve and conservation — derived from Big Hole River										
10	Ruby River	48	14.3	11.7	0	0.90	0.88	0	0	0.1777
11	Axolotl Lake	55	15.0	11.8	0	0.87	0.88	4	9	0.1750
12	BFTC	48	13.7	10.8	1	0.85	0.85	1	1	0.2095
Introduced — other sources										
13	Odell Lake	46	14.0	11.0	2	0.84	0.83	0	0	0.1989
14	Fuse Lake	47	10.8	8.5	6	0.74	0.75	0	0	0.2675
15	Grebe Lake	47	13.7	10.6	2	0.84	0.85	0	0	0.2053
16	Bobcat Lake	47	9.9	8.3	3	0.78	0.80	0	0	0.2713
17	Sunnyslope Canal	50	5	4.5	0	0.62	0.63	0	0	0.4922
Native — Saskatchewan, Canada										
18	Fond du Lac	34	11.7	10.4	7	0.68	0.76	0	0	0.2753

Note: N, sample size; N_A, numbers of alleles; N_A^{36}, rarefaction measure of allelic richness using a sample of 36 genes; N_P, number of private alleles; H_O, observed heterozygosity; H_E, expected heterozygosity; HWE, number of loci not in Hardy–Weinberg equilibrium; LD, pairs of loci with significant linkage disequilibrium; I, mean pairwise relatedness estimates for multilocus genotypes (after Belkhir et al. 2002), where values range from 0 for unrelated individuals to 0.5 for full siblings.

[a] The Big Hole River group (1–5) is the amalgamation of samples populations 1 through 5 (*i.e.*, Steel Creek, Swamp Creek, Big Hole River near Wisdom, Fishtrap Creek, and Lamarche Creek).

[b] Table value for allelic richness estimated using HP-RARE 1.0. Allelic richness estimated using FSTAT 2.9.3.2 was slightly lower (N_A^{36} = 13.24; see Results, Within population diversity).

ulations with presumed historical connectivity, we examined the correlation between the natural log of pairwise fluvial distances (km) and genetic differentiation using Mantel tests implemented in GENEPOP 3.7 (Rousset 1997).

Genetic relationships among populations were inferred by generating an unrooted neighbor-joining (NJ) tree based on Cavalli-Sforza and Edwards' (1967) chord distance. Confidence in the observed topology of the NJ–population tree was assessed using the bootstrap procedure in PHYLIP v3.6 (Felsenstein 1992) based on 1000 resamples across loci. The consensus NJ–population tree was generated in PHYLIP v3.6.

Effective population size

We estimated the long-term effective population size (N_e) using the heterozygosity-based methods of Ohta and Kimura (1973) (eq. 1) and Hartl and Clark (1989) (eq. 2). Both methods assume selective neutrality and predict that at mutation-drift equilibrium, N_e is a function of H_E. Ohta and Kimura (1973) assume a stepwise mutation model (SMM), whereas Hartl and Clark (1989) assume an infinite allele mutation model (IAM). We used the most commonly applied microsatellite mutation rate for fishes, $\mu = 5 \times 10^{-4}$ (Estoup and Angers 1998).

$$(1) \qquad N_{eSMM} = \frac{\left[\left(\frac{1}{1-H_E}\right)^2 - 1\right]}{8\mu}$$

$$(2) \qquad N_{eIAM} = \frac{H_E}{4\mu(1 - H_E)}$$

The true long-term N_e should be between N_{eSMM} and N_{eIAM}, because these two models represent the extremes of the mutation process for microsatellite loci (Busch et al. 2007).

We estimated the contemporary N_e of each population using the single-sample linkage disequilibrium method of Waples (2006) implemented in program LDNe (Waples and Do 2008). This method provides an estimate of the effective number of breeding adults that parented the sampled population. In the analysis, we excluded all alleles with frequencies less than 0.02 and used the jackknife procedure to estimate the 95% confidence intervals.

Table 4. Pairwise F_{ST} (below diagonal) and R_{ST} estimates (above diagonal) for Arctic grayling (*Thymallus arcticus*) at 10 microsatellite

		Population number								
No.	Population	1	2	3	4	5	1–5	6	7	8
1	Steel	—	*−0.0096*	*−0.0083*	*−0.0047*	*−0.0063*	NA	**0.3536**	0.0859	**0.1364**
2	Swamp	*0.0036* a	—	*0.0004*	*−0.0031*	*−0.0106*	NA	0.2905	0.0694	**0.1326**
3	Wisdom	*−0.0027* a	*0.0019* a	—	*−0.0125*	*−0.0054*	NA	**0.381**	0.1167	0.0897
4	Fishtrap	*0.0052*	*0.0019* a	*−0.0052* a	—	*−0.0118*	NA	0.3488	0.0995	0.0861
5	Lamarche	*0.0053*	*0.0055* a	*−0.0019* a	*−0.003* a	—	NA	**0.291**	0.0755	0.116
1–5	Big Hole group	NA	NA	NA	NA	NA	—	**0.2756**	0.086	0.1112
6	Mussigbrod	0.0789	0.0805	0.0772	0.0743	0.0719	0.0719	—	**0.3075**	**0.4784**
7	Miner	0.0789	0.072	0.072	0.0728	0.0777	0.072	0.1199	—	**0.3172**
8	Red Rock	0.0808	0.0747	0.0699	0.0694	0.0782	0.0708	0.1604	0.1501	—
9	Madison–Ennis	0.0725	0.0789	0.0806	0.076	0.0835	0.0726	0.1441	0.1496	0.1739
10	Ruby	0.023	0.0202	0.0128	0.0142	0.0191	0.0171	0.0937	0.075	0.0828
11	Axolotl	0.0232	0.0155	0.0134	0.0138	0.0182	0.0162	0.0981	0.0758	0.0734
12	BFTC	0.0318	0.0233	0.024	0.0237	0.0293	0.025	0.1044	0.086	0.0929
13	Odell	0.0537	0.0579	0.0492	0.0464	0.0568	0.0508	0.1389	0.1329	0.0222
14	Fuse	0.1375	0.1362	0.1399	0.1404	0.1414	0.1301	0.1962	0.1862	0.2021
15	Grebe	0.035	0.0372	0.033	0.0348	0.0392	0.0346	0.1084	0.1144	0.0377
16	Bobcat	0.0577	0.0638	0.0528	0.0557	0.0598	0.0552	0.133	0.1349	0.0739
17	Sunnyslope	0.1551	0.1493	0.1538	0.1484	0.1585	0.135	0.2414	0.2346	0.129
18	Fond du Lac	0.1446	0.1446	0.1454	0.1505	0.1486	0.142	0.206	0.1835	0.2092

Note: See Table 1 for complete population names. Allele frequency tests, based on Fisher's combined probability with a modified false discovery rate detected in all pairs below the diagonal, except those followed by the letter "a", which indicates tests in which the tablewide p values for the null hypothesis that were consolidated into a single Big Hole River population (1–5, Big Hole group). Consequently, NA indicates estimates or tests that are not applicable tified $R_{ST} > F_{ST}$.

Tests for recent population declines

Heterozygosity excess (Cornuet and Luikart 1996) and low ratios of allelic number to allelic size range (M ratio; Garza and Williamson 2001) were used to screen populations for genetic signatures of recent bottlenecks. The two methods are expected to detect bottlenecks on different time scales, allowing us to infer the time period that population decline or recovery occurred (Williamson-Natesan 2005; Spear et al. 2006). The M-ratio method remains sensitive to size reductions even up to 500 generations following the event, whereas the heterozygosity-based method is most powerful at detecting more recent bottlenecks (e.g., 0.2–4.0 N_e generations; Luikart and Cornuet 1998). We expected that (*i*) native Missouri River populations (1–9) would exhibit bottlenecks detectible by both methods because of major habitat alterations 50–100 years ago and subsequent demographic declines, (*ii*) derived conservation populations (10–12) would show more recent bottlenecks if hatchery effects were significant, and (*iii*) introduced populations (13–17) founded >50 years ago may exhibit founder effects (significant M ratio).

Tests for heterozygosity excess were done with the program BOTTLENECK v1.2.02 (Piry et al. 1999) using a two-phase model (TPM) of microsatellite mutation (Di Rienzo et al. 1994) with parameter settings of 95% SMM, 5% IAM, and 12% variance in multistep mutations (i.e., presumed model for microsatellites; Piry et al. 1999; Lippé et al. 2006). Significance of heterozygosity excess observed in a population was evaluated by a one-sided Wilcoxon's signed-rank test ($\alpha = 0.05$) testing the null hypothesis of no significant heterozygosity excess based on 5000 simulation iterations. M ratios were calculated in M_P_VAL (Garza and Williamson 2001). The M ratio is a measure of the number of alleles (k) to the allele size range (r). The M ratio (k/r) is expected to be small in a recently bottlenecked population because k is reduced faster than r. The program M_P_VAL implemented a model of microsatellite evolution assuming 88% one-step mutations (p_g) and 2.8 average-sized non-one-step mutations (Δ_g) (Garza and Williamson 2001). We explored a range of sizes for the prebottlenecked population (N_e = 500 and 5000) and a microsatellite mutation rate of $\mu = 5 \times 10^{-4}$ to estimate θ ($= 4 \times N_e \times \mu$). Statistical significance of the observed M ratio was calculated using the program Critical_M (Garza and Williamson 2001), with the critical value (M_c) for each sample such that 95% of 10 000 simulations of an equilibrium population had M ratio > M_c.

Results

Within-population diversity

We observed moderate to high levels of genetic diversity in Arctic grayling across all 10 microsatellite loci. Expected heterozygosites (H_E) over all loci ranged from 0.63 in Sunnyslope Canal to 0.89 in four Big Hole River samples (Table 3; see also Supplemental Table S1[3]) and averaged 0.80 across all samples The number of alleles per locus (N_A) ranged from 5.0 in Sunnyslope Canal to 16.7 in loci.

---

[3] Supplementary data for this article are available on the journal Web site (http://cjfas.nrc.ca) or may be purchased from the Depository of Unpublished Data, Document Delivery, CISTI, National Research Council Canada, Building M-55, 1200 Montreal Road, Ottawa, ON K1A 0R6, Canada. DUD 5273. For more information on obtaining material, refer to http://cisti-icist.nrc-cnrc.gc.ca/eng/ibp/cisti/collection/unpublished-data.html.

9	10	11	12	13	14	15	16	17	18
0.0628	0.0058	0.0043	0.0089	0.1088	**0.4796**	0.065	**0.2461**	0.1111	**0.5147**
0.0638	0.0096	0.0032	−0.008	0.1059	**0.476**	0.0669	**0.2541**	0.1188	**0.5037**
0.0547	0.0128	0.0069	0.0015	0.0664	**0.4335**	0.0373	**0.2**	0.0674	**0.4738**
0.0509	0.0097	0.0026	0.0038	0.0657	**0.4336**	0.038	**0.1944**	0.0728	**0.4677**
0.0586	0.0102	−0.0006	0.0087	0.0902	**0.4713**	0.0583	**0.2429**	0.1174	**0.5039**
0.0506	0.0129	0.0066	0.0037	0.086	**0.4416**	0.0498	**0.2259**	0.0842	**0.466**
0.4246	**0.3291**	0.2894	0.2896	0.4484	**0.7275**	**0.4499**	**0.6208**	0.5513	**0.7661**
0.1975	0.0921	0.071	0.0895	**0.288**	**0.5945**	**0.2497**	**0.4081**	0.3224	**0.6104**
0.1442	**0.1315**	**0.1299**	0.113	−0.0015	**0.3536**	0.0264	0.1077	0.0348	**0.4075**
—	0.078	0.0618	0.0597	0.0956	**0.5021**	0.0868	**0.2964**	0.1448	**0.5521**
0.0987	—	−0.0044	0.0059	0.102	**0.4923**	0.0546	**0.2197**	0.1212	**0.5153**
0.0938	0.0013 a	—	0.0037	0.0993	**0.4767**	0.06	**0.2319**	0.1242	**0.4953**
0.1023	0.0089	0.0107	—	0.0877	**0.4627**	0.0489	**0.2319**	0.0996	**0.4902**
0.1246	0.0675	0.0579	0.0805	—	**0.3916**	0.0062	**0.1365**	0.0387	**0.4405**
0.1876	0.1578	0.1525	0.1624	0.1827	—	**0.4582**	**0.3486**	0.3814	0.0395
0.0772	0.0512	0.0448	0.0662	0.0162	0.1608	—	**0.1527**	0.045	**0.5132**
0.1106	0.0682	0.0663	0.0783	0.045	0.191	0.037	—	0.1306	**0.4139**
0.2262	0.1513	0.1497	0.1705	0.1234	0.2894	0.1261	0.1704	—	0.4547
0.1974	0.1624	0.156	0.166	0.1883	0.0196	0.1669	0.2022	0.3046	—

(FDR) (*n* = 166 total pairwise tests, tablewide *α* = 0.05), were conducted for all sample pairs. Statistical heterogeneity in allele frequencies was of panmixia was not rejected. Italics denote comparisons made among demes from within the Big Hole River (sample populations 1 through 5) because the Big Hole group contains sample populations 1–5. Bold type indicates sample pairs in which the allele size permutation test iden-

Swamp Creek (a tributary to the Big Hole River) and averaged 12.7 across all samples. The Big Hole River group exhibited higher allelic richness, using a sample of 36 genes (N_A^{36} = 13.24) and H_E (0.89), than the other native populations combined (i.e., populations 6–9; N_A^{36} = 9.46 and H_E = 0.79, $p < 0.05$ for both comparisons).

Genotypic frequencies were in HWE for 175 of 180 tests. Only Axolotol Lake (11), Miner Lake (7), and Bozeman Fish Technology Center (12) were out of HWE for 3 loci, 1 locus, and 1 locus, respectively (Table 3). Significant linkage disequilibrium was observed at only 10 of 801 pairs of loci tested over all populations, and all but one of linked pairs occurred in Axolotl Lake (*n* = 9 pairs of loci).

Individuals within sample populations did not appear to be highly related to one another, with a few exceptions. None of the populations violated the test assumption of being more related than expected based on a random draw of individuals from a panmictic population (lowest one-sided *p* value = 0.053, average *p* value = 0.56, SD = 0.32). Most populations had relatedness coefficients (*I*) less than 0.25 (i.e., analogous to half siblings; Table 3). Fish sampled in the Big Hole River were less related on average (mean *I* = 0.14) than fish sampled from the other native Missouri River populations (mean *I* = 0.25). The Sunnyslope Canal was nearly consistent with a population of full siblings (*I* = 0.49).

Population structure

We observed substantial genetic subdivision among grayling populations outside of the connected Big Hole River (Table 4). Pairwise F_{ST} estimates generally mirrored the differences in allele frequencies: genetic differentiation among demes within the connected Big Hole River was minimal ($F_{ST} \leq 0.0055$, homogeneity in allele frequencies in 8 of 10 comparisons), whereas differentiation between the Big Hole River group (i.e., populations 1–5) and all other wild native and naturalized populations was greater ($F_{ST} \geq 0.035$, heterogeneity in allele frequencies in 10 of 10 cases). The greatest differentiation was generally observed between Canadian-origin populations (Fuse Lake, Fond du Lac) and those from the Missouri River system (range F_{ST} = 0.13–0.31). Canadian-origin populations contained many alleles not found in any of the Montana populations, a high frequency of private alleles at six loci, and a very different distribution of allele size ranges (see Supplemental Table S2[1]). Pairwise F_{ST} values between the five native grayling populations in Montana (populations 1–5, 6, 7, 8, and 9) ranged from at least 0.071 between the combined Big Hole River group (1–5) and all other populations, to 0.174 between the Red Rock lakes (8) and the Madison River – Ennis Reservoir (9).

The global R_{ST} of 0.25 (95% CI 0.17–0.33; *n* = 14 populations (group 1–5 and populations 6–18)) was much larger than the corresponding global F_{ST} of 0.10 (95% CI 0.07–0.15), indicating that F_{ST} underestimates the actual levels of genetic structure in some comparisons. The allele size permutation test identified 41 of 91 pairwise comparisons of populations in which $R_{ST} > F_{ST}$ (Table 4; the 91 comparisons exclude individual estimates for sample sites within the connected Big Hole River group (populations 1, 2, 3, 4, and 5). Pairwise R_{ST} values were largest between Canadian-origin populations (14, 18) and the upper Missouri River populations (1–9), with the largest value (R_{ST} = 0.76) observed between Mussingbrod Lake (6) and Fond du Lac (18). Mussingbrod Lake (6) was the most genetically distinct among the native Missouri River populations (1–9) based on pairwise R_{ST} estimates. The introduced population in Bobcat Lake (16) had $R_{ST} > F_{ST}$ for all comparisons except when compared with Red Rock lakes (8).

The NJ dendrogram revealed five genetically distinct groups (Fig. 2). Distinctiveness of the Canadian-origin populations was highly supported with a 100% bootstrap support for the separation of these two populations from all others. The Big Hole River group was also very distinct with a 96% bootstrap support. Three moderately supported groups consisting of Red Rock Creek, Madison River, and the two isolated lakes in the Big Hole River watershed were also identified, although the relationships of these three groups to one another was not well defined. Affinity of the naturalized populations with their sources was apparent in the topology of dendrogram. Overall levels of genetic differentiation were greater among natural populations than among naturalized populations and their source populations.

Clusters of individuals from native grayling locations in the Missouri River (populations 1–9) identified using the Bayesian method of STRUCTURE (Pritchard et al. 2000) were consistent with patterns of population structure observed with genic tests, F_{ST}, R_{ST}, and the phylogenetic analysis (see Supplemental Table S3[3]). Evaluation of the assignment of individuals to six clusters had a clear biological interpretation based on geography and physical isolation. There was little support for population structure within the connected Big Hole River (populations 1–5); however, fish from this system did form a cluster that was distinct from the other locations sampled. Fish collected from Mussingbrod Lake (6), Miner Lake, Red Rock lakes (7), Madison River (8), and Fuse Lake (14) all formed distinct genetic clusters.

We did not detect a statistically significant isolation-by-distance effect based on based on genetic differentiation that considered mutation (R_{ST}, $n = 10$, Spearman's $r_S = 0.164$, Mantel p value = 0.35) among the five presumed native populations in the upper Missouri River system (see Supplemental Table S4[3]). Differentiation based on genetic drift (F_{ST}) did indicate isolation-by-distance (Supplemental Table S4[3]); however, F_{ST} underestimates differentiation among sample pairs that include Miner and Mussigbrod lakes, where differences are due, in part, to mutation (Table 4).

Effective population size

Historical N_e of native Missouri River grayling ranged from ~1800 to 20 000 and was highest for the Big Hole River group (~4000 – 20 000) and derived populations (Table 5). Estimates of contemporary N_e were generally much lower (11 of 15 populations < 500), though precision was low in some cases and six populations had estimates or upper confidence limits that were infinite. Contemporary N_e for most native Missouri River populations were typically between 150 and 300 (range 162.3–286.3), with the exception of Mussigbrod Lake ($N_e = 1496.8$). Effective size for the Big Hole River group was 207.6, but N_e for two derived populations (Axolotl Lake, Bozeman FTC) was much less (29.5 and 38, respectively).

Fig. 2. Genetic differentiation of Arctic grayling (*Thymallus arcticus*) populations from Canada, Montana, and Wyoming. Unrooted neighbor-joining dendrogram based on Cavalli-Sforza and Edwards (1967) chord distance (CSE) are calculated from allele frequencies at 10 microsatellite loci. Bootstrap probabilities, based on 1000 replicates, provide a measure of statistical confidence for each of the indicated clusters; the numbers leading to each cluster represent the percentage of times that the indicated samples clustered together in the simulated, random sampling replicates. Population symbols and numbers as are in Fig. 1, but with native Missouri River populations emphasized by solid triangles. Groups of populations inferred to share a common origin are enclosed by ellipses.

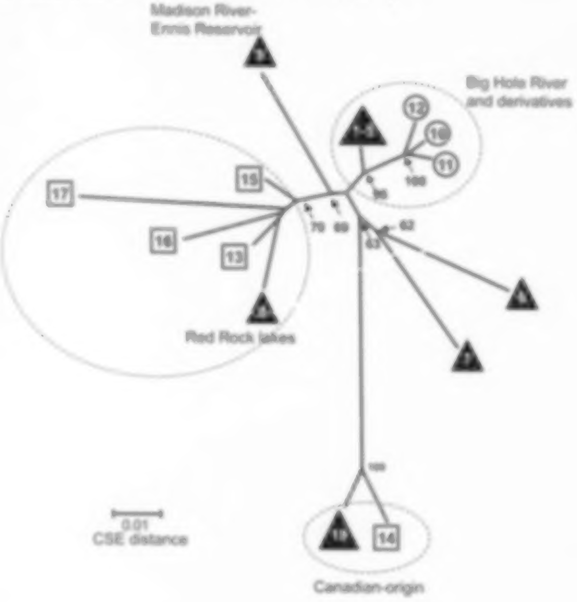

Six populations stood out in a bivariate plot of the mean number of alleles per locus versus the mean number of private alleles per locus (Fig. 3). Both Sunnyslope Canal and Madison River had low number of alleles and low level of private alleles, suggesting that these populations have small N_e relative to the rest of the populations and that they are genetically similar to the other Montana populations. The Canadian-origin populations had the highest levels of private alleles and an intermediate level of mean number of alleles, indicating long-term genetic isolation relative to Montana populations. Among Montana populations, Miner Lake had the most private alleles per locus, suggesting that it has had a relatively low level of gene flow with the other native Montana populations. The highest number of alleles was observed in the Big Hole River group, which is consistent with this population having a comparatively large N_e.

Population bottlenecks

The Ruby River and Axolotl Lake samples experienced recent bottlenecks based on the heterozygosity excess test. Thirteen of 14 sample populations exhibited bottlenecks by the M-ratio test using at least one of the presumed θ values. Only the Big Hole River group did not, though its M-ratio estimate (0.818) was close to the critical value at $\theta = 1$ ($M_c = 0.813$).

Table 5. Effective population sizes and genetic signatures of population bottlenecks in 14 populations of Arctic grayling (*Thymallus arcticus*).

		Effective population size			*M*-ratio bottleneck test		
		Long-term				M_C	
No.	Population	N_{eIAM}	N_{eSMM}	Contemporary N_e (95% CI)	*M* ratio	$\theta = 1$	$\theta = 10$
Native — upper Missouri River basin							
Upper Big Hole River watershed							
1–5	Big Hole River group	4045	20 411	207.6 (175.6–250.9)	0.818	0.813	0.796
6	Mussigbrod Lake	1773	4915	1496.8 (262.3–infinite)	0.747	0.802**	0.752*
7	Miner Lake	2278	7466	286.3 (142.8–4692.6)	0.787	0.801*	0.738
Red Rock lakes, Beaverhead River							
8	Red Rock Creek	2000	6000	228.2 (140.7–546.7)	0.772	0.802*	0.754
Madison River							
9	Madison River – Ennis Reservoir	1423	3448	162.3 (75.5–infinite)	0.653	0.795***	0.718**
Captive reserve and conservation — derived from Big Hole River							
10	Ruby River	3667	17 111	166.5 (119.4–265.6)	0.670[a]	0.805***	0.754***
11	Axolotl Lake	3667	17 111	29.5 (26.3–33.3)	0.695[a]	0.805***	0.760**
12	Bozeman FTC	2833	10 861	38.0 (32.8–44.5)	0.660	0.804***	0.753***
Introduced — other sources							
13	Odell Lake	2441	8400	576.9 (222.8–infinite)	0.794	0.804*	0.752
14	Fuse Lake	1500	3750	163.8 (88–694.1)	0.694	0.805**	0.752**
15	Grebe Lake	2833	10 861	–1013.7[b] (1011.1–infinite)	0.753	0.803**	0.752*
16	Bobcat Lake	2000	6000	252 (114.3–infinite)	0.694	0.803***	0.752**
17	Sunnyslope Canal	851	1576	32.5 (22.9–49.3)	0.575	0.805***	0.756***
Native — Saskatchewan, Canada							
18	Fond du Lac	1583	4090	131.8 (42.8–infinite)[c]	0.676	0.801**	0.735**

Note: Long-term effective population sizes were estimated with heterozygosity-based methods assuming either a stepwise (N_{eSMM}) or infinite allele mutation model (N_{eIAM}), which are presumed to bound the true long-term N_e. Contemporary N_e was based on the linkage disequilibrium estimator of Waples (2006). An estimated *M* ratio < the critical value (M_C) indicates a population bottleneck. Theta (θ) values of 1 and 10 correspond to prebottleneck effective population sizes of 500 and 5000, respectively, assuming a microsatellite mutation rate of 5×10^{-4}. Statistical significance: *, $p \leq 0.05$; **, $p \leq 0.01$; ***, $p \leq 0.001$.

[a] Sample populations that also exhibited genetic signatures of a population bottleneck based on heterozygosity excess included Ruby River ($p \leq 0.001$) and Axolotl Lake ($p \leq 0.01$).

[b] A negative point estimate for effective population size using program LDNe (Waples and Do 2008) means that there is no evidence for any disequilibrium caused by genetic drift due to a finite number of parents, i.e., N_e is infinite.

[c] Contemporary effective size estimate based on seven loci. Three loci (Tar110, Tar114, and Tar115) were removed for analysis because of missing data.

Discussion

Ancestry and population structure in Missouri River Arctic grayling

Microsatellite DNA markers confirm earlier findings that Arctic grayling from the upper Missouri River have been separated from Canadian populations for a long time, perhaps even before the most recent glacial advance (Redenbach and Taylor 1999). Private alleles in the Canadian populations were at high frequency with size distributions distinct from Montana samples, and very high R_{ST} values indicate that mutation, in addition to genetic drift, is responsible for the differentiation.

Arctic grayling from the connected Big Hole River form a genetic group distinct from other native populations in the Madison River – Ennis Reservoir and Red Rock lakes. In turn, there is also moderate support that these latter two populations each form discrete genetic groups. Population groupings based on protein electrophoresis previously found no genetic distinction between Big Hole River and Madison River grayling (Everett 1986; R. Leary, Montana Fish, Wildlife and Parks, University of Montana, Division of Biological Sciences, Missoula, MT 59812, USA, unpublished data), perhaps because only 2 of 39 allozyme loci were polymorphic.

With the exception of the Canadian-origin Fuse Lake population, naturalized lacustrine Arctic grayling populations in the data set appear to trace their ancestry to adfluvial grayling from Red Rocks lakes. This differs from the historical interpretation that fish from Madison River made a significant genetic contribution to naturalized populations derived from the Georgetown Lake and Washoe Park Hatchery populations (Kelly 1931; Everett 1986; Kaya 1990). These now-extinct stocks were a major source of further grayling introductions in Montana (Kaya 2000; MFWP 2005*b*). We were not able to locate archived tissue from Georgetown and Washoe grayling so the genetic composition of the stocked fish is unknown, but the most direct explanation for genetic similarity among naturalized populations is a common origin. We hypothesize that a founder effect from stocking fish of Red Rock origin is the reason for high R_{ST} in Bobcat Lake relative to all other populations except for Red Rock lakes. The distribution of allele sizes in Bobcat Lake grayling was consistent with other Missouri River samples, and Bobcat Lake grayling also cluster with Missouri River populations (and not those from Canada).

Fig. 3. Mean number of alleles and mean number of private alleles per locus over 10 loci for Arctic grayling (*Thymallus arcticus*) populations in Canada, Montana, and Wyoming. Error bars represent the standard error of the mean across loci. The location of a population on the mean number of alleles per locus axis is an indirect measure of the relative N_e among the sampled populations, and its location on the mean number of private alleles per locus axis is directly related to the degree of genetic distinction that population has relative to the other sampled populations. Both measures of genetic diversity were computed according to the rarefaction method of Kalinowski (2004) and a subsample of 36 chromosomes. See Table 1 for population numbers.

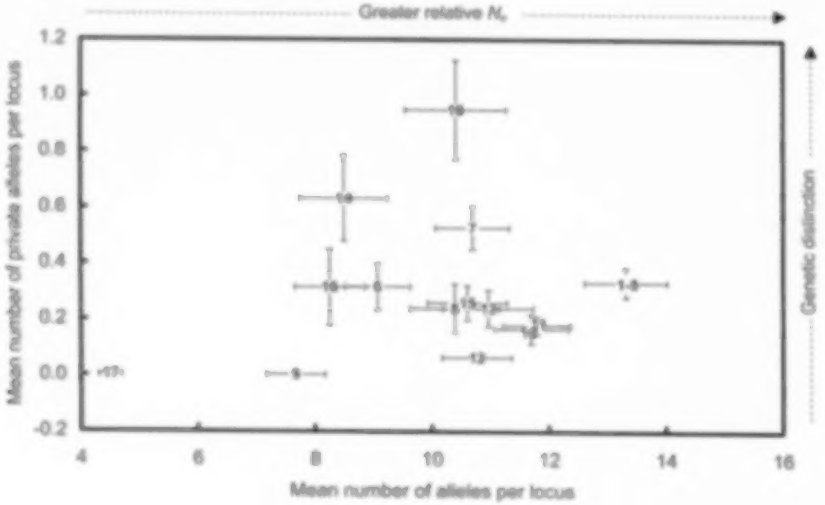

Genetic and biogeographic data suggest that Arctic grayling in Miner and Mussigbrod lakes may be remnant native populations. The level of genetic differentiation in these populations also indicates that they have been demographically independent for some time. Mussingbrod Lake had $R_{ST} > F_{ST}$ relative to the connected Big Hole River and Miner Lake, indicating that it has been isolated long enough for mutation to have contributed to its genetic distinction. In contrast, Miner Lake had $R_{ST} = F_{ST}$ relative to the connected Big Hole River, indicating that genetic drift has caused the observed differentiation and that the population has been isolated for less time than the Mussingbrod Lake population. Stocking of hatchery fish could also account for large R_{ST} values in these lakes; however, both Miner and Mussigbrod lakes were strongly differentiated from the Red Rock lakes population, with $R_{ST} > F_{ST}$ for both comparisons (F_{ST} = 0.15–0.16; R_{ST} = 0.32–0.48). In addition, Miner and Mussigbrod lakes did not cluster with other naturalized populations apparently derived from Red Rock lakes. Such differentiation would be unlikely if Red Rocks grayling were stocked in those waters and made a significant genetic contribution to the extant population. Presence of other native fishes in high-elevation lakes in the upper Big Hole River watershed (e.g., Vincent 1963) demonstrates historical connectivity with the mainstem river. Indigenous burbot (*Lota lota*) and longnose sucker (*Catostomus catostomus*) populations in Miner and Mussigbrod lakes (B. Snyder, Montana Fish, Wildlife and Parks, 1420 East Sixth Avenue, Helena, MT 59620-0701, USA, personal communication, 2006) implies that natural colonization by grayling was also possible. Consequently, we conclude that grayling populations in Miner and Mussigbrod lakes are not solely derived from stocking. The timing of the initial colonization of these lakes by grayling and other native fishes is unknown and warrants further investigation.

We found no evidence for introgression of Canadian-origin fish in Missouri River grayling samples. Moreover, we did not find any indication that extant native Arctic grayling in the Big Hole River, Madison River – Ennis Reservoir, or Red Rock lakes interbred with stocked fish originating from within the Missouri River basin or that these native populations now represent genetic admixtures. Genetic homogenization could be one consequence of interbreeding with hatchery grayling derived from a single source (e.g., Red Rock lakes). In contrast, all of the native Missouri River populations appear to form distinct genetic groups. Everett (1986) also concluded that stocking was not successful or contributed little to the spawning population in the Big Hole River and that geographic structuring was the most direct explanation for genetic (allozyme) differences among grayling in Montana and Wyoming.

Thymallus populations influenced by intraspecific stocking sometimes exhibit greater genetic diversity than unaltered native populations because of the introduction of nonnative genes and Wahlund effects (e.g., Gum et al. 2003). The Big Hole group was the most diverse sample population, but to attribute this to admixture from stocking, one would have to discount landscape genetic arguments that greater diversity in the Big Hole population (relative to other native populations) could be a function of multiple spawning locations and greater habitat extent (e.g., Neville et al. 2006) or habitat connectivity (e.g., Costello et al. 2003; Taylor et al. 2003; Wofford et al. 2005). A direct test of introgression (e.g., Koskinen et al. 2002*b*; Gum et al. 2006) was not possible for indigenous Missouri River grayling because we did not have any samples collected before stocking. Theoretically, stocking from different sources, or stocking from a single source following by genetic drift, could have affected the genetic characteristics of Big Hole River grayling. This appears unlikely given our data and considering that most attempts to introduce Arctic grayling into riverine habitats generally have not been successful (Northcote 1995; Kaya 2000; MFWP 2004).

Little or no recent gene flow has occurred among grayling populations in the Big Hole, Madison, and Beaverhead river subbasins or between Mussigbrod and Miner lakes in the Big Hole River watershed. In contrast, the data suggest recent genetic exchange among spawning sites within the connected Big Hole River, as the demes sampled were largely panmictic. The spatial scale of population structuring for Missouri River grayling (over hundreds of kilometres) is similar to observation of Arctic grayling from rivers in Alaska (Hop and Gharrett 1989) and British Columbia (Stamford and Taylor 2005). Landscape genetic variation in stream salmonids is driven by historical and contemporary factors such as glaciation and habitat modification (e.g., Costello et al. 2003; Taylor et al. 2003; Stamford and Taylor 2005); species-specific differences in behavior and life history (e.g., Wenburg et al. 1998; Heggenes et al. 2006; Neville et al. 2006), and ecological context (e.g., Haugen and Vøllestad 2000; Koskinen et al. 2001). Population genetic structure in *Thymallus* has been more frequently detected among subbasins (Koskinen et al. 2002*a*; Gum et al. 2003; but see Koskinen et al. 2001) relative to other salmonids that show differentiation at finer scales, such as among or within tributary streams (e.g., Carlsson et al. 1999; Taylor et al. 2003; Young et al. 2004).

We infer that the contemporary landscape genetic pattern observed in native Missouri River grayling represents historical population structure but recognize that dams may have fostered some of the observed differentiation among Big Hole, Madison, and Red Rock populations. Restricted gene flow promotes genetic drift, and habitat fragmentation can strongly influence genetic differentiation and diversity in stream fishes (Costello et al. 2003; Wofford et al. 2005), especially those such as Arctic grayling (e.g., Stamford and Taylor 2005) that can move hundreds of kilometres among complementary habitats (Armstrong 1986; Northcote 1995; MFWP 2003). Analysis of museum specimens may help determine whether contemporary factors have altered the genetic architecture that existed among Missouri River grayling populations prior to Euro-American settlement.

Demographic status and population declines inferred from genetic data

Arctic grayling in the Missouri River system were historically very abundant, with long-term N_e ranging from a few thousand to tens of thousands. There is some uncertainty as to the time frame and demographic scale associated with long-term estimates of effective population size (Waples 1991), but most authors agree that these estimates can be interpreted as the harmonic mean of the N_e in each generation among populations within a geographic region (Kalinowski and Waples 2002). In this case, the long-term estimates are best interpreted as N_e for Arctic grayling populations in the Missouri basin since the Wisconsin glacier receded approximately 10 000 years ago. Contemporary N_e for individual populations was significantly less than the long-term N_e. Most populations did not exhibit inbreeding (i.e., contemporary $N_e > 50$), but N_e were low enough to raise concern about maintaining adaptive potential.

Most populations showed genetic signatures of recent population declines, but the approximate timing of these bottlenecks varied. This study was correlative, so we cannot directly attribute a bottleneck to a specific causal factor, but the observations were generally consistent with the demographic histories of some populations. The most recent bottlenecks (heterozygosity excess) were detected in Axolotl Lake and Ruby River grayling, so we presume that 20 years of captivity and hatchery culture are proximate cause. Bottlenecks from declines occurring two or more decades ago (*M* ratio, e.g., Spear et al. 2006) were detected in every sample except the Big Hole River group.

We expected to find a bottleneck in the Big Hole group given that the population is at low abundance. Perhaps the genetic signatures of a bottleneck are not apparent, despite a demographic decline (e.g., see Busch et al. 2007), or the decline has been more gradual or smaller compared with other native populations. Arctic grayling still spawn in multiple locations in the Big Hole River and the mainstem migratory corridor is largely intact. In contrast, fragmentation of mainstem habitats likely contributed to bottlenecks observed in Red Rock lakes and the Madison River. In the Red Rock River system, grayling were extirpated from numerous tributary streams during the last 100 years, and the remaining adfluvial population in the headwater lakes was isolated by a barrier installed in 1957 (Nelson 1954; Vincent 1962; Mogen 1996). In the Madison River, the construction of impassible Ennis Dam >100 years ago constrained, if not eliminated, any expression of the fluvial life history for grayling (Vincent 1962; Kaya 1992). The residual (adfluvial) Madison River population may have been further affected by drawdowns of Ennis Reservoir in the 1960s–1980s, which reduced surface area by up to 15%–50% (MFWP 1990).

The Miner Lake and Mussigbrod Lake grayling populations have not been extensively monitored, so the causes of abrupt population decline are unknown. Loss of connection to the mainstem Big Hole River, winter oxygen deficits (die-offs), or competition with stocked grayling are possible factors. Few demographic data are available for naturalized lake populations, but the timing of bottlenecks suggests possible founder effects. The genetically depauparate and inbred Sunnyslope Canal population has been affected by irrigation management and seasonal dewatering (Barndt and Kaya 2000).

Conservation implications

Arctic grayling within the connected Big Hole River should tentatively be considered a single population because we detected no, to very low levels of, molecular divergence between putative demes within that system. This apparent panmixia could be a very recent development or a consistent pattern over the past few decades (W.R. Ardren and D.P. Peterson, unpublished data). The native Big Hole, Madison, Red Rock, Miner, and Mussigbrod populations in the Missouri River basin are demographically independent from one another. Genetic approaches to defining conservation and management units have been proposed (e.g., Crandall et al. 2000; Palsbøll et al. 2007), but anthropogenic isolation (especially in Big Hole, Madison, and Red Rock), and long-term reproductive isolation (e.g., Mussigbrod and Miner) among native populations dictates that they be managed as separate units. We presume that the native Missouri River populations were historically linked by occasional gene flow and must have exhibited some metapopulation-like structure (e.g., Rieman and Dunham 2000). In the future, facilitating habitat connectivity among subbasins occupied by native populations would help reduce genetic and stochastic risks. The challenge in doing this, however, will be considerable given existing fragmentation and habitat alteration and possible threats from further nonnative trout invasions (Fausch et al. 2009).

The Big Hole River population represents an important genetic reservoir for the species within the Missouri River basin and is also the last example of the riverine, migratory (fluvial) ecotype in the coterminous US (Kaya 1992). Genetic and life history diversity should help buffer populations against environmental variation, catastrophe, and anthropogenic stressors (e.g., Rieman and McIntyre 1993; Crandall et al. 2000; Fausch et al. 2006). By these criteria, the Big Hole River should be a high conservation priority. US state and federal agencies are working with private landowners in the upper Big Hole River basin to implement a conservation agreement to augment streamflows, restore riparian habitats, remove migration barriers, and reduce entrainment in irrigation ditches (MFWP 2006).

Efforts to use captive populations to re-establish wild fluvial populations in indigenous waters will probably continue to challenge grayling restoration biologists. Drought, nonnative trout, and a lack of imprinting by stocked fish may have limited reintroduction success of fluvial Arctic grayling in Montana (MFWP 2003, 2007). A general lack of connected, mainstem river habitats accessible to grayling may further constrain expression of a migratory life history at translocation sites. The genetic data suggest that additional factors may warrant investigation. First, genetic effects of captivity and culture may be unavoidable (e.g., Frankham 2008), and a slight reduction in genetic diversity has occurred in the ancestors of the captive population derived from Big Hole River grayling. There are no data to indicate that these observations are directly related to translocation success, but an examination of behavioral and physiological differences between wild and captive grayling (e.g., in a common-garden setting) or measurable changes in fitness (e.g., in captive or hatchery fish released into their indigenous habitats) would provide a more rigorous evaluation. Second, divergence among populations measured by molecular markers can potentially indicate differences in behavior, ecology, life history, and physiology (Stamford and Taylor 2005) that influence survival in specific habitats (Merilä and Crnokrak 2001; e.g., in *Thymallus*, see Koskinen et al. 2001; Salonen 2005). If genetic differentiation in the Big Hole River group is concordant with local adaptation (Taylor 1991), then a lack of ecological exchangeability (sensu Crandall et al. 2000) between subbasins may, in part, explain why translocations using Big Hole River grayling have yet to establish a self-sustaining population in another river. Common-garden experiments that test for unique or population-specific traits would provide insight into local adaptation. A systematic evaluation of factors influencing translocation success that also considers downscaled climate projections could generate spatially explicit decision support models to help guide future translocation efforts.

Although introductions using Big Hole River stock have not yet produced a self-sustaining fluvial population, few alternatives exist for ongoing translocations. Adfluvial Arctic grayling have not been successfully transplanted into rivers in Montana (Kaya 1992), and heritable behavioral differences exist between adfluvial and fluvial stocks (e.g., Kaya 1991; Kaya and Jeanes 1995). Madison River grayling are extremely rare (MFWP 2007), no brood reserve exists for the population, and the contemporary N_e (162.3) is based mostly on fish captured one or two generations ago. Moreover, these fish now exhibit an adfluvial life history, and it is unclear whether their descendents would re-express a fluvial life history. In the Missouri River basin, Big Hole River grayling theoretically provide a broader template for adaptation to novel environments or future environmental challenges because of their greater genetic diversity (Franklin and Frankham 1998; Lynch and Lande 1998). On the other hand, genetically depauperate populations can persist (e.g., Sunnyslope Canal). If maintaining diversity in captive populations of Big Hole grayling is important, then supplementation from the wild population is needed to limit genetic erosion. Adult grayling are presently at low abundance in the Big Hole River (MFWP 2005*a*, 2007), so genetic augmentation of the captive stocks awaits a demographic recovery of the Big Hole River population.

Acknowledgements

The authors dedicate this manuscript to the memory of Rebecca J. Everett. D. Campton (US Fish and Wildlife Service (USFWS)) provided a thoughtful literature review and synthesis that framed many of the questions addressed in this study. R. Leary (University of Montana and Montana Fish, Wildlife and Parks (MFWP)) provided a helpful review of the original study proposal. D. Campton and two anonymous reviewers provided helpful comments that improved the manuscript. M. Diggs completed the study's laboratory work. Erik Olsen provided database support. USFWS Region 6 and the US Bureau of Reclamation provided funding. M. Wilson (USFWS) provided administrative guidance during project conception. US Forest Service, MFWP, and numerous volunteers helped collect Arctic grayling fin clips in Montana. A. Steed (Montana State University) contributed samples from Grebe Lake, Yellowstone National Park, and J. Merkowsky provided samples from northeastern Saskatchewan, Canada. The findings and conclusions in the article are those of the authors and do not necessarily represent the views of the US Fish and Wildlife Service.

References

Allendorf, F.W., and Phelps, S.R. 1981. Use of allelic frequencies to describe population structure. Can. J. Fish. Aquat. Sci. **38**(12): 1507–1514. doi:10.1139/f81-203.

Allendorf, F.W., Leary, R.F., Spruell, P., and Wenburg, J.K. 2001. The problems with hybrids: setting conservation guidelines. Trends Ecol. Evol. **16**(11): 613–622. doi:10.1016/S0169-5347(01)02290-X.

Armstrong, R.H. 1986. A review of Arctic grayling studies in Alaska, 1952–1982. Biol. Papers Univ. Alaska, **23**: 3–17.

Barndt, S.A., and Kaya, C.M. 2000. Reproduction, growth, and winter habitat of Arctic grayling in an intermittent canal. Northwest Sci. **74**(4): 294–305.

Belkhir, K., Castric, V., and Bonhomme, F. 2002. IDENTIX, a software to test for relatedness in a population using permutation methods. Mol. Ecol. Notes, **2**(4): 611–614. doi:10.1046/j.1471-8286.2002.00273.x.

Bernatchez, L., and Wilson, C.C. 1998. Comparative phylogeography of Nearctic and Palearctic fishes. Mol. Ecol. **7**(4): 431–452. doi:10.1046/j.1365-294x.1998.00319.x.

Busch, J.D., Waser, P.M., and Dewoody, J.A. 2007. Recent demographic bottlenecks are not accompanied by a genetic signature in banner-tailed kangaroo rats (*Dipodomys spectabilis*). Mol. Ecol. **16**(12): 2450–2462. doi:10.1111/j.1365-294X.2007.03283.x. PMID:17561905.

Campton, D.E. 2006. Should Arctic grayling in the Big Hole River, Montana, be considered a distinct population segment (DPS) under the U.S. Endangered Species Act? An evaluation of existing genetic information. Report to Montana Field Office, US Fish and Wildlife Service. Conservation Genetics Laboratory, Abernathy Fish Technology Center, US Fish and Wildlife Service, Longview, Wash.

Carlsson, J., Olsén, K.H., Nilsson, J., Øverli, Ø., and Stabell, O.B. 1999. Microsatellites reveal fine-scale genetic structure in stream-living brown trout. J. Fish Biol. **55**(6): 1290–1303. doi:10.1111/j.1095-8649.1999.tb02076.x.

Cavalli-Sforza, L.L., and Edwards, A.W.F. 1967. Phylogenetic analysis: models and estimation procedures. Evolution, **21**(3): 550–570. doi:10.2307/2406616.

Cornuet, J.M., and Luikart, G. 1996. Description and power analysis of two tests for detecting recent population bottlenecks from allele frequency data. Genetics, **144**(4): 2001–2014. PMID:8978083.

Costello, A.B., Down, T.E., Pollard, S.M., Pacas, C.J., and Taylor, E.B. 2003. The influence of history and contemporary stream hydrology on the evolution of genetic diversity within species: an examination of microsatellite DNA variation in bull trout, *Salvelinus confluentus* (Pisces: Salmonidae). Evolution, **57**(2): 328–344. PMID:12683529.

Crandall, K.A., Bininda-Emonds, O.R.P., Mace, G.M., and Wayne, R.K. 2000. Considering evolutionary processes in conservation biology. Trends Ecol. Evol. **15**(7): 290–295. doi:10.1016/S0169-5347(00)01876-0. PMID:10856956.

Di Rienzo, A., Peterson, A.C., Garza, J.C., Valdes, A.M., Slatkin, M., and Freimer, N.B. 1994. Mutational processes of simple-sequence repeat loci in human populations. Proc. Natl. Acad. Sci. U.S.A. **91**(8): 3166–3170. doi:10.1073/pnas.91.8.3166. PMID:8159720.

Diggs, M.D., and Ardren, W.R. 2008. Characterization of 12 highly variable tetranucleotide microsatellite loci for Arctic grayling (*Thymallus arcticus*) and cross amplification in other *Thymallus* species. Mol. Ecol. Resour. **8**(4): 828–830. doi:10.1111/j.1755-0998.2007.02081.x.

Estoup, A., and Angers, B. 1998. Microsatellites and minisatellites for molecular ecology: theoretical and empirical considerations. *In* Advances in molecular ecology. *Edited by* G.R. Carvlho. NATO Science Series, IOS Press, Amsterdam, the Netherlands. pp. 55–36.

Everett, R.J. 1986. The population genetics of Arctic grayling (*Thymallus arcticus*) of Montana. M.Sc. thesis, University of Montana, Missoula, Montana.

Fausch, K.D., Rieman, B.E., Young, M.K., and Dunham, J.B. 2006. Strategies for conserving native salmonid populations at risk from nonnative fish invasions: tradeoffs in using barriers to upstream movement. USDA For. Serv. Rocky Mtn. Res. Stn. RMRS-GTR-174, Ft. Collins, Colo. Available at http://www.fs.fed.us/rm/boise/publications/fisheries/rmrs_gtr174.pdf.

Fausch, K.D., Rieman, B.E., Dunham, J.B., Young, M.K., and Peterson, D.P. 2009. Invasion versus isolation: trade-offs in managing native salmonids with barriers to upstream movement. Conserv. Biol. **23**(4): 859–870. doi:10.1111/j.1523-1739.2008.01159.x. PMID:19210302.

Felsenstein, J. 1992. PHYLIP (Phylogeny Inference Package). Version 3.5C. Department of Genetics, SK-50, University of Washington, Seattle, Washington.

Frankham, R. 2008. Genetic adaptation to captivity in species conservation programs. Mol. Ecol. **17**(1): 325–333. doi:10.1111/j.1365-294X.2007.03399.x. PMID:18173504.

Franklin, I.R., and Frankham, R. 1998. How large must populations be to retain evolutionary potential? Anim. Conserv. **1**(1): 69–70. doi:10.1111/j.1469-1795.1998.tb00228.x.

Froufe, E., Knizhin, I., and Weiss, S. 2005. Phylogenetic analysis of the genus *Thymallus* (grayling) based on mtDNA control region and ATPase 6 genes, with inferences on control region constraints and broad-scale Eurasian phylogeography. Mol. Phylogenet. Evol. **34**(1): 106–117. doi:10.1016/j.ympev.2004.09.009. PMID:15579385.

Garza, J.C., and Williamson, E.G. 2001. Detection of reduction in population size using data from microsatellite loci. Mol. Ecol. **10**(2): 305–318. doi:10.1046/j.1365-294x.2001.01190.x. PMID:11298947.

Goudet, J. 2001. FSTAT, a program to estimate and test gene diversities and fixation indices (version 2.9.3) [updated from Goudet 1995]. Available at www2.unil.ch/popgen/softwares/fstat.html [updated 23 August 2005].

Gum, B., Gross, R., Rottmann, O., Schröder, W., and Kühn, R. 2003. Microsatellite variation in Bavarian populations of European grayling (*Thymallus thymallus*): implications for conservation. Conserv. Genet. **4**(6): 659–672. doi:10.1023/B:COGE.0000006106.64243.e6.

Gum, B., Gross, R., and Kuehn, R. 2006. Discriminating the impact of recent human mediated stock transfer from historical gene flow on genetic structure of European grayling *Thymallus thymallus* L. J. Fish Biol. **69**(Suppl. C): 115–135. doi:10.1111/j.1095-8649.2006.01264.x.

Guo, S.W., and Thompson, E.A. 1992. Performing the exact test of Hardy–Weinberg proportion for multiple alleles. Biometrics, **48**(2): 361–372. doi:10.2307/2532296. PMID:1637966.

Hardy, O.J., and Vekemans, X. 2002. SPAGeDi: a versatile computer program to analyze spatial genetic structure at the individual or population levels. Mol. Ecol. Notes, **2**(4): 618–620. doi:10.1046/j.1471-8286.2002.00305.x.

Hardy, O.J., Charbonnel, N., Freville, H., and Heuertz, M. 2003. Microsatellite allele sizes: a simple test to assess their significance on genetic differentiation. Genetics, **163**: 1467–1482. PMID:12702690.

Hartl, D.L., and Clark, A.G. 1989. Principles of population genetics. 2nd ed. Sinauer & Associates, Sunderland, Massachusetts.

Haugen, T.O., and Vøllestad, L.A. 2000. Population differences in early life-history traits in grayling. J. Evol. Biol. **13**(6): 897–905. doi:10.1046/j.1420-9101.2000.00242.x.

Hedrick, P.W. 1999. Perspective: highly variable loci and their interpretation in evolution and conservation. Evolution, **53**(2): 313–318. doi:10.2307/2640768.

Heggenes, J., Qvenild, T., Stamford, M.D., and Taylor, E.B. 2006. Genetic structure in relation to movements in wild European grayling (*Thymallus thymallus*) in three Norwegian rivers. Can. J. Fish. Aquat. Sci. **63**(6): 1309–1319. doi:10.1139/F06-028.

Hendry, A.P., Castric, V., Kinnison, M.T., and Quinn, T.P. 2004. The evolution of philopatry and dispersal: homing and straying in salmonids. *In* Evolution illuminated — salmon and their relatives. *Edited by* A.P. Hendry and S.C. Stearns. Oxford University Press, New York. pp. 52–91.

Hop, H., and Gharrett, A.J. 1989. Genetic relationships of Arctic grayling in the Koyukuk and Tanana Rivers, Alaska. Trans. Am. Fish. Soc. **118**(3): 290–295. doi:10.1577/1548-8659(1989)118<0290:GROAGI>2.3.CO;2.

Hubbs, C.L., and Lagler, K.F. 1949. Fishes of the Great Lakes Region. Bull. No. 26, Cranbrook Institute of Science, Bloomfield Hills, Michigan.

Kalinowski, S.T. 2004. Counting alleles with rarefaction: private alleles and hierarchical sampling designs. Conserv. Genet. **5**(4): 539–543. doi:10.1023/B:COGE.0000041021.91777.1a.

Kalinowski, S.T. 2005. HP-RARE 1.0: a computer program for performing rarefaction on measures of allelic richness. Mol. Ecol. Notes, **5**(1): 187–189. doi:10.1111/j.1471-8286.2004.00845.x.

Kalinowski, S.T., and Waples, R.S. 2002. The ratio of effective to census size in fluctuating populations. Conserv. Biol. **16**(1): 129–136. doi:10.1046/j.1523-1739.2002.00134.x.

Kaya, C.M. 1990. Status report on fluvial Arctic grayling (*Thymallus arcticus*) in Montana. Report to Montana Fish, Wildlife and Parks, 1420 E. 6th Avenue, P.O. Box 200701, Helena, MT 59620, USA.

Kaya, C.M. 1991. Rheotactic differentiation between fluvial and lacustrine populations of Arctic grayling (*Thymallus arcticus*), and implications for the only remaining indigenous population of fluvial Montana grayling. Can. J. Fish. Aquat. Sci. **48**(1): 53–59. doi:10.1139/f91-008.

Kaya, C.M. 1992. Review of the decline and status of fluvial Arctic grayling, *Thymallus arcticus*, in Montana. Proc. Mont. Acad. Sci. **1992**: 43–70.

Kaya, C.M. 2000. Arctic grayling in Yellowstone: status, management and recent restoration efforts. Yellowstone Sci. **8**(3): 12–17. Available at www.nps.gov/yell/planyourvisit/yellsci-issues.htm.

Kaya, C.M., and Jeanes, E.D. 1995. Retention of adaptive rheotactic behavior by F1 fluvial Arctic grayling. Trans. Am. Fish. Soc. **124**(3): 453–457. doi:10.1577/1548-8659(1995)124<0453:NROARB>2.3.CO;2.

Kelly, J.L. 1931. Nation watches Montana grayling. Mont. Wildl. **3**(8): 9–11.

Koskinen, M.T., Piironen, J., and Primmer, C.R. 2001. Interpopulation genetic divergence in European grayling (*Thymallus thymallus*, Salmonidae) at a microgeographic scale: implications for conservation. Conserv. Genet. **2**(2): 133–143. doi:10.1023/A:1011814528664.

Koskinen, M.T., Knizhin, I., Primmer, C.R., Schlötterer, C., and Weiss, S. 2002*a*. Mitochondrial and nuclear DNA phylogeography of *Thymallus* spp. (grayling) provides evidence of ice-age mediated environmental perturbations in the world's oldest body of fresh water, Lake Baikal. Mol. Ecol. **11**(12): 2599–2611. doi:10.1046/j.1365-294X.2002.01642.x. PMID:12453243.

Koskinen, M.T., Sundell, P., Piironen, J., and Primmer, C.R. 2002*b*. Genetic assessment of spatiotemporal evoluationary relationships and stocking effects in grayling (*Thymallus thymallus*, Salmonidae). Ecol. Lett. **5**(2): 193–205. doi:10.1046/j.1461-0248.2002.00302.x.

Liknes, G.A., and Gould, W.R. 1987. The distribution, habitat and population characteristics of fluvial Arctic grayling (*Thymallus arcticus*) in Montana. Northwest Sci. **61**(2): 122–129.

Lippé, C., Dumont, P., and Bernatchez, L. 2006. High genetic diversity and no inbreeding in the endangered copper redhorse, *Moxostoma hubbsi* (Catostomidae, Pisces): the positive sides of a long generation time. Mol. Ecol. **15**(7): 1769–1780. doi:10.1111/j.1365-294X.2006.02902.x. PMID:16689897.

Luikart, G., and Cornuet, J.-M. 1998. Empirical evaluation of a test for identifying recently bottlenecked populations from allele frequency data. Conserv. Biol. **12**(1): 228–237. doi:10.1046/j.1523-1739.1998.96388.x.

Lynch, M., and Lande, R. 1998. The critical effective size for a genetically secure population. Anim. Conserv. **1**(1): 70–72. doi:10.1111/j.1469-1795.1998.tb00229.x.

Meldgaard, T., Nielsen, E.E., and Loeschcke, V. 2003. Fragmentation by weirs in a riverine system: a study of genetic variation in time and space among populations of European grayling (*Thymallus thymallus*) in a Danish river system. Conserv. Genet. **4**(6): 735–747. doi:10.1023/B:COGE.0000006115.14106.de.

Merilä, J., and Crnokrak, P. 2001. Comparison of genetic differentiation at marker loci and quantitative traits. J. Evol. Biol. **14**(6): 892–903. doi:10.1046/j.1420-9101.2001.00348.x.

Montana Fish, Wildlife and Parks. 1990. Ennis Reservoir/Madison River fisheries investigation: draft final report 1990. Report to Montana Power Company. Montana Fish, Wildlife, and Parks, 1400 S. 19th Avenue, Bozeman, MT 59718, USA.

Montana Fish, Wildlife and Parks. 1995. Montana fluvial Arctic grayling recovery plan. Report to the Montana Fluvial Arctic Grayling Workgroup. Montana Fish, Wildlife and Parks, 1420 E. 6th Avenue, P.O. Box 200701, Helena, MT 59620, USA.

Montana Fish, Wildlife and Parks. 2003. Movement and habitat selection of Arctic grayling, brook trout, and mountain whitefish during drought conditions in the Big Hole River, Montana. Montana Fish, Wildlife and Parks, 1400 S. 19th Avenue, Bozeman, MT 59718, USA.

Montana Fish, Wildlife and Parks. 2004. Reintroducing fluvial Arctic grayling (*Thymallus arcticus*) to the upper Ruby River, MT — a progress report. Montana Fish, Wildlife, and Parks, 730 N. Montana Street, Dillon, MT 59725, USA. Available at http://fwp.mt.gov/content/getItem.aspx?id=17931.

Montana Fish, Wildlife and Parks. 2005*a*. Fluvial Arctic grayling monitoring report 2004. Montana Fish, Wildlife, and Parks, 730 N. Montana Street, Dillon, MT 59725, USA. Available at http://fwp.mt.gov/content/getItem.aspx?id=10698.

Montana Fish, Wildlife and Parks. 2005*b*. Montana fish plants. Electronic database, version VB6-A2K-CR85-01262005. Montana Fish, Wildlife and Parks, 1400 S. 19th Avenue, Bozeman, MT 59718, USA.

Montana Fish, Wildlife and Parks. 2006. Candidate conservation agreement with assurances for fluvial Arctic grayling in the upper Big Hole River. Montana, Fish, Wildlife and Parks, 1420 E. 6th Avenue, P.O. Box 200701, Helena, MT 59620, USA. Available at http://fwp.mt.gov/content/getItem.aspx?id=11428.

Montana Fish, Wildlife and Parks. 2007. Arctic grayling recovery program — Montana Arctic grayling monitoring report 2006. Montana Fish, Wildlife, and Parks, 730 N. Montana Street, Dillon, Montana 59725, USA. Available at http://fwp.mt.gov/content/getItem.aspx?id=28962.

Mogen, J.T. 1996. Status and biology of the spawning population of Red Rock Lakes Arctic grayling. M.Sc. thesis, Montana State University, Bozeman, Montana.

Morris, W.F., and Doak, D.F. 2002. Quantitative conservation biology: theory and practice of population viability analysis. Sinauer Associates, Inc., Sunderland, Massachusetts.

Narum, S.R. 2006. Beyond Bonferroni: less conservative analyses for conservation genetics. Conserv. Genet. **7**(5): 783–787. doi:10.1007/s10592-005-9056-y.

Nei, M. 1987. Molecular evolutionary genetics. Columbia University Press, New York.

Nelson, P.H. 1954. Life history and management of the American grayling (*Thymallus signifer tricolor*) in Montana. J. Wildl. Manage. **18**(3): 324–342. doi:10.2307/3797019.

Neville, H.M., Dunham, J.B., and Peacock, M.M. 2006. Landscape attributes and life history variability shape genetic structure of trout populations in a stream network. Landsc. Ecol. **21**(6): 901–916. doi:10.1007/s10980-005-5221-4.

Nielsen, E.E., Hansen, M.M., and Loeschcke, V. 1999. Genetic variation in time and space: microsatellite analysis of extinct and extant populations of Atlantic salmon. Evolution, **53**(1): 261–268. doi:10.2307/2640938.

Northcote, T.G. 1995. Comparative biology and management of Arctic and European grayling (Salmonidae, *Thymallus*). Rev. Fish Biol. Fish. **5**(2): 141–194.

Ohta, T., and Kimura, M. 1973. A model of mutation appropriate to estimate the number of electrophoretically detectable alleles in a finite population. Genet. Res. **22**(2): 201–204. PMID: 4777279.

Palsbøll, P.J., Bérubé, M., and Allendorf, F.W. 2007. Identification of management units using population genetic data. Trends Ecol. Evol. **22**(1): 11–16. doi:10.1016/j.tree.2006.09.003.

Pearse, D.E., and Crandall, K.A. 2004. Beyond F_{ST}: analysis of population genetic data for conservation. Conserv. Genet. **5**(5): 585–602. doi:10.1007/s10592-003-1863-4.

Pielou, E.C. 1991. After the Ice Age: the return of life to glaciated North America. The University of Chicago Press, Chicago, Illinois.

Piry, S., Luikart, G., and Cornuet, J.-M. 1999. BOTTLENECK: a computer program for detecting recent reductions in the effective population size using allele frequency data. J. Hered. **90**(4): 502–503. doi:10.1093/jhered/90.4.502.

Pritchard, J.K., Stephens, M., and Donnelly, P. 2000. Inference of population structure using multilocus genotype data. Genetics, **155**(2): 945–959. PMID:10835412.

Randall, L.C. 1978. Red Rock Lakes National Wildlife Refuge: an aquatic history 1988–1977. US Fish and Wildlife Service, 780 Creston Hatchery Road, Kalispell, MT 59901, USA.

Raymond, M., and Rousset, F. 1995. GENEPOP (version 1.2): population genetics software for exact tests and ecumenicism. J. Hered. **86**(3): 248–249.

Redenbach, Z., and Taylor, E.B. 1999. Zoogeographical implications of variation in mitochondrial DNA of Arctic grayling (*Thymallus arcticus*). Mol. Ecol. **8**(1): 23–35. doi:10.1046/j.1365-294X.1999.00516.x. PMID:9919695.

Rice, W. 1989. Analyzing tables of statistical tests. Evolution, **43**(1): 223–225. doi:10.2307/2409177.

Rieman, B.E., and Dunham, J.B. 2000. Metapopulations and salmonids: a synthesis of life history patterns and empirical observations. Ecol. Freshwat. Fish, **9**(1–2): 51–64. doi:10.1034/j.1600-0633.2000.90106.x.

Rieman, B.E., and McIntyre, J.D. 1993. Demographic and habitat requirements for conservation of bull trout. USDA For. Serv. GTR-INT-302, Boise, Idaho.

Rousset, F. 1997. Genetic differentiation and estimation of gene flow from *F*-statistics under isolation by distance. Genetics, **145**(4): 1219–1228. PMID:9093870.

Salonen, A. 2005. Behavioural and morphological variation in European grayling, *Thymallus thymallus*, populations. Ph.D. thesis, University of Helsinki, Finland. Available at http://ethesis.helsinki.fi/julkaisut/bio/bioja/vk/salonen/behaviou.pdf.

Scott, W.B., and Crossman, E.J. 1973. Freshwater fishes of Canada. Bull. Fish. Res. Board Can. No. 184.

So, N., Maes, G.E., and Volckaert, F.A.M. 2006. High genetic diversity in cryptic populations of the migratory sutchi catfish *Pangasianodon hypophthalmus* in the Mekong River. Heredity, **96**(2): 166–174. doi:10.1038/sj.hdy.6800781. PMID:16369576.

Spear, S.F., Peterson, C.R., Matocq, M.D., and Storfer, A. 2006. Molecular evidence for historical and recent population size reductions of tiger salamanders (*Ambystoma tigrinum*) in Yellowstone National Park. Conserv. Genet. **7**(4): 605–611. doi:10.1007/s10592-005-9095-4.

Stamford, M.D., and Taylor, E.B. 2004. Phylogeographical lineages of Arctic grayling (*Thymallus arcticus*) in North America: divergence, origins and affinities with Eurasian *Thymallus*. Mol. Ecol. **13**(6): 1533–1549. doi:10.1111/j.1365-294X.2004.02174.x. PMID:15140096.

Stamford, M.D., and Taylor, E.B. 2005. Population subdivision and genetic signatures of demographic changes in Arctic grayling (*Thymallus arcticus*) from an impounded watershed. Can. J. Fish. Aquat. Sci. **62**(11): 2548–2559. doi:10.1139/f05-156.

Taylor, E.B. 1991. A review of local adaptation in Salmonidae, with particular reference to Pacific and Atlantic salmon. Aquaculture, **98**(1–3): 185–207. doi:10.1016/0044-8486(91)90383-I.

Taylor, E.B., Stamford, M.D., and Baxter, J.S. 2003. Population subdivision in westslope cutthroat trout (*Oncorhynchus clarki lewisi*) at the northern periphery of its range: evolutionary inferences and conservation implications. Mol. Ecol. **12**(10): 2609–2622. doi:10.1046/j.1365-294X.2003.01937.x. PMID:12969465.

US Fish and Wildlife Service. 2007. Endangered and threatened wildlife and plants: revised 12-month finding for Upper Missouri River Distinct Population Segment of Fluvial Arctic Grayling. Fed. Regist. **72**(78): 20305–20314.

Vincent, R.E. 1962. Biogeographical and ecological factors contributing to the decline of Arctic grayling (*Thymallus arcticus*) in Michigan and Montana. Ph.D. thesis, University of Michigan, Ann Arbor, Michigan.

Vincent, R.E. 1963. The native range of lake trout (*Salvelinus namaycush*) in Montana. Copeia, **1963**(1): 188–189. doi:10.2307/1441313.

Waples, R.S. 1991. Genetic methods for estimating the effective size of cetacean populations. *In* Genetic ecology of whales and dolphins. Special issue No. 13. *Edited by* A.R. Hoelzel. International Whale Commission, London, UK. pp. 279–300.

Waples, R.S. 2006. A bias correction for estimates of effective population size based on linkage disequilibrium at unlinked gene loci. Conserv. Genet. **7**(2): 167–184. doi:10.1007/s10592-005-9100-y.

Waples, R.S., and Do, C. 2008. LDNe: a program for estimating effective population size from data on linkage disequilibrium. Mol. Ecol. Resour. **8**(4): 753–756. doi:10.1111/j.1755-0998.2007.02061.x.

Waples, R.S., and Gaggiotti, O. 2006. What is a population? An empirical evaluation of some genetic methods for identifying the number of gene pools and their degree of connectivity. Mol. Ecol. **15**(6): 1419–1439. doi:10.1111/j.1365-294X.2006.02890.x. PMID:16629801.

Weir, B.S., and Cockerham, C.C. 1984. Estimating *F*-statistics for the analysis of population structure. Evolution, **38**(6): 1358–1370. doi:10.2307/2408641.

Weiss, S., Persat, H., Eppe, R., Schlötterer, C., and Uiblein, F. 2002. Complex patterns of colonization and refugia revealed for European grayling, *Thymallus thymallus*, based on complete sequencing of the mitochondrial DNA control region. Mol. Ecol. **11**(8): 1393–1407. doi:10.1046/j.1365-294X.2002.01544.x. PMID:12144660.

Weiss, S., Knizhin, I., Kirillov, A., and Froufe, E. 2006. Phenotypic and genetic differentiation of two major phylogeographical lineages of Arctic grayling, *Thymallus arcticus*, in the Lena River and surrounding Arctic drainages. Biol. J. Linn. Soc. **88**(4): 511–525. doi:10.1111/j.1095-8312.2006.00621.x.

Wenburg, J.K., Bentzen, P., and Foote, C.J. 1998. Microsatellite analysis of genetic population structure in an endangered salmonid: the coastal cutthroat trout (*Oncorhynchus clarki clarki*). Mol. Ecol. **7**(6): 733–749. doi:10.1046/j.1365-294x.1998.00386.x.

Williamson-Natesan, E.G. 2005. Comparison of methods for detecting bottlenecks from microsatellite loci. Conserv. Genet. **6**(4): 551–562. doi:10.1007/s10592-005-9009-5.

Wofford, J.E., Gresswell, R.E., and Banks, M.A. 2005. Influence of barriers to movement on within-watershed genetic variation of coastal cutthroat trout. Ecol. Appl. **15**(2): 628–637. doi:10.1890/04-0095.

Young, S.F., McLellan, J.G., and Shaklee, J.B. 2004. Genetic integrity and microgeographic population structure of westslope cutthroat trout, *Oncorhynchus clarki lewisi*, in the Pend Oreille Basin in Washington. Environ. Biol. Fishes, **69**(1–4): 127–142. doi:10.1023/B:EBFI.0000022886.47243.bf.

Hierarchical Bayesian analysis to incorporate age uncertainty in growth curve analysis and estimates of age from length: Florida manatee (*Trichechus manatus*) carcasses

Lisa K. Schwarz and Michael C. Runge

Abstract: Age estimation of individuals is often an integral part of species management research, and a number of age-estimation techniques are commonly employed. Often, the error in these techniques is not quantified or accounted for in other analyses, particularly in growth curve models used to describe physiological responses to environment and human impacts. Also, noninvasive, quick, and inexpensive methods to estimate age are needed. This research aims to provide two Bayesian methods to (*i*) incorporate age uncertainty into an age–length Schnute growth model and (*ii*) produce a method from the growth model to estimate age from length. The methods are then employed for Florida manatee (*Trichechus manatus*) carcasses. After quantifying the uncertainty in the aging technique (counts of ear bone growth layers), we fit age–length data to the Schnute growth model separately by sex and season. Independent prior information about population age structure and the results of the Schnute model are then combined to estimate age from length. Results describing the age–length relationship agree with our understanding of manatee biology. The new methods allow us to estimate age, with quantified uncertainty, for 98% of collected carcasses: 36% from ear bones, 62% from length.

Résumé : L'estimation de l'âge des individus fait souvent partie intégrante de la recherche sur la gestion des espèces et plusieurs méthodes d'estimation de l'âge sont en usage courant. Il arrive souvent que l'on ne mesure pas l'erreur associée à ces méthodes ou qu'on n'en tienne pas compte dans les autres analyses, particulièrement dans les modèles de courbe de croissance utilisés pour décrire les réactions physiologiques aux impacts environnementaux et anthropiques. De plus, il existe un besoin de méthodes non invasives, rapides et peu coûteuses d'estimation de l'âge. Notre recherche vise à fournir deux méthodes bayésiennes pour (*i*) incorporer l'incertitude associée à l'âge dans un modèle de croissance âge–longueur de Schnute et (*ii*) produire, à partir du modèle de croissance, une méthode pour estimer l'âge à partir de la longueur. Nous avons ensuite utilisé les méthodes sur des carcasses de lamantins de Floride (*Trichechus manatus*). Après avoir déterminé l'incertitude dans la technique de détermination de l'âge (dénombrement des couches de croissance des osselets de l'oreille), nous avons ajusté les données d'âge–longueur au modèle de croissance de Schnute séparément en fonction du sexe et de la saison. Nous avons ensuite combiné des renseignements a priori indépendants au sujet de la structure en âge de la population aux résultats du modèle de Schnute pour estimer l'âge à partir de la longueur. Les résultats qui décrivent la relation âge–longueur s'accordent avec notre compréhension actuelle de la biologie des lamantins. Les nouvelles méthodes nous ont permis d'estimer l'âge, avec une incertitude connue, de 98 % des carcasses récoltées : 36 % à partir des osselets de l'oreille et 62 % à partir de la longueur.

[Traduit par la Rédaction]

Introduction

Age estimation of individuals is often an integral part of population dynamics research because species may have age-specific survival and reproductive rates that are vital components in determining population growth rates, and population age structure can be important in determining extinction probabilities (Caswell 2001). Many techniques exist to estimate age when secondary physiological characteristics, e.g., sizes of bones or counts of growth layers in various tissues or structures, are the only source of data to estimate age. However, such methods give rise to error through limited resolution, inconsistencies, or biases in measurements or via inherent variability in the process (Gil-

---

Received 13 October 2008. Accepted 8 July 2009. Published on the NRC Research Press Web site at cjfas.nrc.ca on 13 October 2009.
J20817

Paper handled by Associate Editor Steven Campana.

L.K. Schwarz.[1,2] Environmental Statistics Group, Department of Ecology, Montana State University, Bozeman, MT 59717-3460, USA.
M.C. Runge. US Geological Survey Patuxent Wildlife Research Center, 12100 Beech Forest Road, Laurel, MD 20708, USA.

[1] Corresponding author (e-mail: schwarz@biology.ucsc.edu).

[2] Present address: Department of Ecology and Evolutionary Biology, Earth and Marine Sciences A308, University of California – Santa Cruz, Santa Cruz, CA 95064, USA.

Can. J. Fish. Aquat. Sci. **66**: 1775–1789 (2009) doi:10.1139/F09-117 Published by NRC Research Press

bert and Stolt 1970; Hohn 1990; Stewart et al. 2006). Interactions between resolution and age can produce further biases (Leberg et al. 1989). Overlooking such error in age measurements can create inaccuracies in growth, recruitment, and mortality analyses, leading to significant consequences for species management (Beamish and McFarlane 1983; Kimura and Lyons 1991; Campana 2001). In particular, some methods have incorporated age error into growth curve models (Leberg et al. 1989; Cope and Punt 2007), but growth curve research often does not account for age uncertainty (Demirhan and Can 2009; Moura et al. 2009; Uehara et al. 2009).

In addition, although some techniques may provide more precise age estimates than others, the procedures can be time-consuming and expensive. Tissue collection methods may also be invasive, or tissue samples may only be available postmortem. Thus, a noninvasive, field-readable metric that is correlated with age would be valuable.

This research provides two Bayesian methods to (*i*) incorporate quantified age uncertainty into Schnute growth curve analysis and (*ii*) use results from the growth curve analysis in conjunction with independent data on population age structure to produce estimates of age from length. The models can be developed for any species when error in the aging technique is quantified and when some age–length and life history data are available. The total-body-length method may provide less precise age estimates compared with other aging techniques, particularly for longer animals that have reached their maximum length. However, length is easy to measure and can be an effective aging method when other methods are not feasible.

We then employ the methods using data from carcasses collected by the Florida Manatee (*Trichechus manatus latirostris*) Carcass Recovery and Necropsy Program, an important potential source of population dynamics information for scientists and managers working to protect this endangered species. After quantifying error in the aging technique (measured as counts of ear bone growth layers), we estimate Schnute growth curve parameters based on measured total body length and ear bone age estimates. Lastly, we construct methods to estimate age, with quantified error, from length.

The Florida Manatee Carcass Recovery and Necropsy Program has collected and necropsied almost all carcasses reported since 1974, leading to a data set of over 5800 specimens through 2005. The manatee's unique physiological characteristics, namely tooth replacement and bone resorption, make age estimation particularly challenging for this species. However, Marmontel et al. (1996) established a technique to estimate ages of Florida manatee carcasses via counts of bone layers in ear bones. Although the precise physiological mechanism for ear bone layer formation is not known, Marmontel et al. (1996) were able to show that the bone layers form annually. They calibrated their ear bone age estimates using carcasses of known age ($n_{\text{known age}} = 7$) and carcasses of animals marked with tetracycline at a known interval before death ($n_{\text{tetracycline marked}} = 10$). Although the calibration sample size was small, there was strong evidence for one growth layer group per year. Variable environmental factors may affect the physical characteristics of growth layer groups, but the actual formation of growth layers appears to be based on endogenous rhythms rather than on environmental effects such as seasonal fluctuations in temperature or food availability. Namely, manatees that spent either a portion or all of their lives in captivity, where environmental conditions were constant, exhibited the same growth layer patterns as noncaptive individuals (Marmontel et al. 1996). However, manatee bone resorption may be correlated with environmental conditions (Marmontel et al. 1996). Since the introduction of this technique, age has been estimated from ear bone growth layer counts for about one-third of the collected Florida manatee carcasses. The age determination method is complex and time-consuming, and sampling has been sporadic and nonrandom over the years (Schwarz 2004).

The ear bone aging method may include several sources of error. Marmontel et al. (1996) suggested that variability in the number of ear bone growth layers for the animals of the same age (process error) may be large because of individual variations in resorption of growth layers. In addition, measurement error increases with age as bone is resorbed and becomes more difficult to "read", and resorption is more common in females. Lastly, because ear bone growth layer counts measure age on an annual scale, they provide poor resolution of age for young animals when birth month is not known.

Uncertainty in the ear bone aging technique has never been quantified, and because the subsample of ear-bone-aged carcasses is nonrandom, there is a strong need to estimate ages of carcasses that have not been ear-bone-aged. Ninety-eight percent of carcasses have been measured for total body length, so length could be an effective way to estimate age in the carcass subsample that lacks ear bone age estimates. After quantifying error in the ear bone aging technique, we use the proposed Bayesian approach to fit a Schnute curve to age–length data, incorporating uncertainty in the ear bone aging technique. Lastly, Schnute curve estimates of length given age are combined with an independent prior on probability of age in a second Bayesian model to provide estimates of age from length. Although the resulting growth model should not be directly applied to the living population, results provide the first quantitative growth curve for manatees. The methods also allow us to estimate age, with quantified uncertainty, for 98% of all collected Florida manatee carcasses.

Materials and methods

We first present Bayesian methods to estimate Schnute growth curve parameters when ages are estimated. Then, a second Bayesian model is developed to estimate age from length using the results from the growth curve fitting procedure combined with independent estimates of population age structure. Lastly, after quantifying error in the aging technique, we use the proposed methods to fit a Schnute growth curve to age–length data and then create probability distributions for age at death given length for Florida manatee carcasses.

Schnute growth curve model

The Schnute equation creates a mathematically flexible growth curve relating length to age (Schnute 1981):

$$(1)\qquad Y(t) = f(t) = \left[y_1^b + (y_2^b - y_1^b)\frac{1 - e^{-a(t-\tau_1)}}{1 - e^{-a(\tau_2-\tau_1)}}\right]^{\frac{1}{b}}$$

where t represents age, $Y(t)$ is length at age t, τ_1 and τ_2 are chosen and fixed ages, respectively (usually minimum and maximum possible values), y_1 and y_2 are length at ages τ_1 and τ_2, respectively, and a and b are Schnute curve parameters.

Age is the independent variable, and length is the dependent variable. The lengths at ages τ_1 and τ_2 (y_1 and y_2) and the Schnute parameters (a and b) are the parameters to be estimated. Parameters a and b represent the rate of the relative growth rate, assuming a linear acceleration or deceleration in growth rate with age. Parameter a is the negative intercept of the linear process describing the relative change in growth rate with age, and parameter b is the negative slope. Special values or ranges of a and b represent often-used simplifications of the Schnute curve that have straightforward biological interpretations (Schnute 1981). The estimated curve is insensitive to the choice of fixed reference ages τ_1 and τ_2, although they are typically chosen as the minimum possible age ($\tau_1 = 0$) and some age at which growth rate approaches zero (τ_2 is really old). The reference age τ_2 must be larger than the age of the oldest individual (Schnute 1981).

Hierarchical Bayesian estimation of Schnute parameters with age error

Bayesian analysis of the Schnute model provides several advantages over frequentist methods. First, joint posterior samples of Schnute parameters (that include correlations) can be used to estimate length from age without needing a defined marginal distribution for each parameter (usually assumed normal). Second, the Bayesian Schnute models produce a range of parameter values with their respective probabilities. In testing all possible combinations of parameters, Bayesian analysis provides the likelihood of all traditional simplifications and variations of the Schnute model without a need to statistically compare different models. Lastly, it is relatively easy to incorporate information about age error into the posterior distribution of the Schnute curve parameters estimated from a sample of individuals with measured length and estimated age. This last procedure is accomplished in a model in which the "hidden" state variable of true age is represented as a separate explicit parameter for each individual carcass. In its most simplistic form, the final model consists of a product of two probability functions.

The first probability is the likelihood function that describes process error in the Schnute age–length relationship. The process error in this relationship represents variation in length calculated from the Schnute model, for the same age. If data show a relatively normal and homoscedastic distribution of length given age, the process error (ε_Y) for variation in length given age is assumed normal and additive with mean = 0 and unknown variance (σ_Y^2) and is incorporated into eq. 1:

$$(2)\qquad Y(t_{\text{true}}) = f(t_{\text{true}}) + \varepsilon_Y$$

where

$$(3)\qquad \varepsilon_Y \sim \text{N}(0, \sigma_Y^2)$$

Variable t_{true} represents the true (not estimated) age of an individual. With a simple rearrangement of eq. 2, it follows that

$$(4)\qquad Y(t_{\text{true}}) \sim \text{N}(\mu_Y, \sigma_Y^2)$$

where

$$(5)\qquad \mu_Y = \left[y_1^b + (y_2^b - y_1^b)\frac{1 - e^{-a(t_{\text{true}}-\tau_1)}}{1 - e^{-a(\tau_2-\tau_1)}}\right]^{\frac{1}{b}}$$

The likelihood function is therefore a product of n normal distributions, where n equals the number of individuals in the length–age data set:

$$(6)\qquad L = p\left(\underline{Y(t_{\text{true}})}|\mu_Y, \sigma_Y^2\right) = \prod_{i=1}^{n}\frac{1}{\sigma_Y\sqrt{2\pi}}\cdot\exp\left[-\frac{1}{2}\left(\frac{Y(t_{\text{true}}) - \mu_Y}{\sigma_Y}\right)^2\right]$$

Length measurement error can be separated from process error if it is known. For simplification purposes, the present analysis does not separate process error from measurement error.

When age is known exactly, the Bayesian analysis ends with the above likelihood. Priors are set for the four Schnute parameters (y_1, y_2, a, and b) and σ_Y^2. Observed data consist of exact known ages and total body lengths.

In some cases, however, true age is not known and is instead represented by a distribution based on error in the aging technique. Therefore, an additional probability function corresponds to independent age error (ε_A) for individual animals. The function describing age error in relation to true age and measured age (t_{meas}) is dependent on the aging technique. Ideally, ε_A should be independently quantified with a sample of animals of known age, comparing known ages with measured age estimates (Campana 2001). Some simple examples might describe age error as additive with a normal distribution, or if error increases with age, it could be multiplicative with a lognormal (LN) distribution.

$$(7)\qquad t_{\text{meas}} = t_{\text{true}} + \varepsilon_A \quad \text{or} \quad t_{\text{meas}} = t_{\text{true}}\cdot\varepsilon_A$$

where

$$(8)\qquad \varepsilon_A \sim \text{N}(\mu_A, \sigma_A^2) \quad \text{or} \quad \log(\varepsilon_A) \sim \text{N}(\mu_A, \sigma_A^2)$$

respectively. So,

$$(9)\qquad p(\varepsilon_A|\mu_A, \sigma_A^2) = \text{N}(\mu_A, \sigma_A^2) \quad \text{or} = \text{LN}(\mu_A, \sigma_A^2)$$

In any case, parameters of ε_A (here, μ_A and σ_A^2) must already be either quantified from an independent analysis or assumed.

When true age is not known, but measured ages and the distribution of ε_A are known, the function linking the three values can be rewritten to provide values of true age. In the example case, we rearrange eq. 7:

$$(10)\qquad t_{\text{true}} = t_{\text{meas}} - \varepsilon_A \quad \text{or} \quad t_{\text{true}} = \frac{t_{\text{meas}}}{\varepsilon_A}$$

The "link" between the likelihood function (eq. 6) and the age error probability is the equation that represents the estimate of true age (eq. 10). The age estimates produced from that equation are used as a substitute for exact known age in eq. 5.

The final Bayesian posterior probability function for Schnute parameters with uncertainty in age measurements is a product of the likelihood function, the probability of age error, and the priors.

$$(11)\qquad p\left(y_1, y_2, a, b, \sigma_Y^2 \middle| \underline{Y(t)}, \underline{t_{\mathrm{meas}}}, \underline{\varepsilon_A}\right) \propto p\left(\underline{Y(t)} \middle| y_1, y_2, a, b, \sigma_Y^2, \underline{\varepsilon_A}, \underline{t_{\mathrm{meas}}}\right) \times \pi(y_1)\cdot\pi(y_2)\cdot\pi(a)\cdot\pi(b)\cdot\pi(\sigma_Y^2)\cdot p(\underline{\varepsilon_A})$$

In the simple example case,

$$(12)\qquad p(\underline{\varepsilon_A}) = p(\underline{\varepsilon_A}|\mu_A, \sigma_A^2) = \prod_{i=1}^{n} p(\varepsilon_A|\mu_A, \sigma_A^2)$$

Note that the parameters of ε_A that define the probability of age error may also have inherent uncertainty. In such a case, additional linked probability functions can be added.

With some restrictions, priors on the Schnute parameters (y_1, y_2, a, b, and σ_Y^2) can be assumed independent and relatively vague. Parameters a and b cannot equal 0, and $y_1 < y_2$. If uniform priors are chosen for a and b, limits on the priors should be wide enough to prevent truncation of the posterior distributions of the parameters due to the bounds of the uniform priors. However, lower and upper bounds of y_1 and y_2 must be restricted and realistic for the species. Otherwise, all variability in length is assigned to the posterior distribution of σ_Y^2. Data are measured length and measured (not true) ages.

After analysis, joint posterior samples of y_1, y_2, a, b, and σ_Y^2 from the Schnute curve analysis along with a random sample of ε_Y drawn from a normal distribution with variance σ_Y^2 can be used in eqs. 1 and 2 to derive posterior distributions of p(length | age) for any age. This type of sampling can also be used to represent p(length | age) in a Bayesian model to estimate age from length.

Estimates of age from length

Estimation of age from length requires an additional Bayesian step.

$$(13)\qquad p(\mathrm{age}_i|\mathrm{length}) = \frac{p(\mathrm{length}|\mathrm{age}_i)\cdot p(\mathrm{age}_i)}{\sum_{j=1}^{\mathrm{MaxAgeBin}} p(\mathrm{length}|\mathrm{age}_j)\cdot p(\mathrm{age}_j)}$$

To successfully estimate age from length, an independent prior on age (p(age$_i$)) is needed. The prior can come from a number of sources: age distributions of similar species, mark–recapture studies, a random sample of the population to determine age distribution, etc. The analysis can be done on a continuous scale. However, the process becomes computer intensive. In addition, length is often measured with limited precision, and independent informative priors for age (p(age$_i$)) may not be available on a continuous scale. Therefore, binning the derived posterior distributions of p(length | age) from the Schnute model into length categories that appropriately reflect precision in length measurements and creating age categories based on either limited prior information or appropriate management decision making is a viable option.

Length and age categories also allow us to determine the probability distribution of age given length through relatively simple random sampling. Estimates of p(length | age) are created using results from the growth curve analysis. Random samples are drawn from three distributions: the joint posterior Schnute analysis parameters (y_1, y_2, a, b, and σ_Y^2), process error (ε_Y) from a normal distribution with a mean of zero and variance of σ_Y^2, and age, limited between a defined age range. The random samples are then used in eqs. 1 and 2 to estimate length. After many repeated random samples, the probability that an animal of a given length is a particular age is estimated using the proportion of counts in each age bin for that length. Thus, eq. 13 becomes

$$(14)\qquad p(\mathrm{age}_i|\mathit{length}_j) = \frac{\dfrac{x_{ij}}{\sum_{j=1}^{l} x_{ij}}\cdot z_i}{\sum_{k=1}^{m}\dfrac{x_{kj}}{\sum_{j=1}^{l} x_{kj}}\cdot z_k}$$

where x_{ij} is the count of "hits" in age class i for a specific length j, $z_i = p(\mathrm{age}_i)$, l is the total number of length groups, and m is the total number of age classes.

Overall, the age distribution for a given length is limited by the likelihood function (p(length | age$_i$)). If the prior is a distribution instead of a point estimate, the variability of that distribution will define the level of uncertainty in the probability of a given age class.

Application to Florida manatee carcasses

Previous research describes the methods used to determine the probability that an animal died within about two weeks of birth vs. later in life (Schwarz 2008), so this analysis focuses on providing age estimates for collected carcasses of animals known to have lived at least two weeks (nonperinatal). First, error is quantified for the ear bone aging technique on an annual scale. Age on an annual scale provides poor resolution for very young animals, and age categories used in management models and decision making require estimates of age on a monthly scale (Table 1). Therefore, uncertainty in age estimates also includes uncertainty in month of birth and incorporates known month of carcass recovery. Second, age–length data of carcasses that have been ear-bone-aged are used to fit a Schnute growth curve model, and the uncertainty in age estimates calculated from the first step is incorporated into the second step. Because length at age can be different by sex, and because there appeared to be a seasonal difference in the length-at-age relationship, analysis of the Schnute curve was performed separately by sex and season. The joint posterior distribution of the Schnute parameters allows us to estimate length given age. Those estimates are then combined with an independent prior on the probability of age, resulting in estimates of age from length for carcasses that were not ear-bone-aged. Due to differences in environment and varying levels of uncertainty, the independent priors on the probability of age are different by region: Atlantic, Northwest, Southwest, and Upper St. Johns (US Fish and Wildlife Service 2001). Therefore, results estimating age given length are shown by sex, season, and region.

Table 1. Age classes and their respective ages used in mark–recapture studies and subsequent management models (Langtimm et al. 2004; Runge et al. 2004).

Age class	Age (years)
0	0.04 (2 weeks) to 0.5
1	0.5 to 1.5
2	1.5 to 2.5
3	2.5 to 3.5
4	3.5 to 4.5
A	>4.5

Different analyses provide results at different length and age resolutions. Schnute curve results are shown on a continuous scale. Although incorporation of error in the aging technique provides age estimates on a monthly scale, age estimation from ear bones are simplified to show the probability of true age binned by the age categories used in management models and decision making (Runge et al. 2004, 2007). The probability that a carcass died at a certain age was binned by 1-year increments starting at six months old. Animals over 4.5 years old were combined into one age class (Table 1). Although Schnute curve results provide estimates of *p*(length | age) on a continuous scale, age estimates from length are produced on an annual scale because prior information on age distribution is limited to an annual scale. However, for simplification, probability distributions of age given length are also shown using the age categories of Table 1. Length measurements are on a 1 cm scale (the maximum resolution of length measurements).

In addition, although true age probability distributions can be calculated for any ear bone age, only results for ear bone ages (count of growth layer groups) of 0, 2, and 4 with carcass collection months of March and October are shown for simplification. The simplified results still provide enough information to describe the overall pattern in true age with increasing ear bone age and the effects of birth month uncertainty on true age estimates. Likewise, true age probability distributions from length can be calculated for any length on a 1 cm scale, but only results for lengths of 175, 240, and 275 cm are shown for simplification. The lengths represent boundaries of very general age classes based on length. Subadults have been defined as animals between 175 and 275 cm long (O'Shea et al. 1985; Ackerman et al. 1995), although both males and females may be sexually mature around lengths of 240–250 cm (Hernandez et al. 1995; Marmontel 1995). Animals < 175 cm have been labeled as calves, whereas animals > 275 cm were considered adults.

Lastly, when estimating age from length, maximum possible true age was set at 80.5 years old. Because of the asymptotic nature of growth and the very low probability that an animal reaches the maximum age before death, and because the defined age class bins focus on younger age classes, change in the maximum possible true age does not dramatically affect the probability a carcass was in a particular age class (maximum probability change ± 0.0028 with ±20 year change in maximum age). Uncertainty in the maximum possible age had a negligible impact on the uncertainty in age given length, so it was not included in this analysis.

Table 2. Data used to estimate error in the ear bone aging technique.

Carcass ID no.	Known age (years)	Ear bone growth layer count	c^*_{ia}
M311	1	1	1
KDL8827	7	7	1
MJAV8921	1	1	1
SWFTM9002	3	3	1
UCF9131	7	7	1
SWFTM7918	12	11	0.917
SWFTM8321	9	11	1.222
MSW9547[a]	3	2	0.667

[a] New data point found from review of the necropsy database. All other data points are from Marmontel et al. (1996).

Data

The Fish and Wildlife Research Institute under the Florida Fish and Wildlife Conservation Commission currently runs the Florida Manatee Carcass Recovery and Necropsy Program. They necropsy all reported manatee carcasses and maintain all hard copies and digital versions of necropsy reports, as well as an electronic database that provides some necropsy information for each reported carcass. Within the manatee carcass data set, Marmontel et al. (1996) determined that seven animals were of known age, either born in captivity or first identified alive as calves. A review of the manatee necropsy database revealed one other carcass of known age that had also been ear-bone-aged (Table 2). The true age for the animals in this sample ranged from 1 to 12 years old, with ear bones exhibiting no to moderate resorption. Data from those eight animals were used in this study to estimate error in the ear bone aging technique by quantitatively comparing true ages with counts of ear bone growth layer groups. Marmontel et al. (1996) showed that bone resorption is more common and of a higher degree in females, which may lead to different biases and uncertainty in ear bone age estimates by sex. However, sample size was too small to estimate ear bone aging error separately by sex.

In addition to the eight carcasses of known age, ages of 2063 Florida manatee carcasses have been estimated from ear bones for the period of 1978 to 2005. During the same time period, almost all carcasses were measured for length (5717 of 5865 carcasses). We used carcasses of known length and measured ear bone age to estimate Schnute growth curve parameters.

To ensure that the resulting Schnute curve applied only to animals greater than two weeks old, carcass data were filtered based on perinatal criteria (Schwarz 2008). The data subset used in the Schnute analysis consisted of carcasses ≤ 160 cm long classified as nonperinatal based on physiological data, plus all carcasses > 160 cm long. Growth curves often vary by sex, so Schnute curve parameters were estimated separately for males and females.

The subsample used to estimate the Schnute growth curve parameters does not provide a uniform distribution of animals across all age classes (Table 3). Also, the ear bone aging method has not been used to estimate ages of a random subsample of the carcasses. However, nonuniform and nonrandom sampling by age does not strongly affect estimation of growth curve parameters, particularly when sample

Table 3. Sample size for estimation of Schnute growth curve parameters by sex, season, and ear bone age.

	Female		Male	
Ear bone age	Winter	Non-winter	Winter	Non-winter
0	59	36	67	43
1	81	39	116	53
2	58	28	70	29
3	34	37	39	28
4	15	19	27	23
5	23	22	22	24
6	20	20	29	28
7	20	34	25	21
8	14	18	18	22
9	14	16	14	17
10	11	16	18	14
11	12	9	11	8
12	11	10	8	9
13	4	5	12	14
14	2	9	14	12
15	6	2	10	6
16	5	12	4	6
17	7	2	8	6
18	3	3	8	7
19	3	7	5	5
20	2	1	1	6
21	3	1	5	4
22		2	3	2
23	3	1	1	1
24	3	3	4	6
25	5	4	2	4
26	2	3	3	1
27	1	2	2	3
28	2	1	4	2
29	1	3		2
30		1		2
31		2		
32			1	
33		1		1
34		1		
35	1	1	1	4
36	1		1	
37			2	
38			1	
39		2		
43				1
48		1		
59		1		
Total	426	375	556	414

size is large (Leberg et al. 1989; Cope and Punt 2007). Sample sizes used to estimate Schnute growth curve parameters, stratified by sex and season, ranged from 375 to 556 (Table 3).

Age estimation: quantification of ear bone error and incorporation of month of birth uncertainty

Although process and measurement error for ear bone age estimates have not been formally measured, Marmontel et al. (1996) described an increase in both the occurrence and intensity of ear bone resorption with age. Consequently, process error increases with age. Those increases were also coupled with an increase in within-reader variability with age (Marmontel et al. 1996). Therefore, a multiplicative ear bone error was assumed, combining both reading (measurement) error and process variation:

Fig. 1. Derived posterior distribution of multiplicative ear bone error calculated from a lognormal distribution using joint posterior samples of μ and σ^2. Data counts of measured ear bone error ($\varepsilon^*_{\mathrm{EB}}$) used in the analysis are shown as open circles (total $n = 8$). See Table 2 for data to calculate $\varepsilon^*_{\mathrm{EB}}$.

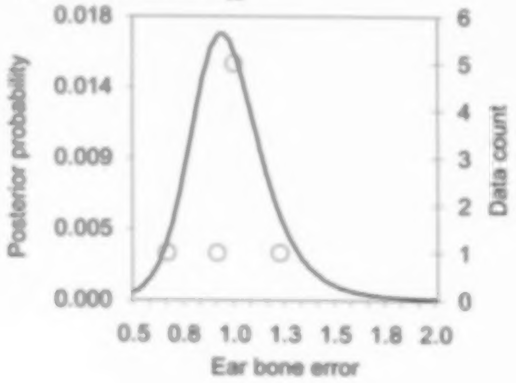

$$t_{\mathrm{earbone}} = t_{\mathrm{trueEB}} \cdot \varepsilon_{\mathrm{EB}} \tag{15}$$

where t_{earbone} is the measured ear bone age, t_{trueEB} is the true age on a yearly scale, and $\varepsilon_{\mathrm{EB}}$ is the ear bone error. Ear bone error, and thus a Bayesian likelihood, was represented by a lognormal distribution with parameters μ and σ^2:

$$L = p(\varepsilon_{\mathrm{EB}}|\mu, \sigma^2) = \mathrm{LN}(\mu, \sigma^2) \tag{16}$$

The calibration model for the estimation of ear bone aging error utilizes the eight known age animals, comparing true and measured ear bone ages. Observed ear bone error was calculated for each of the eight animals as the ratio of measured to "known" actual age, both on a year scale ($\varepsilon^*_{\mathrm{EB}}$; Table 2; Fig. 1).

Assuming prior independence of the parameters of interest, μ and σ^2, we set a vague uniform prior density on (μ, $\log \sigma^2$) (Gelman et al. 1995). The prior transforms to the following probability density:

$$\pi(\mu, \sigma^2) \propto \frac{1}{\sigma^2} \tag{17}$$

Thus, the Bayesian joint posterior distribution for μ and σ^2 is

$$p(\mu, \sigma^2|\underline{\varepsilon^*_{\mathrm{EB}}}) = \frac{p(\underline{\varepsilon^*_{\mathrm{EB}}}|\mu, \sigma^2) \cdot \pi(\mu, \sigma^2)}{\iint p(\underline{\varepsilon^*_{\mathrm{EB}}}|\mu, \sigma^2) \cdot \pi(\mu, \sigma^2) \mathrm{d}\mu \mathrm{d}\sigma^2} \propto \left[\prod_{i=1}^{8} \frac{1}{\varepsilon^*_{\mathrm{EB}i} \sigma \sqrt{2\pi}} \exp\{-[\ln(\varepsilon^*_{\mathrm{EB}i}) - \mu]^2/2\sigma^2\}\right] \cdot \frac{1}{\sigma^2} \tag{18}$$

The derived posterior distribution of ear bone error on an annual scale is then represented as random draws from a lognormal distribution with parameters μ and σ^2 drawn from their posterior distributions. To prevent extreme ear bone error values and based on the work of Marmontel et al. (1996), the posterior values of the derived ear bone error were limited to the range of 0.5 to 2.0. Because all known ear bone errors fall within that range, limiting the posterior ear bone error distribution (either within the likelihood or as a posterior limitation) does not affect the probability of ear bone error within the range. In addition, even with the small sample size and vague priors, results showed such a truncation removed only 0.65% of the derived posterior distribution of ear bone error.

Between-reader variability, although potentially present, is most likely quite small in this case. Only three researchers have ear-bone-aged Florida manatees, and each researcher goes through extensive training and qualitative comparison of their ear bone readings with previous work before reading new ear bones. Although never quantified, between-reader variability is assumed negligible compared with other sources of uncertainty and is not included in this analysis.

Combining growth layer counts with probability of birth month and knowledge of month of carcass recovery can refine ear bone age estimates to a monthly scale. Monthly scale age estimates are needed for the Florida manatee carcasses to coincide with age classes used in management models (Table 1). Considerable anecdotal evidence from aerial surveys, mark–recapture studies, radio-tagged animals, and reproductive studies all show a fairly broad distribution of date of birth during the warm months (Hernandez et al. 1995; Rathbun et al. 1995; Reid et al. 1995). Because of the inconsistent nature of the available data, as well as small sample sizes, a formal analysis of birth month probabilities was not performed. However, based loosely on the evidence, the probability of month of birth for months March through November was set as relatively diffuse: equal for months May through September, decreasing monthly by 50% out to March and November (Table 4). Births do occur in winter. However, such births are probably preterm deliveries, and the likelihood of such small calves surviving to two weeks is probably very low (Marmontel 1995). Because the data selection criteria and the model only include animals that lived for at least two weeks, birth month probability for months December through February was set to zero.

Both the joint posterior distribution on μ and σ^2 and the distribution of birth month were used to characterize age error. Assuming that ear bone layers are deposited on an animal's birthday, real-valued true age (t_{true}, in months) becomes a function of the integer true ear bone age (t_{trueEB}, in years), birth month (M_{B}), and month of carcass recovery (M_{R}):

$$M_{\text{R}} > M_{\text{B}}: t_{\text{true}} = (12 \cdot t_{\text{trueEB}}) + (M_{\text{R}} - M_{\text{B}}) \tag{19}$$

$$M_{\text{R}} < M_{\text{B}}: t_{\text{true}} = [12 \cdot (t_{\text{trueEB}} + 1)] - (M_{\text{B}} - M_{\text{R}}) \tag{20}$$

$$M_{\text{R}} = M_{\text{B}}: t_{\text{true}} = (12 \cdot t_{\text{trueEB}}) \tag{21}$$

Because ear bone error represents error in age estimation on an annual scale, true ear bone age in the above equations is the largest integer not greater than measured ear bone age over ear bone error:

Table 4. Month and the probability that an animal that survived more than two weeks was born in that month.

Month	Probability born in month
March	0.038
April	0.077
May	0.154
June	0.154
July	0.154
August	0.154
September	0.154
October	0.077
November	0.038

$$t_{\text{trueEB}} = \left\lfloor \frac{t_{\text{earbone}}}{\varepsilon_{\text{EB}}} \right\rfloor \tag{22}$$

The model assumes that carcasses are reported and collected in the same month that the animals die. Decomposition rates have not been quantified for manatee carcasses, although the warm, humid environment lends itself to rapid decomposition. A rapid decomposition rate coupled with the proportion of carcasses collected in relatively fresh condition lead us to believe that carcasses are most likely reported within a month of death or not reported at all. A high proportion of carcasses are "badly decomposed" at necropsy (0.56), a state that can easily occur within a few days of death, compared with the proportion of carcasses labeled as "skin and bones" (0.02). All other carcasses are collected before they reach the badly decomposed state (Schwarz 2004).

The derived posterior distribution of true age was calculated for measured ear bone ages based on the inference. The natural log of ear bone age error, truncated between 0.5 and 2.0, was drawn from a normal distribution with parameters μ and σ^2, which were in turn drawn from the joint posterior samples of μ and σ^2 from the inference on the ear bone age calibration data. Because ear bone age estimates are on an annual scale, measured ear bone age was divided by ear bone error and rounded down to the nearest integer (eq. 22). A random month of birth was drawn in relation to the probability of birth month (Table 4). Along with known month of carcass recovery, true age was calculated using eqs. 19–21. Results represent age estimates with process and measurement error in the ear bone aging technique and uncertainty in the month of birth. The simulation was run 100 000 times for each ear bone age and each carcass recovery month. The simulation described above can be used to determine true age for each ear-bone-aged carcass. True age estimates can then be incorporated into models to determine the probability of length given age.

Schnute curve analysis

The parameters of the Schnute curve were estimated separately by sex and season. Males and females often have different growth patterns, and animals dying between November and March are somewhat smaller than animals with the same ear bone age dying between April and Octo-

Fig. 2. Length vs. measured ear bone age (growth layer group categories) for (*a*) females and (*b*) males separated into winter (November–March; shaded squares) and nonwinter periods (April–October; solid diamonds). Points are means, and bars represent ± 1 standard deviation. * Measured ear bone age = 0 only represents nonperinatal carcasses (known to have lived at least two weeks). Graph has been truncated at age 10 to emphasize differences at younger ages. See Table 3 for sample sizes.

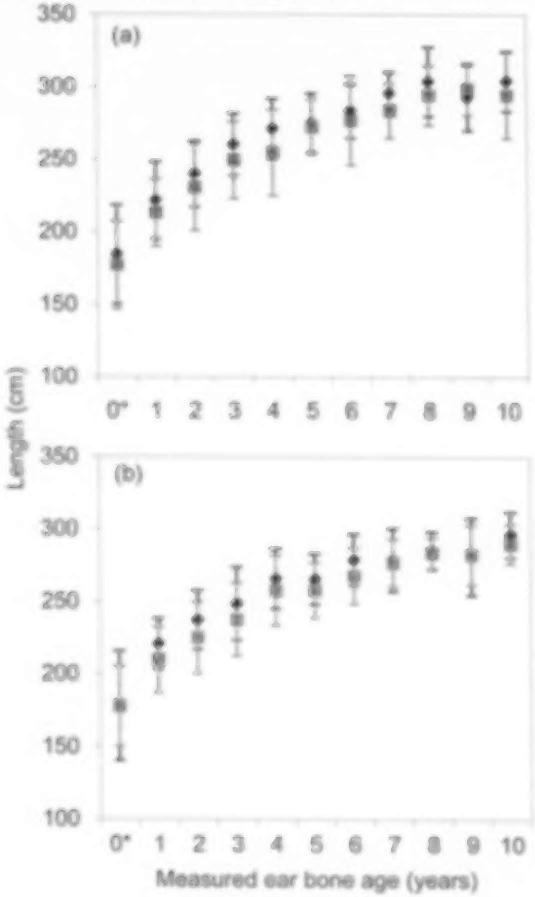

ber (Fig. 2). Marmontel et al. (1996) showed that growth layers are not formed due to seasonal effects, and the results of several simulation exercises (not shown) demonstrated that any potential seasonal effects in growth layer formation could not explain the observed seasonal pattern in the age–length relationship. Hence, seasonally variable causes of mortality related to size are more likely to create the observed patterns. Therefore, data were also separated into winter (November–March) and nonwinter (April–October) periods, and each growth layer group was assumed to represent one year of life.

To estimate Schnute growth curve parameters for Florida manatee carcasses, the Bayesian models described in eqs. 2–12 needed to be customized. Inspection of the data showed a relatively normal and homoscedastic distribution of length given age (Fig. 2). Therefore, the process error (ε_Y) for variation in length given age was assumed normal and additive with mean = 0 and unknown variance (σ_Y^2), and eqs. 2 through 6 were appropriate in this case. Length measurement error has never been quantified for Florida manatees. However, it is probably quite small (maximum ±5 cm) compared with process variation in the Schnute relationship. For the present analysis, it was inseparable from process error.

Error in age estimation for Florida manatee carcasses is slightly more complex than the error that we first presented. The set of probability functions corresponding to independent age error for individual carcasses is a product of two "subfunctions" representing ear bone error and uncertainty in birth month. Both ear bone error and birth month uncertainty vary independently from each other and for each individual carcass, so the probability function of all age error is a multiplicative function of the probability of ear bone error (eq. 16) and birth month probability (Table 4) for all *n* individuals:

$$(23)\qquad p(\underline{\varepsilon_{\mathrm{EB}}}|\mu,\sigma^2)\cdot p(\underline{M_{\mathrm{B}}}) = \prod_{j=1}^{n} p(\varepsilon_{\mathrm{EB}_j}|\mu,\sigma^2)\cdot p(M_{\mathrm{B}_j})$$

The age estimates produced from eqs. 19–21 are used as a substitute for exact known age in eq. 1. A fourth and final probability function (eq. 18) is needed as the parameters μ and σ^2 that define the probability of ear bone error have inherent uncertainty. Overall, the equations that define age error ($p(\varepsilon_A)$) in the hierarchical Bayesian Schnute model (eq. 11) are

$$(24)\qquad p(\underline{\varepsilon_{\mathrm{A}}}) = p(\underline{\varepsilon_{\mathrm{EB}}}|\mu,\sigma^2)\cdot p(\underline{M_{\mathrm{B}}})\cdot p(\mu,\sigma^2|\underline{\varepsilon^{*}_{\mathrm{EB}}})$$

Priors on the Schnute parameters (y_1, y_2, a, b, and σ_Y^2) were assumed independent and relatively vague:

$$(25)\qquad \pi(y_1)\quad\text{and}\quad \pi(y_2) \sim \mathrm{UNIF}(80, 420)$$

$$(26)\qquad \pi(a)\quad\text{and}\quad \pi(b) \sim \mathrm{UNIF}(-100, 100)$$

$$(27)\qquad \pi(\sigma_Y^2) \propto \sigma_Y^{-2}$$

Limits on the uniform priors of *a* and *b* were wide enough to prevent truncation of the posterior distributions of the parameters due to the bounds of the uniform priors. The smallest carcass known to have lived more than two weeks was 82 cm long (Schwarz 2008). The largest Florida manatee carcass ever reported was 411 cm long (Florida Fish and Wildlife Research Institute, Marine Mammal Pathobiology Lab, 3700 54th Avenue South, St. Petersburg, FL 33711, unpublished data), so lengths were limited to between 80 cm and 420 cm. Reference age τ_1 was set to zero, and reference age τ_2 was set to 1420 months, twice the maximum ear bone age ever recorded. For the Schnute analysis, age was in units of months. Data are ear bone ages on a year scale, total body length (in centimetres), and month of carcass recovery.

Posterior distributions and joint posterior samples of all variables were determined using the program MTG (Metropolis within Gibbs) developed by Daniel Goodman of Montana State University (Schwarz 2008). To maximize computer efficiency and improve estimates, simulations

Table 5. Posterior statistics on parameters of the lognormal distribution describing error in the ear bone age estimation technique.

	Marginal				
Parameter	Mode	Mean	SD	Joint mode	Correlation
μ	–0.038	–0.035	0.071	–0.038	0.035
σ^2	0.018	0.041	0.032	0.018	

were performed on orthogonally transformed parameters when correlation between parameters was high (y_2, *a*, and *b*). Simulations were set for a rejection rate near 0.7, a subsampling (thinning) of 1 in 900, and a burn-in period of 900, continuing for a subsample size of 10 000 for each inference (see Cowles and Carlin 1995). The resulting lag-1 autocorrelations were < 0.1, and independent chains with different parameter starting values gave indistinguishable results. To verify convergence and stationarity within the final chains, we used the Heidelberger and Welch convergence diagnostic available from the CODA package in R using standard 10% increments and $p \leq 0.05$ (Heidelberger and Welch 1983; Plummer et al. 2006).

Posterior samples of y_1, y_2, *a*, *b*, and σ_Y^2 from the Schnute curve analysis along with a random sample of ε_Y drawn from a normal distribution with variance σ_Y^2 can be plugged into eqs. 1 and 2 to derive posterior distributions of *p*(length | age) for any age. One billion joint posterior samples of Schnute parameters and σ_Y^2 were drawn randomly and combined with random draws of age between 0.5 months to 80.5 years to calculate length at age. Results are shown as length vs. age graphs by sex and season. This type of sampling can also be used to represent *p*(length | age) in a final Bayesian model to estimate age from length.

Estimates of age from length

Derived posterior distributions of *p*(length | age) from the Schnute model were binned into increments of 1 cm lengths and annual age categories out to the defined maximum age (0.5–1.5 years, 1.5–2.5 years, …, 79.5–80.5 years) except for the first age bin (2 weeks to 0.5 years). Age categories were based on available independent information about *p*(age$_i$), which relies on survival and reproductive rate estimates from mark–recapture studies and management models (Kendall et al. 2004; Langtimm et al. 2004; Runge et al. 2004). Mark–recapture studies collect data during winter months when animals are roughly 0.5, 1.5, 2.5, …, 80.5 years old. The values and levels of uncertainty in demographic variables are different by geographic location, so the informative priors for age (*p*(age$_i$)) were stratified by the four regions defined in the Florida manatee recovery plan: Atlantic, Northwest, Southwest, and Upper St. Johns (US Fish and Wildlife Service 2001). We provide more information on the methods used to develop the informative prior on the proportion of carcasses in each age class (see Supplemental Appendix S1[3]).

The probability that an animal of a given length was a particular age was estimated using the proportion of counts in each age bin for that length (eq. 14). Although the models provide estimated probability of age for any length on a 1 cm scale, resulting estimates of age at death are only presented for males and females in winter and nonwinter months and by region for several lengths that have traditionally been used as cutoffs for different life stages (175, 240, and 275 cm long).

Fig. 3. Posterior distribution of age at death given carcass-measured ear bone ages (*a* and *d*) 0, (*b* and *e*) 2, and (*c* and *f*) 4 and months of carcass recovery, (*a*, *b*, and *c*) March and (*d*, *e*, and *f*) October. Age classes: 0, 2 weeks – 0.5 years; 1, 0.5–1.5 years; 2, 1.5–2.5 years; 3, 2.5–3.5 years; 4, 3.5–4.5 years; A, 4.5 years and older.

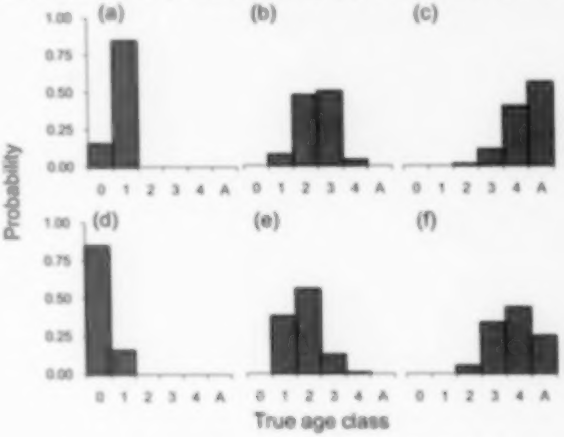

Results

Age estimation: ear bone error with month of birth uncertainty

Using the eight known true-age carcasses to estimate ear bone error, posterior distributions of parameters μ and σ^2 are not highly correlated, and σ^2 is left-skewed (Table 5). The posterior distribution of ear bone error resulting from joint samples of μ and σ^2 has a mode of 0.94, mean of 0.99, and standard deviation of 0.22 (Fig. 1). The results indicate that measured ear bone ages slightly underestimate true ear bone ages.

Values of the posterior probability of age at death given carcass-measured ear bone age and month of carcass recovery reflect the uncertainty in the ear bone aging technique and birth month (Fig. 3). Increased ear bone growth layer counts lead to a general increase in the true age distribution. Carcasses with an ear bone growth layer count ≥ 8 (not shown) have a 100% probability of true age falling within the adult age class (true age ≥ 4.5 years). Carcasses with a given ear bone age are most likely the youngest when recovered in October and the oldest when recovered in March. The seasonal pattern of variability is a reflection of the variability in birth month.

---

[3] Supplementary data for this article are available on the journal Web site (http://cjfas.nrc.ca) or may be purchased from the Depository of Unpublished Data, Document Delivery, CISTI, National Research Council Canada, Building M-55, 1200 Montreal Road, Ottawa, ON K1A 0R6, Canada. DUD 5263. For more information on obtaining material, refer to http://cisti-icist.nrc-cnrc.gc.ca/eng/ibp/cisti/collection/unpublished-data.html.

Table 6. Marginal posterior distributions of Schnute curve parameters.

		Parameter				
Sex	Season	y_1	y_2	a	b	σ_Y^2
Female	Nonwinter	114.1 (19.3)	391.8 (14.3)	0.0016 (0.0009)	6.62 (0.39)	400.5 (44.7)
	Winter	112.8 (18.9)	383.9 (17.5)	0.0026 (0.0012)	5.57 (0.39)	505.3 (44.7)
Male	Nonwinter	97.1 (12.0)	336.2 (7.2)	0.0047 (0.0011)	6.46 (0.36)	311.9 (27.7)
	Winter	105.7 (16.3)	345.8 (12.1)	0.0033 (0.0011)	6.19 (0.33)	358.0 (27.4)

Note: Numbers are means with standard deviations in parentheses.

Table 7. Posterior correlations between Schnute growth curve parameters for the four models separated by sex and season.

			Correlation				
Sex	Season		y_1	y_2	a	b	σ_Y^2
Female	Nonwinter	y_1	1.00	–0.13	0.18	–0.27	0.10
		y_2	—	1.00	–0.95	0.64	–0.10
		a	—	—	1.00	–0.82	0.08
		b	—	—	—	1.00	–0.02
		σ_Y^2	—	—	—	—	1.00
	Winter	y_1	1.00	–0.24	0.35	–0.55	0.14
		y_2	—	1.00	–0.94	0.68	–0.06
		a	—	—	1.00	–0.85	0.06
		b	—	—	—	1.00	–0.05
		σ_Y^2	—	—	—	—	1.00
Male	Nonwinter	y_1	1.00	–0.03	0.05	–0.10	0.09
		y_2	—	1.00	–0.93	0.66	0.00
		a	—	—	1.00	–0.84	–0.03
		b	—	—	—	1.00	0.09
		σ_Y^2	—	—	—	—	1.00
	Winter	y_1	1.00	–0.16	0.24	–0.41	0.11
		y_2	—	1.00	–0.94	0.72	0.00
		a	—	—	1.00	–0.86	0.00
		b	—	—	—	1.00	0.01
		σ_Y^2	—	—	—	—	1.00

Schnute growth curve model

Marginal posterior distributions of the Schnute parameters imply that female carcasses collected during the cold season are somewhat longer than females of the same age collected in the warm season, whereas the opposite is true for males (Table 6). However, posterior correlations between y_2, a, and b (the estimated length at age = τ_2 and the two growth rate parameters) are particularly strong (Table 7). Age–length curves produced from the joint posterior sample of Schnute parameters indicate that overall length estimates are shorter in winter months compared with nonwinter months for animals of the same age, regardless of gender (Fig. 4). In addition, females tend to be slightly longer than males of the same age (roughly 10% larger after 4 years of age).

Estimates of age from length

Using results of the Schnute model to estimate age, the "subadult" length category (175–275 cm long) includes carcasses of all age classes. A carcass 175 cm long still has a relatively high probability of being less than six months old, and a 275 cm long carcass has a high probability of being more than 4.5 years old (Fig. 5). The length of 240 cm (the length at which Florida manatees may be sexually mature) represents all but the youngest age class (Fig. 5).

In addition, posterior probabilities indicate that carcasses of the same length have different age class probabilities depending on sex and season (Fig. 5). In general, carcasses collected in winter months are older than carcasses of the same length collected in nonwinter months. Males are older than females of the same length. Regional differences are a reflection of differences in survival and reproductive rate estimates that determine the proportion of carcasses in each age class used as prior information in the Bayesian model (see Supplemental Appendix S1[3]). Overall, regional differences do not appear to be very strong. However, posterior uncertainty is slightly lower for the Upper St. Johns region where certainty in survival and reproductive rates is higher (leading to a narrower prior on probability of age).

Discussion

Whether performed using age–length data from carcasses or live animals, the Bayesian results provide two very important conclusions about growth curve analyses. First,

Fig. 4. Length vs. age curves calculated from joint posterior samples of Schnute parameters for (*a*) females and (*b*) males separated into winter (November–March; shaded lines) and nonwinter (April–October; black lines) periods. Thicker, solid lines are mean values of length given age. Thinner lines represent 95% posterior intervals (winter, shaded lines; nonwinter, broken lines). Graph has been truncated at age 10 to emphasize differences at younger ages.

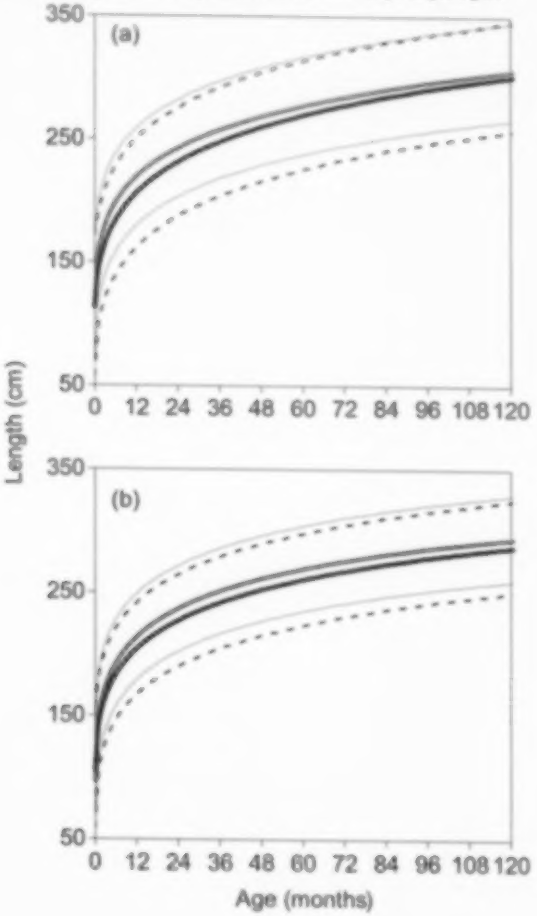

strong posterior correlations between growth-curve parameters indicate that very different combinations of the parameters can produce almost the same growth curve. In addition, given the high variability in individual growth rates, age–length data tend to be diffuse, so different combinations of parameters that produce similar curves have similar posterior probabilities. Some researchers have confused the phenomenon with the idea that an individual's growth rate is correlated with its asymptotic length (Sainsbury 1980; Wang and Thomas 1995; Pilling et al. 2002). Although such a biological correlation may be true, the posterior correlations are a function of the Schnute model combined with diffuse data and do not indicate any within-individual variability in behavior or process.

Second, given the high posterior correlations, marginal posterior distributions for each parameter can be misleading. For example, mean posterior values of the Schnute parameters implied that comparisons of length from age by season were not the same for females as for males. However, when sampling highly correlated parameters jointly, the resulting length estimates from age were consistently longer during nonwinter months, regardless of sex. Mean and modal (not shown) marginal posterior values do not provide a complete picture of the relationship between parameters or how parameter interactions produce different probabilities of length at age.

This research was partially devoted to estimation of error in the ear bone aging process incorporating uncertainty in birth month. Ideally, uncertainty in the ear bone aging technique should be quantified using a substantial sample of animals of known age and multiple readings of the same ear bone by all readers to estimate within- and between-reader variability and bias (Campana 2001). Sample size was too small to estimate uncertainty in the ear bone aging technique by sex, even though error is most likely larger for females. In addition, the calibration sample did not include ear bones with high levels of resorption, so resulting variability and (or) bias in ear bone error may be too low. New studies could also investigate potential patterns in resorption by region to help determine any correlations with resorption and environmental variability. However, despite a small sample size and vague priors, error estimates were relatively precise, showing that ear bone growth layers may slightly underestimate carcass age. The findings are consistent with current information on bone resorption, which removes layers due to remodeling (Marmontel et al. 1996).

A more rigorous quantification of the probability of birth month and an improved understanding of the time between death and carcass recovery are needed. Given the high level of uncertainty in annual ear bone counts, incorporating variability into the birth month probabilities does not affect results. However, if the assumed values are incorrect, age-from-length estimates could be biased either high or low, particularly for very young and very small animals in which age probabilities on a monthly scale are influenced more by uncertainty in birth month than in ear bone age. If carcasses are actually collected in the month following death (or months later), our current assumption that carcasses are collected in the same month in which the animals die leads to an overestimate of age at death. Because decomposition rate is likely rapid, such a bias is probably very small.

The goal of evaluating the Schnute growth curve was to quantify the relationship between length and ear bone age using data of some carcasses to estimate ages of other carcasses using only length measurements. Because a sample of dead animals was used, sex and seasonal differences could represent life history and environmental differences linked to the relationship between age, length, and cause of death, particularly cold stress in smaller animals. Smaller animals are probably more likely to die from cold stress due, perhaps, to a large surface-to-volume ratio compared with that of larger animals of the same age (Buergelt et al. 1984; Reynolds and Wilcox 1986; Ackerman et al. 1995). Therefore, mortalities in winter are probably somewhat size-specific.

Posterior distributions of *a* and *b* show two alternative options other than the Schnute model for the Florida manatee

Fig. 5. Marginal probabilities for age at death given sex, season, region of carcass recovery, and three total body lengths: (*a*) 175 cm, (*b*) 240 cm, and (*c*) 275 cm. Bars are means and whiskers are one standard deviation. Age classes: 0, 2 weeks – 0.5 years; 1, 0.5–1.5 years; 2, 1.5–2.5 years; 3, 2.5–3.5 years; 4, 3.5–4.5 years; A, 4.5 years and older. Regions: Atl, Atlantic; NW, Northwest; SW, Southwest; USJ, Upper St. Johns.

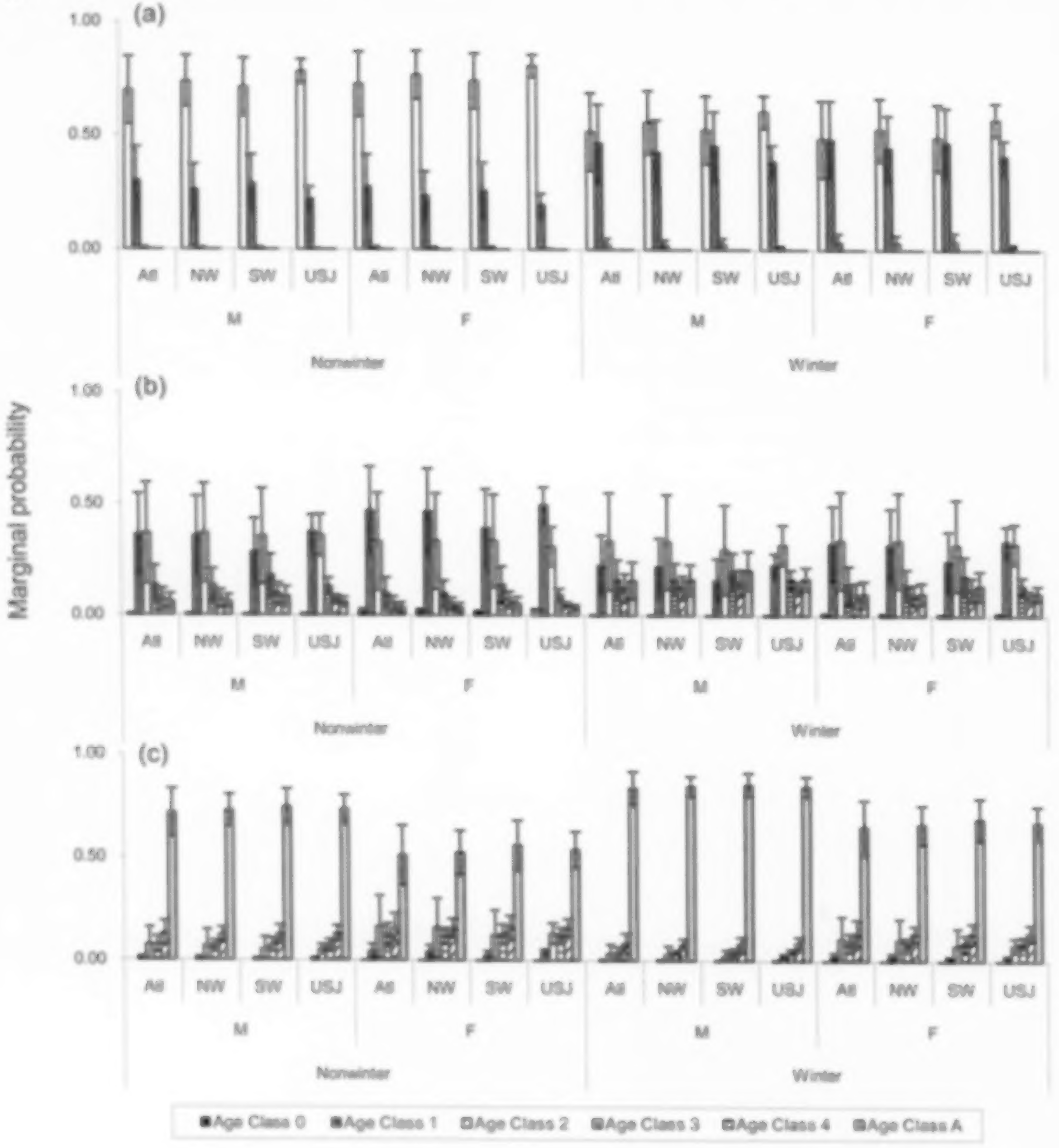

carcass data. Neither parameter falls below zero, suggesting that a generalized von Bertalanffy (GVB) equation may be an appropriate variation (Schnute 1981). The GVB equation is simply a modification of several values in the Schnute model: instead of estimating length at age = 0 (τ_1), GVB estimatesa hypothetical age at length = 0. Instead of estimating length at age = τ_2, GVB estimates asymptotic length. Results would not change if the GVB model was used in place of the Schnute model.

Because the posterior distribution for parameter *a* is near zero, a simplification of the Schnute equation could be considered (eq. 17 in Schnute 1981):

$$(28)\qquad Y(t) = \left[y_1^b + (y_2^b - y_1^b)\frac{t-\tau_1}{\tau_2-\tau_1}\right]^{\frac{1}{b}}$$

The above growth model has no inflection point and implies that manatees never reach an asymptotic length (Schnute 1981). Although continuous growth throughout life is not biologically reasonable for the manatee, the results most likely reflect size-selective mortality, with larger animals more likely to reach an older age.

The resulting Schnute curves calculated for the carcass population might not be appropriate when applied to live animals. For example, shorter lengths in winter do not represent "shrinking" animals during cold periods. In addition, animals dying in winter do not necessarily grow differently than animals dying at other times. Separate models by season account for differences when using the models to estimate age at death from carcass body length but should not imply differences in growth rates or length–age relationships in living animals. Likewise, the implication that manatees do not reach an asymptotic length illustrates that the final Schnute curves fit to carcass data do not necessarily represent true growth trajectories of living individuals.

However, general patterns seen in both the Schnute curve analysis and age-from-length models are consistent with our knowledge of manatee biology. Growth trajectories are similar to those found in a small sample of known-age live animals (O'Shea and Reep 1990). Adult males are slightly smaller than adult females, and the mating system may favor such a disparity. Manatee mating is considered scramble promiscuity with sperm competition, indicating that smaller, more agile males may have a slight advantage when vying for access to females (Rathbun et al. 1995; Anderson 2002; Reynolds et al. 2004). Ralls (1976) suggests that larger females may have higher reproductive success. The difference in overall length at age between males and females has been observed in other species and is probably due to a mixture of both natural and selective pressures (Ralls and Mesnick 2002). Although resulting Schnute curves do not show strong differences by season or sex when estimating length from age, those differences become much more pronounced when the curve is mathematically flipped to estimate age from length.

Results of age estimates for lengths representing the subadult category (175–275 cm) and the length at which some animals become mature (240 cm) generally coincide with manatee life history research using the carcass necropsy data. Newborns can be as long as 160 cm, and the lower 175 cm limit on the subadult category has been used as a very rough estimate of the size at which a calf becomes independent from its mother, between one and two years of age (O'Shea et al. 1985; Ackerman et al. 1995; Schwarz 2008). The probability that a carcass of length 175 cm is between two weeks and 1.5 years old is almost 100%, with some differences to account for sex and season. Although there is a high level of variability in age estimates at 240 cm long, overall results are consistent with studies showing spermatogenesis as young as two years old (237 cm long) and fully spermatogenic testes at two to three years old (252 cm) (Hernandez et al. 1995). Males of length 240 cm are most likely between 0.5 and 2.5 years old. The upper limit on the subadult category was loosely based on the length at which most female manatees are sexually mature. Research on female reproduction shows that the youngest and smallest sexually mature females are represented by a small number of three year olds (average length = 280 cm) and all five year olds (average length unknown) (Marmontel 1995). Female carcasses of length 275 cm are most likely 4.5 years old or older, although there is a small probability that a female of that length is as young as one year old (0% to 8%, depending on season and region).

Uncertainty in the marginal posterior probability of age given length reflects the uncertainty in the age distribution prior and, in this case, can be reduced when uncertainty in survival and reproductive rates is lower. Likewise, the resulting age-from-length models are consistent with the high degree of variability seen in the age–length relationship. The posterior range of possible age classes for a given length is due to the uncertainty in length given age from the Schnute model. Analyses not presented in this research showed that incorporation of age error into the Schnute model did not strongly affect those ranges. However, age uncertainty (with or without bias in age estimates) did depress the resulting curve slightly, meaning that the ranges of possible age classes for given lengths were ultimately shifted somewhat older. Reduced uncertainty in ear bone age estimates, which could also mean inclusion of more animals of known birth year, would ultimately lead to a slightly younger age estimate from length. However, the range of possible age classes for a given length is a function of the high levels of individual variability in length at age and cannot be reduced.

Even with the high levels of uncertainty seen in these results, estimates of age for all collected Florida manatee carcasses can be invaluable when investigating reproduction, survival, and potential age-specific sources of mortality. Results of this study will allow researchers to estimate age, with quantified uncertainty, for 98% of the collected carcasses: 36% by ear bones, 62% by length. Through additional models, future research will use the resulting age estimates to refine survival rate estimates for the youngest age classes, estimates unattainable through mark–recapture studies. Those survival rate estimates can then be used in Florida manatee population viability analysis, currently a key component in manatee management. The incorporated uncertainty will more accurately reflect our current knowledge of the future of the species.

Because numerous species reach an asymptotic length by a relatively young age, many researchers forgo use of length to estimate age, particularly for older (longer) individuals. As an alternative, analyses may use length classes instead of age classes. However, population models require some knowledge of the probability of an individual leaving a smaller length class to enter a larger one for a given time step. Such a requirement still necessitates an understanding of age at length.

Several methods, including age–length keys, are used to estimate age from length in fish (Morton and Bravington 2008), although such techniques are rarely utilized in mammalian research. The methods to estimate age from length described in this research have several advantages over other techniques. In addition to incorporation of age uncertainty, the method does not require a random sample of age–length data. Theoretically, the method allows for estimation of age from length on a continuous scale, but the scale can be altered to fit the limitations of the age and (or) length measurements or to coincide with age classes used in management. In addition, overall precision in age estimates from length are based on the chosen age and length categories, the posterior distribution of the function describing animal growth, and prior information on age distribution, whereas other techniques are highly dependent on sample size by age and length (Morton and Bravington 2008). Lastly, with the exception of defining the distribution of process error (normal) in the length-from-age relationship, the method presented here does not make any assumptions about the distributions of any growth parameters or age-from-length probabilities.

Some very accurate age estimation techniques become infeasible due to limitations of time, money, and invasiveness of procedures, whereas other techniques are disregarded because they are less accurate and (or) biased (Gilbert and Stolt 1970). Therefore, many studies, both in fisheries and in mammalian research, only estimate age for a subsample of data using the more accurate technique. Estimation of age from total body length provides an easy-to-use alternative, and the models to do so can be applied to any species when some age–length and life history data are available. Although the age-from-length method may not be as accurate as other techniques, uncertainty in the method can be quantified and incorporated into other analyses. Estimation of age for the entire data set, which may be possible when a more efficient age estimation technique is available, is particularly important when the subsample of aged individuals using the more accurate technique is nonrandom. Overall, the new methods provide a flexible means to estimate age from length, which can be an invaluable tool when other ageing methods are costly, invasive, or time-intensive.

In addition, growth model results are often used to investigate many species' physiological responses to environmental variability. Bayesian analysis of the Schnute growth curve function provides a novel approach to growth curve estimation by incorporating age error and providing the likelihood of all traditional simplifications and variations of the Schnute model without a need to statistically compare different models. However, given the high posterior correlation between parameters, one should be cautious when interpreting results as true biological processes.

Whether age is estimated via counts of bone or tooth growth layers, tooth wear, otolith rings, body length, shell or tree rings, etc., uncertainty in age estimates from secondary physiological characteristics should be quantified. As adaptive management becomes increasingly prevalent, quantification of various types of uncertainty becomes more and more important, and uncertainty in individual age estimation should not be ignored when addressing age-related species management needs.

Acknowledgements

Dr. Daniel Goodman read several drafts of this manuscript and gave statistical advice and computer software support. Ken Arrison maintained the Florida manatee necropsy data and provided us with the much-needed necropsy reports and updates of the carcass recovery database. The USGS Sirenia Project and Florida Fish and Wildlife Research Institute provided access to their mark–recapture database to cross-reference carcasses with known-age animals. Eric Archer and Shannon Rankin reviewed an earlier draft of this manuscript. This research was funded by the Marine Mammal Commission and Florida Fish and Wildlife Research Institute.

References

Ackerman, B.B., Wright, S.D., Bonde, R.K., Odell, D.K., and Banowetz, D.J. 1995. Trends and patterns in mortality of manatees in Florida, 1974–1992. *In* Population biology of the Florida manatee. National Biological Service Information and Technology Report 1. *Edited by* T.J. O'Shea, B.B. Ackerman, and H.F. Percival. National Biological Service, Washington, D.C. pp. 223–258.

Anderson, P.K. 2002. Habitat, niche, and evolution of sirenian mating systems. J. Mamm. Evol. **9**(1–2): 55–98. doi:10.1023/A:1021383827946.

Beamish, R.J., and McFarlane, G.A. 1983. The forgotten requirement for age validation in fisheries biology. Trans. Am. Fish. Soc. **112**(6): 735–743. doi:10.1577/1548-8659(1983)112<735:TFRFAV>2.0.CO;2.

Buergelt, C.D., Bonde, R.K., Beck, C.A., and O'Shea, T.J. 1984. Pathologic findings in manatees in Florida. J. Am. Vet. Med. Assoc. **185**(11): 1331–1334. PMID:6511576.

Campana, S.E. 2001. Accuracy, precision and quality control in age determination, including a review of the use and abuse of age validation methods. J. Fish Biol. **59**(2): 197–242. doi:10.1111/j.1095-8649.2001.tb00127.x.

Caswell, H. 2001. Matrix population models. 2nd ed. Sinauer Associates, Inc., Sunderland, Mass.

Cope, J.M., and Punt, A.E. 2007. Admitting ageing error when fitting growth curves: an example using the von Bertalanffy growth function with random effects. Can. J. Fish. Aquat. Sci. **64**(2): 205–218. doi:10.1139/F06-179.

Cowles, M.K., and Carlin, B.P. 1995. Markov Chain Monte Carlo diagnostics: a comparative review. J. Am. Stat. Soc. **91**: 883–904.

Demirhan, S.A., and Can, M.F. 2009. Age, growth and food composition of *Scorpaena porcus* (Linnaeus, 1758) in the southeastern Black Sea. J. Appl. Ichthyology, **25**(2): 215–218. doi:10.1111/j.1439-0426.2009.01217.x.

Gelman, A., Carlin, J.B., Stern, H.S., and Rubin, D.B. 1995. Bayesian data analysis. 2nd ed. Chapman and Hall/CRC, Boca Raton, Fla.

Gilbert, F.F., and Stolt, S.L. 1970. Variability in aging Maine white-tailed deer by tooth-wear characteristics. J. Wildl. Manage. **34**(3): 532–535. doi:10.2307/3798858.

Heidelberger, P., and Welch, P.D. 1983. Simulation run length control in the presence of an initial transient. Oper. Res. **31**(6): 1109–1144 . [INFORMS.] doi:10.1287/opre.31.6.1109.

Hernandez, P., Reynolds, J.E., III, Marsh, H., and Marmontel, M. 1995. Age and seasonality in spermatogenesis of Florida manatees. *In* Population biology of the Florida manatee. National Biological Service Information and Technology Report 1. *Edited by* T.J. O'Shea, B.B. Ackerman, and H.F. Percival. National Biological Service, Washington, D.C. pp. 84–97.

Hohn, A.A. 1990. Reading between the lines: analysis of age estimation in dolphins. *In* The bottlenose dolphin. *Edited by* S. Leatherwood and R.R. Reeves. Academic Press, San Diego, Calif. pp. 575–586.

Kendall, W.L., Langtimm, C.A., Beck, C.A., and Runge, M.C.

2004. Capture–recapture analysis for estimating manatee reproductive rates. Mar. Mamm. Sci. **20**(3): 424–437. doi:10.1111/j.1748-7692.2004.tb01170.x.

Kimura, D.K., and Lyons, J.J. 1991. Between-reader bias and variability in the age-determination process. Fish. Bull. (Washington, D.C.), **89**(1): 53–60.

Langtimm, C.A., Beck, C.A., Edwards, H.H., Fick-Child, K.J., Ackerman, B.B., Barton, S.L., and Hartley, W.C. 2004. Survival estimates for Florida manatees from the photo-identification of individuals. Mar. Mamm. Sci. **20**(3): 438–463. doi:10.1111/j.1748-7692.2004.tb01171.x.

Leberg, P.L., Brisbin, I.L., Smith, M.H., and White, G.C. 1989. Factors affecting the analysis of growth-patterns of large mammals. J. Mammal. **70**(2): 275–283. doi:10.2307/1381508.

Marmontel, M. 1995. Age and reproduction in female Florida manatees. *In* Population biology of the Florida manatee. National Biological Service Information and Technology Report 1. *Edited by* T.J. O'Shea, B.B. Ackerman, and H.F. Percival. National Biological Service, Washington, D.C. pp. 98–119.

Marmontel, M., O'Shea, T.J., Kochman, H.I., and Humphrey, S.R. 1996. Age determination in manatees using growth-layer-group counts in bone. Mar. Mamm. Sci. **12**(1): 54–88. doi:10.1111/j.1748-7692.1996.tb00305.x.

Morton, R., and Bravington, M. 2008. Comparison of methods for estimating age composition with application to Southern Bluefin Tuna (*Thunnus maccoyii*). Fish. Res. **93**(1–2): 22–28. doi:10.1016/j.fishres.2008.02.009.

Moura, P., Gaspar, M.B., and Monteiro, C.C. 2009. Age determination and growth rate of a *Callista chione* population from the southwestern coast of Portugal. Aquat. Biol. **5**(1): 97–106. doi:10.3354/ab00119.

O'Shea, T.J., and Reep, R.L. 1990. Encephalization quotients and life-history traits in the Sirenia. J. Mammal. **71**(4): 534–543. doi:10.2307/1381792.

O'Shea, T.J., Beck, C.A., Bonde, R.K., Kochman, H.I., and Odell, D.K. 1985. An analysis of manatee mortality patterns in Florida, 1976–81. J. Wildl. Manage. **49**(1): 1–11. doi:10.2307/3801830.

Pilling, G.M., Kirkwood, G.P., and Walker, S.G. 2002. An improved method for estimating individual growth variability in fish, and the correlation between von Bertalanffy growth parameters. Can. J. Fish. Aquat. Sci. **59**(3): 424–432. doi:10.1139/f02-022.

Plummer, M., Best, N., Cowles, K., and Vines, K. 2006. CODA: Convergence Diagnosis and Output Analysis for MCMC. R News, **6**(1): 7–11.

Ralls, K. 1976. Mammals in which females are larger than males. Q. Rev. Biol. **51**(2): 245–276. doi:10.1086/409310. PMID: 785524.

Ralls, K., and Mesnick, S.L. 2002. Sexual dimorphism. *In* Encyclopedia of marine mammals. *Edited by* W.F. Perrin, B. Würsig, and J.G.M. Thewissen. Academic Press, San Diego, Calif. pp. 1071–1078.

Rathbun, G.B., Reid, J.P., Bonde, R.K., and Powell, J.A. 1995. Reproduction in free-ranging Florida manatees. *In* Population biology of the Florida manatee. National Biological Service Information and Technology Report 1. *Edited by* T.J. O'Shea, B.B. Ackerman, and H.F. Percival. National Biological Service, Washington, D.C. pp. 135–156.

Reid, J.P., Bonde, R.K., and O'Shea, T.J. 1995. Reproduction and mortality of radio-tagged and recognizable manatees on the Atlantic coast of Florida. *In* Population biology of the Florida manatee. National Biological Service Information and Technology Report 1. *Edited by* T.J. O'Shea, B.B. Ackerman, and H.F. Percival. National Biological Service, Washington, D.C. pp. 171–191.

Reynolds, J.E., III, and Wilcox, J.R. 1986. Distribution and abundance of the West Indian manatee (*Trichechus manatus*) around selected Florida power plants following winter cold fronts — 1984–85. Biol. Conserv. **38**(2): 103–113. doi:10.1016/0006-3207(86)90068-6.

Reynolds, J.E., III, Rommel, S.A., and Pitchford, M.E. 2004. The likelihood of sperm competition in manatees — explaining an apparent paradox. Mar. Mamm. Sci. **20**(3): 464–476. doi:10.1111/j.1748-7692.2004.tb01172.x.

Runge, M.C., Langtimm, C.A., and Kendall, W.L. 2004. Stage-based model of manatee population dynamics. Mar. Mamm. Sci. **20**(3): 361–385. doi:10.1111/j.1748-7692.2004.tb01167.x.

Runge, M.C., Sanders-Reed, C.A., Langtimm, C.A., and Fonnesbeck, C.J. 2007. A quantitative threats analysis for the Florida manatee (*Trichechus manatus latirostris*). US Geological Survey Open-File Report 2007-1086. Available online at http://www.pwrc.usgs.gov/resshow/manatee/documents/OFR2007-1086.pdf.

Sainsbury, K.J. 1980. Effect of individual variability on the von Bertalanffy growth equation. Can. J. Fish. Aquat. Sci. **37**(2): 241–247. doi:10.1139/f80-031.

Schnute, J. 1981. A versatile growth-model with statistically stable parameters. Can. J. Fish. Aquat. Sci. **38**(9): 1128–1140. doi:10.1139/f81-153.

Schwarz, L.K. 2004. Understanding uncertainty in aging techniques: the Florida manatee. Report presented to Florida Fish and Wildlife Conservation Commission, Fish and Wildlife Research Institute, Marine Mammal Research Program, St. Petersburg, Fla. Copy available from the lead author.

Schwarz, L.K. 2008. Methods and models to determine perinatal status of Florida manatee carcasses. Mar. Mamm. Sci. **24**(4): 881–898.

Stewart, R.E.A., Campana, S.E., Jones, C.M., and Stewart, B.E. 2006. Bomb radiocarbon dating calibrates beluga (*Delphinapterus leucas*) age estimates. Can. J. Zool. **84**(12): 1840–1852. doi:10.1139/Z06-182.

Uehara, M., Imai, H., and Tachihara, K. 2009. Age and growth of two gizzard shads, *Nematalosa come* and *N. japonica*, in coastal waters around Okinawa Island, southwestern Japan. Fish. Sci. **75**(2): 295–301. doi:10.1007/s12562-008-0042-4.

US Fish and Wildlife Service. 2001. Florida manatee recovery plan (*Trichechus manatus latirostris*). 3rd revision. US Fish and Wildlife Service, Atlanta, Ga.

Wang, Y.G., and Thomas, M.R. 1995. Accounting for individual variability in the von Bertalanffy growth model. Can. J. Fish. Aquat. Sci. **52**(7): 1368–1375. doi:10.1139/f95-132.

Otolith chemistry analyses indicate that water Sr:Ca is the primary factor influencing otolith Sr:Ca for freshwater and diadromous fish but not for marine fish

Randy J. Brown and Kenneth P. Severin

Abstract: Water chemistry is thought to be the primary factor influencing fish otolith chemistry. Experimental results with freshwater and diadromous fish have been consistent with this paradigm, but with marine fish, they have often been ambiguous or contradictory. A review of water chemistry data indicated that Sr:Ca (mmol:mol) levels were higher in marine water than in most freshwater systems and that Sr:Ca variability was lower in marine water than in most freshwater systems. We therefore hypothesized that lifetime otolith Sr:Ca profiles of freshwater fish would exhibit low levels of Sr:Ca with moderate variability, of diadromous fish would exhibit highly variable Sr:Ca levels, and of marine fish would exhibit high levels of Sr:Ca with low variability. Otolith Sr:Ca profiles from 81 species of freshwater, diadromous, and marine fish revealed that freshwater fish had low levels of Sr:Ca and lower variability than expected relative to marine fish, diadromous fish had Sr:Ca levels and variability that were consistent with expectations, and marine fish had high maximum Sr:Ca levels, as expected, and high Sr:Ca variability, similar in magnitude to diadromous fish, which was not expected. These findings indicate that water Sr:Ca is the primary factor influencing otolith Sr:Ca variation for freshwater and diadromous fish but not for marine fish.

Résumé : On croit que la chimie de l'eau est le facteur principal qui influence la chimie des otolithes de poissons. Les études expérimentales utilisant des poissons d'eau douce ou des poissons diadromes s'accordent à ce paradigme, mais celles faites sur les poissons marins sont souvent ambiguës ou contradictoires. Un examen des données de chimie de l'eau indique que les valeurs de Sr:Ca (mmol:mol) sont plus élevées dans les eaux marines que dans la plupart des systèmes d'eau douce et que la variabilité de Sr:Ca est plus faible dans les eaux marines que dans la plupart des systèmes d'eau douce. Nous avons donc émis l'hypothèse selon laquelle les profils Sr:Ca des otolithes des poissons d'eau douce sur l'ensemble de leur vie présentent de faibles valeurs de Sr:Ca avec une variabilité modérée, ceux des poissons diadromes des valeurs de Sr:Ca très variables et ceux des poissons marins de fortes valeurs de Sr:Ca avec une faible variabilité. L'étude des profils de Sr:Ca de 81 espèces de poissons dulcicoles, diadromes et marins montre que les poissons d'eau douce ont de valeurs faibles de Sr:Ca et une variabilité plus faible qu'attendu par comparaison aux poissons marins, que les poissons diadromes ont des valeurs de Sr:Ca et une variabilité qui correspondent aux attentes et que les poissons marins ont des valeurs maximales fortes de Sr:Ca, tel qu'attendu, et une forte variabilité de Sr:Ca, de même importance que celle des poissons diadromes, ce qui n'était pas prévu. Ces observations indiquent que le Sr:Ca de l'eau est le facteur principal qui influence la variation de Sr:Ca chez les poissons dulcicoles et diadromes, mais pas chez les poissons marins.

[Traduit par la Rédaction]

Introduction

Fish populations around the world are being profoundly impacted by exploitation, development activities, and climate change (Hilborn et al. 2003). Understanding fish populations is essential to effective management and long-term preservation of these resources. The science of fish otolith chemistry is being used increasingly to improve our understanding of fish populations by identifying qualities such as essential habitats, migration patterns, and population structure (Campana 1999). Some applications of fish otolith chemistry are becoming almost routine, but there continues to be active research into environmental and physiological factors influencing the incorporation of trace elements into otoliths in the hopes of expanding our capabilities with the science.

The underlying paradigm of almost all otolith chemistry studies is that water chemistry is the primary factor influencing otolith chemistry. Strontium (Sr) has been the most important trace element investigated for several reasons: (*i*) its concentration (or molar ratio to calcium (Ca)) is rela-

Received 20 January 2009. Accepted 8 July 2009. Published on the NRC Research Press Web site at cjfas.nrc.ca on 13 October 2009.
J21005

Paper handled by Associate Editor Steven Campana.

R.J. Brown.[1] US Fish and Wildlife Service, 101 12th Avenue, Room 110, Fairbanks, AK 99701, USA.
K.P. Severin. Department of Geology and Geophysics, University of Alaska Fairbanks, Box 755780, Fairbanks, AK 99775-5780, USA.

[1] Corresponding author (e-mail: randy_j_brown@fws.gov).

Can. J. Fish. Aquat. Sci. **66**: 1790–1808 (2009)　doi:10.1139/F09-112　Published by NRC Research Press

tively stable within but varies widely among aquatic habitats; (*ii*) it is metabolically inert and thought to move passively across membrane barriers separating water from blood and blood from endolymph; (*iii*) it has a 2^+ valence in solution and substitutes for Ca in precipitating otolith mineral; and (*iv*) it is found in relatively high concentrations in water and otoliths compared with other trace elements (Campana 1999; Secor and Rooker 2000). But, does this paradigm hold equally true for all teleost fish?

Experimental studies with juvenile diadromous fish have established unambiguous, positive correlations between the salinity of ambient water and the resulting otolith Sr concentration or molar ratio of Sr to Ca (Sr:Ca) (e.g., Secor et al. 1995; Farrell and Campana 1996; Zimmerman 2005). Field investigations with known life history, diadromous species, often using salinity as a proxy for Sr concentration or Sr:Ca in the water, have produced results consistent with experimental findings (e.g., Limburg 1995; Zimmerman and Reeves 2000; Arai et ai. 2003). Practical applications of otolith Sr analyses with diadromous species have reportedly been successful in describing complex life history details and migration patterns for certain fish populations (e.g., Limburg et al. 2003; Yang et al. 2006; Brown et al. 2007).

Experimental studies with juvenile marine fish have not established consistent positive correlations between salinity treatment levels and otolith Sr concentration or Sr:Ca levels, or there have been significant interactive effects between salinity and environmental or physiological factors (e.g., Bath et al. 2000; Elsdon and Gillanders 2002; Martin et al. 2004). Field investigations of marine species with samples from known locations or life history qualities have produced more ambiguous results than for diadromous species. Many authors have suggested that temperature or physiological events such as spawning interact with water chemistry in complex ways to influence otolith chemistry for marine species (e.g., Campana et al. 1994; FitzGerald et al. 2004; Ashford et al. 2005). Practical applications of otolith Sr analyses with marine species are sometimes reported to be successful in describing life history details such as stock origins or geographic distribution for certain fish populations; however, they usually required the consideration of additional information including concentrations of multiple elements, isotopes, temperature data, and demographic information (e.g., Severin et al. 1995; Thorrold et al. 1998; Rooker et al. 2003). Although physiology is frequently identified as a factor influencing otolith chemistry of marine fish, it is rarely considered to be a factor for freshwater or diadromous fish.

Campana (1999) and Secor and Rooker (2000), in their reviews of the otolith chemistry literature, showed that average otolith Sr levels reported in the literature were greatest in marine, least in freshwater, and intermediate in diadromous fish. This pattern supports the general understanding that Sr levels and Sr:Ca are greater in marine water than in freshwater. Most marine teleost fish species maintain slightly greater fluid solute concentrations than freshwater fish, but both average close to one-third that of marine water (Black 1957). Fish are therefore hypotonic to marine water, where they must work to reduce solute uptake and retain water, and hypertonic to freshwater, where they must work to retain solutes and reduce water uptake. Diadromous species migrate between marine and fresh water and would experience a wider range of osmotic and Sr:Ca conditions than other life history categories. Though it is well established that Sr precipitation in otoliths is a competitive process among 2^+ valence ions in the endolymph (Campana 1999; Kraus and Secor 2004), the different osmotic conditions faced by fish in these different environments may affect the manner in which Sr ions become available to the endolymph.

Summaries of average water chemistry parameters indicate that freshwater systems (e.g., Livingston 1963; Martin and Meybeck 1979; Goldstein and Jacobsen 1987) are uniformly lower in Sr concentration and Sr:Ca molar ratios than marine systems (e.g., Culkin and Cox 1966). Early work by Odum (1957) and more recent work by Kraus and Secor (2004), however, indicate that freshwater Sr:Ca levels are variable among drainage systems and that a small percentage of rivers exhibit Sr:Ca levels greater than reported for marine water. We reviewed water chemistry data for freshwater and marine systems from online databases and from the formal literature to clarify the nature of Sr:Ca environments faced by fish living within these two habitats. We then modeled the estuarine Sr:Ca levels from a small number of river systems to illustrate this transitional environment. This review provides a more comprehensive understanding of Sr:Ca level and variability among habitats, as they relate to fish and otolith chemistry, than was previously available.

We tested patterns of otolith Sr:Ca in freshwater, diadromous, and marine categories of fish for consistency with the paradigm that water chemistry was the primary factor influencing otolith chemistry. Mature-sized, wild fish from these three life history categories were selected. Lifetime Sr:Ca profiles were created with core-to-margin transects to examine Sr:Ca level and variability for each fish. Unknown temperature and physiological effects were expected to influence Sr incorporation into otoliths of all three categories of fish and were considered to be common background factors. Based on our understanding of Sr:Ca differences between freshwater and marine environments, we hypothesized that freshwater fish would exhibit relatively low levels of otolith Sr:Ca with moderate variability, diadromous fish would exhibit high maximum Sr:Ca levels and high variability, reflecting the large range of Sr:Ca environments that they encounter, and marine fish would exhibit relatively high levels of otolith Sr:Ca with low variability.

Materials and methods

Water chemistry review

We reviewed water chemistry data from the United States Geological Survey (USGS 2007) database (n = 4138) and from the geochemistry literature (citations in Appendix A; n = 1861) to improve our understanding of the within-system variability and among-category differences of Sr and Ca in freshwater rivers and lakes, marine systems, and estuaries. Only the dissolved components of Sr and Ca were considered. They were standardized to mg·kg^{-1}, converted to molar concentrations, and presented as the molar ratios of Sr to Ca (Sr:Ca) reported in units of mmol Sr to mol Ca.

Strontium and Ca concentration data were found for 58 lake systems and 786 mainstem and tributary rivers from all continents except Antarctica. Data from closed-basin salt or alkaline lakes were not included in our analyses or figures because the extreme chemistry in these environments often precludes fish occupation and the outlier Sr:Ca values presented scaling problems in our figure. Marine water chemistry data consisted of 171 individual records from published accounts of voyages into most of the major oceans and seas of the world, low and high latitudes, from surface waters to depths of more than 5000 m, and from coral reefs in coastal areas to mid-ocean regions. Data from mid-ocean vents and black smokers were not included. In all, almost 6000 individual measurements of water Sr and Ca concentrations were compiled. Sr:Ca level and variability within and among freshwater and marine habitats were illustrated with a histogram.

The variability of Sr:Ca within individual river systems was examined and graphically compared with the marine system using box plots. Sr:Ca data from 20 rivers were examined. Ten large river drainages from several continents for which Sr:Ca data were available from many mainstem and tributary sites were selected to illustrate the Sr:Ca variability within a drainage. Ten large North American rivers for which Sr:Ca data were available for multiple years and seasons from lower-drainage, mainstem sampling sites were selected to illustrate the Sr:Ca variability within a limited reach of a drainage over a long period of time. All 171 marine Sr:Ca observations were included.

Three rivers with median Sr:Ca levels less than marine water and one river with a median Sr:Ca level greater than marine water were selected to illustrate the relationship between Sr:Ca and salinity in estuary waters. The selected rivers included the Indigirka (Sr:Ca = 2.32) and the Indus (Sr:Ca = 3.58), which had relatively low levels of dissolved solutes, and the Mississippi (Sr:Ca = 2.01) and St. Johns (Sr:Ca = 13.83), which had relatively high levels of dissolved solutes. Concentrations of Sr and Ca were modeled across an estuarine salinity gradient from 0 to 35 practical salinity units (psu) with a progressive series of complementary mixing fractions of fresh and salt water using the following equation:

$$c_{ai} = [(c_{fi}) \cdot (1 - p)] + [(c_{mi}) \cdot (p)]$$

where c_{ai} is the concentration (mg:kg) of element i in ambient estuarine water, c_{fi} is the concentration of element i in freshwater, c_{mi} is the concentration of element i in marine water, i represents dissolved Sr or Ca, and ambient salinity is $p \cdot 35$, where p ranges from 0 to 1. Freshwater Sr and Ca concentrations used in this model were median values for the selected rivers. Average marine water Sr and Ca concentrations from our literature sources were 7.64 (standard deviation (SD) = 0.53) and 405.87 (SD = 27.49) $\mathrm{mg \cdot kg^{-1}}$, respectively, and the mean Sr:Ca level was 8.61 mmol:mol. The variable "p" ranged from 0 to 1 and reflected ambient salinity as a proportion of marine salinity, which was modeled at 35 psu. End-member concentrations of Sr and Ca were used to model Sr:Ca (mmol:mol) values and were plotted against salinity.

Fish otolith selection, preparation, and analysis

Otoliths from 28 freshwater, 21 diadromous, and 32 marine fish species were examined in this study (Appendix B). Taxonomy and nomenclature in this paper are consistent with Fishbase (2008). Mature-sized, wild-caught fish were used in all cases. They were collected from locations and in circumstances ensuring they had lived only in freshwater, in both freshwater and marine water, or only in marine water, respectively. One sample per species was included in among-habitat analyses. Within-species variability was explored with additional analyses of 20 individuals each from freshwater drum (*Aplodinotus grunniens*), a freshwater species, Bering cisco (*Coregonus laurettae*), a diadromous species, and sablefish (*Anoplopoma fimbria*), a marine species.

One otolith from each fish was thin-sectioned through the core and mounted on a glass slide. Most were sectioned in the transverse plane, but some unusually shaped otoliths were sectioned in other planes. Each section was 200–300 μm thick, and growth increments from the core region to the margin were visible with transmitted light. They were polished on a lapidary wheel with 1 μm diamond abrasive and coated with a conductive layer of carbon in preparation for microprobe analyses.

A wavelength-dispersive electron microprobe (microprobe) was used for chemical analyses of otoliths. The technology functions by directing a focused beam of electrons to points on a sample surface. Atoms within the material are ionized by the electron beam and emit X-rays unique to each element. Spectrometers are tuned to count the X-rays from elements of interest. The electron beam used here was 5 μm in diameter and was operated at an accelerating voltage of 15 kilo-electron volts and a nominal current of 20 nanoamperes. According to Gunn et al. (1992), the electron beam penetrates less than 3 μm into otolith material. Strontium and Ca X-rays were counted for 25 s at each point along a core-to-margin transect (core precipitated early in life, margin precipitated late in life) for each otolith. Center-to-center distance between points was 8 μm. Element-specific X-ray counts at each point are proportional to the concentration of the element in the sampled material (Reed 1997; Goldstein et al. 2003). Strontianite and calcite standards were used with established quantitative procedures to develop conversion factors between X-ray count data and elemental concentration estimates in units of $\mathrm{mg \cdot kg^{-1}}$, as detailed by Brown et al. (2007). Elemental concentrations of Sr and Ca were converted to molar concentrations using the following equivalencies:

$$\left(\frac{\mathrm{Sr_{moles}}}{\mathrm{kg}}\right) = \left(\frac{\mathrm{Sr_{mg}}}{\mathrm{kg}}\right)\left(\frac{1_{\mathrm{mole}}}{87.620_{\mathrm{g}}}\right)\left(\frac{1_{\mathrm{g}}}{1000_{\mathrm{mg}}}\right)$$

and

$$\left(\frac{\mathrm{Ca_{moles}}}{\mathrm{kg}}\right) = \left(\frac{\mathrm{Ca_{mg}}}{\mathrm{kg}}\right)\left(\frac{1_{\mathrm{mole}}}{40.078_{\mathrm{g}}}\right)\left(\frac{1_{\mathrm{g}}}{1000_{\mathrm{mg}}}\right)$$

Calcium is found in much greater concentration than Sr in fish otoliths and behaves as a constant in the ratio of Sr:Ca (Campana 1999; Secor and Rooker 2000). Variability in otolith Sr:Ca is, therefore, due almost exclusively to variation in Sr concentration. Consistent with this understanding, we observed a relatively constant Ca concentration among samples at approximately 389 000 $\mathrm{mg \cdot kg^{-1}}$, with a standard error (SE) of approximately 0.23%, or about 900 $\mathrm{mg \cdot kg^{-1}}$. Stron-

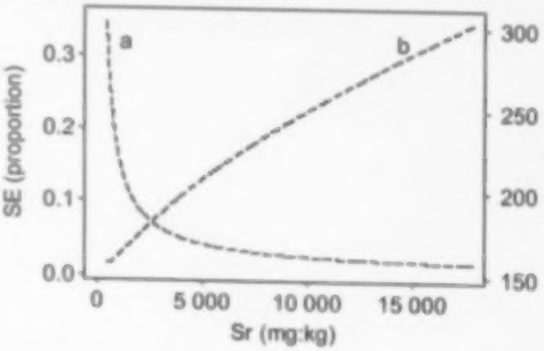

Fig. 1. Standard error (SE) variation across a wide range of otolith Sr concentration estimates expressed in (*a*) proportion of the estimate and (*b*) units of mg:kg.

tium concentration varied widely, ranging from just over our detection limit of approximately 330 mg·kg^{-1} to more than 17 000 mg·kg^{-1}. The SEs of the Sr concentration estimates were proportionally greater near detection limits than at higher concentrations, resulting in approximately 150 mg·kg^{-1} near detection limits and 300 mg·kg^{-1} at the greatest concentrations (Fig. 1).

Three measures of otolith Sr and Sr:Ca variability were analyzed: (*i*) an index of the coefficient of variation (CV) of Sr X-ray count data, which is a function of each data point in a profile relative to the mean value; (*ii*) the range of Sr:Ca, which is a function of only two data points within each profile; and (*iii*) an index of the total variation of each profile, which was an additive function of the Sr:Ca differences between each sequential pair of data points (see Riesz et al. 1990, p. 10, eq. 3). Raw X-ray count data (without the background removed) from homogeneous material are Poisson-distributed, with a mean equal to the variance (Goldstein et al. 2003). An index of the CV of Sr X-ray count data (CVI) was calculated as

$$\mathrm{CVI} = \left(\frac{s}{\bar{X}}\right) \cdot \left(\frac{\sqrt{\bar{X}}}{\bar{X}}\right)^{-1} = \left(\frac{s}{\sqrt{\bar{X}}}\right)$$

where $\left(\frac{s}{\bar{X}}\right)$ was the actual CV and $\left(\frac{\sqrt{\bar{X}}}{\bar{X}}\right)$ was the CV expected from homogeneous material. If an otolith were homogeneous for Sr, the CVI would equal approximately one, and if Sr concentration varied widely across an otolith, the CVI would be much larger than one. The Sr:Ca range statistic was simply the difference between the greatest and lowest values in each profile. The total variation of Sr:Ca (T_v) across each profile was calculated as

$$T_v = \sum_{2}^{n} |(x_k) - (x_{k-1})|$$

where n is the number of sample points in the profile, x is the Sr:Ca value, and $k = 2, 3, \ldots, n$. Standardized residuals from the least-squares linear regression of all T_v were used as the index statistics to account for the wide variation in n among profiles. One-way analysis of variance (ANOVA) procedures were used to test null hypotheses that mean values of CVI, range Sr:Ca, and the index of total variation from the six sample groups of fish were equal versus the alternative hypothesis that at least one group was different. Prior to analysis, the CVI and range Sr:Ca statistics were $\log_{10}$-transformed (log(statistic + 1)) to normalize distributions and equalize variances among categories. Tukey's honestly significant difference (HSD) method of multiple comparisons was conducted a posteriori with a family error rate of 0.05 to determine the relative positions of the groups.

Two measures of otolith Sr:Ca level were analyzed: median and maximum Sr:Ca, which are single-point data values within each profile. Median Sr:Ca was selected rather than mean Sr:Ca because the median value better represents the bulk of data in skewed distributions and is very similar to the mean in normally distributed data. One-way ANOVA procedures were used to test null hypotheses that mean values of log-transformed median and maximum Sr:Ca data from the six sample groups of fish were equal versus the alternative hypotheses that at least one group was different. Following significant results, a posteriori analyses using Tukey's HSD method of multiple comparisons with a family error rate of 0.05 were conducted to determine the relative positions of the groups.

Otolith chemistry studies of diadromous species identify ontogenetic trends in Sr or Sr:Ca to infer migrations between freshwater and marine water (e.g., Brenkman et al. 2007; Brown and Severin 2007). Based strictly on our understanding of Sr:Ca variability in water, freshwater and marine categories of fish were not expected to have distinct or predictable ontogenetic Sr:Ca trends. Instead, it was hypothesized that their Sr:Ca levels would exhibit relatively low variation around a mean value due to annual temperature patterns, physiological effects, and small within-habitat water chemistry fluctuations. Despite these expectations, ontogenetic trends in marine fish otolith chemistry have been detected previously and were thought to be the result of physiological factors rather than water chemistry variation (Brophy et al. 2004; Morales-Nin et al. 2005; Miller 2007). To characterize ontogenetic trends in otolith Sr:Ca, we used the slope parameter from the least-squares linear regression of Sr:Ca for each profile as an indicator. We tested the null hypothesis that mean slope parameters for all six groups of fish were equal with a one-way ANOVA. Upon significant results, a posteriori analysis using Tukey's HSD method of multiple comparisons with a family error rate of 0.05 were conducted to determine the relative positions of the groups.

Characteristic otolith Sr and Sr:Ca variability, Sr:Ca levels, and ontogenetic trends in Sr:Ca among freshwater, diadromous, and marine fish species were illustrated based on a principal components analysis (Jolliffe 1986). Analytical factors from each fish included log-transformed CVI, range, median, and maximum Sr:Ca data, and the total variation index and slope factors. The eigenvalues and eigenvectors for the principal components were tabulated, and the essential variation among life history groups and representative species was illustrated with an ordination plot of the first two principal components.

Graphs of otolith Sr:Ca variation across core-to-margin transects, lifetime Sr:Ca profiles, illustrate ontogenetic trends and have been widely used to describe migrations be-

Fig. 2. Histogram (not stacked) illustrating Sr:Ca (mmol:mol) variability in marine (darkly shaded bars; $n = 171$), river (lightly shaded bars; $n = 786$), and lake (open bars; $n = 58$) habitats.

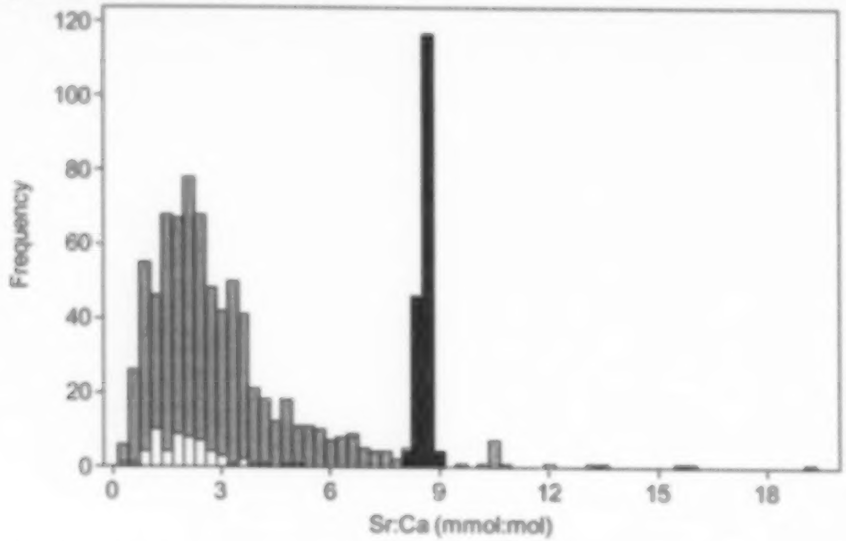

Fig. 3. Sr:Ca variability within 10 large river drainages (upper section), 10 lower mainstem reaches (middle section), and the marine environment (lower section). Sample sizes for each river and for the marine system are indicated in parentheses. All box plots in this paper include median line, interquartile range box, and whiskers that encompass more than 95% of data points. No outliers are shown.

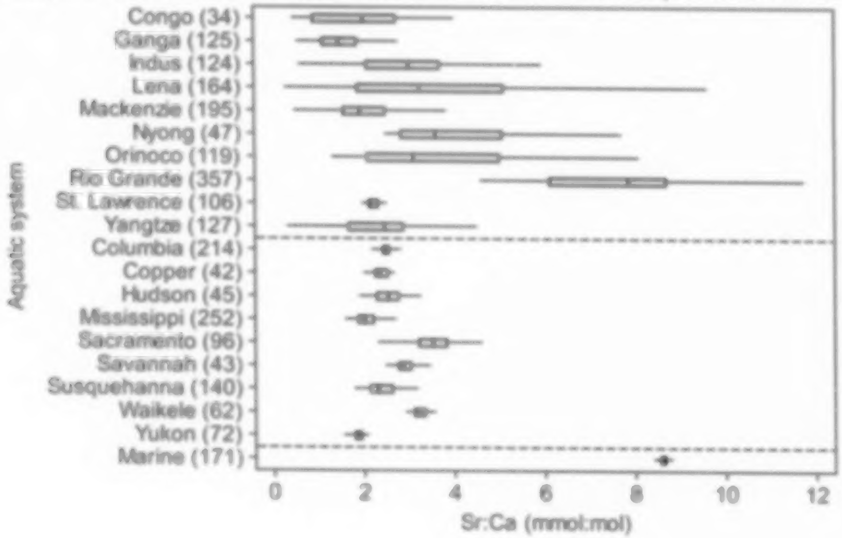

tween freshwater and marine environments (e.g., Tzeng 1996; Howland et al. 2001; Brenkman et al. 2007). General trends in otolith Sr:Ca common to each category were illustrated with a representative selection of species. Several species were represented in both freshwater and diadromous categories, and the Sr:Ca profiles of some of these pairs are presented to illustrate category-specific patterns. Several families were represented by multiple species, and Sr:Ca profiles of some of these family groups are presented to illustrate common patterns. Several additional unique or unusual otolith Sr:Ca profiles are presented and discussed. Because the total number of sample points varied widely among otolith core-to-margin transects, profiles were created with Sr:Ca values plotted against the proportion of the core-to-margin transect for each point.

The partition coefficient for Sr was calculated as

$$D_{Sr} = \left(\frac{Sr}{Ca}\text{otolith}\right) \cdot \left(\frac{Sr}{Ca}\text{water}\right)^{-1}$$

When used in otolith chemistry studies, it is an indicator of the osmoregulatory resistance that an element encounters

Fig. 4. Modeled estuary mixing curves of Sr:Ca versus salinity (psu) for (*a*) Indigirka, (*b*) Indus, (*c*) Mississippi, and (*d*) St. Johns rivers.

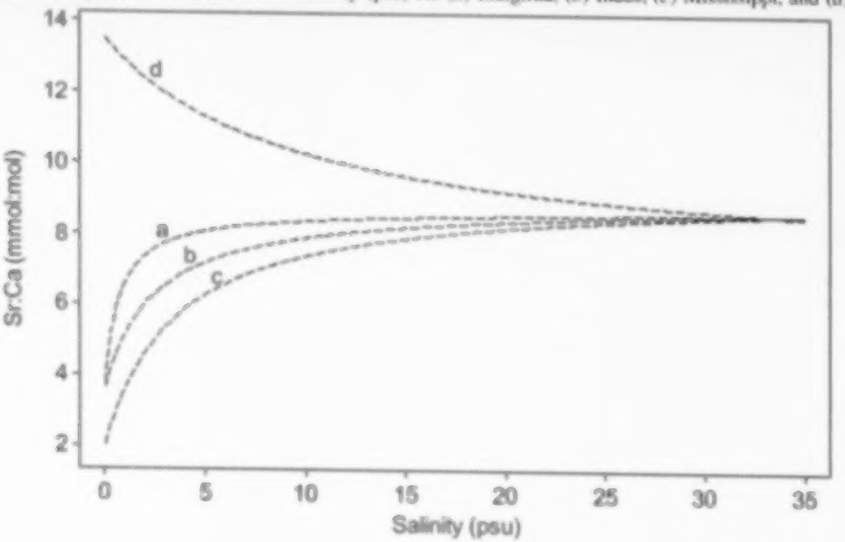

Fig. 5. Box plots illustrating characteristic patterns of otolith Sr and Sr:Ca variability, levels, and ontogenetic trends among freshwater, diadromous, and marine fish as indicated with CVI, Sr:Ca range, the total variation index, maximum and median Sr:Ca data, and slope coefficients. Lettering on the right of each panel indicates results of Tukey's multiple comparisons procedures. Sample groups that are similar are indicated with the same letter and those that are significantly different are indicated with different letters.

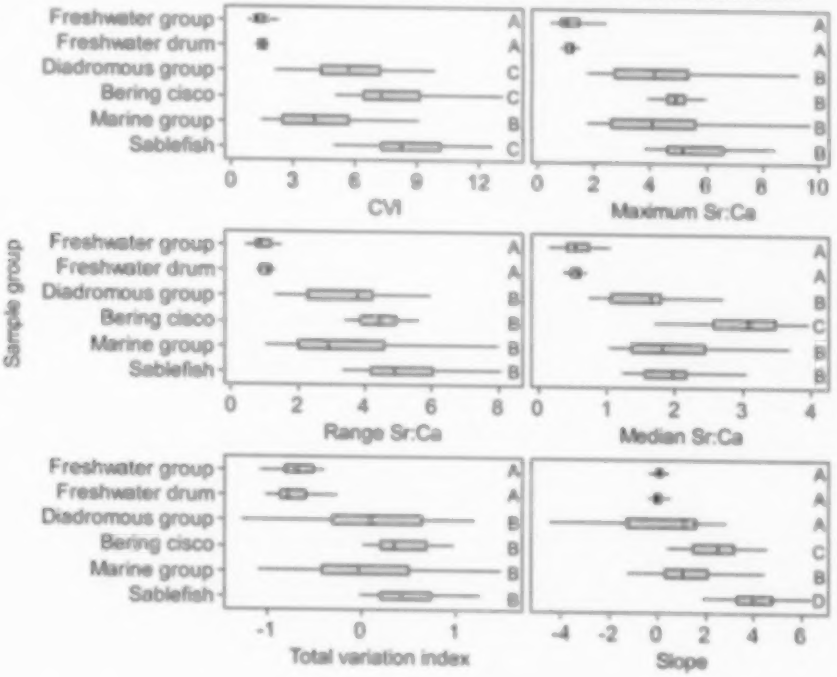

when moving from the water, through the blood, into the endolymph, and eventually to a precipitation site on the otolith. Values near one indicate little resistance relative to Ca, and values approaching zero indicate high resistance (Campana 1999). Water Sr:Ca levels experienced by freshwater and diadromous species in this study were not known with enough confidence to calculate D_{Sr} values. Marine fish, however, were considered to have experienced a relatively constant Sr:Ca environment of approximately 8.61 mmol:mol throughout life. A D_{Sr} profile was therefore prepared for each marine fish, including the sablefish group. Lifetime variability of D_{Sr} values for the marine species were illu-

Table 1. Eigen analysis of the correlation matrix and loading table for the first five principal components of log-transformed CVI, range, median, and maximum Sr:Ca data, and the total variation index and slope coefficient factors from the otoliths of freshwater, diadromous, and marine fish species.

Variable	PC1	PC2	PC3	PC4	PC5
Eigenvalue	4.47	0.92	0.34	0.23	0.05
Proportion	0.75	0.15	0.06	0.04	0.01
Cumulative proportion	0.75	0.90	0.95	0.99	1.00
CVI	–0.46	0.03	0.23	–0.38	0.74
Range Sr:Ca	–0.46	–0.05	0.13	–0.36	–0.29
Total variation index	–0.36	–0.57	0.35	0.65	0.03
Median Sr:Ca	–0.41	0.08	–0.84	0.29	0.18
Maximum Sr:Ca	–0.46	–0.08	–0.08	–0.25	–0.57
Slope	–0.27	0.81	0.32	0.39	–0.10

Fig. 6. Ordination diagram of the first two components from a principal components analysis of log-transformed CVI, range, median, and maximum Sr:Ca data, and the total variation index and slope coefficient factors from the otoliths of six groups of fish; freshwater species (△), freshwater drum (+), diadromous species (○), Bering cisco (●), marine species (□), and sablefish (×). Approximately 90% of the variability among groups was encompassed by these two principal components. One outlier from the diadromous group was located outside of the scales presented at $X = -5.90$, $Y = -6.42$.

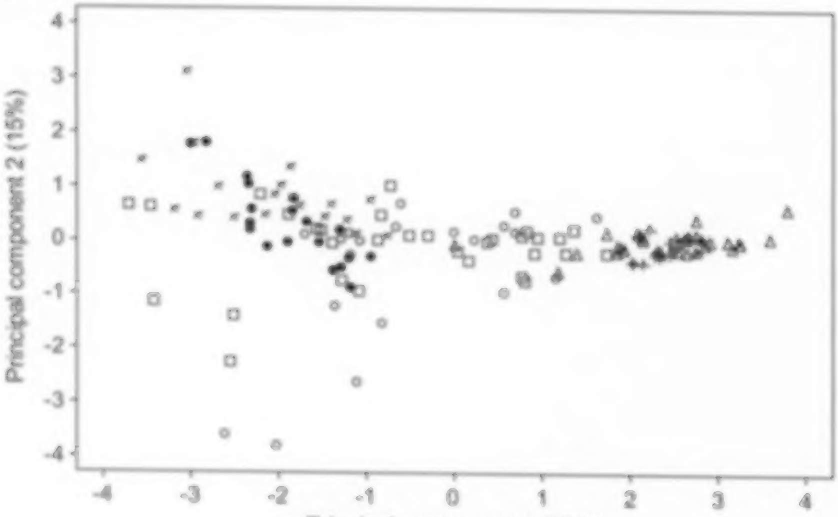

strated with box plots and discussed. Maximum otolith Sr:Ca levels of marine species were thought to reflect their minimum osmoregulatory resistance to Sr while experiencing marine Sr:Ca levels. Distributions of maximum D_{Sr} values for marine species and for the sablefish group were illustrated with a box plot.

Results

Water chemistry

River and lake environments varied across a wider range of Sr:Ca than did marine environments (Fig. 2). Median river (2.39) and lake (1.92) Sr:Ca levels were much lower than the marine level (8.61). Sr:Ca levels ranged from 0.27 to 19.18 in rivers, 0.20 to 5.02 in lakes, and 8.17 to 8.87 in marine water. Less than 3% of the 786 rivers reviewed here, and none of the lakes, had median Sr:Ca levels that exceeded minimum marine levels. Sr:Ca variability within entire drainages was clearly greater than in limited reaches of drainages (Fig. 3), and marine waters were comparatively invariable.

Mixing curves modeled across the estuarine salinity gradients from the four selected rivers revealed a high rate of Sr:Ca change at low salinity levels that declined exponentially as salinity increased (Fig. 4). Surge and Lohmann (2002) derived this same pattern empirically across three estuaries in Florida, and Zimmerman (2005) measured it in his experimental Sr:Ca habitats as well. Rivers with lower dissolved-solute concentrations (Indigirka and Indus rivers) approached marine Sr:Ca levels more precipitously than those with higher dissolved-solute concentrations (Mississippi and St. Johns rivers). The mixing curve for the St.

Fig. 7. Sr:Ca profiles of four pairs of freshwater (first and third columns) and anadromous (second and fourth columns) conspecifics including (*a* and *b*) threespine stickleback (*Gasterosteus aculeatus*), (*c* and *d*) striped bass (*Morone saxatilis*), (*e* and *f*) kokanee and sockeye salmon (*Oncorhynchus nerka*), and (*g* and *h*) humpback whitefish (*Coregonus pidschian*).

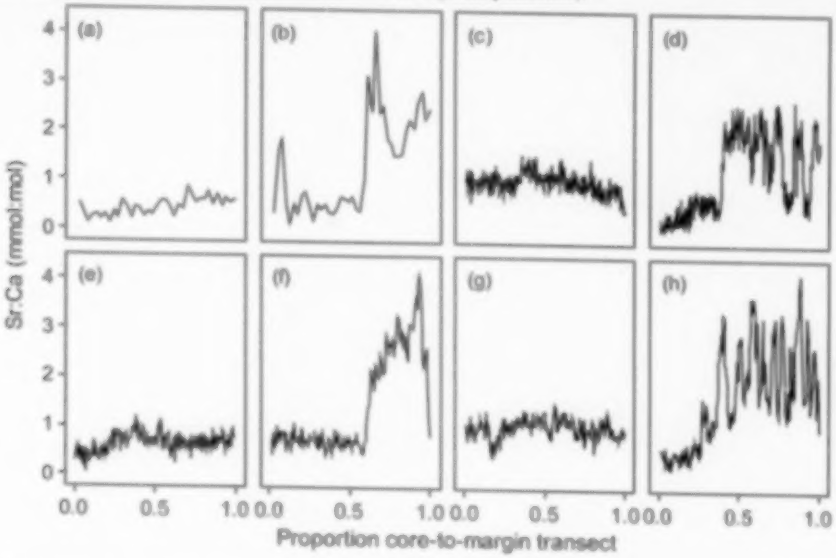

Johns River, one of the rare rivers with Sr:Ca levels greater than marine levels, declined to the marine Sr:Ca level, whereas the other rivers rose to the marine level. These data indicate that diadromous fish moving through an estuary would experience greater Sr:Ca change between salinities 0 and 10, when they are hypertonic to the environment, than between salinities 10 and 35, as they become hypotonic to the environment.

Fish otoliths

Statistics

Initial ANOVA tests of all three otolith Sr and Sr:Ca variability statistics, the two otolith Sr:Ca level statistics, and the ontogenetic trend statistic among the six groups of fish were all highly significant ($P < 0.001$ in all tests). Subsequent contrasts between groups were significant at the family error level of $\alpha = 0.05$. All measures of variability and level indicated that freshwater species exhibited significantly less otolith Sr and Sr:Ca variability and significantly lower levels of otolith Sr:Ca than diadromous or marine species (Fig. 5). The freshwater species and freshwater drum groups exhibited similar measures of otolith Sr and Sr:Ca variability and otolith Sr:Ca level. Freshwater species groups exhibited no particular ontogenetic trend, as indicated by the slope statistic. The freshwater species and freshwater drum groups had similar mean slopes to the diadromous species group, which included several catadromous species, but had significantly lower mean slopes than the Bering cisco, marine species, and sablefish groups.

Diadromous and marine species groups exhibited general similarity in measures of Sr and Sr:Ca variability and Sr:Ca level, and although they differed significantly in mean slopes, all exhibited substantial variability in ontogenetic trends compared with the freshwater species groups (Fig. 5). All four diadromous and marine species groups had statistically similar range Sr:Ca and total variation index measures of Sr:Ca variation, and maximum measures of Sr:Ca levels. The marine species group had a significantly lower CVI statistic than other diadromous or marine species groups, which were similar. The Bering cisco group had a significantly higher median Sr:Ca statistic than other diadromous or marine species groups, which were similar. Mean slopes of Bering cisco, marine species, and sablefish groups were all positive and significantly greater than freshwater species groups.

Principal components analysis

The principal components analysis was effective at consolidating 90% of the essential variability of the six comparative measures that we examined into the first two principal components (Table 1). The ordination plot of the first two principal components illustrated the domains of, or area occupied by, each group relative to the others (Fig. 6). The freshwater species and freshwater drum groups shared a common domain in a relatively discrete region of the plot. The Bering cisco and sablefish groups shared a common regional domain that substantially intersected with the domains of diadromous and marine species groups, but not with the domains of the freshwater species groups. The diadromous and marine species groups occupied the largest regional domains in the plot, intersecting with each other over a substantial region, and with all other groups, except freshwater drum, to some extent. Consistent with the statistical results of our six measures of Sr and Sr:Ca variability, level, and ontogenetic trends, the principal components analysis illustrated that the Sr:Ca profiles of the freshwater species groups were distinctly different than those of the diadromous and marine species groups, which were more similar than they were different.

Sr:Ca profiles

Sr:Ca profiles of pairs of freshwater and anadromous conspecifics revealed a visually distinctive pattern of Sr:Ca variation between categories. All four of the Sr:Ca profiles from the freshwater category had relatively low Sr:Ca levels and low variation (Fig. 7, first and third columns). This contrasted with the Sr:Ca profiles of their anadromous conspecifics that had low Sr:Ca levels initially, reflecting their natal origins in fresh water, followed by significantly elevated Sr:Ca levels later, reflecting their subsequent migrations to marine environments (Fig. 7, second and fourth columns). The Sr:Ca spike in the core region of the anadromous threespine stickleback (*Gasterosteus aculeatus*; Fig. 7*b*) is thought to be an indicator of an anadromous mother, a phenomenon documented for other anadromous species (Kalish 1990; Volk, et al. 2000; Zimmerman and Reeves 2000). The oscillating pattern of Sr:Ca peaks and nadirs in the profiles of the anadromous striped bass (*Morone saxatilis*; Fig. 7*d*) and humpback whitefish (*Coregonus pidschian*; Fig. 7*h*) indicated repeated migrations between marine and freshwater environments as discussed by Secor and Piccoli (2007) for striped bass.

Family groups of species exhibited similar ontogenetic patterns of Sr:Ca variability, level, and distribution, at least within life history categories. Rockfish species (Sebastidae; Fig. 8, top row), exhibited consistently low Sr:Ca levels compared with many other marine species as reflected by maximum Sr:Ca levels of approximately 3 mmol:mol or less. Flatfish species (Pleuronectidae; Fig. 8, second row), exhibited greater variation than rockfish with distinct ontogenetic trends in their Sr:Ca profiles towards higher values later in life. The maximum Sr:Ca level within the flatfish samples was approximately 4 mmol:mol in Pacific halibut (*Hippoglossus stenolepis*; Fig. 8*f*). Sculpin species (Cottidae; Fig. 8, third row) included one freshwater and two marine representatives. The freshwater species, slimy sculpin (*Cottus cognatus*; Fig. 8*g*), exhibited a consistently low level of Sr:Ca with no ontogenetic trend. By contrast, the marine sculpins' Sr:Ca profiles ranged from low levels early in life to relatively high levels later in life that reached a maximum of approximately 8 mmol:mol in a fourhorn sculpin (*Triglopsis quadricornis*; Fig. 8*i*). Similar to the sculpins, cod species (Gadidae; Fig. 8, bottom row) included one freshwater and two marine representatives. Burbot (*Lota lota*) are classified in the family Gadidae by the American Fisheries Society (2004) but in the family Lotidae in Fishbase (2008). We placed burbot with Gadidae species in this figure to highlight the contrast between the patterns of otolith Sr:Ca exhibited by closely related freshwater and marine species. Burbot exhibited a relatively constant low level Sr:Ca profile with no ontogenetic trend (Fig. 8*j*). The marine cod species ranged from very low levels early in life to relatively high levels later in life that reached a maximum of approximately 9.7 mmol:mol in a Pacific cod (*Gadus macrocephalus*; Fig. 8*l*). These data suggest that closely related species within a life history category exhibit similar patterns of otolith Sr:Ca variability, level, and distribution.

The St. Johns River in northern Florida has an extraordinarily high level of Sr:Ca, with a median value of 13.83 mmol:mol (USGS 2007). Several Clupeidae species spawn in the St. Johns River, including anadromous blueback herring (*Alosa aestivalis*) and hickory shad (*A. mediocris*) (Harris et al. 2007). Otolith Sr:Ca profiles of blueback herring and hickory shad from the St. Johns River are presented in contrast to the profile of an anadromous American shad (*A. sapidissima*) from the Hudson River, which has a median Sr:Ca level of 2.49 mmol:mol (USGS 2007). The ontogenetic patterns of Sr:Ca for the American shad (Fig. 9*a*) is consistent with that observed in other anadromous species (see Fig. 7), with low levels in the otolith core region reflecting the chemistry of the freshwater natal environment followed by a distinct rise in Sr:Ca levels reflecting migration to sea. The blueback herring (Fig. 9*b*) and the hickory shad (Fig. 9*c*) from the St. Johns River exhibited Sr:Ca patterns more typical of catadromous species (see Fig. 10), with high levels in their core regions reflecting the unusually high Sr:Ca environment of their natal river followed by a drop in otolith Sr:Ca when they migrated to sea. These data support Kraus and Secor's (2004) contention that water Sr:Ca molar ratios are more predictive than salinity of otolith Sr:Ca levels.

Sr:Ca data from the otolith of a black crappie (*Pomoxis nigromaculatus*) exhibited the greatest variability and the highest levels of all freshwater species examined. It was an outlier in the principal components analysis (Fig. 6, the triangle located close to the 0,0 position), grouping more with the diadromous and marine species groups than with the freshwater species group. The Sr:Ca profile of the black crappie (Fig. 9*e*) is presented in contrast with the profiles of an Alaska blackfish (*Dallia pectoralis*; Fig. 9*d*), exhibiting a typical freshwater fish profile, and an Arctic cisco (*Coregonus autumnalis*; Fig. 9*f*), exhibiting a typical anadromous fish profile. The oscillating pattern of Sr:Ca variation in the profile of the black crappie is clearly more similar in form and magnitude to that from anadromous species than from freshwater species. The black crappie used in this study was captured in Echo Canyon Reservoir in the state of Colorado, USA. The reservoir goes through a dramatic annual cycle of high water after the annual snowmelt, followed by a progressive decline in water level through the rest of the year. Although the Sr and Ca chemistry of Echo Canyon Reservoir is not known, it is thought that the variation in annual water level results in dramatic cycles of diluted and concentrated dissolved solutes, which in turn are reflected in the otolith Sr:Ca profiles of the fish living there.

High ontogenetic variation and maximum levels of otolith Sr:Ca were observed in the Sr:Ca profiles for some diadromous and marine species. The highest otolith Sr:Ca value recorded among the species in this study, 21.80 mmol:mol, was from an anadromous broad whitefish (*Coregonus nasus*; Fig. 10*c*) from Northwest Alaska. Quantitative analyses of this otolith showed that the maximum concentration of elemental Sr was approximately 17 900 mg:kg (95% CI = 17 300 – 18 500 mg:kg). The core region had a uniformly low level of Sr:Ca, consistent with the freshwater natal environment of the species, followed by a region of dramatic peaks and nadirs, consistent with multiple migrations between environments. The fish apparently returned to freshwater to stay at some point later in life, based on a drop in Sr:Ca back towards natal levels. The Sr:Ca profiles of two catadromous species, Atlantic tarpon (*Megalops atlanticus*;

Fig. 8. Sr:Ca profiles of three species within each of four families. Sebastidae species (top row) include (*a*) rougheye rockfish (*Sebastes aleutianus*), (*b*) yelloweye rockfish (*S. ruberrimus*), and (*c*) quillback rockfish (*S. maliger*). Pleuronectidae species (second row) include (*d*) Bering flounder (*Hippoglossoides robustus*), (*e*) Arctic flounder (*Liopsetta glacialis*), and (*f*) Pacific halibut (*Hippoglossus stenolepis*). Cottidae species (third row) include (*g*) slimy sculpin (*Cottus cognatus*), (*h*) Arctic staghorn sculpin (*Gymnocanthus tricuspis*), and (*i*) fourhorn sculpin (*Triglopsis quadricornis*). Gadidae species (fourth row) include (*j*) burbot (*Lota lota*; see discussion in text on family classification of burbot), (*k*) saffron cod (*Eleginus gracilis*), and (*l*) Pacific cod (*Gadus macrocephalus*). Note that the *Y* scale is consistent within family groups, but different among them.

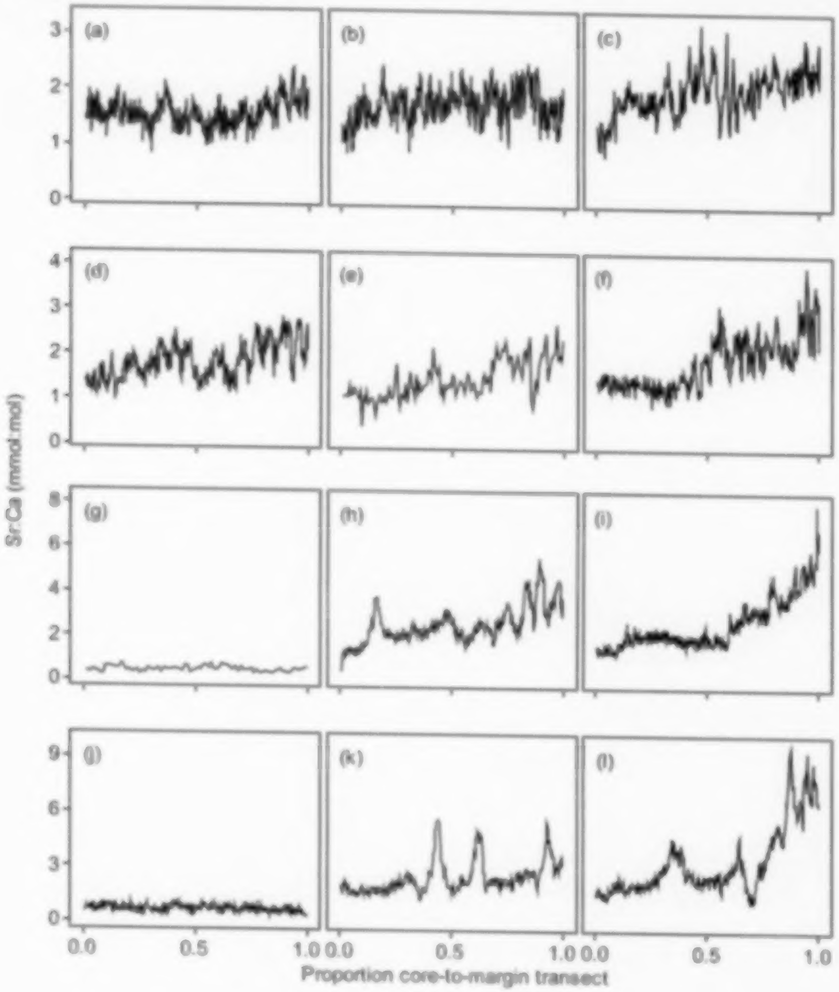

Fig. 10*a*) and European eel (*Anguilla anguilla*; Fig. 10*b*), revealed high levels of Sr:Ca in the core regions of their otoliths, consistent with their marine origins, followed by precipitous declines in Sr:Ca to low levels, consistent with their migrations into freshwater environments. Atlantic tarpon are not obligated to migrate into freshwater environments, but the sample in this study was collected from Lake Nicaragua, a large freshwater lake located approximately 190 km by river from the sea.

The highest otolith Sr:Ca value recorded among marine species in this study, 13.93 mmol:mol, was from the core region of a stout eelblenny (*Anisarchus medius*; Fig. 10*f*) collected during an offshore, benthic-sampling expedition in the Chukchi Sea. Quantitative analyses of this otolith showed that the maximum concentration of elemental Sr was approximately 11 500 mg:kg (95% CI = 11 000 – 12 000 mg:kg). The Sr:Ca profile of a sablefish (Fig. 10*d*) exhibited an ontogenetic pattern similar to that observed in anadromous species such as the humpback whitefish (Fig. 7*h*) presented earlier, with low Sr:Ca levels in the core region, followed by an oscillating series of peaks and nadirs through the rest of its life. The Sr:Ca profile of an Antarctic toothfish (*Dissostichus mawsoni*; Fig. 10*e*) exhibited an ontogenetic trend and maximum level of otolith Sr:Ca similar to those of the fourhorn sculpin (Fig. 8*i*) and Pacific cod (Fig. 8*l*) presented earlier. They all had low levels of Sr:Ca in the core regions followed by progressive increases in Sr:Ca that attained maximum levels in excess of 8 mmol:mol late in life.

Fig. 9. Sr:Ca profiles of six anadromous and freshwater species that illustrate some unusual effects of extraordinary freshwater environments on otolith chemistry. The first row highlights three anadromous Clupeidae species: (*a*) American shad (*Alosa sapidissima*) came from the Hudson River, which has a median Sr:Ca level of 2.49 mmol:mol; (*b*) blueback herring (*A. aestivalis*) and (*c*) hickory shad (*A. mediocris*) originated in the St. Johns River in Florida, which has an unusually high median Sr:Ca level of 13.83 mmol:mol. The second row includes Sr:Ca profiles of (*d*) Alaska blackfish (*Dallia pectoralis*), a typical freshwater species, (*e*) black crappie (*Pomoxis nigromaculatus*), a freshwater species captured in an impoundment that experiences widely fluctuating water level cycles each year, and (*f*) Arctic cisco (*Coregonus autumnalis*), a typical diadromous fish.

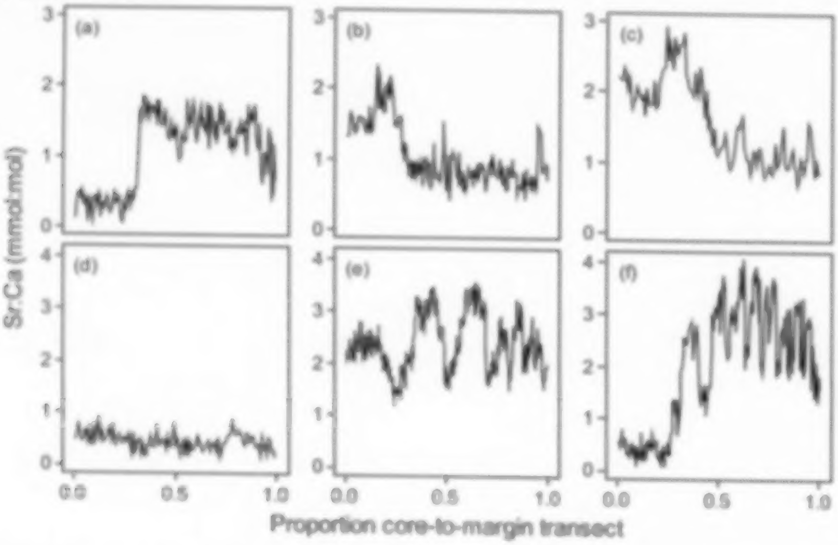

Fig. 10. Sr:Ca profiles of diadromous (top row) and marine (bottom row) species with unusually high Sr:Ca variation and high maximum Sr:Ca levels. Note that the *Y* scale is unique for each profile. (*a*) Atlantic tarpon (*Megalops atlanticus*) and (*b*) European eel (*Anguilla anguilla*) are catadromous and (*c*) broad whitefish (*Coregonus nasus*), which had the highest maximum Sr:Ca value of any fish examined (21.80 mmol:mol), is anadromous. The Sr:Ca profile of the sablefish had the appearance of a typical anadromous species such as the humpback whitefish, with relatively low Sr:Ca levels in the core followed by a series of oscillating peaks and nadirs across the rest of the profile. (*e*) Antarctic toothfish (*Dissostichus mawsoni*) exhibited a progressive ontogenetic trend towards very high Sr:Ca levels that peaked at over 9 mmol:mol. (*f*) Stout eelblenny (*Anisarchus medius*) had extraordinarily high Sr:Ca levels in the core region of its otolith (almost 14 mmol:mol).

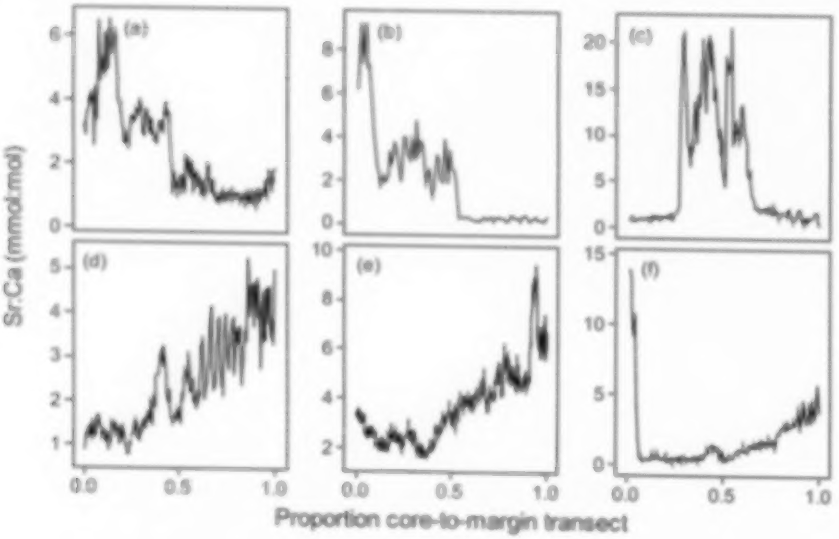

Fig. 11. Box plots illustrating the variability of D_{Sr} in marine fish (ordered as in Appendix B). The distribution of maximum D_{Sr} for the sablefish and marine species groups are displayed in the lower two box plots. Note that no outliers are presented with these box plots for clarity due to scaling issues. As a result, the maximum D_{Sr} box plot extends beyond the upper range of those for individual fish.

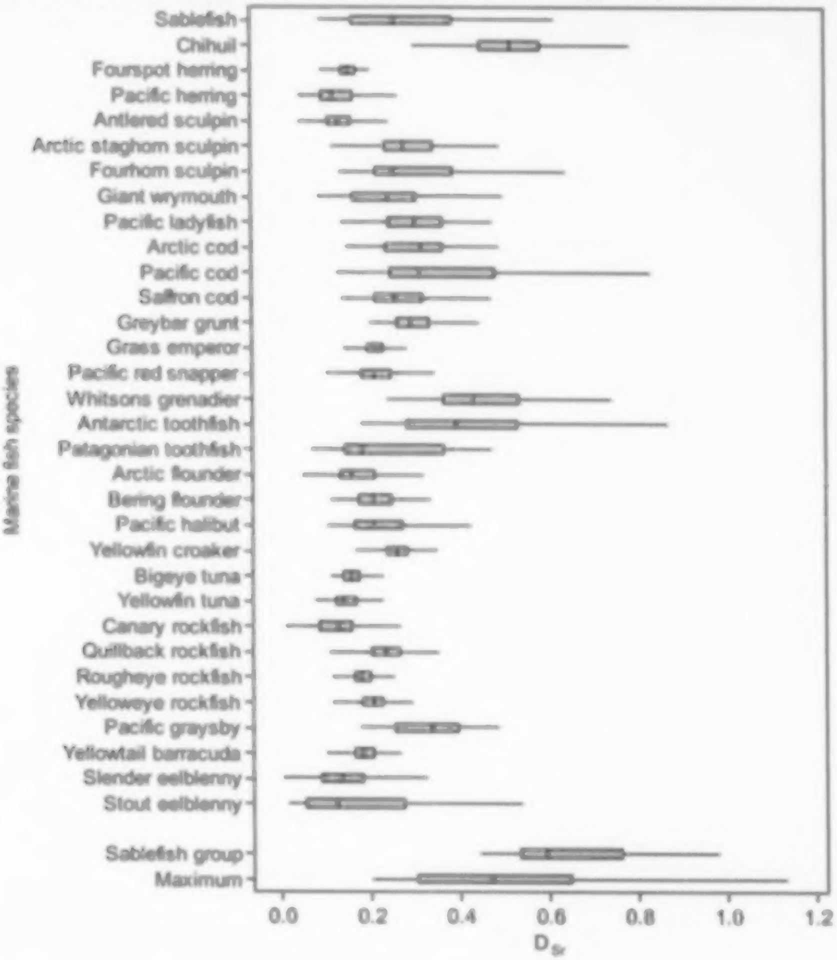

D_{Sr}

Substantial variability of D_{Sr} values was evident within individual otoliths of marine species, as well as among species (Fig. 11). Maximum D_{Sr} for marine species ranged from 0.20 for the fourspot herring (*Herklotsichthys quadrimaculatus*) to 1.62 for the stout eelblenny. Maximum D_{Sr} for the sablefish species group ranged from 0.44 to 0.98, well within the range for the marine species group. The average level of the statistic was 0.54 for the marine species group and 0.66 for the sablefish group. Otolith Sr:Ca levels greater than 8.61 in marine species produce D_{Sr} greater than 1, indicating that Sr concentration is being enhanced in the endolymph relative to marine Sr:Ca levels or that Ca movement into the endolymph is being specifically restricted. Three marine species had maximum Sr:Ca levels greater than 8.61. Only two, the stout eelblenny and the Pacific cod, had sufficiently high maximum Sr:Ca levels that the difference could not be attributed to error in the measurements of otolith Sr and Ca concentrations.

Discussion

The paradigm that water chemistry is the primary factor influencing otolith chemistry appears to apply reasonably well to freshwater and diadromous species and less well to marine species, at least for Sr:Ca. Freshwater species had the lowest otolith Sr:Ca levels of the three life history groups, which was expected. They exhibited significantly less lifetime otolith Sr:Ca variation than diadromous or marine species, even though marine species were expected to exhibit the least variability. Marine species exhibited nearly the same otolith Sr:Ca variability as diadromous species, which was unexpected given the relative homogeneity of Sr:Ca in marine environments and the high variability of environmental Sr:Ca experienced by diadromous fish. Diadromous and marine species groups exhibited similar median and maximum levels of otolith Sr:Ca. Diadromous fish were expected to have lower median levels than marine fish, which these data did not support, and similar maximum levels, which these data did support. All measures of otolith

Sr:Ca variability and level between freshwater and diadromous species were consistent with expectations. Inconsistencies with expected otolith Sr:Ca variability between marine and freshwater species and marine and diadromous species, as discussed above, suggest that factors other than water chemistry influence Sr:Ca variation in otoliths of marine species, a concept previously considered by Secor and Rooker (2000).

Controlled laboratory experiments testing the effects of water chemistry and other environmental factors on otolith chemistry have used juvenile fish almost exclusively with the explicit or implied assumption that their findings applied to the species through life. The reasons for using juvenile fish are obvious, particularly for long-lived species: large numbers of small individuals can be reared in various treatments and the material that precipitates during treatment can easily be identified and sampled (e.g., Zimmerman 2005). A shortcoming of using juveniles to identify factors influencing lifetime patterns of trace element incorporation in otoliths, analogous to extending a regression line beyond the data range, became apparent when ontogenetic trends in otolith chemistry were reported for older fish living in the relatively homogeneous marine environment (e.g., Brophy et al. 2004; Morales-Nin et al. 2005). We identified positive ontogenetic trends in otolith Sr:Ca from most of the marine species examined in this study. Extreme otolith Sr:Ca differences between core and margin regions of marine species exceeded 6 mmol:mol, which is comparable with extreme differences for diadromous species. This magnitude of variation can be explained based on water chemistry for diadromous species but not for marine species.

Based on his work on seasonal variation in blood and endolymph chemistry of a marine fish, Kalish (1991) argued that physiology was a major factor influencing otolith chemistry. He proposed that the concentration of dissolved proteins in the blood affected the availability of dissolved cations, including Sr, to the endolymph because of the tendency of the cations to bind with proteins. A higher concentration of proteins in the blood resulted in less dissolved cations being available to the endolymph and the precipitating otolith. He presented data indicating that the concentration of dissolved proteins in the blood was related to physiological stages associated with life history events such as feeding periods and gonad development. Although these events were correlated with temperature, Kalish (1991) argued that temperature influenced physiology, which in turn affected the availability of Sr to the otoliths, rather than affecting the kinetic energy of dissolved ions, which is considered to be a primary mechanism for temperature effects of abiotic precipitation of aragonite (Kinsman and Holland 1969).

Kinsman and Holland (1969) showed that the coprecipitation of Sr in abiotic aragonite was in equilibrium with ambient water chemistry in a temperature-dependent manner. Increasing temperature increased the kinetic energy of ions in solution. The incorporation of ions into the precipitating mineral created a microzone concentration gradient that was repopulated through diffusion at a rate described by the distribution coefficient, which was influenced by temperature. They estimated a D_{Sr} of 1.12 for abiotic aragonite precipitated at 25 °C and determined that there was a negative correlation with temperature. Assuming similar equilibrium dynamics for biogenic aragonite, the D_{Sr} of coral aragonite was used to estimate historical ocean surface water temperatures (Smith et al. 1979; Beck et al. 1992; de Villiers et al. 1994). More recent work suggested that algal symbionts with some coral species were responsible for as much as 65% of the observed variation in Sr:Ca, complicating what appeared to be a simple calculation of previous water temperature from the chemistry of coral aragonite (Cohen et al. 2002). Similar efforts to correlate temperature and otolith Sr:Ca in fish have produced ambiguous results overall, indicating significant physiological controls on otolith chemistry that appear to vary considerably by species and perhaps through ontogeny (i.e., Sadovy and Severin 1994; Martin et al. 2004; Rooker et al. 2004).

Campana (1999) discussed temperature, major life history transitions, somatic growth rate, and the rate of crystal formation as factors other than water chemistry that may influence otolith Sr:Ca variation in a homogenous environment such as the sea. Somatic growth rate is positively correlated with overall protein synthesis in fish. Campana (1999) proposed that high rates of system-wide protein synthesis extended to endolymph proteins, which are thought to dictate otolith growth. High growth rates are thought to reduce Sr incorporation into otoliths, whereas low growth rates are thought to enhance Sr incorporation (e.g., Sadovy and Severin 1994). Somatic growth rate may be influenced by temperature or life history events such as metamorphosis or spawning or simply through ontogeny as a long-lived fish approaches maximum size. Although temperature variation and physiological events may be responsible for the high otolith Sr:Ca variability observed in many of the marine species examined here, freshwater species that experience similar lifetime temperature variation and physiological events do not exhibit similarly high otolith Sr:Ca variation. It is clear that the factors affecting Sr incorporation into fish otoliths differ fundamentally in effect or magnitude for the three life history categories of fish.

Data presented here demonstrate that there is no unified theory of Sr incorporation in fish otoliths that can be applied to all fish everywhere. Factors influencing Sr incorporation into fish otoliths are different in either effect or magnitude for different species, families, and life history categories. The positive correlation of water Sr:Ca on otolith Sr:Ca for diadromous fish moving between freshwater and marine environments appears to be universal, although the magnitude of the effect may vary by species (Secor and Rooker 2000; Zimmerman 2005) or family. Our water chemistry review indicated that the marine Sr:Ca environment was more homogeneous than either freshwater or brackish environments. Therefore, factors influencing otolith Sr:Ca variation in marine species are more likely to be physiological in nature, as discussed by Kalish (1991), Campana (1999), and Secor and Rooker (2000), rather than the result of exposure to heterogenous environments. Physiological factors do not appear to influence otolith Sr:Ca variation in freshwater species or the influence may be so minor that it is not recognized. Physiological factors may have an influence on otolith Sr:Ca variation in diadromous species when they are in the sea and hypotonic to the environment like marine species. If so, it is not identified because we almost always interpret otolith Sr:Ca variation in diadromous species as an indication of migration between freshwater, estuarine, and marine environments (Howland et al. 2001; Arai et al. 2003; Yang et al. 2006). Despite this possibility, most scientists are comfortable interpreting the migration histories of freshwater and diadromous species based on their Sr:Ca profiles. The distinct patterns observed in the Sr:Ca profiles of marine species are chemical records of life history events that we are not yet able to interpret with confidence. Carefully designed field or long-term experimental studies may be required to identify major factors responsible for otolith Sr:Ca variation in marine species, which would allow interpretation of the life history stories they contain.

Acknowledgements

This investigation would not have been possible without the contributions of otolith samples from the collections of many different fisheries scientists and other interested individuals. They include J. Adams (US Fish and Wildlife Service (USFWS)), J. Akaran (USFWS), J. Baker (US Geological Survey (USGS)), N. Bickford (University of Alaska Fairbanks), B. Carter (USFWS), F. DeCicco (Alaska Department of Fish and Game (ADFG)), N. de Graff (Can-nic-a-nick Environmental Sciences, Canada), P. Horn (National Institute of Water and Atmospheric Research (NIWAR), New Zealand), K. Howland (Fisheries and Oceans Canada), K. Limburg (State University of New York), S. Maclean (Alaska Department of Natural Resources), P. Martinez (Colorado Division of Wildlife), R. McBride (Florida Fish and Wildlife Conservation Commission), A. McDougall (Northern Fisheries Center, Australia), M. Millard (USFWS), J. Miller (Mequon, Wisconsin), J. Moreland (Seward Sealife Center, Alaska), R. Morris (Colorado Division of Wildlife), K. Munk (ADFG), K. Niemela (USFWS), T. Otis (ADFG), T. Reinert (Georgia Cooperative Fish and Wildlife Research Unit), C. Sutton (NIWAR, New Zealand), F. Von Hippel (University of Alaska Anchorage), J. Wexler (Inter-American Tropical Tuna Commission, California), and C. Zimmerman (USGS). Water chemistry data that were not presented in Alexander et al. (2001) were graciously provided by J. Alexander. Constructive reviews of two earlier drafts helped to focus, refine, and improve this manuscript. We greatly appreciate these material, data, and conceptual contributions.

References

Alexander, J., Fielding, C.R., Wakefield, S.J., George, M.T., and Cottnam, C.F. 2001. Fluvial geochemistry through a short-duration, tropical-cyclone induced discharge event in the Burdekin River and Hann Creek, North Queensland, Australia. Aquat. Geochem. **7**(4): 275–293. doi:10.1023/A:1015203127320.

American Fisheries Society. 2004. Common and scientific names of fishes from the United States, Canada, and Mexico. 6th ed. Am. Fish. Soc. Spec. Publ. No. 29, Bethesda, Maryland.

Arai, T., Goto, A., and Miyazaki, N. 2003. Use of otolith microchemistry to estimate the migratory history of the threespine stickleback, *Gasterosteus aculeatus*. J. Mar. Biol. Assoc. U.K. **83**: 223–230.

Ashford, J.R., Jones, C.M., Hofmann, E., Everson, I., Moreno, C., Duhamel, G., and Williams, R. 2005. Can otolith elemental signatures record the capture site of Patagonian toothfish (*Dissostichus eleginoides*), a fully marine fish in the Southern Ocean? Can. J. Fish. Aquat. Sci. **62**(12): 2832–2840. doi:10.1139/f05-191.

Bath, G.E., Thorrold, S.R., Jones, C.M., Campana, S.E., McLaren, J.W., and Lam, J.W.H. 2000. Strontium and barium uptake in aragonitic otoliths of marine fish. Geochim. Cosmochim. Acta, **64**(10): 1705–1714. doi:10.1016/S0016-7037(99)00419-6.

Beck, J.W., Edwards, R.L., Ito, E., Taylor, F.W., Recy, J., Rougerie, F., Joannot, P., and Henin, C. 1992. Sea-surface temperature from coral skeletal strontium/calcium ratios. Science (Washington, D.C.), **257**(5070): 644–647. doi:10.1126/science.257.5070.644. PMID:17740731.

Black, V.S. 1957. Excretion and osmoregulation. *In* The physiology of fishes. Vol. 1. Metabolism. *Edited by* M.E. Brown. Academic Press, Inc., New York. pp. 163–205.

Brenkman, S.J., Corbett, S.C., and Volk, E.C. 2007. Use of otolith chemistry and radiotelemetry to determine age-specific migratory patterns of anadromous bull trout in the Hoh River, Washington. Trans. Am. Fish. Soc. **136**(1): 1–11. doi:10.1577/T05-285.1.

Brophy, D., Jeffries, T.E., and Danilowicz, B.S. 2004. Elevated manganese concentrations at the cores of clupeid otoliths: possible environmental, physiological, or structural origins. Mar. Biol. (Berl.), **144**(4): 779–786. doi:10.1007/s00227-003-1240-3.

Brown, R.J., and Severin, K.P. 2007. A preliminary otolith microchemical examination of the diadromous migrations of Atlantic tarpon *Megalops atlanticus*. *In* Biology and management of the world tarpon and bonefish fisheries. *Edited by* J.S. Ault. CRC Press, New York. pp. 259–274.

Brown, R.J., Bickford, N., and Severin, K. 2007. Otolith trace element chemistry as an indicator of anadromy in Yukon River drainage Coregonine fishes. Trans. Am. Fish. Soc. **136**(3): 678–690. doi:10.1577/T06-040.1.

Campana, S.E. 1999. Chemistry and composition of fish otoliths: pathways, mechanisms and applications. Mar. Ecol. Prog. Ser. **188**: 263–297. doi:10.3354/meps188263.

Campana, S.E., Fowler, A.J., and Jones, C.M. 1994. Otolith elemental fingerprinting for stock identification of Atlantic cod (*Gadus morhua*) using laser ablation ICPMS. Can. J. Fish. Aquat. Sci. **51**(9): 1942–1950. doi:10.1139/f94-196.

Cohen, A.L., Owens, K.E., Layne, G.D., and Shimizu, N. 2002. The effect of algal symbionts on the accuracy of Sr/Ca paleotemperatures from coral. Science (Washington, D.C.), **296**(5566): 331–333. doi:10.1126/science.1069330. PMID: 11884719.

Culkin, F., and Cox, R.A. 1966. Sodium, potassium, magnesium, calcium and strontium in sea water. Deep-Sea Res. **13**: 789–804.

de Villiers, S., Shen, G.T., and Nelson, B.K. 1994. The Sr/Ca-temperature relationship in coralline aragonite: influence of variability in $(\mathrm{Sr/Ca})_{\mathrm{seawater}}$ and skeletal growth parameters. Geochim. Cosmochim. Acta, **58**: 197–208. doi:10.1016/0016-7037(94)90457-X.

Elsdon, T.S., and Gillanders, B.M. 2002. Interactive effects of temperature and salinity on otolith chemistry: challenges for determining environmental histories of fish. Can. J. Fish. Aquat. Sci. **59**(11): 1796–1808. doi:10.1139/f02-154.

Farrell, J., and Campana, S.E. 1996. Regulation of calcium and strontium deposition on the otoliths of juvenile tilapia, *Oreochromis niloticus*. Comp. Biochem. Physiol. Part A Physiol. **115**(2): 103–109. doi:10.1016/0300-9629(96)00015-1.

Fishbase. 2008. FishBase [online resource]. Available at www.fishbase.org [accessed 24 January 2008].

FitzGerald, J.L., Thorrold, S.R., Bailey, K.M., Brown, A.L., and

Severin, K.P. 2004. Elemental signatures in otoliths of larval walleye pollock (*Theragra chalcogramma*) from the northeast Pacific Ocean. Fish. Bull. (Washington, D.C.), **102**: 604–616.

Goldstein, S.J., and Jacobsen, S.B. 1987. The Nd and Sr isotopic systematics of river-water dissolved material: implications for the sources of Nd and Sr in seawater. Chem. Geol. **66**: 245–272.

Goldstein, J.I., Newbury, D.E., Echlin, P., Joy, D.C., Lyman, C.E., Lifshin, E., Sawyer, L., and Michael, J.R. 2003. Scanning electron microscopy and X-ray microanalysis. 3rd ed. Kluwer Academic/Plenum Publishers, New York.

Gunn, J.S., Harrowfield, I.R., Proctor, C.H., and Thresher, R.E. 1992. Electron probe microanalysis of fish otoliths — evaluation of techniques for studying age and stock discrimination. J. Exp. Mar. Biol. Ecol. **158**(1): 1–36. doi:10.1016/0022-0981(92)90306-U.

Harris, J.E., McBride, R.S., and Williams, R.O. 2007. Life history of hickory shad in the St. Johns River, Florida. Trans. Am. Fish. Soc. **136**(6): 1463–1471. doi:10.1577/T06-187.1.

Hilborn, R., Branch, T.A., Ernst, B., Magnusson, A., Minte-Vera, C.V., Scheuerell, M.D., and Valero, J.L. 2003. State of the world's fisheries. Annu. Rev. Environ. Resour. **28**(1): 359–399. doi:10.1146/annurev.energy.28.050302.105509.

Howland, K.L., Tonn, W.M., Babaluk, J.A., and Tallman, R.F. 2001. Identification of freshwater and anadromous inconnu in the Mackenzie River system by analysis of otolith strontium. Trans. Am. Fish. Soc. **130**(5): 725–741. doi:10.1577/1548-8659(2001)130<0725:IOFAAI>2.0.CO;2.

Jolliffe, I.T. 1986. Principal component analysis. Springer-Verlag New York Inc., New York.

Kalish, J.M. 1990. Use of otolith microchemistry to distinguish the progeny of sympatric anadromous and non-anadromous salmonids. Fish. Bull. (Washington, D.C.), **88**: 657–666.

Kalish, J.M. 1991. Determinants of otolith chemistry: seasonal variation in the composition of blood plasma, endolymph and otoliths of bearded rock cod *Pseudophycis barbatus*. Mar. Ecol. Prog. Ser. **74**: 137–159. doi:10.3354/meps074137.

Kinsman, D.J.J., and Holland, H.D. 1969. The co-precipitation of cations with CaCO$_3$ — IV. The co-precipitation of Sr^{2+} with aragonite between 16° and 96°C. Geochim. Cosmochim. Acta, **33**(1): 1–17. doi:10.1016/0016-7037(69)90089-1.

Kraus, R.T., and Secor, D.H. 2004. Incorporation of strontium into otoliths of an estuarine fish. J. Exp. Mar. Biol. Ecol. **302**(1): 85–106. doi:10.1016/j.jembe.2003.10.004.

Limburg, K.E. 1995. Otolith strontium traces environmental history of subyearling American shad *Alosa sapidissima*. Mar. Ecol. Prog. Ser. **119**: 25–35. doi:10.3354/meps119025.

Limburg, K.E., Wickstrom, H., Svedang, H., Elfman, M., and Kristiansson, P. 2003. Do stocked freshwater eels migrate? Evidence from the Baltic suggests "yes". *In* Biology, management, and protection of catadromous eels. *Edited by* D.A. Dixon. Am. Fish. Soc. Symp. No. 33, Bethesda, Maryland. pp. 275–284.

Livingston, D.A. 1963. Chemical composition of rivers and lakes. *In* Data of geochemistry. 6th ed. Chapter G. *Edited by* M. Fleischer. Geological Survey Professional Paper No. 440-G. United States Government Printing Office, Washington, D.C.

Martin, J.-M., and Meybeck, M. 1979. Elemental mass-balance of material carried by major world rivers. Mar. Chem. **7**(3): 173–206. doi:10.1016/0304-4203(79)90039-2.

Martin, G.B., Thorrold, S.R., and Jones, C.M. 2004. Temperature and salinity effects on strontium incorporation in otoliths of larval spot (*Leiostomus xanthurus*). Can. J. Fish. Aquat. Sci. **61**(1): 34–42. doi:10.1139/f03-143.

Miller, J.A. 2007. Scales of variation in otolith elemental chemistry of juvenile staghorn sculpin (*Leptocottus armatus*) in three Pacific Northwest estuaries. Mar. Biol. (Berl.), **151**(2): 483–494. doi:10.1007/s00227-006-0477-z.

Morales-Nin, B., Swan, S.C., Gordon, J.D.M., Palmer, M., Geffen, A.J., Shimmield, T., and Sawyer, T. 2005. Age-related trends in otolith chemistry of *Merluccius merluccius* from the north-eastern Atlantic Ocean and the western Mediterranean Sea. Mar. Freshw. Res. **56**(5): 599–607. doi:10.1071/MF04151.

Odum, H.T. 1957. Strontium in natural waters. Publ. Inst. Mar. Sci. Univ. Tex. **IV**(2): 22–37.

Reed, S.J.B. 1997. Electron microprobe analysis. 2nd ed. Cambridge University Press, Cambridge, Massachusetts.

Riesz, F., Szokefalvi-Nagy, B., and Boron, L.F. 1990. Functional analysis. Courier Dover Publications, Mineola, New York.

Rooker, J.R., Secor, D.H., Zdanowicz, V.S., De Metrio, D., and Relini, L.O. 2003. Identification of Atlantic bluefin tuna (*Thunnus thynnus*) stocks from putative nurseries using otolith chemistry. Fish. Oceanogr. **12**(2): 75–84. doi:10.1046/j.1365-2419.2003.00223.x.

Rooker, J.R., Kraus, R.T., and Secor, D.H. 2004. Dispersive behaviors of black drum and red drum: is otolith Sr:Ca a reliable indicator of salinity history. Estuaries, **27**(2): 334–341. doi:10.1007/BF02803389.

Sadovy, Y., and Severin, K.P. 1994. Elemental patterns in red hind (*Epinephelus guttatus*) otoliths from Bermuda and Puerto Rico reflect growth rate, not temperature. Can. J. Fish. Aquat. Sci. **51**(1): 133–141. doi:10.1139/f94-015.

Secor, D.H., and Piccoli, P.M. 2007. Oceanic migration rates of upper Chesapeake Bay striped bass (*Morone saxatilis*), determined by otolith microchemical analysis. Fish. Bull. (Washington, D.C.), **105**: 62–73.

Secor, D.H., and Rooker, J.R. 2000. Is otolith strontium a useful scalar of life cycles in estuarine fishes? Fish. Res. **46**(1–3): 359–371. doi:10.1016/S0165-7836(00)00159-4.

Secor, D.H., Henderson-Arzapalo, A., and Piccoli, P.M. 1995. Can otolith microchemistry chart patterns of migration and habitat utilization in anadromous fish? J. Exp. Mar. Biol. Ecol. **192**(1): 15–33. doi:10.1016/0022-0981(95)00054-U.

Severin, K.P., Carroll, J., and Norcross, B.L. 1995. Electron microprobe analyses of juvenile walleye pollock, *Theragra chalcogramma*, otoliths from Alaska: a pilot stock separation study. Environ. Biol. Fishes, **43**(3): 269–283. doi:10.1007/BF00005859.

Smith, S.V., Buddemeier, R.W., Redalje, R.C., and Houck, J.E. 1979. Strontium–calcium thermometry in coral skeletons. Science (Washington, D.C.), **204**(4391): 404–407. doi:10.1126/science.204.4391.404. PMID:17758014.

Surge, D.M., and Lohmann, K.C. 2002. Temporal and spatial differences in salinity and water chemistry in SW Florida estuaries: effects of human-impacted watersheds. Estuaries, **25**(3): 393–408. doi:10.1007/BF02695982.

Thorrold, S.R., Jones, C.M., Swart, P.M., and Targett, T.E. 1998. Accurate classification of juvenile weakfish *Cynoscion regalis* to estuarine nursery areas based on chemical signatures in otoliths. Mar. Ecol. Prog. Ser. **173**: 253–265. doi:10.3354/meps173253.

Tzeng, W. 1996. Effects of salinity and ontogenetic movements on strontium:calcium ratios in the otoliths of the Japanese eel, *Anguilla japonica* Temminck and Schlegel. J. Exp. Mar. Biol. Ecol. **199**(1): 111–122. doi:10.1016/0022-0981(95)00185-9.

US Geological Survey. 2007. Water quality samples for USA: sample data [online resource]. Available at http://nwis.waterdata.usgs.gov/nwis/qwdata (site numbers available on request) [last accessed 15 December 2007].

Volk, E.C., Blakley, A., Schroder, S.L., and Kuehner, S.M. 2000.

Otolith chemistry reflects migratory characteristics of Pacific salmonids: using otolith core chemistry to distinguish maternal associations with sea and freshwaters. Fish. Res. **46**(1–3): 251–266. doi:10.1016/S0165-7836(00)00150-8.

Yang, J., Arai, T., Liu, H., Miyazaki, N., and Tsukamoto, K. 2006. Reconstructing habitat use of *Coilia mystus* and *Coilia ectenes* of the Yangtze River estuary, and of *Coilia ectenes* of Taihu Lake, based on otolith strontium and calcium. J. Fish Biol. **69**(4): 1120–1135. doi:10.1111/j.1095-8649.2006.01186.x.

Zimmerman, C.E. 2005. Relationship of otolith strontium-to-calcium ratios to salinity: experimental validation for juvenile salmonids. Can. J. Fish. Aquat. Sci. **62**(1): 88–97. doi:10.1139/f04-182.

Zimmerman, C.E., and Reeves, G.H. 2000. Population structure of sympatric anadromous and nonanadromous *Oncorhynchus mykiss*: evidence from spawning surveys and otolith microchemistry. Can. J. Fish. Aquat. Sci. **57**(10): 2152–2162. doi:10.1139/cjfas-57-10-2152.

Appendix A

Table A1. Literature sources of water chemistry data, habitat types, and geographic regions examined.

Citation	Habitat	Geographic region
Alexander et al. 2001	River	Australia
Andersson et al. 1994	River	Europe
Blum et al. 1994	River	North America
Cameron et al. 1995	River	North America
Culkin and Cox 1966	Marine	Oceans worldwide
Dalai et al. 2003	River	Asia
Dessert et al. 2001	River	Asia
de Villiers 1999	Marine	Atlantic and Pacific oceans
de Villiers et al. 1994	Marine	Atlantic and Pacific oceans
Edmond et al. 1995	River	South America
Edmond et al. 1996	River	South America
Fabricand et al. 1967	Marine	Atlantic Ocean
Faure et al. 1967	Marine, river, and lake	North America and Atlantic Ocean
Gaillardet et al. 1997	River	South America
Gislason et al. 1996	River	Iceland
Goldstein and Jacobsen 1987	River and lake	Worldwide
Han and Liu 2004	River	Asia
Huh and Edmond 1999	River	Asia
Huh et al. 1998a	River	Asia
Huh et al. 1998b	River	Asia
Karim and Veizer 2000	River	Asia
Katz et al. 1977	River	Middle East
Krishnaswami et al. 1992	River	Asia
Livingston 1963	River and lake	North America and Europe
Martin and Meybeck 1979	River	Worldwide
Millot et al. 2003	River	North America
Moon et al. 2007	River	Asia
Negrel et al. 1993	River	Africa
Odum 1957	River and lake	North America and Pacific Islands
Pande et al. 1994	River and lake	Asia
Petelet et al. 1998	River	Europe
Qin et al. 2006	River	Asia
Reeder et al. 1972	River and lake	North America
Trivedi et al. 1995	River	Asia
USGS 2007	River	North America
Viers et al. 2000	River	Africa
Wadleigh et al. 1985	River	North America
Wu et al. 2005	River and lake	Asia
Xu and Liu 2007	River	Asia
Yang et al. 1996	River and lake	North America

References

Alexander, J., Fielding, C.R., Wakefield, S.J., George, M.T., and Cottnam, C.F. 2001. Fluvial geochemistry through a short-duration, tropical-cyclone induced discharge event in the Burdekin River and Hann Creek, North Queensland, Australia. Aquat. Geochem. **7**(4): 275–293. doi:10.1023/A:1015203127320.

Andersson, P.S., Wasserburg, G.J., Ingri, J., and Stordal, M.C. 1994. Strontium, dissolved and particulate loads in fresh and brackish waters: the Baltic Sea and Mississippi Delta. Earth Planet. Sci. Lett. **124**(1–4): 195–210. doi:10.1016/0012-821X(94)00062-X.

Blum, J.D., Erel, Y., and Brown, K. 1994. ^{87}Sr/^{86}Sr ratios of Sierra Nevada stream waters: implications for relative mineral weathering rates. Geochim. Cosmochim. Acta, **58**: 5019–5025.

Cameron, E.M., Hall, G.E.M., Veizer, J., and Krouse, H.R. 1995. Isotopic and elemental hydrogeochemistry of a major river system: Fraser River, British Columbia, Canada. Chem. Geol. **122**(1–4): 149–169. doi:10.1016/0009-2541(95)00007-9.

Culkin, F., and Cox, R.A. 1966. Sodium, potassium, magnesium, calcium and strontium in sea water. Deep-Sea Res. **13**: 789–804.

Dalai, T.K., Krishnaswami, S., and Kumar, A. 2003. Sr and ^{87}Sr/^{86}Sr in the Yamuna River system in the Himalaya: sources, fluxes, and controls on Sr isotope composition. Geochim. Cosmochim. Acta, **67**(16): 2931–2948. doi:10.1016/S0016-7037(03)00203-5.

Dessert, C., Dupre, B., Francois, L.M., Schott, J., Gaillardet, J., Chakrapani, G., and Bajpai, S. 2001. Erosion of Deccan Traps determined by river geochemistry: impact on the global climate and the ^{87}Sr/^{86}Sr ratio of seawater. Earth Planet. Sci. Lett. **188**(3–4): 459–474. doi:10.1016/S0012-821X(01)00317-X.

de Villiers, S. 1999. Seawater strontium and Sr/Ca variability in the Atlantic and Pacific oceans. Earth Planet. Sci. Lett. **171**(4): 623–634. doi:10.1016/S0012-821X(99)00174-0.

de Villiers, S., Shen, G.T., and Nelson, B.K. 1994. The Sr/Ca-temperature relationship in coralline aragonite: influence of variability in $(\mathrm{Sr/Ca})_{\mathrm{seawater}}$ and skeletal growth parameters. Geochim. Cosmochim. Acta, **58**: 197–208. doi:10.1016/0016-7037(94)90457-X.

Edmond, J.M., Palmer, M.R., Measures, C.I., Grant, B., and Stallard, R.F. 1995. The fluvial geochemistry and denudation rate of the Guayana Shield in Venezuela, Colombia, and Brazil. Geochim. Cosmochim. Acta, **59**(16): 3301–3325. doi:10.1016/0016-7037(95)00128-M.

Edmond, J.M., Palmer, M.R., Measures, C.I., Brown, E.T., and Huh, Y. 1996. Fluvial geochemistry of the eastern slope of the northeastern Andes and its foredeep in the drainage of the Orinoco in Colombia and Venezuela. Geochim. Cosmochim. Acta, **60**(16): 2949–2976. doi:10.1016/0016-7037(96)00142-1.

Fabricand, B.P., Imbimbo, E.S., and Brey, M.E. 1967. Atomic absorption analyses for Ca, Li, Mg, K, Rb, and Sr at two Atlantic Ocean stations. Deep-Sea Res. **14**: 785–789.

Faure, G., Crocket, J.H., and Hurley, P.M. 1967. Some aspects of the geochemistry of strontium and calcium in the Hudson Bay and the Great Lakes. Geochim. Cosmochim. Acta, **31**(3): 451–461. doi:10.1016/0016-7037(67)90053-1.

Gaillardet, J., Dupre, B., Allegre, C.J., and Negrel, P. 1997. Chemical and physical denudation in the Amazon River basin. Chem. Geol. **142**(3–4): 141–173. doi:10.1016/S0009-2541(97)00074-0.

Gislason, S.R., Arnorsson, S., and Armannsson, H. 1996. Chemical weathering of basalt in southwest Iceland: effects of runoff, age of rocks and vegetative/glacial cover. Am. J. Sci. **296**: 837–907.

Goldstein, S.J., and Jacobsen, S.B. 1987. The Nd and Sr isotopic systematics of river-water dissolved material: implications for the sources of Nd and Sr in seawater. Chem. Geol. **66**: 245–272.

Han, G., and Liu, C.-Q. 2004. Water geochemistry controlled by carbonate dissolution: a study of the river waters draining karst-dominated terrain, Guizhou Province, China. Chem. Geol. **204**(1–2): 1–21. doi:10.1016/j.chemgeo.2003.09.009.

Huh, Y., and Edmond, J.M. 1999. The fluvial geochemistry of the rivers of Eastern Siberia: III. Tributaries of the Lena and Anabar draining the basement terrain of the Siberian Craton and the Trans-Baikal Highlands. Geochim. Cosmochim. Acta, **63**(7–8): 967–987. doi:10.1016/S0016-7037(99)00045-9.

Huh, Y., Tsoi, M.-Y., Zaitsev, A., and Edmond, J.M. 1998*a*. The fluvial geochemistry of the rivers of Eastern Siberia: I. Tributaries of the Lena River draining the sedimentary platform of the Siberian Craton. Geochim. Cosmochim. Acta, **62**(10): 1657–1676. doi:10.1016/S0016-7037(98)00107-0.

Huh, Y., Panteleyev, G., Babich, D., Zaitsev, A., and Edmond, J.M. 1998*b*. The fluvial geochemistry of the rivers of Eastern Siberia: II. Tributaries of the Lena, Omoloy, Yana, Indigirka, Kolyma, and Anadyr draining the collisional/accretionary zone of the Verkhoyansk and Cherskiy ranges. Geochim. Cosmochim. Acta, **62**(12): 2053–2075. doi:10.1016/S0016-7037(98)00127-6.

Karim, A., and Veizer, J. 2000. Weathering processes in the Indus River basin: implications from riverine carbon, sulfur, oxygen, and strontium isotopes. Chem. Geol. **170**(1–4): 153–177. doi:10.1016/S0009-2541(99)00246-6.

Katz, A., Kolodny, Y., and Nissenbaum, A. 1977. The geochemical evolution of the Pleistocene Lake Lisan – Dead Sea system. Geochim. Cosmochim. Acta, **41**(11): 1609–1626. doi:10.1016/0016-7037(77)90172-7.

Krishnaswami, S., Trivedi, J.R., Sarin, M.M., Ramesh, R., and Sharma, K.K. 1992. Strontium isotopes and rubidium in the Ganga–Brahmaputra river system: weathering in the Himalaya, fluxes to the Bay of Bengal and contributions to the evolution of oceanic ^{87}Sr/^{86}Sr. Earth Planet. Sci. Lett. **109**(1–2): 243–253. doi:10.1016/0012-821X(92)90087-C.

Livingston, D.A. 1963. Chemical composition of rivers and lakes. *In* Data of geochemistry. 6th ed. Chapter G. *Edited by* M. Fleischer. Geological Survey Professional Paper No. 440-G, United States Government Printing Office, Washington, D.C.

Martin, J.-M., and Meybeck, M. 1979. Elemental mass-balance of material carried by major world rivers. Mar. Chem. **7**(3): 173–206. doi:10.1016/0304-4203(79)90039-2.

Millot, R., Gaillardet, J., Dupre, B., and Allegre, C.J. 2003. Northern latitude chemical weathering rates: clues from the Mackenzie River basin, Canada. Geochim. Cosmochim. Acta, **67**(7): 1305–1329. doi:10.1016/S0016-7037(02)01207-3.

Moon, S., Huh, Y., Qin, J., and van Pho, N. 2007. Chemical weathering in the Hong (Red) River basin: rates of silicate weathering and their controlling factors. Geochim. Cosmochim. Acta, **71**(6): 1411–1430. doi:10.1016/j.gca.2006.12.004.

Negrel, P., Allegre, C.J., Dupre, B., and Lewin, E. 1993. Erosion sources determined by inversion of major and trace element ratios and strontium isotopic ratios in river water: the Congo Basin case. Earth Planet. Sci. Lett. **120**(1–2): 59–76. doi:10.1016/0012-821X(93)90023-3.

Odum, H.T. 1957. Strontium in natural waters. Publ. Inst. Mar. Sci. Univ. Tex. **IV**(2): 22–37.

Pande, K., Sarin, M.M., Trivedi, J.R., Krishnaswami, S., and Sharma, K.K. 1994. The Indus River system (India–Pakistan): major-ion chemistry, uranium and strontium isotopes. Chem. Geol. **116**(3–4): 245–259. doi:10.1016/0009-2541(94)90017-5.

Petelet, E., Luck, J.-M., Othman, D.B., Negrel, P., and Aquilina, L. 1998. Geochemistry and water dynamics of a medium-sized watershed: the Herault, southern France. 1. Organization of the different water reservoirs as constrained by Sr isotopes, major, and trace elements. Chem. Geol. **150**(1–2): 63–83. doi:10.1016/S0009-2541(98)00053-9.

Qin, J., Huh, Y., Edmond, J.M., Du, G., and Ran, J. 2006. Chemical and physical weathering in the Min Jiang, a headwater tributary of the Yangtze River. Chem. Geol. **227**(1–2): 53–69. doi:10.1016/j.chemgeo.2005.09.011.

Reeder, S.W., Hitchon, B., and Levinson, A.A. 1972. Hydrogeochemistry of the surface waters of the Mackenzie River drainage basin, Canada — I. Factors controlling inorganic composition.

Geochim. Cosmochim. Acta, **36**(8): 825–865. doi:10.1016/0016-7037(72)90053-1.

Trivedi, J.R., Pande, K., Krishnaswami, S., and Sarin, M.M. 1995. Sr isotopes in rivers of India and Pakistan: a reconnaissance study. Curr. Sci. **69**: 171–178.

US Geological Survey. 2007. Water quality samples for USA: sample data [online resource]. Available at http://nwis.waterdata.usgs.gov/nwis/qwdata (site numbers available on request) [last accessed 15 December 2007].

Viers, J., Dupre, B., Braun, J.-J., Deberdt, S., Angeletti, B., Ngoupayou, J.N., and Michard, A. 2000. Major and trace element abundances, and strontium isotopes in the Nyong basin rivers (Cameroon): constraints on chemical weathering processes and elements transport mechanisms in humid tropical environments. Chem. Geol. **169**(1–2): 211–241. doi:10.1016/S0009-2541(00)00298-9.

Wadleigh, M.A., Veizer, J., and Brooks, C. 1985. Strontium and its isotopes in Canadian rivers: fluxes and global implications. Geochim. Cosmochim. Acta, **49**(8): 1727–1736. doi:10.1016/0016-7037(85)90143-7.

Wu, L., Huh, Y., Qin, J., Du, G., and van Der Lee, S. 2005. Chemical weathering in the upper Huang He (Yellow River) draining the eastern Qinghai–Tibet Plateau. Geochim. Cosmochim. Acta, **69**(22): 5279–5294. doi:10.1016/j.gca.2005.07.001.

Xu, Z., and Liu, C.-Q. 2007. Chemical weathering in the upper reaches of Xijiang River draining the Yunnan–Guizhou Plateau, southwest China. Chem. Geol. **239**(1–2): 83–95. doi:10.1016/j.chemgeo.2006.12.008.

Yang, C., Telmer, K., and Veizer, J. 1996. Chemical dynamics of the "St. Lawrence" riverine system: δD_{H2O}, $\delta^{18}O_{H2O}$, $\delta^{13}C$ δ_{DIC}, $\delta^{34}S_{sulfate}$, and dissolved $^{87}Sr/^{86}Sr$. Geochim. Cosmochim. Acta, **60**: 851–866. doi:10.1016/0016-7037(95)00445-9.

Appendix B

Table B1 follows.

Table B1. Freshwater, diadromous, and marine fish species examined in this study ordered by family and common name.

Freshwater		Diadromous		Marine	
Common name	Species	Common name	Species	Common name	Species
Longnose sucker	*Catostomus catostomus*	European eel	*Anguilla anguilla*	Sablefish	*Anoplopoma fimbria*
Black crappie	*Pomoxis nigromaculatus*	Barramundi	*Lates calcarifer*	Chihuil	*Bagre panamensis*
Green sunfish	*Lepomis cyanellus*	American shad	*Alosa sapidissima*	Fourspot herring	*Herklotsichthys quadrimaculatus*
Smallmouth bass	*Micropterus dolomieu*	Blueback herring	*Alosa aestivalis*	Pacific herring	*Clupea pallasii*
Prickly sculpin	*Cottus asper*	Hickory shad	*Alosa mediocris*	Antlered sculpin	*Enophrys diceraus*
Slimy sculpin	*Cottus cognatus*	Atlantic tarpon	*Megalops atlanticus*	Arctic staghorn sculpin	*Gymnocanthus tricuspis*
Lake chub	*Couesius plumbeus*	Ninespine stickleback	*Pungitius pungitius*	Fourhorn sculpin	*Triglopsis quadricornis*
Northern pike	*Esox lucius*	Threespine stickleback	*Gasterosteus aculeatus*	Giant wrymouth	*Cryptacanthodes giganteus*
Burbot	*Lota lota*	Striped bass	*Morone saxatilis*	Pacific ladyfish	*Elops affinis*
Threespine stickleback	*Gasterosteus aculeatus*	Rainbow smelt	*Osmerus mordax*	Arctic cod	*Boreogadus saida*
Channel catfish	*Ictalurus punctatus*	Arctic cisco	*Coregonus autumnalis*	Pacific cod	*Gadus macrocephalus*
Striped bass	*Morone saxatilis*	Bering cisco	*Coregonus laurettae*	Saffron cod	*Eleginus gracilis*
Yellow perch	*Perca flavescens*	Broad whitefish	*Corgonus nasus*	Greybar grunt	*Haemulon sexfasciatum*
Trout-perch	*Percopsis omiscomaycus*	Chinook salmon	*Oncorhynchus tshawytscha*	Grass emperor	*Lethrinus laticaudis*
Arctic char	*Salvelinus alpinus*	Coho salmon	*Oncorhynchus kisutch*	Pacific red snapper	*Lutjanus peru*
Arctic grayling	*Thymallus arcticus*	Dolly Varden	*Salvelinus malma*	Whitson's grenadier	*Macrourus whitsoni*
Broad whitefish	*Coregonus nasus*	Humpback whitefish	*Coregonus pidschian*	Antarctic toothfish	*Dissostichus mawsoni*
Dolly Varden	*Salvelinus malma*	Inconnu	*Stenodus leucichthys*	Patagonian toothfish	*Dissostichus eleginoides*
Humpback whitefish	*Coregonus pidschian*	Least cisco	*Coregonus sardinella*	Arctic flounder	*Liopsetta glacialis*
Inconnu	*Stenodus leucichthys*	Sockeye salmon	*Oncorhynchus nerka*	Bering flounder	*Hippoglossoides robustus*
Kokanee	*Oncorhynchus nerka*	Steelhead	*Oncorhynchus mykiss*	Pacific halibut	*Hippoglossus stenolepis*
Lake trout	*Salvelinus namaycush*			Yellowfin croaker	*Umbrina roncador*
Lake whitefish	*Coregonus clupeaformis*			Bigeye tuna	*Thunnus obesus*
Least cisco	*Coregonus sardinella*			Yellowfin tuna	*Thunnus albacares*
Rainbow trout	*Oncorhynchus mykiss*			Canary rockfish	*Sebastes pinniger*
Round whitefish	*Prosopium cylindraceum*			Quillback rockfish	*Sebastes maliger*
Freshwater drum	*Aplodinotus grunniens*			Rougheye rockfish	*Sebastes aleutianus*
Alaska blackfish	*Dallia pectoralis*			Yelloweye rockfish	*Sebastes ruberrimus*
				Pacific graysby	*Cephalopholis panamensis*
				Yellowtail barracuda	*Sphyraena flavicauda*
				Slender eelblenny	*Lumpenus fabricii*
				Stout eelblenny	*Anisarchus medius*

Modelling the distribution of fish accounting for spatial correlation and overdispersion

Peter Lewy and Kasper Kristensen

Abstract: The spatial distribution of cod (*Gadus morhua*) in the North Sea and the Skagerrak was analysed over a 24-year period using the Log Gaussian Cox Process (LGCP). In contrast to other spatial models of the distribution of fish, LGCP avoids problems with zero observations and includes the spatial correlation between observations. It is therefore possible to predict and interpolate unobserved densities at any location in the area. This is important for obtaining unbiased estimates of stock concentration and other measures depending on the distribution in the entire area. Results show that the spatial correlation and dispersion of cod catches remained unchanged during winter throughout the period, in spite of a drastic decline in stock abundance and a movement of the centre of gravity of the distribution towards the northeast in the same period. For the age groups considered, the concentration of the stock was found to be constant or declining in the period. This means that cod does not follow the theory of density-dependent habitat selection, as the concentration of the stock does not increase when stock abundance decreases.

Résumé : Nous avons analysé la répartition spatiale de la morue (*Gadus morhua*) dans la mer du Nord et le Skagerrak sur une période de 24 ans à l'aide du processus log-gaussien de Cox (LGCP). Contrairement aux autres modèles spatiaux de répartition des poissons, le LGCP évite les problèmes reliés à l'absence d'observations et inclut la corrélation spatiale entre les observations. Il est, par conséquent, possible de prédire et d'interpoler les densités non mesurées dans n'importe quel site dans la région. Cela est important pour obtenir des estimations non erronées de la concentration du stock et d'autres mesures qui dépendent de la répartition dans la région toute entière. Les résultats montrent que la corrélation spatiale et la dispersion des captures de morues restent inchangées durant l'hiver pendant toute la période, malgré un déclin spectaculaire de l'abondance du stock et un déplacement vers le nord-est du centre de gravité de la répartition durant la même période. Pour les groupes d'âge considérés, la concentration du stock est demeurée constante ou a décliné durant la période. Cela signifie que les morues ne se conforment pas à la théorie de la sélection des habitats dépendante de la densité, puisque la concentration du stock n'augmente pas lorsque l'abondance du stock diminue.

[Traduit par la Rédaction]

Introduction

Knowledge of the spatial distribution of fish and the temporal changes are important for the fishery and fishery management and for understanding the mechanisms of fish behaviour. The distribution of cod (*Gadus morhua*) has been analysed in several studies (Perry et al. 2005; Rindorf and Lewy 2006). These analyses used a single point, the centre of gravity, as an overall measure to describe changes in the spatial distribution. However, if we want to study the spatial distribution of stock abundance in the entire area, another type of modelling is required.

Previously, fishery or scientific survey data have been analysed assuming that observations are independent, irrespective of trawl position, and distributed according to either extensions of the lognormal (Stefánsson 1996) or negative binomial distributions (O'Neill and Faddy 2003; Kristensen et al. 2006). Hrafnkelsson and Stefánsson (2004) presented extensions of the multinomial distribution to account for dispersion and correlation in length measurement samples. To avoid the assumptions of independent observations, other authors used kriging to account for spatial correlation in the analysis of trawl and acoustic survey data (Rivoirard et al. 2000; Stelzenmüller et al. 2005). Estimating parameters using kriging methods, however, requires that data follow a multivariate normal distribution, an assumption that usually is not fulfilled, at least not when part of the data consists of zeroes. The log(catch + constant) transformation is often applied to avoid this problem, a solution which is problematic because the results depend heavily on the choice of the constant. Here we instead use a counting model to describe the discrete catch in number of observations (including the zero catch observations) and to account for the spatial correlation between catches. This model, the so-called Log Gaussian Cox Process, LGCP (K. Kristensen, unpublished; Møller et al. 1998; Diggle and Ribeiro 2007), is also known as the multivariate Poisson–lognormal distribution (Aitchison and Ho 1989) and is a mixture of Poisson-distributed observa-

Received 20 November 2008. Accepted 22 June 2009. Published on the NRC Research Press Web site at cjfas.nrc.ca on 13 October 2009.
J20889

Paper handled by Associate Editor Terrance Quinn II.

P. Lewy[1] and K. Kristensen. National Institute of Aquatic Resources, Technical University of Denmark, Charlottenlund Castle, 2920 Charlottenlund, Denmark.

[1] Corresponding author (e-mail: pl@aqua.dtu.dk).

doi:10.1139/F09-114

Published by NRC Research Press

tions with mean densities following a multivariate lognormal distribution. The Poisson process can be regarded as the sampling process generated by the fishing process. The spatial correlation is included by assuming correlation between densities to be a decreasing function of the distance between them.

The focus of Kristensen (unpublished) was to develop methods for and implementation of maximum likelihood (ML) estimation of the parameters in the LGCP, which hitherto had been estimated by Markov chain Monte Carlo (Møller and Waagepetersen 2004). Aspects of predictions and interpolation were not included. These aspects are crucial when estimating total biomass or the biomass in specified areas, a prerequisite to evaluating the effects of spatial closures and temporal changes of stock concentration.

The objective of this paper is to develop ML-based methods for predicting the unobserved densities at any point in space and to enable goodness-of-fit tests. The use of the model was illustrated by an analysis of the distribution of North Sea and Skagerrak cod in 1983–2006. The temporal change in the dispersion and spatial correlation was examined, and the effect of a range of local hydrographical parameters was investigated. Contour plots of the spatial distribution of age group 1 were produced by interpolation. The theory of density-dependant habitat selection as formulated by MacCall (1990) was investigated, i.e., if the spatial distribution of a stock contracts (expands) when stock abundance decreases (increases). The analysis will be based on the measure of concentration, *D95* (Swain and Sinclair 1994), calculated from interpolations of densities.

Statistical model

Let X_i be the catch in number from haul i with a known position, let λ_i be the unknown true density at the same position, let a and d be dispersion parameters, and let b be a spatial correlation parameter. Further, let $\boldsymbol{X} = (X_1, \ldots, X_n)'$ be the vector of n catch samples covering the area, and let $\boldsymbol{\lambda} = (\lambda_1, \ldots, \lambda_n)'$ be the corresponding true densities, where $\prime$ denotes the transposition of a matrix. It is assumed that the durations of the hauls are the same.

The model considered is a compound Poisson distribution in which the conditional distribution of the catches, X_i, given the density, λ_i, are independent Poisson-distributed variables and $\boldsymbol{\lambda}$ follows a multivariate lognormal distribution:

$$(1)\qquad X_i|\lambda_i \sim \mathrm{Poisson}(\lambda_i)$$

$$\eta = \begin{pmatrix} \eta_1 \\ \vdots \\ \eta_n \end{pmatrix} = \begin{pmatrix} \ln(\lambda_1) \\ \vdots \\ \ln(\lambda_n) \end{pmatrix} \sim N(\mu, \boldsymbol{\Sigma})$$

where

$$\mu = \overbrace{(\mu \ldots, \mu)'}^{n}$$

The variance–covariance matrix $\boldsymbol{\Sigma}$ is defined by

$$\boldsymbol{\Sigma}_{ii} = \mathrm{VAR}(\eta_i) = a + d, \quad a \geq 0 \wedge d \geq 0$$

where $a + d$ is the dispersion of the model. This implies that $E(\lambda_i) = e^{\mu+(a+d)/2}$, $i = 1, \ldots, n$.

The covariance between two densities is assumed to be a decreasing function of distance between the haul positions such that it approaches zero when distance increases:

$$(2)\qquad \boldsymbol{\Sigma}_{ij} = \mathrm{COV}(\eta_i, \eta_j) = a \cdot e^{-b\cdot\mathrm{dist}(i,j)} + d \cdot I_{\mathrm{dist}(i,j)=0}$$

where I is the indicator function and dist(i,j) denotes the distance (in kilometres) on the surface of a sphere between positions i and j. The interpretation of the covariance model, eq. 2, is described below. The relationship between the distance between two points (in kilometres) and the corresponding longitudes and latitudes (lon and lat) is

$$\begin{aligned} \mathrm{dist}(i,j) &= \mathrm{dist}(lon_i, lat_i, lon_j, lat_j) \\ &= 6378.1 \cdot \mathrm{acos}\{\sin(\mathrm{lat}_i \cdot c) \cdot \sin(\mathrm{lat}_j \cdot c) \\ &\qquad + \cos(\mathrm{lat}_i \cdot c) \cdot \cos(\mathrm{lat}_j \cdot c) \\ &\qquad\qquad \times \cos[(\mathrm{lon}_i - \mathrm{lon}_j) \cdot c]\} \end{aligned}$$

where $c = \pi/180$ (Meeus 1998). The correlation between log densities is

$$(3)\qquad \mathrm{COR}(\eta_i, \eta_j) = \frac{a}{a+d} e^{-b\cdot\mathrm{dist}(i,j)}, \quad i \neq j$$

If d is zero, the correlation is $e^{-b\cdot\mathrm{dist}(i,j)}$, independent of a. The model contains the four parameters $\theta = \{\mu, a, b, d\}$ and the unobserved random effects densities, η.

Differences in the duration of the hauls have been ignored and are implicitly included in the small-scale, nugget effect (see below).

The interpretation of the model

First, the observed numbers caught in a haul given the density is assumed to follow a Poisson distribution. This process is interpreted as the fishery sampling process, for instance, due to variation of the behaviour of the trawl or fish movements.

Second, the densities in the sea are assumed to follow a multivariate lognormal distribution in which the correlation between densities is a decreasing function of the distance between them. The mean (E) and variance (V) of observations in the LGCP are as follows:

$$E = E(X_i) = E(\lambda_i) = e^{\mu+(a+d)/2}$$

$$V = V(X_i) = V(X_i|\lambda_i) + V(\lambda_i) = E + (e^{a+d} - 1)E^2$$

where the last term in the equation is the variance of a lognormally distributed variable with log mean E and log variance $a + d$. If the variance of log densities, $a + d$, is positive, then the variance of X is greater than the variance of the Poisson process. Hence, $a + d$ can be regarded as overdispersion parameters relative to the Poisson process. The variance–mean relation of LGCP corresponds to that of the negative binomial distribution, for which $V = E + \mathrm{constant}\cdot E^2$.

Third, the covariance defined in eq. 2 consists of a sum of the two terms, which can be considered as large- and small-scale components, respectively, of the process. The large-scale component includes the large-scale variance a and the parameter b (≥ 0) measuring the strength of the spatial correlation. When b is small, the large-scale correlation between densities is high, and vice versa. The scaling of the correlation is measured by $1/b$, which is the distance for which the spatial correlation is 0.37 (if $d = 0$). The small-scale variance is d, which corresponds to the so-called "nugget" effect in geostatistics, which may, for instance, be due to fish movements. The clear large-scale variation due to "spatial" correlation is illustrated for the case in which the "nugget" effect is excluded (Fig. 1, bold line) and the superimposed small-scale variation due the "nugget" effect (Fig. 1, broken line) blurs the large-scale effect.

Fig. 1. Simulation of a LGCP without a "nugget", the small-scale variation effect (bold line), and the same process including a positive "nugget" effect (broken line).

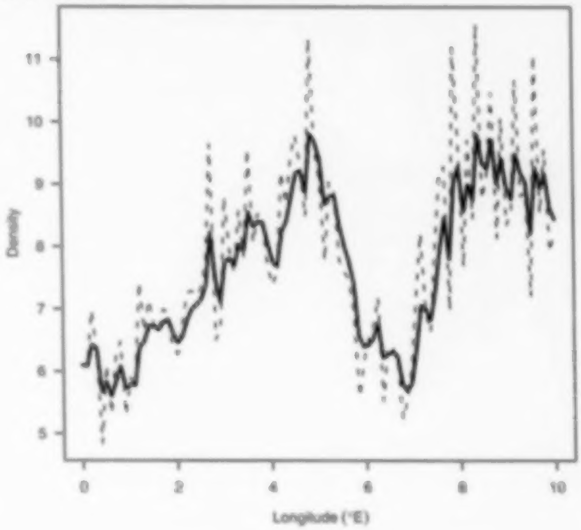

Predictions of unobserved densities at positions with observations available

The likelihood function of X of the LGCP expressed as a function of the parameters, θ, is

$$(4)\qquad L(\theta) = \int P(X, \theta, \eta)\mathrm{d}\eta = \int \mathrm{e}^{-l(X,\theta,\eta)}\mathrm{d}\eta$$

where $l(X, \theta, \eta)$, the negative log-likelihood of (X, η) is

$$l(X, \theta, \eta) = \mathrm{e}^{\sum_{i=1}^{n} \eta_i} - \sum_{i=1}^{n} X_i\eta_i + \frac{1}{2}\ln(\det(\mathbf{\Sigma})) + \frac{1}{2}(\eta - \mu)'\mathbf{\Sigma}^{-1}(\eta - \mu) + \frac{n}{2}\ln(2\pi) + \sum_{i=1}^{n} \ln(X_i!)$$

Laplace approximations have been used to calculate $L(\theta)$ in eq. 4 for ML estimation of $\widehat{\theta}$ and to test hypotheses (K. Kristensen, unpublished data).

For the positions where observations are available, estimates $\widehat{\eta}_\theta(X)$ of log densities $\eta | X$ for given observations X can be obtained by maximizing $l(X, \theta, \eta)$ defined by eq. 4, i.e., $\widehat{\eta}_\theta(X) = \arg\max_\eta l(X, \theta, \eta)$. As indicated, the estimate depends on θ and X. As the estimate of η, we use $\widehat{\eta}(X) = \widehat{\eta}_{\widehat{\theta}}(X)$.

Let $l(\eta|X) = l(X, \widehat{\theta}, \eta)$ denote the likelihood of $\eta | X$. The distribution of $\eta | X$ is now approximated by the normal distribution with mean $\widehat{\eta}(X)$ using a Taylor expansion of $l(\eta | X)$:

$$l(\eta|X) - l\left(\widehat{\eta}(X)\right) \cong 0.5 \cdot (\eta - \widehat{\eta}(X))' \left(\frac{\partial^2 l(\eta \mid X)}{\partial\eta_i \partial\eta_j}\right)^{-1}_{\eta=\widehat{\eta}(X)} (\eta - \widehat{\eta}(X))$$

$$= 0.5 \cdot (\eta - \widehat{\eta}(X))'(\mathbf{\Sigma}^{-1} - D_{\widehat{\eta}(X)})(\eta - \widehat{\eta}(X))$$

where

$$D_{\widehat{\eta}(X)} = \begin{pmatrix} \mathrm{e}^{\widehat{\eta}_1(X)} & & 0 \\ & \ddots & \\ 0 & & \mathrm{e}^{\widehat{\eta}_n(X)} \end{pmatrix}$$

i.e., the distribution of $\eta | X$ is approximated by the quadratic approximation

$$(5)\qquad \eta|X \sim N(\widehat{\eta}(X), (\mathbf{\Sigma}^{-1} + D_{\widehat{\eta}(X)})^{-1})$$

Calculations using "realistic" parameters indicate that this is a good approximation to the true distribution.

Assuming that the approximation holds, the estimator $\widehat{\eta}(X)$ equals $E(\eta | X)$, which is the posterior minimum variance unbiased estimator of η for given X.

Using that

$$\begin{aligned}\mathbf{\Sigma} = V(\eta) &= V(E(\eta|X)) + E(V(\eta|X)) \\ &\cong V(\widehat{\eta}(X)) + E((\mathbf{\Sigma}^{-1} + D_{\widehat{\eta}(X)})^{-1})\end{aligned}$$

we find that

$$(6)\qquad \begin{aligned}V(\widehat{\eta}(X)) &\cong \mathbf{\Sigma} - (\mathbf{\Sigma}^{-1} + D_{\widehat{\eta}(X)})^{-1} \\ &\cong \mathbf{\Sigma}_{\widehat{\theta}} - (\mathbf{\Sigma}_{\widehat{\theta}}^{-1} + D_{\widehat{\eta}(X),\widehat{\theta}})^{-1}\end{aligned}$$

Spatial interpolation

By analogy to the kriging method, the LGCP can be used to spatially interpolate the density at positions where no observations exist. The best unbiased prediction of any function of the unobserved density is the conditional mean given the observations. In the analyses below, we assume that the formulas of the conditional means and variances are based on the true value of the parameters. In practice, the true values are replaced by the MLEs.

Assume that we want to predict the densities $\lambda_{\mathrm{new}} = (\lambda_1, \ldots, \lambda_m)' = (e^{\eta_1}, \ldots, e^{\eta_m})'$ for m new positions without observations. First, the log densities $\eta_{\mathrm{new}} = \log(\eta_{\mathrm{new}}) = (\eta_1, \ldots, \eta_m)'$ are predicted.

According to eq. 1, the combined set of η and η_{new} are distributed as

$$\begin{pmatrix} \eta \\ \eta_{\mathrm{new}} \end{pmatrix} \sim N\left(\begin{pmatrix} \mu \\ \mu_{\mathrm{new}} \end{pmatrix}, \begin{pmatrix} \boldsymbol{\Sigma} & \boldsymbol{\Sigma}_{12} \\ \boldsymbol{\Sigma}_{12} & \boldsymbol{\Sigma}_{22} \end{pmatrix}\right)$$

where $\mu_{\mathrm{new}} = \overbrace{(\mu, \ldots, \mu)'}^{m}$ and $\boldsymbol{\Sigma}_{12}$ are defined similarly as $\boldsymbol{\Sigma}$.

We know that the conditional distribution of $\eta_{\mathrm{new}} | \eta$ is normal with mean and variance

$$(7) \qquad E(\eta_{\mathrm{new}} | \eta) = \mu_{\mathrm{new}} + \boldsymbol{\Sigma}_{21} \boldsymbol{\Sigma}^{-1} (\eta - \mu)$$

$$(8) \qquad V(\eta_{\mathrm{new}} | \eta) = \boldsymbol{\Sigma}_{22} - \boldsymbol{\Sigma}_{12} \boldsymbol{\Sigma}^{-1} \boldsymbol{\Sigma}_{12}$$

By analogy with the predictions of $\eta | X$, we want to use $E(\eta_{\mathrm{new}} | X)$ for spatially interpolation. From the definition of the LGCP, the conditional distribution of $X | \eta_{\mathrm{new}}, \eta$ only depends on the densities in the points with observations η. According to Brémaud (1999, p. 12), this implies that η_{new} and X are conditionally independent given η and, hence, $E(\eta_{\mathrm{new}} | \eta, X) = E(\eta_{\mathrm{new}} | \eta)$. This implies that

$$\begin{aligned} (9) \qquad E(\eta_{\mathrm{new}} | X) &= E(E(\eta_{\mathrm{new}} | \eta, X) | X) = E(E(\eta_{\mathrm{new}} | \eta) | X) \\ &= E(\mu_{\mathrm{new}} + \boldsymbol{\Sigma}_{21} \boldsymbol{\Sigma}^{-1} (\eta - \mu) | X) \\ &= \mu_{\mathrm{new}} + \boldsymbol{\Sigma}_{21} \boldsymbol{\Sigma}^{-1} (E(\eta | X) - \mu) \\ &\cong \mu_{\mathrm{new}} + \boldsymbol{\Sigma}_{21} \boldsymbol{\Sigma}^{-1} (\hat{\eta}(X) - \mu) \end{aligned}$$

$$\begin{aligned} (10) \qquad V(\eta_{\mathrm{new}} | X) &= V(E(\eta_{\mathrm{new}} | \eta) | X) + E(V(\eta_{\mathrm{new}} | \eta) | X) \\ &\cong \boldsymbol{\Sigma}_{12} \boldsymbol{\Sigma}^{-1} V(\eta | X) \boldsymbol{\Sigma}_{12} \boldsymbol{\Sigma}^{-1} \\ &\qquad + \boldsymbol{\Sigma}_{22} - \boldsymbol{\Sigma}_{12} \boldsymbol{\Sigma}^{-1} \boldsymbol{\Sigma}_{12} \\ &\cong \boldsymbol{\Sigma}_{12} \boldsymbol{\Sigma}^{-1} (\boldsymbol{\Sigma}^{-1} + D_{\hat{\eta}(X)}) \boldsymbol{\Sigma}^{-1} \boldsymbol{\Sigma}_{12} \\ &\qquad + \boldsymbol{\Sigma}_{22} - \boldsymbol{\Sigma}_{12} \boldsymbol{\Sigma}^{-1} \boldsymbol{\Sigma}_{12} \end{aligned}$$

Having determined log density $\eta_{\mathrm{new}}(X)$, the interpolated values of the density $\lambda_{\mathrm{new}}(X) = E(\lambda_{\mathrm{new}} | X)$ can be approximated using a Gaussian posterior approximation based on eqs. 9 and 10:

$$(11) \qquad E(\lambda_{\mathrm{new}} | X) = \exp(E(\eta_{\mathrm{new}} | X) + \mathrm{diag}(V(\eta_{\mathrm{new}} | X))/2)$$

We also wish to predict nonlinear functions of $\lambda_{\mathrm{new}}(X)$ such as the measure of stock concentration, *D95*, defined below. $E(f(\lambda_{\mathrm{new}}) | X) = E(f(e^{\eta_{\mathrm{new}}}) | X)$ and the variance is calculated by simulation by drawing 100 times from the Gaussian posterior approximation based on eqs. 9 and 10 and calculating the mean and variance of simulated values of $f(e^{\eta_{\mathrm{new}}})$.

The spatial interpolation is performed on a regular fine-scaled grid. The scale should be chosen sufficiently fine to obtain a good approximation to the continuous random field.

Other distribution measures

The ability of the LGCP to perform spatial interpolations of the (unobserved) population densities makes it possible to obtain unbiased estimates of stock characteristics based on densities in the entire space. A measure of stock concentration is considered. The measure, *Dx*, introduced by Swain and Sinclair (1994), is defined as the proportion of the minimum area containing x% of the stock, i.e., $D95_{\mathrm{true}}$ (say) is

$$D95_{\mathrm{true}} = \inf_{A \subseteq E} \left\{ \frac{|A|}{|E|} : \frac{\int_A \lambda(y) \mathrm{d}y}{\int_E \lambda(y) \mathrm{d}y} = 0.95 \right\}$$

where E indicates the entire area in consideration, and A, any subarea of E.

If the area is divided into n equally sized subareas and λ_i represents the density in subarea i, then *D95* can be approximated by

$$D95 = \frac{m + \frac{0.95 - z(m)}{z(m+1) - z(m)}}{n}$$

where

$$z(m) = \frac{\sum_{i=1}^{m} \lambda_{(i)}}{\sum_{i=1}^{n} \lambda_i}, \quad m \leq n$$

where m fulfills $z(m) \leq 0.95 \leq z(m+1)$ and where $\lambda_{(i)}$, $i = 1, \ldots, n$, are the densities sorted in descending order.

D95 is greater than zero and less than 0.95. *D95* is inversely proportional to the stock concentration, i.e., the concentration of a stock increases when *D95* decreases. *D95* approaches zero when concentration increases and equals 0.95 if the density is constant in the entire space, i.e., when the concentration is minimal.

The validity of the theory of density-dependant habitat selection was investigated by comparing the relation between *D95* and stock abundance for 1983–2006, for which the abundance drastically was reduced. According to the theory formulated by MacCall (1990), individuals first occupy habitats with the highest suitability, but as realized suitability of these habitats declines due to increasing population density, other previously less suitable unoccupied habitat become colonized. Hence the distribution is characterized by spatially equal realized suitability. If the theory holds, *D95* should increase when the stock abundance increases.

Calculation of *D95* has been based on predicted densities performed on the regular 50 × 50 grid consisting of 808 points as described above. This procedure ensures that an unbiased estimate of *D95* is obtained (see Appendix A).

Analysis of residuals and goodness-of-fit tests

The residuals can be calculated as $X - e^{\hat{\eta}(X)}$. Maximizing the log-likelihood $l(X, \theta, \eta)$ (eq. 4) with respect to η shows that $\hat{\eta}(X) - \mu = \boldsymbol{\Sigma}^{-1}(X - e^{\hat{\eta}(X)})$and hence the quantity $R = (\hat{\eta}(X) - \mu)$ can be regarded as residuals on a log scale, which is a linear transformation of the original residuals. We prefer to apply these transformed residuals, which express the deviation between predicted log density and the mean. To obtain standardized residuals of R, the variance of R is needed:

$$V(R) = V(\hat{\eta}(X) - \mu) = \mathbf{\Sigma} - E((\mathbf{\Sigma}^{-1} + D_{\hat{\eta}(X)})^{-1})$$

As the last term in the expression of the variance is not known, we instead use $R^{\circ} = R + u$, where $u \sim N(0, (\mathbf{\Sigma}^{-1} + D_{\hat{\eta}(X)})^{-1})$ and for which $V(R^{\circ}) = \mathbf{\Sigma}$ as modified residuals to circumvent this problem. We now assume that $R^{\circ} \sim N(0, \mathbf{\Sigma})$, and accordingly, $U^{\circ} = L^{-1}R^{\circ}$ is used as normal, standardized, and independent residuals, where L is the lower Choleski triangle of $\mathbf{\Sigma}$.

Now assume that we want to examine if residuals are independent of some specified spatial characteristics, for instance, the longitude and latitude. We know that R° is related to the longitude, whereas U° is not. However, if the absolute value of $(L^{-1})_{ij}$ is decreasing as the distance between the points i and j increases, then a specific element $U_i^{\circ} = \sum_j (L^{-1})_{ij} R_j^{\circ}$ of U° only depends on the residuals close to the specified observation. This implies that the residuals may be considered as area-specific residuals, which was applied to examine model deviations according to the longitude and latitude.

Goodness-of-fit tests for validation of the model have been based on the estimated values of log density, $\hat{\eta}$, and the MLE of the other parameters, $\hat{\theta}$. Two tests were considered, T_1 and T_2.

$$T_1 = (\hat{\eta}(X) - \hat{\mu})' V(\hat{\eta}(X))^{-1} (\hat{\eta}(X) - \hat{\mu})$$

where the variance–covariance matrix is determined by eq. 6.

The second test is based on the Kolmogorov–Smirnov test quantity and the quantity $U = L_{V(\hat{\eta})}^{-1}(\hat{\eta} - \hat{M})$

$$T_2 = \max_x |F_U(x) - N(x)|$$

where $L_{V(\hat{\eta})}$ is the lower Choleski triangle of $V(\hat{\eta})$, F_U is the empirical distribution function of U, and N is the distribution function of the normal distribution.

If log density $\eta(X)$ for given observations X is normally distributed, i.e., $\eta | X \sim N(\hat{\eta}, V(\hat{\eta}))$, then T_1 and T_2, respectively, follow the χ^2 and Kolmogorov distributions. Even that the assumption of normality probably is reasonable, implying that the two distributions may be used as test probabilities, we instead simulate the exact distributions of T_1 and T_2. Firstly, estimate the parameters in the model and calculate T_1 and T_2. Secondly, simulate new sets of parameters from the normal distribution $N(\hat{\theta}, \hat{\mathbf{\Sigma}})$ 100 times using the parameters estimated. Thirdly, calculate T_1 and T_2 for each of the 100 repetitions.

The first test should be two-sided, and the second, one-sided. Hence, the test probabilities $p_1 = P(T_1 > T_{1,\text{obs}})$ and $p_2 = 2\cdot\min(q_2, 1 - q_2)$, where $q_2 = P(T_2 \geq T_{2,\text{obs}})$, were calculated. The model is accepted if p is greater that 0.05. The likelihood ratio test was applied to test successive hypotheses regarding the parameters.

Application

The LGCP was applied to cod catch rates from the International Bottom Trawl Survey (IBTS) in the North Sea and the Skagerrak in February 1983–2006. IBTS is coordinated by the International Council for the Exploration of the Sea (ICES) and data are available on www.ices.dk/datacentre/datras/public.asp. The area is confined within 4°W and 13°E longitude and 50°N and 62°N latitude. The period 1983 and onwards was chosen because the coverage and survey gear standardization was better compared with those of previous years. For the first-quarter survey, the annual number of hauls lies between 322 and 534, with a mean of 390. The area contains 186 statistical rectangles (1° longitude × 0.5° latitude), which were covered twice or more. The gear used is a bottom trawl and the haul positions within the rectangles are randomly selected among trawlable areas. The haul duration is, on average, 30 min, but in 12% of the hauls taken before 1999, the duration was about 1 h, which may introduce a bias.

The length of the cod caught was recorded and used to determine age using age–length keys. The spatial distribution using LGCP was studied for each of the age groups 1, 2, and 3 years and older.

The hydrographical data (depth, bottom temperature, and salinity by haul) were provided by ICES' hydrographical database. Data for the stock numbers by year and age were obtained from the ICES Working Group Report (ICES 2006).

Results

The model was used separately for each combination of age groups 1, 2, and 3+ and years 1983–2006, i.e., for 3 × 24 = 72 combinations. First, the model LGCP was used to investigate if the position, depth, temperature, and salinity could describe the variation of the catch-per-unit-effort (CPUE), i.e., for given age and year, it is assumed that

$$\begin{aligned} \text{(12)} \qquad \ln(E(X_{\text{age,year},i})) = \alpha &+ \text{poly}(\text{lon}_{\text{age,year},i}, 2) \\ &+ \text{poly}(\text{lat}_{\text{age,year},i}, 2) + \text{poly}(\text{depth}_{\text{age,year},i}, 2) \\ &+ \text{poly}(t_{\text{age,year},i}, 2) + \text{poly}(\text{sal}_{\text{age,year},i}, 2) \end{aligned}$$

where i denotes the sample number for a given age and year; "lon", the longitude; "lat", the latitude; depth, the bottom depth (in metres); t, the temperature (in °C); "sal", the salinity (in ppm); "poly(·, 2), a second-degree polynomial; and α, a parameter. Why the covariates enter the right-hand side of eq. 10 as a second-degree polynomial is because this enables the existence of, for instance, a preferred temperature with a decreasing preference when moving away from the optimum. The assumption of a log-linear mean structure was made to ensure that mean CPUE remains positive.

MLEs of the parameters in eq. 12 and their confidence intervals obtained from the Hessian matrix were used to test the significance of the parameters. For all years, age groups, and parameters, the confidence intervals contained zero. One more run with the model with the second-degree terms removed gave the same result. Hence, for all age groups and years, it was concluded that none of the effects associated with the covariates was found to be significant, i.e., log of

Fig. 2. (*a*) Plots of the relationship between the elements of the inverse of the lower Choleski triangle, L^{-1}, and the distance between corresponding points and (*b*–*c*) residuals plotted against (*b*) longitude and (*c*) latitude for age group 1 in 1994.

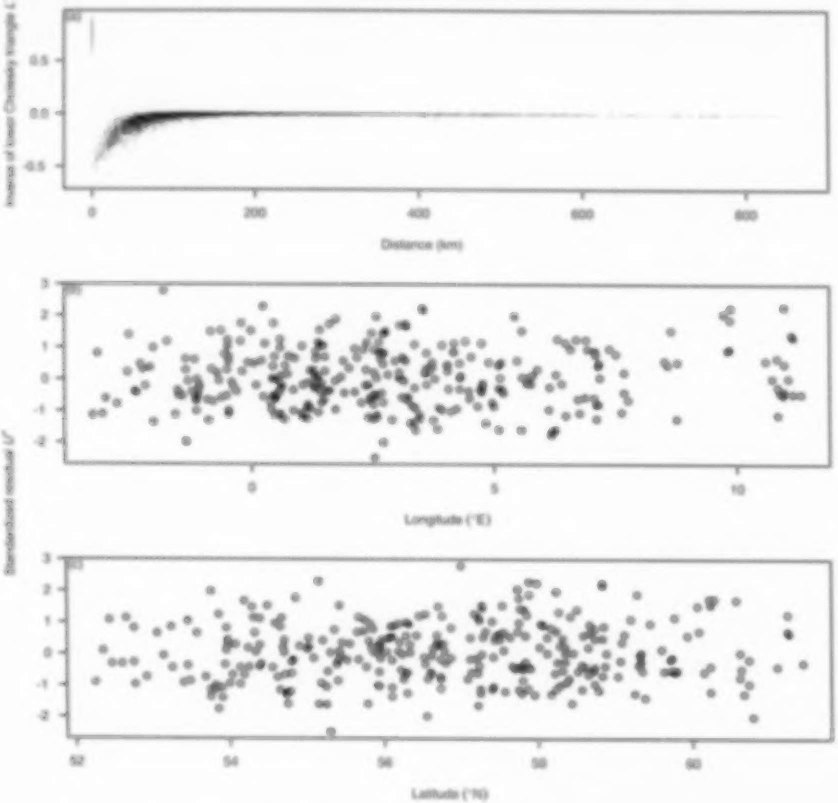

Table 1. Estimated parameters and the 95% confidence limits (lower (L95%) and upper (U95%)) by age.

	Age 1			Age 2[a]			Age 3+[b]		
	L95%	Mean	U95%	L95%	Mean	U95%	L95%	Mean	U95%
$1/b$[c]	179.1	242.0	327.0	66.2	87.2	114.5	44.8	58.9	77.3
a	4.08	4.98	6.07	2.11	2.41	2.75	0.98	1.12	1.27
d	1.26	1.42	1.58		1.02[d]			0.71[d]	

[a] 1999, 2001, and 2005 excluded.

[b] 1983, 1984, 1988, 1994, 2001, and 2005 excluded.

[c] $1/b$, the characteristic distance, is the distance in kilometres for which the correlation between log densities is 0.37.

[d] $\exp(\overline{\log(d)})$.

the expected value, μ, is constant throughout the area independent of any of the explaining covariates. For this model and for all ages and years, the four parameters μ, a, b, and d have been estimated.

Regarding the residual analysis, the elements of the inverse Choleski, $(L^{-1})_{ij}$, was plotted against the distance between points for all three age groups and all 24 years. For all 72 plots, the functional relation between the inverse Choleski and the distance is very similar. As an example, age group 1 in the middle of the period from 1983 to 2006, i.e., 1994, has been selected. The result is illustrated (Fig. 2*a*), showing that the absolute values of the inverse Choleski elements actually decrease when the distance increases. It appears that outside a circle of 100 km, the corresponding residuals R^* can be neglected, indicating that only residuals U^* within the circles are correlated. The residuals U^* were plotted against longitude and latitude. No trend or systematic pattern was found for any of the residual plots (plots again for age group 1 in 1994 are shown in the middle and lower panels of Fig. 2).

The validity of the model has been tested using both goodness-of-fit test statistics T_1 and T_2. Both tests resulted in the model not being rejected for all age groups and years using a level of significance of 5%.

Fig. 3. Contour plots for 1-year-old cod in the North Sea and the Skagerrak in 1983–2006 based on interpolation onto a 50 × 50 grid. The shading scale indicates log density. (Figure 3 is concluded on the next page.)

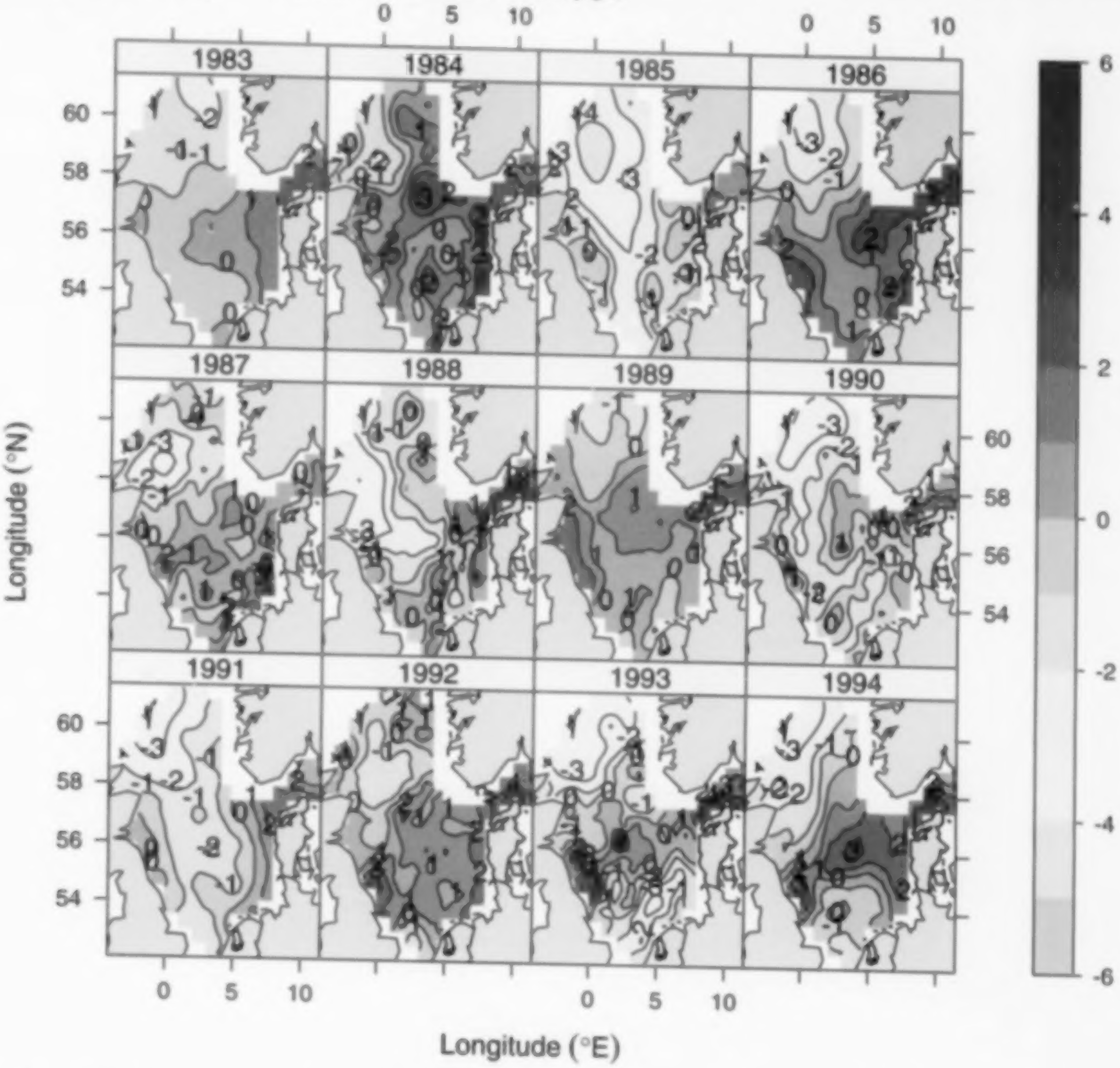

For each age group separately, we tested the hypothesis that the parameters *a*, *b*, and *d* remain constant over years using the likelihood ratio test in the following way. Let $l_y(\theta) = -\log(L_y(\theta))$ denote the likelihood function for year *y*, let $\hat{\theta}_y$ denote the MLE of the parameters, and let $\hat{H}_y = H_{y,\theta=\hat{\theta}_y}$ denote the estimated Hessian matrix. For each year, we approximate the likelihood function with the second-order approximation, i.e.,

$$l_y(\theta_y) - l_y(\hat{\theta}_y) \cong (\theta_y - \hat{\theta}_y)' \hat{H}_y (\theta_y - \hat{\theta}_y)$$

Using this approximation, the simultaneous likelihood function including all years can be approximated by

$$(13) \qquad l(\theta) - l(\hat{\theta}) \cong (\theta - \hat{\theta})' \hat{H} (\theta - \hat{\theta})$$

where

$$(14) \qquad \hat{H} = \begin{pmatrix} \hat{H}_1 & 0 & \\ & \ddots & \\ 0 & & \hat{H}_n \end{pmatrix} \quad \textit{and } \theta = (\theta_1, \ldots, \theta_n)'$$

For the likelihood function approximated in eq. 13, linear hypotheses of the form $\theta = A\beta$ can be tested by the likelihood ratio test and using $\hat{\beta} = (A'\hat{H}A)^{-1}A'\hat{H}\hat{\theta}$. The homogeneity of the parameters over years, i.e., $\theta_y = \theta$ for all *y*, was tested by setting $A = (\theta, \ldots, \theta)'$.

Fig. 3 (concluded).

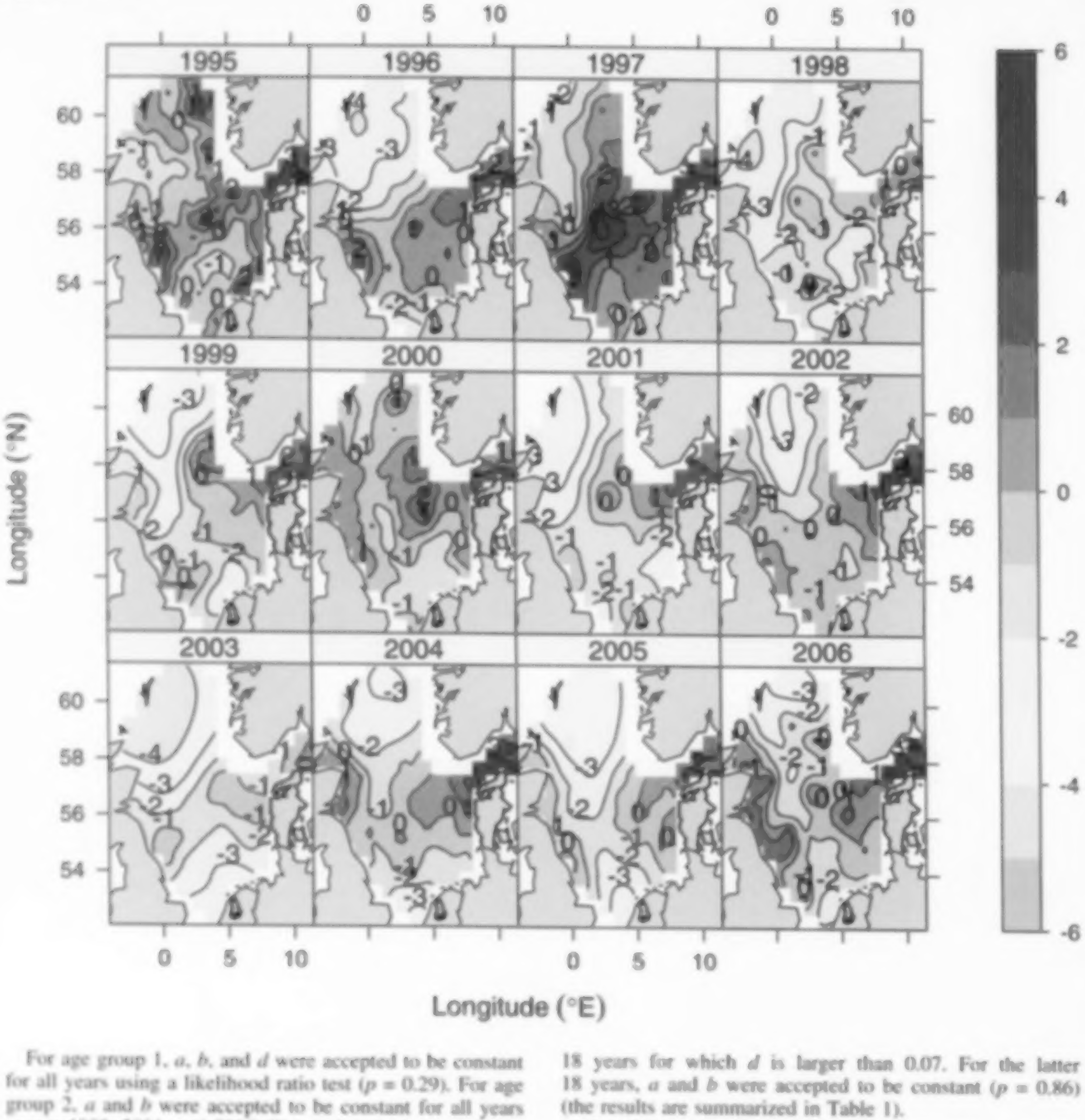

For age group 1, *a*, *b*, and *d* were accepted to be constant for all years using a likelihood ratio test ($p = 0.29$). For age group 2, *a* and *b* were accepted to be constant for all years except 1999, 2001, and 2005. The analyses of age groups 1 and 2 are the most important because the main part of the data consists of positive catches. This is in contrast to age 3+ for which the zero proportion is large as it increases from about 40% to about 60% of the hauls. Hence, the results for these age groups should be treated with caution. For age 3+, 1983 clearly was an outlier, which was excluded from the analysis. For the remaining years, two levels of parameter *d* appear to divide the years into two groups: 1984, 1988, 1994, 2001, and 2005 for which the nugget effect, *d*, was not significantly different from zero, and the remaining 18 years for which *d* is larger than 0.07. For the latter 18 years, *a* and *b* were accepted to be constant ($p = 0.86$) (the results are summarized in Table 1).

The characteristic distance 1/*b*, the large-scale *a*, and the small-scale variation *d* are decreasing by increasing age, indicating that both the spatial correlation and the overdispersion or patchiness declines for increasing age (Table 1).

Contour plots and *D*95 were calculated based on interpolated values of stock density for a regular 50 × 50 grid covering the North Sea and the Skagerrak (confined within 4°W and 13°E longitude and 50°N and 62°N latitude). This corresponds to areas of about 27 × 24 km^2. The areas covering land have been removed, which leaves us with a total of 808 positions for which the densities should be predicted

Fig. 4. Minimum area occupied by 95% of the stock, *D95*, by age plotted against stock number for cod in the North Sea and the Skagerrak in 1983–2006 (bold lines) and 95% confidence limits (broken lines): (*a*) age group 1; (*b*) age group 2; and (*c*) age group 3+. The straight lines indicate linear regression lines.

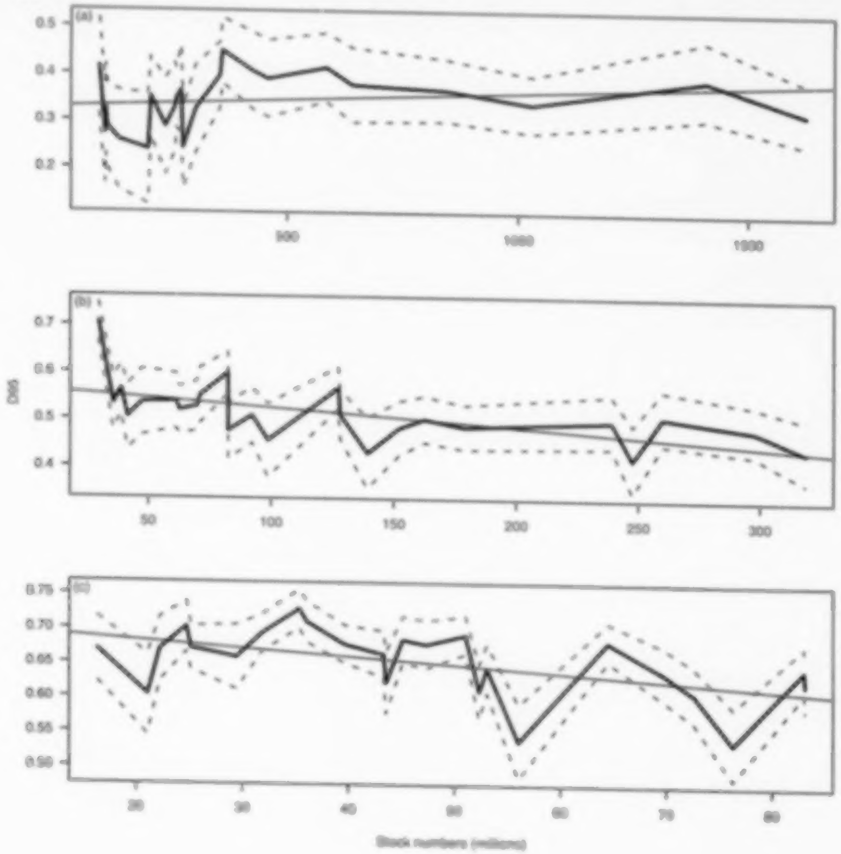

compared with the average of 390 observations available for each of the years 1983–2006. We also tried the finer 70 × 70 grid. The deviations between the two cases with respect to both the mean density and the measure of concentration mentioned below were less than 2%, indicating that the 50 × 50 grid results in reliable estimates functions of λ_{new}.

Contour plots are provided for age 1 (Fig. 3). Until 1997, age group 1 was mainly situated in the southern North Sea and the Skagerrak but has since changed such that a major part is situated in the Skagerrak. It should be noted that this geographical change of distribution is not in contradiction with the unchanged concentration measured using *D95*. This may take place if, for instance, high-density areas geographically change place. Similarly, for age group 2, the high-density area was the northern North Sea and the Skagerrak before 2002 but mainly in the Skagerrak thereafter.

The validity of the theory of density-dependent habitat selection

Plots of *D95* and the 95% confidence limits vs. abundance and year are shown for the age groups 1, 2, and 3+ (Fig. 4). For age 1, linear regression analysis indicates that *D95* is independent of stock abundance, whereas *D95* seems to decline slightly with increasing abundance for age 2 and older. This means that although stock abundance is decreasing drastically during the period, the concentration remains unaffected or decreases and accordingly the theory of density-dependent habitat selection for cod in the North Sea in February–March does not hold.

Discussion

The LGCP applied to analyse the spatial distribution of fishery survey data is a flexible counting model that was able to describe the spatial distribution of cod in the North Sea and the Skagerrak. The model does not assume that observations are independent, but accounts for possible spatial correlation and enables modelling of separate small- and large-scale variations. Problems with zero catches are avoided by the discreteness of the LGCP. A method for calculating residuals related to latitude and longitude enabling graphical validation of the model has been developed, which makes it possible to examine possible geographical deviations from the model. Finally, two simulated exact tests have been formulated and implemented to perform goodness-of-fit tests.

One of the most important features of the LGCP introduced is the ability to predict and interpolate unobserved densities at any location in the area independent of the sampling locations. This ability is important because it is then possible to obtain unbiased estimates of, for instance, the stock concentration in the area (see Appendix A) or the total sum of individuals or biomass. The expected value of the posterior distribution $E(\eta_{\text{new}} | X)$ is used as the basis for interpolation of the spatial distribution of the densities as it is a minimum variance estimator of η_{new} (Diggle and Ribeiro 2007). Many authors (e.g., Møller et al. 1998) have used MCMC to simulate the posterior mean, which has the advantage that the estimates are unbiased. In the present paper, we have instead used a Gaussian approximation to the posterior distribution to estimate posterior means analytically. Simulations indicate that this assumption is reasonable (K. Kristensen, unpublished data). The analytical approach has the advantage that the convergence problems with MCMC for high dimensional data are avoided and the computer time is reduced. The interpolation by sampling from the posterior distribution technique may further be improved using fast Fourier transform and conditioning by kriging (Rue and Held 2005).

The spatial correlation and the large-scale variation of the cod distribution did not change in 1983–2006. This is remarkable in that the conditions of the stock in the same period drastically changed as cod abundance declined by about 75% (ICES 2006), and the centre of gravity of the North Sea component of the stock moved about 200 km northeast (Rindorf and Lewy 2006). This indicates that spatial correlation and variance for cod in the North Sea and the Skagerrak seem to be insensitive to major stock changes in the period.

The stability also applies to the concentration of the stock, which is either unchanged over time (age group 1) or declines slightly (age 2 and older). This implies that the theory of density-dependent habitat selection or other density-dependent theories do not apply to cod in the North Sea and the Skagerrak in winter. This result is in contrast to the results of Blanchard et al. (2005), who analysed data from the English Groundfish Survey in the summer (August–September). The conflicting results may be due to differences in the behaviour of cod in the winter and summer or it could be caused by bias in the estimation of *D95* using raw or smoothed data, especially for small mean catch rates (see Appendix A).

From the point of view of fishery management, it is crucial that the concentration does not increase with declining abundance. Other things being equal, this means that the mean catch rates will not be retained in the commercial fishery when cod abundance declines. If a concentration took place, it could lead to an overestimation of the stock size, as was the case for cod off Newfoundland (Hutchings 1996; Atkinson et al. 1997).

Analyses of possible relations between local cod occurrence and local hydrographical parameters such as temperature, salinity, depth, latitude, and longitude, etc., showed that none of the variables affected the cod distribution. Especially, this means that there was no evidence that adult cod locally move to avoid high or low temperature in the winter, for which the range of temperature is −1 to 9 °C. This is in agreement with the results of Rindorf and Lewy (2006) that the centre of gravity for adult fish was not affected by average temperature and wind.

The effect of the spatial distribution of the fishery on distribution of the stock is not included in the analyses because of lack of data. If bycatch and discard of age group 1 is limited, the effect is of minor importance as the fishing mortality rate for trawl and gill net fishery is only about half of the natural mortality in the period. For fish 2 years old and older, the effect may be important as the fishing mortality is about 50% greater than the natural mortality in the period (ICES 2006).

The interpolated densities indicate that age group 1 shifted from being located mainly in the southern North Sea and the Skagerrak to being mainly in the Skagerrak. This indication of temporal correlation would be valuable to incorporate into the model. If such a model with positive temporal correlation were accepted, it would enable annual or seasonal predictions of the spatial distribution of fish stocks.

In conclusion, LGCP is a flexible model of the spatial distribution of fish accounting for spatial correlation between densities and avoiding problems with zero observations. It is therefore possible to interpolate the densities at any location in the area, which could be used, for instance, in connection with evaluation of the effects of closed areas. This model can be used to test the significance of relations between fish occurrence and hydrographical or climatic factors.

Acknowledgements

The work was partly funded by the Danish National project SUNFISH. We thank A. Nielsen, A. Rindorf, and two referees for helpful comments that improved the paper considerably.

References

Aitchison, J., and Ho, C.H. 1989. The multivariate Poisson – log normal distribution. Biometrika, **76**(4): 643–653. doi:10.1093/biomet/76.4.643.

Atkinson, D.B., Rose, G.A., Murphy, E.F., and Bishop, C.A. 1997. Distribution changes and abundance of northern cod (*Gadus morhua*), 1981–1993. Can. J. Fish. Aquat. Sci. **54**(Suppl. 1): 132–138. doi:10.1139/cjfas-54-S1-132.

Blanchard, J.L., Mills, C., Jennings, S., Fox, C.J., Rackham, B.D., Eastwood, P.D., and O'Brien, C.M. 2005. Distribution–abundance relationships for North Sea Atlantic cod (*Gadus morhua*): observation versus theory. Can. J. Fish. Aquat. Sci. **62**(9): 2001–2009. doi:10.1139/f05-109.

Brémaud, P. 1999. Markov chains, Gibbs fields, Monte Carlo simulation, and queues. Springer, New York.

Diggle, P.J., and Ribeiro, P.J., Jr. 2007. Model-based geostatistics. Springer, New York.

Hrafnkelsson, B., and Stefánsson, G. 2004. A model for categorical length data from groundfish surveys. Can. J. Fish. Aquat. Sci. **61**(7): 1135–1142. doi:10.1139/f04-049.

Hutchings, J.A. 1996. Spatial and temporal variation in the density of northern cod and a review of hypotheses for the stock's collapse. Can. J. Fish. Aquat. Sci. **53**(5): 943–962. doi:10.1139/cjfas-53-5-943.

International Council for the Exploration of the Sea. 2006. Report of the Working Group on the Assessment of Demersal Stocks in the North Sea and Skagerrak. ICES ACFM:35.

Kristensen, K., Lewy, P., and Beyer, J.E. 2006. How to validate a length-based model of single species fish stock dynamics. Can. J. Fish. Aquat. Sci. **63**(11): 2531–2542. doi:10.1139/F06-135.

MacCall, A.D. 1990. Dynamic geography of marine fish populations. Washington Sea Grant Program, Seattle, Washington.

Meeus, J. 1998. Astronomical algorithms. Willmann-Bell Inc., Richmond, Virginia.

Møller, J., and Waagepetersen, R.P. 2004. Statistical inference and simulation for spatial point processes. Chapmann & Hall/CRC, Boca Raton, Florida.

Møller, J., Syversveen, A., and Waagepetersen, R. 1998. Log Gaussian Cox processes. Scand. J. Stat. **25**(3): 451–482. doi:10.1111/1467-9469.00115.

O'Neill, M.F., and Faddy, M.J. 2003. Use of binary and truncated negative binomial modelling in the analysis of recreational catch data. Fish. Res. **60**(2-3): 471–477. doi:10.1016/S0165-7836(02)00101-7.

Perry, A.L., Low, P.J., Ellis, J.R., and Reynolds, J.D. 2005. Climate change and distribution shifts in marine fishes. Science (Washington, D.C.), **308**(5730): 1912–1915. doi:10.1126/science.1111322.

Rindorf, A., and Lewy, P. 2006. Warm, windy winters drive cod north and homing of spawners keeps them there. J. Appl. Ecol. **43**(3): 445–453. doi:10.1111/j.1365-2664.2006.01161.x.

Rivoirard, J., Simmonds, J., Foote, K.G., Fernandes, P., and Bez, N. 2000. Geostatistics for estimating fish abundance. Blackwell Science, Oxford, UK.

Rue, H., and Held, L. 2005. Gaussian Markov random fields: theory and applications. Chapman & Hall/CRC Boca Raton, Florida.

Stefánsson, G. 1996. Analysis of groundfish survey abundance data: combining the GLM and delta approaches. ICES J. Mar. Sci. **53**(3): 577–588. doi:10.1006/jmsc.1996.0079.

Stelzenmüller, V., Ehrich, S., and Zauke, G.-P. 2005. Effects of survey scale and water depth on the assessment of spatial distribution patterns of selected fish in the northern North Sea showing different levels of aggregation. Mar. Biol. Res. **1**(6): 375–387. doi:10.1080/17451000500361009.

Swain, D.P., and Sinclair, A.F. 1994. Fish distribution and catchability: what is the appropriate measure of distribution? Can. J. Fish. Aquat. Sci. **51**(5): 1046–1054. doi:10.1139/f94-104.

Appendix A

When calculating the index related to stock concentration, *D95*, one has to ensure that the estimate is nonbiased. The amount of bias of *D95* will be examined here assuming that data follow the LGCP and that the estimation of *D95* is based on the estimated LGCP parameters and interpolation onto a 50 × 50 grid. Further, it will be shown that using the raw or smoothed observations as the basis for estimating *D95* may result in biased estimates for small values of the mean catch rate. Finally, it will be demonstrated that *D95* is closely related to the dispersion and spatial correlation of data. The simulation experiments are performed as follows.

Estimation of *D95*

D95 *estimated based on LGCP predictions*

An area confined by longitudes 0°E to 10°E and latitudes 50°N to 60°N has been considered for which the maximum distance between the corners is 1280 km. For a regular 51 × 51(= 2601) grid with longitudes (0°, 0.2°, …, 10°) and latitudes (50°, 50.2°, …, 60°), one realization of the densities, $\lambda = (\lambda_1, \ldots, \lambda_{2601})'$, for the 2601 grid points has been simulated assuming that they follow a LGCP with known parameters μ (the common log density), a (the overdispersion), and b (the spatial correlation parameter). A nugget effect is not included. The simulations are performed by first calculating the distances between the 2601 points and, based on that, the variance–covariance matrix, $\mathbf{\Sigma}$, using the known parameters a and b and eq. 2. Then the 2601 log densities, $\eta = (\eta_1, \ldots, \eta_{2601})'$, are simulated by randomly drawing from the multivariate normal distribution, $N(M, \mathbf{\Sigma})$ where

$$M' = \overbrace{(\log(\mu) - a/2, \ldots, \log(\mu) - a/2)}^{2601}$$

The densities are then $\lambda = e^{\eta} = (e^{\eta_1}, \ldots, e^{\eta_{2601}})'$ for which $E(\lambda_i) = \mu$, $i = 1, \ldots, 2601$. Based on the 2601 values of λ, *D95* has been calculated. For the selected values of the parameters, it has been shown that a 51 × 51 grid is sufficient to obtain an estimate of the true *D95* with the error less than 0.01. Hence we consider this estimate, $D95_{\text{true}}$, as the true *D95* for the realized distribution of densities.

We now simulate the catches $X = (X_1, \ldots, X_{121})'$ on the 11 × 11 (= 121) grid with longitudes (0°, 1°, …, 10°) and latitudes (50°, 51°, …, 60°), which is a regular subset of the 51 × 51 grid. This grid approximately corresponds to one haul being taken in a statistical square of 60 × 60 nautical miles, which is a rough grid with a poor covering of the area considered. The catches are simulated by randomly drawing from the independent Poisson distributions with means equal to the corresponding subset, $\lambda_{11 \times 11}$, of λ. From the simulated catches, X, the estimates of the parameters, $\widehat{\mu}$, $\widehat{a}$, and $\widehat{b}$ have been obtained by ML, and based on that, the predictions on the 51 × 51 grid of the log densities $\widehat{\eta}_{\text{predicted}} = (\widehat{\eta}_1, \ldots, \widehat{\eta}_{2601})'$ and the variance have been calculated using eqs. 9 and 10. In principle, an estimate of $\widehat{\lambda}_{\text{predicted}} = \exp(\widehat{\eta}_{\text{predicted}} + \widehat{a}/2)$ could be obtained, but as this may be seriously biased (Aitchison and Brown 1976), we instead simulate an unbiased estimate by (1) drawing from the multivariate normal distribution $\widehat{\eta}_{\text{sim}} = N(\widehat{\eta}_{\text{predicted}}, \text{VAR}(\widehat{\eta}_{\text{predicted}}))$, (2) calculating $\widehat{D95}_{\text{sim}} = D95(\exp(\widehat{\eta}_{\text{sim}}))$, and (3) repeating steps 1 and 2 1000 times and calculating the $\widehat{D95}_{\text{LOC}}$ equal to the mean of $\widehat{D95}_{\text{sim}}$. The possible bias of $\widehat{D95}_{\text{LOC}}$ has been calculated as $\widehat{D95}_{\text{LOC}}/D95_{\text{true}} - 1$.

D95 *estimates based on the observations*

As some authors use the observations or smoothed value of these as basis for estimating *D95* (Swain and Sinclair 1994; Atkinson et al. 1997; Blanchard et al. 2005), we also examine the possible bias by calculating $D95_{\text{observations}}(X)$ based on the (raw) 121 observations and two alternatives based on smoothed values. The first estimate, $D95_{81}(X)$, based on smoothed observations is obtained by dividing the latitude and longitude ranges [0, 10] and [50, 60], defining the area considered into nine intervals each and calculating the mean of the observations in each of the 9 × 9 (= 81) rectangles defined. Correspondingly, $D95_{25}(X)$ is obtained by dividing the area into five intervals.

Fig. A1. Relative bias of estimated *D95* versus mean catch rate: bold solid line, estimates based on predictions using the LGCP; solid line, estimates based on raw catch observations; broken lines, estimates based on smoothed catch observations. See text in the appendix.

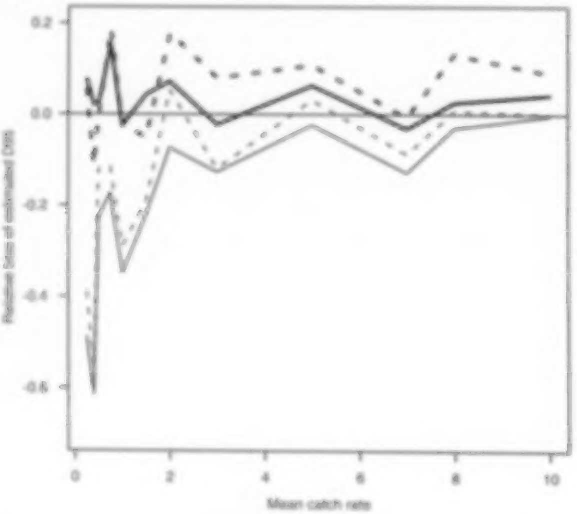

The relationship between D95 *and the spatial correlation and the dispersion*

To examine the above relationship, $D95_{true}$ has been calculated for a range of values of $1/b$ with fixed dispersion a, and vice versa.

Results: estimation of D95

To examine the effect of varying mean catch rate, the following sets of simulations have been performed for fixed values of a and b for the following values: $a = 1.5$, $b = 0.005$, catch rates = (0.25, 0.4, 0.50, 0.75, 1, 1.5, 2, 3, 5, 7, 8, 10), *i.e.*, $\mu = \ln(\text{catch rate})$.

For $b = 0.005$, the characteristic spatial correlation distance $1/b$ equals 200 km, the distance at which the spatial correlation equals 0.37. For the case considered, the proportion of the points for which the distance is less than 200 km is about 10%, indicating that observations are available for estimating the parameters in the model. The coefficient of variation of the densities λ is $\sqrt{1.5} = 1.22$.

The results of the simulations are illustrated, showing the relationship between the relative bias of estimates of *D95* and the mean catch rate (Fig. A1). This figure shows that in general, $\widehat{D95}_{LGC}$ is the least biased estimator of *D95* and that the bias is less than 5% for mean catch rates larger than 1. For mean catch rates less than 1, the relative bias is less than 15%. The smoothed estimate, $D95_{S1}$ is the second-best estimator, with a relative bias less than 10% for mean catch rates larger than 2. For mean catch rates less than 2, however, the relative bias is tremendous, up to about – 60%. In general, the bias of $D95_{25}$ seems to be positive, up to 20%. For small values of mean catch rates, the bias is still limited, below 10%. $D95_{observations}$ is negatively biased, and the bias is especially huge (up to –60%) for small values of the mean catch rate.

Fig. A2. The relationship between *D95* and (*a*) 1/*b* and (*b*) the variance of log density *a*.

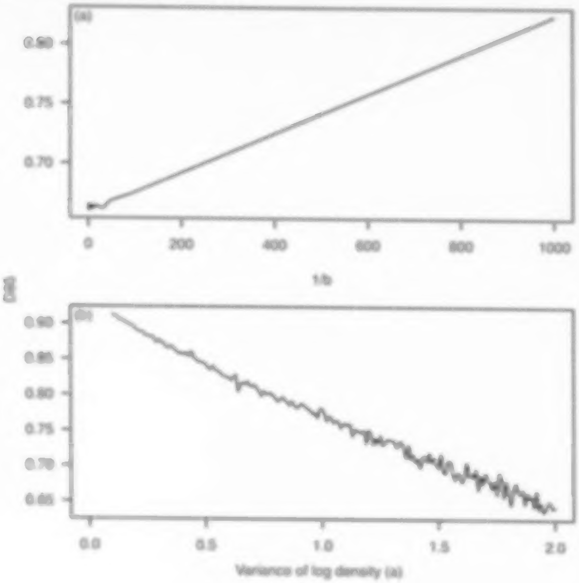

We conclude that the LGCP estimator, $\widehat{D95}_{LGCP}$, is the best estimator. Smoothing of the observations may lead to satisfactory *D95* estimates for mean catch rates larger than 1 or 2. Raw observations should not be used for estimation of *D95*.

Results: the relationship between D95 *and spatial correlation and dispersion*

The results are illustrated showing the relationship between *D95* and $1/b$ for fixed values of the mean catch rate of 10 and $a = 1.5$ (Fig. A2*a*), as well as the relationship between *D95* and a for a mean catch rate of 10 and $b = 0.02$ (Fig. A2*b*). The figure shows that *D95* depends on the spatial correlation, the dispersion, and the log densities. Hence, changes in the concentration of a stock ($1 - D95/0.95$) may be caused by changes either in the dispersion or the spatial correlation or in both stock characteristics. The quantity $1 - D95/0.95$ is a measure of the concentration, which lies between 0 and 1.

References

Aitchison, J., and Brown, J.A.C. 1976. The lognormal distribution. Cambridge University Press, Cambridge, UK.

Atkinson, D.B., Rose, G.A., Murphy, E.F., and Bishop, C.A. 1997. Distribution changes and abundance of northern cod (*Gadus morhua*), 1981–1993. Can. J. Fish. Aquat. Sci. **54**(S1): 132–138. doi:10.1139/cjfas-54-S1-132.

Blanchard, J.L., Mills, C., Jennings, S., Fox, C.J., Rackham, B.D., Eastwood, P.D., and O'Brien, C.M. 2005. Distribution–abundance relationships for North Sea Atlantic cod (*Gadus morhua*): observation versus theory. Can. J. Fish. Aquat. Sci. **62**(9): 2001–2009. doi:10.1139/f05-109.

Swain, D.P., and Sinclair, A.F. 1994. Fish distribution and catchability: what is the appropriate measure of distribution? Can. J. Fish. Aquat. Sci. **51**(5): 1046–1054. doi:10.1139/f94-104.

Evaluating the demographic significance of genetic homogeneity using a coalescent-based simulation: a case study with gag (*Mycteroperca microlepis*)

Elizabeth L. Cushman, Nathaniel K. Jue, Allan E. Strand, and Erik E. Sotka

Abstract: Gag (*Mycteroperca microlepis*) from the eastern Gulf of Mexico and northwestern Atlantic are managed as separate stocks, although evidence for their demographic isolation remains equivocal. Several hundred individuals were genotyped at 11 microsatellite loci and it was found that gag across these regions were genetically indistinguishable ($F_{ST} < 0.001$). A coalescent-based computer simulation was employed to quantitatively assess the relative importance of dispersal rate, population size, and time since divergence on gag genetic homogeneity. Using empirical estimates of long-term effective population size (16 500), a range of dispersal rates and divergence times (500 to 500 000 generations) was modeled, and it was concluded that present-day genetic homogeneity must be maintained by dispersal rates of at least 20–30 migrants per generation and up to hundreds or thousands per generation. This study also documents the absence of significant temporal genetic structure and inbreeding in the Atlantic when comparing cohorts separated in time from weeks to 20 years. This suggests that the long-standing practice of overfishing gag has yet to manifest as an inbreeding effect. Overall, gag dispersal rates remain uncertain, and consequently, this study can neither support nor refute management schemes that independently regulate gag in the eastern Gulf of Mexico and northwestern Atlantic.

Résumé : Les badèches baillou (*Mycteroperca microlepis*) de l'est du golfe du Mexique et du nord-ouest de l'Atlantique sont gérées comme des stocks distincts, bien que les données sur leur isolement démographique restent équivoques. Nous avons déterminé le génotype à 11 locus microsatellites de plusieurs centaines d'individus et nous n'arrivons pas à distinguer génétiquement les badèches baillou dans l'ensemble de ces régions ($F_{ST} < 0{,}001$). Une simulation sur ordinateur basée sur la coalescence nous à servi à évaluer quantitativement l'importance relative du taux de dispersion, de la taille de la population et du temps depuis la divergence pour l'homogénéité génétique de la badèche. En utilisant des estimations empiriques de la taille effective de la population à long terme (16 500), nous avons modélisé une gamme de taux de dispersion et de temps depuis la divergence (500 à 500 000 générations); il en ressort que l'homogénéité génétique actuelle doit être maintenue par des taux de dispersion d'au moins 20–30 migrants par génération jusqu'à des centaines ou des milliers de migrants par génération. Notre étude note aussi l'absence de structure génétique temporelle significative et de consanguinité dans l'Atlantique dans des comparaisons de cohortes séparées dans le temps par des périodes allant de semaines à 20 années. Cela indique que la pratique de longue date de surpêche de la badèche baillou ne s'est pas encore manifestée comme un effet de consanguinité. Globalement, les taux de dispersion de la badèche demeurent incertains et, en conséquence, notre étude ne peut ni appuyer, ni rejeter les propositions de gestion qui contrôlent de façon indépendante les badèches baillou de l'est du golfe du Mexique et du nord-ouest de l'Atlantique.

[Traduit par la Rédaction]

Introduction

Fisheries managers use several criteria to determine whether species should be managed as a single stock or as multiple units (Begg and Waldman 1999; Fraser and Bernatchez 2001). From the biological perspective, management units (or populations and stocks) are groups of individuals that are demographically independent from others (Waples and Gaggiotti 2006). However, identifying which groups are demographically isolated depends on describing patterns of connectivity across space (Fogarty and Botsford 2007), which itself is extremely difficult for most marine populations because of the biological and oceanographic complexity inherent to dispersal processes (Shanks 1995).

One approach to describing patterns of connectivity is to measure gene flow, which has the distinct advantage of al-

---

Received 1 September 2008. Accepted 8 July 2009. Published on the NRC Research Press Web site at cjfas.nrc.ca on 13 October 2009.
20756

Paper handled by Associate Editor Anti Vasemägi.

E.L. Cushman, A.E. Strand, and E.E. Sotka.[1] College of Charleston, Grice Marine Laboratory, 205 Ft. Johnson Rd, Charleston, SC 29412, USA.
N.K. Jue. Florida State University, Department of Biological Science, 4079 King Building (4295), Tallahassee, FL 32306, USA.

[1] Corresponding author (e-mail: sotkae@cofc.edu).

Can. J. Fish. Aquat. Sci. 66: 1821–1830 (2009) doi:10.1139/F09-140 Published by NRC Research Press

lowing scientists to evaluate patterns of effective dispersal across multiple generations (Hauser and Carvalho 2008). Unfortunately, the genetic approach often yields ambiguous interpretation when fisheries species exhibit weak differentiation across broad spatial scales (Ward et al. 1994; Waples 1998). This is because it can be difficult to tease apart the primary demographic and evolutionary causes of genetic homogeneity: stabilizing selection, nonequilibrium between drift and migration since subpopulations diverged, and ongoing gene flow. Moreover, even modest levels of gene flow (hundreds of individuals per generation) can yield values of differentiation (or F_{ST}) that are swamped by the sampling error of most studies (Waples and Gaggiotti 2006; Cano et al. 2008). To address these limitations, novel genetic and analytical methods are needed to help tease apart the causes of the weak genetic differentiation that characterizes many fisheries species (Selkoe et al. 2008).

The gag (*Mycteroperca microlepis*; Goode and Bean 1879) is a large (maximum ~1.2 m total length), protogynous grouper commonly found in the northwestern Atlantic, Gulf of Mexico, and off the coast of Brazil (Heemstra et al. 2002), and is one of the most commercially and recreationally important grouper species in the southeastern United States (Bullock and Smith 1991). Gag are currently managed as two separate stocks: the eastern Gulf of Mexico (Gulf) and the northwestern Atlantic off the southeastern US coast (Atlantic), with the delineation at the Florida Keys. Two studies have employed molecular techniques to address gag population genetic structure. Jue (2006) sampled the Gulf and documented no temporal or spatial genetic differentiation across several yearly cohorts. Chapman et al. (1999) found patchy genetic differentiation among sampling locations for gag from the Atlantic and the Gulf, but the number of samples and genotyped loci were modest and preclude strong statistical inference.

Eleven microsatellite loci were genotyped to address three main objectives: (*i*) to determine whether spatial and temporal genetic differences exist among yearly cohorts of gag taken from different regions within the Atlantic; (*ii*) to determine whether spatial differentiation exists between the Atlantic and Gulf; and (*iii*) to employ a coalescent-based simulation approach to evaluate the biological significance of the lack of genetic differentiation between the Gulf and Atlantic. These analytical simulations explicitly address the degree to which nonequilibrium processes or ongoing gene flow are responsible for genetic homogeneity, an issue that confounds many studies of marine fisheries genetics.

Materials and methods

Sample collection and DNA isolation

Four sets of spatially and temporally segregated samples were collected: offshore Atlantic adult and subadult gag from several year classes, 2005 year-class juvenile gag from North Carolina estuaries, 1985 year-class gag postlarvae (~15 mm) from South Carolina estuaries, and offshore adult Gulf gag from several unknown year classes (Table 1; Fig. 1). Tissue samples from Atlantic adult and subadult gag were collected in April and May of 2005 from offshore North Carolina, South Carolina, and the eastern coast of Florida by the Marine Resources Monitoring, Assessment, and Prediction (MARMAP) Program of the South Carolina Department of Natural Resources (SCDNR), with the help of hook-and-line commercial (bandit reel) and recreational (rod and reel) fisherman. Young-of-the-year gag were collected from North Carolina estuaries from 1 August to 2 September 2005 by the National Oceanic and Atmospheric Administration (NOAA), using dock-mounted traps placed at the Center for Coastal Fisheries and Habitat Research (CCFHR) on Pivers Island near Beaufort, North Carolina. Young-of-the-year gag were collected using 1 m × 2 m frame neuston nets (1–2 mm mesh) from Breach Inlet, a barrier island inlet located just north of Charleston, South Carolina, between Sullivan's Island and the Isle of Palms. These postlarvae were collected by SCDNR on a weekly basis from 22 March to 6 June 1985. Offshore adult Gulf gag were collected in 2004–2006 from two regions of the eastern Gulf of Mexico representing the northwestern (above Tampa Bay or 27.5°N latitude) and southwestern (below Tampa Bay or 27.5°N latitude) coasts of Florida, respectively.

Tissue samples were preserved in a sarcosyl–urea solution (1% sarcosyl, 8 mol·L^{-1} urea, 20 nmol·L^{-1} sodium phosphate, 1 mmol·L^{-1} EDTA, pH 6.8) before extraction. A SPRINTPrep magnetic bead procedure (Agencourt, Inc., Beverly, Massachusetts) was used to isolate genomic DNA.

Genotyping

A suite of 11 microsatellite loci developed for several grouper species including gag (Chapman et al. 1999), black grouper (*Mycteroperca bonaci* (Poey); Zatcoff et al. 2002), and Hawaiian grouper (*Epinephelus quernus* Seale; Rivera et al. 2003) were genotyped (for further information on microsatellite loci including locus names and sequences, see Supplemental Table S1, available online from the NRC Data Depository[2]). These loci were chosen because they were polymorphic, demonstrated clear and consistent amplification, and had been used successfully for *M. microlepis* in previous studies (Chapman et al. 1999; Jue 2006). For the offshore Atlantic adult and juvenile gag and the North Carolina juveniles (Pivers Island samples), eight of these 11 loci (GAG023, GAG038, GAG045, MBO029, MBO048, MBO086, CA2, CA6) were assayed with fluorescently labeled forward primers (IDTDNA, Applied Biosystems (ABI), Foster City, California) at Florida State University (FSU) in Tallahassee, Florida (P.I. Dr. Don Levitan). These eight loci were genotyped on an ABI 3130xl Genetic Analyzer with capillary electrophoresis. ABI Genemapper Software version 4.0 was used to read and determine final scores for the resulting data. Accuracy of scores was assessed by adherence of sample peaks to a predetermined locus-specific binning system in Genemapper, and a subset of 95 samples was analyzed by a second human reader to confirm score consistency. PCR amplifications for these eight

---

[2] Supplementary data for this article are available on the journal Web site (http://cjfas.nrc.ca) or may be purchased from the Depository of Unpublished Data, Document Delivery, CISTI, National Research Council Canada, Building M-55, 1200 Montreal Road, Ottawa, ON K1A 0R6, Canada. DUD 5275. For more information on obtaining material, refer to http://cisti-icist.nrc-cnrc.gc.ca/eng/ibp/cisti/collection/unpublished-data.html.

Table 1. Number of genotyped samples from each site and year class.

	Site					
Year class	EFL	SC	NC	NWFL	SWFL	Total
2005[*]	—	—	30	—	—	30
2002	2	—	4	—	—	
2001	4	43	82	—	—	129
2000	7	49	69	—	—	125
1999	13	32	10	—	—	55
1998	11	—	—	—	—	11
1997	2	—	—	—	—	2
1995	1	—	—	—	—	1
1994	3	—	—	—	—	3
1993	7	—	—	—	—	7
Unknown	1	—	—	211	131	343
1985[†]	—	158	—	—	—	158
Total	51	282	195	211	131	870

Note: Sites: EFL, eastern coast of Florida; SC, South Carolina; NC, North Carolina; NWFL, northwestern coast of Florida; SWFL, southwestern coast of Florida)

[*] NC young-of-the-year juveniles (Pivers Island).

[†] SC young-of-the-year postlarvae (Breach Inlet).

Fig. 1. Map of the southeastern coast of the United States (Atlantic) and the eastern Gulf of Mexico. General collecting locations for offshore adult and juvenile gag are indicated by ellypses. NC, North Carolina; SC, South Carolina; EFL, eastern coast of Florida; SWFL, southwestern coast of Florida; NWFL, northwestern coast of Florida. Coordinates for the majority of the Atlantic samples were provided, and individual collecting sites are indicated by solid circles. Estuarine sampling sites for North Carolina juvenile gag (Pivers Island) and South Carolina postlarvae (Breach Inlet) are indicated by shaded stars.

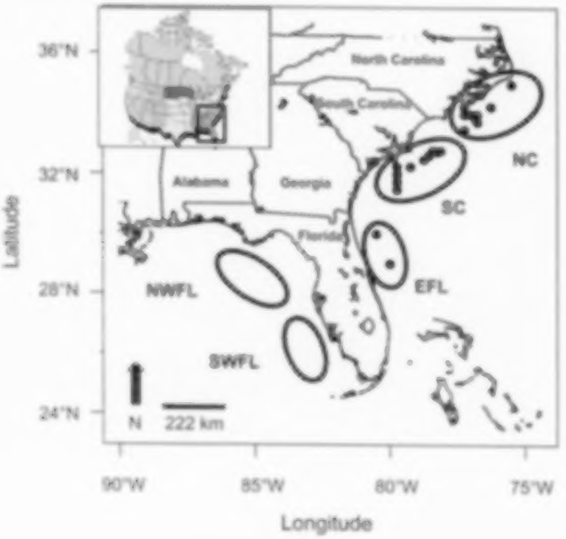

loci contained sample DNA (~2.5 ng·µL^{-1}), water, 5× Colorless GoTaq Reaction Buffer (1×, pH 8.5), MgCl$_2$ (2 mmol·L^{-1}), BSA (0.5 µg·µL^{-1}), dNTPs (0.2 mmol·L^{-1}), forward and reverse primer (0.3 µmol·L^{-1} each), and Promega GoTaq DNA polymerase (0.03 U·µL^{-1}) for a total reaction volume of 20 µL. For the Gulf offshore adults (NWFL and SWFL), all 11 loci were genotyped on the ABI system using the protocols described above. Genotyping for the remaining Atlantic samples was performed on an eight-capillary Beckman Coulter CEQ-8000 Genetic Analyzer (CEQ) at College of Charleston's (CofC) Molecular Core Facility. This includes the offshore adults and juveniles and the 2005 Pivers Island juveniles at three loci (GAG007, GAG010, MB088) and all of the 1985 South Carolina postlarvae (Breach Inlet samples) at six loci (GAG007, GAG023, GAG038, GAG045, MBO029, MBO048). Only these six loci could be amplified with any consistency for the 1985 SC postlarvae, possibly due to quality of the sample DNA after 20 years of storage. Loci genotyped on the CEQ were assayed with fluorescently labeled forward primers (SIGMA-Proligo, The Woodlands, Texas). Data were visualized and hand-scored using CEQ 8000 Fragment Analysis Software version 8.0, and a subset of samples for each locus was confirmed by a second human reader. PCR amplifications for the CEQ analyzed loci contained DNA (~2.5 ng·µL^{-1}), water, 10× AccuBuffer (1×, pH 8.3), BSA (0.5 µg·µL^{-1}), dNTPs (0.8 mmol·L^{-1}), forward and reverse primer (0.3 µmol·L^{-1} each), and BIOLINE Accuzyme DNA polymerase (0.013 U·µL^{-1}) for a final reaction volume of 20 µL (for locus-specific PCR protocols, see Supplemental Table S2[2]).

Because results from genotyping can differ between locations, machines, and reagents, the consistency of genotyping for each locus was tested on a subset of samples analyzed on both the ABI and CEQ systems: 30 samples at three loci (GAG007, GAG010, MB088) and 10 samples at five other loci (GAG023, GAG038, GAG045, MBO029, MBO048). It was noted that samples genotyped on the CEQ always scored 1–4 base pairs higher (depending on the locus) than the same samples genotyped on the ABI system. This discrepancy between systems was consistent among samples and was corrected before the analysis.

Rates of genotyping errors were not directly estimated, but it can be assumed that their effects on the results of this study were negligible for several reasons. No locus systematically deviated from Hardy–Weinberg equilibrium or was in linkage disequilibrium with other loci. Many suggested protocols were followed to minimize genotype errors (see Bonin et al. 2004), including amplifying negative controls, discarding samples with problems of amplification or repeatability, replicating amplifications for a subset of samples, cross-reading data with multiple eyes, and checking all data by hand. Moreover, Bonin et al. (2004) suggest that genotyping errors are more problematic for individual-based analyses (e.g., kinship, relatedness) than for the population-structure questions, which are the primary focus of this study.

Statistical analysis

Tests for Hardy–Weinberg equilibrium (HWE), linkage disequilibrium, and null alleles were performed for all loci within each group (site or year class) and for all loci across the entire data set. Tests for deviations from HWE were conducted using exact tests performed with Markov chain randomization in the program Arlequin (version 3.11; Excoffier et al. 2005). Chains had 200 000 steps with a 10 000 step burn-in. Tests for linkage equilibrium between all microsatellite pairs were executed in Arlequin using 20 000 permutations. Tests for the presence of null alleles and large-allele drop-out were performed with the program MICROCHECKER (version 2.2.3; van Oosterhout et al. 2004).

Spatial, temporal, and regional level comparisons were performed using analysis of molecular variation (AMOVA) procedures (Excoffier et al. 1992), pairwise Φ_{ST} estimation (Weir and Cockerham 1984), and a series of Markov chain Monte Carlo exact tests (Raymond and Rousset 1995) within Arlequin. The significance level for the first two tests was determined by 20 000 permutations. The number of steps in the Markov chain for the exact tests was 200 000, with a burn-in of 10 000 steps, as recommended by Arlequin. Significance levels (α value) for all analyses were adjusted using a sequential Bonferroni correction (Rice 1989). For the spatial analysis, adults and juveniles from North Carolina (33.5°N–34.5°N latitude, n = 165), South Carolina (31.5°N–32.8°N latitude, n = 124), and eastern Florida (28°N–30°N latitude, n = 51) were compared with one another and with two Gulf of Mexico locations (northwestern Florida, above 27.5°N latitude, n = 211, and southwestern Florida, below 27.5°N latitude, n = 131) at 11 loci. For the temporal analysis within the Atlantic, fish from the 2001 year class (n = 129), the 2000 year class (n = 125), and the 1999 year class (n = 55) were compared with one another and with the 2005 North Carolina young-of-the-year (Pivers Island samples, n = 30) with all 11 microsatellite loci, and with the 1985 South Carolina young-of-year postlarvae (Breach Inlet samples, n = 158) with 6 microsatellite loci. In addition, the 1985 samples were collected on a weekly basis, allowing postlarvae from two different time points of the 1985 larval ingress period into Breach Inlet (23 April and 9–11 May) to be compared to assess for within year class variation (for the 1985 sampling strategy, see Supplemental Figure S1[2]).

The relative influence of mutation and genetic drift rate on genetic differentiation was assessed by a comparison of R_{ST} values with F_{ST} values using the software SPAGeDi and following Hardy (2003). There was no significant difference between the two measures (data not shown), indicating that mutation does not have an overwhelming effect on levels of differentiation.

To contrast genetic diversity between Atlantic sites and the Atlantic and the Gulf of Mexico, standard diversity estimates were generated using Arlequin (for spatial and temporal diversity indices including the sample size, number of alleles, allelic size range, observed and expected heterozygosity, and probability of deviation from Hardy–Weinberg equilibrium for each locus, see Supplemental Tables S3–S5[2]), and a coalescent-based estimate of theta (Θ) was generated using MIGRATE (version 2.3; Beerli and Felsenstein 2001).

Allele frequencies of the microsatellites appeared to follow the expectations of a stepwise mutation pattern (for locus-specific allele frequencies, see Supplemental Figs. S2 and S3[2]), so a Brownian stepwise mutational model was utilized for all runs. To ensure that estimates of Θ for the Atlantic would be comparable with previous estimates of these parameters in the Gulf of Mexico, MIGRATE runs were modeled according to the methodology of Jue (2006): Θ had a uniform prior distribution over the interval [0, 50.0], the simulation incorporated a Bayesian approach, runs were composed of 10 independent chains sampling 10 000 genealogies using a multiple Markov static heating scheme, and loci mutational rates were scaled by the number of alleles per locus across the entire sample set; the only exception was that initial runs (10 replicate runs of 20 random individuals) were done by site rather than by year of samples. Bayesian posterior distributions of all runs were examined for stability. As in Jue (2006), when spatial and temporal differentiation proved to be negligible, final estimates for Θ and its credible intervals (2.5%–97.5%) for the entire Atlantic were found by taking the average median scores of Θ and the average credible intervals across all loci for 10 replicate runs of 40 randomly selected individuals (500 "bins" posterior distribution) from the combined Atlantic data set. Replicate runs using independent starting values were performed to ensure stability of the results, and median values were examined as these will give the most stable and reliable estimates of the true value of Θ with this method (Beerli 2006).

Once the average median Θ values and credible intervals (2.5%–97.5%) were obtained, long-term N_e and its credible intervals were calculated for each Atlantic site and for the entire Atlantic (all sites and all year classes) using $\Theta = 4N_e\mu$. For the same 11 microsatellite loci, Jue (2006) estimated a mutation rate of $\mu = 2 \times 10^{-4}$ using the methodology of Turner et al. (2002). To conservatively reduce bias in the final estimates of long-term effective population size, the author utilized half of this value ($\mu = 1 \times 10^{-4}$) to calculate the long-term N_e for the Gulf (Jue 2006). Here, both mutation rates were used to estimate long-term N_e in the Atlantic.

Calculated in this manner, Θ is a broad-based, long-term measure of diversity generated from the mutation-drift equilibrium acting across hundreds if not thousands of generations and is therefore influenced by historical population dynamics. Despite this limitation of the coalescent approach, using Θ estimates from MIGRATE is likely conservative with regard to underestimation of N_e when populations are recently subdivided and is preferable to other methods when N_e is large because of the low statistical power of other methods (e.g., temporal F_{ST}; Turner et al. 2002).

Gene flow simulations

To estimate the degree to which migration and time since divergence impact genetic differentiation, coalescent-based simulations were generated using SIMCOAL (Excoffier et al. 2000). These simulations utilized the average effective population size estimated from MIGRATE-derived Θ and the fastest mutation rate (~16 500 diploid individuals), but doubling the estimate of N_e did not change our overall conclusions (data not shown). An ancestral population was allowed to diverge into two equally sized populations of 16 500 each between 500 and 500 000 generations ago. The range in the number of generations took into account uncertainties in the generation time of gag (3–10 years; calculations drawn from SCDNR unpublished data and Morris et al. 2000), the indeterminate timing of the split between the Gulf and the Atlantic, which likely occurred during the Pleistocene epoch (11 500 – 1.8 million years ago; Avise 1992), and any possible bias in the underestimation of N_e in the results. Starting immediately after divergence and continuing until the present, the two populations were then allowed to disperse at a rate (i.e., N_m) of between zero and 50 individuals per generation, tracking 11 microsatellite loci for each individual. One-hundred simulation replicates under each combination of parameters were run. At the end of each simulation replicate, Rmetasim (Strand 2002; http://cran.r-project.org) sampled 300 individuals per population, approximating the number of genotyped fish samples, and calculated the average Weir and Cockerham's Φ_{ST}. The mean Φ_{ST} across replicates and its 2.5% and 97.5% quantiles were then visualized. These simulations should be considered as a first-order approximation of gag evolution, given that gag demography (particularly overlapping generations and unequal sex ratio) violates the underlying assumptions of the coalescent approach implemented in SIMCOAL. A simultaneous estimate of gene flow and migration using MIGRATE was attempted but the estimates were unreliable because likelihood surfaces were extremely flat (data not shown).

Results

Statistical analysis

When samples were pooled, all loci met Hardy–Weinberg expectations. Site and year-class level tests for the Atlantic and the western coast of Florida (eastern Gulf of Mexico) showed departures from HWE in one instance (MBO88 locus in the Florida population) after Bonferroni correction. MICROCHECKER detected the presence of null alleles for three loci (GAG023, MBO48, and MBO086); however, the signal was not consistent across sites or year classes, suggesting that this may be a sampling artifact. No loci were found to be affected by linkage disequilibrium or large-allele drop-out after Bonferroni correction.

AMOVA procedures revealed no genetic differentiation at any spatial or temporal scale within the Atlantic (all $F_{ST} < 0.005$, all $p > 0.05$) or any spatial differentiation between the Gulf and Atlantic groups ($F_{ST} = -0.0002$, $p = 1.0$) (for complete spatial and temporal AMOVA results, see Supplemental Tables S6–S8[2]). For all AMOVAs, virtually all of the total variance was explained by within-group variation (97%–100%) rather than by among-group variation. An analysis of pairwise Φ_{ST} between locations and year classes yielded low, insignificant values before and after Bonferroni corrections (Table 2). Similarly, exact tests on allele frequencies also yielded no significant differences ($p > 0.05$; results not shown).

Significant differences in genetic diversity between sets of locations and year classes were not detected (see Supplemental Tables S3–S5[2]). Observed and expected heterozygosity averaged ~0.73–0.79 for each location and year class in the Atlantic and Gulf, and theta (Θ) estimates did not differ between sites in the Atlantic or between the Atlantic and the Gulf (Fig. 2). The average median Θ value and average credible intervals (2.5%–97.5%) for each site were as follows: EFL = 12.07 (8.21–16.04), SC = 12.82 (8.95–17.37), and NC = 13.83 (9.86–17.83). The Θ value and credible intervals (2.5%–97.5%) for the entire Atlantic (all sites combined) was 14.51 (9.81–18.76). Using $\Theta = 4N_e\mu$, the long-term N_e and its credible intervals for the entire Atlantic was 18 138 (12 263 – 23 450) at $\mu = 2 \times 10^{-4}$ and 36 275 (24 525 – 46 900) at $\mu = 1 \times 10^{-4}$ (see Materials and methods). The estimates of Θ did not differ significantly from the Gulf values (Fig. 2), as was originally reported in Jue (2006): $\Theta = 12.39$ (9.1–15.24) yields $N_e = 15\,488$ (11 375 – 19 050) at $\mu = 2 \times 10^{-4}$ or 30 975 (22 750 – 38 100) at $\mu = 1 \times 10^{-4}$.

Gene flow simulations

The coalescent-based simulations provide an estimate of the lowest amount of migration that could maintain genetic homogeneity between regions under nonequilibrium conditions. Assuming that gag have a diploid effective population size of ~16 500 (the average N_e when assuming fastest mutation rates; see above), the expected level of genetic differentiation between the Gulf and the Atlantic should be low but detectable when migration ceases and time of divergence is between 5000 to 500 000 generations (Fig. 3). Increases in migration rate yields declines in Φ_{ST}, regardless of the time since divergence, but the confidence intervals do not include Φ_{ST} ~0.001 until migration rates reach 20–30 individuals per generation or more. Therefore, assuming that the microsatellite sampling in this study could detect levels of $\Theta_{ST} = 0.001$ (e.g., Rose et al. 2006; see Discussion), the gag genetic homogeneity between Atlantic and Gulf regions could be maintained by as few as 20–30 migrants per generation. The upper estimate of migrants per generation cannot be assessed using these simulations and could theoretically be hundreds to thousands of individuals.

Discussion

This analysis of 11 microsatellite loci from 870 gag from the northwestern Atlantic and eastern Gulf of Mexico among four year classes (1984, 1999, 2000, and 2001) indicates genetic homogeneity across broad temporal (~20 years) and spatial (~2000 km) scales. In all cases, the majority of total genetic variation could be found within, rather than between, locations or year classes (97%–100%). These conclusions do

Table 2. Φ_{ST} values for pairwise spatial (site) and temporal (year-class) comparisons.

(*a*) Spatial comparisons.

Site	EFL (51)	SC (124)	NC (165)	NWFL (211)	SWFL (131)
EFL	0				
SC	–0.0009	0			
NC	–0.0002	–0.0005	0		
NWFL	–0.0003	–0.0003	–0.0007	0	
SWFL	–0.0003	0.0002	0.0001	0.0006	0

(*b*) Temporal comparisons.

	11 Loci				6 Loci				
Year class	1999 (55)	2000 (125)	2001 (129)	2005 (30)	1985 (158)	1999 (55)	2000 (125)	2001 (129)	2005 (30)
1985					0				
1999	0				–0.0007	0			
2000	–0.0005	0			–0.0003	–0.0004	0		
2001	0.0003	0.0008	0		–0.0006	0.0004	0.0006	0	
2005	0.0006	0.0026	0.0035	0	–0.0001	0.0003	0.0032	0.0004	0

Note: The total number of individuals is given in parentheses following the site or year class; both 6 loci (including the 1985 SC postlarvae) and 11 loci (excluding the 1985 SC postlarvae) results are shown for the temporal tests. Sites: EFL, eastern coast of Florida; SC, South Carolina; NC, North Carolina; NWFL, northwestern coast of Florida; SWFL, southwestern coast of Florida. No comparisons were statistically significant.

Fig. 2. Average median theta (Θ) values and average credible intervals (2.5% and 97.5%) as estimated by MIGRATE (Beerli and Felsenstein 2001) for each Atlantic site and the Atlantic and eastern Gulf of Mexico (Gulf) as a whole. Theta (Θ) estimates did not differ significantly between sites in the Atlantic or between the Atlantic and the Gulf of Mexico. EFL, eastern coast of Florida; SC, South Carolina; NC, North Carolina.

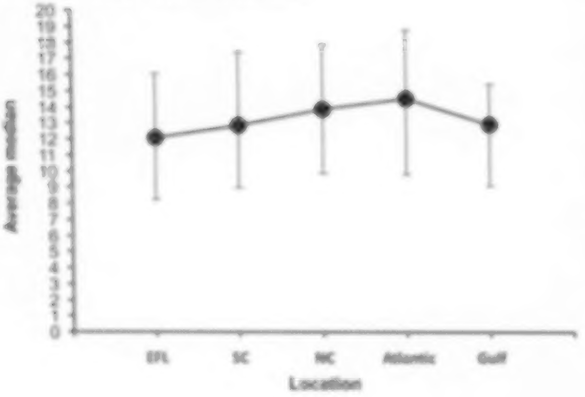

not confirm Chapman et al. (1999), the only other population genetic treatment of gag from both Gulf of Mexico and Atlantic sites. Using a subset of the microsatellite loci in this study (GAG010, GAG023, GAG038) and a smaller number of sample locations and genotypes, Chapman et al. (1999) report patchy genetic structure among populations and significant departures from Hardy–Weinberg equilibrium due to inflated inbreeding coefficients (F_{IS} = 0.02 to 0.44; mean F_{IS} = 0.27) at two of three loci. In contrast, this study found uniformly homogenous genetic structure, no consistent deviations from HWE, and low, nonsignificant levels of F_{IS} (–0.01) within and among locations. It is likely that the causes of these discrepancies are methodological, as the present study used modern genotyping methods (automated capillary-based genotyping versus gel scoring), a greater sample size (870 versus 246), and a greater number of genetic loci (11 vs. 3). The large-scale homogeneity found in this study does, however, mirror a similar conclusion of Jue (2006), which also reported no temporal or spatial genetic differentiation within the eastern Gulf of Mexico using these same 11 microsatellites. In addition, no significant difference in genetic diversity (as measured by theta and heterozygosity) was detected between the northwestern Atlantic and the eastern Gulf of Mexico in this study (see Supplemental Tables S3–S5[2]), suggesting that the effective population sizes are similar among regions. These data imply then that gag stocks from the northwestern Atlantic and eastern Gulf of Mexico belong to a single genetically panmictic population.

However, the lack of genetic differentiation between the eastern Gulf of Mexico and the Atlantic may be the consequence of (*i*) the low statistical power of our data to resolve genetic structure, (*ii*) migration between regions, (*iii*) nonequilibrium between gene flow and drift since populations diverged, or some combination of these three explanations. Low F_{ST} values are particularly common for marine fishes (Ward et al. 1994; Waples 1998) and elevate concerns about the statistical power necessary to infer the degree of gene flow among marine populations. A first-approximation power analysis was generated using the program POWSIM (Ryman and Palm 2006) and indicated that there was a 99.5% chance of detecting a significant difference at an F_{ST} of 0.001 with 11 loci and a sample size of 300 per region. Coupled with the consistency of the values across loci, cohorts, and statistical tests, we have confidence that the absolute levels of differentiation obtained in this study (F_{ST} < 0.001) are biologically real.

It is possible that low levels of genetic differentiation are maintained by effective long-distance migration of gag. Gag larvae have a relatively long planktonic existence (mean 43 days; Keener et al. 1988), and surface-drogue evidence indicates that surface currents can travel from the Florida Keys to the eastern coast of Florida within 45 days (Hare and Walsh 2007). In addition, substantial numbers of adult

Fig. 3. Predicted level of genetic differentiation (Weir and Cockerham's Φ_{ST}) for 11 microsatellite loci with varying numbers of migrants per generation (N_m) after an ancestral population (diploid N_e = 16 500) splits into two subpopulations (N_e = 16 500 each). *t*, number of generations since divergence. Error bars represent the 95% confidence interval of 100 replicate runs under each combination of parameters (varying migrations rates and generation times). Simulations show that even after as many as 500 000 generations, migration rates (N_m) as low as 20–30 individuals per generation yield Φ_{ST} values near 0 (error bars extend to 0).

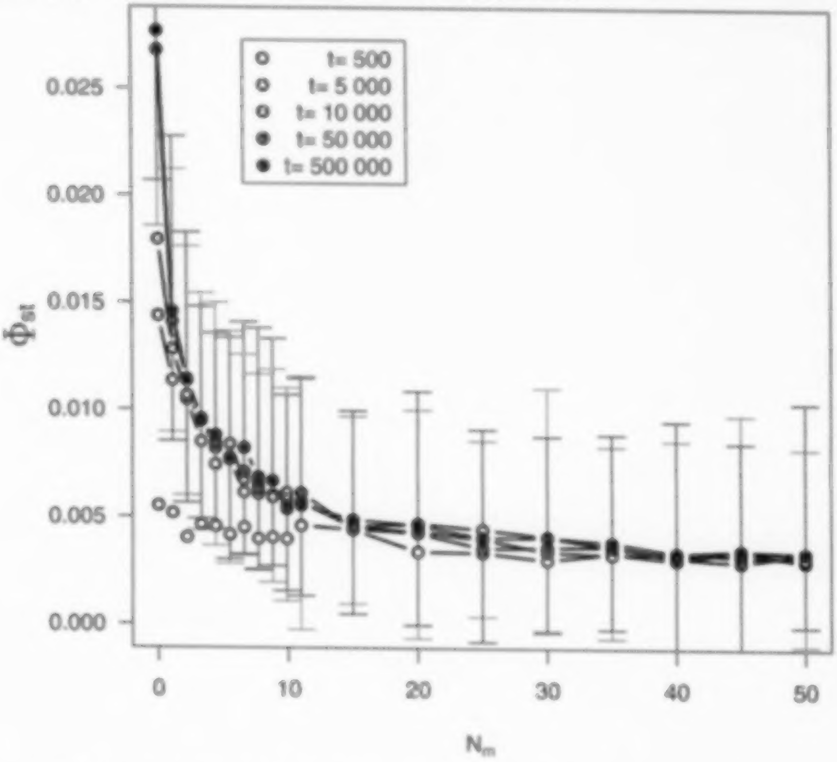

Table 3. Studies of marine fishes that have compared the Gulf of Mexico with the Atlantic.

Fish	Loci	F_{ST}	Reference
Vermillion snapper	Msats (7)	0.001 (ns)	Bagley et al. 1999
Red grouper	Msats (4)	<0.000 (ns)	Zatcoff et al. 2004
Scamp	Msats (6)	<0.000 (ns)	Zatcoff et al. 2004
Striped mullet	mtDNA (1)	<0.000 (ns)	Rocha-Olivares et al. 2000
Red snapper	mtDNA (1)	<0.000 (ns)	Garber et al. 2004
Red porgy	Msats (6)	0.000 (ns)	Ball et al. 2007

Note: Msats, microsatellites; mtDNA, mitochondrial control region. The number of loci used is given in parentheses; ns, nonsignificant.

and subadult gag are known to move among reefs within the Gulf (Heinisch and Fable 1999; Lindberg et al. 2006; Southeast Data, Assessment, and Review (SEDAR) 2006*b*) and the Atlantic (McGovern et al. 2005), and a small proportion of these are moving between regions. McGovern et al. (2005) tagged 3876 gag largely from North carolina and South Carolina and recovered 435 (11.2%) tagged individuals. Of these individuals, five gag moved into the eastern Gulf of Mexico, or almost 1.15% of recovered individuals. If this rate approximated the average number of adult or subadult individuals that moved between regions (i.e., migration rate *m*), then with a census size (N_C) of 1–3 million (following Jue 2006), approximately 12 000 to 35 000 adult or juvenile individuals move from the Atlantic to the Gulf per generation. There are several assumptions underlying this estimate, including bias in recapture (McGovern et al. 2005), but it seems reasonable to assume that hundreds to thousands of gag are able to move among regions per generation. To affect the population genetics, however, at least some of these migrants must be reproducing. A tentative estimate of adult gene flow can be generated by calculating the effective size of this migrant pool, given the tagging-based estimate of migration (1.15%). Assuming an N_e/N_C ratio of 10^{-2} (Jue 2006), the effective number of migrants (or N_em) based on the McGovern et al. tagging data is between 120 to 350. Acknowledging that one should be cautious in using F_{ST} to estimate N_m (Whitlock and McCauley 1999), it is interesting to note that this estimate is consistent with the genetic data presented in this study: a simplistic analysis of the tagging-based migrant pool yields F_{ST} of 0.0007 to 0.0021, a level of F_{ST} that is at or below the limit of detectable signal using our genetic sampling.

The third possible explanation for the lack of genetic differentiation between the Gulf of Mexico and the Atlantic is that these regions are not at an evolutionary equilibrium between genetic drift and gene flow. When a subdivided population has not had enough time since divergence to differentiate via lineage sorting, genetic homogeneity between sampling locations would be an artifact of past connectivity rather than present isolation and one could mistakenly infer larger migration rates than the true rates (Whitlock and McCauley 1999). Such nonequilibrium conditions are especially likely among large marine populations (Grosberg and Cunningham 2001). Computer-based simulations were utilized to assess the degree to which lineage sorting (which for a given N_e is determined by the time since divergence), gene flow or both can be responsible for neutral genetic homogeneity between locations. Such analyses are emerging as powerful tools in analyzing empirical population genetic data (e.g., Strand and Niehaus 2007; Selkoe et al. 2008) in large part because they allow alternative evolutionary hypotheses to be evaluated quantitatively. Here, the effect of time since divergence and effective migration rates on Φ_{ST} was modeled using the coalescent simulator in SIMCOAL. The results suggest that even after a conservatively long time since divergence (500 000 generations or ~1.5–5 million years for gag), effective migration rates as low as 20 to 30 individuals per generation yield levels of genetic differentiation that were measured (i.e., $\Phi_{ST} < 0.001$). Our simulations and other coalescent analyses (data not shown) indicate that providing a more precise estimate of genetic differentiation is not possible given our genetic and population sampling. This suggests that genetic homogeneity between Gulf and Atlantic gag results from either broad dispersal (hundreds to thousands of individuals per generation) or dispersal rates as low as approximately 20–30 per generation when populations are not in genetic equilibrium.

Our study highlights an important aspect of computer-based simulations, which is to estimate the lower bound of dispersal between regions when populations reveal genetic homogeneity. Simulations could be more broadly used to provide lower bounds of the number of migrants per generation among a suite of marine species. This includes a number of commercially important fish species that reveal no Gulf–Atlantic genetic separation (Table 3) as we have seen in gag: red snapper (*Lutjanus champechanus*; Garber et al. 2004), vermillion snapper (*Rhomboplites aurorubens*; Bagley et al. 1999), red porgy (*Pagrus pagrus*; Ball et al. 2007), red grouper (*Epinephelus morio*; Zatcoff et al. 2004), scamp (*Mycteroperca phenax*; Zatcoff et al. 2004), and striped mullet (*Mugil cephalus*; Rocha-Olivares et al. 2000). Similar to gag, these fish have large census sizes (hundreds of thousands) and show low, nonsignificant levels of differentiation between regions. Because simulations provide quantification of gene flow and time since divergence, the approach dramatically improves on the qualitative assessment that has been pursued by previous studies. For example, authors have suggested only general guidelines (e.g., 1/*m* generations to reach equilibrium; Bagley et al. 1999; for theory, see Slatkin 1995) to assess the degree by which nonequilibrium is important in driving population genetics. The advantage of simulations is their ability to quantify the synergistic effects among population size, time since divergence, and migration rate in predicting levels of genetic divergence, while providing quantitative measures of migration that can be compared with empirical data.

The data presented in this study suggest at least two implications for fisheries management. First, there is no evidence that overfishing has had demonstrable consequences on the neutral population genetics of gag over the period of time examined. The South Atlantic Fisheries Management Council (SAFMC) and the Gulf of Mexico Fisheries Management Council (GOMFMC) consider gag to be overfished (i.e., the current fishing mortality rate is above that which maintains a maximum sustainable yield; SEDAR 2006*a*, 2006*b*). Overfishing has led to female-biased sex ratios in these regions as gag are protogynous hermaphrodites that become male when large (Coleman et al. 1996; McGovern et al. 1998; Harris and Collins 2000). Shifts in sex ratios, in addition to the lowered census sizes, will have detrimental long-term effects on gag populations by lowering effective sizes (or N_e) and, as a consequence, increasing rates of genetic drift and inbreeding. The results from this study do not reveal clear genetic effects of fishing pressure only to the extent that there is no significant signal of inbreeding; however, we caution that the relatively long generation time of gag (3–10 years) will delay the appearance of fishing-related losses in genetic diversity.

Second, the data presented in the study address the long-standing strategy of managing gag fisheries in the United States as two separate stock units, with the Atlantic stock unit (North Carolina to Key West) managed by the South Atlantic Fishery Management Council and the Gulf of Mexico stock unit managed by the Gulf of Mexico Fishery Management Council (Key West to Mexico) (SEDAR 2006*a*, 2006*b*). Current management schemes take into account the greater population size and the larger fishing industry in the Gulf of Mexico when compared with the Atlantic (Koenig et al. 2000; SEDAR 2006*a*, 2006*b*), yet there is a need to understand effective migration rates between the zones. These genetic data indicate low divergence between the Atlantic and the Gulf of Mexico, which implies substantial connectivity between these regions and would support their combination into a single genetically homogenous management unit. However, because of general concerns with statistical power and nonequilibrium in large marine populations, many authors have now cautioned against using panmixia (i.e., genetic homogeneity) as the sole standard by which management units are determined for marine organisms (Taylor and Dizon 1996; Taylor and Dizon 1999; Palsbøll et al. 2007). Simulations were used to conclude that the rates of dispersal between the eastern Gulf of Mexico and Atlantic regions could be as low as approximately 20–30 per generation or as high as hundreds to thousands per generation, and distinguishing these possibilities will likely require greater sampling of both individuals and the gag genome. Given the imprecision, this study can neither support nor refute current management schemes that independently regulate gag in the Gulf and the Atlantic.

Acknowledgements

The authors thank NOAA researcher Erik Williams in Beaufort, North Carolina, and members of the South Carolina Department of Natural Resources in Charleston, South Carolina, including Patrick Harris, George Sedberry, Marcel Reichert, David Wyanski, Dan Machowski, and Byron White, for the collection of Atlantic samples. The authors appreciate the assistance of Robert Chapman, Brandon Eleby, and Amy Ball with methodology. The authors also thank Don Levitan and the members of the Levitan lab at Florida State University in Tallahassee, Florida, for use of materials, equipment, and laboratory space. Funding for this research was generously provided by South Carolina Sea Grant and by the US Environmental Protection Agency (US EPA) under the Science to Achieve Results (STAR) Graduate Fellowship Program. The US EPA has not officially endorsed this publication and the views expressed herein may not reflect the views of the US EPA.

References

Avise, J.C. 1992. Molecular population structure and the biogeographic history of a regional fauna: a case history with lessons for conservation biology. Oikos, **63**: 62–76. doi:10.2307/3545516.

Bagley, M.J., Lindquist, D.G., and Geller, J.B. 1999. Microsatellite variation, effective population size, and population genetic structure of vermillion snapper, *Rhomboplites aurorubens*, off the southeastern USA. Mar. Biol. (Berl.), **134**(4): 609–620. doi:10.1007/s002270050576.

Ball, A.O., Beal, M.G., Chapman, R.W., and Sedberry, G.R. 2007. Population structure of red porgy, *Pagrus pagrus*, in the Atlantic Ocean. Mar. Biol. (Berl.), **150**: 1321–1332. doi:10.1007/s00227-006-0425-y.

Beerli, P. 2006. Comparison of a Bayesian and maximum-likelihood inference of population genetic parameters. Bioinformatics, **22**: 341–345. doi:10.1093/bioinformatics/bti803. PMID:16317072.

Beerli, P., and Felsenstein, J. 2001. Maximum likelihood estimation of a migration matrix and effective population sizes in *n* subpopulations by using a coalescent approach. Proc. Natl. Acad. Sci. U.S.A. **98**: 4563–4568. doi:10.1073/pnas.081068098. PMID:11287657.

Begg, G.A., and Waldman, J.R. 1999. A holistic approach to stock identification. Fish. Res. **43**: 35–44. doi:10.1016/S0165-7836(99)00065-X.

Bonin, A., Bellemain, E., Bronken Eidesen, P., Pompanon, P., Brochmann, C., and Taberlet, P. 2004. How to track and assess genotyping errors in population genetics studies. Mol. Ecol. **13**: 3261–3273. doi:10.1111/j.1365-294X.2004.02346.x. PMID:15487987.

Bullock, L.H., and Smith, G.B. 1991. Seabasses (Pisces: Serranidae). Memoirs of the Hourglass Cruises VII (part II). Marine Research Laboratory, Florida Department of Natural Resources, St. Petersburg, Florida.

Cano, J.M., Shikano, T., Kuparinen, A., and Merilä, J. 2008. Genetic differentiation, effective population size and gene flow in marine fishes: implications for stock management. J. Integr. Field Sci. **5**: 1–10.

Chapman, R.W., Sedberry, G.R., Koenig, C.C., and Eleby, B.M. 1999. Stock identification of gag, *Mycteroperca microlepis*, along the southeast coast of the United States. Mar. Biotechnol. **1**: 137–146. doi:10.1007/PL00011761. PMID:10373622.

Coleman, F.C., Koenig, C.C., and Collins, L.A. 1996. Reproductive styles of shallow-water groupers (Pisces: Serranidae) in the eastern Gulf of Mexico and the consequences of fishing spawning aggregations. Environ. Biol. Fishes, **47**: 129–141. doi:10.1007/BF00005035.

Excoffier, L., Smouse, P., and Quattro, J. 1992. Analysis of molecular variance inferred from metric distance among DNA haplotypes: application to human mitochondrial DNA restriction data. Genetics, **131**: 479–491. PMID:1644282.

Excoffier, L., Novembre, J., and Schneider, S. 2000. SIMCOAL: a general coalescent program for the simulation of molecular data in interconnected populations with arbitrary demography. J. Hered. **91**(6): 506–510. doi:10.1093/jhered/91.6.506. PMID:11218093.

Excoffier, L., Laval, G., and Schneider, S. 2005. Arlequin ver. 3.0: an integrated software package for population genetics data analysis. Evolutionary Bioinformatics Online, **1**: 47–50. Software available at http://cmpg.unibe.ch/software/arlequin3/#Downloads [accessed September 2007].

Fogarty, M.J., and Botsford, L.W. 2007. Population connectivity and spatial management of marine fisheries. Oceanography (Washington, D.C.), **20**(3): 112–123.

Fraser, D.J., and Bernatchez, L. 2001. Adaptive evolutionary conservation: towards a unified concept for determining conservation units. Mol. Ecol. **10**: 2741–2752. PMID:11903888.

Garber, A.F., Tringali, M.D., and Stuck, K.C. 2004. Population structure and variation in red snapper (*Lutjanus campechanus*) from the Gulf of Mexico and Atlantic coast of Florida as determined from mitochondrial DNA control region sequence. Mar. Biotechnol. **6**: 175–185. doi:10.1007/s10126-003-0023-7. PMID:14586768.

Grosberg, R., and Cunningham, C.W. 2001. Genetic structure in the sea: from populations to communities. *In* Marine community ecology. *Edited by* M. D. Bertness, S. Gaines, and M.E. Hay. Sinauer Associates, Sunderland, Mass. pp. 61–84.

Hardy, O.J. 2003. Estimation of pair-wise relatedness between individuals and characterization of isolation-by-distance processes using dominant genetic markers. Mol. Ecol. **12**: 1577–1588. doi:10.1046/j.1365-294X.2003.01835.x. PMID:12755885.

Hare, J.A., and Walsh, H.J. 2007. Planktonic linkages among marine protected areas on the south Florida and southeast United States continental shelves. Can. J. Fish. Aquat. Sci. **64**: 1234–1247. doi:10.1139/F07-089.

Harris, P.J., and Collins, M.R. 2000. Age, growth and age at maturity of gag, *Mycteroperca microlepis*, from the southeastern United States during 1994–1995. Bull. Mar. Sci. **66**(1): 105–117.

Hauser, L., and Carvalho, G.R. 2008. Paradigm shifts in marine fisheries genetics: ugly hypotheses slain by beautiful facts. Fish Fish. **9**(4): 333–362.

Heemstra, P.C., Anderson, W.D., Jr., and Lobel, P.S. 2002. Serranidae. *In* The living marine resources of the western central Atlantic. Volume 2. Bony fishes. Part 1 (Ascipenseridae and Grammatidae). *Edited by* K.E. Carpenter. FAO Species Identification Guide for Fishery Purposes, American Society of Ichthyologists and Herpetologist Special Publication 5, Rome, Italy. pp. 1308–1369.

Heinisch, B.V., and Fable, W.A., Jr. 1999. Movement of gag, *Mycteroperca microlepis*, in and from St. Andrew Bay, Florida. Bull. Mar. Sci. **64**(3): 501–508.

Jue, N.K. 2006. Exploring the structure of genetic variation and the influences of demography on effective population size in the gag grouper *Mycteroperca microlepis* (Goode and Bean). J. Fish Biol. **69**(Suppl. C): 217–224. doi:10.1111/j.1095-8649.2006.01273.x.

Keener, P., Johnson, G.D., Stender, B.W., Brothers, E.B., and Beatty, H.R. 1988. Ingress of postlarval gag, *Mycteroperca microlepis* (Pisces: Serranidae), through a South Carolina barrier island inlet. Bull. Mar. Sci. **42**(3): 376–396.

Koenig, C.C., Coleman, F.C., Grimes, C.B., Fitzhugh, G.R., Scanlon, K.M., Gledhill, C.T., and Grace, M. 2000. Protection of fish spawning habitat for the conservation of warm-temperate reef-fish fisheries of shelf-edge reefs of Florida. Bull. Mar. Sci. **66**: 593–616.

Lindberg, W.J., Frazer, T.K., Portier, K.M., Vose, F., Loftin, J., Murie, D.J., Mason, D.M., Nagy, B., and Hart, M.K. 2006. Density-dependent habitat selection and performance by a large mobile reef fish. Ecol. Appl. **16**(2): 731–746. doi:10.1890/1051-0761(2006)016[0731:DHSAPB]2.0.CO;2. PMID:16711059.

McGovern, J.C., Wyanski, D.M., Pashuk, O., Manooch, C.S., III, and Sedberry, G.R. 1998. Changes in the sex ratio and size at maturity of gag, *Mycteroperca microlepis*, from the Atlantic coast of the southeastern United States during 1976–1995. Fish. Bull. (Washington, D.C.), **96**: 797–807.

McGovern, J.C., Sedberry, G.R., Meister, H.S., Westendorff, T.M., Wyanski, D.M., and Harris, P.J. 2005. A tag and recapture study of gag, *Mycteroperca microlepis*, off the southeastern US. Bull. Mar. Sci. **76**(1): 47–59.

Morris, A.V., Roberts, C.M., and Hawkins, J.P. 2000. The threatened status of groupers (Epinephelinae). Biodivers. Conserv. **9**: 919–942. doi:10.1023/A:1008996002822.

Palsbøll, P.J., Bérubé, M., and Allendorf, F.W. 2007. Identification of management units using population genetic data. Trends Ecol. Evol. **22**(1): 11–16. doi:10.1016/j.tree.2006.09.003. PMID:16982114.

Raymond, M., and Rousset, F. 1995. An exact test for population differentiation. Evolution, **49**: 1280–1283. doi:10.2307/2410454.

Rice, W.R. 1989. Analyzing tables of statistical tests. Evolution, **43**(1): 223–225. doi:10.2307/2409177.

Rivera, M.A., Graham, G.C., and Roderick, G.K. 2003. Isolation and characterization of nine microsatellite loci from the Hawaiian grouper *Epinephelus quernus* (Serranidae) for population genetic analyses. Mar. Biotechnol. **5**: 126–129. doi:10.1007/s10126-002-0093-y. PMID:12876647.

Rocha-Olivares, A., Garber, N.M., and Stuck, K.C. 2000. High genetic diversity, large inter-oceanic divergence and historical demography of the striped mullet. J. Fish Biol. **57**: 1134–1149. doi:10.1111/j.1095-8649.2000.tb00476.x.

Rose, C.G., Paynter, K.T., and Hare, M.P. 2006. Isolation by distance in the eastern oyster, *Crassostrea virginica*, in Chesapeake Bay. J. Hered. **97**(2): 158–170. doi:10.1093/jhered/esj019. PMID:16489144.

Ryman, N., and Palm, S. 2006. POWSIM: a computer program for assessing statistical power when testing for genetic differentiation. Mol. Ecol. **6**: 600–602. doi:10.1111/j.1471-8286.2006.01378.x.

Selkoe, K.A., Henzler, C.M., and Gaines, S.D. 2008. Seascape genetics and the spatial ecology of marine populations. Fish Fish. **9**: 363–377.

Shanks, A.L. 1995. Mechanisms of cross-shelf dispersal of larval invertebrates. *In* Ecology of marine invertebrate larvae. *Edited by* L. McEdward. CRC Press, Boca Raton, Florida. pp. 323–368.

Slatkin, M. 1995. A measure of population subdivision based on microsatellite allele frequencies. Genetics, **139**: 457–462. PMID:7705646.

Southeast Data, Assessment, and Review. 2006*a*. SEDAR 10. Stock assessment report 1. South Atlantic gag grouper. Available at http://www.sefsc.noaa.gov/sedar/ [accessed August 2008].

Southeast Data, Assessment, and Review. 2006*b*. SEDAR 10. Stock assessment report 2. Gulf of Mexico gag grouper. Available at http://www.sefsc.noaa.gov/sedar/ [accessed August 2008].

Strand, A.E. 2002. METASIM 1.0: an individual-based environment for simulating population genetics of complex population dynamics. Mol. Ecol. Notes, **2**: 373–376. doi:10.1046/j.1471-8286.2002.00208.x.

Strand, A.E., and Niehaus, J.M. 2007. KERNELPOP, a spatially explicit population genetic simulation engine. Mol. Ecol. Notes, **7**: 969–973. doi:10.1111/j.1471-8286.2007.01832.x.

Taylor, B.L., and Dizon, A.E. 1996. The need to estimate power to link genetics and demography for conservation. Conserv. Biol. **10**(2): 661–664. doi:10.1046/j.1523-1739.1996.10020661.x.

Taylor, B.L., and Dizon, A.E. 1999. First policy then science: why a management unit based solely on genetic criteria cannot work. Mol. Ecol. **8**(Suppl. 1): S11–S16. doi:10.1046/j.1365-294X.1999.00797.x. PMID:10703548.

Turner, T.F., Wares, J.P., and Gold, J.R. 2002. Genetic effective size is three orders of magnitude smaller than adult census size in an abundant, estuarine-dependent marine fish (*Sciaenops ocellatus*). Genetics, **162**: 1329–1339. PMID:12454077.

van Oosterhout, C., Hutchinson, W.F., Wills, D.P.M., and Shipley, P. 2004. Micro-Checker: software for identifying and correcting genotyping errors in microsatellite data. Mol. Ecol. Notes, **4**: 535–538. Software available at http://www.microchecker.hull.ac.uk/. doi:10.1111/j.1471-8286.2004.00684.x.

Waples, R.S. 1998. Separating the wheat from the chaff: patterns of genetic differentiation in high gene flow species. J. Hered. **89**(5): 438–450. doi:10.1093/jhered/89.5.438.

Waples, R.S., and Gaggiotti, O. 2006. What is a population? An empirical evaluation of some genetic methods for identifying the number of gene pools and their degree of connectivity. Mol. Ecol. **15**: 1419–1439. doi:10.1111/j.1365-294X.2006.02890.x. PMID:16629801.

Ward, R.D., Woodward, M., and Skibinski, D.O.F. 1994. A comparison of genetic diversity levels in marine, freshwater, and anadromous fishes. J. Fish Biol. **44**: 213–232. doi:10.1111/j.1095-8649.1994.tb01200.x.

Weir, B.S., and Cockerham, C.C. 1984. Estimating *F*-statistics for the analysis of population structure. Evolution, **38**: 1358–1370. doi:10.2307/2408641.

Whitlock, M.C., and McCauley, D.E. 1999. Indirect measures of gene flow and migration: $F_{ST} \neq 1/(4Nm+1)$. Heredity, **82**: 117–125. doi:10.1038/sj.hdy.6884960. PMID:10098262.

Zatcoff, M.S., Ball, A.O., and Chapman, R.W. 2002. Characterization of polymorphic microsatellite loci from black grouper, *Mycteroperca bonaci* (Teleostei: Serranidae). Mol. Ecol. Notes, **2**: 217–219. doi:10.1046/j.1471-8286.2002.00194.x.

Zatcoff, M.S., Ball, A.O., and Sedberry, G.R. 2004. Population genetic analysis of red grouper, *Epinephelus morio*, and scamp, *Mycteroperca phenax*, from the southeastern U.S. Atlantic and Gulf of Mexico. Mar. Biol. (Berl.), **144**: 769–777. doi:10.1007/s00227-003-1236-z.

NRC CNRC
CISTI - ICIST

RIGHTSLINK
Copyright Clearance Center

NRC Research Press is pleased to announce our partnership with the Copyright Clearance Center

Les Presses scientifiques du CNRC annoncent fièrement leur partenariat avec le Copyright Clearance Center

With Copyright Clearance Center's Rightslink® service, it's faster and easier than ever before to secure permission from NRC Research Press Journals titles to be reused in a book / textbook, journal/ magazine, newspaper/newsletter, coursepack / classroom materials, CD-ROM/ DVD, promotional materials/pamphlet, presentation/slide kit, corporate intranet, or photocopy. Rightslink is also able to handle your requests for offprints as well as digital and paper reprints.

The process for permissions to reproduce content from Monographs remains unchanged and instructions can be found in the Contact Us & Customer Support section on our website.

Rightslink can be accessed by clicking on the "Reprints and Permissions" link in the table of contents of the article in question.

Le service Rightslink® du Copyright Clearance Center permet d'obtenir plus rapidement et plus facilement que jamais l'autorisation de réutiliser du contenu des revues des Presses scientifiques du CNRC dans des livres, des manuels, des revues, des magazines, des journaux, des bulletins, de la documentation pédagogique, des CD-ROM, des DVD, de la documentation promotionnelle, des diaporamas, l'intranet d'une entreprise ou une photocopie.*Rightslink* peut aussi traiter vos demandes pour des tirés à part ainsi que pour des réimpressions d'articles numériques et imprimés.

Le processus d'autorisation des reproductions de contenu des monographies demeure le même. Vous trouverez les instructions à la section Coordonnées et soutien à la clientèle.

On peut accéder à Rightslink en choisissant le lien « réimpressions et autorisations » dans la table des matières pour l'article voulu.

For questions about using the Rightslink service, please call Customer Support at 1-877-622-5543 (toll-free) or 978-777-9929, or e-mail customercare@copyright.com

Pour toute question à propos de l'utilisation du service Rightslink, communiquez avec le soutien à la clientèle au 1-877-622-5543 (sans frais) ou au 978-777-9929, ou par courriel à customercare@copyright.com.

National Research Council Canada | Conseil national de recherches Canada

Canadä

NRC·CNRC

National Research Council Canada
Conseil national de recherches Canada

Canadian Journal of Fisheries and Aquatic Sciences 1980–1995 back issues now available on the Web!

Archives du Journal candien des sciences halieutiques et aquatiques (1980–1995) maintenant accessibles sur le Web!

NRC Research Press is currently taking orders for the one-time purchase of the *Canadian Journal of Fisheries and Aquatic Sciences* back files (1980–1995), 15 years of fully indexed digitized articles are available!

This monthly journal publishes manuscripts reporting significant new knowledge and understanding of fisheries and aquatic sciences. They cover a range of disciplines including biology and ecology of marine and freshwater organisms, limnology, oceanography, physiology, toxicology, genetics, economics, disease, and management. CJFAS is one of 16 journals published by NRC Research Press, Canada's foremost scientific publisher.

Since this is a cost-recovery initiative, once costs are fully recovered, we would like to make our content more widely available by making the back files completely open in late 2009. We hope that libraries and the STM community share this goal and will partner with us to make this initiative a success.

ISSN: 1205-7533

CJFAS Web site: cjfas.nrc.ca

Frequency: Monthly (12 times/year)

Price: $2000.00

Les Presses scientifiques du CNRC acceptent maintenant les commandes pour l'achat en bloc des archives du *Journal canadien des sciences halieutiques et aquatiques* (1980–1995), 15 années d'articles numérisés et indexés!

Cette revue mensuelle publie des articles contribuant, via l'apport de nouvelles connaissances d'importance ou d'une compréhesion approfondie, à l'enrichissement des sciences halieutiques et aquatiques. Ceux-ci traitent de disciplines variées, y compris la biologie et l'écologie des organismes d'eau douce et d'eau salée, la limnologie, l'océanographie, la physiologie, la toxicologie, la génétique, l'économie, les maladies et la gestion. Elle est l'une des 16 revues des Presses scientifiques du CNRC, la maison d'édition scientifique la plus importante au Canada.

Il s'agit d'une initiative en recouvrement de coûts. Ainsi, nous aimerions élargir l'accès à nos collections en offrant les archives tout à fait gratuitement vers la fin de 2009, une fois les coûts entièrement recouvrés. Nous espérons que le milieu STM et les bibliothèques appuieront notre objectif et contribueront au succès de cette initiative.

ISSN : 1205-7533

Site Web : jcsha.cnrc.ca

Fréquence : mensuelle (12 numéros par année)

Tarif : 2000 $

Contact **Mike Boroczki** at **613-993-9108**
or mike.boroczki@nrc-cnrc.gc.ca for further information.

Communiquez avec **Mike Boroczki** au **613-993-9108**
ou mike.boroczki@nrc-cnrc.gc.ca pour obtenir des renseignements supplémentaires.

Contents (concluded) / Table des matières (suite et fin)

Kevin L. Pangle and Scott D. Peacor	**1748–1757**	Light-dependent predation by the invertebrate planktivore *Bythotrephes longimanus*
Douglas P. Peterson and William R. Ardren	**1758–1774**	Ancestry, population structure, and conservation genetics of Arctic grayling (*Thymallus arcticus*) in the upper Missouri River, USA
Lisa K. Schwarz and Michael C. Runge	**1775–1789**	Hierarchical Bayesian analysis to incorporate age uncertainty in growth curve analysis and estimates of age from length: Florida manatee (*Trichechus manatus*) carcasses
Randy J. Brown and Kenneth P. Severin	**1790–1808**	Otolith chemistry analyses indicate that water Sr:Ca is the primary factor influencing otolith Sr:Ca for freshwater and diadromous fish but not for marine fish
Peter Lewy and Kasper Kristensen	**1809–1820**	Modelling the distribution of fish accounting for spatial correlation and overdispersion
Elizabeth L. Cushman, Nathaniel K. Jue, Allan E. Strand, and Erik E. Sotka	**1821–1830**	Evaluating the demographic significance of genetic homogeneity using a coalescent-based simulation: a case study with gag (*Mycteroperca microlepis*)

National Research Council Canada
Ottawa, Canada
K1A 0R6

Conseil national de recherches Canada
Ottawa, Canada
K1A 0R6

Postage paid at Ottawa
Publications mail
Registration No. 40062591

Port payé à Ottawa
Poste-publication
Enregistrement n° 40062591

USPS periodical postage paid at Plattsburgh, NY 12901, USA

Canadian Journal of

FISHERIES AND AQUATIC SCIENCES

Volume 66, Number 10, October 2009

Journal canadien des

SCIENCES HALIEUTIQUES ET AQUATIQUES

Volume 66, numéro 10, octobre 2009

ARTICLES / ARTICLES

Julie Breton, Catherine Vallières, and Isabelle Laurion 1635–1648 Limnological properties of permafrost thaw ponds in northeastern Canada

Marcos Paulo Figueiredo-Barros, Adriano Caliman, João J. F. Leal, Reinaldo L. Bozelli, Vinicius F. Farjalla, and Francisco A. Esteves 1649–1657 Benthic bioturbator enhances CH_4 fluxes among aquatic compartments and atmosphere in experimental microcosms

Timothy Copeland and David A. Venditti 1658–1665 Contribution of three life history types to smolt production in a Chinook salmon (*Oncorhynchus tshawytscha*) population

Guðmundur J. Óskarsson and Christopher T. Taggart 1666–1681 Spawning time variation in Icelandic summer-spawning herring (*Clupea harengus*)

M. Catherine Eimers, Shaun A. Watmough, Andrew M. Paterson, Peter J. Dillon, and Huaxia Yao 1682–1692 Long-term declines in phosphorus export from forested catchments in south-central Ontario

Elvar H. Hallfredsson and Torstein Pedersen 1693–1706 Effects of predation from juvenile herring (*Clupea harengus*) on mortality rates of capelin (*Mallotus villosus*) larvae

Olaf P. Jensen, David J. Gilroy, Zeb Hogan, Brant C. Allen, Thomas R. Hrabik, Brian C. Weidel, Sudeep Chandra, and M. Jake Vander Zanden 1707–1718 Evaluating recreational fisheries for an endangered species: a case study of taimen, *Hucho taimen*, in Mongolia

Heidi Pardoe, Anssi Vainikka, Gudmundur Thórdarson, Gudrun Marteinsdóttir, and Mikko Heino 1719–1733 Temporal trends in probabilistic maturation reaction norms and growth of Atlantic cod (*Gadus morhua*) on the Icelandic shelf

Matthew L. Keefer, Christopher A. Peery, and Brett High 1734–1747 Behavioral thermoregulation and associated mortality trade-offs in migrating adult steelhead (*Oncorhynchus mykiss*): variability among sympatric populations

Continued on inside back cover / Suite au verso

Front cover: Iboko Saito/Toshiyuki Tajima/Dex Image/Getty Images.

Page couverture : Iboko Saito/Toshiyuki Tajima/Dex Image/Getty Images.

Canada

Printed in Canada by / Imprimé au Canada par
NRC Reprographic Services / Service de reprographie CNRC
Page production by / Mise en page par
NRC Research Press / Presses scientifiques du CNRC

0706-652X(200910)66:10;1-I